APPROCHES MICROSCOPIQUE ET MACROSCOPIQUE DES DETONATIONS

2ème Atelier International

Saint-Malo (Palais du Grand Large) France

2 - 7 OCTOBRE 1994

DTIC
ELECTE
OCT 2 6 1995
F

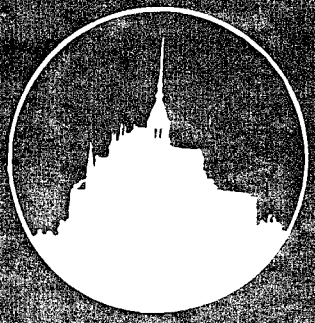

19951012 054

Éditeur scientifique S.ODIOT

les editions de physique

DISTRIBUTION STATEMENT A
Approved for public release;
Distribution Unlimited

JOURNAL DE PHYSIQUE IV

Volume 5 | Colloque C4 | Mai 1995

Supplément au Journal de Physique III, n°5

Approches microscopique et macroscopique des détonations

2ème atelier international

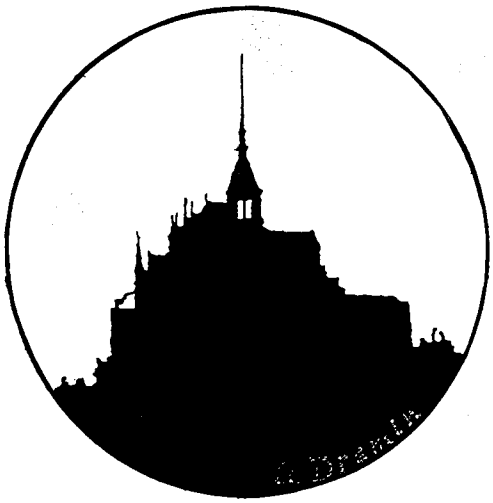

St. Malo, Palais du grand large
2-7 octobre 1994

les éditions de physique

Avenue du Hoggar
Zone Industrielle de Courtaboeuf
B.P. 112
91944 Les Ulis cedex A, France

Accesion For
NTIS CRA&I ☑
DTIC TAB ☐
Unannounced ☐
Justification .....
By .....
Distribution /
Availability Codes
Dist | Avail and / or Special
A-1

APPROCHES MICROSCOPIQUE ET MACROSCOPIQUE DES DETONATIONS

2 eme Atelier International

Sous le haut patronage du CEA/DAM, Centre d'Etudes de Vaujours-Moronvilliers

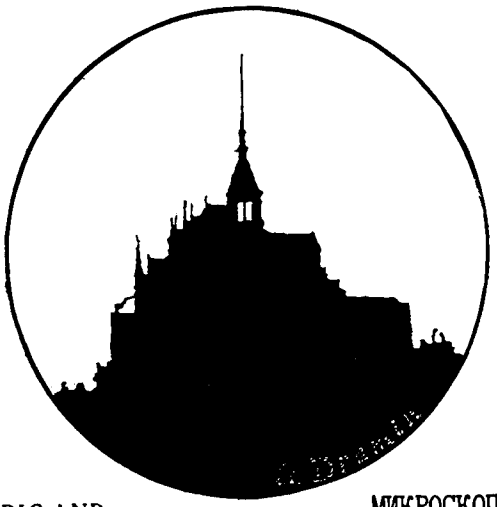

MICROSCOPIC AND MACROSCOPIC APPROACHES TO DETONATION

2 nd International Workshop

МИКРОСКОПИЧЕСКИЙ И МАКРОСКОПИЧЕСКИЙ ПОДХОДЫ К ИССЛЕДОВАНИЮ ДЕТОНАЦИИ

II международное рабочее совещание

This work is subject to copyright. All rights are reserved, whether the whole or part of the material is concerned, specifically the rights of translation, reprinting, re-use of illustrations, recitation, broad-casting, reproduction on microfilms or in other ways, and storage in data banks. Duplication of this publication or parts thereof is only permitted under the provisions of the French Copyright law of March 11, 1957. Violations fall under the prosecution act of the French Copyright Law.

© Les Editions de Physique Les Ulis 1994

Printed in France

Sous le haut patronage du CEA/DAM, Centre de Vaujours-Moronvilliers et avec le concours du Laboratoire d'Energétique et de Détonique de l'ENSMA

Présidents

Ron Armstrong (USA), Anatoly Dremin (Russie), Simone Odiot (France)

Comité d'accueil local

Jean-Claude Adenis, Hedwige Van Tiggelen

Comité d'organisation

J.C. Adenis (France), J.Ph. Choquin (France), S. Coffey (USA), M. Cook (Grande Bretagne), A. Fauconnier (France), C. Fauquignon (France), D. Jones (Australie), J. Lee (Canada), D. Liebenberg (USA), Y. de Longueville (France), Ch. Michaud (France), T. Pivina (Russie), H.N. Presles (France), A. Van der Steen (Pays-Bas), W. Tao (USA), F. Volk (Allemagne), F. Walker (USA)

Coordination

S. Odiot

Comité scientifique

R. Amiable (DGA/DME), J. Boileau (DGA/DRET), A. Delpuech (CEA/CER), P. Donguy (CEA/CEVM), S. Fliszar (Université de Montréal), V.I. Goldanskii (Institut Semenov de Chimie Physique), R. Miller (NRL), P. Rigny (CNRS), R. Troyanowski (S.C.F. section Chimie Physique), P. Urtiev (Livermore), P. Veyrié (CEA/CEVM)

Support financier de l'atelier

Nous remercions les organismes suivants qui ont permis par leur contribution financière, le bon déroulement de cette manifestation.

France

Association Française de Pyrotechnie, AFP
CEA, Centre d'Etudes de Vaujours-Moronvilliers
CEA, Centre d'Etudes du Ripault
CNRS
DGA, Direction des Recherches Etudes et Techniques
Les Editions de Physique

E.U.

Office of Naval Research, European Office
US Army Research
Development standardization Group

PREFACE

Je garde un très bon souvenir de l'Atelier de Megève de 1987, car, à cette occasion, étaient réunis les meilleurs spécialistes sur le thème de la détonation. Dès le début de ces réunions, une invitation avait été formulée par Madame ODIOT de sortir des sentiers battus, par la suite, de longues discussions ont permis d'approfondir ce sujet. Elles ont contribué de façon certaine à enrichir les connaissances scientifiques des participants. Cet atelier a permis d'améliorer les approches théorique et expérimentale. La modélisation des mécanismes de détonation a progressé.

En ce qui me concerne, j'avais pu bénéficier du savoir des spécialistes de modèles et de comprendre certains phénomènes qui apparaissent dans les foyers où la combustion se stabilise dans un écoulement supersonique : les calculs avaient montré, en aval de l'onde de choc, une formation de structure tourbillonnaire qui était, dans mon cas bénéfique, car mélangeant le combustible injecté à la paroi avec l'air amont et cette formation expliquait pourquoi la stabilisation de la combustion dans un écoulement à grande vitesse était possible.

L'Atelier de 1994 a le même souci :

1) en rassemblant des spécialistes mondiaux avec, en particulier, la présence de scientifiques russes réputés comme DREMIN, BORISOV,...

2) en évaluant les progrès réalisés depuis le dernier Atelier

3) en analysant des sujets essentiels comme :

   a) la réponse à une onde de choc d'un explosif idéal en phase condensée,
   b) la description et l'analyse fine de l'évolution chimique dans l'espace et le temps : transition choc-détonation, stabilité de l'onde de détonation, arrêt de la combustion...

Ce n'est pas mon rôle d'entrer dans le détail des exposés et des discussions. Dans ce court préambule, je me propose de souligner quelques points que j'ai particulièrement appréciés.

* Le thème fondamental demeure le calcul de la vitesse de propagation de l'onde explosive. Lorsque pour la première fois j'ai abordé ce problème, j'ai été surpris par la simplicité de la théorie basée sur les équations du bilan fortement simplifiées, limitées aux conditions amont et surtout aval (hypothèse de condition sonique) et donnant, dans le cas des mélanges gazeux, des vitesses de propagation théoriques peu éloignées de l'expérience, alors que j'ai peiné et peine encore sur le calcul de la vitesse de propagation de la déflagration (valeur propre du système) compliqué, lourd et parfois incertain.

  Les modèles classiques de l'onde de détonation idéale sont connus comme étant les modèles C.J. (CHAPMAN, JOUGUET) et Z.N.D. (ZELDOVITCH, NEUMANN, DOERING), améliorés par BRUN et CHERET, pour tenir compte de la courbure de l'onde, de l'écoulement réactif, et de la présence de forts gradients à l'aval dans le cas des explosifs en phase condensée.

  - Il reste néanmoins, comme le signale A.N. DREMIN, de nombreux points d'interrogation relatifs, par exemple, aux problèmes d'initiation, de transition déflagration-détonation, d'extinction, d'instabilités...

- Les phénomènes de détonation se développent dans un système dynamique. Ils ont une vie propre ce qui disqualifie l'hypothèse du stationnaire. Le paramètre temps est nécessairement présent dans tous ces problèmes.

- Les écoulements relaxés de ce système sont essentiellement non-linéaires et un effort doit être poursuivi dans cette direction, la présentation de Paul CLAVIN en est un exemple.

- Je suis toujours intrigué quand on parle de vitesse du son dans un écoulement chimiquement relaxé, car, dans ce cas, il existe plusieurs vitesses du son. Ici, l'hypothèse est faite, comme les phénomènes sont très rapides, de prendre une composition figée, la vitesse du son est donc supposée être celle donnée par la thermodynamique. Dans un milieu hors d'équilibre, à fort gradient, avec la formation très rapide de certaines espèces chimiques, la ligne ou la surface sonique a-t-elle un sens ?

Comme le souligne C. FAUQUIGNON dans son exposé, les discussions sur la théorie de la détonation sont loin d'être closes. C'est le rôle de cet Atelier de faire avancer nos idées dans ce domaine.

* Le problème de l'interaction d'une onde de choc avec la matière condensée explosive, souvent hétérogène, est d'une importance fondamentale dans le cadre des applications en relation avec la sécurité pyrotechnique.

La formation de points chauds, points d'accumulation de l'énergie, la transition choc-détonation, enfin d'une manière générale tout ce qui touche à la compréhension des mécanismes. Ces derniers temps, tous ces thèmes de recherche ont fait des progrès remarquables. Je voudrais dans ce préambule mettre l'accent sur le haut niveau de la physique utilisée. Les recherches sur l'interaction d'un choc avec un cristal explosif (PETN par exemple) constituent un ensemble consistant de la physique fondamentale, à la fois par l'influence de la structure ou, s'il s'agit d'un cristal de sa symétrie, par les modifications que l'onde de choc apporte à cette structure.

La concentration de l'énergie dans la phase d'amorçage en certains points du solide (points chauds dont les dimensions sont de l'ordre de 10^{-1} μm) est un phénomène très important dans le cadre de l'amorçage de la détonation. La sensibilité à la détonation des explosifs est également un problème complexe dont la solution progresse mais qui nécessite de fortes bases scientifiques en chimie quantique et physique moléculaire.

* Les résultats exposés au cours de cet Atelier sur la spectroscopie ultra-rapide sont étonnants. Ces dernières années, les méthodes de diagnostics par des techniques optiques ont été considérablement améliorées. Ce succès est dû en partie à l'utilisation des lasers et au développement exponentiel de l'informatique.

J'ai pu constater que ces améliorations des performances des techniques de mesure se retrouvent également dans les recherches, pourtant complexes, sur la détonation.

Les performances ont été améliorées dans deux domaines : d'une part dans la microanalyse des parties ultimes de la matière, d'autre part dans la rapidité de la mesure utilisant des impulsions allant jusqu'à la femtoseconde (10^{-15} s.).

Ces prouesses doivent permettre d'avoir une meilleure compréhension des phénomènes, d'élucider certains mécanismes et de valider les différents modèles. Le processus de détonation est caractérisé par de très hautes pressions et très hautes températures, l'analyse du rayonnement émis ou absorbé à différentes longueurs d'onde est riche en informations variées, d'où le succès des techniques spectrométriques ultra-rapides en temps réel, donnant de précieuses informations :

- sur la rupture des liaisons chimiques,

- sur le transfert et les échanges d'énergie à différent niveaux électroniques et vibrationnels,

- sur les réarrangements des espèces réagissantes,

- sur les différentes séquences des réactions chimiques irréversibles dans la matière condensée et en particulier dans les cristaux,

- sur les temps caractéristiques des réactions en chaîne pour la formation des espèces hautement activées (temps de l'ordre de 10^{-12} à 10^{-14} s.). Le processus de détonation pour les réactions majeures est de l'ordre du dixième de picoseconde, l'appareillage impressionnant développé par le CEA, TRISP (Time Resolved Infrared Spectral Photography) par spectrographie d'absorption permet de détecter les espèces chimiques formées au début de la décomposition de l'explosif et de les suivre dans les premières dizaines de nanosecondes pendant cette décomposition.

Avec tout l'appareillage sophistiqué évoqué précédemment, la structure microscopique de l'onde garde toujours un certain mystère malgré les remarquables exposés et les sérieuses discussions de ces quelques jours studieux passés à Saint-Malo.

Cela tient à la complexité du problème, la chimie quantique et la physique moléculaire fournissent quelques réponses sur la rupture des liaisons, sur la sensibilité au choc de certaines molécules, sur la propagation de l'énergie libérée d'une molécule à une autre dans l'édifice cristallin.

Tout cet aspect microscopique est en pleine évolution. Les réunions futures auront encore, dans ce domaine, de nombreux sujets de discussion.

Marcel BARRÈRE

PREFACE

I keep in mind a good memory of the 1987 MEGEVE workshop where the best scientists concerned with the detonation topic were convened. At the very beginning of the meeting Mrs ODIOT suggested us to get off the beaten track and so afterwards long and thorough discussions followed. This workshop certainly increased our scientific knowledge and improved the theoretical and experimental advances. The detonation mechanism and its modelling has made great strides.

I got much information and profit from modelling specialists for understanding some combustion phenomena which appear in combustor used for supersonic scramjet propulsion system where the combustion is stabilized: computations had shown the formation of vortex structures behind the shocks which are favourable for the mixing process of upstream air with hydrogen injected at the wall and explain the combustion stabilization, in the supersonic flow.

The 1994 workshop has the same purpose:

1) with a worldwide specialist meeting, with the participation of well-known Russian scientists as DREMIN, BORISOV...

2) with an evaluation of new results since the last workshop,

3) with an analysis of major topics such as:

a) The shock-wave response of an ideal condensed phase explosive,

b) The description and precise analysis of the physical and chemical evolution in space and time: shock-detonation transition, detonation stability, extinction process...

My purpose is not to enter into the details of papers and discussions, I would only like to underline some points I particulary appreciated.

The basic aspect of this theme is the detonation velocity computation. When I first met this problem, I was surprised by the theoretical simplicity based on the balance equations highly simplified, bounded on the upstream side conventional conditions and downstream with a sonic condition, these computation results for gaseous mixtures are not so far from the experimental detonation velocity. I met and I still meet some trouble because computing the propagation velocity of a deflagration (eigen value of the system) is complicate, heavy and sometimes imprecise.

The classical models of the ideal detonation wave are known as C.J. model (CHAPMAN, JOUGUET) and Z.N.D. (ZELDOVITCH, NEUMANN, DOERING) improved by BRUN and CHERET, to take into account of the wave curvature and the strong gradient effect in the case of explosive materials in condensed phase.

– Nevertheless, A.N. DREMIN pointed out that many questions have still no answer such as the initiation problem, the transition deflagration - detonation, the extinction, the instability conditions...

– The detonation phenomena spread out in a dynamical system. They have their own life which disqualifies the steady assumption. The time parameter is present in every problem.

– The relaxed flow of this system is fundamentally non-linear and an effort must be made in that direction. Paul CLAVIN's presentation is one example of it.

I am always puzzled when scientists discuss about sound velocity in a chemical relaxed flow because, in this case, many sound velocities can be defined. The simpler assumption is to suppose a frozen composition, for the phenomena are fast, and then the sound velocity is given by thermodynamic. In a non-equilibrium flow, with high gradients, with the fast formation of new species, where is the sonic line or sonic surface ?

As C. FAUQUIGNON underlines it: "Detonation theory is not a closed subject", the purpose of this workshop is to bring our ideas forward in the detonation theory.

The interaction problem of a shock-wave with liquid or solid heterogeneous explosives is of a fundamental importance in the application activities in relation with pyrotechnic security.

Hot spots formation, accumulation points of energy, shock-detonation evolution and finally, from a general point of view, the understanding of various mechanisms: all these topics are now in remarkable progresses. I would like to insist on the high level of the basic physics being used. The shock-wave interaction with an explosive crystal (Pentrite PETN for example) is a coherent view of fundamental physics, at the same time for structure effect or for the symmetry in a crystal and to modify this structure.

The energy concentration during the initiation of detonation in certain points in the solid (spots, dimension about 10^{-1} μm) is an important problem at the beginning of detonation.

The shock sensitivity of explosives is a complex problem, the solution of which being under progress and strong scientific foundations are necessary in quantum chemistry and molecular physic.

The results given at this workshop in ultra-fast spectrometry are surprising. In the past decade, the diagnostic methods by optical technics have improved a lot. This success is due to both the use of lasers and the exponentially increase in computing.

I also noticed that progresses for measurement technics are to be found in other research areas such as detonation. Performances were improved in two domains: on one hand in microanalysis at the ultime scale of the molecule and, on the other hand, a femtosecond pulse sequences to study fast events.

These improvements will allow a better understanding of phenomena clarifying some mechanism, and validating the various models. The detonation process is characteristic of high pressures and high temperatures; the radiation (emission or absorption) at different wave-length is to bring a lot of information from which the succes of real-time ultra fast spectroscopy techniques gives valuable information :

– on the breaking of chemical bonds,

– on the energy transfers at different electronic and vibrationnal levels.

– on the reorganization of reacting species,

– on the chemical evolution in the condensed phase and in particular in the crystal,

– on the characteristic times of chain chemical reactions, species formation of high activation (times in the range $10^{-12} - 10^{-14}$ sec). The detonation process for important chemical reaction is of about tenth picoseconde. The CEA impressive experimental set up, the TRISP (Ultra-fast Time-Resolved Infra-Red Spectral Photography), through absorption spectrometry gives the nature of the chemical species occuring during the explosive decomposition and to follow these molecules during the first ten nanoseconds of this decomposition.

Despite all this sophisticated set up mentioned above the microscopical wave structure still remains a mystery, in spite of the outstanding papers and the serious discussions which were to be heard during this studious week in Saint-Malo.

This is due to the complexity of the problem. Quantum chemistry and molecular physics give anyway some answers on the molecular structure, on molecule shock sensitivity and on the released energy propagation of one molecule to another.

All this microscopic aspect is in rapid evolution, and in the next meetings many other and interesting discussions will come out.

Marcel BARRÈRE

INTRODUCTION

Je viens de relire le compte-rendu du premier atelier de Megève sur les "Approches microscopique et macroscopique des détonations", publié en 1987 par les mêmes Editions de Physique. Trois articles ont retenu plus particulièrement mon attention. Ils sont signés de Numa Manson, Jason Nunziato et Arnold Karo. Je vous convie, ami lecteur, à vous y reporter pour deux raisons. La première, un hommage à leur mémoire ; la seconde, la meilleure des introductions aux travaux de ce deuxième atelier de St Malo et des suivants.

Numa Manson nous conduit à travers les documents anciens (1869 à 1900) vers la découverte de l'onde de détonation dont il fait l'historique critique avec son regard de physicien.

Jason Nunziato, dans une approche macroscopique de la détonation des explosifs hétérogènes (grains), brosse avec grande concision l'état de connaissance sur les processus physiques, "points chauds", et chimiques qui engendrent l'initiation et le développement de la détonation. Il souligne les points faibles d'une chimie par trop globale qui, désormais, devrait prendre en considération les espèces et réactions élémentaires intermédiaires avec leur cinétique ; étude fondamentale de la chimie des explosifs, à haute pression dynamique, que les récents progrès en spectroscopie et chimie quantique permettent d'envisager.

Arnold Karo passe en revue les simulations numériques, par dynamique moléculaire, de la propagation d'un choc dans les systèmes condensés. L'analyse qu'il donne des processus de transferts d'énergie induits par choc dans les matériaux énergétiques révèle son travail de pionnier sur la structure et la stabilité du front de choc. "C'est de la compréhension, dit-il en conclusion, des processus microscopiques impliqués dans l'initiation par choc des explosifs puissants, que se développera une image plus complète du ou des chemins de décomposition explosive sous choc mécanique."

Tout est ainsi réuni pour introduire les sujets traités en 1994 à l'atelier de St Malo, dont l'objectif à plus ou moins court terme focalise les questions posées, en conclusion de l'atelier de Megève, sur la réponse d'un explosif condensé au choc, qui engendre l'onde de détonation et lui confère caractéristiques et structure, objectif sur lequel Anatoly Dremin nous exhortera, inlassablement, tout au long de cet atelier, à faire porter notre effort.

L'étonnante performance des techniques expérimentales en spectroscopie ultrarapide rend aujourd'hui envisageable le suivi en temps réel des processus élémentaires hors équilibre, suggérés par une simulation numérique en dynamique moléculaire toujours plus performante, calculés par une chimie théorique qui contrôle déjà la phase condensée à haute pression statique et qui devra, nécessairement, un jour, s'adapter au choc. La spectroscopie de la subpicoseconde, nouveau fleuron de St Malo, donne à rêver ; des expériences possibles sortent du domaine de l'utopie. Mais comment la technique surmontera-t-elle les difficultés que pose la synchronisation du choc avec

l'enregistrement de la réponse du matériau ?

Il manquait à Megève des spécialistes, non détoniciens, des transferts d'énergie dans les cristaux et dans les liquides, de thermodynamique statistique, dont l'autorité peut contrôler ou provoquer nos idées. De tels spécialistes en la personne de Salvatore Califano et Savo Bratos étaient présents à St Malo.

On doit à Paul Vieille et Ya.B.Zel'dovich, le modèle fondamental hydrodynamique qui sert de base à la plupart des théories macroscopiques actuelles des détonations. Elles sont utilisées pour interpréter nombre d'observations expérimentales et notamment celles relatives aux conditions critiques d'existence du régime autonome de détonation. La modélisation des comportements dynamiques de la détonation par les méthodes de perturbation singulière n'avait pas été envisagée à Megève. Ces idées, introduites rappelons-le par Ya.B.Zel'dovich en théorie des flammes, font une apparition remarquée et prometteuse pour l'étude des phases gazeuses homogènes dans la limite des grandes énergies d'activation *. Autoriseront-elles aussi celle des phases condensées homogènes ?

Il était encore prématuré à Megève de passer des acquis en recherche fondamentale à l'application : maîtrise de la détonation ou méthodes prédictives compte-tenu du coût d'une nouvelle molécule explosive. A St Malo, des exposés et de vifs échanges ont fait le point sur l'efficacité des codes prévisionnels, macroscopiques - hydrodynamique - et moléculaires avec "pedigree des erreurs" en calculs quantiques - chimie théorique -.

L'atelier a réuni à St Malo 101 personnes : France (52), E.U (20), Grande Bretagne (7), Russie (5), Belgique (4), Suède (3), République Tchéque (3), Allemagne (2), Australie (2), Canada (1), Italie (1), Pays Bas (1), aussi bien universitaires que chercheurs d'organismes publics ou de l'industrie. Cela illustre le vif intérêt en recherche fondamentale pour la "Détonique", science pluridisciplinaire à haute technologie, et la nécessité ressentie unanimement de son développement pour en maîtriser les manifestations. La présence des Russes et des Tchèques, grands absents de Megève, la coprésidence d'Anatoly Dremin et de Ron Armstrong, dynamisèrent le brassage des idées et le développement de collaborations futures.

L'atelier, réparti sur quatre journées, se subdivise dans son compte-rendu en huit parties y compris la conclusion. La conclusion, je la livre au lecteur à l'état brut de nos conclusions individuelles. Elle est l'oeuvre de tous. Faire une synthèse de nos diverses conclusions, c'eût été les enfermer dans un cadre personnel. Les idées sont libérées devant le Grand Large du Palais.

I - Survol des aspects de la détonation

II - Autres conceptions de la détonation

III - Mécanismes de transfert d'énergie dans les matériaux énergétiques. Théories et expériences

IV - Aspects théoriques de la dynamique nonlinéaire de la détonation

V - Du microscopique au macroscopique

VI - Vers une chimie réaliste des processus réactionnels en détonique

VII - L'avenir des simulations numériques de la détonation par dynamique moléculaire

Conclusion

Les nombreuses discussions, questions - réponses et commentaires, qui ont fait l'objet de séances quotidiennes sont difficiles à refléter. Elles apparaissent parfois en fin d'articles, regroupées en synthèse par le modérateur ou retranscrites pêle-mêle. Je remercie vivement Scott Shackelford et Jacques Boileau, Jean-Claude Adenis grâce à qui nous avons pu disposer de documents écrits et enregistrés.

Il reste à vous remercier tous et en votre nom, aussi, nos parrains français et américains. Cet appui, moral et financier, nous le devons à Dick Miller, Pierre Veyrié, Alain Delpuech, Henry-Noël Presles.Tout particulièrement, un grand merci à Jean-Claude Adenis, Président de l'AFP, qui a assuré la logistique de l'atelier, veillé, dans les moindres détails, sur notre bien-être dans ce Palais du Grand Large, dirigé par Olivier Watine, assisté de Anne Blondel, que nous remercions très vivement pour la qualité de leur prestation, et leur remarquable organisation.

Je pense que ceux qui ont connu Olga de Mercouly, Poète de la Mer, se souviennent de la chaleur de son accueil, je lui dis ma reconnaissance.

J'exprime ma gratitude à Louis Brun qui m'a aidée si gentiment de ses conseils avisés.

Simone Odiot, d'Orcières le 31 Mars 1995

*Rédacteurs de ce paragraphe, Daniel Desbordes, Pierre Vidal, Henry-Noël Presles, merci.

INTRODUCTION

I have just read again the report on the first workshop, held at Megève in 1987, on microscopic and macroscopic approaches to detonation, that was published that same year by Les Editions de Physique. I was particularly impressed by three articles, written by Numa Manson, Jason Nunziato, and Arnold Karo. I can only advise you, dear reader, to read them for two reasons. First of all, as a tribute to the memory of these remarkable men; secondly, because these articles are the best introduction possible to the studies of the second workshop, held in St Malo in 1994, and the workshops to come.

Numa Manson leads us via the original documents of the 19th century (1869-1900) towards the discovery of the detonation wave, of which he traces the history with a physicist's critical eye.

Jason Nunziato, in a macroscopic approach to the detonation of heterogeneous explosives (grains), evaluates, with great conciseness, what we know today about physical processes, "hot spots", as well as about chemical processes that cause the initiation and expansion of detonation. He exposes the weaknesses of an approach to chemistry that was too phenomenological, pointing out that chemistry should now take into account the identification of the intermediary basic reactions with their kinetics. This is a fundamental study of the chemistry of energetic material under high dynamic pressure, that recent progress in spectroscopy and quantum chemistry will eventually make possible.

Arnold Karo, goes over the numerical simulations, by molecular dynamics, of shock propagation in condensed systems. His analysis of shock-induced energy transfer in energetic materials shows his pioneer work on shock front structure and stability. He concludes by saying: " It is from an understanding of the microscopic processes involved in the shock initiation of high explosives that a more complete picture of the path or paths to explosive decomposition from mechanical shock loading will be obtained."

This preliminary work, therefore, enables us to introduce the topics studied at the 1994 St Malo workshop, whose aim was, in the short run, to focus on the questions raised in conclusion at the workshop held in Mevège, on condensed explosive shock response triggering the detonation wave and giving it both characteristics and structure, an aim on which Anatoly Dremin relentlessly encouraged us to concentrate all our efforts throughout the workshop.

The astounding performances of experimental techniques in ultrafast spectroscopy now make it possible to envisage real time monitoring of the out of equilibrium basic processes suggested by numerical simulation by increasingly efficient molecular dynamics, calculated by theorical chemistry, which already masters high static pressure, and must, necessarily, adapt itself to the shock. With subpicosecond spectroscopy, the new jewel of St Malo, it is as if all our dreams could become reality; some experiments have become possible, they are no longer utopic, but not so easy to carry out with regard to technical problem of synchronisation, schock and energetic material response.

In Megève, there were no non-detonitian specialists in energy transfers in crystals and liquids, nor in statistical thermodynamics, whose authority could check or provoke our ideas. Such specialists, represented by Salvatore Califano and Savo Bratos, were present at St Malo.

We owe Paul Vieille and Ya. B. Zel'dovich the fundamental hydrodynamic pattern which is now the basis of most macroscopic detonation theories. They are used to interpret many experimental observations, in particular those in connection with critical conditions for the existence of the self-sustaining detonation regime. The modelisation of dynamic behaviours of detonation by singular pertubation methods had not been evoked at Megève. These ideas, introduced by Ya. B. Zel'dovich, in flames theory are very promising for the study of homogenous gaseous phases within the limits of the high activation energies (*). Will they also make that of homogenous condensed phases possible?

It was still too early in Megève to put into practice our knowledge in fundamental research: the mastery of detonation or predictive methods, considering the cost of a new explosive molecule. In St Malo, a certain number of presentations and lively discussions have made it possible to evaluate the efficiency of previsional macroscopic codes in hydrodynamics as well as molecular codes and the pedigree of errors in quantum calculations — theoretical chemistry.

101 people took part in the workshop: France (52), United States of America (20), Great Britain (7), Russia (5), Belgium (4), Czech Republic (3), Germany (2), Australia (2), Canada (1), Italy (1), the Netherlands (1). Some came from universities, others were researchers working for public organisations or the private sector. This is evidence of the appeal in fundamental research of Detonics, a pluridisciplinary, high-technology science, and of the necessity, wished by all, to develop it, so that its manifestations can eventually be mastered. The presence of researchers from Russia and the Czech Republic, who had unfortunately not been present at Megève, of Anatoly Dremin and Ron Armstrong, who co-presided the workshop, have given more energy and new meaning to intellectual exchanges, and future collaboration.

The report on the four-day St Malo workshop is divided into eight parts, including the conclusion. I give this conclusion to the reader, just as it was in St Malo, the work of all of us, as a summary of the conclusion of each participant would have seemed too restrictive and personal. Our ideas were set free in front of "Le Grand Large du Palais".

I. Overall Aspects of Detonation
II. Alternative Views on Detonation Theory
III. Energy Transfer Mechanisms in Energetic Materials — Theories and Experiments
IV. Theoretical Aspects of Non-Linear Dynamics of Detonation
V. From Microscopic to Macroscopic
VI. Towards a Realistic Chemistry of Reactional Processes in Detonics
VII. The Future of Numerical Simulations of Detonation by Molecular Dynamics
Conclusion

It is difficult to make an exact account of all the discussions, questions, answers and comments that flourished every day. In some cases, they are given at the end of the article or the summaries are written by our moderator, in other cases, their contents has, simply, been transcribed.

I would like to express my gratitude to Scott Shackelford and Jacques Boileau, Jean-Claude Adenis, thanks to whom we now have at our disposal, written and recorded documents. I would also like to thank all the participants, and our French and American sponsors. Many thanks to Dick Miller, Pierre Veyrié, Alain Delpuech and Henry-Noël Presles for their financial and moral support.

I want to thank Jean-Claude Adenis, the President of the AFP, who was in charge of the organisation of the workshop, and took great care of us at the Palais du Grand Large.

I am also very grateful to Monsieur Olivier Watine, the manager of the Palais, and his assistant, Madame Anne Blondel, for their remarkable work.

I think that those of you who met Olga de Mercouly, Poet of the Sea, remember her warm welcome. I want to tell her how grateful I am.

Finally, I want to express my gratitude to Louis Brun for his kind help and good advice.

Simone Odiot, d'Orcières, March 31, 1995

(*) The authors of this paragraph are Daniel Desbordes, Pierre Vidal, Henry-Noël Presles.

BIENVENUE A SAINT-MALO AU 2èME ATELIER DE TRAVAIL SUR LES APPROCHES MICROSCOPIQUE ET MACROSCOPIQUE DES DETONATIONS

Simone Odiot

Sept ans auparavant a eu lieu le premier atelier. Comme point d'ancrage, nous avions choisi Megève au pays du Mont Blanc, le plus haut sommet de France, "attracteur étrange", au début du siècle, des amoureux de l'impossible. Aujourd'hui c'est St Malo qui vous accueille, la patrie des découvreurs du Nouveau Monde, des corsaires, barroudeurs des mers, et le signe du Mont Saint Michel, symbole d'harmonie et de lumière, rappelle notre vocation de chercheur, aussi, ne l'oublions pas jeudi lorsque nous irons vers lui.

Un certain nombre de participants de Megève sont ici. D'autres nous ont quittés : Arnold Karo, Jason Nunziato et plus récemment Numa Manson ; ils étaient des pionniers pour introduire, développer, encourager l'approche microscopique des détonations. Je vous serais reconnaissante de bien vouloir honorer leur souvenir, debout, en une minute de silence.

Bien qu'il soit toujours acquis que l'approche macroscopique des théories classiques de la détonation, au niveau de l'application reste fort utile, cette approche cependant est inapte à la prévision d'accidents puisque, en fait, un tel contrôle est hors de sa compétence dans la mesure où elle ne peut répondre à la question fondamentale, "Pourquoi un explosif explose-t-il ?" .

La problèmatique soulevée en conclusion à Megève, impliquait un regroupement possible de nos compétences complémentaires, pour une étude expérimentale et théorique des transferts d'énergie dans le matériau soumis au choc, excitation, relaxation, dissociation, réactions chimiques ainsi que de l'identification des espèces réactives formées, au sein d'un "laboratoire fugace", siège de phénomènes hors équilibre à des pressions dynamiques extrêmes.

La molécule dont les caractéristiques électroniques confèrent certes au matériau ses propriétés détoniques, et la cinétique de ses fragments de dissociation, peuvent être examinées dans leur environnement dense, en temps réel. Aujourd'hui, les progrès en expérimentation et en chimie théorique rendent moins utopique le traitement de telles conditions.

Le développement des spectrographies ultra rapides, des techniques d'analyse des produits réactifs, autorisent, aujourd'hui, la conception d'expériences, impossibles sept ans auparavant,

pour décortiquer les mécanismes de détonation.

L'évolution des simulations de ces processus par dynamique moléculaire peut induire, aujourd'hui, de nouvelles idées.

Puisse cet atelier brasser nos diverses expériences dans ces domaines sus-cités, pour, de l'analyse de nos résultats, dégager une théorie des détonations ou à un niveau plus réaliste et modeste, de nouvelles voies d'approche.

A cet effet, cette manifestation qui est un atelier de travail et non un symposium où chacun prend un juste plaisir à exposer sa pensée et ses travaux, respecte un grand temps de libres discussions autour d'un thème quotidien, préparées par des conférences pléniaires et soutenues durant le temps imparti aux discussions générales par des interventions ponctuelles de très courte durée.

Finalement, j'attire votre attention sur le fait que cet atelier a trois présidents, américain, russe et français. La confrontation entre Est et Ouest ne se transforme-t-elle pas aujourd'hui en collaboration ?

Seven years ago the first workshop took place. As an anchor place, we had chosen Megeve, village located in the heart of White Mount country - the highest summit in Europe, which was in the beginning of the century some "strange attractor" of the lovers of the impossible.Today St Malo city - the fatherland of the discoverers of the New World, the fatherland of the corsairs - adventurers of the sea, is greeting you.
The sign of the Mont Saint Michel - symbol of Harmony and Light recalls our vocation of researcher ; thus, don't forget next thursday when we will go towards the Mount.

Some participants who have been in Megeve are also here.

Some : Arnold Karo and Jason Nunziato and more recently Numa Manson who were pioneers to introduce, elaborate, encourage to treat the microscopic approach to detonations, have unhappily gone. I should be greatly obliged if you kindly recall their memory by standing a minute in silence.

Although it is well known that macroscopic approach of the classical theories to detonation is useful, however, the approach can not predict injuries because, in fact, it is out of its competence since it is not able to answer the fundamental question : "Why does an explosive explode ?"

The problematics, mentioned in Megeve workshop conclusion had implied different group collaborations for theoretical and experimental studies of the process of energy transfer for excitation, relaxation, dissociation, chemical change and so on in shocked energetic material as well as the identification of the reactive species formed behind the shock front inside this "detonation short-lived laboratory" - the centre of highly non-equilibrium phenomena under extreme dynamic pressure conditions.

The molecule, electronic characteristics of which confer to the material its detonic properties, and chemical kinetics of dissociation and originated fragments reactions have to be investigated taking into account this severe environment.

Nowadays, progress in theoretical chemistry allows to treat such conditions.

Nowadays, the fast-expanding of ultra fast spectroscopies and reactive product analysis techniques might allow us to think of experimental realisation study on detonation mechanisms, in real time.

Nowadays, the molecular dynamics simulations of processes can induce new ideas.

Let this workwhop be able to mix our various experiences in order to bring out a theory of detonation or if we stay more realistic and modest, some ways for new approach.

Thus to do that, this meeting which is a workshop but not a symposium where everyone takes pleasure in explaining his own thinking and works, has to preserve a long time for free discussions around a daily topic previously prepared by plenary lectures and sustained during the time given to general discussions by some ponctual, short-time consuming, interventions.

Finally, one should mention that the workshop has three co-chairmen, american, russian and french and it means that the previous confrontation between East and West is changing for East and West collaboration.

Anatoly Dremin

Detonation Science originated in the previous century. You know that Alfred Nobel invented in 1860 some initiator based on primary explosives in order to reach reliable initiation of secondary explosives explosion.

The invention resulted in considerable increase of the explosion effect in comparison with that usually observed before at explosion initiation by black powder flame. Nobody knew at that time that the invention in fact had involved into human beings use the phenomenon which was named later, after its official discovering by french scientists Berthelot & Vieille and Malard & Le Chatelier in the beginning of the 80thies of that century, as the DETONATION phenomenon. As the matter of fact the discovery was the Detonation Science origin. Many outstanding scientists in France and other countries were involved in the phenomenon study, during the all past period till the present days french scientists being constantly in the first lines of the phenomenon researches.

First hydrodynamic theory of the phenomenon was developed in France - by Jouguet (1905), in England - by Chapman (1900), and in Russia - by Michelson (1889). They represented detonation wave as a shock wave with exothermic chemical reaction inside its front. It was the most significant step in the phenomenon theory progress. The theory turned out to be good for calculations of kinematic parameters of ideal detonation. However, the theory is unable to interpret detonation limits : SDT, instability, and failure diameter since, it had not proposed any mechanism of EMs' transformation at detonation.

Grib (1939), Zel'dovich (1940), von Neuman (1942), and Döring (1944) developed new hydrodynamic theory of detonation. It appeared as some response to the need for the theory capable to interpret the limits. The notion of the finite size chemical spike in the detonation wave front is the main point of the mechanism proposed by the ZND detonation theory. With few exception the chemical spike has been observed experimentally in many powder explosives and the ZND detonation wave model has got in this respect strong evidence. But the limits interpretations on the basis of the mechanism proposed were not completely successful. It turned out that the theory needs further development even for the stable detonation wave characteristic of powder explosives. However, one has to stress that although the model of the instable detonation wave characteristic of weak homogeneous explosives has nothing to do with the ZND detonation model, reliable knowledge of the regularities of EMs explosion energy release under the shock effect is important for both, power and weak explosives detonation.

The realization of the importance and the necessity of the study of the process of the shock mechanical energy transfer to explosive molecules is the main progress of the Detonation community activity during the last 10-15 years. Many scientists - Walker, Karo and Hardy, Coffey, Armstrong, Toton, Zerilli, Tsai, Trevino, Fayer, Dlott, Kim, Tokmakoff, E.Oran, Lambrakos, Boris, Gupta, Sharma and others - all of them stimulated the problem origin and its foundation.

But one should mention once again that French scientists, I would assemble here only some names : S.Odiot & M.Peyrard, A.Delpuech & S.Dufort, - they have played in the business especially remarkable role. Their pioneering extremely stimulating theoretical and experimental studies of explosive single crystals detonation phenomenon have given a strong impulse to the business as a whole.They were the first who realized the problem in its present understanding. And I believe that the first International Workshop on Microscopic and Macroscopic Approaches to Detonation arranged by french scientists in Megeve 7 years ago was the bright manifestation of the fact recognition. On the other hand, taking into account the recognition, nevertheless we have at present to be thankful to our french colleagues and especially to P.Veyrié, J.Boileau, Ch.Michaud, C.Fauquignon, G.Presles, G.Dupré for their efforts and support to arrange this workshop. In the course of past 7 years new results have been obtained, new interpretations have been done to some old experimental findings inconsistent with the ZND detonation theory. However, it should be mentioned that although the problem of shock mechanical energy transfer to explosive molecules at detonation has already attracted definite attention at some international meetings (for example, at the late Gordon Conference on Energetic Materials in New Hampton, 26 June - 1 July, 1994, USA), the problem is still in its infant state.

The Workshop Organising Committee and we, - S.Odiot, R.Armstrong, and myself as the Workwshop Co-chairmen believe that the time has come to discuss the results and findings as well as the possibilities of all available experimental, theoretical and computational methods to be used in the problem study in order to look for better detonation physical model. In my practice I came across with some theories of the same shock induced phenomena, each of them working well at different conditions. However, as the matter of fact, it turned out that the phenomenon nature, its intrinsic mechanism had not been revealed yet. I hope that sometime EMs' transformation mechanism at detonation will be understood sufficiently to develop unique detonation theory. Let our Workshop will be the first step towards this aim.

Mesdames et Messieurs,

Ouvrir une session d'un atelier scientifique, lancer une conversation entre amis lors d'une réception, ressortent du même point de vue. Il faut casser la glace.
Beaucoup de la réussite des ateliers scientifiques résulte des premiers instants. Pourvu que la mayonnaise prenne.

Il nous faudra beaucoup de modestie et d'écoute. Cette dernière épithète est certes à la mode mais elle est profondément justifiée.
Il y a ceux qui exploitent l'efficacité des modèles hydrodynamiques, c'est-à-dire macroscopiques. Ce sont des moyennes qui suivant la finesse des observations expérimentales lachent pied progressivement. D'autres font un dogme de la description détaillée des phénomènes moléculaires, lesquels sont les seuls à prendre en compte la totalité de la physique. Mais ceux là doivent peut être se limiter à décrire des configurations simples vu la complexité de plus en plus inextricable des phénomènes.

Je vous invite donc à vous écouter les uns les autres très honnêtement. Peut-être trouverez-vous un langage commun, peut-être pas. Mais en tous cas les chercheurs se seront rencontrés et peut-être se seront compris.

Pierre Veyrié

LISTE DES PARTICIPANTS
LIST OF PARTICIPANTS

Adenis Jean-Claude, CEA, B.P. 7, 77181 Courtry, France

Almström Henrik, National Defence Research Est., S-17290 Stockholm, Suède

Amiable René, DGA/DME/ST3S, 00460 Armées, France

Armstong Ronald W., Univ. of Maryland, College Park, MD 20742-3035, U.S.A.

Bardo Richard D., Naval Surface Warfare Center, 10901 New Hampshire Ave., MD 20903-5000, Silver-Spring, U.S.A.

Barrère Marcel, Onera, B.P. 72, 92322 Châtillon cedex, France

Baudin Gérard, DGA/DRET, 46500 Gramat, France

Bauer Pascal A., ENSMA, B.P. 109 Chasseneuil du Poitou, 86960 Futuroscope cedex, France

Becuwe Alain, SNPE, B.P. 2, 91710 Vert Le Petit, France

Belmas Robert, CEA, B.P. 16, 37260 Monts, France

Boileau Jacques, 15 rue des Lions Saint Paul, 75004 Paris, France

Boris Jay P., Naval Research Lab., DC 20375-5000 Washington, U.S.A.

Borisov A.A., Institute of Chemical Physics, 4 Kosygin St., 117997 Moskva, Russie

Braithwaite Martin, ICI Explosives PLC, Scotland KA20 3LN, Stevenson, Ayrshire, Royaume Uni

Branka Ruddy, Ineris, B.P. 2, 60550 Verneuil en Halatte, France

Bratos Sava, Université Pierre et Marie Curie, 75752 Paris cedex 05, France

Brown David, University of California, 9500 Gilman Drive, CA 92093-0402, La Jolla, U.S.A.

Brun Louis, CEA, B.P. 7, 77181 Courtry, France

Burgan Jean-Robert, CEA, B.P. 7, 77181 Courtry, France

Byers Brown William, Univ. of Manchester, Lancashire M13 9PL, Manchester, Royaume Uni

Califano Salvatore, Universita Di Firenze, Via Gino Cappooni, Firenze, Italie

Chaisse Francis, CEA, B.P. 7, 77181 Courtry, France

Charrue Pierre, CEA, B.P. 16, 37260 Monts, France

Cheret Roger, CEA, B.P. 510, 75752 Paris cedex 15, France

Chevallier Jean-Marc, CEA, B.P. 2, 33114 Le Barp, France

Choquin Jean-Philippe, CEA, B.P. 7, 77181 Courtry, France

Clavin P., CNRS, Case 252, 13397 Marseille cedex 20, France

Coffey Steve, Naval Surface Warfare Center, 10901 New Hampshire Ave., MD 20903 Silver Spring, U.S.A.

Cook Malcom, Defence Research Agency, Kent TN14 7BP, Sevenoaks, Royaume Uni

Courtecuisse Stéphane, CEA, B.P. 7, 77181 Courtry, France

Danel Jean-François, CEA, B.P. 7, 77181 Courtry, France

Davis William C., Los Alamos National Lab., P.O. Box 1663, NM 87545, Los Alamos, U.S.A.

Delpeyroux Didier, CEA, B.P. 16, 37260 Monts, France

Delpuech Alain, CEA, B.P. 16, 37260 Monts, France
Deng Junhua, Svebefo, P.O. Box 49153, S-100 29, Suède
Desbordes D., ENSMA, B.P. 109 Chasseneuil du Poitou, 86960 Futuroscope cedex, France
Dick Jerry J., Los Alamos National Lab., P.O. Box 1663, NM 87545, Los Alamos, U.S.A.
Dlott Dana, Univ. of Illinois, 505 S. Mathews Ave., IL 61801, Urbana, U.S.A.
Doyle Robert, Naval Research Lab., 4555 Overlook Ave. S.W., DC 20375-5000, Washington, U.S.A.
Dremin Anatoly N., Institute of Chemical Physics, Chernogolovka, 142432, Moskva, Russie
Dufort Serge, CEA, B.P. 16, 37260 Monts, France
Dupré Gabrielle, CNRS/CRCCHT, Avenue de la Recherche Scientifique, 45071 Orléans cedex, France
Fabre Denise, CNRS, Avenue J.B. Clément, 93430 Villetaneuse, France
Fauconnier Alain, T.B.A., 45240 La Ferté Saint Aubin, France
Fauquignon Claude, I.S.L., B.P. 34, 68301 Saint Louis cedex, France
Félix Sébastien, DGA/DRET/SDR/GT, 00460 Armées, France
Fliszar Sandor, Université de Montréal, CP 6210 Succ A, Québec H3C 3V1, Montréal, Canada
Gamezo Vadim, Université Pierre et Marie Curie, Place Jussieu, 75252 Paris cedex 05, France
Goutelle Jacques, DGA/CEG, 46500 Gramat, France
Gupta Yogendra M., Washington State University, WA 99164-2814, Pullman, U.S.A.
Haskins Peter J., DRA, Kent TN14 7BP, Sevenoaks, Royaume Uni
He Longting, Université Aix Marseille I, Rue Henri Poincaré, 13397 Marseille cedex 04, France
Jones David A., Dept. of Defence, DSTO, P.O. Box 50, Vic 3032 Melbourne, Ascot Vale, Australie
Kennedy David L., ICI Australia, P.O. Box 196, 2327, Kurri Kurri, Australie
Kernen Patrick, NATO/NIMIC, B-1110, Brussels, Belgique
Klein Ruppert, Institut Fuer Techn. Mech., Templergraben 64, D-5100, Aashen, Allemagne
Kondrikov Boris, Mendeleev University of Chemical Tech., 9 Mlusskaja SQ., 125190, Moskva A190, Russie
Kunz Albert, Michigan Technological Univ., 1400 Townsend Av., MI 49931, Houghton, U.S.A.
Lafon André, DGA/DRET, 00460 Armées, France
Lehky Ladislav, Synthesia AS, Vupch, Vyzkumny Ustav Prumyslove, 532 17, Pardubice-Semtin, République Tchèque
McAfee John M., Los Alamos National Lab., P.O. Box 1663, NM 87545, Los Alamos, U.S.A.
Melius Carl, Sandia National Lab., P.O. Box 969, CA 94551, Livermore, U.S.A.
Mialocq J.C., CEA, 91991 Gif-sur-Yvette cedex, France
Miller Richard, Office of Naval Research, 800 N. Quincy Street, VA 22217-5000, Arlington, U.S.A.
Nelson Keith, MIT, 77 Massachusetts Ave. Room 6231, MA 02139, Cambridge, U.S.A.
Odiot Simone, 3 Quai de la Tournelle, 75005 Paris, France
Oran Elaine, Naval Research Lab., Code 4410, DC 20375-5000, Washington, U.S.A.
Petitet Jean, CNRS, 93430 Villetaneuse, France
Pivina Tatiana S., ND Zelinsky Institute of Organic Chem., Leninsky Prosp. 47, 117913, Moskva, Russie
Plancon Michel, CEA, B.P. 6, 92260 Fontenay aux Roses, France
Plotard Jean-Paul, CEA, B.P. 7, 77181 Courtry, France

Pommeret Stanislas, CEA, Bât. 125, 91191 Gif-sur-Yvette, France
Poyet Jean-Michel, CEA, B.P. 7, 77181 Courtry, France
Presles Henri Noel, ENSMA, B.P. 109 Chasseneuil du Poitou, 86960 Futuroscope cedex, France
Proud William, Cambridge University, Madingley Road, CB3 OHE, Cambridge, Royaume Uni
Rajchenbach Corinne, Université de Bordeaux 1, 33405 Talence cedex, France
Ramsay John B., Los Alamos National Lab., P.O. Box 1663, NM 87545, Los Alamos, U.S.A.
Rauch Armand, CEA, B.P. 7, 77181 Courtry, France
Rigny Paul, CNRS, 3 rue Michel Ange, 75749 Paris cedex 16, France
Roucou J., CEA, B.P. 2, 33114 Le Barp, France
Rullière C., Université de Bordeaux 1, 351 cours de la Libération, 33405 Talence cedex, France
Russell Thomas P., Naval Research Laboratory, code 6110, DC 20375, Washington, U.S.A.
Samirant Michel S., I.S.L., B.P. 34, 68301 Saint Louis cedex, France
Sanderson A., NATO/NIMIC, JB 102, B-1110, Brussels, Belgique
Shackelford Scott A., FJ Seiler Research Laboratory NC, CO 80840-6528, San Diego, Royaume Uni
Simonetti Philippe, CEA, B.P. 16, 37260 Monts, France
Soulard Laurent, CEA, B.P. 7, 77181 Courtry, France
Swift Damian, M.O.D. (P.E.) AWE, H12, Awe Aldermaston, Berks RG7 4PR, Reading, Royaune Uni
Turkel Marie-Laure, CEA, B.P. 7, 77181 Courtry, France
Van Den Steen Albert, Prins Maurits Laboratory TNO, Lange Kleiweg 137, P.O. Box 45, NL-2280 AA, Rijswijck, Pays-Bas
Van Tiggelen Pierre J., Université Catholique de Louvain, Place Louis Pasteur, B-1348, Louvain La Neuve, Belgique
Van Tiggelen Edwige, 13 av. Meute, B-1470, Bousbal, Belgique
Vauthier Edouard, Université Pierre et Marie Curie, 4 Place Jussieu, 75252 Paris cedex 05, France
Vavra Pavel, Synthesia AS, Vupch, Vyzkumny Ustav Prumyslove, 532 17, Pardubice-Semtin, République Tchèque
Veyrie Pierre, CEA, B.P. 7, 77181 Courtry, France
Vidal Pierre, ENSMA, B.P. 109, 86960 Futuroscope cedex, France
Volk Fred, ICT Fraunhofer Institut, Postfach 1240, D-7507, Pfinztal-Berghausen, Allemagne
Walker Franklin E., Interplay, 18 Shadow Oak Road, CA 94256, Danville, U.S.A.
Wättestam Anders, National Defence Research Est., S-172 90, Stockholm, Suède
White Stephen, M.O.D. (P.E.) AWE, Aldermaston, Berks RG7 4PR, Reading, Royaume Uni
Winter Christine, CEA, B.P. 7, 77181 Courtry, France
Zeman Svatopluk, University of Pardubice, CW-532 10, Pardubice, République Tchèque

CONTENTS

I. OVERALL ASPECTS OF DETONATION C4-1

I.1. Solids C4-2

I.1.1. Classical Theory of Detonation C4-2

Classical Theory of Detonation
W.C. Davis and C. Fauquignon C4-3

I.1.2. Statements from Laboratories: Success and Failure of the Classical Theory C4-23

On the Detonation Wave Propagation
J.-M. Chevalier C4-25

An Evaluation of Detonation Models
D.C. Swift and S.J. White C4-37

Some Features of the Curvature of a Two-Dimensional Detonation Shock Front at a Simple Refraction Locus
P. Vidal, E. Bouton and H.-N. Presles C4-49

Quelques Points Importants en Détonique Classique
F. Chaisse C4-57

I.1.3. Shock Wave Interaction with Energetic Materials C4-59

Physical Origin of Hot Spots in Pressed Explosive Compositions
R. Belmas and J.-P. Plotard C4-61

Dislocation Mechanisms for Shock-Induced Hot Spots
R.W. Armstrong C4-89

Shock-Wave Behavior in Explosive Monocrystals
J.J. Dick C4-103

Shock Wave Interaction with Composite Materials
A. van der Steen C4-107

I.1.4. Discussion C4-119

I.2. Liquid and Gases C4-124

I.2.1. Detonation Initiation and Self-Sustained Regime in Homogeneous Media C4-125

Structure of Gaseous Detonation Waves and Chemical Kinetics
P.J. Van Tiggelen C4-127

On the Energy Evolution in Gaseous Detonation Waves
A.A. Borisov, O.I. Mel'nichuk, A.R. Kasimov, B.A. Khasainov, K.Ya. Troshin and V. Kosenkov C4-129

Detonation Generation and Propagation in Homogeneous Liquid Explosives
H.N. Presles and P. Vidal C4-143

I.2.2. Statements from Laboratories: Success and Failure of the Classical Theory C4-153

Critical Initiation Conditions for Gaseous Diverging Spherical Detonations
D. Desbordes C4-155

The Limits of Applicability of Usual Kinetic Relations to the Detonation Waves Chemistry. Homogeneous Explosives
B.N. Kondrikov C4-163

I.2.3. Discussion C4-171

I.3. Final Discussion C4-177

I.3.1. Statements from Laboratories on Non-Ideal Behaviour of Energetic Materials C4-177

Characterization of High-Explosive Initiation and Safety at Los Alamos
J.M. McAfee C4-179

Research into the Detonation of Non Ideal Versus Ideal Explosives
R.S. Miller and J.M. Goldwasser C4-189

The Challenge of Non-Ideal Detonation
D.L. Kennedy C4-191

Williamsburg Equation of State for Modelling Non-Ideal Detonation
W. Byers Brown, Z. Feng and M. Braithwaite C4-209

I.3.2. Discussion C4-215

Proposed New Nomenclature for Steady Detonation
D.L. Kennedy C4-220

The Ideal Detonation
L. Brun C4-225

II. ALTERNATIVE VIEWS ON DETONATION C4-229

A Comparison of the Classical and a Modern Theory of Detonation
F.E. Walker C4-231

Towards Detonation Theory
A.N. Dremin C4-259

III. ENERGY TRANSFER IN CONDENSED ENERGETIC MATERIALS (EMs) THEORIES AND EXPERIMENTS C4-277

III.1. General Lectures C4-278

Phonon Lifetimes in Molecular Crystals with Isotopic Impurities
S. Califano C4-279

Energy Transfer in Molecular Liquids
S. Bratos C4-283

Single-Shot Femtosecond Spectroscopy of Reactive Organic Molecular Crystals
W. Wang, D.D. Chung, J.T. Fourkas, L. Dhar and K.A. Nelson C4-289

III.2. Molecular Mechanisms of Energy Transfer in EMs C4-300

Les Méthodes Prédictives pour le Développement de Nouvelles Molécules Explosives
S. Dufort C4-303

A New Kinetics and the Simplicity of Detonation
F.E. Walker C4-309

III.3. Shock Response of Condensed EMs - Experiments C4-334

Picosecond Dynamics Behind the Shock Front
D.D. Dlott C4-337

Recent Developments to Understand Molecular Changes in Shocked Energetic Materials
Y.M. Gupta C4-445

III.4. General Discussion C4-357

III.4.1. Statements from Laboratories on the Experimental Assessment of the Molecular Mechanisms C4-358

A Raman Spectroscopic Study of Nitromethane up to 350 °C and 35 GPa
S. Courtecuisse, F. Cansell, D. Fabre and J.-P. Petitet C4-359

Sub-Picosecond Time-Resolved Spectroscopy of Energetic Materials: the Nitromethane and Nitro-Stilbenes
C. Rajchenbach, G. Jonusauskas and C. Rulliere C4-365

Experimental Study of Photon-Phonon Interactions in an Explosive by Laser Probe Mass Spectrography
J.F. Eloy and A. Delpuech C4-379

Influence of Initiation Strength, Ambient Inert Gas, Al-Content and Polymeric Binder on the Detonation Products of High Explosives
F. Volk C4-383

Sulfuric Acid Influence on the Nitrocompounds Detonation Reactions
V.N. Gamezo, S.M. Khoroshev, B.N. Kondrikov and G.D. Kozak C4-395

Carbon in Detonation Products. A "Three-Phase" Modelisation
M.-L. Turkel and F. Charlet C4-407

Rearrangements of Ammonium Nitrate Cluster Ions with High Internal Energy
R.J. Doyle and B.I. Dunlap C4-417

III.4.2. Discussion C4-423

IV. THEORETICAL ASPECTS OF NON-LINEAR DYNAMICS OF DETONATION C4-427

Direct Initiation of Gaseous Detonations
P. Clavin and L. He C4-431

Analysis of Accelerating Detonation Using Large Activation Energy Asymptotics
R. Klein C4-443

Spontaneous Localization of Vibrational Energy
D.W. Brown and L. Bernstein C4-461

V. FROM MICROSCOPIC TO MACROSCOPIC C4-475

A Transition from a Microscopic to a Macroscopic Approach to Steady State Detonation
C.S. Coffey C4-477

A General Concept Concerning Energetic Material Sensitivity and Initiation
S.A. Shackelford C4-485

A Theoretical Approach to Energetic Materials
M.D. Cook C4-501

"Microscopic" and "Macroscopic" Level of the Errors for Detonation Characteristics Calculations: Pedigree of the Errors
T.S. Pivina, E.A. Arnautova, M.S. Molchanova and V.V. Shcherbukhin C4-505

VI. TOWARDS A REALISTIC CHEMISTRY OF THE REACTIONAL PROCESSES IN DETONATION C4-519

VI.1. Study of the Energetic Behaviour of Energetic Compounds C4-520

Etude du Comportement Energétique de l'Explosif à l'Echelle Moléculaire. Approche Théorique et Expérience TRISP
D. Delpeyroux, C. Lafon, D. Mathieu, Ph. Simonetti, F. Cansell, D. Fabre and J.P. Petitet C4-521

Thermochemistry and Reaction Mechanisms of Nitromethane Ignition
C.F. Melius C4-535

Microscopic Experimental Approaches to High Pressure Chemistry
T.P. Russell, T.M. Allen, J.K. Rice and Y.M. Gupta C4-553

Reaction Mechanisms in Shocked, Intercalated Graphite and Boron Nitride
R.D. Bardo C4-561

VI.2. Applications for Engineering C4-571

What Makes a Useable New Energetic Material?
A.J. Sanderson C4-573

The Use of Predictive Methods for the Design of New Explosive Molecules
A. Delpuech C4-581

VI.3. Discussion C4-585

VII. THE FUTURE OF NUMERICAL SIMULATIONS OF THE DETONATION BY MOLECULAR DYNAMICS C4-593

Molecular Dynamics Studies of Initiation in Energetic Materials
P.J. Haskins C4-595

Molecular Dynamics Analysis of an Energetic System under Thermal and Shock Sollicitations
L. Soulard C4-599

The Limits of Molecular Dynamics Applied to Condensed-Phase Energetic Materials
E.S. Oran and J.P. Boris C4-609

Conclusion C4-623

Author Index C4-635

I OVERALL ASPECTS OF DETONATION

1 SOLIDS

1-1 Classical Theory of Detonation

1-2 Statements from Laboratories : Success and Failure of the Classical Theory

1-3 Shock Wave Interaction with Energetic Materials

1-4 Discussion

2 LIQUIDS AND GASES

2-1 Detonation Initiation and Self-sustained Regime in Homogeneous Media

2-2 Statements from Laboratories : Success and Failure of the Classical Theory

2-3 Discussion

3 FINAL DISCUSSION

3-1 Statements from Laboratories on Non-ideal Behaviour of Energetic Materials

3-2 Discussion

1 SOLIDS

Chairman : Pierre Veyrié, Directeur du Centre d'Etudes de Vaujours - Moronvilliers (CEA /DAM)

Ladies and Gentlemen,

It is universally admitted that several experimental results have been understood thanks to the C.J.model and its physical interpretation the ZND (ZELDOVICH, VON NEUMAN, DORING) detonation description.

Unfortunately, anyone who wants to take upon account detonation dimension limited materials, to take care of growth from initiation to detonation to describe lateral emergence distance, and many other important data, knows that the CJ model fails to explain all those experiments.

Much more sophistication is required in the theory.

Then shall this sophistication be macroscopic following a more precise and pertinent hydrodynamic explanation or be a microscopic description of the behaviour of constitutive molecules and crystals ? We have to discuss. This is the challenge that we have to face.

Bill Davis and Claude Fauquignon are now going to introduce the workshop around that point.

Then Ron Armstrong, Robert Belmas, Jerry Dick and Albert Van der Steen will emphasize heterogeneous effects in explosive compositions.

Representatives of major Laboratories will tell us their experience on the success and failure of the theory later on.

1-1 Classical Theory of Detonation

Classical Theory of Detonation, a Review ; **W.C.Davis - C.Fauquignon**

JOURNAL DE PHYSIQUE IV
Colloque C4, supplément au Journal de Physique III, Volume 5, mai 1995

Classical Theory of Detonation

W.C. Davis and C. Fauquignon*

Energetic Dynamics Los Alamos, 693 46th Street, Los Alamos, NM 87544, U.S.A.
** French-German Research Institute, 5 rue du Général Cassagnou, 68301 Saint-Louis cedex, France*

Abstract

In a first part is presented the model of the Ideal Detonation. Emphasis is placed on the physical assumptions made in the setting and resolution of the continuum mechanics equations to be used. The basic elements of computations of ideal detonation parameters will be described. The experiments performed to check the predictions, and their results, will be reported. Some discussion of explosives in which chemical equilibrium is not reached, due to slow diffusive mixing of the reactants or to conditions where some of the reactions are very slow, will also be given. These explosives are often called non-ideal explosives. Obviously, when the reaction zone is not very thin relative to system dimensions, or when it is not very short relative to system times, the Ideal Detonation model, restricted to plane, steady flow, is inadequate. The third part of the paper is concerned with curved detonation fronts, and with time dependent processes. The steady detonation of small-diameter cylindrical cartridges will be discussed as one example, and the initiation of detonation in the shock-to-detonation transition as another. Detonation theory is not a closed subject, and much effort is currently being spent to extend classical theory. Some of the newer ideas will be introduced in a concluding part.

1. THERMO-HYDRODYNAMIC DESCRIPTION OF DETONATION

(C. Fauquignon)

1.1 Introduction

An explosive is defined as a substance which can deliver very quickly a large amount of energy and produce a large amount of gas. The energy has generally a chemical origin and the reactions progress in the surrounding material by drawing a part of the energy previously produced.

According to the processes of the energy transfer in the non reacted material, two regimes are defined, deflagration and detonation, which are differentiated from the usual combustion by their velocities of propagation (some mm/s for the usual combustion, several hundred m/s for the deflagration and several thousand m/s for the detonation). It follows that the flow of the high pressure reaction products is the acting agent of the energy transfer and of the self sustaining of the combustion. As a consequence, the description of the process calls in the fluids mechanics associated with the thermo-chemistry for the setting of the energy balance.

In this presentation, we will only consider the case of the detonation in which, contrary to the deflagration, the energy transfer in the non reacted material is supersonic. The detonation is characterised by the existence of a shock wave in the front of which the reactions start.

The model of the Ideal thermo-hydrodynamic Detonation which will be presented does not take into account the physico-chemical processes in the shock front or in its neighbourhood and which may require revision of the assumption of the discontinuity of the shock front considered as the frontier between two states at thermodynamic equilibrium.

1.2 Model of the Ideal Detonation

The model considers (Figure 1a) a reactive supersonic flow, self sustained by the shock wave, steady as far as the end of the reactions : all the exo-energetic reactions are assumed to reach an equilibrium at the same time, this equilibrium being a function of the temperature and of the pressure. Beyond this point, an unstationnary rarefaction takes place being controlled by the boundary conditions of the explosive charge. In this downstream flow,the composition of the products may change as a function of p, V, T, but no energy can be transfered upstream and influence the characteristics of the detonation.

The set of the conservation equations to be solved in building the model neglect the conductive and radiation effects and assume a laminar non viscous flow.

The steady state condition means that the shock front and the plane of the end of reaction propagate at the same velocity D in a plane semi-infinite geometry. The indexes 0 and 1 correspond respectively to the non reacted and totally reacted material.

If we consider that the plane of the end of reaction is the head of an unstationnary rarefaction, the condition of a steady state upstream is fulfilled if this plane is sonic, $D = \hat{u} + \hat{a}$, where $\hat{u}$ and $\hat{a}$ are the material velocity and the sound speed at this plane. This condition was found by Chapman [1] and Jouguet [2] who have shown its consequences in the thermodynamic (p, v) plane (Figure 1b). In the (p, v) plane, 0 represents the fresh explosive and the locus of the possible final states of the reaction products is the curve (H) obtained by solving the conservation equations :

$$H(p, v) = \tfrac{1}{2} (p + p_0) (v_0 - v) + E(p, v) - E_0 (p_0, v_0) = 0$$

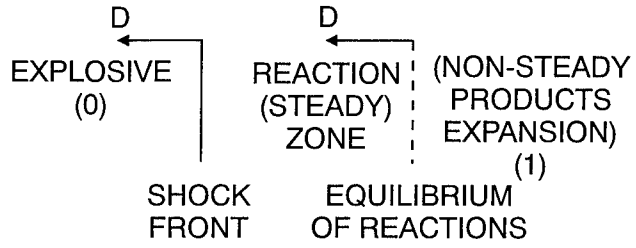

FIG. 1a : SPATIAL SCHEME

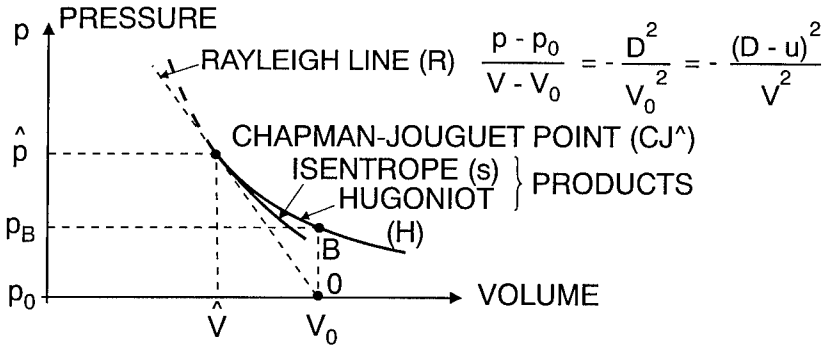

FIG. 1b : CHAPMAN-JOUGUET MODEL (p, V)

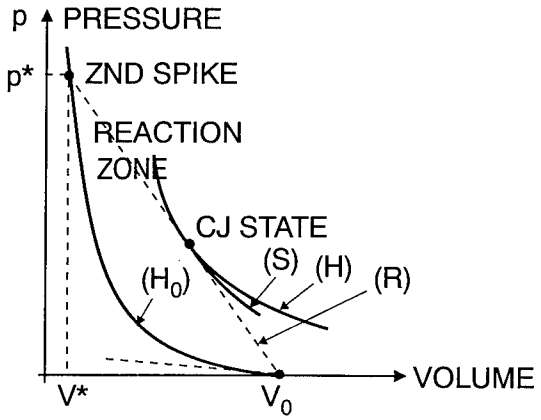

FIG. 1c : COMPLETE DESCRIPTION (p, V)

FIG. 1 : IDEAL THERMO-HYDRODYNAMIC DETONATION

The basic difference from an Hugoniot for non-reacted explosive is in the meaning of E =

$E_o = E'_o$ (internal energy of the fresh material + q_o
(energy of formation of the explosive molecule)

$E = E'$ (internal energy of the reaction products + q
(energy of formation of the products)

As a consequence (p_o, v_o) is not on (H) and the ordinate on (H) for $V = V_o$ is a point B such that $p_B - p_o$ is the increase of the pressure for a constant volume reaction at $V = V_o$.

By solving the conservation equations it is possible to express the velocities D, u as functions of p and V:

$$-\frac{D^2}{V_o^2} = -\frac{(D-u)^2}{V^2} = \frac{p-p_o}{V-V_o} \quad (R)$$

As a consequence, any final state on (H) corresponds a velocity D as a result of the intersection of (H) and of (R) called the Rayleigh line.

It is shown that the steady state condition for the Ideal Detonation is fulfilled when (R) is tangent with H; At the tangent point, called CJ point, (R) is also tangent with the isentrope S the slope of which is $-\frac{a^2}{V^2}$. As a consequence, at the CJ point

$$D = \hat{u} + \hat{a}$$

It is also interesting to note that the CJ detonation velocity is the minimal velocity which can be reached.

Until now, the reaction zone has been neglected or assumed to have no thickness. It will be seen later (see part 2) that the present description of the Ideal Detonation is sufficient for computation of the detonation parameters.

1.3 A more complete description : The ZND model

A description of the complete structure of detonation with propagation of the shock in the fresh explosive has been proposed quasi-simultaneously in 1942 by Doering, Zeldovitch and von Neumann [3], [4], [5]. The construction in the (p, v) diagram needs to know the Hugoniot H_o of the non reacted explosive (Figure 1c).

The steady state condition and the use of the Rayleigh line (R) show that (p_o, v_o), (p^*, v^*) and (p, û) are aligned on a straight line of slope equal to $-\frac{D^2}{V_o^2}$. In the reaction zone the pressure drops steeply from a maximum value p^*, called the ZND spike, to the CJ pressure $\hat{p}$. The simplest interpretation of the model would be to calibrate the $p^* - \hat{p}$ segment in the extent of reaction λ, from $\lambda = 0$ at p^* to $\lambda = 1$ at $\hat{p}$. However, we enter here into the most controversial part of the model as we will see now.

1.4 First consideration on the limits of the model

The following considerations deal with the simplicity of the physical assumptions and with the reality of one dimensional plane and semi-infinite geometry.

a) The existence of a non-reacted Hugoniot is questionnable if out of equilibrium effects and early decomposition occur. The main consequence would be to modify the reaction scheme and would have a major influence in the build-up to detonation following a shock of a short duration.

b) The validity of the assumption of a single reaction rate and of the absence of diffusion effects between the species has been roughly considered in the comparison between computations and experiments and is used to divide the explosives in non-ideal and ideal compositions. This point will be examined in part 3 at the same time as the coïncidence of a sonic state with the end of the exo-energetic reactions.

c) The validity of the plane semi-infinite assumption for most of charges designed for military and civil applications is a question of time and space scale : The thinner the reaction zone the better the assumption. It is mainly the requirement for insensitive explosives in the last decades which has made it necessary to re-examine the question and to bridge between non-ideal geometries and non-ideal explosives mainly where the model is used as a tool for the design of charges.

References part 1

[1] Chapman D.L., *Lond.Edi.nb.Dubl.Phil.Mag.* 47(1899) 90
[2] Jouguet E., *J.Math.pures.Appl. Paris* 60(1905) 347
[3] Zeldovich Ya.B., NACA Tech.Memo.(1950) N° 1261 (also "Selected works" p. 411)
[4] von Neumann J., OSRD Report (1942) N° 549
[5] Döring W., Burkhardt G., Air Material Command Technical Report - F-TS-1227-IA (GDAM A9-T46)(1949)

2. APPLICATIONS OF CLASSICAL DETONATION THEORY

(W. C. Davis)

In the preceeding chapter Dr. Fauquignon has presented the classical theory of detonation. This simple theory is the basis for almost all calculations made for the design of devices driven by high explosives. Here we will examine how it is used, and describe some tests of the theory.

In some applications of explosives, say an aerial bomb, the important quantities for design are the velocity of the case fragments and the strength of the shock wave at relatively large distances for the bomb. The partition of energy between fragments and gas does not depend strongly on the details of the detonation and the interaction of waves with the metal, and is not at all sensitive to the method used to calculate the performance of the system. Many approximate methods [1] have been developed for such problems. Results of such calculations do not provide a test of the applicability of the theory. On the other hand, understanding small details of the system, such as spalling of the case of the bomb, require detailed calculations, and it is important to get the details of the flow of the detonation products reasonably correct. These calculations do provide a test of the applicability of the theory.

The classical model [2] gives the state of the detonation products at the end of the chemical reaction zone, and shows further that the state does not depend on the details of the chemical reaction, but simply on the energy released. The state, usually called the Chapman-Jouguet or CJ state and designated here by a subscript j, is described by

$$\mathbf{p}_j = \frac{\rho_0 \mathbf{D}^2}{\gamma_j + 1} \qquad \rho_j = \rho_0 \frac{\gamma_j + 1}{\gamma_j} \qquad \mathbf{u}_j = \frac{\mathbf{D}}{\gamma_j + 1} \qquad \mathbf{c}_j = \frac{\gamma_j \mathbf{D}}{\gamma_j + 1}$$

where p is the pressure, ρ is the density and subscript 0 denotes the initial state, D is the CJ detonation wave velocity, γ is the dimensionless sound velocity to be discussed below, u is the particle velocity, and c is the sound velocity. The dimensionless sound velocity γ is a thermodynamic state variable and is given by

$$\gamma = \frac{\rho \mathbf{c}^2}{\mathbf{p}},$$

with the square of the sound speed defined as $\mathbf{c}^2 = (\partial \mathbf{p} / \partial \rho)_s$, for all ρ and p, not just at the CJ state. Note that γ in hydrodynamics is not the ratio of specific heats, and is not a constant except in special cases.

The classical model has the detonation wave running at constant speed; therefore if one knows, or assumes, its location at an instant of time, one can calculate [3] its location and shape at a later time. The model gives the state of the detonation products at the wave front from the formulas above. The flow of the products, an inert flow with the only possible chemical changes being shifts in equilibrium composition as the state changes, can be computed from the usual equations [2] of hydrodynamics. The only processes that produce appreciable entropy are shock waves in the flow of the products; if there are no shocks, the flow is isentropic. If there are shocks, they move the state off the isentrope, in most cases only

slightly. The material description needed to complete the formulation of the flow of the products gases is required only near the isentrope through the CJ point (called the principal isentrope).

While it may seem straightforward to model detonation by advancing the wave at each time step, and setting the state to the CJ state at that position, this procedure often causes numerical difficulties [4]. Since the state at the end of the chemical reaction is independent of the details of the reaction, any method for reacting the explosive to its products will give the same end state. In modeling, any scheme that reacts the explosive quickly and does not introduce numerical difficulties will be satisfactory. Many schemes have been used; some work better than others. Most calculations are made using one of the schemes for burning the explosive; there is no attempt to model the real reaction zone.

Any thoughtful person must ask why it is necessary to introduce this artificiality. Why not just model the reaction zone following all the details of the chemical reactions? The answer is that it is not practical to do that. To get even a reasonably accurate model of the reaction zone requires at least 30 calculational cells in the reaction zone. The device will usually have a characteristic size that is 100 to 1000 or more reaction zone lengths, to be far enough from the critical size, or failure size, for the system to be robust. While one-dimensional calculations are possible with 10 000 or more cells, two- and three-dimensional calculations with 10^8 or 10^{12} cells, the ones of interest, are not. Attempts to model the reaction zone in a real system take more than a day on the fastest computers.

Whether the front is advanced and the state set using the classical theory, or by using an artificial burning, a description of the properties of the detonation products is required in every calculation. The explosive driven system must be considered as an engine, differing from more conventional engines in that the parts are deformed as well as moved and that the cycle is not repeated. The detonation products are the working fluid for the engine. The description [5-7] of the products is usually called an "equation of state". The quantities that are required are two derivatives:

$$\gamma(\mathbf{p},\rho) \equiv (\rho / \mathbf{p})(\partial \mathbf{p} / \partial \rho)_s \qquad \Gamma(\mathbf{p},\rho) \equiv (1/\rho)(\partial \mathbf{p} / \partial E)_\rho$$

where E is the specific internal energy. Values are needed only in the immediate neighborhood of the principal isentrope that passes through the CJ point, because little entropy is produced in the weak shocks that may occur in the system after detonation.

The material description for calculations is almost always obtained by calibrating a convenient fitting form to experiments as much like the system to be calculated as possible. Sometimes the fitting includes results from equations of state calculated by statistical mechanics using assumed intermolecular force laws, and other theoretical equations of state. Simple expansions of the equation of state such as a virial expansion are of limited use. The densities are so high that the intermolecular interaction energy is very large compared with the thermal energy. Typically in the region of most of the energy transfer from products to inert parts one has $p/\rho RT>10$. The results are presented as

$$p = p(\rho,E)$$

and the necessary derivatives for the hydrodynamic calculations are obtained from this expression. The "equation of state" is incomplete (a function of ρ and E rather than of ρ and S) because it is calibrated from mechanical measurements that yield no information about temperature or entropy.

One sees from this description of how the classical theory is used, to provide a model for fitting the measurements, that its success for this purpose does not provide a real test of the theory. The fact that the calibration experiments can be quite different from the system being modeled indicates that the classical model is probably qualitatively correct. A definitive test must use other data.

The first reassuring fact [8,9] is that most, but not all [10, 11], detonations do in fact propagate with a leading shock wave that is reasonably smooth, followed by a decrease in pressure as the chemical reaction takes place, and then, if the back boundary condition is proper, followed by an expansion wave. These observations show that the classical model is at least qualitatively correct. The measured reaction zone in practical explosives ranges from about 10 μm to about 10 mm, a range of 1000. Explosives with reaction zones smaller than 10 μm are too dangerous to handle safely, and ones with reaction zones larger than 10 mm fail to propagate except in very large sizes.

Experiments [12] providing a severe test of the theory were carried out using liquid nitric oxide NO as a prototype explosive. The description of the detonation products was obtained from shock wave measurements made on liquid oxygen, liquid nitrogen, and liquid mixtures of oxygen and nitrogen. A careful study, using the best theory available to help the analysis was made. No calibration to detonation measurements was required. Then the results of measurements of detonation velocity and CJ pressure were compared with the predictions of the theory, and the agreement was found to be very satisfactory. The really important conclusion to be reached, which could not be supported otherwise, was that the assumption that the detonation products reach chemical and thermal equilibrium in the detonation reaction zone is an excellent approximation.

Another set of experiments [13], however, testing the theory by the "inverse method", showed that the theory is not exactly correct. This method requires that the initial state of the explosive is varied to provide values for derivatives of detonation velocity with respect to initial density and energy about a standard initial state. For TNT the energy was varied by using solid and liquid TNT so the energy was different by the heat of fusion, and the density was varied by using solid TNT pressed to different densities, or by varying the temperature of the liquid. For liquid nitromethane the energy was varied by mixing it with a mixture of nitric acid, acetonitrile, and water that had the same atomic composition but different energy, and the density was varied by changing the temperature. The results for the derivatives allowed the pressure to be calculated, and this inferred value was compared with measurements of detonation pressure. In these experiments agreement was not obtained; the values differed by several standard deviations.

The main support for belief that the classical theory is a good approximation to actuality comes from its use in predicting the behavior of an explosive, perhaps even an explosive that has never been made. It was recognized [14] at least 75 years ago that if the simple theory is correct one need know only the atomic composition of the explosive and its heat of formation

to calculate its detonation properties. The atomic composition determines the composition of the products, since they are (by assumption) in chemical equilibrium. Most of the heat comes from the formation of the products, so the dependence on an exact figure for the heat of formation of the explosive is relatively weak. For most common explosives, the major products are N_2, H_2O, CO_2, CO, and C(soot), with minor amounts of NO, NH_3, CH_4, H_2, O_2, HCOOH, etc. Sometimes other elements besides CHNO are present. If an equation of state for each species is available, and a mixing rule is known, the free energy can be minimized to give the composition of the products and the state variables. There need be no calibration to detonation experiments.

While simple in concept, this procedure is complex and tedious in execution. Many workers [15-17] have made schemes for doing it, and many equations of state with various calibration data have been used, and different mixing rules have been tried. Other minor constituents have been considered. Obviously, different schemes give slightly different results. However, all reasonable schemes give surprisingly good predictions, usually within a few per cent of the measured values. Rarely in science and engineering has it been possible to make predictions of the detailed properties of complex materials as well as has been done for explosives. The value of the classical simple theory is proven by these results.

Reading the current papers on explosives one soon sees that workers are not satisfied with the available predictions. To make a decision about whether or not to invest the large amount of effort and funds needed to develop a new explosive for practical application, the accuracy of a few per cent is not good enough. The gain in performance from a new explosive is never more than a few per cent above the old ones. While refining the equations of state and the mixing rules, or trying new minor constituents, seems to help a little, studying the deficiencies and errors soon leads one to believe that there is an underlying additional cause of error. The most likely cause is that the products do not go completely to equilibrium in a short enough time in all explosives. There is strong evidence for very slow heat release near the end of the reaction zone. Perhaps the slow reactions can be identified and predicted, with subsequent improvement of the prediction of explosive performance.

This brief review describes how the classical theory of detonation, in its simplest form, is applied to practical problems. Almost all calculations of the behavior of explosive driven systems are based on the theory. Predictions of the performance of new explosives are based on the theory. The theory has been tested in many ways, not all of them described here. It is not perfect, nor is it complete, but it is extremely useful and is very widely used.

References part 2

[1] G. E. Jones, J. E. Kennedy, and L. D. Bertholf, Ballistic calculations of R. W. Gurney, Am. J. Phys. 48, 264-9 (1980).

[2] W. Fickett and W. C. Davis, Detonation, U. of California Press, 1979, Chap. 2.

[3] J. B. Bdzil and D. S. Stewart, Modeling two-dimensional detonations with detonation shock dynamics, Phys. Fluids A 1, 1261-7 (1989), Sect. IIIA. For more detail, see J. Bdzil and W. Fickett, DSD technology : a detonation reactive Huygens code, Los Alamos Report LA-12235-MS, 1992.

[4] C. L. Mader, Numerical modeling of detonation, U. of California Press, 1979.

[5] W. C. Davis, Equation of State for Detonation Products, Eighth Symposium (International) on Detonation, NSWC MP 86-194, 1985, pp. 785-795.

[6] R. Menikoff and B. J. Plohr, The Riemann problem for fluid flow of real materials, Rev. Mod. Phys. 61, 75-130 (1989).
[7] W. C. Davis, Equation of state for detonation products, Tenth Symposium (International) on Detonation, preprints pp. 112-3, 1993.
[8] J. B. Bdzil and W. C. Davis, Los Alamos Report, LA-5926-MS, 1975.
[9] J. B. Bdzil, Perturbation Methods applied to problems in detonation physics, Sixth Symposium (International) on Detonation, ACR-221, 1976, pp. 352-370.
[10] L. V. Altshuler, Shock waves and extreme states of matter, Shock Compression of Condensed Matter, Williamsburg APS Meeting, 1991, pp. 3-14. See Figs. 2 & 3.
[11] W. Fickett and W. C. Davis, Detonation, U. of California Press, 1979, Chap. 5.
[12] G. L. Schott, W. C. Davis, and W. C. Chiles, Initiation and detonation measurements on liquid nitric oxide, Ninth Symposium (International) on Detonation, OCNR 113291-7, 1989, pp. 1335-1345.
[13] W. C. Davis, B. G. Craig, and J. B. Ramsay, Failure of the Chapman-Jouguet theory for liquid and solid explosives, Phys. Fluids 8, 2169-2182 (1965).
[14] R. Becker, Impact waves and detonations, Zeit. Phys. 8, 321-362 (1922), English trans. NACA TM 505 and TM 506, March 1929.
[15] J. Taylor, Detonation in condensed explosives, Clarendon Press, 1952.
[16] C. L. Mader, Numerical modeling of detonations, U. California Press, 1979, Chap. 2.
[17] Detonation Symposium Volumes. There are more than 150 papers listed under the heading EOS in the index to the first nine Symposia.

3. DETONATION IN A NON IDEAL GEOMETRY

(C. Fauquignon)

Some usual cases are :

- Divergent and convergent 1-D detonation (the planar condition is not respected)

- Steady detonation in a cylindrical stick

- Mach detonation : In theory it is a special 1D detonation, but its existence results from 2D boundary conditions.

We shall concentrate here on the steady detonation in a cylindrical stick for which a large amount of accurate experimental results on the detonation velocity and on the front curvature as a function of the diameter is available.

3.1 Sketch of the reactive flow

Figure 2a features some stream lines, the curved shock front, the sonic surface which corresponds to a barrier for acoustic waves propagating upstream toward the shock front, the surface where the reactions end.

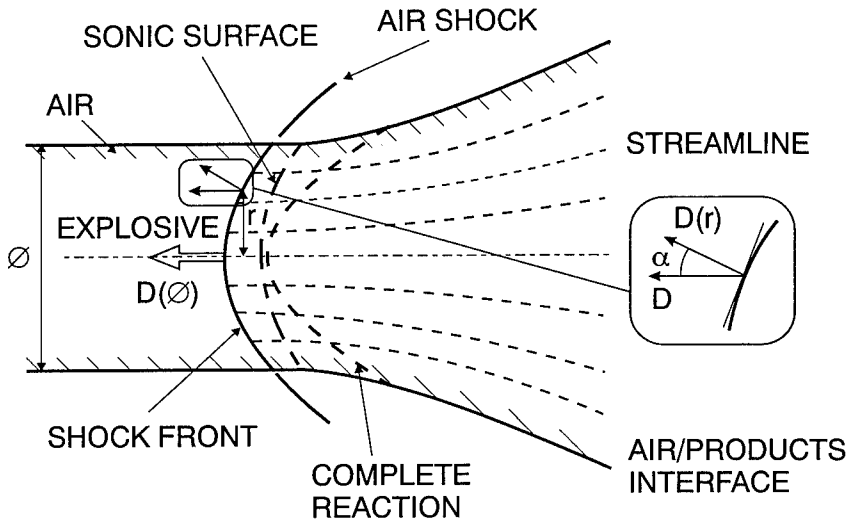

FIG. 2a : PHENOMENOLOGY OF THE REACTIVE FLOW

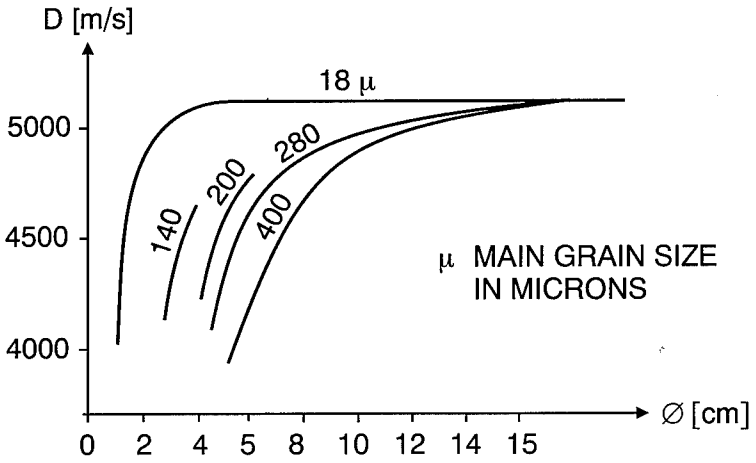

FIG. 2b : DETONATION VELOCITY D VERSUS STICK DIAMETER ∅
PRESSED TNT ρ_0 = 1.2 g × cm^{-3}

FIG. 2 : DETONATION OF A CYLINDRICAL STICK

The local curvature of the front determines the initiation conditions for the reactions along the stream line passing through this point. The intensity of the shock is given by its velocity $D\cos\alpha$. In the steady self-sustained detonation, the shock intensity also depends on the energy delivered on the stream line between the shock and the sonic surface. The energy delivered downstream between the sonic surface and the surface of end of reactions mainly supplies the lateral expansion.

As the diameter of the stick decreases, the part of the energy delivered to sustain the shock decreases and, finally the failure diameter is reached.

A first observation is that the steady state is not strictly governed by the sonic condition but depends strongly on the lateral expansion. A second observation is that the detonation prediction, for instance of its velocity, depends not only on the reaction kinetics, on the equation of state of the intermediate species (needed to calculate the sound velocity) but also on the thermo-mechanical processes involved in the shock front to initiate the reactions.

As a consequence of the overlapping of all these factors, most of them being poorly known, the theoretical and numerical approaches call upon global phenomenological models with fitting parameters based on detonation velocity or front curvature measurements.

In the case of the physically heterogeneous solid explosives, approaches similar to those used in Shock to Detonation Transition analysis (see 3.4) are performed. They use the three step scheme :

(a) Formation of hot spots
(b) Collapse of the reacting hot spots
(c) Burning.

Sometimes this scheme is concentrated in a two step process, Ignition and Build up.

3.2 Some experimental observations

One of the first observations is the major role of the physical heterogeneities illustrated by Figure 2b which represents the velocity versus the stick diameter for different TNT grain sizes, with the loading density, i.e. the energy, being constant. To interpret the results it is to be noted that the grain size has opposite effects in the three step scheme. The larger the grain size the more energetic are the hot spots but the longer is the burning time. Such experimental observations have been used some decades ago, to test a grain burning model with arbitrary burning rate function of the pressure, but as the role of the grain size in the ignition was neglected the agreement with the experiment was relatively poor.

An interesting experimental study aiming at an independant variation of the influence parameters of (a) and (c) has been performed using a mixture of nitromethane either with a physical sensitizer (silica particles) or with a liquid chemical catalyst the diethylene-triamine (DETA) [1] which influences only the burning rate.

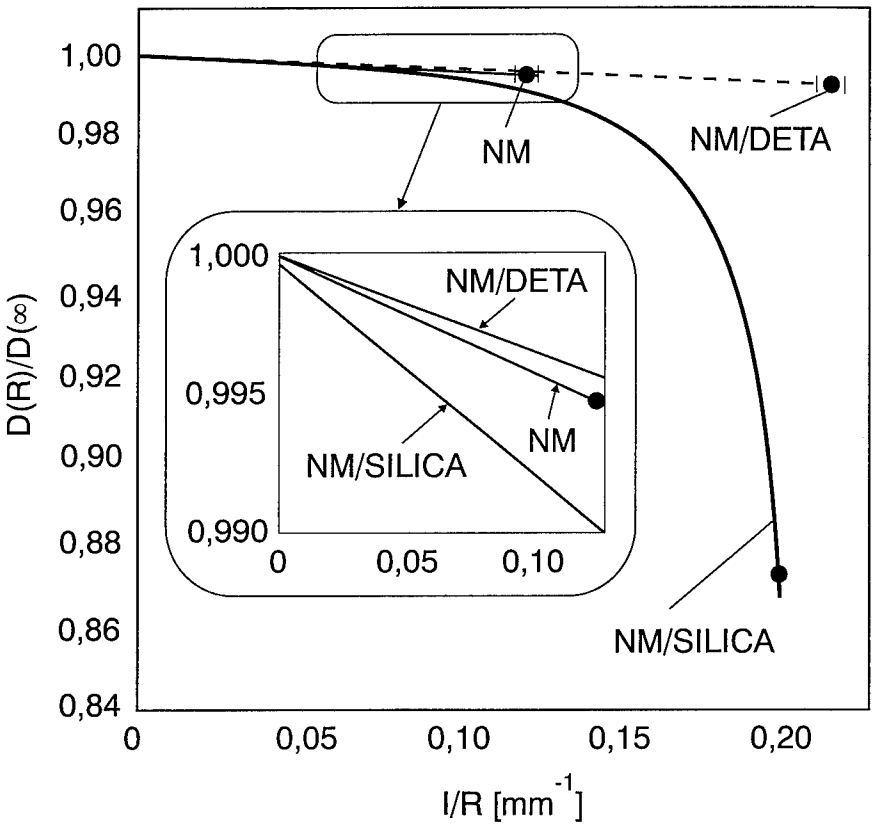

FIG. 3 : DETONATION VELOCITY OF NITROMETHANE (NM) MIXTURES VS RADIUS OF THE CHARGE

Figure 3 presents the results which confirm the expected phenomenology :

- The silica particles absorb a part of the explosive energy but allow the detonation to be self sustained even at low detonation velocities, i.e. at low shock pressure.

- DETA shortens the burning time, i.e. the reaction zone, without changing the energy much.

- Both agents allow the mixtures to reduce the failure diameter to comparable values as they follow independent modes of action.

In spite of the large amount, the variety and the quality of the experimental observations, they give global information, the detonation velocity and the front curvature, and can only be used in the frame of an a priori scheme.

The present studies concerning the hot spots which will be presented in this meeting will help to a better understanding of the initial conditions in the shock front of most of the military and civil compositions. However, the transfer of the energy to the bonds of the molecules remains a question which cannot be tackled with the same methods due to a major difference in the time scale of the thermo-mechanical and of the physico-chemical processes.

3.3 Theoretical approaches

Specific studies aim mainly at taking into account multi-dimensionnal effects, using as a reference the plane CJ or ZND model, in order to improve the codes for numerical modeling.

These models refer to the fluid mechanics applied to an homogeneous material, and to a simple single reaction rate. They mainly differ in the mathematical formulation of multi-dimensionnal effects represented by transverse waves and flow along the curved front surface.

A description of these studies is beyond of the aim of this meeting and we just mention some recent references [2], [3]. However, following a similar path, L. Brun has brought a new generalized mechanical description of the detonation which will be presented in this meeting.

As has been noted before the reactive flow is too complex to evidence any chemical kinetics law directly from the experiment. An a priori prediction of a detonation in a multi-dimensionnal geometry requires to use in the numerical code a kinetics law determined in a specific experiment and it seems that the Shock to Detonation Transition (SDT) in plane geometry is the best way to get it.

3.4 The shock to detonation : A time dependant process

The SDT in an efficient tool to analyse the detonation mechanism for at least three reasons :

- The initial conditions, i.e., the shock pressure and duration are well defined and can vary from one experiment to another.

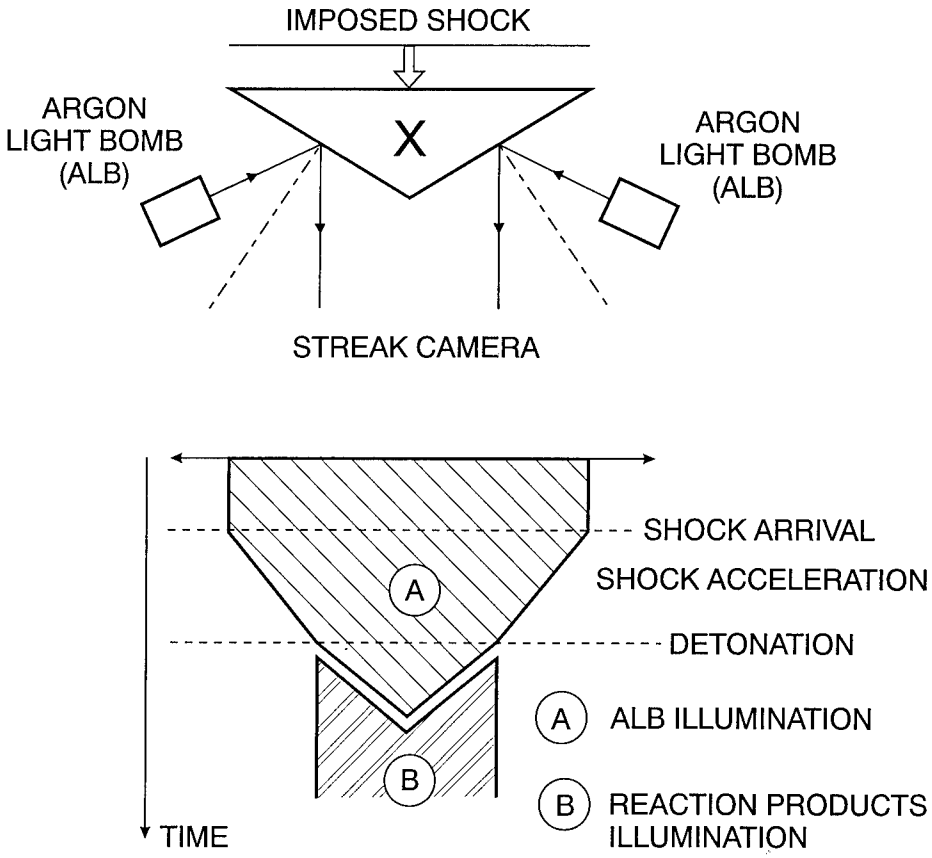

FIG. 4 : EXPERIMENTAL STUDY OF SDT BY THE DOUBLE EXPLOSIVE WEDGE TECHNIQUE

- At pressures much lower than the ZND pressure, the SDT experiment gives an enlarged picture of the reactive flow from the initial shock compression up to a quasi steady detonation.

- The experiment requires a small amount of explosive that is suitable for fine measurements.

For about 35 years, the wedge technique (Figure 4) [4] has been used with some refinements.

The phenomenological reactive models which have been developed using measurements of the path vs time of the accelerating reactive shock [5] are based on the two step ignition and build up process for explosives assuming that hot spots are responsible of the initial heating. A survey of some of this models is given in [6].

Lagrangian analysis of the pressure or of the particle velocity in the build up zone is also used with success to check the validity of reactive models.

In spite of the efficiency of the method a more accurate knowledge of the initial conditions behind the shock front, i.e. of the microscopic heating processes and of the microstructure of the explosive specimens or of some out of equilibrium molecular processes is required to get a true chemical kinetics law. However, the reactive models are efficiently used by the designers of charges after having fitted the parameters with SDT experiments on the explosive composition to be used.

References part 3

[1] Engelke R., Phys. Fluids 22 (1979) pp. 623-630
[2] Bdzil J.B., Fickett W., 9th Symposium on Detonation - OCNR 113291-7 (1989) pp. 730-742
[3] Lambourn B.D., Swift D.C., 9th Symposium on Detonation - OCNR 113291-7 (1989) pp. 784-797
[4] Campbell A.W., Davis W.C., Ramsay J.B., Travis J.R., Phys. Fluids 4(1961) pp. 511-521
[5] Moulard H., Kury J.W., Delcos A., 8th Symposium on Detonation (1985) NSWC-MP 86-194 Report, pp. 902-913
[6] Fauquignon C., *Journal de Physique,* Colloque C4 Supplément au n° 9, Tome 48, Sept. 1987, pp. 39-65.

4 - FRONTIERS OF DETONATION THEORY

(W.C. Davis)

All detonation studies involve the interaction of chemistry and mechanics. In the detonation reaction zone the flow is not smooth and laminar, and consequently the shock wave is not smooth. The result is that the explosive is not heated uniformly, and the chemical reaction rate, an extremely non-linear function of temperature, is much more non-uniform. Reaction is fast in some small regions, usually called hot spots, and, relatively, almost nonexistent elsewhere until it spreads from the hot spots.

In cast solid explosives, pressed polycrystalline explosives, emulsions and slurries, and in loosely packed powders, most of the hot spots are in the neighborhood of lower density regions. Where the density is low, the motion is greater, and more work is done on the material by the motion. The internal energy rises there, and the temperature is higher. The scale of the hot spots is related to the size of the crystallites or the rate of cooling when casting, etc., and these sizes are determined by such considerations as convenience for handling. How much reaction takes place at a hot spot depends of the rate of reaction and the rate of diffusion of heat away from the hot spot. In two explosives with crystallites the same size but reaction rates very different, the apparent effect of the hot spots may be very different.

In liquid explosives, it might seem that there will be no hot spots. Nature is not so kind. The flow in a detonation in a liquid explosive is still not smooth and laminar, because the burning is hydrodynamically unstable [1], and generates transverse waves spontaneously. (The solid explosives discussed in the preceeding paragraph also have these instabilites, and they compete with the ones generated by inhomogeneity). The scale and the spacing of these hot spots is related to the scale of the chemical reaction zone; the details are not understood, and are a subject for future research. The structures that have been studied seem to have a spacing of a few, 3 to 10, reaction zone lengths.

Detonation in gases [1] produces very strong transverse waves, often with a shock wave collision called a Mach stem, where the pressure and temperature are far above the average. In some cases almost half the gas flows through this interaction region. It is as if the detonation, unable to propagate in a laminar flow, created superchargers for itself to ensure propagation. Gas detonations have been studied extensively (they do not destroy the equipment, the equations of state are known, the flow is transparent, and the transverse wave structures can be made large by reducing the initial pressure) and much is known about the details of the transverse waves. It is tempting to believe that structures in condensed phase explosives are analogous to those in gases. After all, if one explosive is not more like another explosive than anything else, there can be no science of explosives. But probably gases are different from liquids and solids. The spacings are 100 or more reaction zone lengths. The mechanical details are very different because of the differences in the equations of state.

The published papers [2] on detonation abound with papers on hot spots. It has been known for a very long time that imperfections and inhomogeneities strongly influence the critical size below which detonation will not propagate, and that many explosives must have hot spots to be useful. Two batches of explosive with identical chemical composition may differ enough in their hot spot behavior to make one batch useful and the other useless. Obviously, producers of explosives have learned to control the hot spots. The knowledge is all empirical.

One result of the current inability to model the effects of all the varied phenomena lumped together under the heading hot spots is that there is no way to take any available knowledge of chemical reaction rates for well-defined chemical explosive and predict what a particular formulation will do. For example, in one long list comparing the sensitivity of explosives in the gap test, a cast TNT formulation was the least sensitive explosive, and a pressed TNT formulation was the most sensitive. When the behavior of the explosive is accurately described by the simple classical theory discussed in Parts 1 & 2 of this introduction, that is,

when the effective reaction zone length is small relative to system dimensions, the reaction rate has little effect on performance. Part 3 made it clear that safer explosives with long reaction zones cannot be described so simply, and the details of the phenomena in the reaction zone are important. When transient behavior is important, as in initiation of detonation intentionally, and even more in accidental initiation, the reaction zone in all its multi-dimensional detail, is even more important.

The difference between the classical theory of Parts 1 & 2, and the more complex ideas of Part 3 & 4, is that the classical model has only one important space scale, the reaction zone length. In most of Part 3 the dimensions of the charge provide another space scale. Above in Part 4 a scale of inhomogeneity was added. There are many space scales that are important in some detonation problems; fortunately not all of them are important in all detonation problems. When the flow is steady or nearly steady, that is, a wave moves but changes only slowly with time, space and time scales are simply related. When the transients are considered, space and time scales are not so neatly interchangeable.

A list of some important space scales is given in Table I. It is just an evaluation of the order of magnitude of these scales, and is arbitrary in many respects. However, it shows an enormous range. Modeling, whether analytical or computational, for systems where the ratio of important space scales is large presents great difficulties.

New developments in detonation theory are needed to incorporate treatments of all the important processes at their disparate scales. The new approaches discussed in Part 3 are a start. This meeting, with its title "Microscopic and Macroscopic Approaches to Detonation", is directed to the frontiers of detonation science.

TABLE I

Item	Scale(meter)
Charge size	10^{-1}
Reaction zone length	10^{-5}-10^{-2}
Crystallites, dendrites, emulsions	10^{-5}-10^{-3}
Hot spots	10^{-7}-10^{-4}
Shock roughness	10^{-7}-10^{-4}
Shock thickness	10^{-8}
Atoms and molecules	10^{-10}

References Part 4

[1] W. Fickett and W. C. Davis, Detonation, U. California Press, 1979, Chaps. 6 & 7.

[2] S. L. Crane, W. E. Deal, J. B. Ramsay, A. M. Roach, and B. E. Takala, Index for the proceedings of the Symposia (International) on Detonation, 1951-1989, Tenth Symposium (International) on Detonation, preprints p. 473, 1993. There are 75 entries under the heading "hot spots".

1-2 Statements from Laboratories : Success and Failure of the Classical Theory

On the Detonation Wave Propagation ; J.M. Chevalier

An Evaluation of Detonation Models **D.C. Swift** and S.J. White

Some Features of the Curvature of a Two-dimensional Detonation Shock Front at a Simple Refraction Locus ; **P.Vidal**, E.Bouton and H.N.Presles

Quelques points importants en détonique classique ; F.Chaissé

JOURNAL DE PHYSIQUE IV
Colloque C4, supplément au Journal de Physique III, Volume 5, mai 1995

On the Detonation Wave Propagation

J.-M. Chevalier(1)

Commissariat à l'Energie Atomique, CEV-M, BP. 7, 77181 Courtry, France

A new theoretical approach of the unsteady detonation in condensed explosives was developped. The first experimental results presented in this paper confirm that the evolution of the front can be described by the propagation of front-waves, as predicted by the model. It seems, also, that the speed of these waves is a decreasing function of detonation velocity and doesn't depend on the confinement of the explosive.

INTRODUCTION

A new model describing the detonation front propagation in condensed explosives (named Jr model) has been recently proposed by L. Brun [1-2]. First macroscopic model of the unsteady detonation, the Chapman-Jouguet model [3] assumes an instantaneous and complete decomposition across a downstream sonic discontinuity. But the condition of a detonation propagation at constant velocity doesn't agree with the curved steady revolution detonation (SRD) fronts observed on condensed explosives. The Zeldovitch-Von Neuman-Döring model ZND [4-5] assumes that the decomposition goes on behind a non reactive and hence subsonic discontinuity. The ZND model agrees for interpretations of the SRD [6], but appears difficult to extend to unstationnary cases like spherically diverging detonation.

In Jr model, the front acceleration is related to its curvature by two functions of the local detonation velocity: the characteristic curvature, which has been already studied (Aveillé,Bdzil) [7-11], and a new function, the characteristic speed, which describes the propagation of front-waves.

Original experiments was performed in order to check the model, in TATB and HMX based compositions, to confirm the front-waves propagation.

THE Jr MODEL

Three assumptions govern the model. The detonation front is assimilated to an infinitely thin and downstream sonic discontinuity. But this model does not suppose, as Jouguet's did, a total decomposition within the front, and thus accordingly releases Jouguet's condition $D=D_{cj}$ [1]. The acceleration of a self-sustained detonation wave front is given by the relation:

$$\delta D/\delta t = 2\, C^2(D)\, [K(D) - \mathscr{C}],$$

where $\mathscr{C}$ is the curvature of the front, C(D) the velocity of the front-waves and K(D) the celerity-curvature relationship.

(1) At present, Commissariat à l'Energie Atomique, CESTA, BP. 2, 33114 Le Barp, France

The associated boundary condition is:

$$B(\theta_b, D_b)=O,$$

where θ_b is the front inclination on the unperturbed interface and D_b the front velocity at the boundary.

The characteristic angle connects the front-wave speed with the detonation velocity by the relation:

$$tg\ \varphi = C(D)/D$$

ASSOCIATED EXPERIMENTS

The Jr model can easily be used to describe what would happen in a cylindrical geometry: if a steady detonation propagates in an explosive cylinder, a sudden reduction of the diameter generates a circular perturbation which propagates inwards.

As shown figure 1, the model tells that, if the perturbation starts at time t_O, at t_O+dt a length Cdt of the front will be modified. The TT' surface is not yet affected, and is determined by a translation of the NN' surface.

These phenomena must be experimentaly observed in order to check the model.

FIGURE 1 : DISPLAY PRINCIPLE OF FRONT WAVES

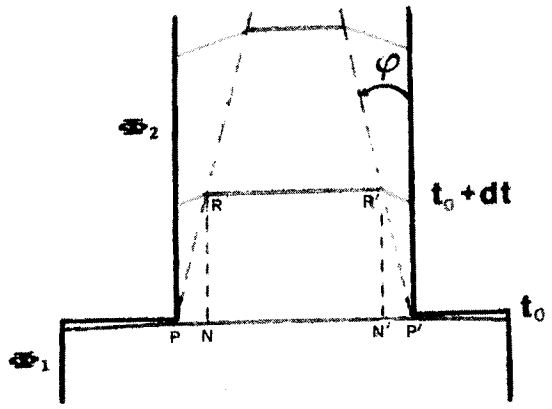

EXPERIMENTAL SET-UP

The experimental set-up used to observe the detonation front and to measure the front-wave speed is presented figure 2.

A plane wave generator initiates a detonation wave in an unconfined explosive cylinder (diameter ϕ_1). Its length H_1 is chosen in order to achieve a steady detonation. The cylinder free surface is metallized for the optical recording of the front motion.

An argon flash-light is reflected by the surface and focused on a streak camera. When the

detonation wave interacts with the surface, the damage of the metal spray is recorded on the film.

In another experiment a cylinder of diameter ϕ_2 ($\phi_2<\phi_1$) and length H_2 is added to the previous one, and the detonation front is observed by using the same technics. Comparison of the shapes of the waves which emerge from both cylinders yields the velocity of the front-waves.

FIGURE 2 - DISPLAY EXPERIMENTAL SET-UP OF FRONT WAVES IN EXPLOSIF.

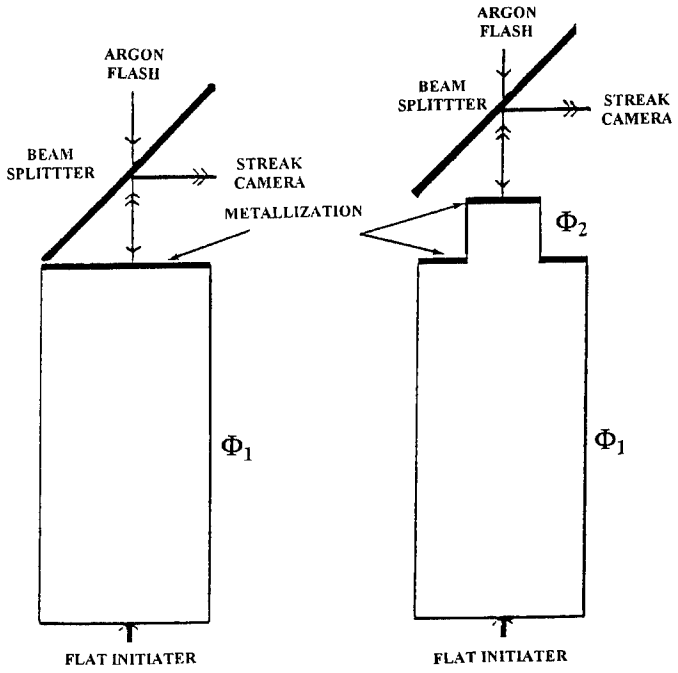

EXPERIMENTAL RESULTS

TATB BASED COMPOSITION T2 (97 % TATB)

In order to study the variation of the front-waves speed C versus the detonation velocity D, several cylinder diameters ϕ_1 have been tested. For T_2 composition, as for others TATB compositions, the detonation velocity is strongly dependent on the cylinder diameter (Aveillé) [10-11].

Figure 3 presents the optical records obtained in one configuration. In the first experiment, the dimensions were ϕ_1=30 mm, H_1=120 mm. In the second experiment, a cylinder ϕ_2=15 mm, H_2=15 mm is added.

No noise perturbs the records. The superposition of the two measurements gives an accurate determination of the front-waves speed. The central part of the front, delimited by the two points T and T', is not yet affected by the perturbations propagated by the front -waves, as predicted by the Jr model.

As defined figure 1, D and C are given by the relation : D=NT/dt, C=PN/dt. C is the average value of the front waves velocity. D is in good agreement with previous measurements [10-11].

The values of C(D), reported in table 1 , show that C is a decreasing function of D [12].

FIGURE 3 - EXTENDING SUPERPOSITION OF T_2 ϕ_1=30 AND ϕ_2=15 WAVES OUT

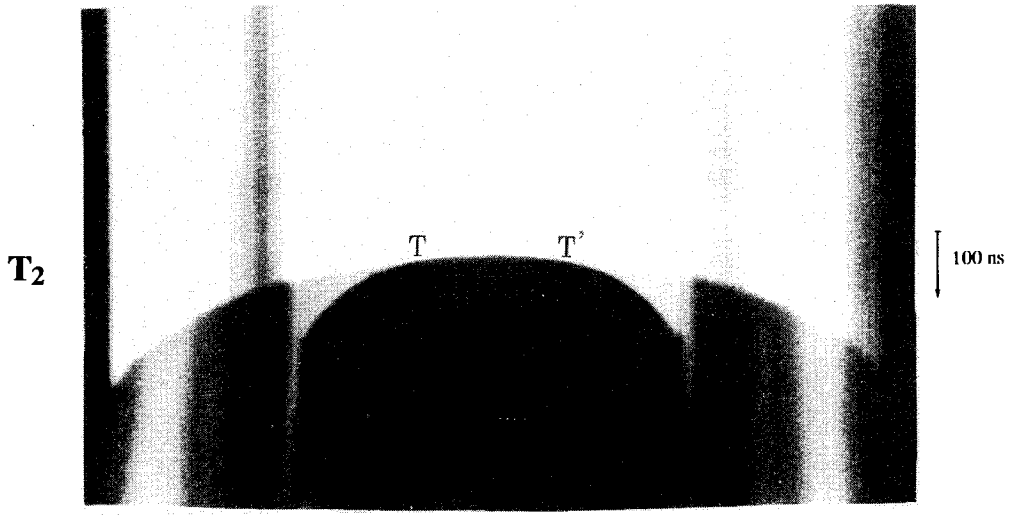

TABLE 1 - MEASURED VALUES ON T_2 COMPOSITION

Φ_1/Φ_2 (mm)	H_2 (mm)	D (m/s)	C(D) (m/s)	φ (°)	ΔD (m/s)	ΔC (m/s)	Δφ (°)
30/15	15	7538	2810	20.4	35	250	2
		7519	2810	20.5	35	250	2
75/50	40	7627	1880	13.8	20	140	1
100/50	40	7603	2170	15.9	20	140	1

To complete the determination of function C(D), a serie of experiments have been realised with cylinder diameters f_1 decreasing from 75 to 10 mm. In these conditions the detonation velocity decreases from 7630 to 7290 m/s [10-11]. The measured values of C(D) are reported on table 2. The variations of front-waves speed C versus the detonation velocity are recorded on figure 4. These results confirm that C is decreasing function of D. The last value seems to

express that the front-wave speed increases strongly near the critical diameter (ϕ_c=8.5 mm for T_2 composition). Neverthless, this value needs to be confirm.

TABLE 2 - STUDY OF THE C(D) FUNCTION ON T_2 COMPOSITION

Φ_1/Φ_2 (mm)	H_1 (mm)	H_2 (mm)	D (m/s)	C(D) (m/s)	φ (°)	ΔD (m/s)	ΔC (m/s)	Δφ (°)
75/50	510	40	**7626**	**1990**	**14.6**	8	100	0.8
60/40	370	30	**7612**	**1990**	**14.7**	10	130	1
40/20	240	14	**7560**	**2320**	**17.1**	20	140	1
30/15	160	10	**7558**	**2490**	**18.2**	30	200	1.5
20/14	100	9	**7502**	**2670**	**19.6**	30	220	2
15/10	75	4	**7438**	**3350**	**24.2**	70	400	3
		6	**7413**	**3210**	**23.4**	45	270	2
10/6	50	2	**7326**	**5860**	**38.7**	135	840	6

In a second study two experiments series have been performed to observe the variation of front-wave speed C with the time.

In this case, configurations with ϕ_1=50 mm, ϕ_2=30 mm and H_2=10 to 50 mm by 10 mm step has been tested. For this configuration the detonation velocity on the axis wouldn't vary.

The experimental results are reported on table 3. The measured values of C confirm that to one detonation velocity value D is associated one front-wave speed C, taking the experimental accuracy into consideration.

HMX BASED COMPOSITIONS X1 AND X2 (96 ET 94,2% HMX)

These two HMX based compositons differ essentially by their binders. The measured values of C(D) [12] are reported in table 4.

In both compositions, the values are nearly the same, as expected, and lower than those found for the TATB composition.

For the experiments on HMX compositions, decrease of the detonation velocity is not significant enough to check whether function C(D) is decreasing or not.

TABLE 3: MEASURED VALUES OF FRONT-WAVES SPEED VERSUS THE TIME ON T_2 COMPOSITION

Φ_1/Φ_2 (mm)	H_1 (mm)	H_2 (mm)	D (m/s)	C(D) (m/s)	φ (°)	ΔD (m/s)	ΔC (m/s)	Δφ (°)
50/30	300	10	**7612**	**2090**	**15.4**	30	390	3
		20	**7607**	**2020**	**14.9**	15	195	1.5
		30	**7607**	**1990**	**14.7**	10	130	1
		40	**7606**	**2170**	**15.9**	8	65	0.5
		50	**7609**	**2025**	**14.9**	6	40	0.5

Figure 4 - Variation of front-waves speed C versus the detonation velocity

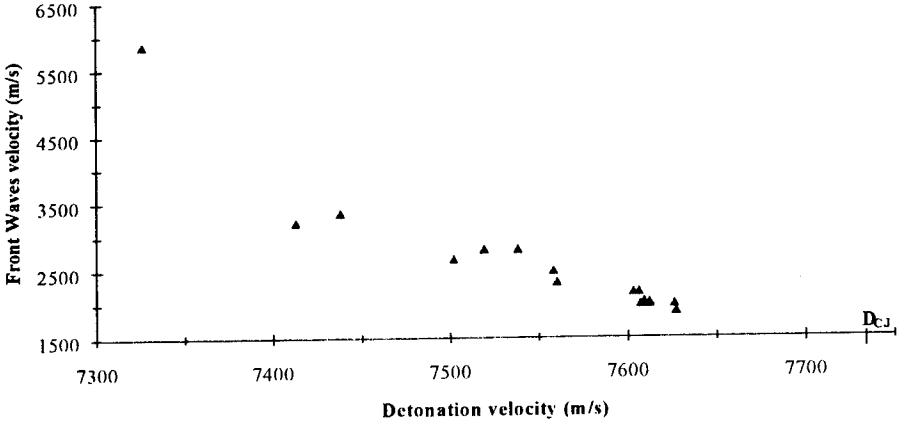

TABLE 4 - MEASURED VALUE ON X_1 AND X_2 COMPOSITION

Composition	Φ_1/Φ_2 (mm)	H_2 (mm)	D (m/s)	C(D) (m/s)	φ (°)	ΔD (m/s)	ΔC (m/s)	Δφ (°)
X_1	**25**/10	20	**8755**	**1450**	**9.4**	40	100	1
X_1	**50**/30	30	**8744**	**1530**	**9.9**	25	100	1
X_2	**100**/50	40	**8767**	**1420**	**9.2**	20	100	1
X_2	**100**/50	80	**8760**	**1320**	**8.5**	10	100	1

INFLUENCE OF THE CONFINEMENT

The Jr model predicts that C is a function of the detonation velocity and will not depend on the boundary conditions. Some experiments were performed with an aluminum case around the second explosive cylinder. The results are given in table 5.

TABLE 5 - INFLUENCE OF THE CONFINEMENT COMPOSITION

Confinement	Φ_1/Φ_2 (mm)	H_2 (mm)	D (m/s)	C(D) (m/s)	φ (°)	ΔD (m/s)	ΔC (m/s)	$\Delta\varphi$ (°)
Air	100/50	40	**8767**	**1420**	**9.2**	20	100	1
2024			**8787**	**1370**	**8.9**	20	100	1
Air	100/50	40	**7603**	**2170**	**15.9**	20	140	1
Steel			**7646**	**2060**	**15.1**	20	140	1
2024			**7651**	**1940**	**14.2**	20	140	1

The measured values of C, with and without confinement, are very close to each other. Of course, the shapes of the detonation fronts are very different : the front-waves move with the same speed, but they do not carry the same information.

UNSTEADY REGIME

In the experiment depicted on figure 5 the detonation was initiated in a cylinder of T_2 composition by a plane detonation making an angle of 74° with the axis. It appears that the detonation in the T_2 cylinder evolves towards the stationnary shape which would be observed when initiation is perpendicular to the axis.

Indeed several configurations have been performed with T_2 cylinders which dimensions are respectively ϕ=50 mm and H=100, 200, 400 and 600 mm. For the first, the optical record presented (figure 6) shows an assymetrical detonation front with regard to the axis. For the third, the detonation front (figure 7) was setted partly, presenting a weak assymetry.

For this configuration, the perturbation due to the diameter reduction and which propagates inwards, is arrived at cylinder center and is came back two times before the detonation emergence. For the last, the recorded detonation front was setted and presents the same characteristics as a detonation front with a perpendicular to the axis initiation.

Figure 5 - Experiences in unsteady detonation field

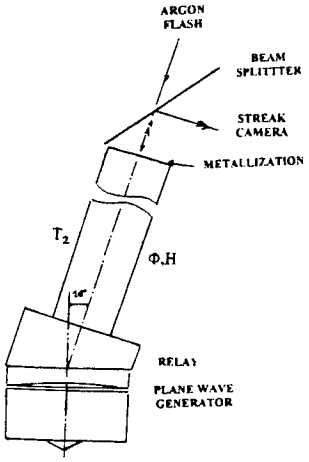

FIGURE 6 - Optical record of detonation in T_2 cylinder (ϕ=50 mm et H=100 mm) initiated by a plane detonation making an angle of 74° with the axis

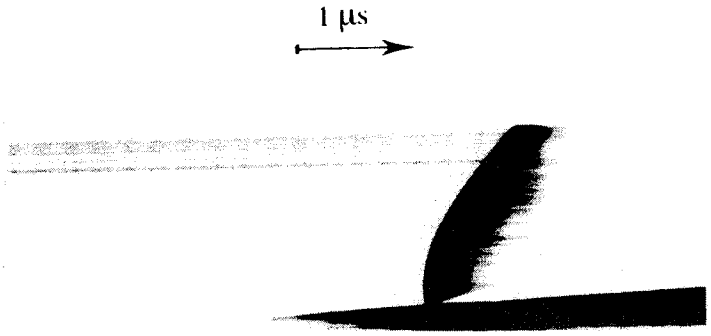

FIGURE 7 - Optical record of detonation in T_2 cylinder (ϕ=50 mm et H=400 mm) initiated by a plane detonation making an angle of 74° with the axis

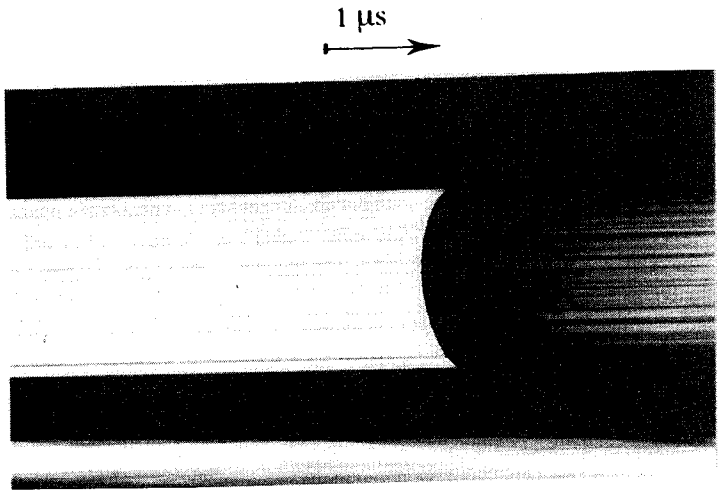

FIGURE 8 - Experimental set-up of the zero method for boundary condition determination

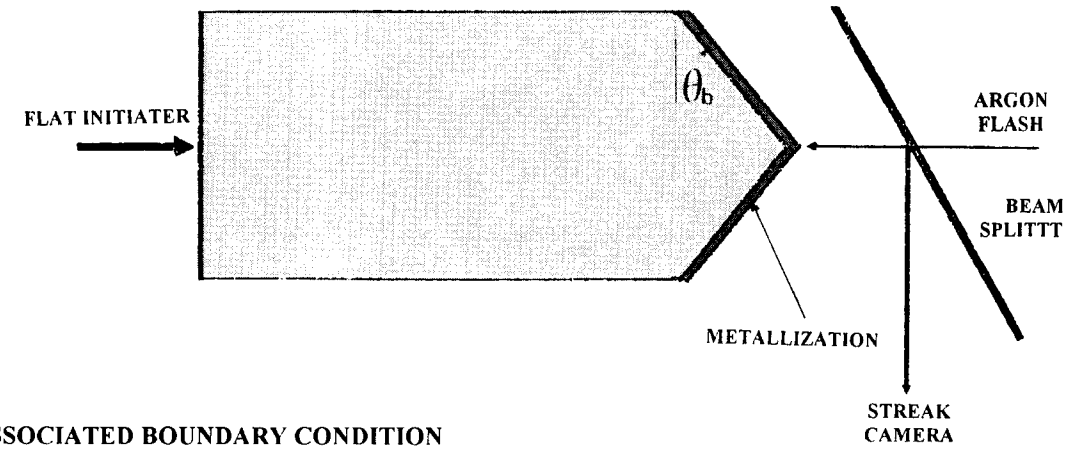

ASSOCIATED BOUNDARY CONDITION

For this study, two methods were used to measure the front inclination. The first (classical method) is based on the front detonation record at the end of explosive cylinder. For the second (zero method), this cylinder is terminated in cone ("pencil") with an inclination q_b corresponding to the presumed value. This method allows a more accurate measure of the motion at this presumed value. The experimental set-up of this method and the optical record obtained for T_2 cylinder with 30 mm diameter are presented respectively figures 8 and 9. Measures were obtained after digitalization and linear approximation on 0.7 mm of boundary front wave. The measured values for T_2 composition are showed on table 6. The boundary detonation velocity is given by the relation $D_b = D.\ cosq_b$, where the D values were measured by Aveillé and Col. [10-11]. The classical method, though less accurate, is given interesting results.

FIGURE 9 - Optical record for T2 "pencil" (ϕ=30 mm et H=180 mm)

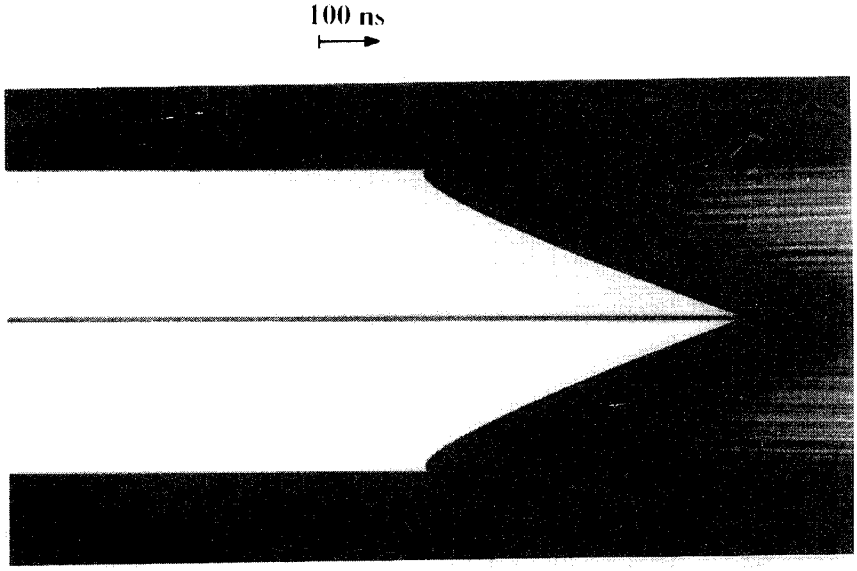

TABLE 6 - MEASURED VALUES OF THE BOUNDARY CONDITION ON T_2 COMPOSITION.

	(Zéro method))		(Classical method)	
Φ (mm)	D_b (m/s)	Θ_b (°)	D_b (m/s)	Θb (°)
50			7145	**20.1**
40			7095	**20.2**
30	7095	**19.8**	7110	**19.8**
20	7020	**20.7**	7065	**19.6**
15	6885	**22.7**	6925	**21.1**
10			6450	**28.3**
9			6340	**29.6**

$$\Delta^{\Theta}{}_{b} \sim 1°$$

CONCLUSION

The experimental results presented in this paper are in general agreement with the front wave propagation phenomena as described by the Jr model. They were obtained for TATB or HMX based compositions, which exhibit very different front curvatures and these preliminary results seem to confirm the basic assumption of a front-wave speed that only depends upon the detonation velocity.

The results on TATB based composition show that C is a decreasing function of D. Experiments performed on HMX based compositions can't lead to same conclusions. Results on TATB (C(D) function associated with the boundary condition values) would certainly allow to treat more physically the detonation in calculations.

REFERENCES

[1] L. Brun *"Une théorie de la détonation dans les explosif condensés fondée sur l'hypothèse de Jouguet"* CEA Report (Unpublished 1989)

[2] L. Brun *"Un nouveau modèle macroscopique de la détonation non soutenue dans les explosifs condensés"* Symposium International Hautes Pressions Dynamiques, la Grande Motte p.103-107, CEA eds (1989)

[3] E. Jouguet *"Mécanique des explosifs"* Doin et fils eds (1917)

[4] R. Courant and K.O. Friedrichs *" Supersonic flow and shock waves"* I.P. (1948)

[5] W. Fickett and D.C. Davis *"Detonation"* University of California Press (1979)

[6] J.B. Bdzil *"Steady-statetwo-dimensional detonation"* J. Fluid. Mech., 108, 195-226 (1981)

[7] J.B. Bdzil and D.S. Stewart *" Modeling two dimensionnal detonations with detonation shock dynamics"* Phys. of fluid, 1,7, P. 1261-67 (1989)

[8] C. Bianchi, N. Carion and J. Aveillé CEA Report (Unpublished 1987)

[9] C. Perennes, C. Bianchi, N. Carion and F.Chaissé CEA Report (Unpublished 1988)

[10] J. Aveillé, J. Baconin, N. Carionand J. Zoé *"Experimental study of spherically diverging detonation waves"* The Eighth Symposium International on Detonation, 523-527, Albuquerque (1985)

[11] F. Chaissé, J.M. Servas, J. Aveillé, J. Baconin, N. Carion and P. Bongrain *"A theoretical analysis of the shape of a steady axisymmetrical reactive shock front in cylindrical charges of high explosive. A curvature-diameter relationship"* The Eighth Symposium International on Detonation, 539-547, Albuquerque (1985)

[12] J-M. Chevalier, N. Carion, J-C. Protat et J-C. Redasse *" Propagation phenomena on the detonation wave front"* Physical Review Letters Vol. 71-5, 710-714 (1993)

JOURNAL DE PHYSIQUE IV
Colloque C4, supplément au Journal de Physique III, Volume 5, mai 1995

An Evaluation of Detonation Models

D.C. Swift and S.J. White

AWE Aldermaston, Reading RG7 4PR, U.K.

Abstract: Detonation models of practical use for large explosive systems have been evaluated against experimental data obtained by AWE. The models considered were Chapman-Jouguet, Whitham-Bdzil-Lambourn and Zeldovich-Neumann-Doering. The experimental data included measurements of detonation wave propagation in various geometries of explosive, pressure and initiation properties. The ZND model performs well over the widest range of problems, but not perfectly. It is not clear whether any shortcomings are from a deficiency in the theory, inadequate attention to its constituent equations of state and reaction rates, or inadequate experimental data.

1. INTRODUCTION

In order to understand hydrodynamic phenomena in explosive-driven systems, accurate models are required for processes occurring in the explosive. These include the motion of the leading shock and subsequent pressure history for full detonation, over and under driving by neighbouring explosives, initiation and unreactive behaviour, desensitisation, detonation quenching and enhancement. The models considered here are applied to heterogeneous high explosives based on HMX and TATB.

An additional constraint on models is that they should be suitable for use in hydrocode calculations of macroscopic systems. Complete resolution of processes at the atomic level is not possible when performing calculations of systems of the order of a metre in size, so reasonable approximations must be found.

2. THE 'REAL' PICTURE OF DETONATION

'Real' detonation starts with a shock wave. In heterogeneous explosives, the variation in material impedance could give the shock an irregular, possibly turbulent structure.

Chemical reactions start in or behind the shock. The metastable molecules of undetonated explosive react, releasing energy. Reaction can continue for a relatively long period, as the reaction products expand and cool.

At some point behind the leading shock, the product molecules can have accelerated to the local speed of sound relative to the leading shock (LS). Reactions taking place in the region between the LS and this sonic point (or sonic surface in 3D) are unaffected – causally disconnected – from the flow downstream. The region between the LS and the sonic surface has been termed the detonation zone (DZ) to distinguish it from the reaction zone (RZ) which may extend beyond the sonic surface.

3. CHAPMAN-JOUGUET THEORY

In the Chapman-Jouguet (CJ) model, the thickness of the DZ is considered to be negligible. Complete reaction is assumed to occur in the resulting laminar shock. A consequence of this is that detonation waves travel with a constant speed D.

Experimentally, when a rod or slab of explosive is initiated with a plane wave, the wave emerging at the other end is curved (Fig. 1) [5]. For HMX charges a few cm across, detonation at the edges can be delayed by several tens of ns with respect to the centre. The effect is several times larger for TATB. Furthermore, detonation waves travel at different speeds along charges of different diameter or thickness.

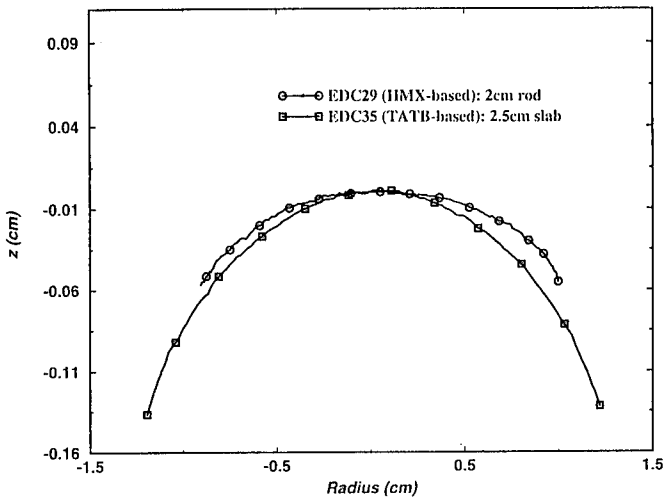

Figure 1: Waveshapes at the end of plane-initiated charges.

The speed of a dynamically expanding wave in the 'logosphere' geometry has been shown to change with time [1]. Similarly, preliminary results on the variation of arrival time of a detonation wave with position on the face of a disc (Fig. 2) seem to indicate an inconstant speed [13].

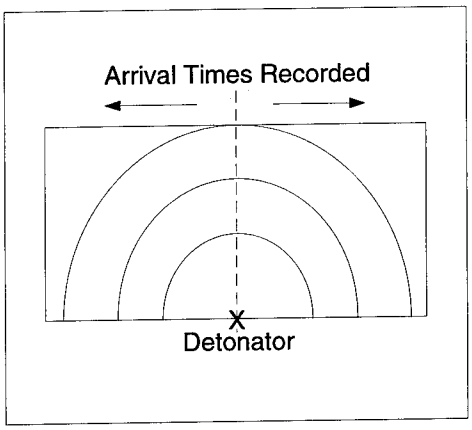

Figure 2: Disc experiments to measure detonation speed.

These effects point to a finite DZ thickness. As well as failing to model such effects, the CJ model provides no explanation for phenomena such as enhancement and quenching, and does not allow initiation properties to be predicted.

4. THE WHITHAM-BDZIL-LAMBOURN MODEL

The Whitham-Bdzil-Lambourn (WBL) model is phenomenological, providing a means of calculating the motion of the LS based on the assumption that the local detonation speed D at any point on the LS depends only on the local wave curvature K. Where the wave makes contact with inert materials adjoining the explosive, the angles it can make with the boundary are constrained. [11, 14] The WBL model is closely related to the Detonation Shock Dynamics (DSD) model [3].

Parameters for the $D(K)$ relation are inferred from the shape of steady waves at the end of long rods and slabs. Linear relations of the form

$$D = D_{CJ}(1 - AK) \tag{1}$$

have been employed usually, where D_{CJ} and A are determined by fitting experimental waveshapes. It has been found that any single waveshape can be matched quite well with a linear $D(K)$ relation, but that the relations from charges of different diameter or thickness are different. This effect is much greater for TATB than for HMX, where the linear $D(K)$ relations deduced from different experiments are similar (Fig. 3). In the case of HMX, the variation with initial temperature is consistent with the density change on thermal contraction.

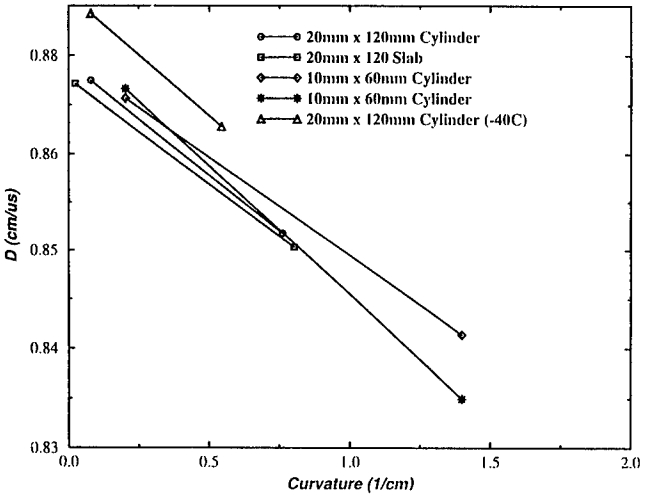

Figure 3: $D(K)$ relations for EDC29 (HMX-based).

The $D(K)$ relations inferred from a series of experiments on the TATB-based EDC35 are shown in Fig. 4. The curvature limits were deduced from the range of curvatures in the theoretical fit to the waveshape, and are somewhat arbitrary. These results demonstrate that a linear $D(K)$ relation is inappropriate for TATB. Preliminary calculations using a $D(K)$ relation based on that for PBX9502 [2] have demonstrated that a non-linear relation can match a wider range of experiments.

Given an reasonable $D(K)$ relation, the WBL model accurately predicts waveshapes in rods and slabs and reproduces the diameter effect. It is a computationally efficient way of tracking the LS.

It is assumed in the WBL model that the $D(K)$ relation can be applied to unsteady detonation waves, and this seems to be borne out in practice when looking at the shapes of detonation waves in charges too short for a steady state to be reached. However, the assumption may only be approximately true. The WBL model was used successfully to calculate the shape of detonation waves in rods of EDC29 which were too short to have reached a steady state. On the other hand, preliminary results [13] from direct speed – time measurements on dynamically expanding waves may not be wholly consistent with WBL calculations. Initial attempts at reactive flow calculations of spherically diverging detonations based on the ZND model do not exhibit a behaviour consistent with the WBL model.

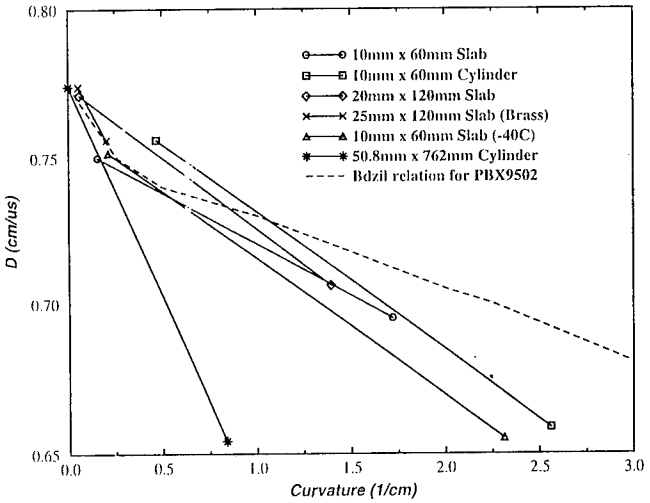

Figure 4: $D(K)$ relations for EDC35 (TATB-based).

As with CJ theory, the WBL model does not attempt to address the initiation of detonation, and provides no explanation for phenomena such as desensitisation.

5. ZELDOVICH-NEUMANN-DOERING THEORY

Zeldovich-Neumann-Doering (ZND) theory is based on the assumption that the LS is laminar and unreactive with no substructure. Reaction occurs in the subsequent expansion of the explosive. The ZND model requires a reaction rate (or rates, if several decomposition processes are modelled) and equations of state (EoS) for unreacted explosive and material in all stages of reaction. If reaction occurs heterogeneously, the EoS must model equilibration processes for pressure and temperature..

5.1 Detonation pressure

A general consequence of the ZND theory is its prediction of a pressure spike well above the CJ value – the von Neumann (vN) spike. This has been observed in Doppler velocimetry experiments, looking through a window of similar impedance to the explosive [12].

Another approach for measuring the vN spike is from the free surface velocity imparted to an inert material [7]. Since shocks in an inert are subsonic with respect to the flow behind, the vN spike erodes during its passage through the inert. The thinner the inert, the greater the effective accelerating pressure and the closer it will be to the value at the LS. Experiments have been performed using a tapering piece of aluminium as the inert material [6]. Its free surface velocity was inferred from the time it took to cross an air gap and cause extinction of total internal reflection in a glass block (Fig. 5).

Initial experiments have indicated the presence of a spike above the CJ value, but its precise value is not clear.

5.2 Oblique shock/inert interactions

Another possible way of inferring the pressure at the LS is to consider the angle between a detonation wave and the interface between the explosive and an inert material. The LS drives a shock into the inert material, and in general a wave is reflected into the RZ. Reflected waves alter the states within the RZ and hence change the rate of reaction. Such changes alter the reactions occurring within the DZ, modifying the speed of the wave and hence its shape.

5.2.1 High-impedance inert materials

If the inert material has a higher shock impedance than the explosive, then depending on the angle

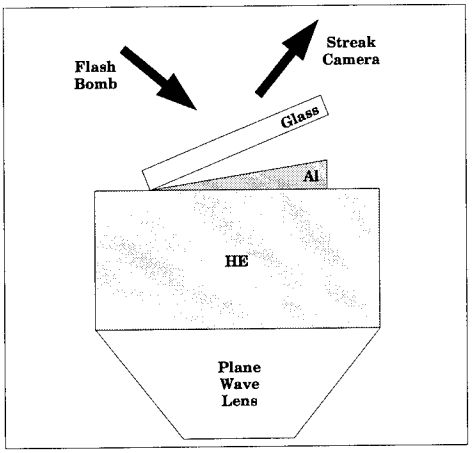

Figure 5: Experimental scheme for measuring detonation pressure.

of incidence of the LS, the reflected wave may be a shock or a rarefaction. At some angle, no wave is reflected. If the detonation wave reaches this state it should persist, since the chemical reactions are unaffected. (It is conceivable that this state is only reached very slowly, i.e. that at other angles, the reflected wave has negligible effect on the reactions.) This angle, ϕ_a, is the value which should be observed in the waveshape at the end of long rods and slabs. Measuring ϕ_a provides some information on the LS, if the Hugoniot of the inert material is known accurately.

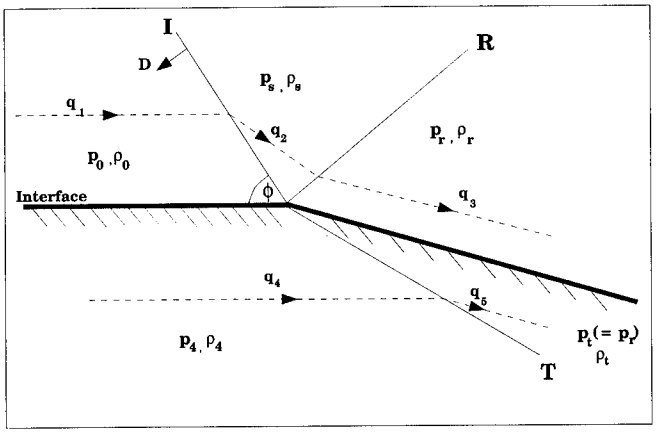

Figure 6: Refraction of the leading shock into a material of high impedance.

Such calculations have been performed for EDC35, using an unreacted EoS of the Jones-Wilkins-Lee (JWL) form with negative second exponential [8], adjusted to match experiments on the unreacted Hugoniot of EDC35 [9, 15]. Calculations were also performed for an incident CJ detonation, using a products JWL in the normal way. The strength of the inert material was neglected.

ϕ_a was found to vary slightly with shock speed. A 'typical' value of D was used in most of the calculations.

Sample results for a variety of inert materials are presented in Table 1. ϕ_a is larger for materials of higher density and impedance, as would be expected intuitively. (ϕ_a would be 90° for a rigid boundary.)

Table 1: Values of the asymptotic boundary angle.

Material	ϕ_a (degrees)			
	Unreacted JWL	CJ JWL	Experiment	
			(waveshape fit)	(fit near edge)
brass	80.25	76.60	78.8	72.5±2.0
copper	81.65	78.60		
steel	82.95	79.60		
tantalum	83.68	81.50		
Ti-6Al-4V	78.95	72.30		

One suitable experiment has been performed so far, EDC35 and brass in a slab geometry (Fig. 1). ϕ_a was estimated in two ways: from the gradient of a function fit to the bulk of the wave, and by estimating the gradient of the wave near its edges. The functional fit did not pick up the slightly steeper 'tails' near the interfaces and therefore overestimates ϕ_a.

It can be seen that the angle seen experimentally is in fact closer to the value inferred from a CJ state than from the ZND model. This appears to be evidence against the ZND model, but may be because of deficiencies in the unreacted EoS or because the shock interaction picture presented here is oversimplified.

5.2.2 Low-impedance inert materials

If the inert material has a lower shock impedance than the explosive then the reflected wave is always a rarefaction. This should reduce the rate of reaction in the DZ, decelerating the wave near the interface.

However, when the detonation wave is close to normally incident on the interface, the rarefaction cannot influence the shape of the LS because information cannot propagate quickly enough to enter the causal domain of the LS in any other part of the explosive: the LS cannot 'see' the interface. The 'causal angle' ϕ_c at which the LS can first be influenced by the interface is found by equating the rate at which the interface sweeps across the LS

$$c_s = \frac{D}{\tan\phi} \tag{2}$$

with the rate at which sound waves of speed c travel around the LS

$$c_w = \sqrt{c^2 - (D - u_s)^2} \tag{3}$$

where u_s is the material speed (Fig. 7).

The shape of a detonation wave in a long charge should be steady if it makes the angle ϕ_c with a surrounding low-impedance medium such as air. Calculated and experimental results for EDC35 are shown in Table 2. The CJ value is a consequence of the fact that the CJ detonation wave is sonic with respect to the flow behind, and is clearly not in agreement with experiment. It has been found difficult to determine an accurate experimental value of ϕ_c, and it is quite possible that future experiments will yield values closer to the ZND prediction.

5.3 Reactive flow calculations

The ZND model has been investigated by performing 1D reactive flow calculations of initiation and detonation on plane and spherically diverging systems. Several rate laws were investigated, but effort was concentrated on a type of Forest Fire law [10]

$$\dot{\lambda} = \dot{\lambda}_0(1-\lambda)\left(\frac{p}{p_{ref}}\right)^r \left[1 + f\left(\frac{p}{p_{ref}}\right)^s\right] \tag{4}$$

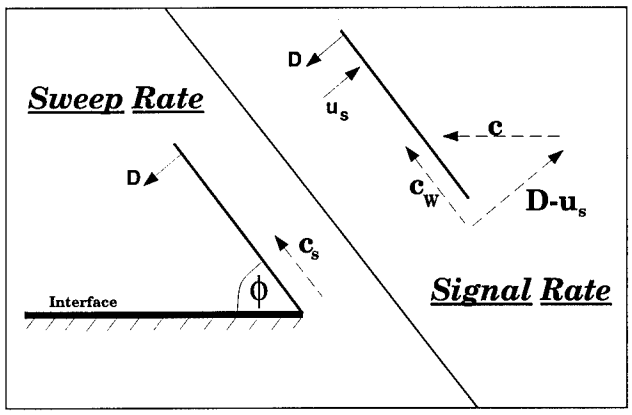

Figure 7: Angle at which a detonation wave just 'sees' an interface.

Table 2: Values of the causal boundary angle.

ϕ_c (degrees)		
Unreacted JWL	CJ JWL	Experiment
49.0	90	60±4

where λ is the single 'fraction reacted' parameter, since this exhibited the most interesting features.

A parameter-free extension to the JWL products EoS was employed to model unreacted and partially reacted states [14]. This has the form

$$p = \frac{\omega e}{v} + A\left[1 - \frac{\omega v_0}{R_1 v}\right] e^{-R_1 v/v_0} + B\left[1 - \frac{\omega v_0}{R_2 v}\right] e^{-R_2 v/v_0} - (1-\lambda)\frac{\omega}{v}(e_0 + e^*) \tag{5}$$

where

$$e^* = \frac{v_0}{\omega}\left[A\left(1 - \frac{\omega}{R_1}\right) e^{-R_1} + B\left(1 - \frac{\omega}{R_2}\right) e^{-R_2} - p_0\right] \tag{6}$$

This EoS is based on constant volume reaction and an offset between the specific internal energies e of the unreacted explosive and its products. The effect of the last term in Eq. 5 is to reduce the pressure to the unshocked value p_0 when the material is uncompressed ($v = v_0$), unreacted ($\lambda = 0$) and cold ($e = e_0$).

The validity of this EoS was tested by using it to calculate the unreacted Hugoniot of EDC35. The Hugoniot was compared with experimental data [9] (Figs 8 and 9). It can be seen that the modified JWL is a reasonable match to the pressure – particle speed data, although not so good for the shock speed.

Two classes of reactive flow calculations were performed: quasisteady and dynamic.

5.3.1 Dynamic calculations

Dynamic reactive flow calculations were made using a 1D Lagrangian finite difference code written especially for this problem. Shock waves were treated with a quadratic artificial viscosity q, and in any cell reaction was not allowed to start until q had begun to decrease. The code was validated by demonstrating an acceptable accuracy in calculating the speed and profile of inert shocks and fully-developed CJ detonation waves.

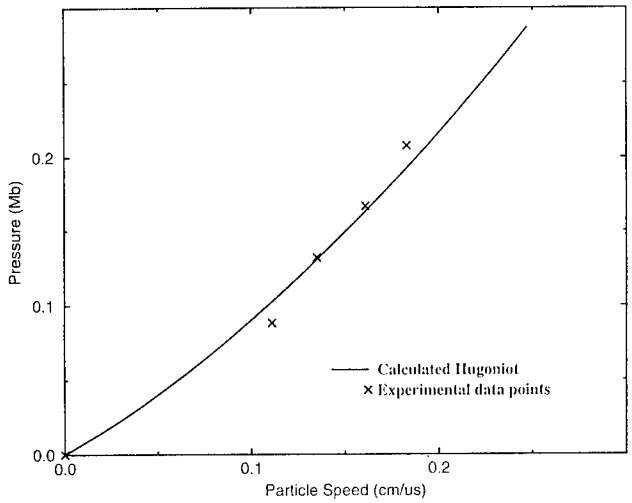

Figure 8: Pressure – particle speed for EDC35.

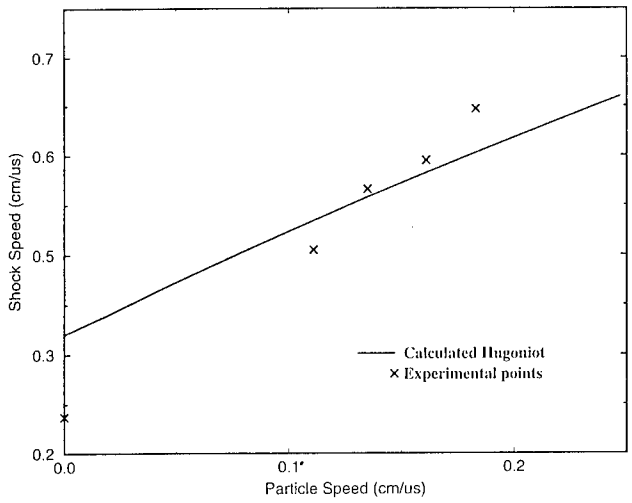

Figure 9: Shock speed – particle speed for EDC35.

It was found that the experimental data on the variation of run distance to detonation with pressure for EDC35 [9] could be reproduced to arbitrary accuracy (Fig. 10) by adjusting the parameters in the reaction rate law (Eq. 4). Calculations were performed with a range of mesh sizes down to 20 μm, and had roughly converged at about 80 μm.

Initial calculations of spherically diverging detonation waves produced detonation speeds more constant than would be consistent with the WBL model's use of a $D(K)$ relation. The means of initiation (e.g. the applied pressure) mattered, and it was not clear how best to model 'real' initiation systems in 1D. Direct experimental verification depends on more accurate measurements of spherically diverging waves, e.g. in the disc geometry described earlier.

5.3.2 Quasisteady calculations

Reactive flow calculations were also performed of quasisteady diverging detonations, similar to the states along streamlines in the steady wave in a long rod or slab. Such calculations had previously been used to find a consistent combination of EoS, $D(K)$ relation and reaction rate [14].

The quasisteady solution scheme was used to find the variation of detonation speed with wave curvature. Using the same EoS and reaction rate as provided a good fit to the EDC35 Pop

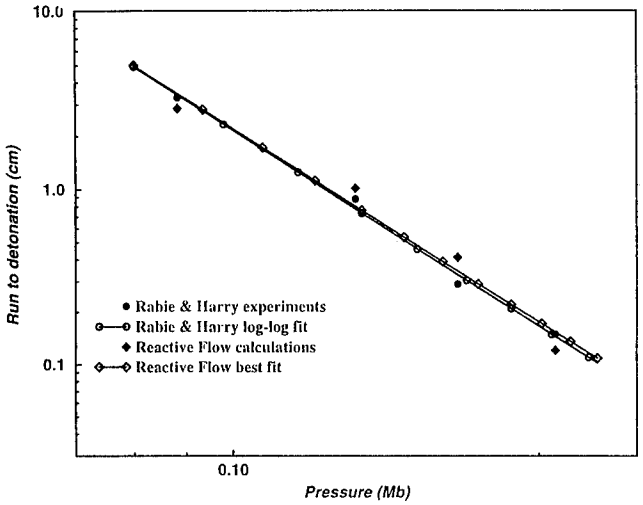

Figure 10: Pop plot for EDC35.

plot data, the quasisteady solution produced a $D(K)$ relation broadly in agreement with the results of the steady waveshape experiments (Fig. 11).

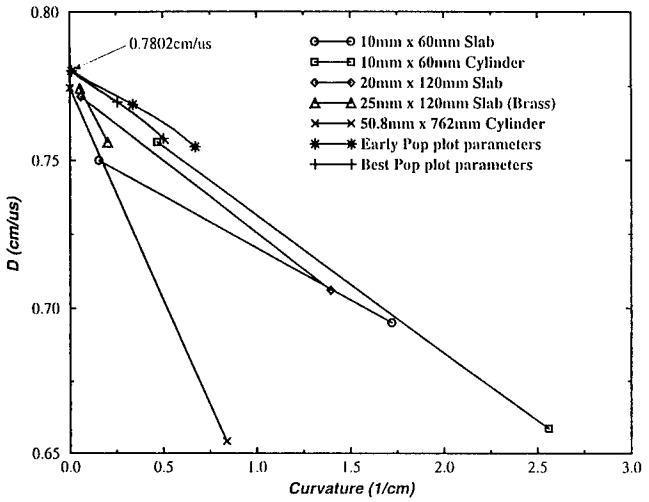

Figure 11: Experimental and reactive flow $D(K)$ relations for EDC35.

The $D(K)$ curves calculated by the quasisteady scheme exhibited detonation failure when $K \sim 1/\text{cm}$. This value turns out to be extremely sensitive to the reaction rate parameters. The difference in Pop plots between the 'early values' and the final fit was barely significant (Fig. 10), yet the $D(K)$ curves diverged considerably at higher curvatures. The conclusion to draw from this study is that adjustments to the form and parameters of the reaction rate should allow an experimental $D(K)$ relation to be reproduced as accurately as desired. Thus ZND theory allows a model for the TATB-based EDC35 to be deduced which is in reasonable agreement with several experiments on initiation and full detonation.

6. CONCLUSIONS

The CJ theory is adequate to a few percent in detonation speed. The variation in speed can occur between experiments in different geometries, or between different regions in a single geometry. It does not allow for non-ideal (non-planar) detonation effects, for instance as caused by the interaction

of detonation waves with inert materials. The CJ theory does not allow non-detonation effects to be calculated.

The WBL model matches the diameter effect and wave profiles much more accurately. It is not certain how applicable a detonation speed – curvature relation for steady waves is for the motion of nonsteady waves. Again, non-detonation effects are not treated.

The ZND theory predicts the existence of a spike of high pressure early in the detonation zone. Such spikes have been observed or inferred, but there is some uncertainty over their precise value. Predictions of angles between detonation waves and interfaces with inert materials seem in approximate agreement with experiment, although there is again some doubt about exact values. The theory appears to make it possible to construct unique models of explosive behaviour which are valid for unreacted, initiation and detonation behaviour. Such models have many degrees of freedom, so it seems likely that even if the model is not strictly accurate (e.g. if the leading shock is partially reactive) then there are enough parameters to allow data to be fitted. Heterogeneity can be built in through the use of exotic reaction rates and EoS. However, the direct use of the ZND model requires calculations to resolve the reaction zone. This is impractical for calculations on large systems.

7. ACKNOWLEDGEMENTS

The authors wish to acknowledge the contributions of Alan Collyer, Adrian Johnson, Paul Selby, Brian Lambourn, John Bdzil and Craig Tarver. They provided the experimental data and many of the ideas without which little of this work would have been possible.

8. REFERENCES

[1] Aveillé J., Baconin J. and Zoé J., "Experimental study of spherically diverging detonation waves", Proc. 8th Symposium (International) on Detonation, (1985).

[2] Bdzil J.B., "DSD characterisation of PBX9502", 10th Symposium (International) on Detonation, Boston MA 12 – 16 July 1993.

[3] Bdzil J.B., Fickett W. and Stewart D.S., "Detonation shock dynamics: a new approach to modeling multi-dimensional detonation waves", Proc. 9th Symposium (International) on Detonation, OCNR 113291-7 (1989).

[4] Brun L., Kneib J.-M. and Lascaux P., "Computing the transient self-sustained detonation after a new model", 10th Symposium (International) on Detonation, Boston MA 12 – 16 July 1993).

[5] Collyer A.M. and Johnson A.M., AWE internal report (1994).

[6] Collyer A.M. (AWE Aldermaston), private communication (1994).

[7] Davis W.C., "Magnetic probe measurements of particle velocity profiles", 6th Symposium (International) on Detonation, ACR-221 (1976).

[8] Green L.G., Tarver C.M. and Erskine D.J., "Reaction zone structure in supracompressed detonating explosives", Proc. 9th Symposium (International) on Detonation, OCNR 113291-7 (1989).

[9] Rabie R.L. and Harry H.H. "Characteristics of British explosives FD16, EDC29, EDC35, EDC37", Los Alamos National Laboratory report LA-UR-92-1928 (1992).

[10] Johnson J.N., Tang P.K. and Forest C.A., "Shock wave initiation of heterogeneous reactive solids", *J. App. Phys.* 57, 9 (1985).

[11] Lambourn B.D. and Swift D.C., "Whitham's shock dynamics model applied to the propagation of divergent detonation waves", Proc. 9th Symposium (International) on Detonation, OCNR 113291-7 (1989).

[12] Tarver C.M. (Lawrence Livermore National Laboratory), private communication (1993).

[13] Selby P.A. (AWE Aldermaston), private communication (1994).

[14] Swift D.C. and Lambourn B.D., "Developments in the W-B-L detonation model", 10th Symposium (International) on Detonation, Boston MA 12 - 16 July 1993).

[15] Wortley S.P., Powell D. and Jones A.G., AWE internal report, (1993).

© British Crown Copyright 1994 /MOD
Published with the permission of Her Britannic Majesty's Stationary Office

JOURNAL DE PHYSIQUE IV
Colloque C4, supplément au Journal de Physique III, Volume 5, mai 1995

Some Features of the Curvature of a Two-Dimensional Detonation Shock Front at a Simple Refraction Locus

P. Vidal, E. Bouton and H.-N. Presles

Laboratoire d'Energétique et de Détonique, URA 193 du CNRS, ENSMA, BP. 109, 86960 Futuroscope cedex, France

We present a theoretical study of the interaction of a constant-velocity two-dimensional detonation wave with its surrounding medium. For the case of pure refraction, we obtain exact expressions for the interface curvatures of the shock fronts in both the explosive (X) and its confinement (C) in terms of the detonation velocity D, the material properties of X and C and, if the flow is cylindrically symmetric, the radius of the explosive charge. These relations are obtained from the constraints imposed on the flow derivatives of the pressure P and the flow turning angle θ by the conservation laws, the boundary conditions at the curved shock fronts and the contact conditions matching P and θ along the interface. This model is used in our numerical analysis of a polytropic explosive with a pressure-dependent decomposition rate and a polytropic confinement. We find that, for a given D, the explosive's interface curvature C_x decreases as the confinement's density increases.

1.INTRODUCTION

Detonation wave front dynamic in condensed explosives is currently studied by using evolution equations which relate the geometrical and kinematical properties of the wave surface. There are essentially two approaches. In the first one [1] the detonation is considered as a generalized CJ wave, specifically a curved partially reactive sonic hydrodynamic discontinuity. Under the assumption that the spatial and time flow derivatives are finite at the reactive side of this discontinuity, the analysis yields an hyperbolic evolution equation which relates the mean curvature, the normal velocity and the normal acceleration of the wave front surface. In the second one [2], the detonation is considered as a generalized ZND structure. Under the assumptions that the flow is quasi-one-dimensional and quasi-steady behind the leading shock, the analysis leads to a parabolic evolution equation which relates the mean curvature and the normal velocity of the detonation shock front surface. These evolution equations have the common feature to be solely dependent on the explosive material properties. To use these models for studying constant velocity curved two-dimensional detonations, it is necessary to first define a relevant boundary condition at the edge of the explosive charge, precisely the detonation wave front slope as a function of its velocity. The shape and the velocity of the detonation wave front are then uniquely determined for a given transverse size of the explosive charge.

In this short communication, attention is focused on a particular boundary condition for a constant velocity curved two-dimensional detonation shock front. Specifically, we study the case of a pure refraction which describe the case where the shock in the explosive (X) and the shock in the confinement (C) of X match whithout any wave reflected in X or C [3]. Further, we shall restrict our analysis to the interaction point I of the shocks in X and C and we shall derive exact expressions for the curvatures of OI and O'I at point I. We then shall present the results of calculations performed with these expressions subjected to the assumptions that X and C are governed by polytropic equations of state and that the chemical energy release rate in X obeys a pressure-dependent law [4,5].

2.ANALYSIS OF THE REFRACTION

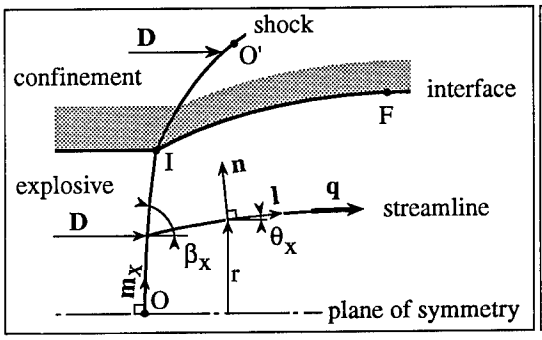

Figure 1. - Confined two-dimensional detonation

β	shock inclination angle
θ	streamline turning angle
P	pressure
ρ	specific mass
q	relative material speed
λ	extent of chemical decomposition
e	specific internal energy
s	specific entropy
t	time
$d^\circ( )/dt$	material derivative ($q\partial( )/\partial l$ if steady-state flow)

Table 1. - Nomenclature

Our study is based upon the two-dimensional (2D) Zeldovich-Von Neuman-Doring (ZND) model [6,7] : a 2D axisymmetric (2DA) or 2D plane (2DP) adiabatic inviscid reactive flow sustains a symmetrically curved shock propagating at constant velocity D in a quiescent explosive. In a SFF, the flows in X and C are steady-state in the vicinity of OI and O'I. We shall use the subscript H to denote a shocked state in X or C and use x and c as subscripts or superscripts to denote states in X and C respectively. We shall omit x and c when referring to X or C indistinctively. Our other notations are given in Table 1. To describe such 2DP (α= 0) or 2DA (α=1) flows in a SFF, we first write the balance equations for mass, momentum and energy in a system of curvilinear orthogonal coordinates defined by the streamlines and their normals as :

$$(\partial \mathrm{Ln}(\rho)/\partial l) + (\partial \mathrm{Ln}(q)/\partial l) + (\partial\theta/\partial n) = -\alpha \sin(\theta)/r \qquad (1)$$

$$(\partial \mathrm{Ln}(q)/\partial l) + (\partial P/\partial l)/(\rho q^2) = 0 \qquad (2)$$

$$(\partial\theta/\partial l) + (\partial P/\partial n)/(\rho q^2) = 0 \qquad (3)$$

$$(-\partial \mathrm{Ln}(\rho)/\partial l) + (\partial P/\partial l)/(\rho c^2) = \sigma.w/q \qquad (4)$$

The (frozen) sound speed c and the thermicity vector σ can be expressed as functions of P, ρ and λ by using a specified e(P, ρ, λ) equation of state. The decomposition rate vector w is also to be considered as depending on P, ρ and λ. In nonreactive media, λ, σ and w are equal to zero.

$$c^2 = (\partial P/\partial \rho)_{\lambda,s} = (P\rho^{-2} - (\partial e/\partial \rho)_{\lambda,P}) / (\partial e/\partial P)_{\lambda,\rho}$$

$$\rho c^2 \sigma = (\partial P/\partial \lambda)_{e,\rho} \quad ; \quad (d^0\lambda/dt) = w(P,\rho,\lambda)$$

We next recall [8] that the shock values of any dependent variable $g = (\rho , q , P, \theta)$ can be expressed as a function of β and D by using the jump relations for an oblique shock and the equation of state of the medium under consideration. λ_H is equal to zero (ZND model). The shock values of the partial derivatives of the latter variables thus satisfy the following geometrical identity (Figure 1) :

$$\cos(\beta-\theta_H)(\partial g/\partial l)_H + \sin(\beta-\theta_H)(\partial g/\partial n)_H = (dg_H/d\beta)C \qquad (5)$$

where $C = (d\beta/dm) = \sin(\beta)(d\beta/dr_H)$ denotes the curvature of a meridian shock line. Applying the identity (5) to the variables P and θ yields two relations which, together with the relations (1) to (4), defines a linear nonhomogeneous system of six equations in the shock values of the six partial derivatives involved in it. Upon resolution, we obtain in particular

$$(\partial P/\partial l)_H = A_p C - B_p \qquad (6)$$

$$(\partial \theta/\partial l)_H = A_\theta C - B_\theta \qquad (7)$$

$$(\rho q^2)_H^{-1}\Delta A_p = \cos(\beta-\theta_H)(dP_H/d\beta)/(\rho_H q_H^2) + \sin(\beta-\theta_H)(d\theta_H/d\beta)$$

$$(\rho q)_H^{-1}\Delta B_p = \sin^2(\beta-\theta_H)\{ \sigma_H w_H/q_H - \alpha\sin(\theta_H)/r_H \}$$

$$\Delta A_\theta = - (1-M_H^2)\sin(\beta-\theta_H)(dP_H/d\beta)/(\rho_H q_H^2) + \cos(\beta-\theta_H)(d\theta_H/d\beta)$$

$$\Delta B_\theta = \cos(\beta-\theta_H)\sin(\beta-\theta_H)\{ \sigma_H w_H/q_H - \alpha\sin(\theta_H)/r_H \}$$

$$\Delta = 1 - M_H^2\sin^2(\beta-\theta_H) \quad ; \quad M = q/c$$

The coefficients A_p, A_θ, B_p, B_θ and Δ are function of β and D. The coefficients B_p and B_θ also depend on r_H for a 2DA explosive charge.

We finally write the contact conditions for X and C by matching the pressures and the flow directions along the interface IF as :

$$P_X = P_C \qquad (8)$$

$$\theta_X = \theta_C \qquad (9)$$

$$(\partial P/\partial l)_X = (\partial P/\partial l)_C \qquad (10)$$

$$(\partial \theta/\partial l)_X = (\partial \theta/\partial l)_C \qquad (11)$$

These matching conditions apply along the interface IF. It is important to acknowledge that they also apply at the intersection point I of shocks OI and O'I when there is no reflected wave in X or C as for a pure refraction. The shock relations (6) and (7) can thus be used to evaluate the derivatives in relations (10) and (11) at point I. This operation yields a linear nonhomogeneous system of two equations in the two interface values, C_X and C_C, of the curvatures of shocks OI and O'I. We obtain

$$C_X = \{ (B_\theta^X - B_\theta^C) A_p^C - (B_p^X - B_p^C) A_\theta^C \} / \bar{\Delta} \quad (12)$$

$$C_C = \{ (B_\theta^X - B_\theta^C) A_p^X - (B_p^X - B_p^C) A_\theta^X \} / \bar{\Delta} \quad (13)$$

$$\bar{\Delta} = A_\theta^X A_p^C - A_p^X A_\theta^C$$

The conditions (8) and (9) define the values of the shock angles β_X and β_C at I as functions of the velocity D and the material shock properties of X and C. The interface values of the curvatures of OI and O'I consequently depend on D, the material shock properties of X and C, the chemical decomposition rates and, for a 2DA explosive charge, on the radius of the explosive charge.

3.RESULTS OF A MODEL CALCULATION

We have specialized the above results to the case of a 2DP explosive charge ($\alpha = 0$) bounded with a nonreactive confinement ($\lambda_C = 0$, $\sigma_C = 0$, $w_C = 0$) and have introduced in our analysis the following simplifying assumptions (the subscript 0 will denote the initial conditions) :

1- The inital pressure P_0 can be neglected with respect to the shock pressure P_H. In condensed explosives, typical P_0/P_H ratios are 10^{-5}.

2- A global irreversible reaction can model the exothermic process in the reaction zone of X:

Explosive $\rightarrow$ Products

Such a reaction is accordingly described by a single scalar variable λ_X that represents the mass fraction of burnt explosive and specifies the fraction of heat released per unit mass of X.

3- The material properties of X and C are governed by polytropic equations of state :

$$e(P, \rho, \lambda) = e_0 - \lambda Q + P/\rho(\gamma - 1) \quad (14)$$

where γ and Q denote the polytropic index and the total amount of heat avalaible per unit mass respectively. Here, Q_C is equal to zero since we have chosen a nonreactive confinement.

4- The global chemical decomposition rate of X obeys a pressure-dependent law in the form :

$$w_X = \tau^{-1}(P_X/P_{ref})^a(1 - \lambda_X)^b \quad (15)$$

where τ is a characteristic chemical time, P_{ref} is a characteristic pressure and a and b are nondimensional constants.

Assumptions 1, 2 and 3 lead to the following one-dimensional SS-DW velocity [6,7]:

$$D^* = \sqrt{2(\gamma_x^2 - 1)Q_x} \qquad (16)$$

The velocity D*, the initial specific mass ρ_{0x} and the characteristic time τ were used to nondimensionalize the other variables and, without loss in generality, the characteristic pressure P_{ref} was set equal to $\rho_{0x}D^{*2}$.

We next used formula (12) to determine how the relationship between the explosive's interface-curvature C_x and the DW velocity D depends on the properties of C and on the parameter a of the decomposition rate (15). The control parameters of our calculations are the nondimensional velocity D/D*, the polytropic indices γ_x and γ_c, the relative density ρ_{0c}/ρ_{0x}, and the parameter a of the decomposition rate. The values of D*, ρ_{0x} , ρ_{0c} , γ_x and γ_c were chosen to model the liquid explosive nitromethane (D*= 0.63 cm/μs, ρ_{0x}= 1.128 gr/cm^3, γ_x = 2.4) confined in steel (ρ_{0c}/ρ_{0x}= 7, γ_c = 2.75)) or titanium (ρ_{0c}/ρ_{0x} = 4, γ_c = 1.54) tubes [9,10]. These materials meet the pure refraction conditions in the range of the selected values for D/D* (0.9-1.0). For polytropic materials, the values of the angles β_x and β_c are independent of D. Here we found:

β_x = 81.15 degrees and β_c = 23.21 degrees for ρ_{0c}/ρ_{0x} = 7

β_x = 73.87 degrees and β_c = 24.43 degrees for ρ_{0c}/ρ_{0x} = 4

Figure 2 presents the qualitative trend of our D-C_x relation for polytropic materials. One observes that, for a given velocity D, the higher the density of the confinement, the smaller the explosive's interface curvature Our numerical results are summarized in Figure 3 which plots the nondimensionalized wave velocity D/D* versus the nondimensionalized interface curvature $\tau D^* C_x$. The curves exhibits the following trends:

1- For a given velocity D, the absolute value of the explosive's interface-shock-curvature, - C_x , decreases as the confinement's density increases. Also, the distance between curves associated with two confinements and the same value of the parameter a decreases as the value of a increases.

2- Depending on the pressure exponent in the decomposition rate, the slope of the curves can be positive infinite or negative.

3- The same considerations apply to the dependence of the normal velocity $D\sin(\beta_x)$ and the explosive's interface curvature.

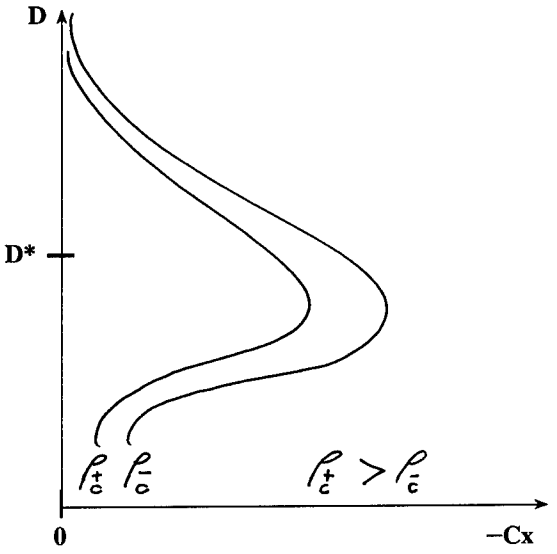

Figure 2. - Qualitative trends of the D-Cx relationship in the case of a polytropic explosive and two polytropic confinements.

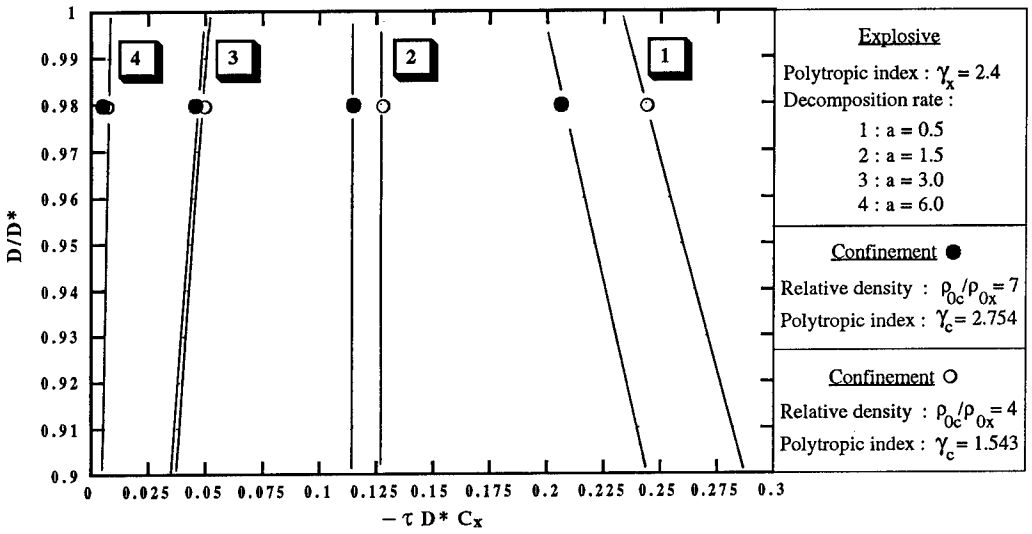

Figure 3. -Plots of the nondimensionalized detonation velocity D/D* versus the nondimensionalized explosive's interface curvature $-\tau D^* C_x$ for a polytropic explosive, two polytropic confinements and the decomposition rate law $w_x = \tau^{-1}(p_x/p_{ref})^a(1-\lambda_x)^\nu$ (two-dimensional plane charge).

CONCLUSIONS

Current modelling of self-sustaining curved two-dimensional detonation shock fronts is based upon a compatibility relationship between the normal velocity (Dn) and the curvature (C) of the detonation shock front that only depends on the properties of the explosive [2,11]. This relationship is obtained by integrating the flow equations between the leading shock and the rear boundary of its domain of dependence (the "sonic locus") under the assumption that the flow which sustain the shock is quasi one-dimensional and quasi steady. Our analysis indicates that there exists a situation where the geometrical characteristics of a curved detonation wave front can be obtained in closed forms from straight geometrical considerations without approximating the flows behind the curved shock fronts and without restricting the forms of the equations of state and the chemical decomposition rates. It also indicates that, in this situation, these characteristics depend on both the explosive and the confinement material properties. Our formula (12)for the explosive's interface shock curvature can thus be used to assess the accuracy of the (Dn-C) relationship, in the close vicinity of the interaction point and to calibrate shock equations of state and decomposition rates in condensed explosives from velocity measurements and shock-front shape records of confined two-dimensional self-sustaining detonation waves.

Finally, we suggest that one should distinguish between two cases of dynamical behavior for detonation shock fronts propagating in two-dimensional charges under the pure refraction boundary condition. In the first case, the explosive has sufficiently short a reaction zone so that only a very narrow domain in the vicinity of the explosive-confinement interface has a significant influence on the detonation shock front geometry. The dynamical behavior of such explosives would consequently be correctly described by evolution equations uniquely determined by the properties of the explosive. In the second case, the explosive has sufficiently long a reaction zone so that a wide domain of the flow in the explosive receives informations from the explosive-confinement interface. In this case, it seems reasonable to expect that the dependence of the detonation shock front geometry on the confinement material properties evidenced in our work is not restricted to the close vicinity of the interaction point but extends to a large part of the detonation shock front and, presumably, even on the explosive charge axis. Consequently, the dynamical behavior of the detonation shock front would here obey more complicated evolution equations than in the first case.

REFERENCES

[1] Brun L., rapport CEA-DAM, CEV-DPM, n° DO879023, (1989).

[2] Klein R., *SIAM J.Appl.Math.*, **53**, 5, (1993) 1401-1435.

[3] Stewart D.S. and Bdzil J.B., "Examples of detonation shock dynamics for detonation wave spread applications", Ninth Symposium (International) on Detonation, OCNR 113291-7,**1**, (1989) 773-783.(See the discussion by Bdzil at the end of the paper).

[4] Vidal P., Cowperthwaite M., Presles H.-N., Fontaine D., *C.R.Acad.Sci.Paris*, t.315, Série II, (1992) 791-794.

[5] Vidal P., Cowperthwaite M., Presles H.-N., Fontaine D., *C.R.Acad.Sci.Paris*, t.316, Série II, (1993) 177-180.

[6] Zeldovich Ya.B., Kompaneets S.A., Theory of detonation, (Academic Press, New York, 1960).

[7] Fickett W., Davis W.C., Detonation, (University of California Press, Berkeley,1979).

[8] Courant R., Friedrichs K., Supersonic flow and shock waves, (Intersciences, 1948).

[9] Marsh S.P., LASL Shock Hugoniot Data, (University of California Press, Berkeley, 1980.

[10] Presles H.-N. , Contribution à l'étude de la détonation de mélanges liquides binaires à base de nitrométhane, (Thèse de doctorat ès sciences physiques, Université de Poitiers, 1979).

[11] Stewart D.S., Bdzil J.B. , *Combustion and flame*, **72**, (1988) 311-323.

JOURNAL DE PHYSIQUE IV
Colloque C4, supplément au Journal de Physique III, Volume 5, mai 1995

Quelques Points Importants en Détonique Classique

F. Chaisse

CEA/CEV-M, BP. 7, 77181 Courtry, France

Abstract

In this discussion we recall two types of experiments, achieved at the CEV-M (CEA), exhibiting specific properties in the detonation dynamics.

In the classical theory of detonation (ZND scheme) it appears some troubles in the interpretation of such experimental results.

Dans le cadre de la détonique classique, des études expérimentales conduites au CEV-M ces dernières années ont fait apparaître des propriétés spécifiques de la dynamique des ondes de détonation qui semblent, à première vue, difficilement explicables dans le cadre du modèle ZND.

Pour cela, nous nous référons aux publications [1] et [2] de MM. J. Aveillé et J.M. Chevalier. Le premier a étudié la détonation sphérique divergente sur deux compositions explosives au TATB (T1 et T2) et sur une composition à l'octogène (X1), le second sur le même type de compositions explosives a mis en évidence l'existence d'onde de front se propageant transversalement sur la surface de l'onde de détonation en symétrie cylindrique.

Dans la publication [1], sur les trois compositions étudiées, on constate que, pour une courbure donnée du front, la célérité du front de détonation en sphérique divergent reste toujours inférieure à celle de la détonation axi-symétrique. La concordance de ces célérités de détonation n'est observée qu'aux faibles courbures.

Dans la publication [2], la célérité C de propagation d'onde de front, associée à une perturbation prenant naissance sur le contour externe de la cartouche cylindrique, possède un caractère fini. Cette célérité C présente la propriété de croître lorsque la célérité axiale du front de détonation diminue.

Une question alors se pose : comment interpréter les résultats des références [1] en [2] d'un point de vue théorique ?

Si l'on se réfère au code DSD (Detonation Shock Dynamics) développé à LOS ALAMOS [3] qui détermine l'évolution spatio-temporelle d'un front d'onde de détonation sans faire appel à

l'écoulement aval, nous avons des difficultés théoriques. Dans le code DSD, la détonation possède la structure usuelle ZND associée à l'existence d'une relation célérité-courbure, et le traitement théorique de ce modèle conduit à une équation d'évolution du front d'onde de type parabolique.

Références :

[1] J. Aveillé and al.
Experimental Study of Spherically Diverging Detonation Waves.
8th Symp. Int. on Detonation - Albuquerque (N.M.) (1985).

[2] J.M. Chevalier and al.
Propagation Phenomena on the Detonation Wave Front.
Physical Review Letters - Vol. 71 - n° 5 - p. 712-714 (1993).

[3] J. Bdzil and W. Fickett.
DSD Technology : A Detonation Reactive Huygens Code.
L.A.N.L. rapport LA.12235.MS (1992).

1-3 Shock Wave Interaction with Energetic Materials

Physical Origin of Hot Spots in Pressed Explosives Compositions, *Macroscopic Approach ;* **R. Belmas** and J.P. Plotard

Dislocation Mechanisms for Shock-induced Hot Spots, *Microscopic Approach* ; R.W.Armstrong

Shock-Wave Behavior in Explosive Monocrystals ; J.J.Dick

Shock Wave Interaction with Composite Materials ; A.Van der Steen

JOURNAL DE PHYSIQUE IV
Colloque C4, supplément au Journal de Physique III, Volume 5, mai 1995

Physical Origin of Hot Spots in Pressed Explosive Compositions

R. Belmas and J.-P. Plotard*

Commissariat à l'Energie Atomique, Centre d'Etudes du Ripault, BP. 16, 37260 Monts, France
** Commissariat à l'Energie Atomique, Centre d'Etudes de Vaujours-Moronvilliers, BP. 7, 77181 Courtry, France*

Abstract : We present a complete experimental and theoretical study of hot spots generation in pressed explosive compositions. First, the results of experiments leading to the identification of the hot spots origin are detailed. Then, using these results, a physical model is developed. Three applications are presented. The firts one is devoted to the study of the sensitivity of mixed HMX/TATB compositions. The second one deals with double shock desensitization. The third one is the development of an efficient SDT kinetics using the hot spot model previously described.

1 - INTRODUCTION

Hot spot generation is now well-recognized as the initial mechanism governing shock-to-detonation transition.
The study of hot spot formation is difficult due to high temperature (~ 1000 K) and pressure (from 0.1 GPa to several 10 GPa) involved in this phenomenon, short duration (from a few ns to a few μs), very small size of the areas of interest (≤ a few microns), opacity of the considered media and decomposition phenomena generating heat, gases and pressure.
To overcome these difficulties, original experiments were carried out in order to identify the origin of the hot spots. The knowledge of this phenomenology then allowed us to develop a physical model of hot spots formation and ignition.
This model itself is a powerful tool which can be used to analyze complex initiation mechanisms like the ones occurring in mixed explosive compositions or in the case of double shocks.
Another application of interest is the association of such a model with a grain burning law in order to develop an efficient and physical kinetics able to simulate all the phenomena involved in the shock-to-detonation transition.

2 - HOT SPOTS : PHENOMENOLOGY - EXPERIMENTS [1]

2.1 Possible origin of hot spots

The hot spots are generated by the interaction between shock waves and heterogeneities of the microstructure of the explosive.

Several heterogeneities can be at the origin of hot spots :
- porosity,
- binder **[2] [3]**.

In the same way, different mechanisms can be invoked, for hot spot formation, during pore collapse :
- hydrodynamic mechanism **[4]**,
- heating of trapped gases **[5][6]**,
- viscoplastic work in the explosive around the pores **[7][8][9]**.

As mentioned in the introduction, direct observation is very difficult and we performed comparative experiments to evaluate the respective importance of each mechanism.

2.2 Relative influence of porosity and binder

Experiments were performed on pressed TATB compositions and pure TATB samples pressed at different densities. In all cases, the same well-characterized TATB powder was used.

Gap-Test : the experimental set-up is presented in ***Figure 1***.

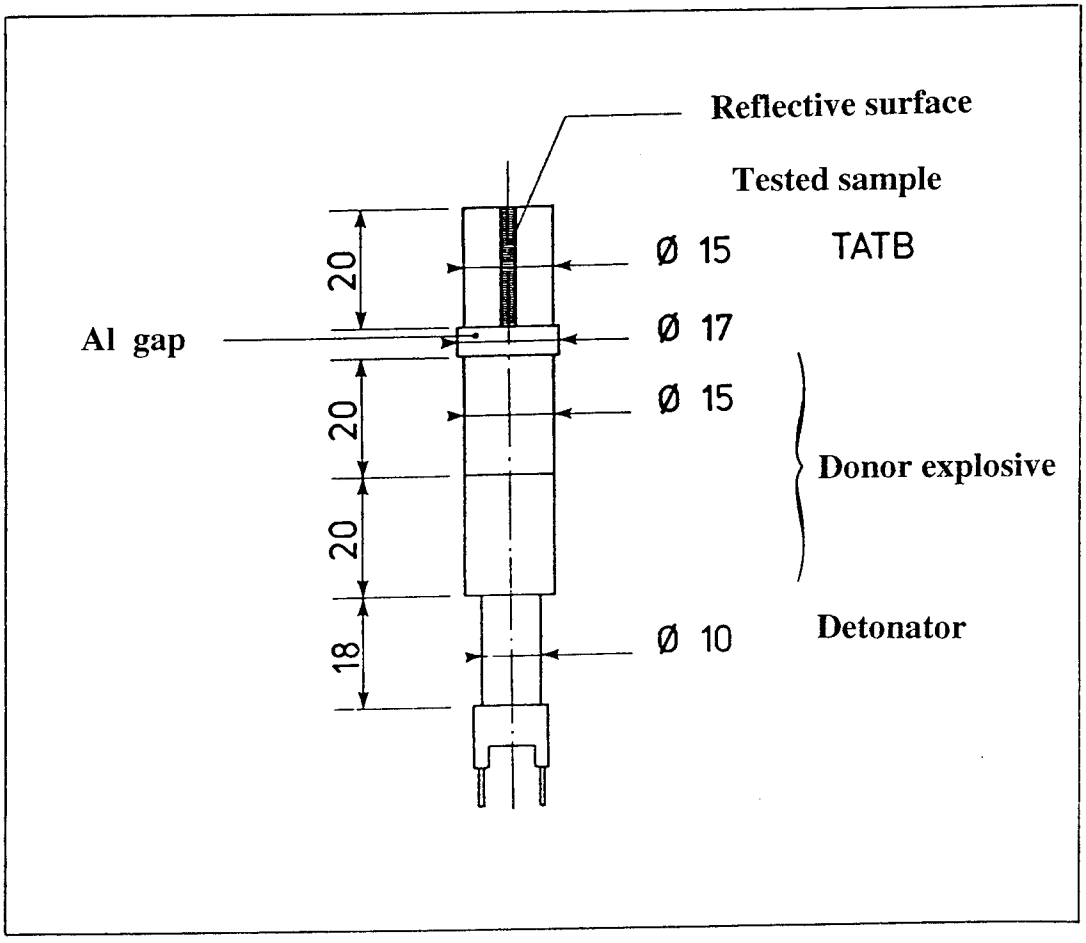

Figure 1 - GAP TEST EXPERIMENTAL SET-UP

In addition to the go-no go results usually obtained with these experiments, we measured the run distance to detonation by observing the side of the sample with a streak camera to determine the (x, t) diagrams. The experimental data are summarized in ***Figures 2 and 3*** for TATB samples with densities between 1.0 and 1.875, and TATB composition T2, which includes TATB powder, a few percent of binder and 2.3 % of porosity. The removal of the binder from T2 leads to a 1.8 in density pure TATB sample.

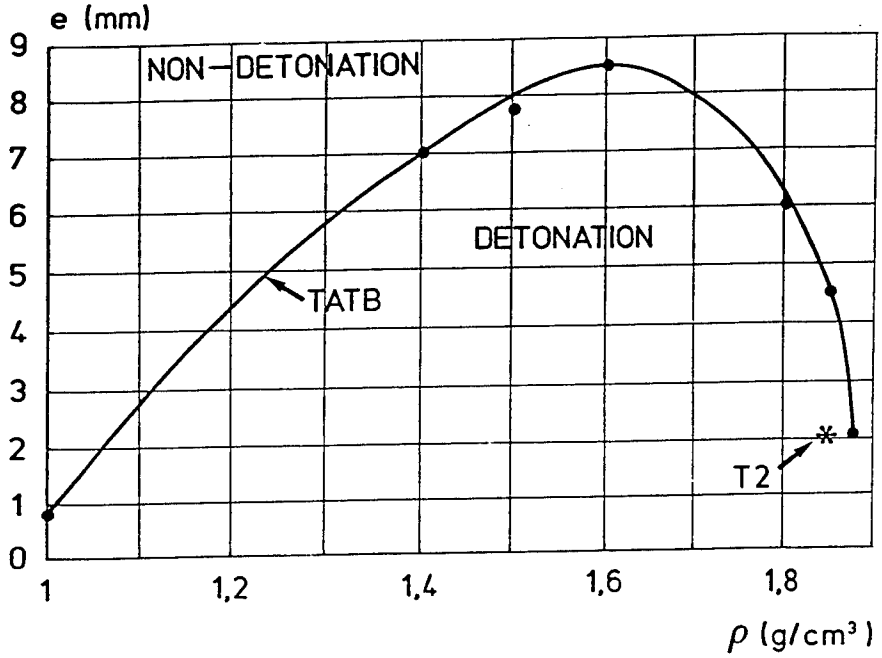

Figure 2 - GAP-TEST DATA

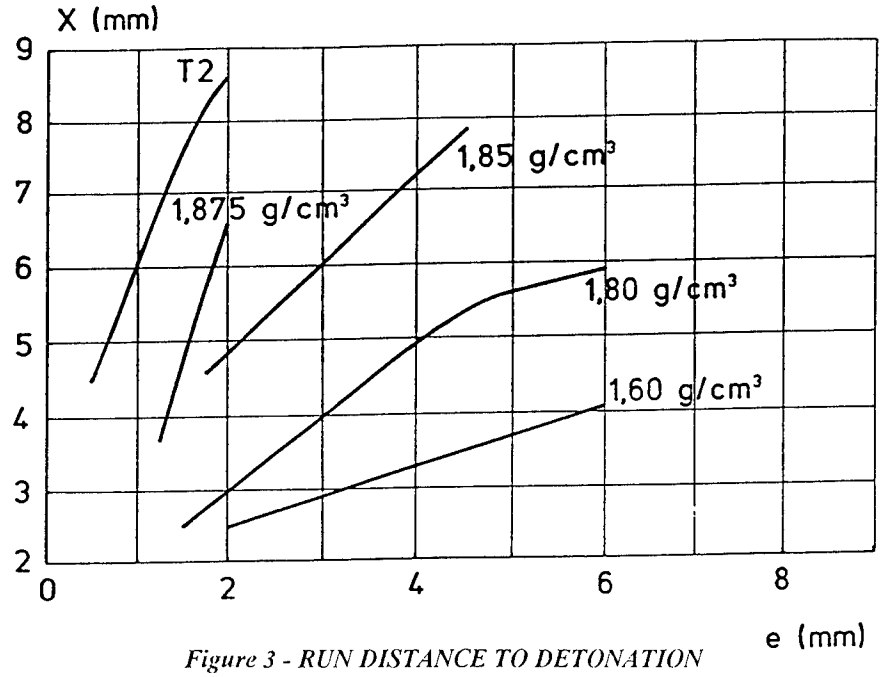

Figure 3 - RUN DISTANCE TO DETONATION

The analysis of ***Figures 2 and 3*** shows that it is easier to initiate the powder without binder than the T2 composition. For the studied case, the binder has a negligible influence on the production of hot spots regarding to the influence of porosity.

Run distance to detonation : We performed wedge test experiments on three different TATB compositions based on the same explosive powder ***(Table 1)***. The three binders have very different chemical and mechanical properties. We obtained the same results ***(Figure 4)*** for T1 and T2, which have the same porosity. The T3 composition, which has a lower porosity, is more difficult to initiate. The results confirm our previous conclusion on the weak influence of the binder on hot spots formation process, regarding to the importance of porosity.

Composition	TATB Powder	Binder	Porosity
T1	50µm	B1	2,6 %
T2	50	B2	2,3 %
T3	50	B3	1,4 %

Table 1 - TATB COMPOSITIONS

Short duration shock initiation : The threshold curves ***(Figure 5)*** obtained for T1, T2 and T3 lead to the same conclusion as before about the relative influence of binder and porosity.

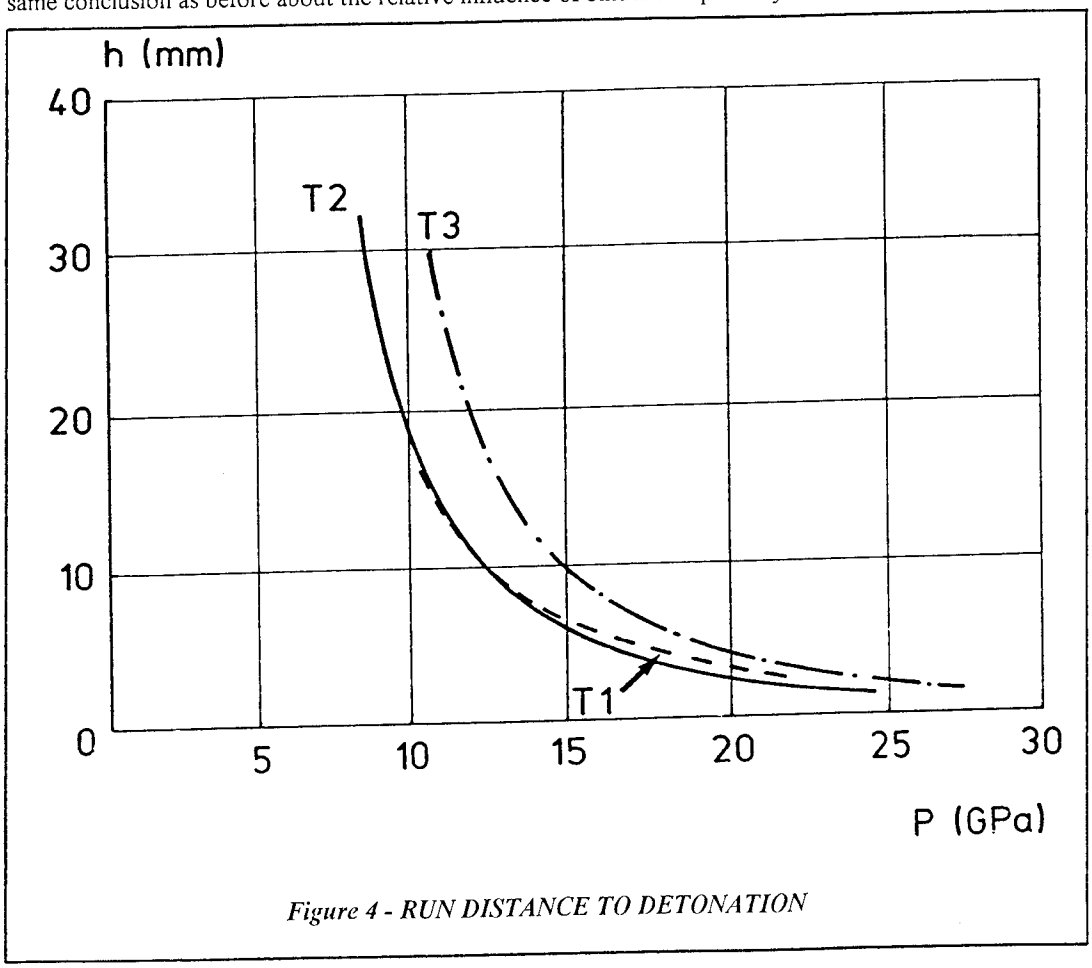

Figure 4 - RUN DISTANCE TO DETONATION

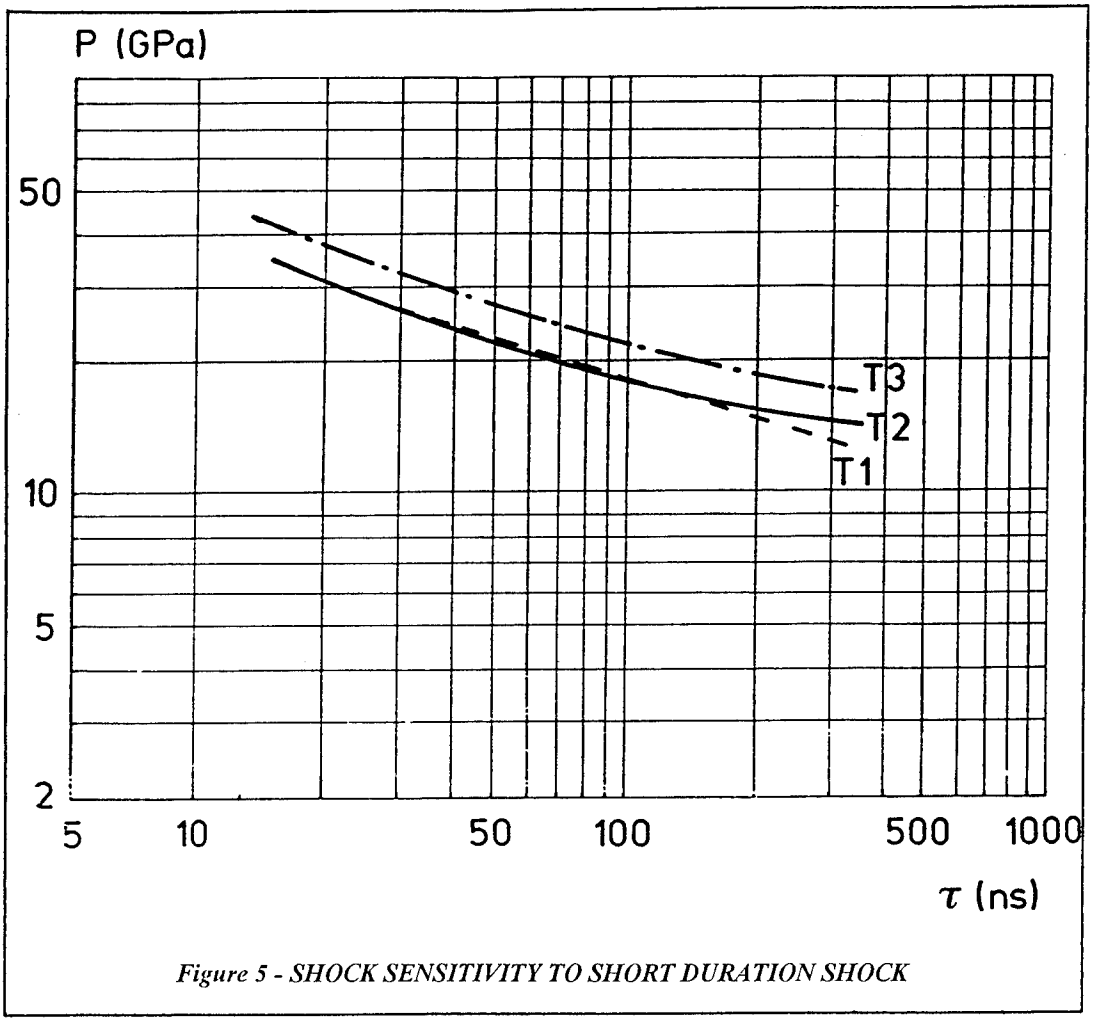

Figure 5 - SHOCK SENSITIVITY TO SHORT DURATION SHOCK

2.3 Effective mechanism governing hot spots formation

We showed that in our pressed explosive compositions, the hot spots are created by the collapse of the pores. Some of the previously presented Gap-Test experiments, which were realised in the room atmosphere, were performed under vacuum. The same results, including the (x, t) diagrams, were obtained. Therefore, the compression of the gas contained in the voids has no influence on the initiation of the explosive.

It is not so easy to have experimental data and make a choice between a hydrodynamic and a viscoplastic collapse of the voids. R.B. FREY **[9]** developed a dimensional analysis of this problem. His conclusion can be summarised as follow :

$$\text{if} \quad N1 = \frac{a_0 \frac{dP}{dt} \sqrt{\frac{\rho}{y}}}{Y}$$

$$\text{and} \quad N2 = \frac{a_0 \sqrt{\rho P}}{\mu}$$

with a_0 : initial pore radius (assumed spherical)
P : pressure
t : time
Y : yield strength
ρ : explosive crystal density
μ : viscosity

then, to have a hydrodynamic mechanism, the two quantities N1 and N2 must be greater than one.
In a shock wave, N1 is always greater than one, but, as shown in ***Figure 6***, the criterion is not fulfilled by N2 in our explosive compositions, in which the pores characteristic size lies between 0.1 µm and 1 µm and the viscosity (not well known), can lie between 100 Pa.s and 1000 Pa.s, as proposed by several authors **[7] [10] [11] [12]**.

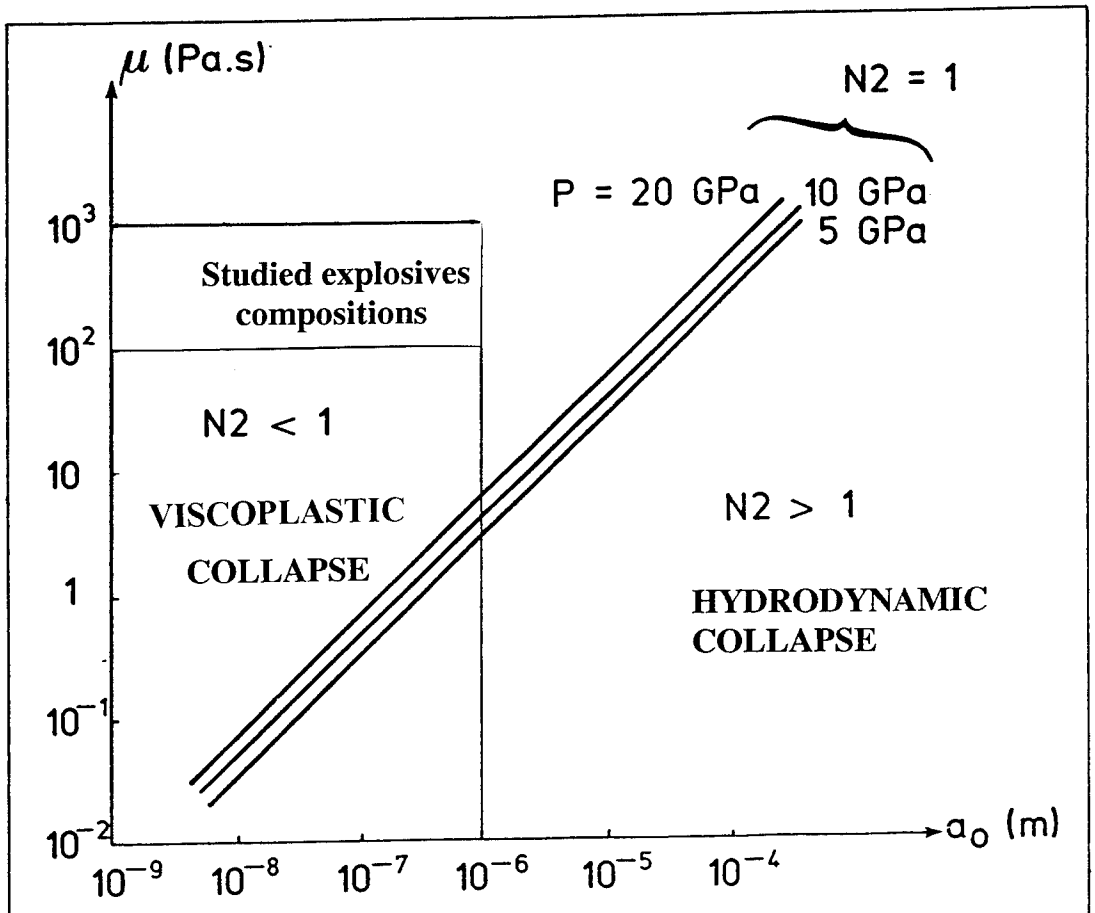

Figure 6 : ANALYSIS OF THE VISCOPLASTIC NATURE OF THE PORE COLLAPSE

Therefore, this analysis, added to the experimental data, shows that in pressed explosive compositions, the hot spots formation process is the result of the viscoplastic collapse of the pores included in the material.

3 - A HOT SPOTS FORMATION AND IGNITION MODEL [13]

3.1. The model

The pores are described as hollow spheres. the comparison of the two typical times, one for the viscous collapse $\tau_c = \frac{4\mu}{P} \geq 10^{-7}$ s, the other for the shock crossing through the pore $\tau_s = \frac{2.a_o}{U} \leq 10^{-9}$s, shows that, at the beginning of the pore collapse, all the thermomechanical quantities are uniform all around the void. Therefore the implosion is spherical and initial values of pressure, density, and temperature are those induced by the shock in the medium surrounding the pore.
A program was written in order to compute the heating of the explosive around the collapsing void, and its time to ignition. Based on the same assumptions and equations than other published models**[7] [8] [9],** it calculates the evolution of a viscoplastic, heat-conducting, incompressible energetic material. The equations are :

$$r^3 - a^3 = r^3_0 - a^3_0$$

$$\rho \ddot{r} = \frac{\delta \sigma_r}{\delta r} - 12\mu \frac{\dot{r}}{r^2} + \frac{2Y}{r}$$

$$\rho Cp \frac{\delta T}{\delta t} = \dot{C} + \dot{Q} + \dot{W}$$

in which
- Cp heat capacity,
- r radius,
- T temperature,
- C thermal conduction term,
- Q heat released by chemical reaction term,
- W heat created by the viscoplastic work term,
- σ_r radial stress.

Therefore :

$$\dot{W} = 2Y - \frac{\dot{r}}{r} + 12\mu \left(\frac{\dot{r}}{r} \right)^2$$

$$\dot{Q} = RZQ \exp(-E/RT)$$

$$\dot{C} = \lambda \left[\frac{\delta T}{\delta r^2} + \frac{2}{r} \frac{\delta T}{\delta r} \right]$$

in which
- R ideal gas constant,
- Z frequency factor,
- Q heat of decomposition,
- E activation energy,
- λ thermal conductivity.

All the parameters of these equations have a physical meaning, and can be determined with a good accuracy but the viscosity. This last parameter can be calibrated by using the hot spots model together with pressure history curves measured with embedded manganin gauges in shocked explosives samples.

3.2 Determination of the viscosity

The experimental set-up is presented in ***Figure 7***. The velocity of the projectile is chosen in order to have the needed shock pressure in the explosive. The pressure versus time curves are measured in the shocked explosive sample ***(Figure 8)***. If the shock pressure is not too high (in the shown example, 9GPa in the TATB composition T2), the curve presents two parts : a plateau followed by an increase of the pressure. The physical meaning of these two parts may be : the initiation of the hot spots followed by an increase of the pressure generated by the decomposition gases.

The extrapolation, up to the zero depth, of the curve which represents the duration of the plateau as a function of the depth of measurement, gives the value of the initiation time of the hot spots for the given pressure. This ignition time was determined for several shock pressures. The comparison of these experimental values with those obtained with the numerical model leads to a given value of the viscosity.

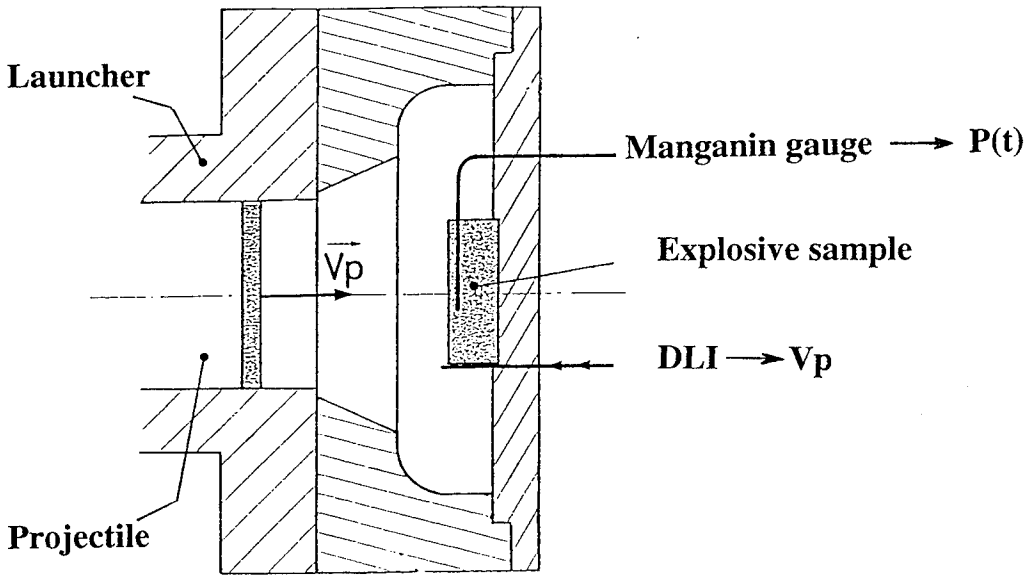

Figure 7 - PRESSURE VS TIME MEASUREMENT SET UP

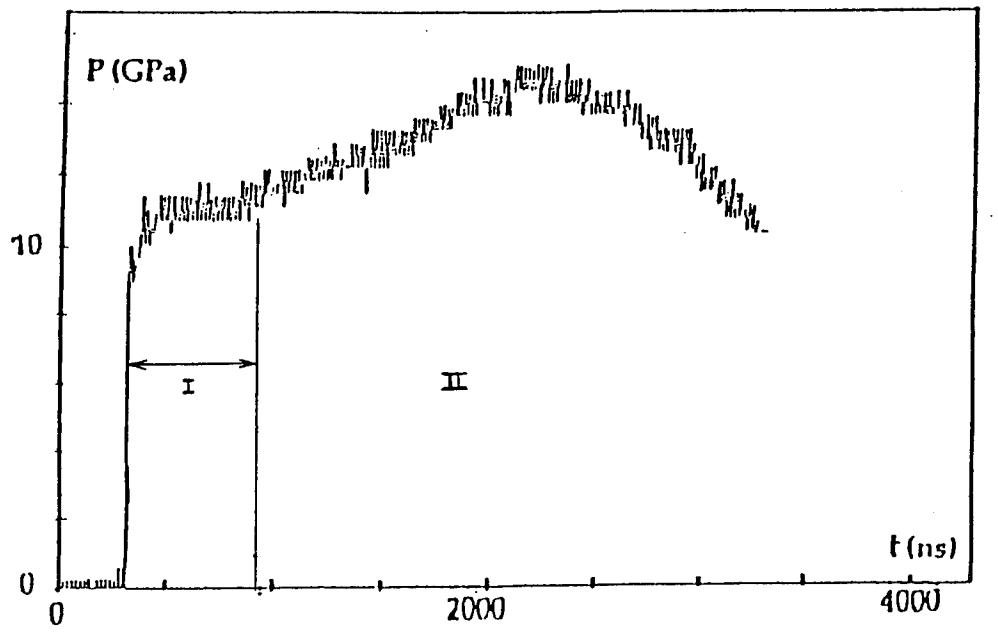

Figure 8 - TYPICAL PRESSURE VS TIME CURVE

But the so calibrated model is not able to simulate other experiments, like double-shocks impacts. In fact, the duration of the first plateau is not only the ignition time of the hot spots ; it includes also the time required to obtain a sufficient amount of gases which leads to a pressure increase in the explosive.
With the same experimental set-up, it is possible to determine the pressure threshold of shock initiation. Using the hot spots model with a given viscosity, it appears that, the larger the pore, the easier the initiation ***(Figure 9)***. Therefore, for a given shock pressure, the initiation time of the composition is the initiation time of the largest voids. The smaller pores, if initiated by the shock, modify the energy release history behind the shock, but have no influence on the first reactions initiation. The model used with the largest voids diameter and the good value of the viscosity will reproduce these threshold values.

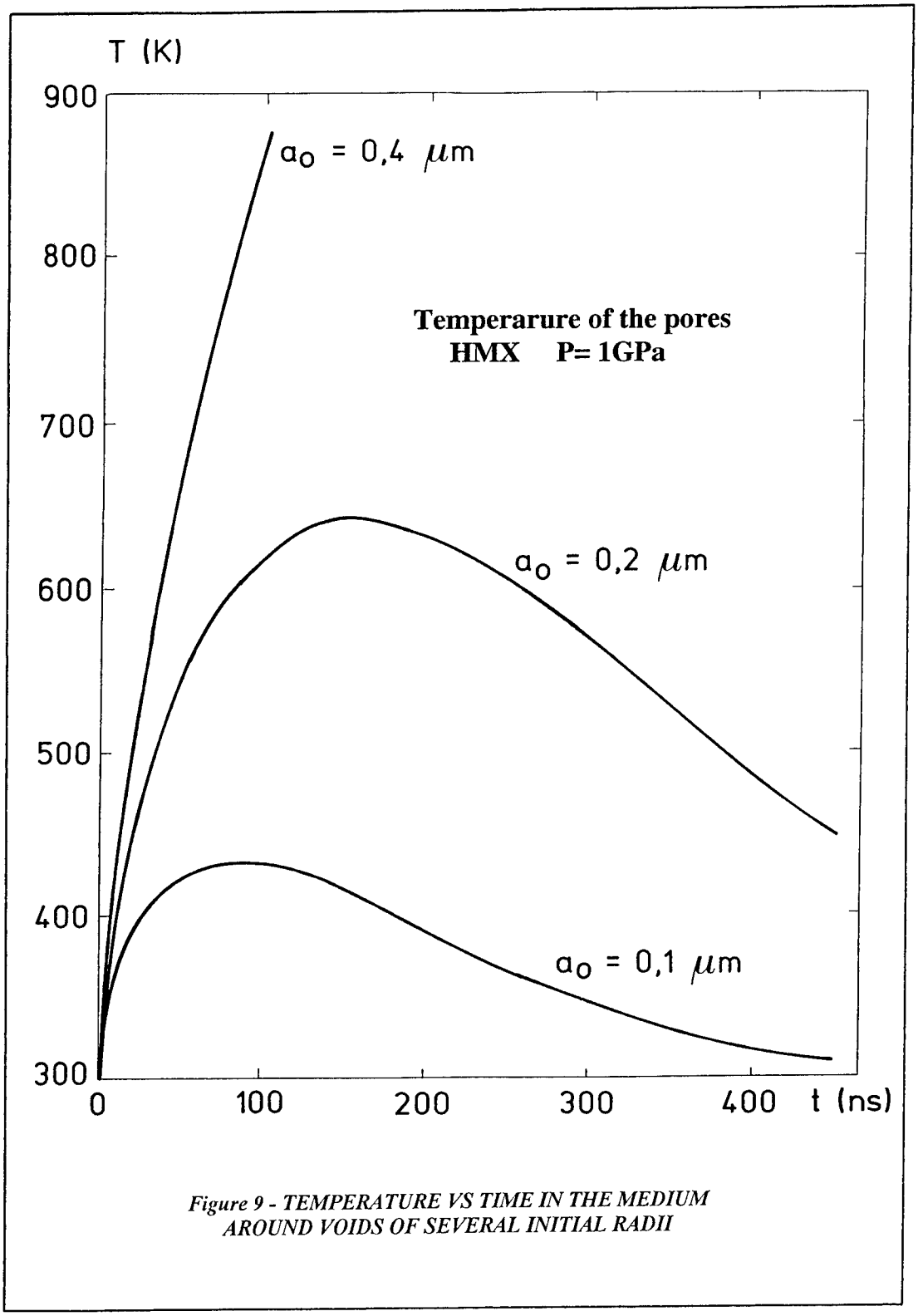

Figure 9 - TEMPERATURE VS TIME IN THE MEDIUM AROUND VOIDS OF SEVERAL INITIAL RADII

The results obtained on two explosives compositions, X1 and T2 (defined in ***Table 2***) are presented. From the pressure measurements reported in ***Figures 10 and 11***, the threshold pressure for X1 and T2 are respectively 1 and 4 GPa. The viscosity of HMX and TATB deduced from these values and the viscosity of the TATB is about five times the HMX one.

Composition	X1	T2	TX1
HMX wt %	96 0-600	0	45 0-100
TATB wt % grain size (μm)	0	97	52
Inert binder wt %	4	3	3
Porosity and pores radii (μm)	1.7 % $a_0 \leq 0.5$	2.3 % $a_0 \leq 0.5$	0.5 % intergranular $a_0 \leq 0.2$ 1.5 % in the TATB $a_0 \leq 0.5$

Table 2 - EXPLOSIVES MICROSTRUCTURE

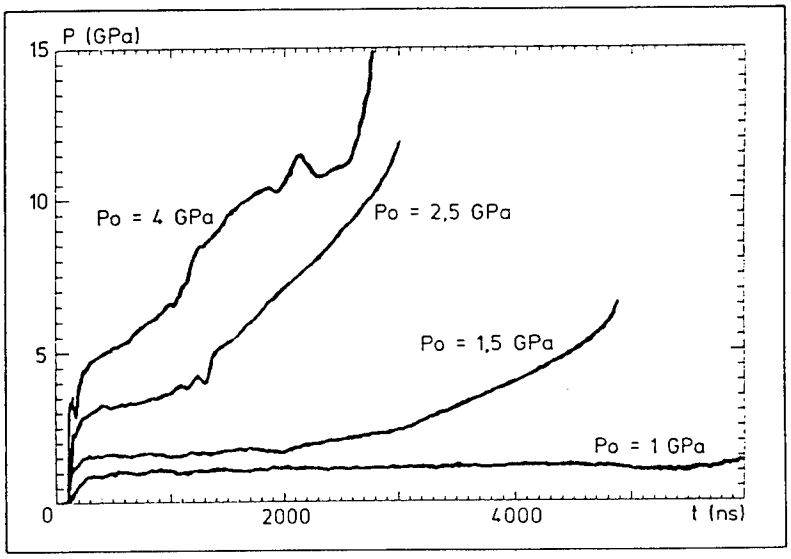

Figure 10 - PRESSURE VS TIME IN X1 COMPOSITION FOR SEVERAL INPUT PRESSURES

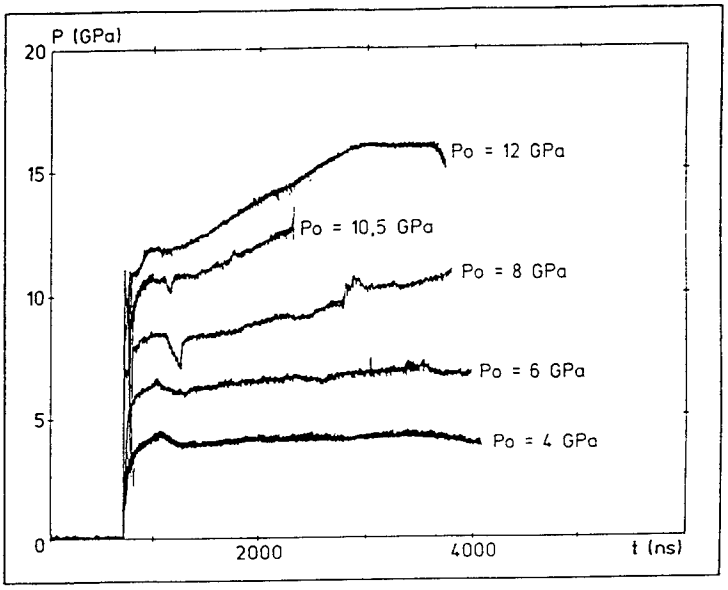

Figure 11 - PRESSURE VS TIME IN T2 COMPOSITION FOR SEVERAL INPUT PRESSURES

3.3 An analytical model

We developed a simplified hot spots model, easier to use in a code and which gives the same results about the evolution of the microvoids (radius, temperature) that those obtained previously, with the reference numerical model.

3.3.1 - Motion equation : The evolution of the radius of the pore is governed by the equation :

$$-\rho a \ddot{a} = P - Py + 4\mu\frac{\dot{a}}{a} + 1.5\rho\dot{a}^2$$

with : a : pore radius,
P_Y : -2/3 Y In ∅,
∅ : porosity.

The asymptotic solution of this equation is :

$$a = a_0 \exp\left[\int_0^t -\frac{P - P_v}{4\mu} dt\right]$$

We use this formula for a(t) in the simplified model because it leads to a very good agreement with the results of the reference model ***(Figure 12)***.

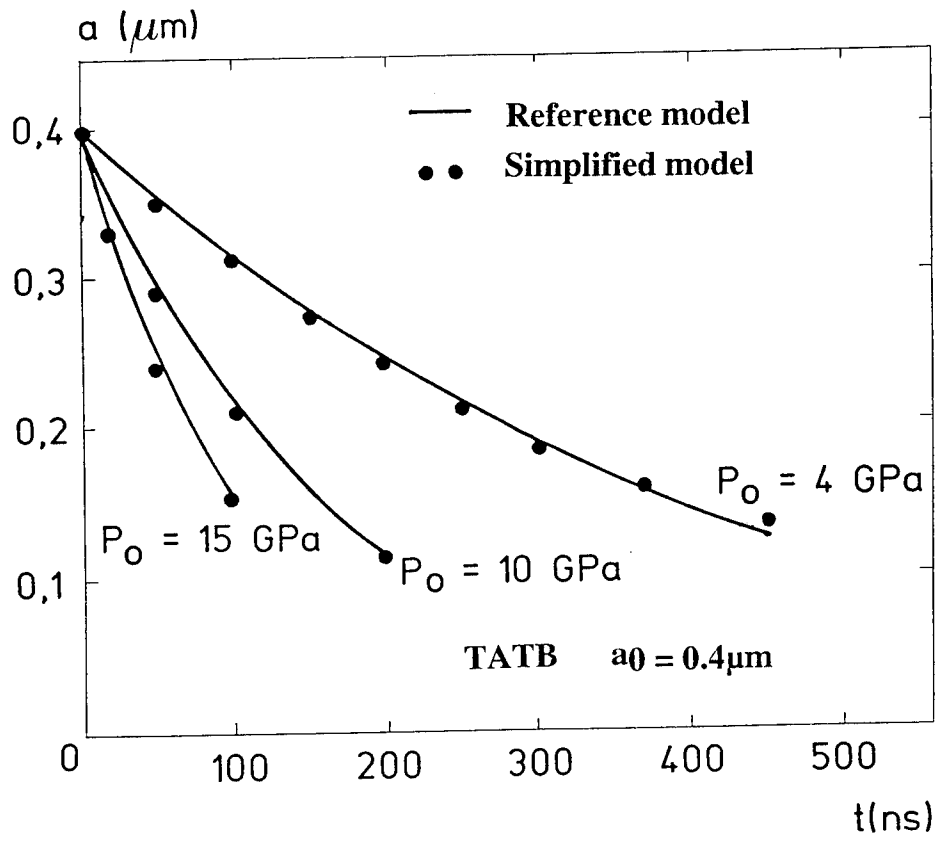

Figure 12 - COMPARISON OF SIMPLIFIED MODEL AND REFERENCE MODEL

3.3.2 Viscoplastic heating and thermal conduction :The pore wall temperature increase, due to the viscoplastic strains of the explosive, is given by :

$$d\theta_{vp} = \left[\frac{12\mu}{\rho C_p} \frac{\dot{a}^2}{a^2} - \frac{2Y}{\rho C_p} \frac{\dot{a}}{a} \right] dt ,$$

where a is given by the motion asymptotic solution.
The cooling of the material, resulting from the thermal conduction, is calculated with a simplified analytical model based on an approximated heat balance in a spherical geometry ***(Figure 13)***.

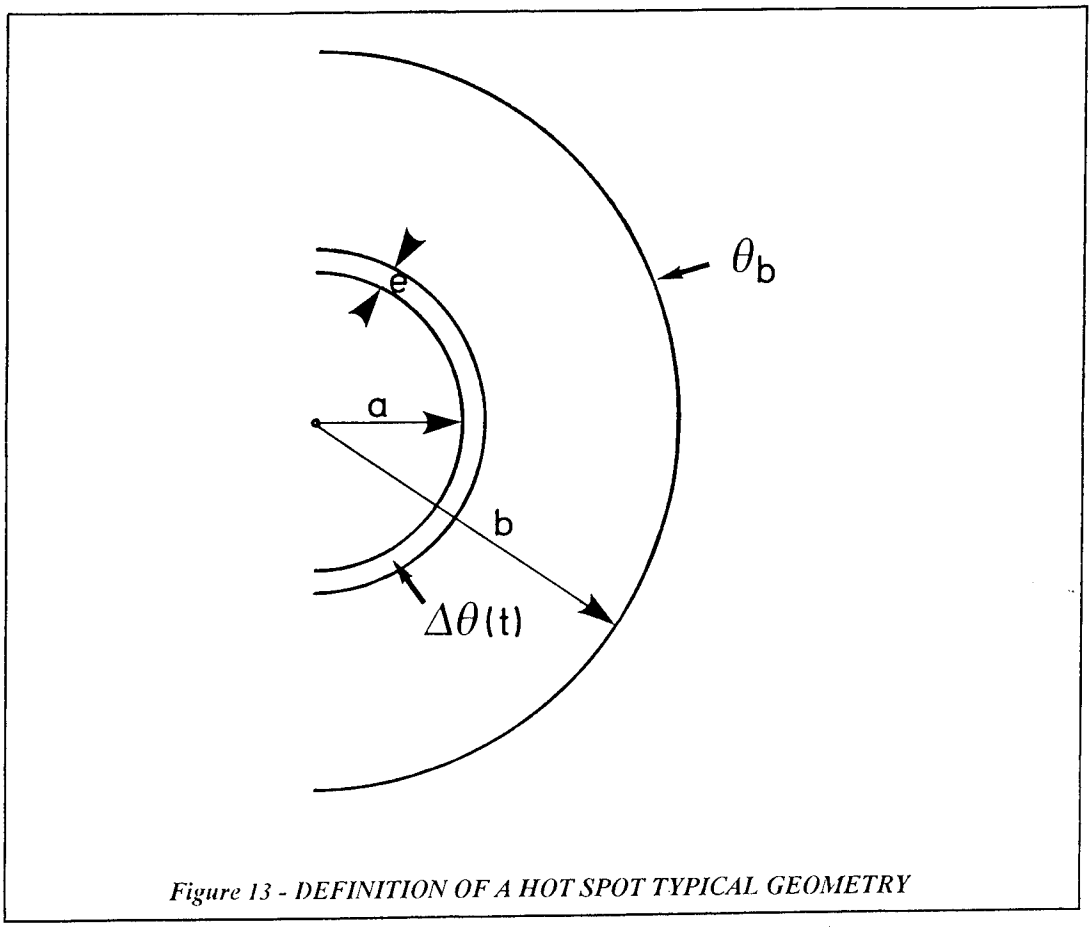

Figure 13 - DEFINITION OF A HOT SPOT TYPICAL GEOMETRY

We calculate the temperature (assumed uniform) in a thin shell (thickness : e) of explosive surrounding the void. During dt, this temperature increases by $d\theta_{vp}$ as a result of viscoplastic heating, and the approximated heat balance is given by :

$$\frac{4\pi\lambda ab}{b-a}\left(\theta(t)+d\theta_{vp}-\theta_0\right)dt = 4\pi\rho C_p a^2 f a_0 d\theta_c$$

where $d\theta_c$ is the cooling due to thermal conduction. Then, the pore wall temperature is given by :

$$\theta(t+dt)=\theta(t)+d\theta_{vp}-d\theta_c+d\theta_d$$

$d\theta_d$ is the increase in temperature produced by the explosive decomposition, and is calculated with a simple zero order Arrhenius kinetics.

The thickness of the shell, e, is equal to $f.a_0$, where f is a function of the non-dimensional variable :

$$x=\frac{\rho C_p}{\lambda}\frac{a^2\dot{a}}{a_0}$$

This function is determined in order to fit the results delivered by the reference hot spot model, as shown in ***Figure 14.***

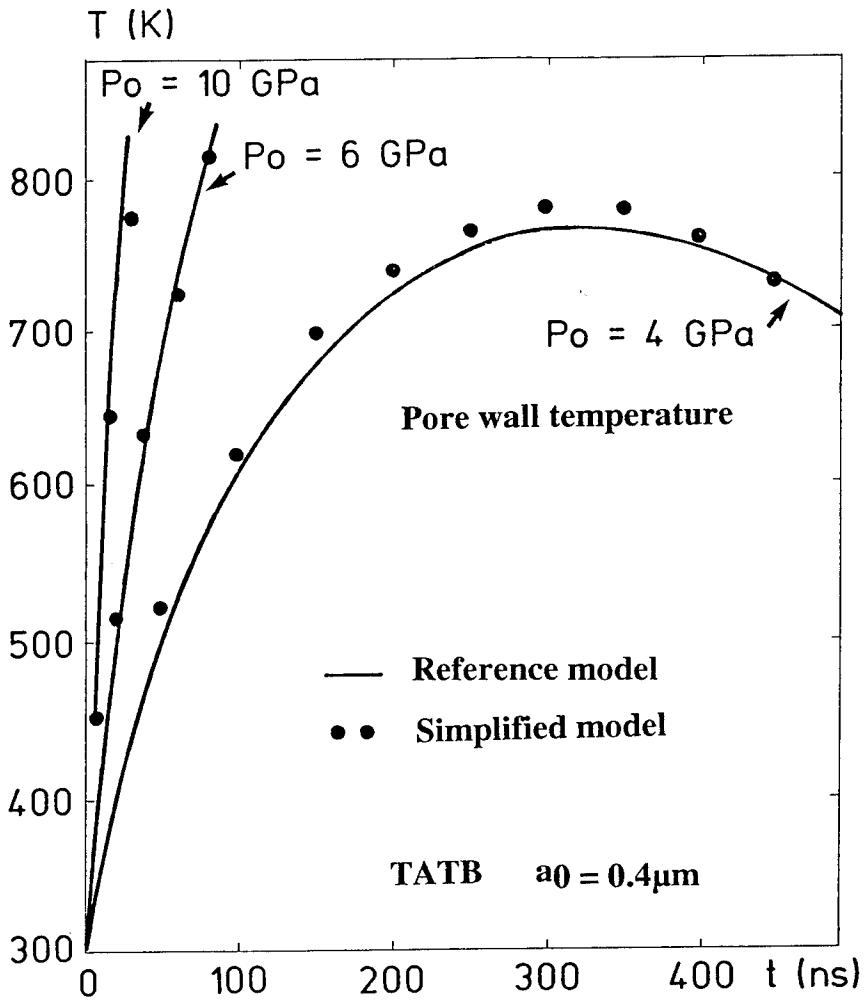

Figure 14 - PORE WALL TEMPERATURE CALCULATED WITH THE SIMPLIFIED MODEL AND THE REFERENCE ONE

3.4 Hot spots in cast explosive compositions :

The porosity is generally very weak in cast compositions. Then, the origin of hot spots cannot be explained exactly as previously.

However a very close approach can be done, the same mechanism can be invoked and the same models apply with slight modifications.

Cast compositions are characterized by high percentage of binder. Thus a schematic representation of the microstructure of these compositions, suitable for modelling, can then be "large" cavities surrounded by explosive and filled with binder. Microscopic observation can give the characteristic size of these cavities and the model must be modified to take into account the compressibility of the binder. This can be done by taking into account, in the motion equation, a cavity internal pressure opposite to the shock pressure and depending on time (degree of collapse) and on the properties of the binder. In this case, the more compressive the binder, the easier the collapse of the cavity.

As a result of this, compositions with compressive binder should be more sensitive.

4 - APPLICATIONS

4.1 Initiation study of a mixed TATB-HMX composition [14] [15]

We studied the shock initiation of composition TX1 ***(see Table 2)***. The experimental pressure threshold measured for TX1 is 2.5 GPa ***(Figure 15)*** The TATB is not initiated by the shock wave, at this pressure ***(Figure 11)*** and the composition is ignited by the HMX. The hot spots model with the viscosity value determined for X1 and 1μm pores diameter predicts the 2.5 GPa value for the threshold pressure of TX1 in which the larger pores are only 0.4 μm in diameter ***(Figure 16)***.

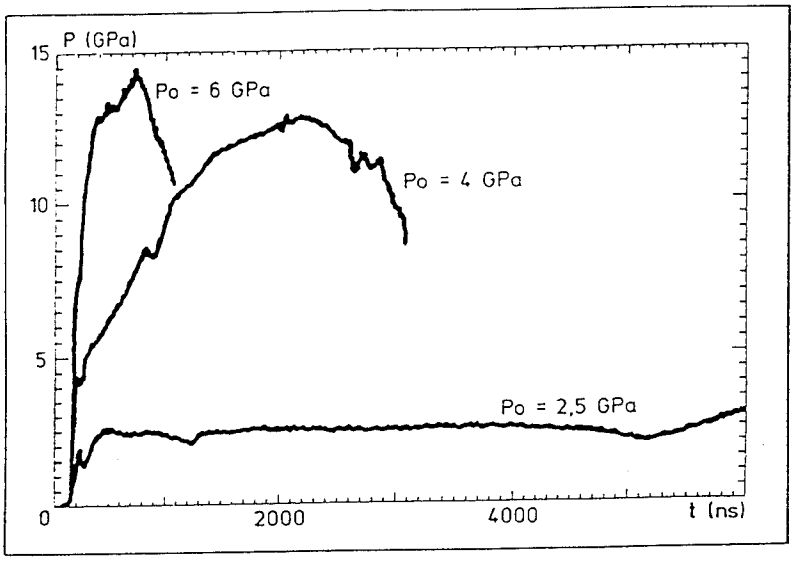

Figure 15 - PRESSURE VS TIME IN TX1 COMPOSITION FOR SEVERAL INPUT PRESSURES

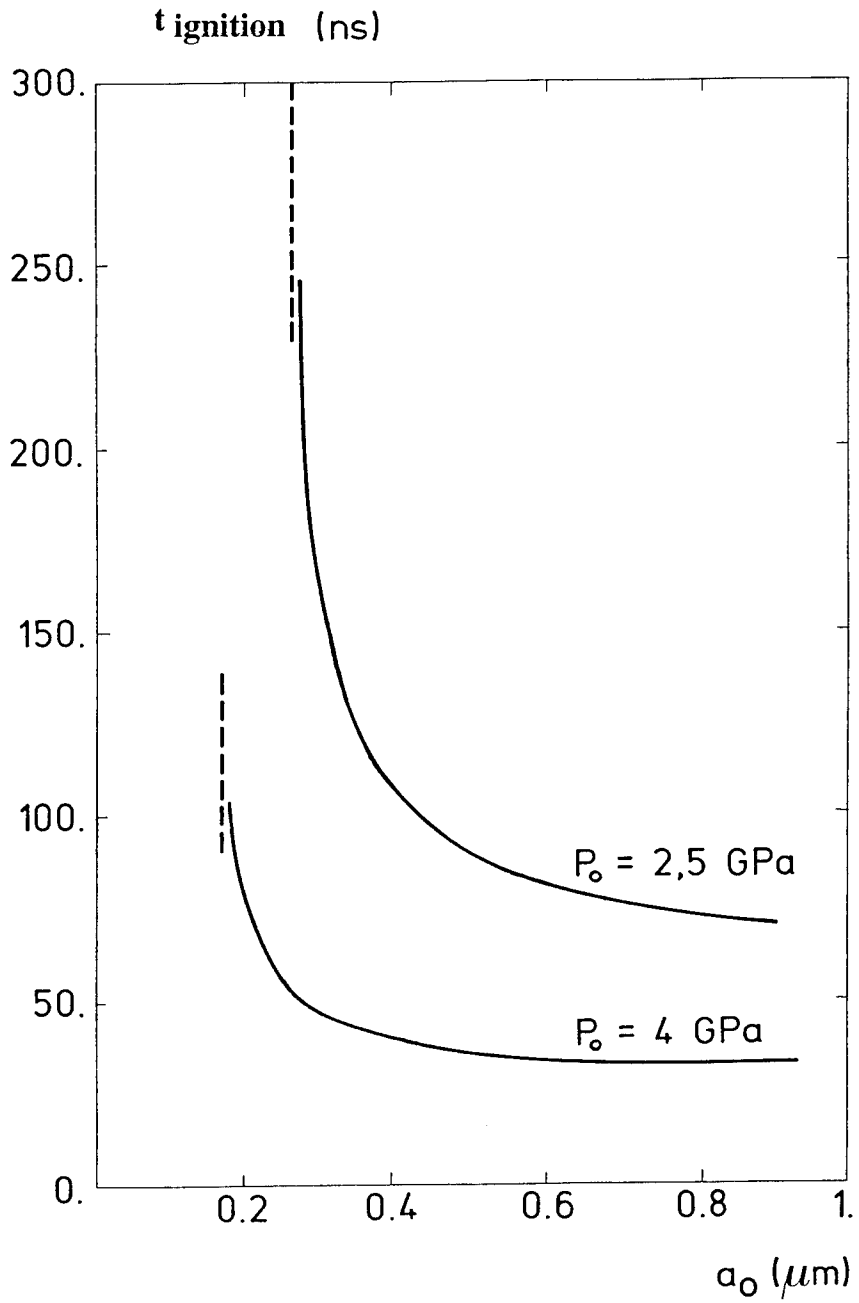

Figure 16 - IGNITION TIME OF INTERGRANULAR HOT SPOTS

4.2 ANALYSIS OF DOUBLE SHOCKS ON HMX, TATB, AND HMX/TATB COMPOSITIONS

If an explosive sample is subjected to a low pressure shock, the pores collapse with a slow heating and, due to cooling by heat conduction, do not ignite. The pore collapse duration is a function of shock pressure, pore diameter and explosive viscosity.

If the explosive is subjected to a second shock ***(Figure 17)*** of a higher pressure, even higher than the threshold pressure previously determined, it can be not initiated. This desensitization phenomenon depends on first shock pressure and duration, and on second shock pressure.

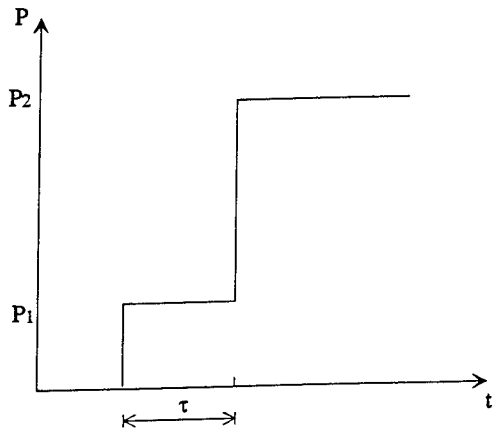

Figure 17 - TYPICAL DOUBLE-SHOCK PROFILE

For example, for X1 composition, if P1=0.5GPa and P2=1.4GPa, comparisons with the hot spots model show that for $\tau > 0.2$ µs, the explosive is desensitized. This numerical value is in good agreement with experimental results ***(Figure 18)***.

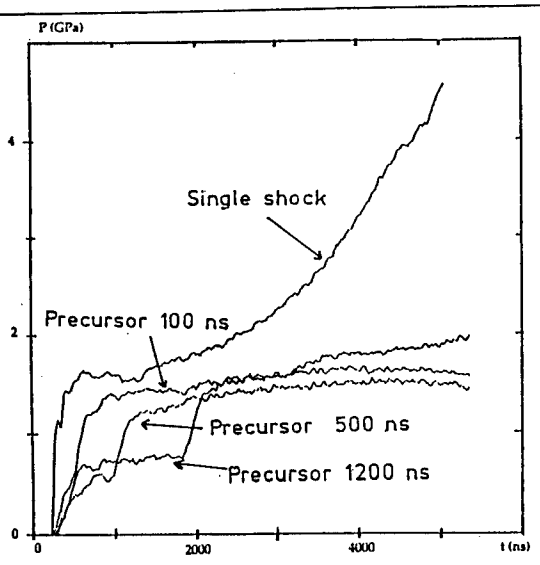

Figure 18 - PRESSURE VS TIME IN X1 SUBJECTED TO DOUBLE SHOCKS

A TATB composition is more difficult to desensitize, because of its higher viscosity. But, as shown in ***Figure 19,*** the same phenomenon can be obtained.

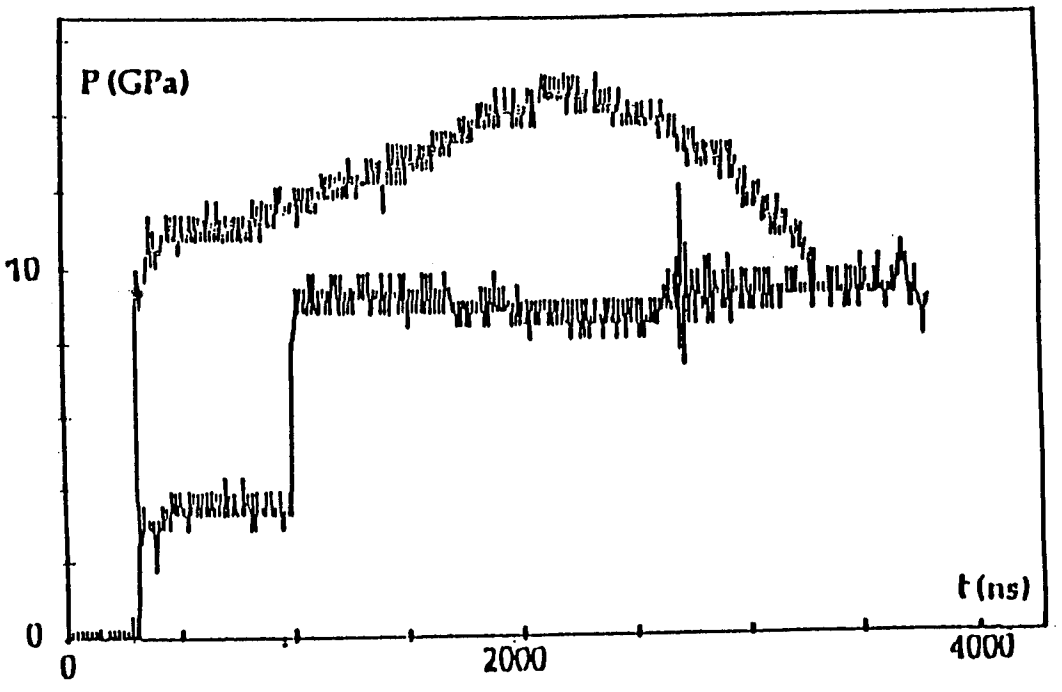

Figure 19 - PRESSURE VS TIME IN T2 COMPOSITION SUBJECTED TO DOUBLE SHOCKS

For a HMX/TATB composition, the initiation process is more complex. Experimental results are presented in ***Figure 20***. In this example, P1 = 1.6 GPa, lower than the initiation threshold pressure of the composition. At this shock pressure, the pores directly connected with the HMX (a_0 = 0.2 μm) are rapidly closed and no hot spot will be created in the HMX by the P2 = 4. GPa shock. The TATB powder is the same than the one used in T2, with 1 μm in diameter pores. As the TATB viscosity is greater than the HMX one, a longer time is required to get the closure of the pores. Therefore, if the duration of the precursor shock is less than 500 ns, the 4 GPa shock induces a heating of the TATB around the voids (800°C). The TATB cannot be initiated, but, by conduction of the thermal energy to an adjoining HMX grain, the TX1 composition is initiated.

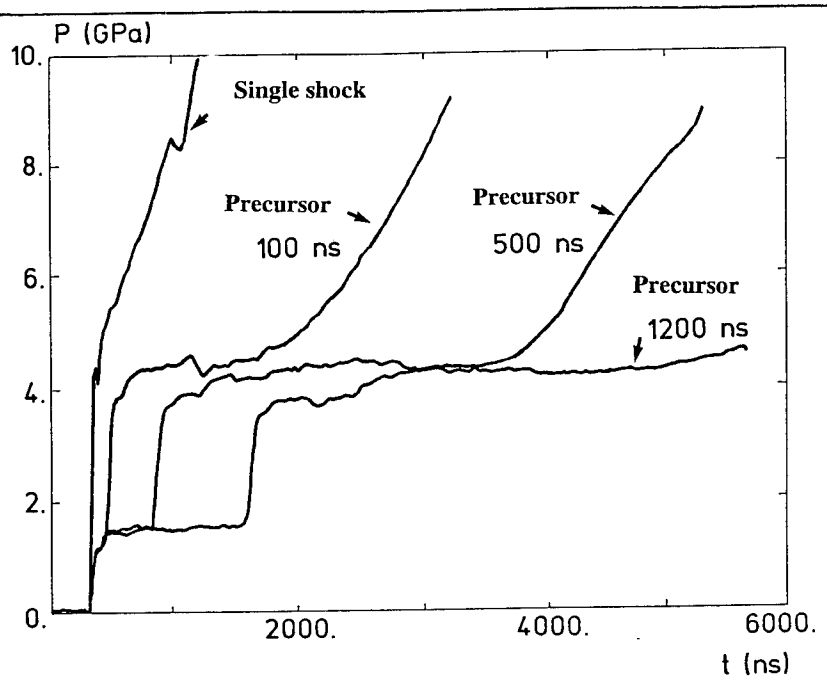

Figure 20 - PRESSURE VS TIME IN TX1 COMPOSITION SUBJECTED TO DOUBLE SHOCKS

4.3 Development of a physical kinetics [15] [16]

The study of the behavior of explosive devices subjected to mechanical stimuli requires numerical modelisation of the shock-to-detonation transition. Several models, able to compute the shock initiation of heterogeneous explosives, were developed in different laboratories. The most famous and used are the Ignition and Growth Model **[17] [18]**, the Forest-Fire Rate and the Explicit Hot Spot Model **[19] [20].** These models are efficient tools but their empirical formulations and, in some cases, the important number of parameters needed, limit their applications.

In another connection, all the laboratories working about the formulation of explosive compositions are looking for insensitive high explosives. A kinetics of decomposition of the explosive, which takes into account the microstructure of the explosive composition, would help the researchers in their choices.

The shock-to-detonation transition is the result of two basic phenomena :
- hot spots formation and ignition,
- explosive burning under high pressure.

As a result, a good kinetic able to simulate all the events involved in the SDT process must be composed of two physical models well-adapted to the description of these two basic phenomena.

The AMORC kinetics has been developed using the previously described analytical hot spots model *(see 3.3)* and an efficient grain burning law.
This kinetics is able to describe all the phenomena involved in shock initiation like :
- SDT for high and low (induction time) incident pressures.
- Explosive desensitization by small pressure precursor or pressure ramp wave.
- Propagation of the detonation, interactions with inert materials.
- Influence of the temperature on the SDT.
- Influence of the microstructure (porosity, grain size, grain morphology).
- Mixed compositions reactive behavior.

4.3.1 Explosive grain burning **[21] [22]** : The influence of grain size on the microstructural burning is well known. Fine grains generally burn faster than coarse ones. In addition, the importance of grain morphology on the decomposition phenomena was demonstrated **[21] [22]**. The assumed mechanism based on these works is composed of three phases : hot-spots ignition on the surface, grain surface growth, and grain burning.

The association of a powder morphology analysis with a grain mathematical erosion method leads to an evolution of the yield, p/S (perimeter/surface of the grains) characteristic of the real powder. As an example, for the TATB powder used in our TATB compositions, the calculated evolution of p/S as a function of the unburned mass fraction W is plotted in **Figure 21**.

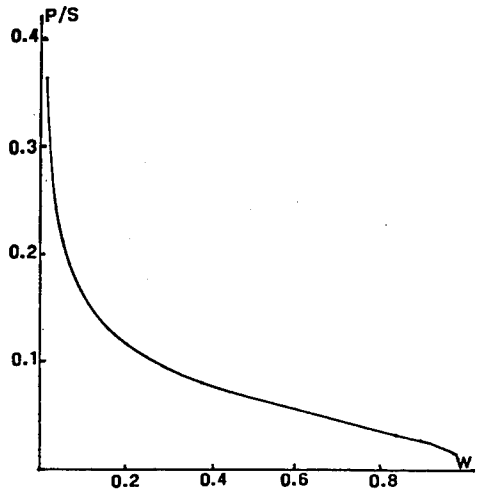

Figure 21 - EVOLUTION OF GRAIN MORPHOLOGY DURING THE DECOMPOSITION

4.3.2 The AMORC kinetics **[15][16]** : As mentioned previously, the AMORC kinetics is the association of the hot spots model with the grain burning law. The decomposition term of the kinetics is given by :

$$-\frac{1}{W}\frac{dW}{dt} = F(N).\frac{p}{S}.V_c(P)$$

where : - F(N) is a function of the number of hot spots, N, calculated by the hot spots model, in which a pore size distribution is introduced.
- $V_c(P)$ is the pressure dependent burning velocity, measured in strand burner tests.

4.3.3 Validation of the AMORC kinetics : The AMORC kinetics is implemented in a one dimensional hydrodynamic code.As seen previously, the hot spots model is able to calculate the threshold initiation shock pressure and to predict the desensitization of the explosive by a precursor shock. The kinetics must reproduce the pressure versus time curves measured at several depths in shocked explosive samples.

In ***Figure 22*** are plotted the profiles of pressure as a function of time, measured with manganin gauges in a TATB composition (T2) for an initial sustained shock of 11 GPa, and calculated with the AMORC kinetics. ***Figure 23*** presents the comparison between measurements and calculations of pressure profiles at 5mm depth in the explosive, for different initial shock pressures.
A good agreement is obtained in all cases. The run distance to detonation as a function of the input pressure was also calculated and agreed well with experiments.

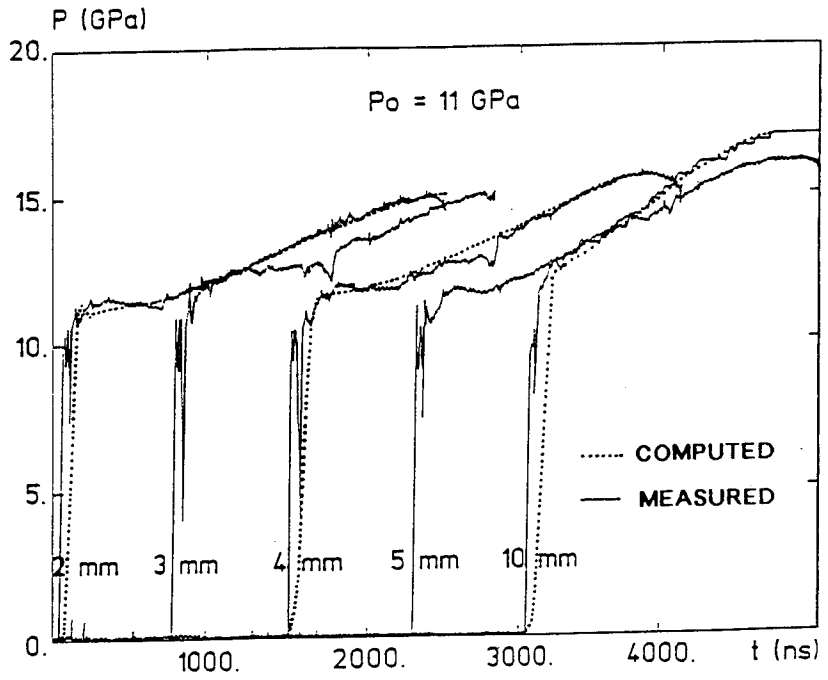

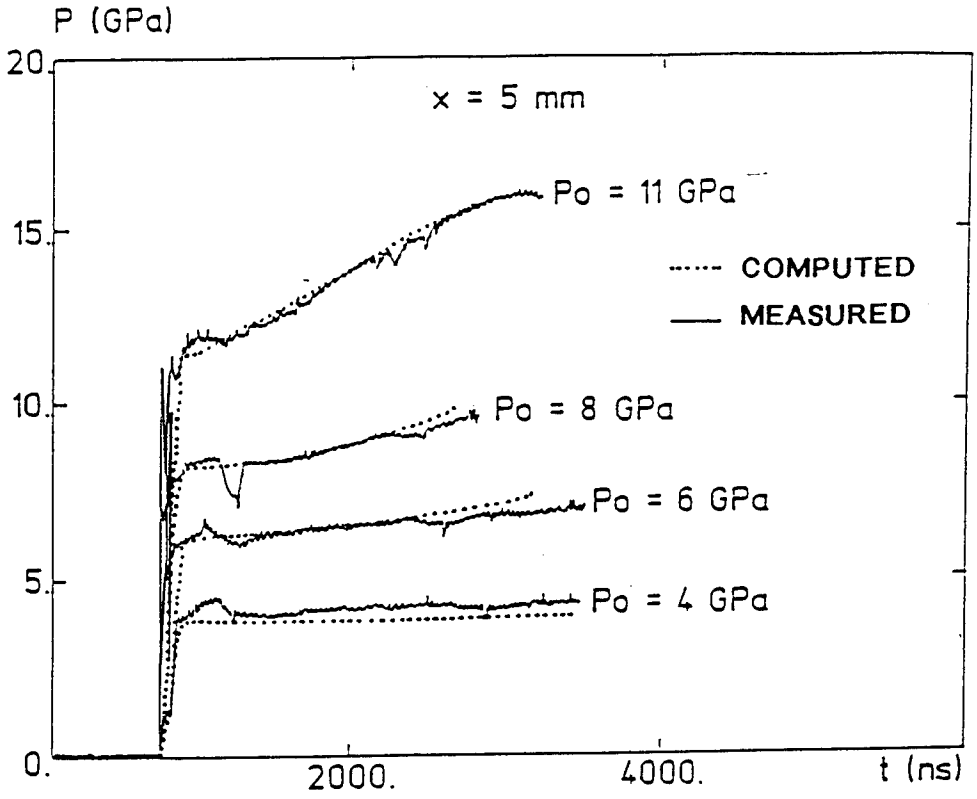

Figures 22 and 23 : COMPARISON BETWEEN MEASURED AND COMPUTED PRESSURE EVOLUTION IN SHOCKED T2 EXPLOSIVE THE CURVES ARE ARBITRARILY POSITIONED ON THE TIME AXIS

As shown in ***Figure 24***, computations with AMORC reproduce the desensitization of the explosive by a precursor shock.

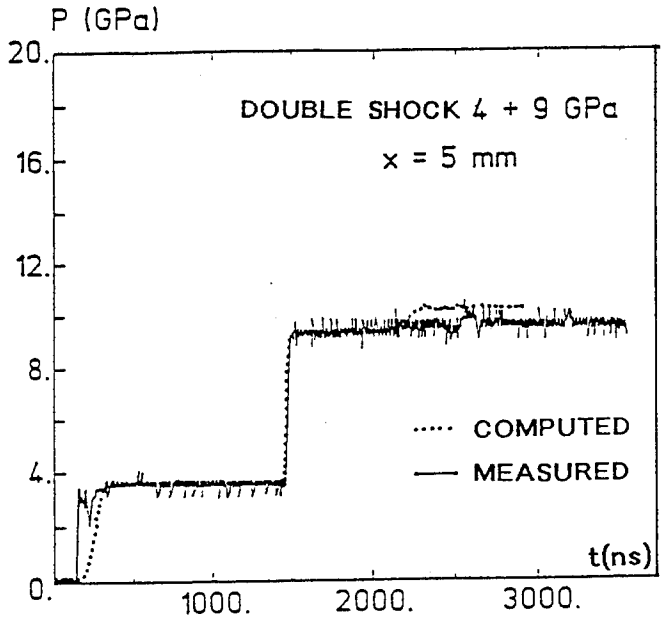

Figure 24 - EXAMPLE OF DESENSITIZATION OF TATB COMPOSITION BY PRESHOCKING

4.3.4 New applications :In the two parts of the kinetics, the microstructure of the explosive is explicitly introduced, and the temperature of the medium is taken into account to determine the ignition of the hot spots. The physical description of the initiation process allows preliminary numerical studies of new explosive compositions, in which the porosity, the grain size or the grain morphology are modified. The explicit calculation of the temperature in the ignition process has an important application in safety studies. Two examples are shown now as an illustration of the AMORC capabilities.

Influence of the initial temperature :

On ***Figure 25***, are plotted the pressure profiles calculated for T2 composition at 300 K or preheated at 500 K and subjected to the same shock. These results exhibit a small but significant sensitization of the explosive when it is heated before impacted.

Influence of the microstructure :

Let C1, C2 and C3 be three TATB compositions composed of spherical grains of three different diameters. These three compositions are defined in ***Table 1***. The smaller the grain size, the smaller the pores. The pressure calculated after a 5 mm propagation of the shock in the explosive samples for a 10 GPa sustained shock are reported in ***Figure 26***.

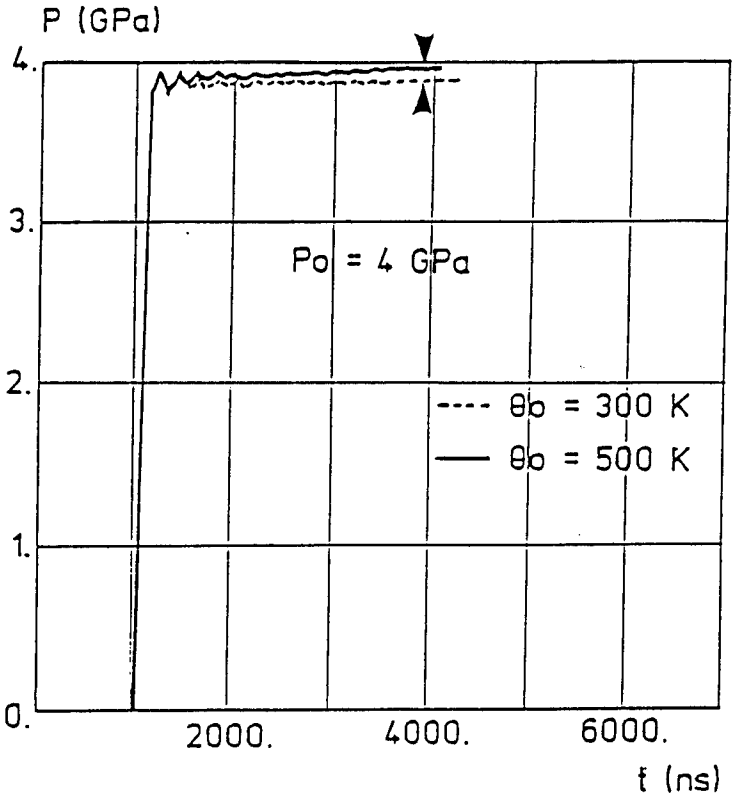

Figure 25 - EFFECT OF THE TEMPERATURE ON THE SENSITIVITY OF EXPLOSIVE COMPOSITIONS

	Grains diameter (μm)	Pores radius (μm)
C1	50	0.4
C2	10	0.2
C3	1	0.1

Table 2 - MICROSTRUCTURE OF THE EXPLOSIVE COMPOSITIONS

For C1 composition, the large pores lead to hot spots ignition and the coarse grains burn slowly. For C2, ignition is also obtained and the smaller grain size results in a faster pressure increase. In this case, the use of smaller grains increases the sensitivity of the explosive composition.

For C3, the voids are to small to produce an ignition of the explosive. In this case, a smaller grain size results in a lower sensitivity of the explosive composition. This phenomenon, called crossing of sensitivity, was previously experimentally observed **[24] [25].**

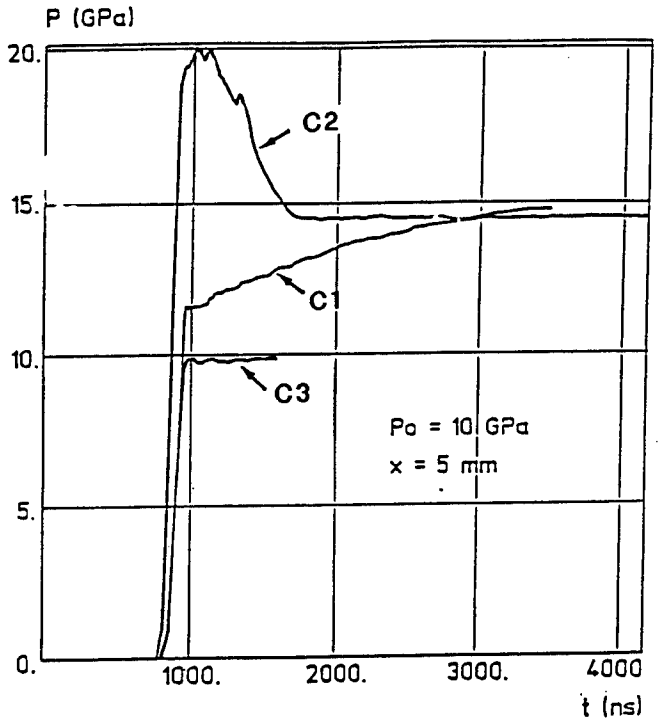

Figure 26 -EFFECT OF THE MICROSTRUCTURE
ON THE SENSITIVITY OF EXPLOSIVE COMPOSITIONS

5 - CONCLUSION

We performed an experimental and theoretical study of hot spots creation in pressed explosive compositions.

Experimentally, it was found that hot spots formation and ignition are the result of the interaction of shock waves with microstructural voids. The mechanism governing the heat generation in the hot spots is the viscoplastic collapse of the porosity.

A physical model of hot spot generation and ignition was developed on the basis of this phenomenology.

Several applications were presented :

- analysis of the complex mechanisms governing the initiation of mixed HMX-TATB compositions,
- study of double-shock desensitization,
- development of a powerful kinetics taking into account the composition microstructure.

In this kinetics, the hot spots model is associated with an efficient grain burning law.

The applications of such a model are in the areas of physics of explosives, safety studies and explosive composition formulation.

AKNOWLEDGEMENTS :

We are deeply indebted with C. CASTILLE and E. GERMAIN who determined the origin of hot spots, M. NICOLLET who performed the impacts experiments, C. BIANCHI, M. LEROY and L. LEJAY who made the programs and performed the calculations.

REFERENCES :

[1] CASTILLE C., GERMAIN E., BELMAS R. - "Origine physique des points chauds dans les compositions explosives pressées au TATB", Propellants, Explosives, Pyrotechnics 17, 249-253 (1992).

[2] WALKER E.H. - "Derivation of the P^2T detonation criterion", 8th symposium (international) on detonation, ALBUQUERQUE (1985).

[3] BELMAS R. - "Amorcage d'une composition explosive par sollicitations mécaniques rapides", 3ème Congrès de Pyrotechnie Spatiale, JUAN-LES-PINS (1987).

[4] MADER C.L., KERSHNER J.D. - "The three dimensional hot spot model applied to PETN, HMX, TATB and NQ", LA-10203-MX UC-45 (Septembre 1984).

[5] PARTOM Y. - "A void collapse model for shock initiation", 7th symposium (international) on detonation, ANNAPOLIS (1981).

[6] BELMAS R. - C.E.A. internal report.

[7] KHASAINOV, BORISOV A.A., ERMOLAYEV B.S.- "Shock wave predetonation processes in porous high explosives", 8th symposium (international) on detonation", ALBUQUERQUE (1985).

[8] MAIDEN D.E.- "A hot spot model for calculating the threshold for shock initiation of pyrotechnics and explosives", 3ème congrès de pyrotechnie spatiale, JUAN-LES-PINS (1987).

[9] FREY R.B. - "Cavity collapse in energetic materials", 8th symposium (international) on detonation, ALBUQUERQUE (1985).

[10] WACKERLE J., JOHNSON J.O., HALLECK P.M. - "Shock initiation of high density PETN", 6th symposium (international) on detonation, Office of Naval Research, ACR-211, ARLINGTON, VA (1970).

[11] HALLECK P.M., WACKERLE J. - "Dynamic elastic-plastic properties of single crystal pentaerythritol tetranitrate", Journal of Applied Physics, Vol 47, N° 3 (1976).

[12] BAER M.R. - "Numerical studies of dynamic compaction of inert and energetic granular materials", Journal of Applied Mechanics 36, Vol. 55 (mars 1988).

[13] BELMAS R., PLOTARD J.P., BIANCHI C., LEROY M., MEILLOT E., "Un modèle de points chauds fondé sur l'implosion de la porosité microstructurale", Propellants, Explosives, Pyrotechnics 18, 217-222 (1993).

[14] NICOLLET M., BELMAS R., PLOTARD J.P., UDIMENT B., LEROY M. - "Amorçage par chocs simples et doubles d'une composition mixte TATB-octogène", Propellants, Explosives, Pyrotechnics 18, 128-131 (1993).

[15] BELMAS R., BIANCHI C., LEROY M. - "AMORC, un modèle physique d'amorçage par choc des explosifs", 4èmes Journées Détonique, BOURGES (1991).

[16] BELMAS R., PLOTARD J.P., BIANCHI C. - "A physical model of shock-to-detonation transition in heterogeneous explosives", Xth symposium (international on detonation), BOSTON (1993).

[17] LEE E.L., TARVER C.M - "Phenomenological model of shock initiation in heterogeneous explosives", Physics of fluids, Vol 4, 511-521 (1980).

[18] TARVER C.M., HALLQUIST J.O., ERICKSON L.M. - "Modeling short pulse duration shock initiation of solid explosives", 8th symposium (international) on detonation, ALBUQUERQUE (1985), NSWC MP 86-194 (1985).

[19] JOHNSON J.N., TANG P.K., FOREST C.A. - "Shock wave initiation of heterogeneous reactive solids", Journal of Applied Physics, Vol 57, 4323-4334 (1985).

[20] TANG P.K., JOHNSON J.N., FOREST C.A. - "Modeling heterogeneous high explosive burn with an explicit hot spot process", 8th symposium (international) on detonation, ALBUQUERQUE (1985),NSWC MP 86-194, 1985.

[21] CHERIN H., GOHAR P. - "The influence of grains morphology on the behavior of explosives", 9th symposium (international) on detonation, PORTLAND (1990).

[22] CHERIN H. - "Influence of microstructure on explosive compositions chemistry", Xth symposium (international) on detonation, BOSTON (1993).

[23] URTIEW P.A., ERICKSON L.M., ALDIS D.F., TARVER C.M. - "Shock initiation of LX-17 as a function of its initial temperature", 9th symposium (international) on detonation, PORTLAND (1990).

[24] MOULARD H. - "Particular aspect of the explosive particule size effect on shock sensitivity of cast PBX formulations", 9th symposium (international) on detonation, PORTLAND (1990).

[25] HONODEL & al C.A. - "Shock initiation of TATB formulations", 7th symposium (international) on detonation, ANNAPOLIS (1981), NSWC MP 82-334 (1981).

-o-

JOURNAL DE PHYSIQUE IV
Colloque C4, supplément au Journal de Physique III, Volume 5, mai 1995

Dislocation Mechanisms for Shock-Induced Hot Spots

R.W. Armstrong

Department of Mechanical Engineering, University of Maryland, College Park, MD 20742, U.S.A.

ABSTRACT

Crystal dislocations provide the ultimate source of localized damage enhancement within solid materials. Vortices are the dislocation counterparts within liquids and gases. For energetic crystals, tubular holes might run along the pre-existent dislocation line lengths and act as shock-induced "in-situ" hot spots. Beyond this consideration, nearly invisible clouds of dislocations are possibly generated at point defects or point defect clusters by the shear stresses at a shock front. Multiple fine scale dislocation movements provide a mechanism for the shock to move to a hydrostatic stress state. Interatomic or intermolecular separations of the order of critical reaction coordinate distances are achievable during the unit dislocation displacements --- without change in material volume. Such nanoscale dislocation predictions connect with microscale experiments in a number of cases where larger scale "defect" considerations are involved. Dislocation pile-ups in slip band avalanches, often associated with cracking, account for very appreciable and localized heating that is deformation rate dependent. Complex dislocation slip band interactions occur within the plastic zones of macroscopic crack tips to control the fracture toughness properties of energetic and related materials.

1. INTRODUCTION

Individual dislocations in energetic crystals have special properties at nanoscale dimensions that relate both to microscopic and macroscopic aspects of detonation. In addition, shock loading produces a nanoscale dislocation network that, depending on the strength of the shock, will influence the generation of hot spots during the follow-on plastic deformation that occurs just behind the shock front. Thus, shock-induced hot spot development involves an added deformation feature that has to be considered when making comparisons with hot spot origins in drop-weight impact tests.

1.1 Energetic crystal dislocations at nanoscale dimensions

The large lattice parameters of energetic crystals lead to an elastic strain energy centered on the dislocation core position that is also relatively large, compared to the crystal surface energy, so that a tubular hole running along the dislocation line is preferred over the occurrence of severely strained molecules at the heart of the dislocation [1]. Figure 1 shows in (a) a unit cell for the orthorhombic crystal structure of cyclotrimethylene-trinitramine (RDX) and in (b) a (002) plane view of a dislocation proposed to explain [100] direction slip on the (040) slip plane. The large size of molecules clearly puts them at out-of-place positions near to the dislocation origin.

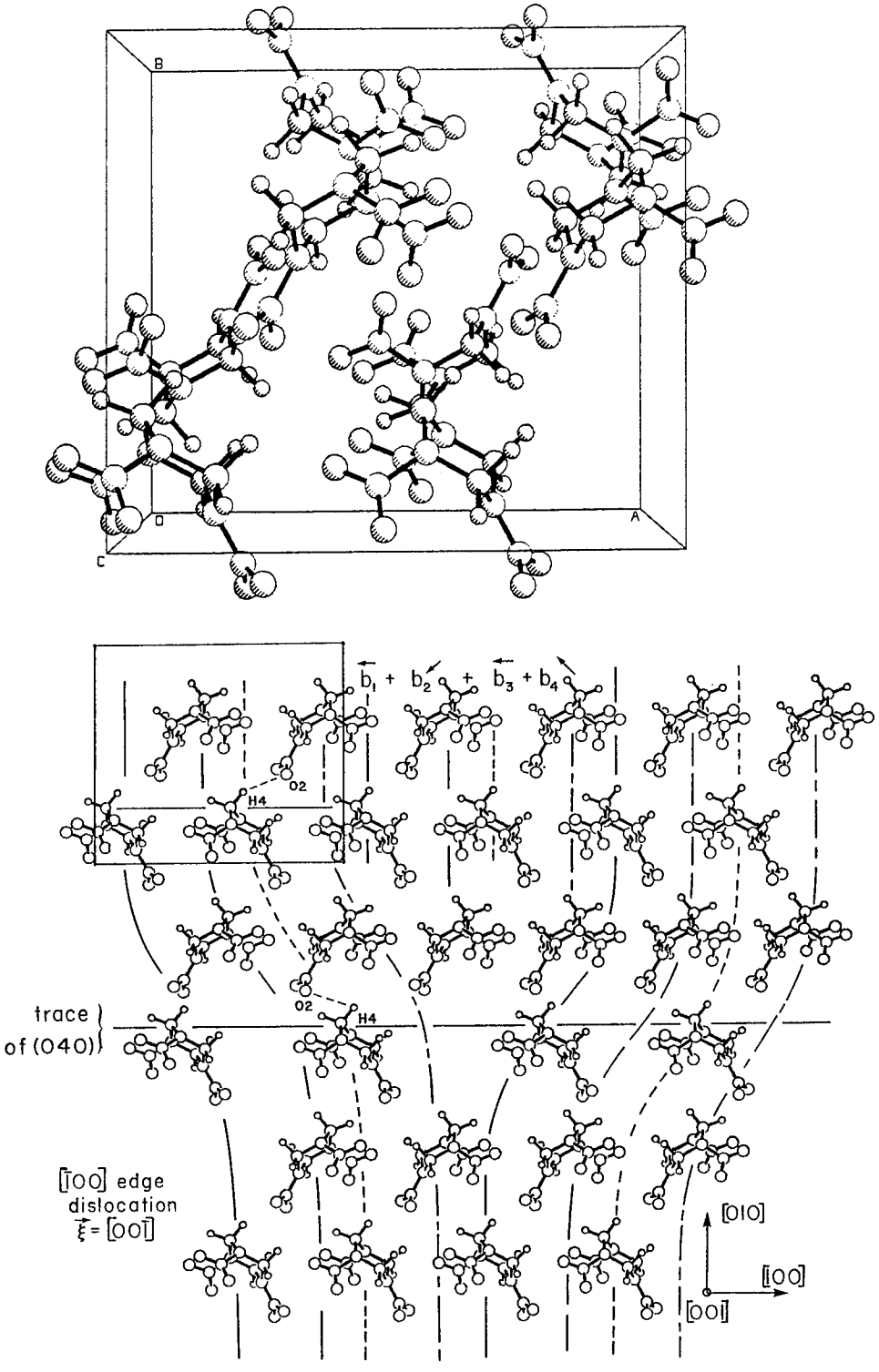

Figure 1a,b. RDX orthorhombic cell and [$\bar{1}$00](040) edge dislocation.

The comparison of dislocation strain energy and surface energy is connected with an intrinsic ductility index of (surface energy divided by the product of shear modulus and dislocation Burgers vector) that is low for energetic materials [2,3]. Also, the rather dense packing of irregularly shaped molecules, for example in RDX, has been shown on an atomic model basis to obstruct the sequential shear displacements that would normally facilitate easy dislocation movement [4], thus explaining measurements of a pronounced resistance to plastic flow at microhardness indentations [5]. In a related important connection, the molecularly "hindered" shear of slip planes in pentaerythritol tetranitrate (PETN) crystals has been proposed to control their sensitivity to shock initiation of detonation [6,7].

1.2 Nanoscale shock structures

The generation of a nanoscale dislocation structure at a propagating shock front was initially proposed in a pioneering study to explain measurements of shock hardening in metals [8]. The model was extended to give estimations of dislocation densities that would match post-shock strengthening measurements [9]. A more recent model involves the periodic generation of nanoscale dislocation loops by shear stresses at the shock front and the reaction of these loops to form a residual nanoscale dislocation dipole structure with resultant Burgers vectors parallel or antiparallel to the shock propagation direction [10]. The model has been related to the previous consideration of shock hardening measurements in metals [11] but, also, the model has been connected with molecular dynamics calculations performed to describe the generation of hot spots by shocks in energetic crystals [12].

1.3 Drop-weight impact tests

Hot spots and the initiation of chemical decomposition were associated with the occurrence of discontinuous load drops in transmitted pressure-time curves measured for drop-weight impact tests on RDX, PETN and related materials [13]. A microscopic explanation of the behavior was given in terms of the hot spots being generated when dislocation pile-up avalanches were released from blocked slip bands at obstacles [14]. On this model basis, the crystal size dependence of drop-height sensitivity measurements was predicted [15] and the mechanically-induced hot spot sizes were compared with direct thermal model calculations [16].

2. DISLOCATION ATTRIBUTES IN ENERGETIC CRYSTALS

The relatively weak molecular or hydrogen bonding of energetic crystal lattices leads to the possibility of numerous dislocations being formed within the lattice structures depending on thermal fluctuations or solute influences that occur during even the most careful crystal growth procedures. For example, a large variety of dislocation Burgers vectors and line vectors has been observed with the method of x-ray diffraction topography applied to mapping dislocation distributions in carefully solution-grown crystals of RDX [17]. The ease with which dislocations might be formed in these materials, however, contrasts with the apparent contradiction that the dislocation strain energies are relatively large compared to the heat of fusion, because of the large Burgers vectors [18].

2.1. Crystal growth observations

A detailed description has been given of the relationship of dislocation Burgers vectors and line vectors to the characteristic internal growth sector microstructures and external polygonal crystal morphologies obtained with the growth-from-solution techniques normally employed for non-metallic crystals [19]. The dislocation lines generally run normal to the growth surface facet planes. Figure 2a,b shows an example of the growth morphology and sectioned internal growth sector microstructure obtained for an individual RDX crystal particle [20]. The resultant facet planes in Figure 2a and previous facet planes in Figure 2b are identified from crystallographic calculations reported for RDX planes and directions [21].

Dislocation structures relating to external growth morphologies observed for RDX were reported previously in another x-ray diffraction topography study [22]. In Figure 2a, probable dislocation line emergence points are marked at A, B, C, and D. Other tabular crystal morphologies and a new growth

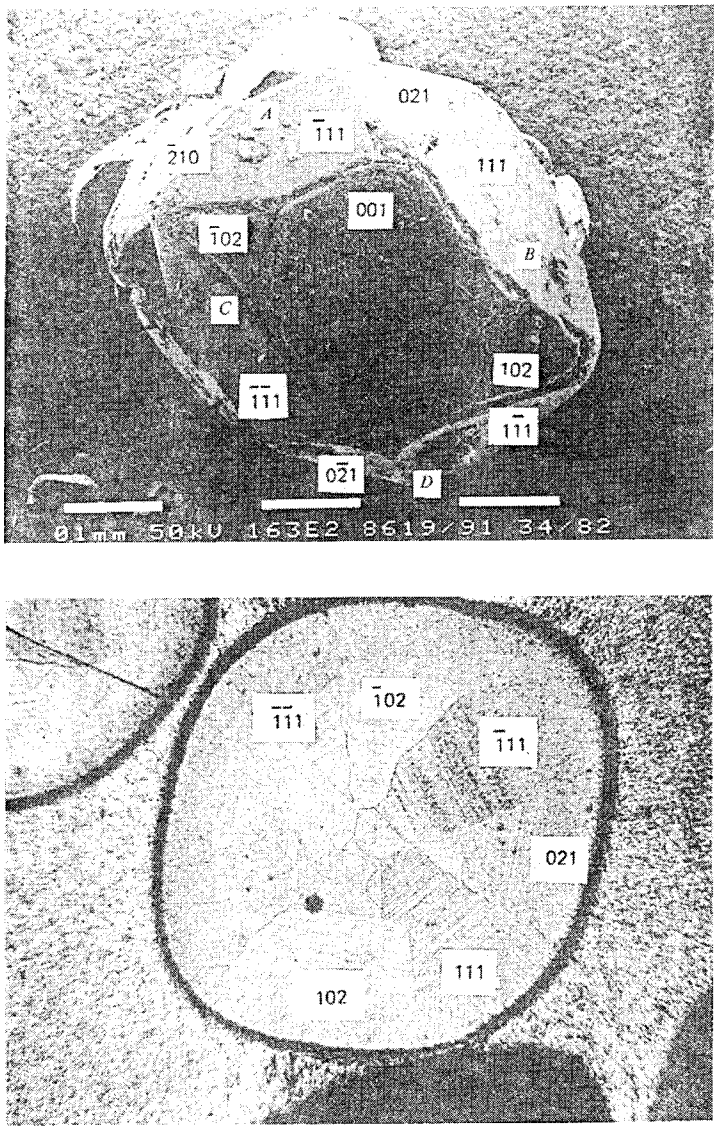

Figure 2a,b. RDX particle morphology and sectioned growth sectors.

morphology were identified for RDX in [21] and, consequently, other dislocation substructures would be included within the crystals. In this way, the variety of growth morphologies observed for RDX crystals provides evidence of the varying dislocation substructures that are contained within the crystals.

2.2 Dislocation "immobility"

The restricted extent of dislocation slip surrounding microhardness indentations in RDX [5, 23] led to the consideration that the interleaved nature of rather complex molecules in the relatively dense lattice structures of energetic materials provided the primary basis for a self-resistance to dislocation movement. On this basis, [100] direction slip in RDX on an (040) slip plane was proposed as an example of a relatively easy slip path to explain previously reported slip observations. Also, limited slip on $(02\bar{1})$ planes was identified at microhardness indentations [24].

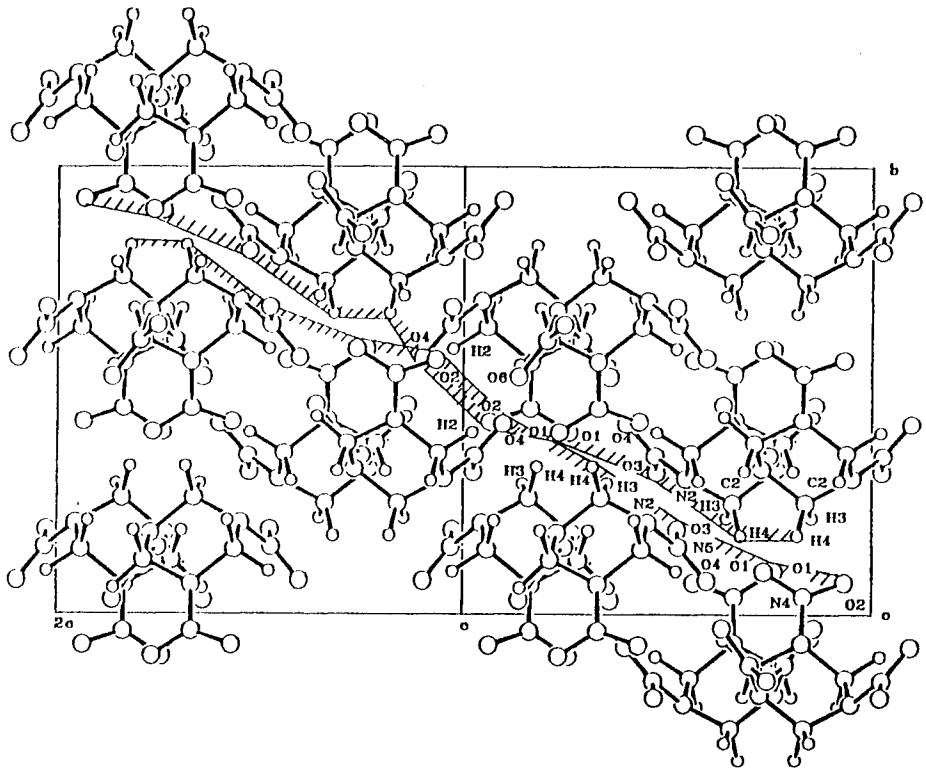

Figure 3. RDX molecule interactions for [100](02$\bar{1}$) slip.

Figure 3 shows a model of [100] slip on the (02$\bar{1}$) plane crossing two unit cells in RDX. At the vertical (001) plane junction of the cells, interactions are shown for two pairs of oxygen atoms in outcropping ONO groups between adjacent molecules. The particular interactions that are shown are those that would be involved in removing one oxygen atom in each case from adjacent ring extensions to form 1,3-dinitroso-5-nitro-1,3,5-triazacyclohexane. This compound was detected in drop-weight impact test specimens of RDX recovered from tests at near initiation drop-heights [25].

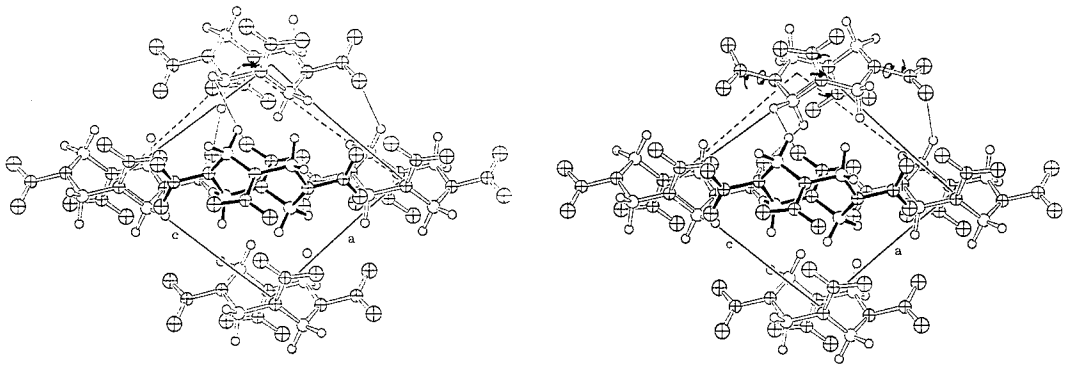

Figure 4. HMX molecule translations and rotations for (101)[10$\bar{1}$] Type II deformation twinning.

An explanation of the difference between slip deformation being observed, though with difficulty, in RDX and deformation twinning being observed as a primary deformation mechanism in (harder) crystals of cyclotetramethylenetetranitramine (HMX) has been proposed to be rooted in the more flexible structure of the larger HMX molecule [26]. Figure 4 shows a possible mechanism for the {110} type II deformation twinning structure that is proposed to occur in the monoclinic HMX crystal lattice. Molecular rotations are indicated to occur within the molecule in addition to the required translational displacements.

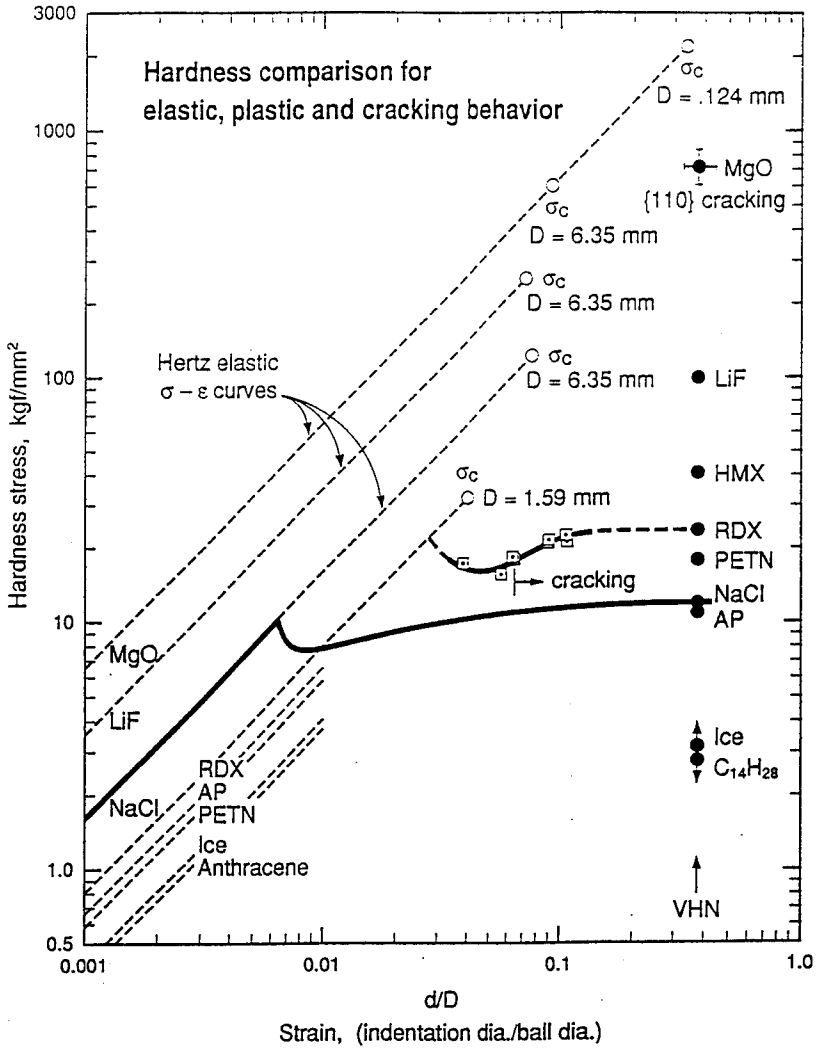

Figure 5. Elastic, plastic and cracking indentation hardnesses.

2.3 Microhardness assessment

The stresses for plastic flow and cracking of energetic crystals are able to be compared on the continuous indentation hardness basis that is shown in Figure 5. The hardness stress is given by the load divided by the projected area of the indentation and the hardness strain is specified as the ratio of contact diameter for a ball indenter divided by the ball diameter. The logarithmic scale for the indentation stress-strain behavior covers a substantial range in stress and strain values that are applicable for the initial (Hertzian) elastic loading response, the onset of progressive plastic flow, and a theoretical limiting elastic cracking condition [27].

The computed linear elastic loading responses of the different materials, indented in each case with a steel ball, are shown along the left edge of Figure 5, beginning at the lowest stress and strain values. For these lines, larger elastic stress values at any strain are indicative of larger elastic moduli, for example, for elastically stiff MgO as compared with elastically compliant anthracene crystals. The low elastic modulus of RDX is significantly less than that of NaCl. A continuous ball indentation test result is shown for an NaCl crystal as the heavy curve leading from elastic loading behavior to plastic flow and eventually matching with a Vickers hardness measurement plotted at an equivalent hardness strain of 0.375. By comparison, separate ball test results are shown for indentations put into an RDX crystal and including a theoretical hardness cracking stress shown on the elastic loading line for the 1.59 mm. diameter ball employed in the measurements. The comparison with NaCl shows that RDX is more compliant but has a higher plastic flow strength, near to the theoretical limiting cracking stress. The comparison is in line with the dislocation structure considerations described in the preceding Sections and with an analysis of the limited intrinsic ductility to be expected for RDX [3].

3. SHOCK DEFORMATIONS ON THE NANOSCALE

Figure 6 shows the dislocation model that has been proposed to explain shock hardening of materials

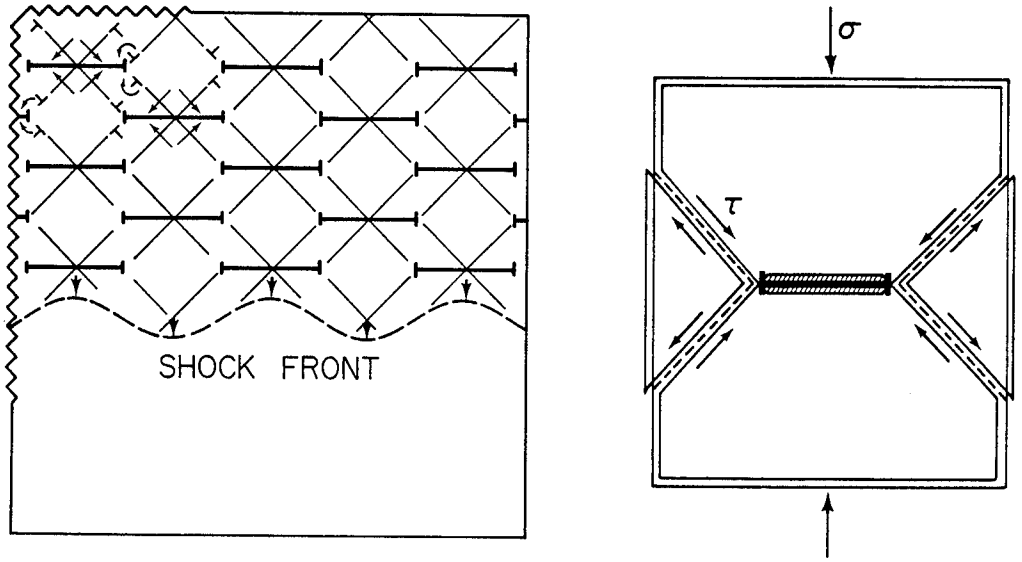

Figure 6. Nanoscale dislocation dipole model for shock damage.

and, in particular, has been proposed to be involved in shock-induced hot spot initiations of energetic materials [10]. For this ideal representation, the large strain induced at all points along the shock front is proposed to initiate numerous elemental shear zones. The sense of shear for the dislocation displacements is determined by the compressive stress. With lateral constraint, the dislocation displacements move the stress state towards a hydrostatic environment. The elemental crossed shears of the individual loops are distributed in a manner to give dislocation reactions at intertwined slip intersections so that a residual state of one-dimensional strain is achieved for the resultant dislocation structure. The proposed nanoscale structure appears to give a reasonable explanation of shock hardening observations [11].

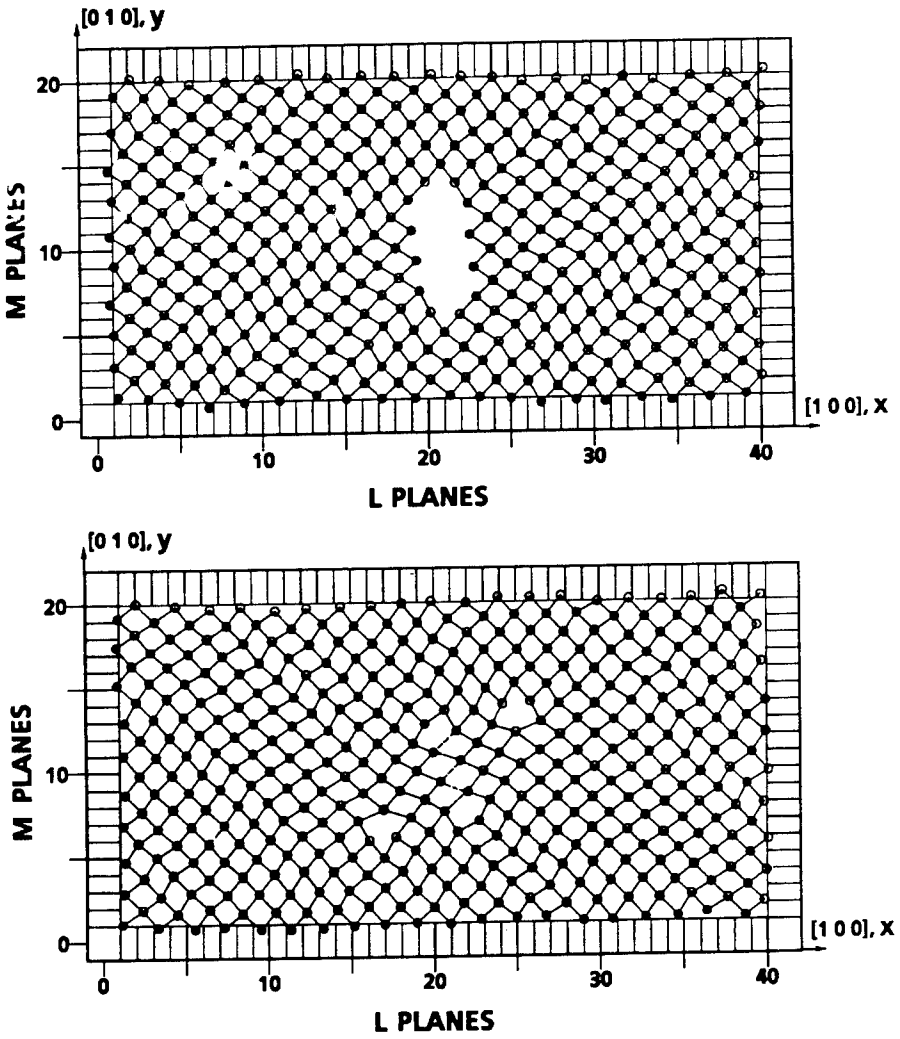

Figure 7a,b. Vacancy cluster collapsed into dislocation dipoles.

3.1. Molecular dynamics assessment

The consideration of events occurring at nanoscale dimensions in shocks has led to a molecular dynamics study of the role that other defects, such as vacancy clusters, may play in generating any proposed dislocation nanostructure [12]. Figure 7 shows a ten atom vacancy cluster in (a) that was found to collapse under imposed shock-type unidirectional displacements to generate a pair of dislocation dipoles in (b). The missing vacancies in (b) are accounted for in the closed planes separating each pair of dislocations constituting the respective dipoles.

An important result that was obtained from monitoring the collapse of the vacancy cluster in Figure 7 and of studying shock influences on other monatomic or molecular vacancy defects [28] was that appreciable hot spot heating always occurred in association with local irreversible plastic relaxation of the structure. Figure 8 shows a representative stress-strain curve for collapse of the vacancy cluster [11]. The method of computing appropriate stresses has been described [29]. Further model calculations of such defect-mediated structural relaxation processes in monatomic and molecular systems have shown that hot spots occur when the potential energy source of the strained lattice is released through an allowed extent of structural relaxation [30].

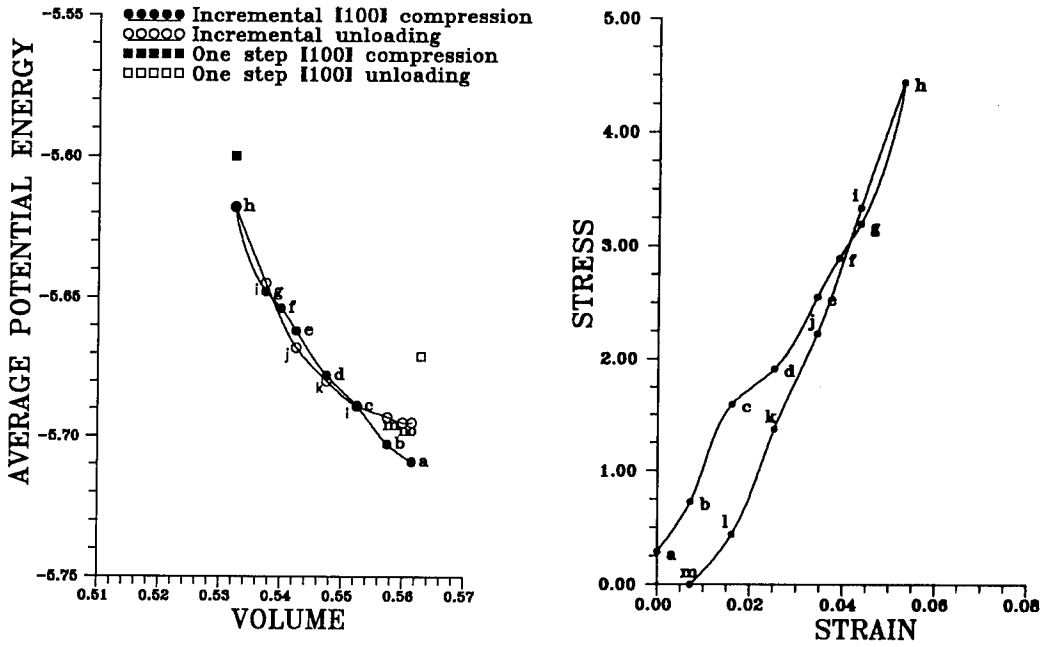

Figure 8. Stress-strain curve for collapse of vacancy cluster.

3.2. Plastic relaxation mechanisms

Depending on the strength of the shock, initiation may occur between two limiting cases: at high stress amplitude where pre-existent defects, including dislocation cores, may operate as "in-situ" hot spots of minor requisite thermal excursion [31] or at low stress amplitudes where more substantial plastic relaxation mechanisms are involved for greater localized temperatures. The latter situation is of more interest and relates to the issue of hot spot temperatures that are proposed even for lessor stress amplitude tests, for example, as occur in drop-weight impact tests.

4. DISLOCATION PILE-UP MECHANICS

As mentioned earlier, a dislocation pile-up mechanism was proposed to explain the generation of hot spots in drop-weight impact tests [14], as indicated schematically in Figure 9. Here, the dislocation pile-ups in obstructed slip bands could easily span a crystal cross-section or a substantial portion of it. Of course, there is an immediate extent of localization associated with the occurrence of individual slip planes because of their being separated by material that is only elastically strained. However, an obstructed slip band pile-up, if released by collapse of the strongest type of localized obstacle that occurs for the theoretical fracture stress, would produce ultrafast dissipation of the pent-up potential energy for generation of a hot spot.

4.1 Impact test results

A proposed susceptibility index for hot spot generation from idealized dislocation pile-up avalanches is displayed graphically in Figure 10. The limiting temperature relationships for different combinations of material parameters are given in the Figure. The main parameters that vary among the different materials are the theoretical microstructural stress intensity for fracturing, k, and the material thermal conductivity, K. The ratio (k/K) appears to provide a useful susceptibility index that is indicated by the slopes of lines that could be drawn to the various material open circle points in the graph. Otherwise actual values of upper limiting hot spot temperatures are given by the slopes of the lines that are drawn to the closed circle points. Expanded scales for the abscissa and ordinate scales

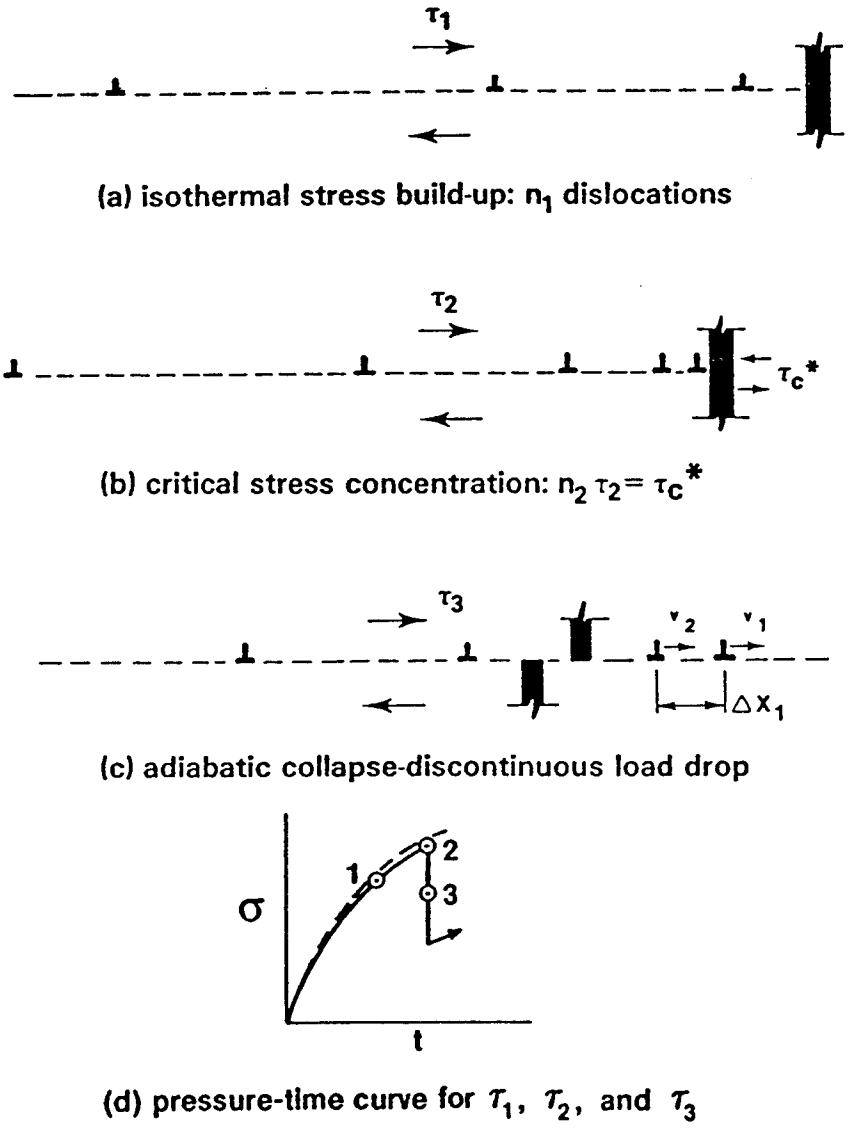

Figure 9. Dislocation pile-up avalanche model for hot spot.

are shown near to the origin for RDX, PETN and ammonium perchlorate (AP) materials. Such calculations have been carried forward to evaluate the longer hot spot lifetimes that occur for RDX as compared with PETN and less so for AP [32].

The microstructurally-based pile-up avalanche model description leads naturally to the expectation of a crystal size dependence for the impact drop-height sensitivity. A predicted increase in drop-height initiation with reduction in crystal size was confirmed for RDX [15]. Figure 11 shows a comparison of results obtained for RDX powder material tested at two laboratories and, also, for tests on octanitrobenzidine (CL-12) material [33]. The vertical spread in Figure 11 of the three RDX drop-height measurements at a crystal size of 250 micrometers is attributed to variations in the microstructures of the specimens that were obtained from different production batches.

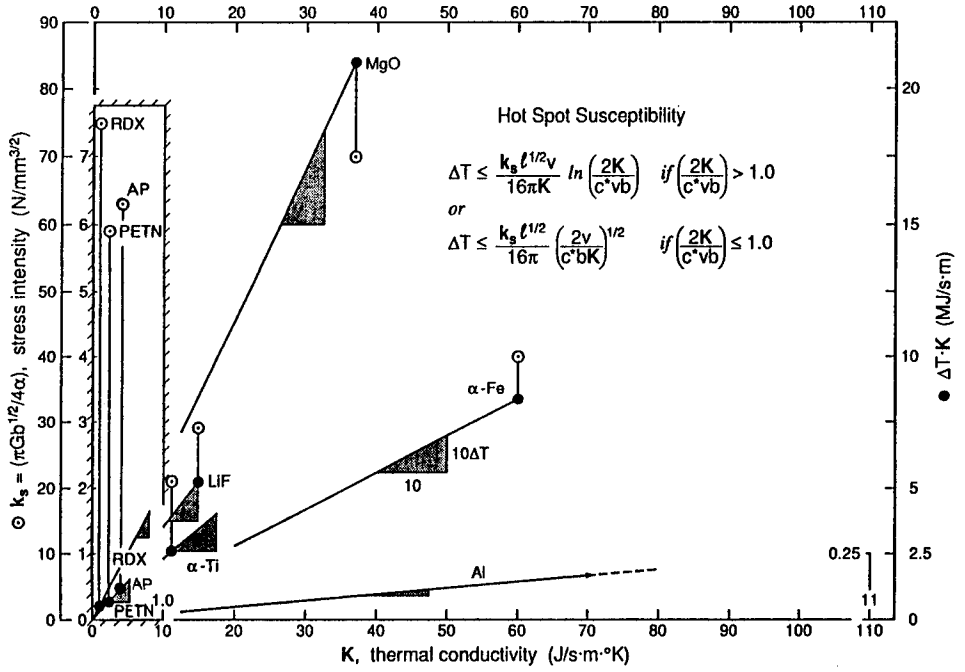

Figure 10. Pile-up based (k/K) ratio for hot spot susceptibility.

A further consideration of the pile-up avalanche model for mechanical generation of hot spots is its relation to model calculations for thermally-induced hot spots. Figure 12 shows the comparison for RDX and PETN on the basis of one thermal model description [15,34]. An interesting result of the comparison is that PETN should be initiated at lower hot spot temperatures than RDX because of the difference in thermal initiation properties.

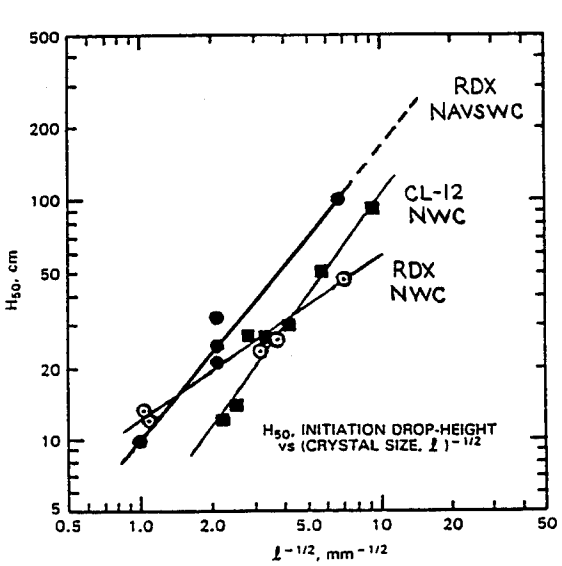

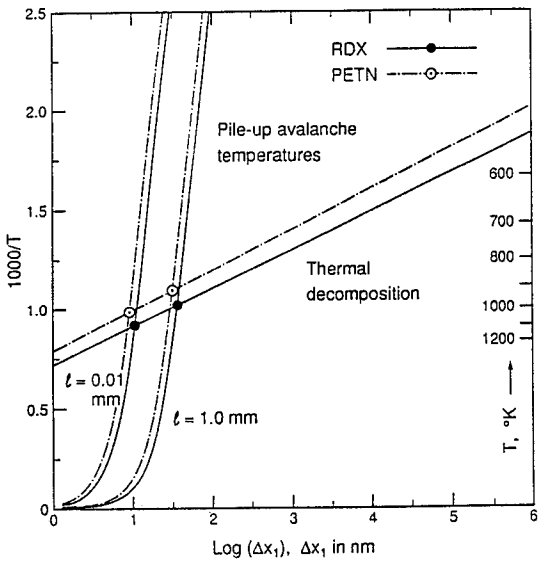

Figure 11. Crystal size dependence for drop-weight sensitivity.

Figure 12. Mechanical and thermal hot spots in RDX and PETN.

4.2 Shock connections
Here, as was mentioned, the interesting case is at low shock amplitudes where the influence of a nanoscale dislocation substructure created in the front is to be encountered immediately by the shock-driven movement of pre-existent slip dislocations. The type of hardening attributed to the nanoscale dislocation network has been measured for shocked AP crystals [35]. In more recent work on AP, shock initiation of chemical decomposition was shown to occur at hardness impressions put into the crystals beforehand [36]. Other work on the occurrence of shear banding in materials bears on the shock hardening issue [37] also in that such hardening is athermal. The strain hardening of the material is unchanged or possibly reduced. Thus, the nanoscale substructure contributes to shear localization or "channeling" of plastic deformation. The result should be an enhancement of hot spot formation. The indication then is that more significant hot spot development would occur for shocked materials than would be expected on the basis of a simple extension of drop-weight impact test results.

5. CONCLUSIONS
5.1 The rather unique character of dislocation generation and movement in energetic materials gives an explanation at nanoscale dimensions of how intermolecular distances can be reduced to critical reaction coordinate distances for the direction-dependent shearing of the low symmetry lattice structures.

5.2 In any case, significant hot spot temperatures are always produced by whatever irreversible plastic relaxation mechanisms may occur.

5.3 The detonation of relatively defect-free shocked crystals is very likely initiated just behind the shock front as a result of the pre-existent dislocations interacting with a nanoscale network of dislocation dipoles being sequentially generated at the travelling front.

5.4 For the shock initiation of energetic materials containing microscopic defects, such as surface notches or voids, there is an implicit role of dislocation-based plasticity involved in further localizing hot spot damage.

Acknowledgements

It is a pleasure to thank Simone Odiot for involving me in this workshop activity and, also, for me to thank colleagues at the Naval Surface Warfare Center (NSWC) for much collaborative work that is reflected in the references cited in this paper and that have shaped my thinking on the topic. Richard Miller is especially thanked for providing support for my work at NSWC and at the University of Maryland, most recently, through Contract N00014-86-K-0286.

References

[1] Frank F.C., Acta Cryst. 4 (1951) 497-501.

[2] Armstrong R.W., Mater. Sci. Eng. 1 (1966) 251-254.

[3] Armstrong R.W. and Elban W.L., Mater. Sci. Eng. A111 (1989) 35-43.

[4] Armstrong R.W. and Elban W.L., "Microstructural Origin of Hot Spots in RDX Crystals", Energetic Material Fundamentals Workshop, Los Alamos National Laboratory, NM, 14-17 October 1986 (Chemical Propulsion Information Agency Publication 475, 1987) pp. 177-182.

[5] Elban W.L. and Armstrong R.W., "Microhardness Study of RDX to Assess Localized Deformation and Its Role in Hot Spot Formation", Seventh (International) Symposium on Detonation, U.S. Naval Academy, Annapolis, MD, 16-19 June 1981 (Naval Surface Weapons Center NSWC MP 82-334, 1982) pp. 976-985.

[6] Dick J.J., Mulford R.N., Spencer W.J., Pettit D.R., Garcia E. and Shaw D.C., J. Appl. Phys. 70 (1991) 3572.

[7] Dick J.J. and Ritchie, J. Appl. Phys. 76 (1994) 2726-2737.

[8] Smith C.S., Trans. Metall. Soc. AIME 212 (1958) 574

[9] Meyers M.A., Scripta Metall. 12 (1978) 21.

[10] Armstrong R.W., Miller R.S. and Sandusky H.W, in "Indentation Hardness, Defect Structure and Shock Model for RDX Explosive Crystals", ONR Workshop on Dynamic Deformation, Fracture and Transient Combustion, Chestertown, MD, 12-14 May 1987 (Chemical Propulsion Information Agency Publication 474, 1987) pp. 77-89.

[11] Bandak F.A., Armstrong R.W. and Douglas A.S., Phys. Rev. B 46 (1992) 3228-3235.

[12] Bandak F.A., Tsai D.H., Armstrong R.W. and Douglas A.S., Phys. Rev. B 47 (1993) 11681-11687.

[13] Heavens S.N. and Field J.E., Proc. Roy. Soc. (London) A338 (1974) 77-83.

[14] Armstrong R.W., Coffey C.S. and Elban W.L., Acta metall. 30 (1982) 2111-2116.

[15] Armstrong R.W., Coffey C.S., DeVost V.F. and Elban, W.L., J. Appl. Phys. 68 (1990) 979-984.

[16] Armstrong R.W., "Dynamic/Shock/Dislocation Aspects of Energetic Crystal Decompositions", Shock, Mechanical, and Thermal Initiation-to-Detonation Workshop, Los Alamos National Laboratory, NM, 16-18 November 1993, in print as a Chemical Propulsion Information Agency Publication.

[17] Halfpenny P.J., Roberts K.J. and Sherwood J.N., Philos. Mag. A53 (1986) 531.

[18] Armstrong R.W. and Elban W.L., Mater. Sci. Eng. A111 (1989) 35-43.

[19] Klapper H., Characterization of Crystal Growth Defects, B.K. Tanner and H.K. Bowen Eds. (Plenum Press, NY, 1980) pp. 133-160.

[20] van der Steen A.C. and Duvalois W., "What Do Explosive Particles Look Like", ONR/TNO Workshop on Desensitization of Explosives and Propellants, Prins Maurits Laboratory, Rijswijk, The Netherlands, 11-13 November 1991, Preprints Volume 3, pp.1.

[21] Elban W.L., Hoffsommer J.C. and Armstrong R.W., J. Mater. Sci. 19 (1984) 552-566.

[22] McDermott I.T. and Phakey P.P., J. Appl. Cryst. 4 (1971) 479.

[23] Halfpenny P.J., Roberts K.J. and Sherwood J.N., J. Mater. Sci. 19 (1984) 1629-1637.

[24] Elban W.L., Armstrong R.W., Yoo K.C., Rosemeier R.G. and Yee R.Y., J. Mater. Sci. 24 (1989) 1273-1280.

[25] Hoffsommer J.C., Glover D.J. and Elban W.L., J. Energetic Mater. 3 (1985) 303.

[26] Armstrong R.W., Ammon H.L., Du Z.Y., Elban W.L. and Zhang X. J., "Energetic Crystal-Lattice-Dependent Responses", Structure and Properties of Energetic Materials, D.H. Liebenberg, R.W. Armstrong and J.J. Gilman Eds. (Materials Research Society, Pittsburgh, PA 1993) pp. 227-232.

[27] Hammond B.L. and Armstrong R.W., Philos. Mag. Lett. 57 (1988) 41-47.

[28] Tsai D.H. and Armstrong R.W., "Molecular Dynamics Modeling of Hot Spots in Monatomic and Molecular Crystals Under Rapid Compression in Different Crystal Directions", International Conference on Shock Waves in Condensed Matter, St. Petersburg, Russia, 18-22 July 1994, (Russian) J. Chem. Phys., in print.

[29] Tsai D.H., J. Chem. Phys. 70 (1979) 1375.

[30] Tsai D.H. and Armstrong R.W., "Defect Enhanced Structural Relaxation Mechanism for the Evolution of Hot Spots in Rapidly Compressed Crystals", J. Phys. Chem., in print.

[31] Armstrong R.W. (Traduction: J. Boileau), Revue Scientifique et Technique de la Défense, 16 (1992) 161-164.

[32] Armstrong R.W. and Elban W.L., "Dislocation Roles in Energetic Crystal Responses", ONR/LANL Workshop on the Fundamental Physics and Chemistry of Combustion, Initiation and Detonation of Energetic Materials, Los Alamos National Laboratory, NM, 3-6 March 1992 (Chemical Propulsion Information Agency Publication 589, 1992) pp. 367-378.

[33] Nielson A.T., Working Group Meeting on Sensitivity of Explosives (Center for Energy Technology and Research, New Mexico Institute of Technology, 1987) pp. 256-276.

[34] Boddington T. Ninth Symposium (International) on Combustion (Academic Press, NY, 1963) pp. 287.

[35] Sandusky H.W., Glancy B.C., Carlson D.W., Elban W.L. and Armstrong R.W., J. Propulsion Power (1991) 518-525.

[36] Elban W.L., Sandusky H.W., Beard B.C. and Glancy B.C., J. Propulsion Power 11 (1995) in print.

[37] Armstrong R.W. and Zerilli F.J., Mech. Mater. 17 (1994) 319-327.

JOURNAL DE PHYSIQUE IV
Colloque C4, supplément au Journal de Physique III, Volume 5, mai 1995

Shock-Wave Behavior in Explosive Monocrystals

J.J. Dick

MS P952, Los Alamos National Laboratory, Los Alamos, New Mexico 87545, U.S.A.

Abstract

The shock response of explosive monocrystals is strongly anisotropic. Shock initiation sensitivity depends strongly on crystal orientation in PETN. This can be understood in terms of steric hindrance to shear during the shock-induced deformation of the molecular crystal. This initiation mechanism appears to be tribochemical rather than thermal. Related work by other researchers is also discussed.

In our work we have observed that the shock sensitivity for initiation of detonation depends strongly on the orientation of the crystal relative to the shock wave.[1,2] This implies that the initiation process in monocrystals is not simply a bulk thermal process, since the shock-induced temperature increase should not depend strongly on orientation. It must be controlled by some anisotropic crystal property. We have been able to explain our observations in terms of anisotropic shear flow in the uniaxial strain of a plane shock wave. The maximum resolved shear stress in a plane shock wave is at 45° to the plane of the shock wave in a homogeneous, isotropic material. In a crystal the shear flow will occur on a crystallographic plane near 45°. In molecular crystals the molecules are able to pass by each other without interference on some planes, but on other planes the molecules present obstacles to each other's passage in the shear flow. In PETN (pentrite) the O-NO_2 arms interfere with each other in some orientations. We have termed this effect steric hindrance to shear. We have found that orientations that have strong hindrance have high sensitivity especially at low stresses. The orientations with low hindrance are insensitive. No detonation has been observed in them up to 19 GPa in crystals up to 10 mm thick.

We have studied four orientations. We have found [100] and [101] orientations to be insensitive and [110] and [001] to be sensitive by shock experiments and by steric hindrance analysis. An example of this orientation-dependent initiation sensitivity is shown in Fig. 1. Laser interferometer (VISAR) records for [100] (insensitive) and [001] (sensitive) orientations shocked to 4.18 GPa are shown. The particle-velocity history for the [100] orientation shows a single wave to the final state. Behind the shock the particle velocity is essentially constant as would be expected for inert behavior. For the [001] orientation there is a double-

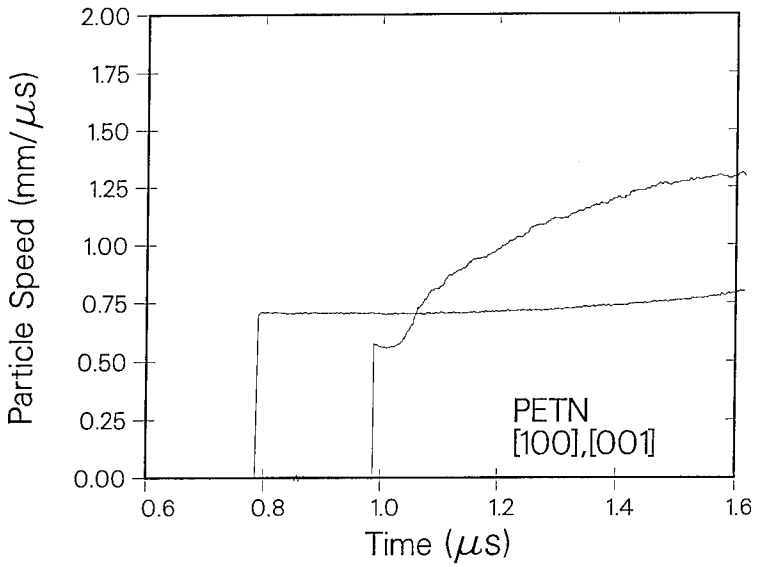

FIG. 1. Particle vs time histories at the PETN/PMMA interface for [100] and [001] orientation crystals shocked to an input stress of 4.18 GPa. The [100] record begins at 0.790 μs and the [001] record begins at 0.988 μs.

wave structure. This is an elastic shock followed by a plastic or inelastic wave to the particle velocity of about 0.7 mm/μs. This elastic-plastic behavior is described in detail in Ref. 3. Behind the plastic wave is a region of constantly increasing particle velocity. This is due to the exothermic decomposition in the initiation process for this sterically hindered case. Luminescent radiation has been observed from the sensitive orientations at this shock strength using image intensifier cameras, photodiodes, and spectrographs. Previous analysis indicates that this radiation is from excited electronic states of NO_2 and possibly NO.[1] Recent analysis indicates that the radiation begins at the base of the plastic wave. This coincides with the onset of the sterically hindered shear and suggests that the first endothermic step in initiation in explosive monocrystals may be tribochemical owing to bond breaking by the sterically hindered shear process.

This orientation-dependent sensitivity has been corroborated by L. Soulard.[4] He studied [111] and [001] orientations of PETN with PVDF gauges at shock strengths from 5 to 11 GPa. His results show considerable more reactivity for the [001] orientation than for the [111] orientation.

Rudel and coworkers have studied the orientation dependence of the favorability for detonation in PETN and nitromethane crystals.[5] They described the favorability in terms of straight chains of N atoms and short inter-nitrogen distances in the shock direction as well as transverse rigidity supported by large N-O bond angles in the crystal. It is interesting that they found favorability in the same orientations that we found to be sensitive to initiation in these explosives.[1,6] It would be interesting to understand the relationship between the two models of steric effects.

At low stresses we have found anomalous sensitivity in that the run distance to detonation is shorter at 4.2 GPa than at 8.5 GPa for the [110] orientation. By studying the induction time for the onset of emission, D. Spitzer has shown that this anomalous sensitivity is strongest at about 5 GPa.[7] We undertook a series of VISAR laser interferometer experiments at 4.2 GPa in order to try to understand the basis for this anomaly. They displayed an elastic-plastic, two-wave structure. The anomaly is apparently associated with this struc-

ture. Our tentative conclusion is that the prestrain generated by the elastic wave makes the sterically hindered shear even more effective in causing explosive initiation chemistry.

M. Samirant has reported detonation velocities for PETN for [100] and [001] orientations.[8] The [100] orientation is one for which no sign of initiation has been observed in our experiments to 19 GPa. The experiments include wedge, VISAR, and image-intensifier camera types. In Samirant's experiments the PETN crystals were initiated by detonating explosive in contact. This implies an input shock strength of about 30 GPa. It seems reasonable that even the insensitive, hindered orientations will detonate if shocked at detonation pressure.

In order to confirm this we have performed some exploratory experiments of mass spectrometry of reaction products of initiating and detonating PETN crystals with N. R. Greiner.[9] Complete mass spectra are obtained at 12 μs intervals in the vacuum chamber. PETN crystals of hindered, sensitive [110] (0.8 mm thick) and unhindered, insensitive [101] (1.1 mm thick) orientations were subjected to pressures of 18 and 30 GPa using 1.55 g/cm^3 TATB and 1.65 g/cm^3 HMX, respectivly, in contact. Two experiments were performed at each pressure with each orientation. The results were not completely reproducible, but the spectra are indicative of final detonation products at 30 GPa for both orientations. At late times there is evidence of undecomposed PETN for the [101] orientation. At 18 GPa for [110] orientation there is early evidence of final detonation products and some unreacted PETN signal at later times. For [101] there are some weak signals of early decomposition products along with unreacted PETN signal at later times. Overall, the results corroborate the results stated in the previous paragraph that all orientations detonate when subjected to detonation pressures even though the initiation sensitivity varies greatly at lower pressures.

The question remains as to whether the first endothermic, bond-scission step is a tribochemical one or due to local molecular thermal excitation by the steric hindrance in terms of phonon-vibron up-pumping. In Fig. 2 are shown radiance spectral data for the two sensitive orientations shocked to about 4.2 GPa. Grey body curves from Planck's law are also shown. The temperatures were chosen so that the curves had peak radiance at about the same wavelength as the radiance data from the shock experiment. The emissivity constants were chosen to match the experimental peak radiance. The temperatures of 5000 and 6000 K are unreasonably high and the experimental data have a different form than that given by Planck's law for a black or grey body. This can be interpreted as more evidence the radiation observed is luminescence from excited electronic states, not thermal radiation. The timing of the luminescence coinciding with the beginning of the plastic wave and shear flow suggests that it may be due to a tribochemical process, (i.e., a mechanical process analagous to friction caused by the stericaly hindered shear flow). The molecules become obstacles to one another and are not able to deform enough to pass by in the time scale involved.[3]

Subsequent processes in the exothermic buildup to detonation may likely be occurring in localized regions of the crystal, perhaps in slip bands. This concentrates the shock energy and subsequent heat release in a small fraction of the crystal during the initial phase of initiation. This failure mechanism under shock conditions may be similar to that observed by Ananin and coworkers[10] in crystalline quartz, a material with similar mechanical properties.

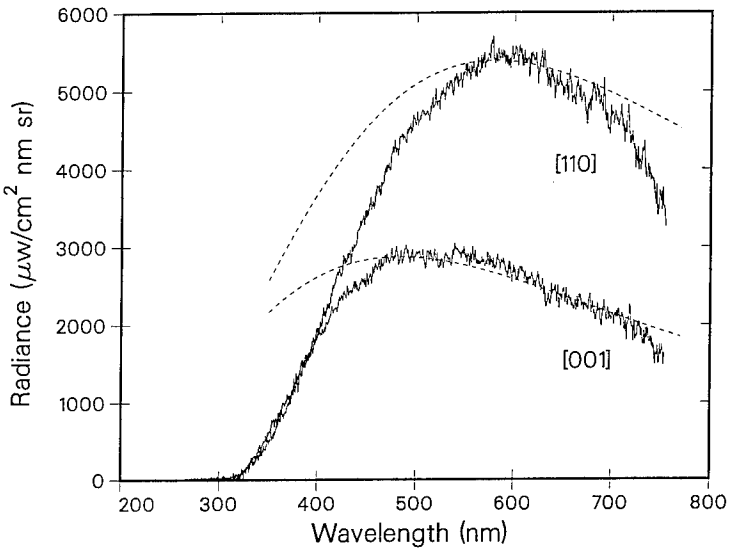

FIG. 2. Emission spectra of [110] and [001] orientations of PETN shocked to 4.2 GPa. Shock position is 1.8 to 2.4 mm during the acquisition of the data. The dashed lines represent grey-body curves from Planck's law. For [110] the grey-body temperature is 5000 K and the emissivity is 0.0042. For [001] the temperature is 6000 K and the emissivity is 0.0009.

REFERENCES

* This work was performed under the auspices of the U. S. Department of Energy and partially supported by the Office of Munitions Memo of Understanding between the Department of Energy and the Department of Defense.

[1] J. J. Dick, R. N. Mulford, W. J. Spencer, D. R. Pettit, E. Garcia, and D. C. Shaw, J. Appl. Phys. **70**, 3572 (1991).

[2] J. J. Dick, Appl. Phys. Lett. **44**, 859 (1984).

[3] J. J. Dick and J. P. Ritchie, J. Appl. Phys. **76**, 2726 (1994).

[4] L. Soulard, thesis, "Etude du Monocristal de Pentrite Soumis a un Choc Plan," L'Universite de Haute-Alsace, 1990; L. Soulard and F. Bauer, in *Shock Compression of Condensed Matter–1989*, edited by S. C. Schmidt, J. N. Johnson, and L. W. Davison (Elsevier, Amsterdam, 1990),p. 817.

[5] P. Rudel, S. Odiot, J. C. Mutin, J. C. Peyrard, J. Chim. Phys. **87**, 1307 (1990).

[6] J. J. Dick, J. Phys. Chem. **97**, 6193 (1993).

[7] D. Spitzer, thesis, "Etude du Role des Defauts de Taille Microscopique dans la Transition Choc-Detonation du Monocristal de Pentrite," Universite Louis Pasteur de Strasbourg, p. 153, 1993.

[8] M. Samirant, J. Phys. (Paris) **48**, C4-85 (1987).

[9] N. R. Greiner and N. C. Blais, *Ninth Symposium (International) on Detonation*, (Office of Naval Research, Arlington, VA, 1989), p. 953. also N. C. Blais, H. A. Fry, and N. R. Greiner, Rev. Sci. Instrum. **64**, 174 (1993) and in Tenth Symposium (International) on Detonation, in press.

[10] A. V. Ananin, O. N. Breusov, A. N. Dremin, S. V. Pershin, and V. F. Tatsii, Fiz. Goreniya Vzryva, **10**, 426 (1974) .

JOURNAL DE PHYSIQUE IV
Colloque C4, supplément au Journal de Physique III, Volume 5, mai 1995

Shock Wave Interaction with Composite Materials

A. van der Steen

TNO Prins Maurits Laboratory, Lange Kleiweg 137, P.O. Box 45, 2280 AA Rijswijk, The Netherlands

Abstract: A large number of physical and chemical parameters determine the sensitivity of explosives. Special emphasis is placed on the influence of the crystal quality on the initiation process. First the crystal size is considered for monomodal and bimodal distributions. It seems that the Lee-Tarver model is not capable to explain all the experimental observations. Other parameters like the crystal shape, the smoothness of the surface of the crystal, internal defects and dislocations (like voids), and the effect of a binder in a PBX are also discussed. From the experimental results known up to now it is clear that an optimised crystal quality can help to obtain less sensitive explosives. For this the study of the crystallisation process is a key item.

1. INTRODUCTION

The sensitivity of explosives is like a balance. On one side the explosive has to be as insensitive as possible to enhance the safety and on the other side the functioning of explosives will be negatively effected if the sensitivity is too low. For those reasons sensitivity has always been a topic in the detonation community.

To describe the sensitivity of explosives is very complicated. First of all it is an intrinsic property of the explosive molecule itself. Enormous progress is being made in relating the chemical structure to the sensitivity. While Kamlet related sensitivity to the composition of organic explosives, later Delpuech and Odiot linked the sensitivity to the properties of the excited electronic state of the molecule [1]. In this way a relatively good estimate of the sensitivity of a new molecule can be obtained before it has ever been sensitised.

On a larger scale the physical properties of the crystal lattice play a role in the sensitivity. Coffey and Armstrong for example relate the mechanical properties of the lattice to the impact sensitivity [2]. They assume that a pile-up of phonons will occur on dislocations in the lattice and will act as ignition sites. Many investigators have related the crystal size to the sensitivity. Moulard has shown the importance of the crystal size in relation to the shock sensitivity of PBX's [3]. Spear has investigated the shock sensitivity of RDX as a function of the crystal size [4]. A more theoretical approach is given by the Lee-Tarver model that describes the ignition and pressure build-up during shock initiation assuming spherical particles with one specific diameter.

However, crystals never behave ideally and most of the time the imperfections in the crystals determine physical properties such as the shock sensitivity. Just as for liquid explosives that can be sensitised by air bubbles, the sensitivity of solid explosives depends strongly on the number and type of dislocations and imperfections in the crystal lattice. Mishra was one of the first who showed experimentally that the impact sensitivity of RDX depends on the solvent used for crystallisation [5]. The different solvents resulted in

different crystal shapes. Also van der Steen et al. have shown the influence of the crystal shape on the shock sensitivity [6]. They have shown that a decrease of the critical initiation pressure of more than 1 GPa can be reached if speroidized crystals with smoothed surfaces are used. Borne has shown that the concentration of voids in RDX crystals effects the sensitivity [7]. The small number of experimental evidence is contrary to the large number of theoretical models describing the creation of hot-spots.

A last but certainly not least important contribution comes from the state in which the explosive is applied. Large single crystals are not used in warheads or boosters. All kinds of different processing techniques are used and processing aids are added to make the explosive applicable: pressing, casting, extruding, mixing (like CompB), addition of waxes or polymers, plasticizers, etc.. Pressed explosives with a minimum of voids between the binder and the explosive have a significantly higher sensitivity than cast-cured explosives. The interaction between the binder and the explosive contributes also to the sensitivity. According to Swallone the mechanical properties of the polymer influence the sensitivity of the PBX [8]. This is also suggested by Shedelbauer [9]. Others have investigated the influence of the impedance mismatch of the binder and the explosive to the sensitivity. Schrader et al. have shown that the decomposition of the polymer followed with catalytic decomposition of the explosive can increase the sensitivity of AP-based rocket propellants [10].

The above shows that there is a large range of interest from the fundamental level of understanding for the explosive molecule until the application of a PBX in a warhead or as a booster. In all stages we have to understand the nature of the sensitivity of explosive. At TNO-PML we are trying to understand and control the sensitivity of RDX-based PBX's by controlling the quality of the RDX crystals. In that way we try to understand the role of the crystal size, crystal defects and imperfections, crystal interaction with the binder and with other crystals, etc. However it seems that each question being solved generates more new questions. In the following chapters a series of examples is given on different factors effecting the sensitivity of explosives.

2. EXPLOSIVE AND TEST METHOD

Most experiments are carried out on cast-cured HTPB-based PBX's with RDX as a high explosive. The solid loading of the PBX varies depending on the use of monomodal (65%) or bimodal (85%) RDX. Standard procedures and binders are used to cast-cure the PBX [6].

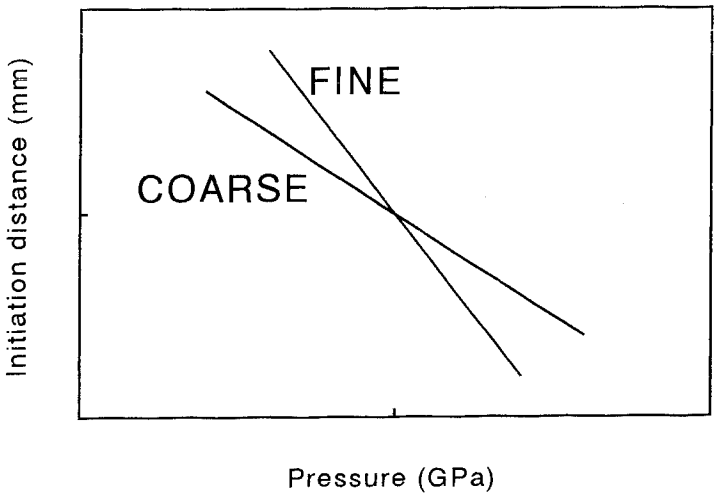

Figure 1: Schematic representation of the initiation distance of an explosive consisting of coarse or fine crystals, as a function of the initiation pressure.

The shock sensitivity of the PBX's is determined with a gap test [6]. It has a diameter of 50 mm, hexocire as a donor explosive (an RDX-wax composition) and a PMMA gap. Using an optical streak camera the distance between the PMMA-acceptor interface and the place the detonation wave emerges from the outer surface of the charge is measured. This initiation distance is slightly different as measured on the central axis of the set-up but this test method allows fast experiments. The initiation distance is measured as a function of the shock pressure in the PMMA at the PMMA-explosive interface. The initiation distance is considered to be a good description of the shock sensitivity of the charge.

3. MONOMODAL RDX

Generally it is accepted that the critical initiation pressure becomes higher if the crystal size decreases. Schematically this is illustrated in Figure 1. It is assumed that at relatively low pressures the composition with the coarser crystals is more sensitive (gives shorter initiation distances) because those crystals are more easily ignited than the finer crystal. In other words the ignition process is the controlling step. At higher pressures the growth of the reaction is controlling and the larger surface area of finer crystals causes a higher sensitivity. This crossing of the sensitivity as a function of the initiation pressure has been found by several investigators. Table 1 lists the particle sizes of four batches of RDX with different crystal sizes (two coarse and two fine batches).

Table 1: Average crystal size (50%), 10% and 90% limits of the crystal size distribution and specific surface of two fine and two coarse RDX batches.

	50% μm	10%-90% μm	Specific surface m^2/cm^3
F1	4.7	2.2-10.7	1.65
F2	47	27-73	0.1567
C1	234	177-315	0.0305
C2	522	416-698	0.0124

In Figure 2 the initiation distances for four PBX's with a solid loading of 65% RDX are given as a function of the initiation pressure. No crossing of the sensitivities is observed at higher pressures. The largest crystals (C2) are not the most sensitive but the sensitivity lies in between the sensitivity of the F2 and C1 crystals.

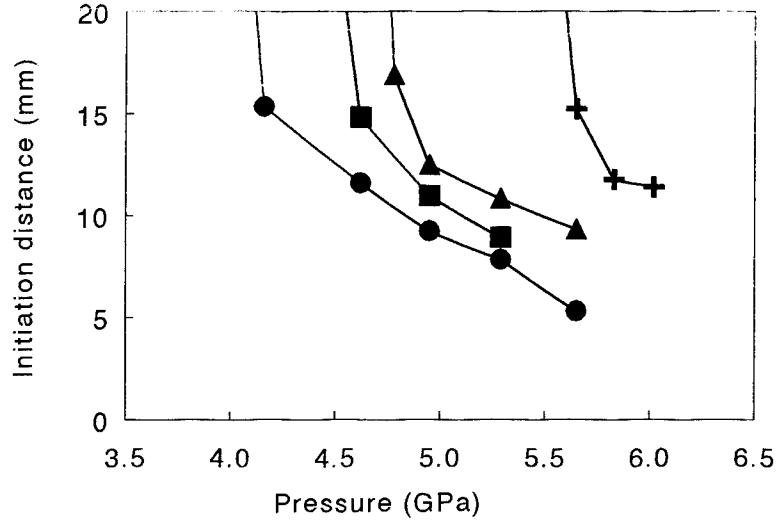

Figure 2 Initiation distances as a function of the initiation pressure for four PBX's with different RDX crystals, see Table I. ● = C1, ■ = C2, ▲ = F2 and + = F1.

Crossing of the sensitivities is observed when the initiation distances are determined with a so-called electric gun. In that case the explosives are initiated by the impact of a thin kapton flyer. For thin flyers the rare-faction waves extinguish the shock waves and therefore much higher pressures are needed to initiate the explosive. Two different thicknesses of flyers (125 μm and 250 μm) are used and the thicker the flyer the more the shock wave will resemble the initiation wave for the gap test. Results are presented schematically in Figure 3. Contrary to the gap test the coarse crystals are the most sensitive for a flyer thickness of 125 μm. The critical pressure for the fine is about 21 GPa and for the coarse 15 GPa. For a flyer of 250 μm these critical pressures lie much closer together although the fine is still the most sensitive (10 and 12 GPa). As has been observed already in Figure 2 the situation is reversed for the gap test experiments although the difference is still very small (about 4 and 6 GPa). More details can be found in reference [11].

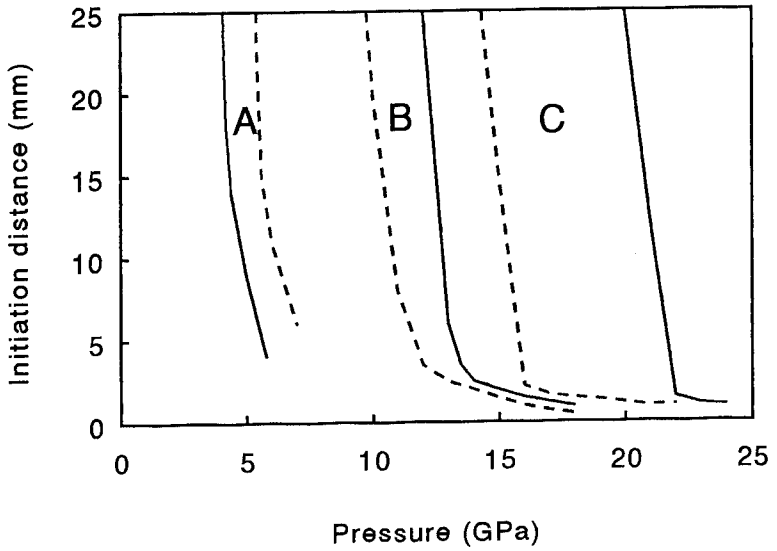

Figure 3: Schematic representation of the initiation distances as a function of the initiation pressure for PBX's with fine (----) and coarse (——) RDX for three different impulses. A: gap test, B: flyer 250 μm, C: flyer 125 μm.

These results for monomodal RDX indicate that in general the model of Figure 1 holds for the sensitivity of explosives. Deviations occur as is demonstrated in Figure 2 and can be found in [11]. Also the length of the pressure pulse has to be taken into account. The influence of the solid loading, all presented experiments have a solid loading of 65%, on the shock initiation process has to be clarified further. It seems that the application of different thicknesses of flyers in the electric gun offers a very simple and fast technique to study the initiation of explosives as a function of the length (impulse) of the shock wave.

4. BIMODAL RDX

Bimodal mixtures of RDX are applied to increase the amount of high explosive in the PBX. To explain the sensitivity for bimodal mixtures becomes however more complicated. Important parameters are - again - the crystal sizes and the ratio of the coarse and fine fraction applied.

In Figure 4 the sensitivities of two PBX's with bimodal RDX are compared. The coarse fraction has in both cases the same diameter (370 μm). The fine fraction is about 20 μm for one sample and 55 μm for the other. The coarse fine ratio is 64/36. It shows that the PBX with the smallest crystals has a critical pressure that is about 0.5 GPa lower than for the larger crystals.

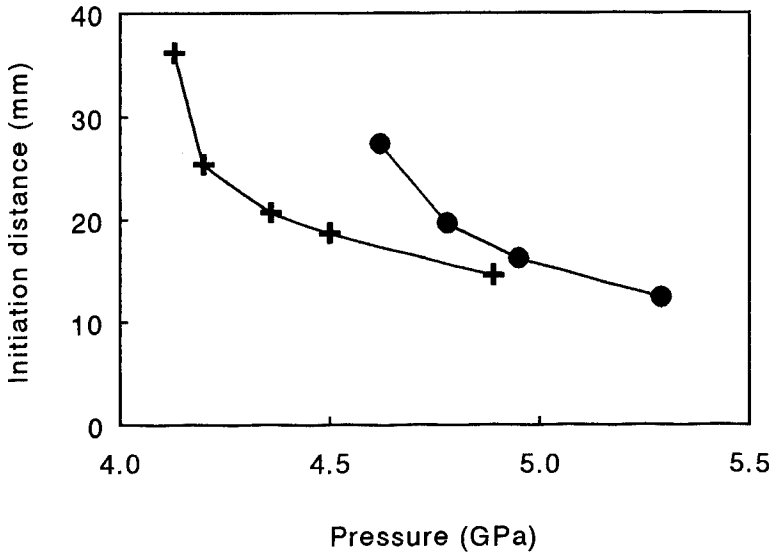

Figure 4 Initiation distances as a function of the initiation pressure for a PBX with a fine fraction of 20 μm (○) and a fine fraction of 55 μm (●). The coarse fraction is the same for both RDX's.

The same is observed by varying the ratio coarse/fine in the PBX. The results for three coarse/fine ratio's are shown in Figure 5. In this case also the PBX with the largest amount of fine crystals is the most sensitive.

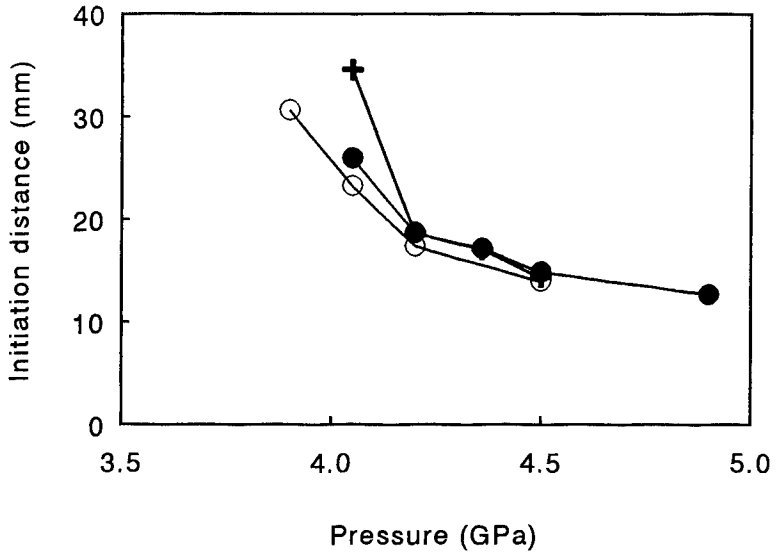

Figure 5 Initiation distance as a function of initiation pressure for PBX's with different ratio's of coarse and fine RDX. O) C/F = 59/41, ●) C/F = 64/36, +) C/F = 76/24.

Both observations seem to be contradictory to the model shown in Figure 1. It assumes that (at relatively low pressures, and that is the case in these examples) the smaller the crystals the less sensitive is the explosive. The reversal in the bimodal samples is caused by the presence of the coarse crystals. If fine and coarse crystals are both present in a PBX it is most likely that the coarse crystal will be ignited at the lowest (critical) pressures. The subsequent build-up to a detonation reaction will be determined by the specific surface of the RDX. Since this is considerably higher for the fine crystals it is not unexpected that

the increase of the amount of fine crystals or the decrease of the crystal size of the fine fraction increases the sensitivity of the PBX.

These results are only qualitatively and many questions remain. For example it is not yet clear how the distance between the coarse and the fine crystals effects the initiation process (how is the energy transfer). Also it is not evident how much of a coarse fraction is needed to ignite the decomposition reaction. And last but certainly not least: why are the coarse crystals the most sensitive?

5. MODELLING

There are many models available to simulate the shock initiation of explosives. The most well known are the Forest Fire and the Lee-Tarver model. The Forest Fire model is very crude and empirical and cannot be applied to parameter studies as are presented above. The model is more suitable for simulating the shock initiation behaviour of different explosives.

The Lee Tarver model is also referred to as the ignition and growth model and is founded on the knowledge that the shock initiation in heterogeneous explosives is based on the formation and subsequent reaction of the hot spots that are created when the shock pulses compresses the solid. In the model one ignition term and two growth terms are applied. The ignition and growth terms can help to understand qualitatively the shock initiation process. They could be an indication for the number of defect where ignition starts and how easily a reaction grows to completion. A disadvantage of the model is that it can only simulate one (spherical) particle size. Bimodal mixtures (two crystal sizes) cannot be simulated. The transfer of the ignition reaction from the coarse crystals to the fine crystals is not yet understood.

The simulation of monomodal explosives gives some interesting result [12]. In these simulations the initiation distance was calculated as a function of the initiation pressure. In Figures 6 the results are given for a variation of the amplitude of the first growth term (G1) and the ignition term (I).

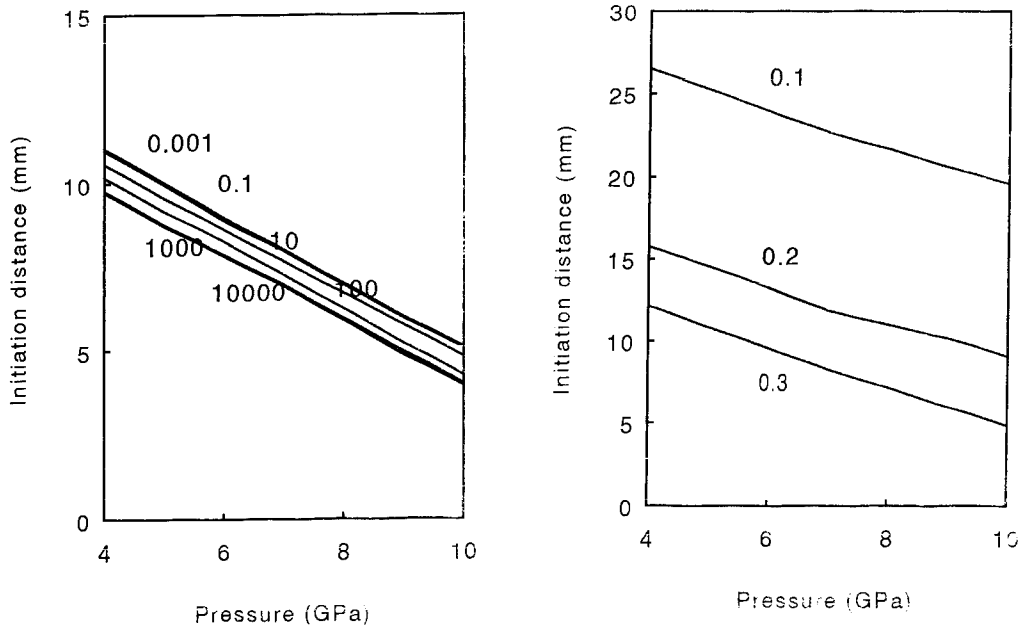

Figure 6. The simulated initiation distance as a function of the initiation pressure for different values of the ignition term (left) and the growth term (right) in the Lee-Tarver model.

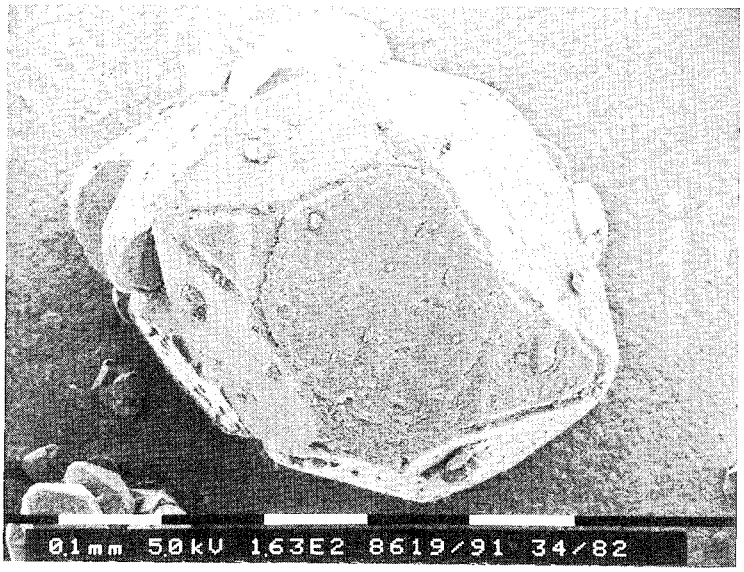

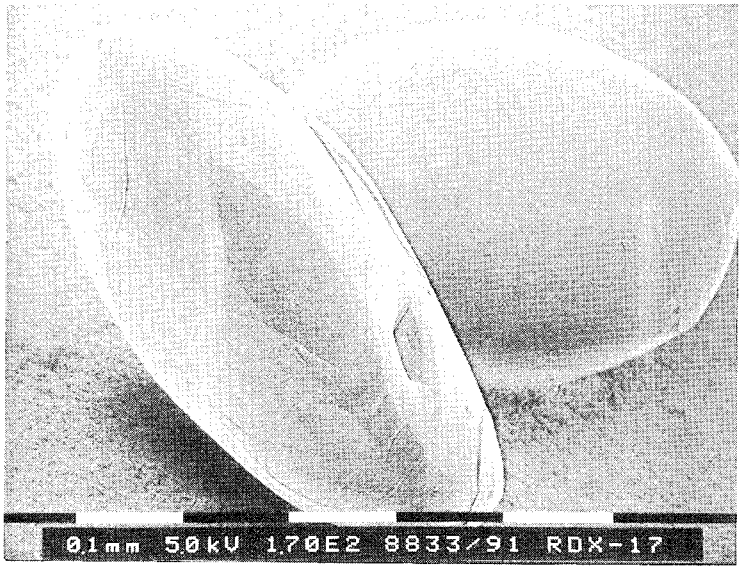

Figure 7: Scanning Electron Micrographs of a typical RDX crystal (top) and a crystal that has been post-treated (bottom) to obtain a better morphology.

These results show that the growth terms dominate the initiation process. A variation of 0.05 to 0.3 in the growth term results in a much larger variation in the initiation distances than a variation of 10^{+7} in the ignition term. This seems to be in accordance with the findings for the bimodal mixtures. For those mixtures it is also found that small variations in the fine material (growth) causes large variations in the sensitivity. On the other hand, these simulations do not explain the results for the monomodal PBX's. Considering the simulations the ignition term plays a minor role and the crossing of the sensitivity curves cannot be explained.

6. CRYSTAL QUALITY

All results presented above are interpreted with respect to the crystal size and the crystal size distribution while the crystals are assumed to be spheres. Unfortunately crystals seldom have the shape of a sphere. This is illustrated in Figure 7 where two Scanning Electron Micrographs (SEM) are given of RDX crystals. Both have about the same diameter. One has the typical structure of an RDX crystal as obtained directly from the recrystallization vessel. The faces of the crystal can be assigned to the different growth directions of the crystal. The other crystal is more oval shaped and has a very smooth surface. This crystal has been post-treated with the solvent ethyl acetate. Its morphology is much more regular and can be defined with only two parameters.

The influence of the morphology of the crystals on the shock sensitivity is shown in Figure 8. PBX's with the same fine fraction (47μm) but with an angular and not post-treated coarse fraction and a coarse fraction that has been post-treated are compared. The diameter of the coarse fraction is 480 μm before the post-treatment and 450 μm afterwards. It shows that especially at the initiation threshold the PBX with the smoother crystal is about 0.4 GPa less sensitive than the angular crystals. The differences are less pronounced for the higher pressures. Unfortunately the sensitivity for monomodal PBX's has not (yet) been measured.

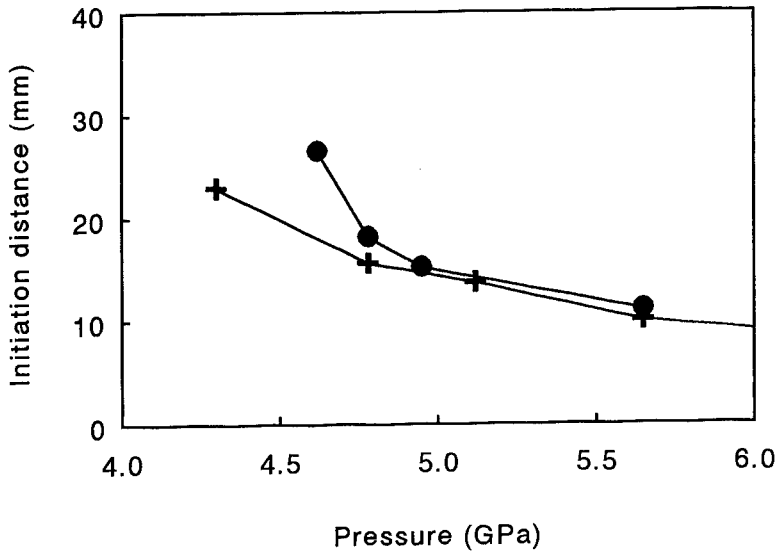

Figure 8: Initiation distances as a function of initiation pressure for a PBX with +) angular crystals and ●) oval shaped crystals as the coarse fraction.

These results show that not only the particle size plays a role in the sensitivity but also the morphology of the crystals. There are several possible explanations for the decreased sensitivity:

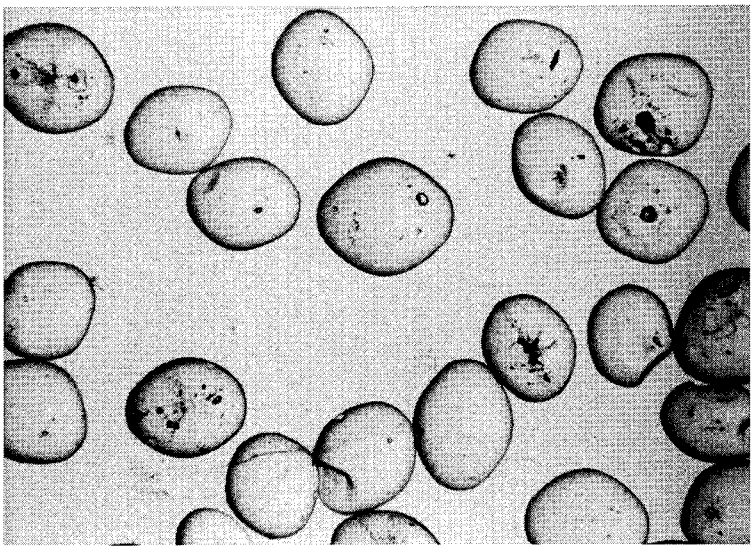

Figure 9: Light microscopy of RDX crystals. Empty and filled voids are visible.

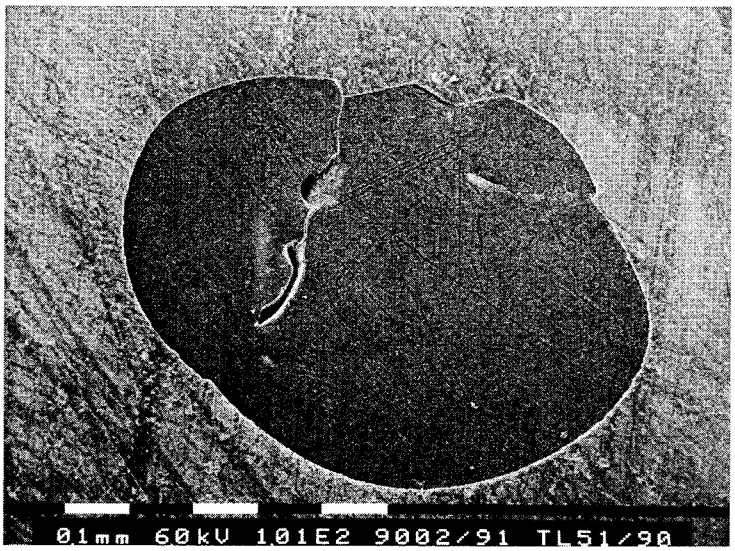

Figure 10: SEM picture of a cross section of an RDX crystal. A void and different crystals orientations are visible.

- The tap density with the spheroidized particles is higher. The increased average distance between the crystals could cause the decreased sensitivity.
- A better contact between the binder and the crystal is possible for smoother crystals, voids could still be present at the interface for the angular crystals and cause ignition.
- Angular crystals are more sensitive than speroidized crystals because ignition occurs at the corners of the crystals.

The morphology tells something about the "outside" of the crystals. Figure 9 shows the "inside" of RDX crystals as can be seen with a light microscope. Voids, sometimes filled with solvent, of all different sizes and shapes can be observed. In Figure 10 a cross section is given of one crystal. An elongated void that was probably filled with the solvent is clearly visible. All these imperfections are caused by the crystallisation process. Depending on the type of crystallisation (cooling, evaporation, etc.) and the growing rate the internal and external quality of the crystal will be influenced. Borne has already indicated that crystals with a higher density, and therefore a smaller number of voids, have a lower initiation threshold [7]. Also Chan has shown that the sensitivity of CL20 can be less by improving the crystallisation method [13]. It is assumed that these voids act as ignition sites. Void collapse, adiabatic heating, plastic flow, etc. are generally considered as the processes to form hot-spots.

Cutting crystals and etching the surfaces yields even more information as can be seen in Figure 11. The different growth directions and the interfaces in between are clearly visible. It can not be excluded that at these interfaces with a relatively high number of dislocations a pile-up of energy occurs as has been described by Coffey and Armstrong [2]. Crystallisation studies and detailed techniques to follow the initiation (or better the ignition and growth) processes have to reveal these questions in the future.

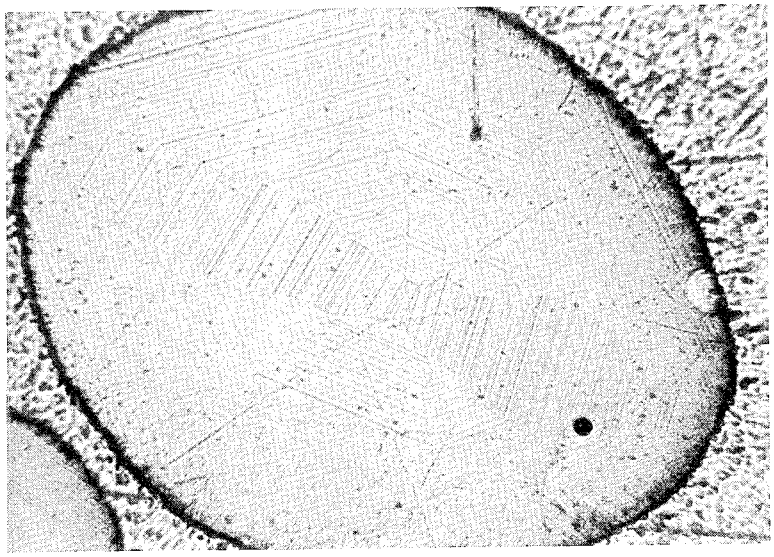

Figure 11: Cross section of an RDX crystal. The growth sectors and a seed crystal in the centre are clearly visible.

7. CONCLUSIONS

Most of the time fundamental studies on sensitivity refer to ideal systems as one molecule or a single crystal. It is impossible to detonate a molecule and from the studies of Dick on PETN [14] we know that it is very hard to detonate a crystal. Recently at Lawrence Livermore National Laboratory it has been shown that initiation in single crystals only occurs after the shock wave has reflected against an interface.

This paper has tried to give some more insight in physical parameters affecting the sensitivity. The results are mainly qualitative and still many questions remain. The most important are:

- How are (coarse) crystals ignited?
- How does the energy transfer between crystals take place?
- How far can we decrease the sensitivity of an RDX based PBX by optimising the crystal quality?

It is this last question that is the most important. Crystallisation of RDX is getting more attention in the detonation community at the moment and hopefully there will be a few answers in the coming years.

Acknowledgements

The research project was carried out under assignment A93KL447 for the Royal Dutch Army. The author would like to thank all his colleagues who contributed to this work: Willem Duvalois, Aat Hordijk, Antoine van der Heijden, Wim Prinse, Murk van Rooijen, Benoit Coleau, Jos Mul, Rene Oostdam, Ries Verbeek en Ed de Jong.

References

1. A. Delpuech, Initiation des explosifs à l'échelle moléculaire, Approches Microscopique et Macroscopique des Détonations (Les éditions de Physique, Megève, 1987), 353 (1987)
   A.E. Delpuech, The use of time-resolved spectrometries in the study of initiation of explosives at molecular level, Proceedings Ninth Symposium (International) on Detonation, Portland, 172 (1989)
   S. Odiot, Mechanisms of detonation in molecular crystals: a review, Approches Microscopique et Macroscopique des Détonations (Les éditions de Physique, Megève, 1987), 225 (1987)
   S. Odiot and M. Peyrard, Why does an explosive explode?, Approches Microscopique et Macroscopique des Détonations (Les éditions de Physique, Megève, 1987), 393 (1987)
2. C.S. Coffey, Energy localization and the initiation and detonation of crystalline explosives by shock or impact, Proceedings Workshop Desensitization of Explosives and Propellants, TNO Prins Maurits Laboratory, Rijswijk, The Netherlands, November 1991
   R.W. Armstrong, Dislocation mechanics aspects of desensitization to impact or shock deformations, Proceedings Workshop Desensitization of Explosives and Propellants, TNO Prins Maurits Laboratory, Rijswijk, The Netherlands, November 1991
   C.S. Coffey and R.W Armstrong, This workshop
3. H. Moulard, J.W. Kury and A Declos, The effect of RDX particle size on the shock sensitivity of cast PBX formulations, Proceedings Eight Symposium (International) on Detonation, Albuquerque, 902 (1985)
   H. Moulard, Particular aspects of the explosive particle size effect on shock sensitivity of cast PBX formulations, Proceedings Ninth Symposium (International) on Detonation, Portland, 18 (1989)
4. R.J. Spear and V. Nanut, Mechanism of and particle size effects on shock sensitivity of heterogeneous pressed explosives: preliminary assessment of binderless RDX in fuze trains, DOD Materials Research Laboratories, Melbourne Australia, MRL-R-1077 (1987)
5. I.B. Mishra and L.J. Vande Kieft, Novel approach to insensitive explosives, 19th International Annual Conference of ICT 1988, Karlsruhe, 25-1 (1988)
6. A.C. van der Steen, H.J. Verbeek and J.J. Meulenbrugge, Influence of RDX crystal shape on the shock sensitivity of PBXes, Proceedings Ninth Symposium (International) on Detonation, Portland, 83 (1989)
   A.C. van der Steen and E. Skjold, RDX particle shape and the sensitivity of PBXes, 1990 Joint Government/Industry Symposium on Insensitive Munitions Technology (Addendum Proceedings), White Oak, 235 (1990)

A.C. van der Steen, E.G. de Jong, W.C. Prinse, A.C. Hordijk and W Duvalois, Crystal quality and shock sensitivity of RDX-based PBXes, Tenth Symposium (International) on Detonation, Boston, (1993) to be published
7. L. Borne, Influence of intragranular cavities of RDX particle batches on the sensitivity of cast plastic bonded explosives, Proceedings Tenth Symposium (international) on Detonation, Boston, (1993) to be published
8. G.M. Swallone and J. Field, Proc. R. Soc. Lond. A., Vol. 379, 389 (1982)
9. F. Schedlbauer and A. Kretschmer, The influence of particle size and mechanical properties on the sensitivity of high explosive charges (PBX), Proceedings Tenth Symposium (International) on Detonation, Boston, (1993) to be published
10. M.A. Schrader, M.W. Leeuw and A.C. van der Steen, The heat sensitivity of solid propellants, AGARD Conference Proceedings No. 367, Hazard studies for solid rocket motors, Lisse, 19 (1984)
11. W. Prinse, M. van Rooijen, B. Coleau, J. Mul, R. Verbeek and A. van der Steen, Shock sensitivity testing of explosives with the gap test and thin flyer impact test, Europyro 1995, to be published
12. R. Verbeek and A. van der Steen, The simulation of shock initiation of less sensitive explosives using the hydrocode autodyn, Proceedings Tenth Symposium (international) on Detonation, Boston, (1993) to be published
13. M. Chan, NAWC, China Lake, Private communications
14. J. Dick, This workshop

1-4 Discussion

Moderator : Claude Fauquignon, Institut de Recherches Franco-Allemand

The preceding lectures have given the generally admitted theory of the Detonation in an ideal (1D-steady) geometry and in non-ideal geometries where boundary effects force us to take into account the reaction zone structure.

As a complement to this macroscopic description, some heating processes in the shock front have been presented.

A discussion is now open on the validity of the models which have just been presented compared to the experience of laboratories concerned with condensed explosives.

Questions-Answers, Comments

Questions - Answers, Comments.

Dremin *A Comment on Chemical Spike profile*

The finding which is of great importance for the ZND detonation theory is the chemical spike experimental observation in condensed explosives stable detonation wave front. The theory has got strong evidence in this respect. However it turned out that the sharp steeply decaying chemical spike profile experimentally observed and Ш-shaped chemical spike predicted by the theory differ principally. The Ш-shaped theoretical profile implies that EMs do not change chemically during their compression inside the detonation wave shock front, that the reaction begins behind the front at a shock compressed state. The steeply decaying profile experimentally observed means that the maximum rate of EMs' explosion energy evolution just behind the front is conditioned by some chemical preparatory processes inside the front. The difference testifies for the necessity of further developing the stable detonation wave physical model

Gupta - Dremin :

Q : It would be helpful to explain qualitatively why the ideal ZND model does one expect a flat top wave behind the von-Neuman spike. In contrast, why does a triangular spike imply reaction in the shock front ?

A : For steady-state process all intermediate states of the transition (from initial to final) zone (at detonation it is the chemical spike) spreads with one and the same velocity (at detonation it is the CJ velocity). Therefore all states are located in (P, V) plane along Rayleigh line ($P = -(D/V_0)^2 \Delta V$). The ZND detonation physical model implies that there is chemical change of EM's molecules during their compression inside the detonation wave shock front, that the reaction begins in some induction time behind the front at EM's shock-compressed state. It means that the shock pressure during the induction time will not change.

Melius - Dremin :

Q : What is a reasonable maximum time limit for chemical reaction to occur after which the classical theory of detonation is no longer meaningful ? Is one microsecond sufficienly fast ? Is 100 nsec ? Is 10 ns ?

A : The ZND detonation theory implies that there is no chemical change with EM's molecules during the material compression inside the detonation shock wave front. It means that there is the shock-compressed material layer in the detonation wave front discontinuity zone.

At present it becomes evident that the notion is invalid. Due to extremly fast loading rate of EM's inside the detonation shock wave discontinuity zone, some highly nonequilibrium material state originates which results in the materials' molecules chemical change with active particles origin (<ns - endothermic zone).

Dick - Swift

Q : Regarding detonation velocity vs curvature models : what is their relationship to ZND theory ?

A : Detonation speed-curvature (D(K)) relations are derived directly from experimental measurements of the steady wave shape in long rods and slabs of explosive.

The ZND model applied to steady 1D diverging detonation predicts a relation between D and K. Its form depends on the explosive's equation of state and reaction rate.

The simple use of a D(K) relation for a non-steady wave is not a direct consequence of the ZND model. It corresponds to an additional approximation i. e. that the reaction-zone has negligible inertia to change.

Miller - Davis

Q : Why do you say that a 1% increase in detonation energy or pressure is important?

A : The discussions I have heard about deciding which candidate new safe explosive to use have centered on whether this one was 10% better than the one in current use, or another one had 11% more energy. An energy increase of 1% is not important, but 1% accuracy would be useful for discriminating among proposed explosives.

Bauer - Davis :

Q : The calculation of thermodynamic properties of detonation products requires an accurate knowledge of the EOS.

According to your presentation there are numbers of thermochemical codes involving all types of EOS that seem to be adequate for such purpose.

Does that mean there is no future for fundamental investigation on this particular aspect ?

Should one consider this as being the only concern of engineers ?

Should one focus on the build up of new simple but physically based codes ?

A : Accurate Equations of State have many uses, for engineering design, for designing experiments and measurements of all kinds, and for fundamental scientific understanding. Their improvement will probably never be finished. While it is true that designers, pressed for time, sometimes modify Equations of State to hide other errors in their computations, that are really used just for interpolation among experiments, these same designers need physically based accurate Equations of State to test their understanding of how their devices work. In the scientific study of how explosives decompose chemically in reaction zones of detonating or initiating explosives, accurate Equations of State for partially reacted mixtures are needed desperately. Methods for treating strongly curved waves especially need good Equations of State.

Veyrié : *a comment*

Measuring E.O.S. of explosive materials is necessary. The question is what materials ?

At pressure under threshold of initiation, it presents both engineering and scientific interest.

At higher pressures, it is difficult to know exactly what is measured in a partially reacted material in

a dynamic variation.
It keeps however a practical engineering interest.

Belmas - Dremin :
Q : You told that for high pressure shock initiation, the microstructure of the explosive had no influence because of a bulk mechanism. How can you explain Dr Davis's experiments (extinction of detonation by preshocking) ? Obviously, this extinction is due to an homogeneisation (pore collapse without ignition) of the medium by the preshock and this phenomenon agrees well with a discrete hotspots theory.
A : Charge structure has no influence on EM's energy release rate at shock intensities larger than some proper P*characteristic for each charge. Dr W.Davis'experiments were done at shock pressures smaller than P*, that is at relatively low shock intensities, when the structure influences the SDT process.

Boileau - Belmas :
Q : Is the effect of void different when they are empty, half gas and solvent or full of solvent ?
A : No difference for 1μ size pores but, may be, for very large pores we can have an influence of the trapped gases.

Miller - Davis :
Q : Do you think that molecular dynamics simulations of vacancy defect effects are practically relevant ?
A : The smallest interesting hot spot, with some heat-conducting explosive around it, involves more than 10^9 molecules. Explosives safe enough to handle need at least 10^{15} molecules to react to achieve initiation. The interaction of the waves generated by the small release of energy at each hot spot must be treated. Very clever use of molecular dynamics will be needed to shed much light on how hot spots really work, and that clever use should be encouraged.
Oran : *General comment on molecular dynamics (MD) and the effects of what is in the voids on the propagation of detonations and sensitivity of explosives.*
Problem with MD is getting to the right scales to answer macroscopic questions. However, with this caveat in mind, mention some preliminary MD calculations that look at effects of what is in the hole. These show that what is in the hole has a large effect on lattice disruption, and therefore sensitivity.

Volk - Belmas :
Q : In your paper you mentioned that explosives with different binders and the same porosity exhibit the same initiation behavior. Does this hold also for extremely different binders in mechanical behavior such as polybutadiene binder compared to polyisobutylene binder ?
A : The binders used have very different chemical, mechanical and thermal properties. We did not

see differences between the results if the porosities were closed.

Boileau - Samirant, Ramsay :

Q : Is there a difference in crystal sensitivity of an energetic material when it contains gas in a defect and when it contains an entrapped liquid in a defect ? For example, recrystallization of cyclic nitramines often could leave solvent molecules entrapped totally or partially within crystal lattice defects (internal forces) - closed porosities.

S : *On the effect of the content of the porosities.*

They have an effect at very low pressure and for this very low pressure there is a large influence of the defects on the structure of the crystrals. If we look by XR around the porosities of the crystal, you can see that deformed area is larger than the porosity, and it is this deformed area which gives the sensitivity and it doesn't depend, at first glance, on the content of the porosity.

For SDT at low pressure the sensitivity does not depend on the size or the type of void in the crystal but on the size of the perturbed zone in the crystal array. This volume gives the number of dislocations that can be blocked by the defect and the energy released in the hot spot.

R : Early work of Travis and Mader showed no relationship between density of inclusions in nitromethane and efficacy of initiation. Also recent work reported at the last Detonation Symposium by Ramsay, Richter and Bernecker showed large differences in sensitivity of elastic material on the basis of porosity induced by tensile damage compared to other porosity.

2 LIQUIDS AND GASES

Chairman : Paul Rigny, Directeur du Département des Sciences Chimiques du C.N.R.S.

Le phénomène de l'explosion reste l'un des plus fascinants de la chimie. S'il intrigue toujours les chercheurs, il motive aussi de nombreux ingénieurs par ses applications pratiques multiples et spectaculaires. Pour la Science fondamentale et appliquée de cette fin du XXème siècle, le problème reste toujours entier. Les magnifiques développements des techniques d'études des laboratoires qu'ont apportés les progrès de l'instrumentation ouvrent l'espoir d'analyses précises au niveau moléculaire ; les progrès de la simulation - et de la chimie théorique en général - font miroiter l'accès à la compréhension prédictive de ces phénomènes. Mais que de chemin encore à parcourir pour relier structure moléculaire et phénomène détonique !

Depuis plusieurs années, les organisateurs des Ateliers "Approches microscopique et macroscopique des détonations" s'emploient à rapprocher les différents acteurs impliqués. Sans découragement, ils surmontent les difficultés culturelles scientifiques et autres (les applications militaires ne sont jamais loin, qui déconcertent bien des scientifiques). Ce deuxième atelier va sûrement, comme le premier, marquer un nouveau progrès dans l'ambitieuse démarche de la maîtrise des mystères de la transformation de la matière ; il sera en tous cas, riche de discussions et d'échanges vifs et salutaires.

Detonation has always been and still is one of the most fascinating phenomena in chemistry. It still puzzles the scientist while it drags the engineer into ever more spectacular uses. For XXth century Science, the problem is still fully present. The outstanding and numerous developments of the instruments and techniques available in laboratories open new hopes of experimentation and interpretation at the molecular level ; the progress of modelling and computing techniques - more generally of theoretical chemistry - let us envision the predictive understanding of these phenomena. But, of course, the gap between detonation and molecular structure is still huge, and not to be filled easily.

For many years, organisers of the workshops" Microscopic and Macroscopic Approaches to Detonation" work to mix the different scientific actors implied in the field. Continuously, they go over cultural (military applications, alien to many scientists, are never very far) and scientific difficulties.This second workshop, I am sure, will set a new step in the ambitious way towards the mastering of the mysteries of the transformation of matter ; it will certainly be rich of lively and sound discussions and exchanges.

2-1 Detonation Initiation and Self-sustained Regime in Homogeneous Media

Structure of Gaseous Detonation Waves and Chemical Kinetics ; P.Van Tiggelen

On the Energy Evolution in Gaseous Detonation Waves ; **A.A.Borisov**, O.I.Mel'nichuk, A.R.Kasimov, B.A.Khasainov, K.Ya.Troshin and V.Kosenko

Detonation Generation and Propagation in Homogeneous Liquid Explosives ; **H.N.Presles** and P.Vidal

JOURNAL DE PHYSIQUE IV
Colloque C4, supplément au Journal de Physique III, Volume 5, mai 1995

Structure of Gaseous Detonation Waves and Chemical Kinetics

P.J. Van Tiggelen

Laboratoire de Physico-Chimie de la Combustion, Université Catholique de Louvain, Louvain-la-Neuve, Belgique

ABSTRACT

The tridimensional unsteady character of the flow field for detonations has been established about thirty years ago. The shock pattern is rather complex and the complete description of the phenomenon remains beyond the power of fast computer even today. However the classical thermodynamic approach allows to grasp what are the dominating factors of the whole process: leading shock inducing an exothermic reaction governed by the chemical kinetic mechanism of the heat release. The dynamics of gaseous detonation is coupled therefore closely to the rate of the heat release which in turn influences the time-dependent shock structure of the front.
Measurements of the detonation velocity (D) are close to the values of the Chapman-Jouguet model of a detonation which is based on full thermodynamic equilibrium. But, the structure as evidenced from the soot records is more sensitive to the initial conditions : pressure, equivalence ratio, diluent nature and percentage, as well as the type of fuels, promoters and inhibitors of combustion processes. From systematic measurements of the length (L) of the detonation cell imprinted on soot for several mixtures, it has been possible to demonstrate the promoting role of hydrogen, and the inhibiting role of halocarbons on the detonation of CO/O2/Ar mixtures. Some detailed studies of OH emission, shock velocity of the unsteady leading shock, pressure inside a cell have shown the self-similar character of the flow field inside one cell. It demonstrates that the detonation phenomenon can be viewed as a periodic reinitiation of reactive shocks at a frequency identical to the reciprocal of the characteristic time as defined by the ratio: L/D. Irregular cell structure can occur in more complex mixtures such as CH4/O2. In that case the higher values of the activation energy of the conversion process induce a much higher sensitivity to the elaborate temperature fluctuations of the flow field. More recently,numerical simulations have allowed to model the unsteady bidimensional model of a detonation. The following papers could be referred to for more details about this approach of the gaseous detonations:
-J.C.LIBOUTON, M.DORMAL,and P.J.VAN TIGGELEN, Progress in Astronautics and Aeronautics, Vol.75 pp 358-369 (1981)
-P.J.VAN TIGGELEN et J.C.LIBOUTON, Annales de Physique ,Vol.14 pp 649-660 (1989)
-M.H.LEFEBVRE, E.S.ORAN, K.KAILASANATH,and P.J.VAN TIGGELEN , Progress in Astronautics and Aeronautics, Vol. 153 pp 64-76 (1992)
-M.H.LEFEBVRE, E.S.ORAN, K.KAILASANATH,and P.J.VAN TIGGELEN, Combustion and Flame Vol. 95 pp 206-218 (1993)

JOURNAL DE PHYSIQUE IV
Colloque C4, supplément au Journal de Physique III, Volume 5, mai 1995

On the Energy Evolution in Gaseous Detonation Waves

A.A. Borisov, O.I. Mel'nichuk, A.R. Kasimov, B.A. Khasainov, K.Ya. Troshin and V. Kosenkov

N. Semenov Institute of Chemical Physics, Russian Academy of Sciences, Moscow 117977, Russia

Abstract

There is a definite inconsistency between the classical ZND theory of detonation and contemporary experimental observations and attempts to model real detonation waves. Nevertheless, the classical onedimensional model of detonation is still extensively used in interpreting measurements because of its simplicity and physical clarity. This naturally raises the questions, what does actually the classical model represent and how one can relate the real multidimensional wave structure to an effective onedimensional detonation? The answer to these questions is extremely important from the practical point of view, because it defines how simple the solution of the criticality problems in detonation could be (i.e. whether one has to solve the very cumbersome three-dimensional nonsteady gasdynamic problem with detailed kinetics of the chemical reaction comprising a few hundreds of elementary steps to predict such parameters as critical initiation energy, critical distances, and concentrations, or the solution of a simplified onedimensional gasdynamic problem with global chemical kinetic equations would suffice?).

The present communication discusses the following t s with the aim of answering partly the above questions. (1) An analysis of the detailed kinetic calculations of the heat evolution rate in some fuel-air mixtures and comparison of these results with experiments reveals that (a) in the majority of detonable mixtures heat release can be described by global equations with an accuracy quite sufficient for assessing the critical detonation parameters, (b) chemical kinetics shows no so-called "recombination" zones with an appreciable heat evolution that follow the main reaction zone, (c) the ratio between the induction and the explosion (within which the major fraction of the stored energy is evolved) times exceeds unity under the conditions corresponding to detonation waves in fuel-air mixtures, which contradicts the shock tube measurements. All these results can be reasonably explained by the fact that the chemical reaction in detonation waves (in shock waves as well) proceeds in a gas with a highly inhomogeneous distribution of the parameters (temperatures, pressures, and particle velocity) which gives rise to the so-called hot-spot mechanism of chemical reactions in gaseous and two-phase media. It is shown that the hot spot ignition is the main reason of instability of detonation waves. Nonsynchronous mixture ignition at different points produces the effect of extended heat evolution zone and reduces the effective induction zone.

Results of measurements of averaged and local parameters behind detonation waves in gases support the idea that the effective heat evolution rate in the onedimensional representation of the wave is much more complicated than that inherent in the chemical reaction alone, because it contains also a significant contribution of the kinetic and thermodynamic energy redistribution within the major reaction zone and downstream of it, which makes the onedimensional structure of detonation waves deviate significantly from the classical pattern leading to nonmonotonic heat release behind the shock front (the possibility of appearance of two or more effective sonic planes and heat rlease maxima).

However, a onedimensional analysis of marginal detonation waves has demonstrated that critical parameters can be estimated quite accurately within simplified models, which is attributable to the fact that the criticality is associated with local termination of the reaction within narrow stream tubes where the flow pattern resembles closely the ZND non-CJ detonation wave structure. Unlike the chemical reaction zone in detonations far away from the limit, which is shorter than the detonation cell size, the reaction zone in marginal detonations is comparable with the cell size.

The results of onedimensional calculations of critical diameters and minimal energies of direct initiation of detonation are compared with experiment.

INTRODUCTION

It is unambiguously proved both theoretically and experimentally that onedimensional detonation waves in gaseous and two phase (sprays or dusty gases) are virtually nonexistent. Nonetheless, the so-called Zeldovich-von Neumann-Döring theory developed originally for essentially onedimensional detonation waves is still extensively used in interpreting experimental data. This can be attributed to three reasons: first, the ZND model is physically clear and simple and always warrants adequate, at least qualitative, explanation of all experimental observations, second, the properties of non-marginal detonation waves are described quite adequately by this model, except the real structure of the von Neumann spike (which is actually of little importance in many cases), and, finally, calculations using three-dimensional models are so scarce and cumbersome that can not be considered as a series basis for interpreting any experimental results. Moreover, the ZND model applies undoubtedly to individual stream tubes even in three-dimensional nonsteady detonation waves in the sense that in narrow stream tubes one can distinguish the initiating shock wave, von Neumann spike, and the surface where the reaction is terminated, but these "elementary" detonation waves are not necessarily CJ waves.

Thus, the state of art in the detonation theory is such that the overidealized ZND model is used by almost everybody, while the realistic three-dimensional model, although clearly formulated, is too inconvenient for common use, and there is actually no intermediate model or even general understanding how the averaged (over space and time) detonation parameters correlate with the three-dimensional wave structure. Of importance is also to find out how adequately the one-dimensional ZND model describes marginal detonation waves and critical conditions for detonation initiation. *A priori,* one can expect that this simplified approach is applicable to treating critical detonation phenomena and calculating the von Neumann spike structure but with some effective averaged kinetic of energy release behind the lead shock front (which may drastically differ from the pure chemical kinetics). This was tacitly assumed in many theoretical works (see, e.g., [1]), where a two-stage reaction or "recombination stage" were introduced in the computational model.

This paper is an attempt to cover the gap between the aforementioned models and to answer the questions how the ZND model could be applied (if so) to at least approximate calculations of the realistic detonation parameters and what kind of kinetic equations should be used in these calculations.

HIGH TEMPERATURE REACTION KINETICS

General analysis of reaction kinetics implies that the reactive mixture has homogeneous properties. Both experiment and calculations with detailed chemical kinetics show clearly an induction period during which the temperature in the system changes only little and a stage of progressively accelerated temperature rise.

First we consider the induction stage, because quite often it constitutes the major part of the overall reaction time and in many cases it is the only parameter which is reliably measured in shock tube experiments. Most of the reactions in detonation waves comprise a great many elementary steps even within the induction period, therefore Arrhenius plots of induction periods t_{ind} are not necessarily straight lines in a wide temperature range. There are examples of both flattening (mostly for hydrocarbons) and steepening (e.g. for hydrogen mixtures) of the t_{ind} versus $1/T$ dependence at lower temperatures. Such a behavior of the Arrhenius plots is associated with a changeover of the dominant mechanisms or rate

controlling steps within the same reaction scheme, and hence can be observed only in systems where concurrent processes with different effective activation energies take place. Fortunately, in practice the characteristic times of changes in the flow parameters (i.e. times available for the reaction) range in rather narrow limits, so that the Arrhenius plots of ignition delays in each particular case may be represented by straight lines with a fairly good accuracy. Therefore one can expect that this reaction stage can be described by a global equation of the Arrhenius type, at least for conditions relevant to detonation processes.

Induction period is only a part of the total time during which heat is released by a chemical reaction. Unfortunately, there is no simple analytical means for calculating t_e , i.e. the time within which the major fraction of the energy stored in the system is evolved. Usually interpretation of detonation phenomena associated with chemical kinetics is based on consideration solely of induction periods. The characteristic feature of t_{ind} is its high temperature sensitivity, therefore the analysis of the shock wave - reaction zone complex leads inevitably to a conclusion that this complex is unstable. In a number of theoretical approaches the heat release pattern is represented even by a step-wise function. Figure 1 [2] demonstrates both the induction and explosion times as functions of temperature for various mixtures as measured in a static apparatus and shock tube. The induction period, as seen from Fig. 2 [2], can be defined quite easily from pressure or luminosity records as, for example, a time to an appreciable rise of the signal or to the inflection point, and t_e may be measured as a time to the maximum pressure or maximum luminosity. This definition of t_e slightly underestimates it, especially when the signal rises slowly, since expansion of the gas may compensate for the signal growth due to the reaction. However for the majority of gasdynamic problems, especially for those relevant to shock wave-exothermic reaction coupling, it is the overall heat release time which is of importance. Figure 1 illustrates clearly that t_{ind} is the principal constituent of the overall heat release time only at rather low temperatures and values of t_{ind} above 10^{-4} s, below the intersection point of the Arrhenius plots for t_{ind} and t_e the heat release profile is no longer of an explosion type. A position of the intersection point depends on the pressure and temperature mainly due to a strong dependence of the induction period on these parameters, since t_e is affected by variations of pressure and temperature only slightly. The effective activation energy of t_e turned out to be only a few kcal/mol and the pressure exponent of about 0.2 - 0.3, whereas for the majority of hydrocarbons the effective activation energy of induction periods ranges between 30 and 50 kcal/mol, while the pressure exponent changes between - 0.7 and - 1.0. It should also be noted that unlike induction periods, t_e are affected (if so) by various chemical additives only insignificantly, which is accounted for by the fact that any additional production of reactive species in the system may change solely that part of the reaction which proceeds under conditions when the radical concentration is not too high. At later reaction stages the thermal production of radicals is so intense that only additives taken in amounts comparable with the concentrations of the initial reagents may influence the reaction rate.

The fact that the heat evolution rate during the explosion part of the temperature profile is slower than the rate which should be expected based on the kinetic parameters (activation energy and preexponential factor) derived from measured ignition delays is reflected in the term "recombination reaction stage" frequently used in detonation literature, though this definition is not precisely adequate (which follows from the considerations presented below). First, since the temperatures in a partially burnt gas are much higher than that at which the reaction has started, the Arrhenius exponents of all the elementary steps during the major fraction of t_e are much less sensitive to temperature variations than at the beginning of the reaction (due to smaller E/RT values).

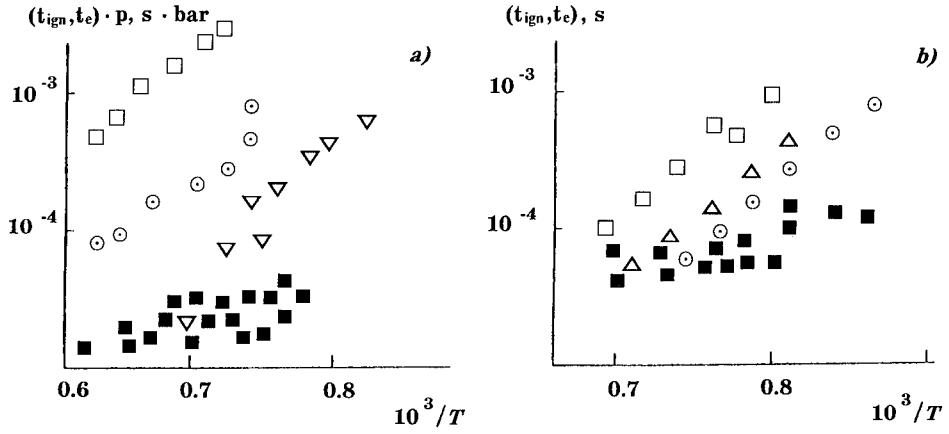

FIGURE 1. Arrhenius plots of the induction periods t_{ind} and explosion times t_e: (*a*) □ 6% methane + 12% O_2 + 82% Ar; ○ 3.3% propane + 16.6% O_2 + 82% Ar; ∇ 1.5% heptane + 16.5% O_2 + 82% Ar; ■ t_e for all the mixtures; (*b*) 4.3% propane + 21.3% O_2 + 74.4% N_2: □ p = 1 bar; Δ p = 2 bar; ○ p = 5 bar; ■ t_e for all the pressures.

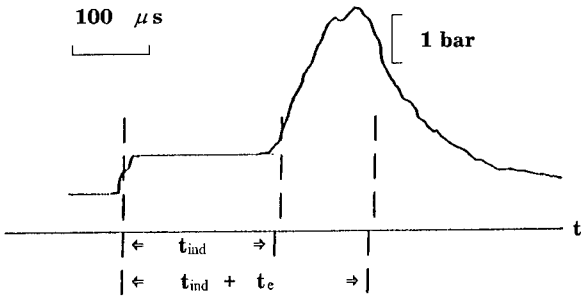

FIGURE 2. An example of pressure record behind the shock wave reflected from a rigid wall in a propane-air mixture. The initial flat portion corresponds to the induction period, and the rising portion is the heat release stage.

Second, the radical concentrations at these reaction stages are very high and therefore elementary reactions involving these reactive particles become dominant. This applies to recombination reactions as well, since it can easily be inferred from a mathematical analysis of the kinetic equations for chain, and even non-chain, reactions that the radical concentrations should pass through a maximum (which is the higher, the greater the contribution of the branching steps to overall radical production) in the course of the reaction, which means that there must exist a radical recombination stage. In the overwhelming majority of mixtures, this latter stage does not produce a significant contribution to the overall heat release, because the energy stored in the radicals formed constitute only a small fraction of the heat content of the reaction products.

That in an isothermal case the time histories of the radicals may peak at the early stage of the process is seen from very simple considerations. Indeed, even non-chain reactions start usually with decomposition of fuel (or oxidizer) molecules, that is with formation of radicals. The difference between chain and non-chain reactions consists in what happens further with the radicals formed: in non-chain reactions they recombine to produce species

with a lower enthalpy of formation than the initial reagents, while in chain reactions they enter into chain propagation processes yielding both the end products and active intermediates (i.e. producing both heat and chemical energy). Of the principal importance is the point that the initial reagents produce radicals and atoms more easily than the end products since the latter have stronger bonds (otherwise the overall heat release will never be positive). Hence, the equilibrium radical concentrations for individual initial components of a combustible mixture may be higher than that for the end reaction products. The faster radical production in a chain branched reaction reduces the fraction of the active species recombined within the induction period, that is why the radical concentration overshoot in chain branched reactions is usually much (up to several orders of magnitude) higher than in other types of explosion reactions. However, under non-isothermal conditions, radical concentration overshoot can be observed only in branched chain reactions because of continuous decomposition of all the species present in the mixture with growing temperature.

Inasmuch as the activation energies of radical-radical and radical-intermediate reactions are lower than those of reactions involving the starting molecules, the overall effective activation energy will drop with the burnt fraction.

It follows from the aforesaid that the *E/RT* factors at later reaction stages are lower than at its beginning and, hence, the role of the reactant depletion will be more prominent. The heat release profile becomes flatter with time due to all the aforementioned factors but not to radical recombination alone. Here we mention only chemical factors that flatten the heat release profile at the later reaction stages.

Now we consider how fast the recombination energy may be evolved. Let radicals be formed instantaneously in combustion products in amount of R_0. Then the characteristic concentration-decay time is $(R_0 k_r M)^{-1}$, where k_r is the recombination rate constant and M is the total concentration of species. This follows from the solution of the kinetic equation for quadratic radical recombination under the aforesaid initial condition. The value of k_r may be set equal to the frequency of triple collisions, i.e. to 10^{16} cm^3/mol·s. This yields for the recombination time a value of $10^{-12}(M/R_0)T^2/P^2$ s. Here P is pressure in atm. As mentioned above, concentrations R_0/M lower than 1% may change the total thermal energy only less than by 1%, therefore for practical estimates we may write that the recombination time should be less than $10^{-4}/P^2$. Thus, at pressures higher than 10 atm this time does not exceed 10^{-6} s, i.e. recombination proceeds very fast in detonation systems. Although the above estimate is very rough, it applies to many practical situations. The main conclusion that can be drawn from this estimate is that variation of the radical concentrations throughout the explosion (intense) portion of the energy release profile should be more or less close to the quasi-steady one (because of very fast recombination). Hence, for radical concentration in the general case of chain branched reaction we may write at this reaction stage:

$$R = (k_I A_2/2k_r)[1 + (1 + 4k_I M k_r/k_b^2 A_2)^{1/2}],$$

where k_I and k_b are the rate constants of the initiation and branching reactions, respectively, and A is the fuel concentration. Thus the heat release rate at this stage is:

$$dq/dt = k_{pr} q_{pr} A_2 R + k_r^2 R q_r + q_I k_I A_2 = (k_{pr} q_{pr} + k_b q_r) A_2 R =$$

$$[k_b A_2/2k_r + (k_I M A_2/k_r)](k_{pr} q_{pr} + k_b q_r) A_2,$$

where q_i are the reaction heats and subscript *pr* signifies a chain propagation step. It is taken into account here that $q_r \approx -q_I$, so that term $k_I A_2 M(q_r + q_I)$ may be neglected not only because of smallness of the initiation rate constant but because of the small energy difference as well. This indicates that explosion proceeds at its later stages as a non-chain process with some effective rate constants and does not show any pronounced recombination stage.

The absence of this stage is also shown by direct calculations of adiabatic explosion with detailed kinetics. Some of the results are presented in Figs. 3 and 4, where the reacting systems are chosen deliberately to demonstrate the possible effect of the recombination stage on heat evolution. As expected from the above rough estimates, no profound recombination stage is observed, moreover, calculations contradict even the shock tube measurements, because the t_e is always (even at high temperatures) much shorter than t_{ind}. The only plausible explanation of this contradiction is that ignition behind shock waves (as well as behind detonation waves) is an essentially inhomogeneous process, that is, gasdynamic fluctuations that inevitably are generated behind shock waves due to flow interaction with the walls (or to detonation wave instability) lead to formation of a great many hot spots in the unburnt mixture. This hot spot ignition was repeatedly observed in shock tubes. Non-synchronous mixture ignition at various points changes the temperature-time history averaged over the tube cross section "stretching" its part corresponding to fast energy release (explosion proper) and decreasing is slope. This suggests that the major factor responsible for two-step kinetics of heat release behind detonation waves is hot-spot mixture ignition, which makes it different from calculations based only on detailed chemical mechanisms under homogeneous conditions. Although hot spot ignition does not affect appreciably the kinetic parameters derived from the ignition delays measured in shock tube experiments because mixtures used in these experiments are highly diluted. But in detonable mixtures this may not be the case, therefore direct transfer of the experimental data obtained in shock tubes to detonation waves requires special consideration. The high scatter of the shock tube data on ignition delays is the well recognized fact. It should naturally be ascribed to inhomogeneous ignition of the mixture. And yet, one can not expect strong deviations of the ignition delays measured in reactive mixtures from those corresponding to a homogeneous reaction, because a direct comparison of the ignition delays measured in individual stream tubes behind the lead shock wave of a spinning detonation with shock tube measurements and chemical kinetic calculations demonstrates their consistency.

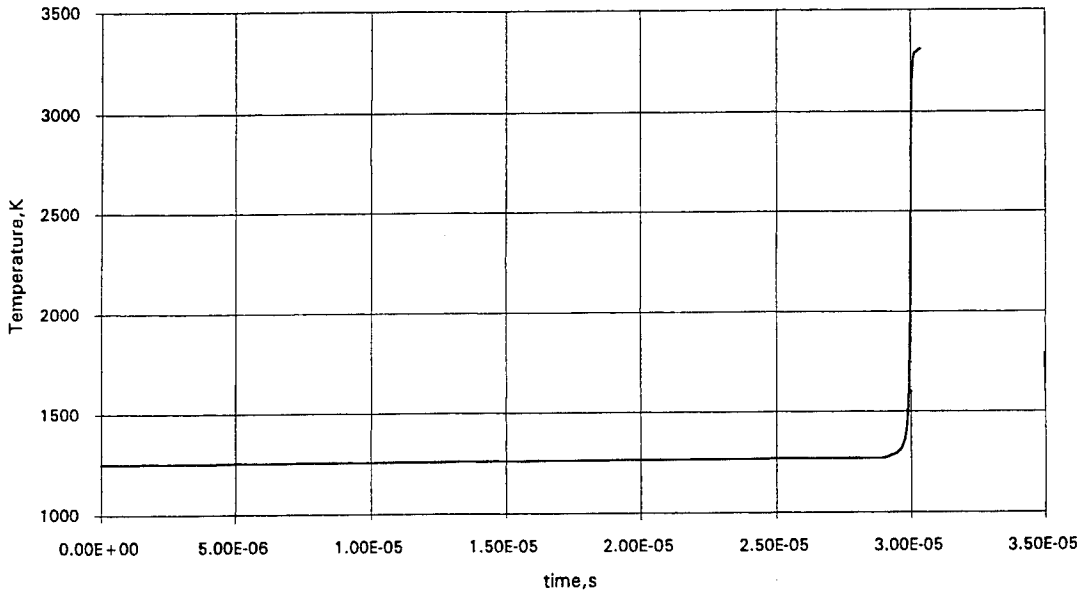

FIGURE 3. Temperature - time history for explosion of an 2.15 H_2 + (O_2 + 3.76 N_2) mixture at T_0 = 1250 K and p_0 = 28.3 bar.

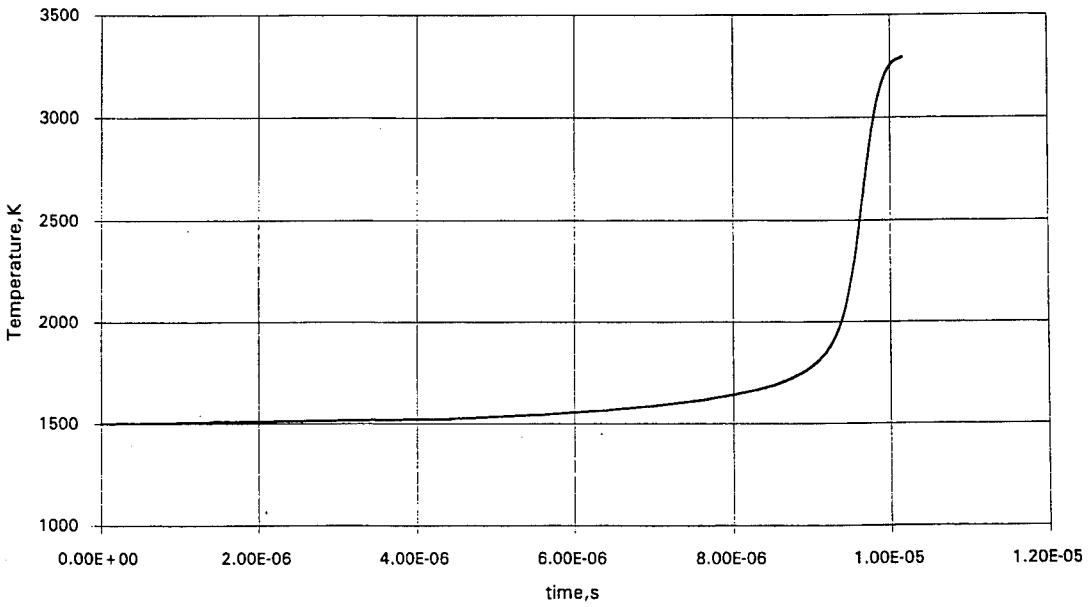

FIGURE 4. Temperature - time history for explosion of an $C_3H_8 + 5(O_2 + 3.76\ N_2)$ mixture at $T_0 = 1500$ K and $p_0 = 28.3$ bar.

Thus, all the onedimensional detonation calculations, in which the heat release rate is averaged over mixture volume, should be performed with an at least realistic reaction kinetics, e.g. that measured in shock tube experiments where the whole energy release profile is monitored. Hence, calculations with a detailed chemical kinetics are meaningful only when no averaging procedure is used, i.e. within three- or two-dimensional hydrocodes in which local temperature fluctuations are automatically taken into account.

However, detailed reaction schemes are inconvenient for complicated three-dimensional gasdynamic calculations because they bring about computational difficulties (which turns out unsurmountable in many cases), on the other hand, they are inapplicable to one-dimensional calculations. The most rational way to cope with this problem is to derive global kinetic equations, deriving them either from detailed reaction schemes for three-dimensional calculations or from shock tube measurements for onedimensional calculations. Below we illustrate both approaches.

The basic parameter for comparison with experiment is the ignition delay which is nearly identical in both cases. The main idea of further calculations is simulation of the entire heat release profile by expressions valid for the delay of thermal explosion. As follows from the theory of thermal explosion, ignition delay is related to the heat release rate at the zero-time conditions:

$$t_{ind} = c_p R T_0^2/(EQw),$$

where c_p is the specific heat, E, Q, and w are the effective activation energy, heat, and relative rate of the reaction, which are not necessarily the same throughout the temperature interval considered. This is illustrated in Fig. 5, where ignition delays for various hydrogen-air mixtures are summarized. Hence, to find the real reaction rate, one needs to express w via t_{ind}, introduce the dependence of w on concentrations of the reagents, and assume the temperature in the expression for t_{ind} variable. This procedure hopefully will allow one to

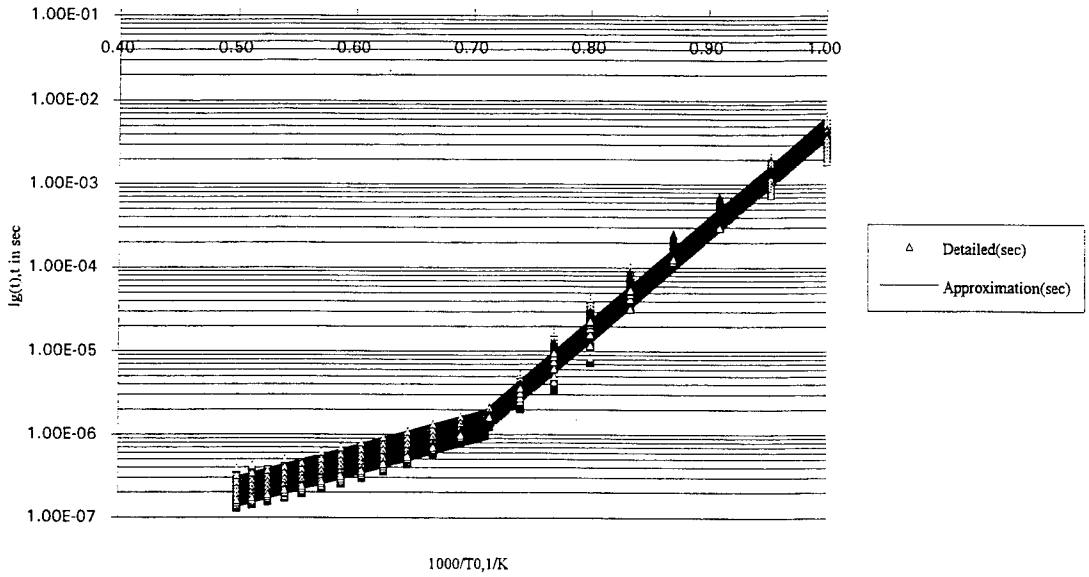

FIGURE 5. Calculated ignition delays of various hydrogen-air mixtures. Symbols are calculations by the detailed reaction mechanism, lines are calculations by the approximating equations. The concentartion and pressure ranges are: 19 - 59% H_2 and 15 - 35 bar, respectively.

use measured induction periods, at least in the region of temperatures and pressures where they could unambiguously be defined, to more or less adequately describe the reaction course. As far as the detailed kinetic calculations are concerned, Fig. 6 compares the exact solution and the temperature profile calculated by the approximate formula. Although the shapes of the curves differ significantly, the most important characteristic - the overall reaction time fits very well. It should be emphasized that even with the effective reaction orders much less than those derived from shock tube experiments the global formula yields lower slopes of the explosion part of the temperature profile, which indicates that any two stage reaction mechanisms are not of the purely chemical nature.

In order to take into account flattening of the effective heat release profile during later stages of an adiabatic thermal explosion (in onedimensional calculations) one may use a parameter which is tacitly assumed not to affect the course of the reaction within the induction period in a mixture with a high chemical energy stored. This parameter is the effective reaction order. As follows from the above considerations, the structure of the final expressions describing both the induction and intense-heat-release reaction stages is not very different for thermal and chain-thermal explosions (except for chain branched reactions with a very low contribution of recombination reactions to the radical concentration variation during the induction period). Thus there is some hope to write a single heat release equation for both stages but with some effective reaction order which will not change the expression for the induction period but will enable one to fit the "explosion part" of the heat release profile to measured t_e. In accord with the above hypothesis one may express the reaction rate as follows:

$$- dA_2/dt = c_{pRT}^2 (A_2/A_2^0)^n / (QEt_{ind}).$$

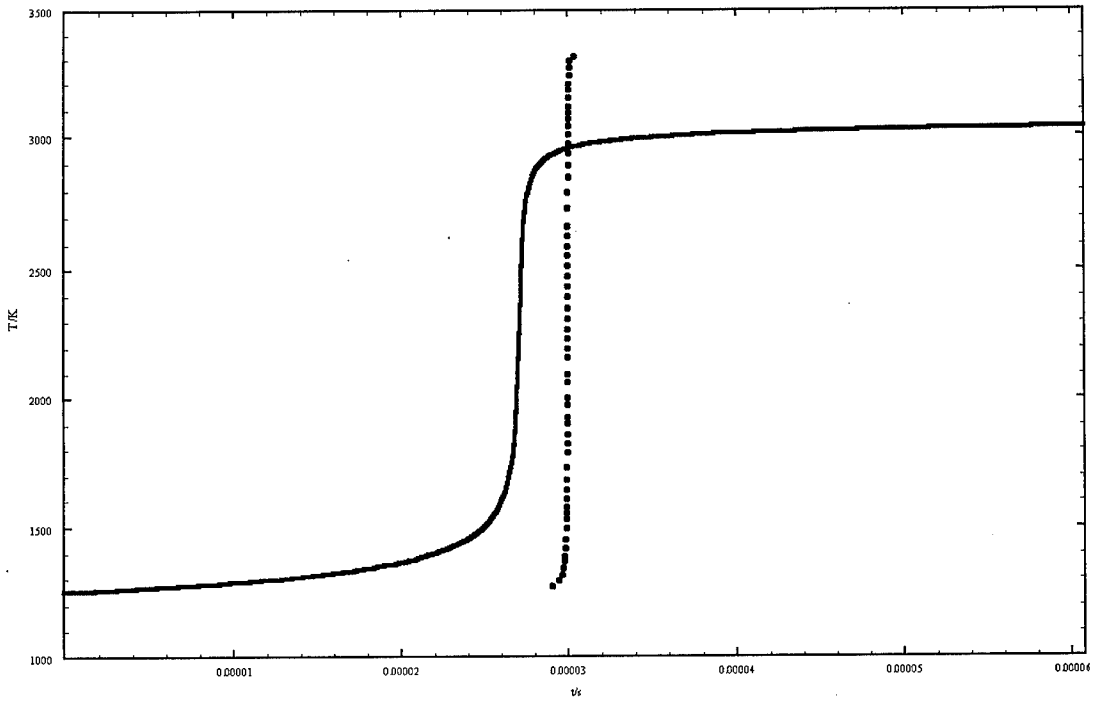

FIGURE 6. Comparison of the temperature profiles calculated by the detailed reaction mechanism and approximate kinetic equation. The conditions are same as in Fig. 3.

Here the temperature in the experimental expression for the ignition delay is assumed to be equal to its instantaneous value (the reagent concentrations in the empirical equation for t_{ign} being retained equal to the initial ones), and factor $(A_2 / A_2^0)^n$ is introduced to allow for the change in the reaction rate at later reaction stages.

The effective reaction order, which allows one to fit the calculated and measured t_{ign} and t_c with a fairly good accuracy turned out to be very weakly dependent on the type of a hydrocarbon fuel, thus for propane- and ethylene- air mixtures it is three, and for methane-air mixtures it is 4.5.

As for chain branched reactions with low efficiency of the chain termination steps, it should be emphasized that this latter approach is hardly to be applicable to description of the whole heat release profile, at least with some realistic activation energies and rate constants. For this reason the two-term formula for the reaction rate [2] could be recommended in this case.

CRITICAL DETONATION PARAMETERS AND THE WAVE STRUCTURE

In order to check validity of the ZND model with effective reaction kinetics we attempted to predict a critical diameter for detonation propagation in tubes and minimum energy of detonation initiation in tubes for a propane-air mixture. Onedimensional calculations were essentially based on the empirical equation for ignition delays and effective reaction order found also from shock tube measurements. Heat and momentum transfer to the tube walls were taken into account.

Figures 7a and 7b shows "go" and "no go" calculations of detonation initiation by two plane point explosion energies evolved instantaneously in the tube. The calculated minimum initiation energy of 4.0 MJ/m2 does not differ very much from its experimental counterpart

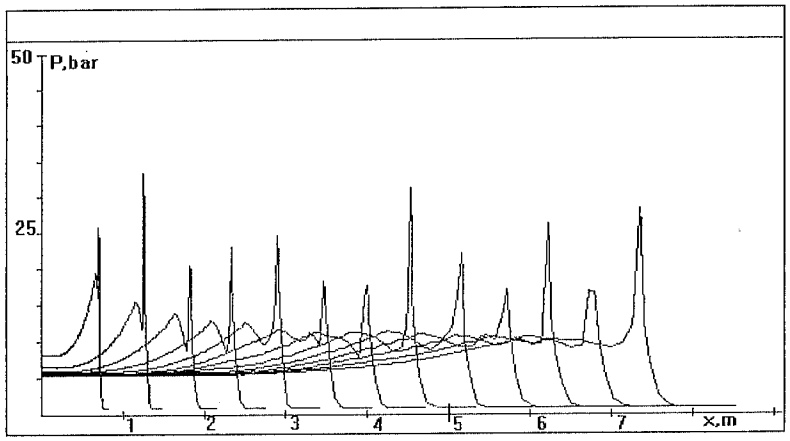

a.

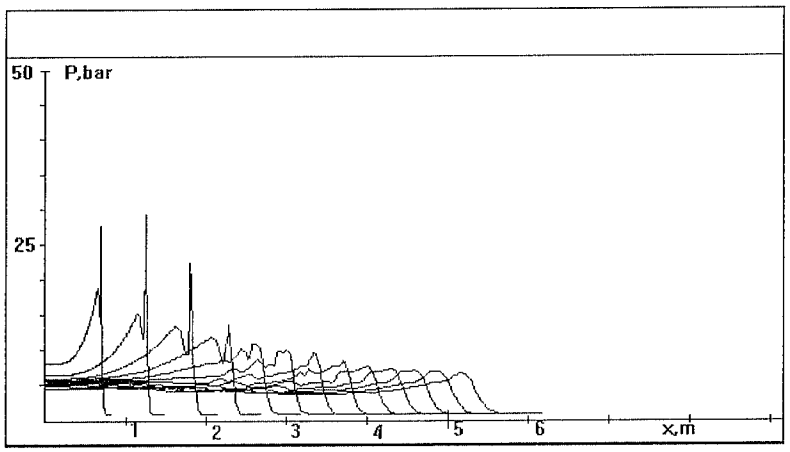

b.

FIGURE 7. Initiation of detonation in a propane-air mixture (point plane explosion): (*a*) go, E_{init} = 4.1 MJ/m^2 (*b*) no go, E_{init} = 3.9 MJ/m^2.

equal to 2.7 MJ/m2 under similar conditions. The estimated critical tube diameter (17 mm) is also consistent with measurements (19 mm).

Calculations revealed also importance of the longitudinal detonation wave fluctuations on the dependence of the concentration limits of detonation on tube diameter. Greater fluctuations of the reaction zone length at larger tube diameters do not allow it to grow unboundedly with the diameter, that is at large tube diameters the lean detonation limit changes only insignificantly, which is in full agreement with experimental observations.

Thus, we can conclude that ZND model can adequately predict critical parameters of detonation waves when the effective reaction kinetics is properly chosen (i.e. takes into account hot spot ignition). It is not surprising, because the critical parameters are governed by the longest reaction zone parts in which the induction period dominates and the hot spot effect, changing mainly the zone of intense energy evolution, is not very critical.

The lack of experimental data on the ignition delays makes often researchers use detonation cell sizes λ as substituents. Although there is some correlation between the

reaction zone and λ, one should be very cautions when deriving kinetic parameters from measured λ values. As we demonstrate below, the major reaction is completed at distances less than the longitudinal detonation cell size (*b*) and there is no grounds to believe that the average reaction zone constitutes a definite fraction of *b*.

Unlike the appropriate graph of ignition delays, the Arrhenius plot of *b* is highly nonlinear. This is illustrated in Fig. 8, where log *b* measured in propane-oxygen mixtures

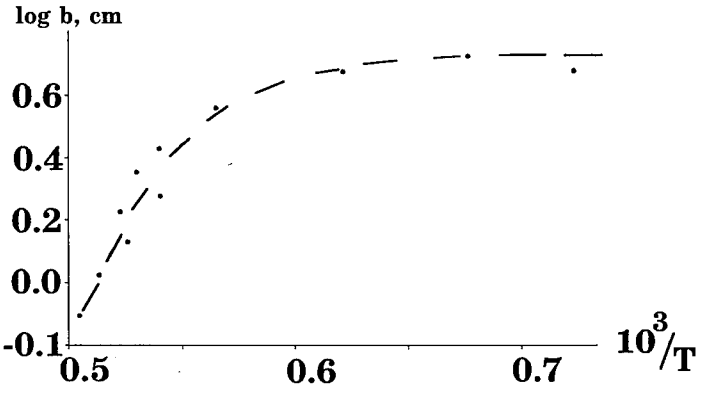

FIGURE 8. Arrhenius plot of the longitudinal detonation cell size for C_3H_8 - O_2 - N_2 mixtures (with variable *x*).

containing different amounts of nitrogen is plotted as a function of the average temperature behind the plane lead shock wave propagating at a detonation velocity. This means that *b* can not be recommended as a precise kinetic parameter.

In contrast to critical detonation characteristics, the ZND model with the above-discussed heat release kinetics is inapplicable to describing the behavior of the averaged parameters behind a detonation wave. Density profiles exhibit the highest deviation from the traditional ZND model. Indeed, Fig. 9 shows measurements of various parameters behind a detonation wave in a propane/oxygen/nitrogen/krypton mixture at atmospheric pressure in a tube 50 mm i.d.. The detonation velocity is 1569 m/s and the transverse detonation cell size is 17 - 18 mm. The X-ray absorption signal is the only truly averaged measured parameter. Instead of the gradually decaying signal profile (predicted by the ZND model), we see a curve with two minima. The first absorption peak should be assigned to the von Neumann spike within which the major reaction is completed. This is supported by the OH emission and ionization current signals that peak also within this period of time (that is, intense generation of excited OH radicals and chemi-ions ceases). The second peak is also seen on all the records. Most likely, this peak corresponds to collision of flappy transverse waves (that is to the end of detonation cells), which is confirmed by measurements of their size. The rise of all the signals after the second minimum is not quite clear as yet. There could be several factors leading to this rise, which we discuss below.

Going back to the first portion of the records, we may state that, within the ZND model, this flow portion has an averaged sonic plane slightly upstream of the absorption signal minimum. The gas density grows after this minimum because part of the kinetic energy of transverse motion is converted into the internal energy, which is equivalent to an additional heat release in the flow averaged over the tube cross section. This effective heat release downstream of the averaged sonic plane (where the flow is supersonic with respect to the lead shock front) produces a compression wave rising the flow parameters (density, temperature, local dissociation and ionization degrees, and pressure), which is clearly shown by all the experimental records. This compression wave is followed by a rarefaction wave (after the second sonic plane).

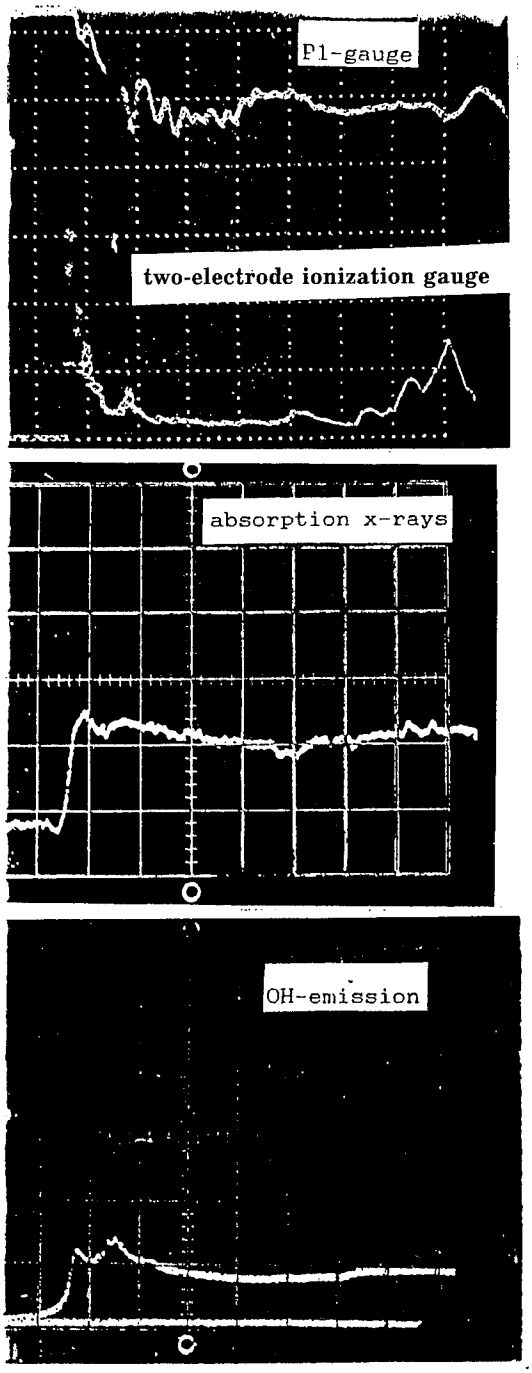

FIGURE 9. Records of pressure, ionization current, X-ray absorption, and OH emission behind a detonation wave in a propane - oxygen - nitrogen -krypton mixture.

The final rise of the effective temperature and density after the second minimum (see the ionization current and OH emission) could be attributed to: (*a*) burning out of tiny fresh-mixture blobs formed in three-dimensional detonation waves (and revealed in gasdynamic calculations); (*b*) continuing redistribution of the energy between the transverse gasdynamic motion and internal degrees of freedom and between hotter stream tubes and colder ones; and (*c*) boundary layer formation. Which of them is dominant can not be decided without additional investigations.

SUMMARY

The above analysis of experimental observations of detonations in gases suggests that the ZND model applied in its traditional one-dimensional form can be used to predict some critical detonation waves (critical diameters, minimum energy of detonation initiation), provided the appropriate kinetics of heat release behind the lead shock wave allowing for hot spot ignition is incorporated in the calculation model.

Calculations of the quasi-onedimensional detonation wave structure requires a more sophisticated heat release model, because redistribution of the energy between the transverse gas motion and internal degrees of freedom and longitudinal flow changes dramatically this structure resulting in a flow with at least two sonic planes (instead of one in the ZND model) behind the lead shock wave.

ACKNOWLEDGEMENT

The research described in this publication was made possible in part by Grant No. M3G000 from the International Science Foundation.

REFERENCES

1. V.A. Levin, V.V. Markov, and S.F. Osinkin, Khimicheskaya Fizika, v. 3, No. 4, pp. 611-614, (1984)).

2. A.A. Borisov et al., Progress in Astronautics and Aeronautics, v.114, pp. 124-139, (1988).

JOURNAL DE PHYSIQUE IV
Colloque C4, supplément au Journal de Physique III, Volume 5, mai 1995

Detonation Generation and Propagation in Homogeneous Liquid Explosives

H.N. Presles and P. Vidal

Laboratoire de Combustion et de Détonique, UPR 9028 du CNRS, ENSMA, BP. 109, 86960 Futuroscope cedex, France

Foreword

The goal of this paper is to present the main features of detonation generation and propagation in liquid explosives. Most of the results are related to Nitromethane (NM) since it is the most studied liquid explosive.

I - Introduction

Depending on whether they are homogeneous or heterogeneous, explosive media have specific detonic properties which are related to different heat release mechanisms. Before describing the ignition, propagation and extinction of a detonation in a liquid explosive charge, it is useful to recall some specific features of liquid explosives.

The latter are homogeneous in normal conditions but by adding heterogeneities, such as solid particles or bubbles, they can exhibit solid explosives properties.

Homogeneous liquid explosives are transparent to the visible light so that the radiations emitted by the detonation products can be recorded while the detonation wave propagates inside the explosive charge.

Liquid explosive densities are of order 1 g/cm^3 so that the detonation pressure is in the range 10 to 20 GPa. With such a pressure level the compressibily of the confinement has a great influence on the shape of the detonation front and on the critical diameter.

When liquid explosives are submitted to a shock or a detonation wave they exhibit a phenomenon called "electrical polarization effect". For instance, this effect is very useful to look at the consecutive events leading to the ignition of a detonation.

If cavitation is generated in the liquid explosive charge under precursor effects propagating through the confinement, an other detonation propagation regime called "low velocity detonation" can be obtained. For safety reasons, it is very important to understand this particular regime.

II - Detonation ignition in liquid explosives submitted to a plane shock wave

The processes involved in the detonation ignition in liquid explosives submitted to a plane shock wave have been clearly established in 1961 by Campbell et al. /1/ after the

preliminary work of Chaiken /2/. Using an other experimental technique, Hardesty in 1976 /3/ confirmed all these processes. When a liquid explosive is submitted to a plane shock wave of proper characteristics, a thermal explosion occurs after an induction time τ (Fig. 1), leading to a detonation wave which propagates into the compressed explosive at a velocity D^* higher than the shock wave velocity U. When this detonation wave overcomes the shock wave it becomes an overdriven detonation propagating in the explosive at rest, its velocity decreasing toward the normal detonation velocity D.

Assuming that the chemical reaction follows an Arrhenius rate law, the induction time can be approximated by the relation

$$\tau = K\, T_c^2 \exp\left(\frac{E}{RT_c}\right)$$

T_c is the shock temperature of the explosive and E the activation energy.

In agreement with this relation, experimental results show a great dependance of the induction delay on the initial temperature T_o of the liquid explosives (T_c depends on T_o).

Measuring τ for different shock strenghts and calculating the corresponding liquid temperature T_c, it has been shown /4/ that the activation energy of NM compressed by a shock wave is about 25 kcal/mole, that is half of the value for the gas-phase unimolecular decomposition.

In most of the studies the diagnostic information during the subsequent events of initiation was obtained from a streak camera looking towards the compressed explosive through the shock wave. In some explosives, like NM, light from the detonation propagating in the compressed explosive is weak but readily photographed. With some other explosives, there is a lack of luminosity. In 1965 TRAVIS /5/ has shown that electrical signals are generated by initiation processes occuring in dielectric liquid explosives filling a plane capacitor. A few years before, EICHELBERGER and HAUVER /6/ and HARRIS /7/ have reported studies on the charge generation by shock in inert dielectric. They have considered the effect to be due to mechanical polarization of the molecules produced at the shock front.

As the initial shock wave enters the liquid explosive and propagates, it polarizes the molecules in a thin layer (Fig. 2). Then the polarization relaxes rapidly. Using the ALLISON theory /8/ to analyse the electrical response of NM compressed by shock waves in the range 3 to 8 GPa, we have shown that the polarization relaxation time is of the order of 10 ns /9/.

When detonation starts at the interface between the barrier and the explosive at time τ, it polarizes a second layer of molecules which leads to a positive signal and when it catches the leading shock wave only one polarized layer remains. A negative signal corresponds to this event. As the detonation wave gets closer to the second metallic plate the electrical pulse rises rapidly because of the rapidly decreasing effective electrode spacing. TRAVIS has shown that the times of occurence of the initiation events measured by both the polarization and optical techniques are the same. This electrical technique is very useful to measure very short induction time.

Mechanical orientation of the dipoles submitted to shock wave is a possible cause of the electrical phenomena associated with shock or detonation propagation, but it has not been proved and some more fundamental researches should be started to really understand it.

III - Detonation propagation

Many experiments have shown that the relationship between explosive charge size and steady state detonation velocity is qualitatively different for homogeneous and heterogeneous explosives.

For both kind of explosives, the detonation pressure is so high that part of the chemical energy is used to produce lateral material motion. As a consequence, the detonation front is curved and its velocity decreases with the charge diameter down to a minimum value called the failure or the critical diameter, below which no steady wave can propagate. The corresponding charge diameter is termed critical diameter.

The detonation velocity of liquid explosives decreases linearly with respect to the reciprocal of the charge diameter (Fig. 3) and is nearly independant of the confinement nature. The detonation velocity decrement between infinite and critical diameter is very small (about 1%). The corresponding curve for heterogeneous explosives shows a strong downward concavity, a larger velocity decrement and a strong sensitivity to the confinement nature.

This is the case with heterogeneous mixtures based on NM and containing beads /10/ or glass micro-balloons (GMB) (Fig. 3) /11/.

Following CAMPBELL and ENGELKE /12/, the differences between the curves for homogeneous liquid and heterogeneous explosives is due to different mechanisms supporting wave propagation.

Homogeneous burn is the mechanism involved in the detonation of homogeneous explosives while in the case of heterogeneous explosives it is re-inforced by "hot spots". The lack of concave part in the homogeneous explosives curve should be due to the lack of the hot spot mechanism.

The influence of chemical sensitization of NM on its steady detonation propagation has also been studied by ENGELKE /13/. He has shown that very small amount of amines (DETA) produces a significant reduction of the NM critical diameter. For instance, adding 0.03 weight per cent of DETA to NM reduces the critical diameter by an amount of 40%. A so small amount of chemical impurity has no influence on the initial density nor on the specific heat of reaction of pure NM so that only the chemical kinetics is altered. From detonation velocity measurements of mixtures containing 0.03 weight per cent of DETA, ENGELKE deduced that the one-dimensional reaction zone length of the detonation in this mixture is 80% of that in pure NM.

The shape of the detonation front can also be used for obtaining information about the chemical kinetics because it is determined by the interaction between fluid mechanics and the heat release rate inside the reaction zone

BDZIL et al /14/, using experimental measurements of detonation wave shape and velocity in combination with a quasi-one dimensional theory of the processes inside the reaction zone, have evaluated the parameters of the Arrhenius law for NM. They got a rather high value of the activation energy (92±23 kcal/mole) in comparison with that obtained from initiation experiments.

About the detonation velocity of NM-DETA mixtures, WALKER /15/ found, with one-dimensional experiments, an increase with DETA up to 0.1 weight per cent. Measuring the detonation velocity and temperature of theses mixtures confined in brass tubes, we observed that these characteristics are continuously decreasing while the DETA concentration is increasing. So these results obtained with two-dimensional axisymetric detonation do not confirm those of WALKER.

IV -Three-dimensional detonation front structure

The detonation front in some liquid explosives such as NM is not smooth /15/ and streak camera records of the emitted light shows a nonuniform burning of the explosive throughout the cross section. One can deduce that detonation in NM is unstable. To discern the details of the detonation structure it is usual to decrease the specific energy of the explosive by diluting it with some non-explosive molecule. For instance NM is usually diluted with acetone /17/ /18/ /19/ . Using such a mixture, we can observe that the detonation wave structure behaves similarly as in gaseous explosive with respect to dilution with an inert additive, to chemical sensitization and to detonation overdriven degree.

For example as shown on fig. 4 adding a small amount of DETA to a NM-acetone mixture reduces greatly the size of the detonation front structure /20/. Thus, as in gaseous explosives, the three-dimensional structure is very sensititive to the chemical kinetics.

From these observations, chemical decomposition processes in homogeneous liquid and gaseous explosives look similar.

V - Detonation failure and critical diameter

Looking with framing or streak camera at the detonation front propagating in liquid explosive charge with size near the critical one, one can observe non luminous areas spreading inward from the confining wall /21/.

Because these areas look like reaction quenching waves they are called failure waves /22/. They appear to be characteristic of homogeneous explosives. When the flow expansion is too large compared to the rate of chemical energy release, a reaction failure wave travels along the detonation front. Quasi-steady, quasi-one dimensional theoretical modellings /26/ associate a critical shock curvature and a critical velocity to this event.

Behind failure waves, there is compressed explosive which can thermally explode and initiate again a detonation.

As the detonation process in charge size near the critical one is unsteady and the starting of failure wave random, the best way to look at the failure mechanism is to submit a steady detonation to a sudden confinement enlargement /17/ (Fig. 5).

When the detonation passes over the corner of the confinement a failure wave takes place at the periphery and propagates symmetrically toward the axis of the charge at a constant velocity.

According to the criterion of DREMIN and TROFIMOV /23/ the critical diameter of the unconfined charge is defined by the tube diameter ϕ for which the re-initiated detonation in the compressed explosive overtakes the failure wave exactly on the axis.

Experiments show that the critical diameter of liquid explosives is very sensitive to the confinement nature (and also to the confinement thickness when this thickness is sufficiently small /27/) and to the initial temperature. For instance, the critical diameter of NM confined in a steel tube is around 2 mm and 14 mm in glass. It decreases as the initial temperature increases with a rate of about 0,43 mm/C /24/.

Using the model of DREMIN and TROFIMOV, ENIG and PETRONE /25/ have shown that this can be explained by the fact the chemical kinetics is of an Arrhenius form.

VI - Conclusion

Due to different heat release mechanisms, liquid homogeneous explosives present some specific detonic properties in comparison with heterogeneous liquid or solid ones.

As there is no possibility to look straight to the chemical kinetics inside the detonation wave of condensed explosives, researches have to be undertaken to solve this problem.

One possible way is through inverse methods based for instance on realistic two-dimensional detonation modelling combined with detonation wave shape measurements.

But as instabilities have been observed in the detonation of some liquid explosives, the next step would be to use a three-dimensional approach in order to understand the real detonation and to determine for instance if there is some similarity between detonation waves in gaseous mixtures and in homogeneous liquid explosives.

VII - References

/1/ CAMPBELL A.W., DAVIS W.C., TRAVIS J.R., Shock initiation of detonation in liquid explosives, 3 rd Symp. on Detonation, ACR 52, 469-498, 1960.

/2/ CHAIKEN R.F., Kinetics theory of detonation of high explosives, Master's thesis, Polytechnic Institute of Brooklyn, 1958.

/3/ HARDESTY D.R., An investigation of the shock initiation of liquid NM, Comb. and Flame, 27, 229-251, 1976.

/4/ CHAIKEN R.F., Correlation of shock pressure, shock temperature and detonation induction time in NM, Symp. HDP, 41-53, 1978.

/5/ TRAVIS J.R., Electrical transducer studies of initiation of liquid explosives, 4th Symp. on Detonation, ACR 126, 609-615, 1965.

/6/ EICHELBERGER R.J., HAUVER G.E., Solid state transducers for recording of intense pressure pulses, Congrès sur les Ondes de détonation, CNRS Paris, 363-381, 1962.

/7/ HARRIS P., Mechanism for the shock polarization in dielectrics, J.Appl. Phys. 36, 739-741, 1965.

/8/ ALLISON F.E., Shock induced polarization in plastics, J. Appl. Phys., 36, 7, 2111-2112, 1965.

/9/ DE ICAZA-HERRERA M., PRESLES H.N., BROCHET C., Polarisation du nitrométhane sous choc, Revue de Physique Appliquée, 547-553, 1978.

/10/ ENGELKE R., Effect of the number density of heterogeneities on the critical diameter of condensed explosives, Phys. Fluids, 26, 9, 2420-2424, 1983.

/11/ H.N. PRESLES, P. VIDAL, J.C. GOIS, B.A. KHASAINOV, B.S. ERMOLAEV, "Influence of glass microballons size on the detonation of NM" bases mixtures, accepted for publication in Shock Wave Journal.

/12/ CAMPBELL A.W., ENGELKE R., The diameter effect in high density heterogeneous explosives, 6th Symp. on Detonation, ACR 221, 642-652, 1976.

/13/ ENGELKE M., Effect of chemical inhomogeneity on steady-state detonation velocity, Phys. Fluids, 23, 5, 875-880, 1980.

/14/ BDZIL J.B., ENGELKE R., CHRISTENSON D.A., Kinetics study of a condensed detonating explosive, J. Chem. Phys., 74, 10, 5694-5699, 1981.

/15/ WALKER F.E., Initiation and detonation studies in sensitized NM, Astronautica Acta, 6, p.807 ..., 1979.

/16/ ZELDOVICH Y.B., KORMER S.B., KRISKEVICH G.V., YUSHKO K.B., Dokl. Akad. Navk. SSSR, 171, 67, 1965.

/17/ DREMIN A.N., ROZANOV O.K., TROFIMOV V.S., On the detonation of NM, Comb. and Flame, 7, 153-162, 1963.

/18/ MALLORY H.D., GREENE G.A., Lunimosity and pressure aberrations in detonating NM solutions, J. of Applied Physics, 40, 12, 4933-4938, 1969.

/19/ URTIEW P.A., KUSUBOV A.S., DUFF R.E., Cellular structure of detonation in NM, Comb. and Flame, 14, 117-122, 1970.

/20/ PRESLES H.N., Nouveau critère d'étude de la sensibilisation d'explosifs liquides, CRAS, 314, II, 575-578, 1992.

/21/ CAMPBELL A.W., MALIN M.E., HOLLAND T.E., Detonation in homogenous explosive, 2nd Symp. on Detonation, 454-477, 1955.

/22/ COTTER T.P., The structure of detonation in some liquid explosives, Dissertation, Cornell University, 1953.

/23/ DREMIN A.N., TROFIMOV V.S., On the nature of the critical diameter, 10th Symp. Int. on Combustion, 839-843, 1965.

/24/ CAMPBELL A.W., MALIN M.E., HOLLAND T.E., Temperature effect in the liquid explosive NM, Journal of Applied Physics, 27, 6, 963, 1954.

/25/ ENIG J.W., PETRONE F.J., The failure diameter theory of Dremin, 5th Symp. Int. on Detonation, ACR 184, 99-104, 1970.

/26/ STEWART D.S., BDZIL J.B., The shock dynamics of stable multi-dimensional detonation, Comb. and Flame, 72, 311-323, 1988.

/27/ FORBES J.W, LEMAR E.R., BAKER R.N., Detonation wave propagation in PBXW-115, IXth Symp. (Int.) on Detonation, OCNR 113291-7, I, 806-815, 1990.

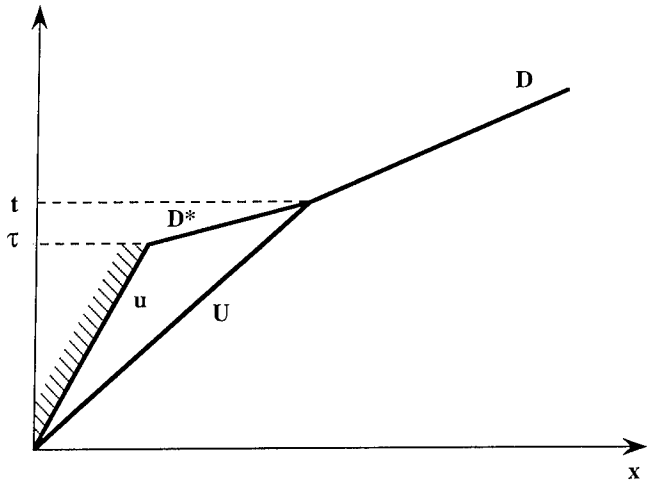

Fig. 1. Space-time representation of the events leading to the generation of a detonation in a homogeneous liquid explosive submitted to a plane shock wave

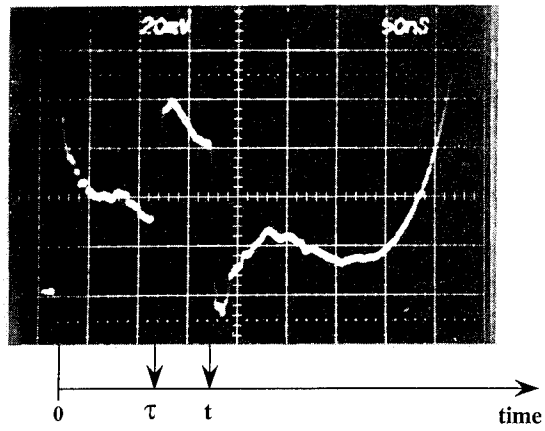

Fig. 2. Electrical signals associated with detonation generation.
At t= 0, the shock wave enters the nitromethane.
τ and t have the same meaning as on Fig. 1.

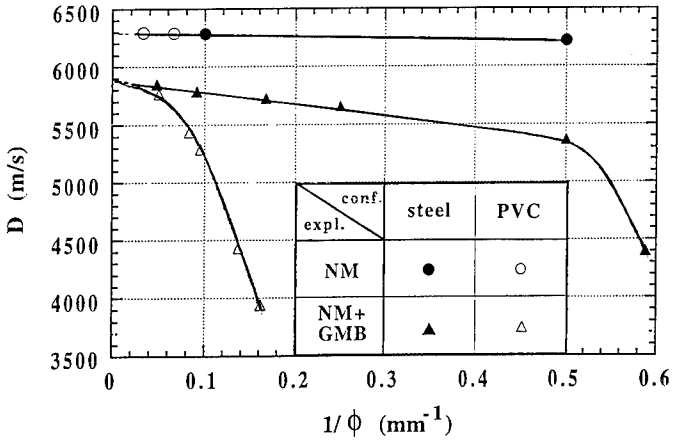

Fig. 3. Detonation velocity with respect to the reciprocal charge diameter for NM and for a heterogeneous mixture made of NM and 2% (mass fraction) of glass micro-balloons (GMB) confined in PVC and steel tubes

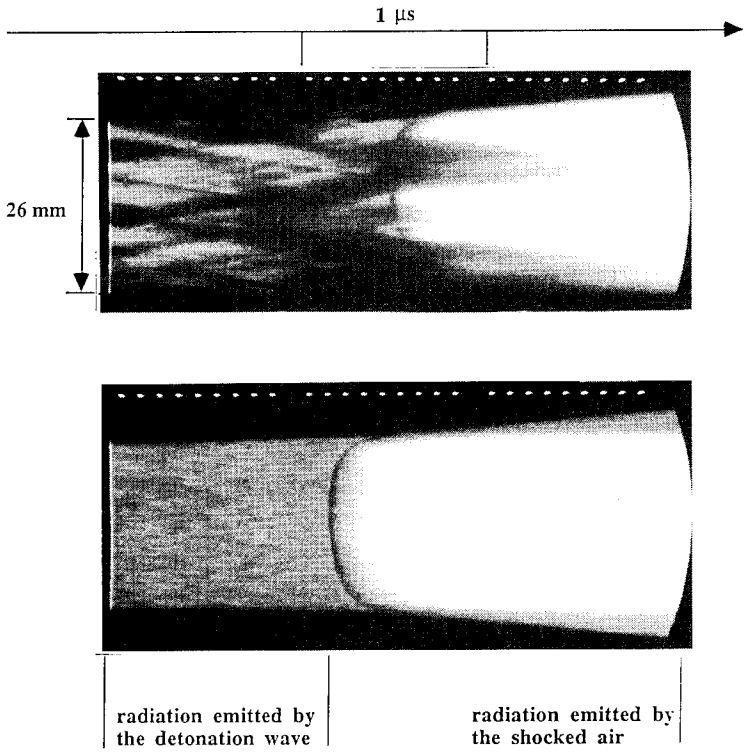

Fig. 4. Streak camera records of the radiation emitted by the detonation wave front propagating in NM-acetone mixture (upper record) and in the same mixture sensitized with DETA (lower record)

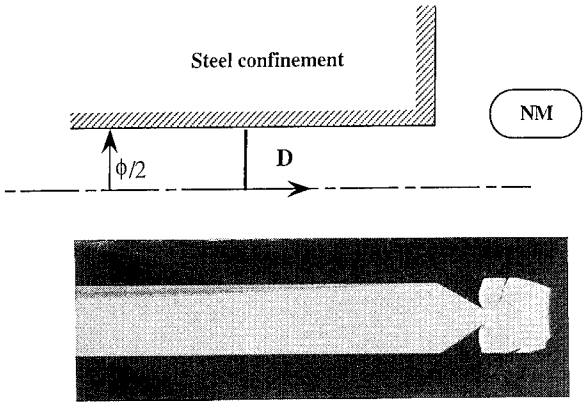

Fig. 5. Streak camera record of a detonation wave submitted to a confinement discontinuity : A conical failure wave moving with constant tranverse velocity reduces the size of the detonation front. Then re-initiation occurs.

2-2 Statements from Laboratories : Success and Failure of the Classical Theory

Critical Initiation Conditions for Gaseous Diverging Spherical Detonations ; D.Desbordes

The Limits of Applicability of Usual Kinetic Relations to the Detonation Waves Chemistry in Homogeneous Explosives ; B.N.Kondrikov

JOURNAL DE PHYSIQUE IV
Colloque C4, supplément au Journal de Physique III, Volume 5, mai 1995

Critical Initiation Conditions for Gaseous Diverging Spherical Detonations

D. Desbordes

Laboratoire d'Energétique et de Détonique, URA 193 du CNRS, ENSMA, Site du Futuroscope, BP. 109, 86960 Futuroscope cedex, France

Abstract : The diverging spherical detonation wave in gaseous explosives is obtained either with a point source of explosion of energy E or through the transmission of a plane detonation from a cylindrical tube of diameter d into a large volume. The mechanism of detonation initiation in both cases is based on the shock to detonation transition.The experimental critical conditions lead to an initiation criterion for detonation resulting from the competition between the expansion behind the leading shock wave on one hand and the shock-induced chemical heat release on the other. Whatever the type of ignition source, the detonation is obtained when the radius of curvature of the wave overcomes a particular critical value R_c whose size includes a constant and large number of cell width λ_{CJ} ($R_c \equiv 20\ \lambda_{CJ}$) and then can be considered as intrinsic to the detonative mixture used. λ_{CJ}, which is the mean size of the cellular structure of a CJ detonation, is proportional to the global chemical induction length L_i, calculated in the ZND scheme, by also a large factor (generally more than 10). Two other criteria define the critical initiation energy E_c and the critical tube diameter d_c for obtaining detonation with respect to this intrinsic length R_c .

1. INTRODUCTION

The direct initiation of the diverging spherical detonation in gaseous explosives, is based on the so-called shock to detonation transition and has been generally studied via two modes of ignition. The first mode consists in the diffraction of a planar CJ or overdriven detonation wave from a tube of i.d. d (or from orifices of different shapes) into a large volume [1] to [7]. The second mode is the deposition in the medium, by a sufficiently powerfull point source of explosion, of an energy E creating quasi-instantaneously a strong decaying spherical shock wave [1], [8] to [11].

The critical onset of the spherical detonation has been widely studied in both cases essentially in order to define the detonability limits of a mixture. These limits must be regarded as intrinsic limits because depending on the reactive mixture for given initial conditions (of pressure p_o and temperature T_o) and only on one well-controlled external parameter, as the critical diameter of transmission d_c of the tube, or on the critical initiation energy E_c of the source.

In this work are summarized all the important features concerning the problem of the critical initiation of a detonation in free space in situations defined above.

2. INITIATION BY DIFFRACTION OF A PLANAR DETONATION - MODE 1

The first idea of Laffitte in 1925, in order to produce the spherical diverging detonation in a gaseous reactive mixture (spherical detonation had never been observed at that time), was to use a plane detonation propagating in a rigid tube, which is generally easy to initiate because of the confining, and to transmit it in a larger volume [12]. Lafitte never succeeded to obtain spherical detonation because of the too smaller size of the diameter of the tube he used with respect to the reactive mixture. Nevertheless,

later on, after the experimental precursor work of Zeldovich et al. (1956) [1], this mode of production of spherical detonation wave was clearly demonstrated.

In this mode, the detonation regime exists in the medium contained in the tube where detonation products expand in constant cross section area. This detonation is submitted to a large perturbation when suddenly the confining disappears. Then, the detonation may :

1) go on, propagating in diverging spherical geometry or,

2) be quenched.

At the exit of the tube of diameter d, when the plane detonation diffracts, the two-dimensional lateral expansion propagates from the edge towards the axis of the tube and under subcritical conditions destroys completely the plane detonation wave as it penetrates into the larger volume. The plane detonation wave turns into a decaying two-dimensional curved shock wave followed by a gradually decoupling flame front.

At critical conditions, when the mean radius of curvature R of the diffracted shock wave has increased to a threshold value, the onset of detonation suddenly occurs on the axis of the tube and goes throught the whole volume before to propagate close to the CJ conditions. A quasi spherical predetonation sphere [7] is then observed with a radius $R = R_c$ (as displayed in Fig. 1).

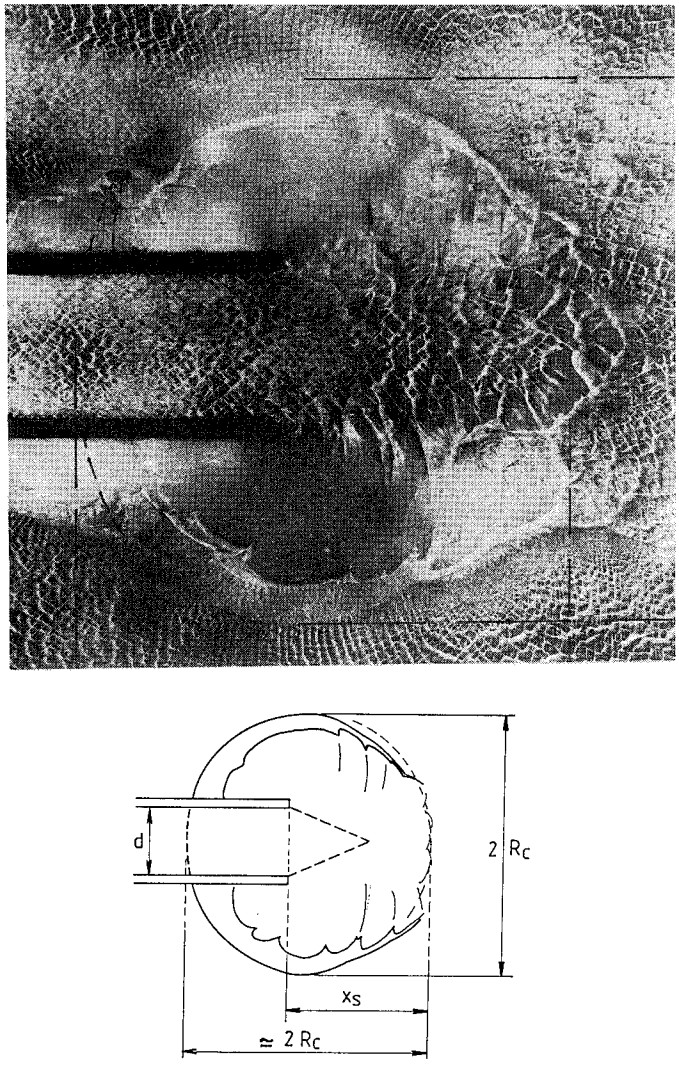

Fig. 1 Smoked-foil record of predetonation sphere of mean radius R_c for critical transmission of a plane detonation into a large volume in $C_2H_2 + 2.5\ O_2$ mixture at $T_o = 293$ K.

For most of the gaseous detonation mixtures currently used (C_nH_m/O_2 and H_2/O_2 or /Air) observations give :

$$R_c \cong 1.6\ d \qquad (1)$$

So, at that mean radius, independently of the mixture used and of the size d of the tube, the shock wave strength is quasi identical if referred to the initial conditions for a plane-CJ diffracted detonation wave. Moreover, many experimental data provide a noteworthy correlation between R_c and the detonation cell size λ_{CJ} of the mixture [13], as :

$$R_c \cong 20\ \lambda_{CJ} \qquad (2)$$

Thus, considering Eqs. (1) and (2), the classical notion of critical tube diameter d_c of transmission of a CJ plane detonation wave into a large volume can be defined and appears as a direct consequence of the $R_c \cong 20\ \lambda_{CJ}$ requirement, i.e. :

$$d_c \cong \frac{20\ \lambda_{CJ}}{1.6} \cong 13\ \lambda_{CJ} \qquad (3)$$

If now we consider the diffraction of a plane overdriven detonation wave which turns into a CJ spherical detonation wave, experiment shows that at critical conditions, the $R_c \cong 20\ \lambda_{CJ}$ rule remains valid [14]. Nevertheless, size of the critical diameter d_c decreases depending on the strength of the plane detonation wave. For not too high values of D/D_{CJ} and depending on the reactive mixture [14], d_c is found a decreasing function of D/D_{CJ} which follows the $d_c = 13\ \lambda$ rule. Detonation cell size λ depends on D/D_{CJ} as the following :

$$\frac{\lambda}{\lambda_{CJ}} \cong \frac{D}{D_{CJ}} \exp \frac{E_A}{RT_{ZND}} \left[\left(\frac{D_{CJ}}{D}\right)^2 - 1\right] \qquad (4)$$

As D/D_{CJ} increases from 1, this kind of source tends progressively towards the ideal point source of explosion (at least in the decreasing part of the relationship).

3. INITIATION BY AN EXPLOSION POINT SOURCE - MODE 2

In his experiment in 1925 [12], Laffitte succeeded for the first time to obtain a spherical diverging detonation wave by the action of high explosive point source. At that time, this diverging propagation of the wave was rejected since 1917 [15] by Jouguet. Neverteheless around the 40's, independantly Taylor [16] and Zeldovich [17] gave a particular solution of the expansion of the detonation products behind such a CJ wave.

In a general way, the critical initiation of spherical detonation does not depend on the type of source if it can be considered as an ideal strong point source of explosion (cf. Taylor [18] and Sedov [19]) as for instance, laser spark, exploding wire or detonation of high explosive. In such conditions, the energy deposition shows the same trend and the resulting shock wave produced and its decay may be scaled by only one parameter, i.e the energy of the source E (for fixed ρ_o). The intense decaying spherical shock wave produced in the reactive mixture turns into an overdriven expanding detonation wave. This detonation presents a very large curvature of its front and is submitted to the action of the intense rear expansion wave and then decays rapidly as R increases. For critical initiation, at a radius $R = R_s$, the detonation is totally quenched. The very fine cellular system observed for $R < R_s$, with cell size $\lambda < \lambda_{CJ}$, disappears [13] (cf. Fig. 2). It can be noticed that when approaching the "CJ" regime of the wave (velocity $D \cong D_{CJ}$) the curved detonation does not resist the rear expansion. A spherical shock followed by a decoupling flame is then observed. As the shock wave propagates up to $R = R_c$ ($> R_s$), the sudden onset of detonation occurs in the whole volume at different locations in the unburned compressed layer located between the shock front and the flame (cf. Fig. 3). As a remarkable result, this radius R_c is correlated to the cell width λ_{CJ}, as in the mode 1 of initiation, by a factor of about 20 for common reactive mixtures used, independently of the type of the energy source if it is strong enough (cf. Fig. 4).

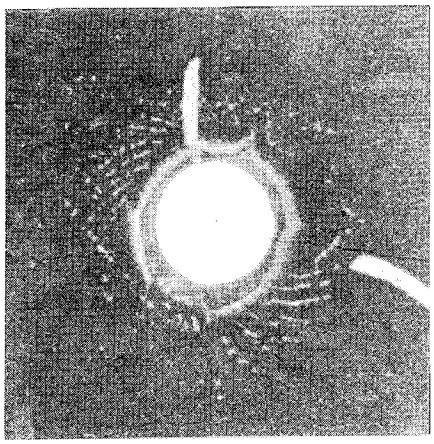

Fig. 2 Smoked-foil record of the detonation cellular structure near the initiation source and its failure in critically initiated spherical detonation in $C_2H_2 + 2.5\ O_2$ mixture at $T_o = 293$ K and $p_o = 30$ torr ($\lambda_{CJ} = 5$ mm - $R^* \equiv 20$ mm).

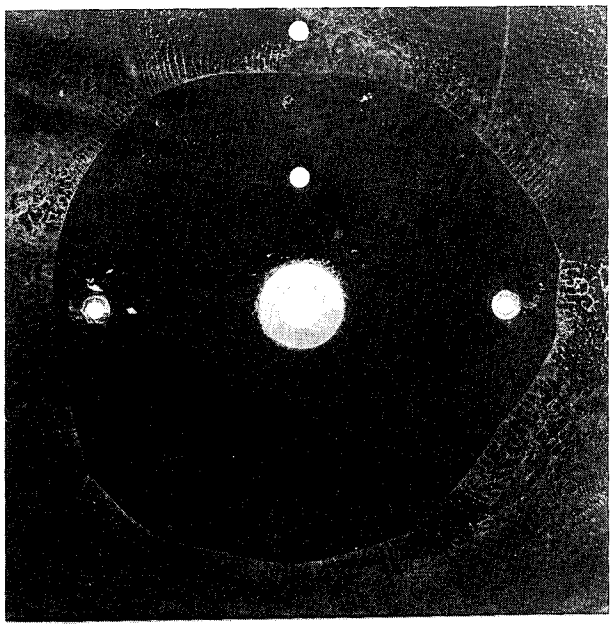

Fig. 3 Smoked-foil record of the predetonation sphere of mean radius R_c for critical detonation initiation in $C_2H_2 + 2.5\ O_2$ mixture at $T_o = 293$ K and $p_o = 40$ Torr ($\lambda_{CJ} = 4$ mm).

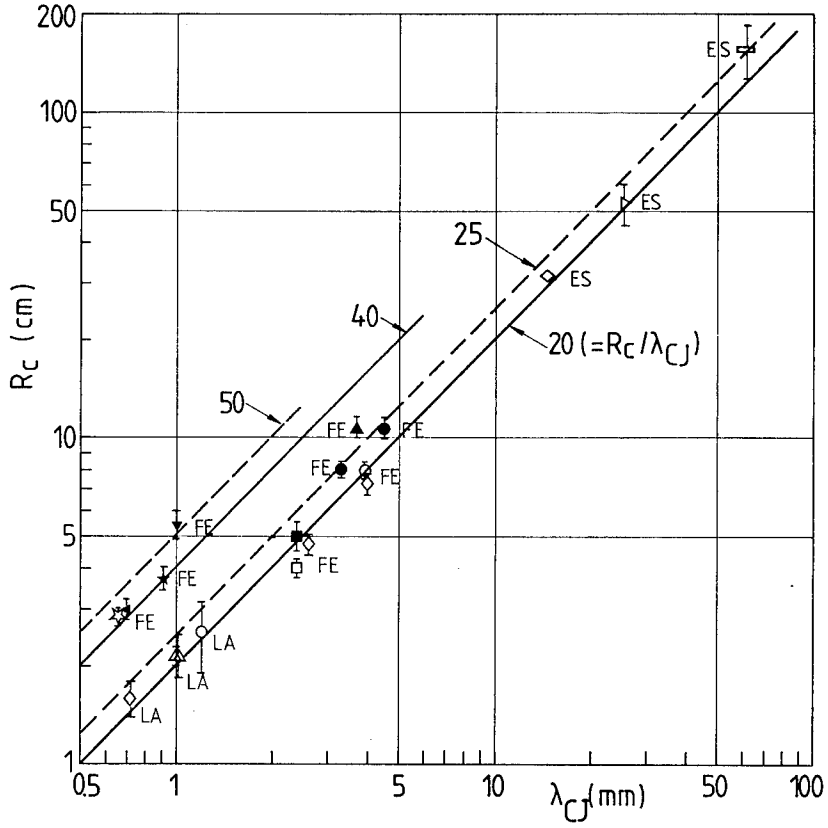

Fig. 4 Critical predetonation radius R_c versus cell size λ_{CJ} in various reactive mixtures for different initiation sources. (FE : Exploding wire - LA : Laser spark - ES : High Explosive) ◆ C_2H_2+ O_2 - ● C_2H_2+ 2.5 O_2 - ▲ C_2H_2 + 2.5 O_2 + 3.5 Ar (50% Ar) ▲ C_2H_2 + 2.5 O_2 + 9 Ar (72% Ar) ★ C_2H_2 + 2.5 O_2 + 10 Ar (75% Ar) ▼ C_2H_2+ 2.5 O_2 + 13 Ar (79% Ar) - ■ C_2H_2+ 2.5 O_2 + 5 N_2 - H_2 + Air (ϕ=1) - C_2H_4 + Air (ϕ=1.3) - C_3H_8+ Air (ϕ = 1) (white point = spherical propagation - black point = hemispherical propagation).

More recently, some experiments [20] [21] have shown that, for some reactive mixtures diluted by a large amount of a monoatomic inert as He, Ar or Kr, the critical radius $R_c = k \lambda_{CJ}$ presents a constant k depending on the amount of diluent and is, for a dilution of 75 to 80%, about twice the common value, i.e. $k \cong 40\text{-}44$. In such mixtures the $R_c = 1.6\ d_c$ rule holds, meaning that similarity concerning thermodynamical characteristics required for initiation is maintained.

In a general way, instabilities that generally arise during the process of chemical energy release in the detonation front depend deeply on the amplitude of the reduced global activation energy E_A/RT_{ZND} of the chemical system and undoubtely at the origin of the cellular and subcellular structure of the detonation wave [22]. For the systems mentionned above of particularly low values of E_A/RT_{ZND} ($\cong 5$) in comparaison with values of common reactive systems, the cellular structure is very regular (based on one particular frequency of instability). Moreover, detonation in such systems propagating in tubes exhibits a three-dimensional structure depending strongly on the rigid boundaries and its failure (initiation) because of lack of instrinsic instabilities of higher frequencies is more easy (difficult) to obtain [23] ([24]) when submitted to an external perturbation. In connexion with that, in diverging propagation the selfsustained detonation appears not so resistant to expansion and requires a larger critical radius of curvature R_c (if referred to λ_{CJ}) and then larger critical tube diameter d_c and critical initiation energy E_c [13] [21].

4. DISCUSSION

In the precursor work of Zeldovich et al. (1956), who studied carefully these two modes of initiation of detonation, is established what we called the "Zeldovich criterion" for initiation. It may be summarized into necessary conditions concerning two parameters (intensive and extensive) of the initiation problem, respectively :

1°) the strength p_s of the shock wave must be larger than a threshold value (to insure at least the self ignition of the reactive mixture), i.e. $p_s \sim p_{ZND} >> p_o$ and,
2°) the radius of curvature R of the wave is at least equal to the chemical induction length L_i[(1)] of the mixture, L_i remaining the sole characteristic length of the problem.

So the critical initiation energy may be written as :

$$E_c \sim p_{ZND} L_i^3 \qquad (5)$$

Experiments on critical initiations performed after that work confirm qualitatively such a criterion [25], but give no quantitative estimation of energy E_c.

In fact, experiments [7]-[11] reported above show clearly that onset of spherical detonation occurs at criticallity for a very large radius of curvature of the wave (at least one order of magnitude higher than the cell size λ_{CJ}).

The physical mechanism for the onset of detonation considering a progressive distance from the source is the following in the two modes [13] :

1°) at the beginning of the process the detonation regime exists (CJ or overdriven plane detonation in mode 1 and overdriven spherical detonation in mode 2).

2°) this detonation is destroyed by the strong negative gradient of the expansion wave behind the curved detonation front by respectively :
- the lateral expansion starting from the corner and converging to the axis of the tube in the case of the sudden disappearing of confining,
- the central spherical expansion in the case of initiation by the point source.

3°) as the wave recovers a small curvature with regard to the cell size λ_{CJ}, the onset of the self-sustained detonation occurs.

For simplicity of analysis, we have considered only the second initiation mode because of point symmetry (notice that for mode 1, diffraction of a highly overdriven plane detonation wave by a very small tube diameter is quite representative of the case considered because in such situation the shape of the source may be ignored). In that case, the curved multiheaded detonation exists for very small R, because of the large strength of the wave ($D/D_{CJ} > 1$ and $p_s >> p_{ZND}$). Inside the sphere of radius R*, where R* is the radius of the spherical shock wave where the energy of the source E is balanced by the chemical energy release, i.e. :

$$R^* = \left(\frac{E}{\frac{4}{3}\pi \rho_o Q}\right)^{1/3} \qquad (6)$$

the motion of the wave is governed by the energy deposition and the combustion observed is the "induced" detonation regime. At $R = R^*$, the detonation regime still exists, because cellular structures are almost recorded. So, the chemical heat release has played a role at that radius equivalent for the propagation of the shock, from the point of view of energy, to the external source. For R ($= R_s$) slightly larger than R*, the three-dimensional structure of the detonation vanishes. Most of the experiments show [13] clearly that in first approximation :

---

(1) The chemical induction length used by Zeldovich and coworkers was certainly a kind of hydrodynamic mean scale separating the shock front and the flame in the detonation structure considered in the ZND frame. A proof of that is reported in the same work where critical tube diameter is correlated to L_i by the relationship $d_c = 15 L_i$ which is very close to the $d_c = 13 \lambda_{CJ}$ rule. So, L_i in that work was representative approximately of the size of the cell spacing of the reactive mixture even if at that time the intrinsic detonation cellular structure had not been yet discovered.

1°) $R_s \cong R^*$ and
2°) R_s is equal to 0.2 R_c, so

$$R_s \cong R^* \cong 0.2\ R_c\ (\cong 4\ \lambda_{CJ}) \qquad (7)$$

Considering Eqs (2) (6) (7) and the approximate relationship $D_{CJ}^2 = 2(\gamma^2 - 1)Q$, the critical energy of initiation can be expressed by :

$$E_c = B\ \rho_o\ D_{CJ}^2\ R_c^3 \qquad (8)$$

where

$$B = \frac{4\pi}{750(\gamma^2 - 1)}$$

This expression gives generally a reasonably good estimation of the energy of real sources [13]-[21] and is very close to those given by Vasiliev and Grigoriev [26], Lee [27] and Knystautas et al [28].

In other respects, the small curvature of the wave front for the existence of the selfsustained detonation is highlighted in the experimental study of Murray et al [29]. Detonations propagate in tube with removing wall (plastic film) of different thicknesses which permit to vary the rear expansion rate. The authors demonstrated clearly that a too strong rear expansion destroys the detonation wave and a criterion for the critical existence of the self-sustained propagation of the "curved" detonation in different chemical systems has been given concerning the radius of the wave front, i.e. $R_c > 16\ \lambda_{CJ}$.

Recently, in correlation with this problem of existence of curved self-sustained detonation wave, He and Clavin [30] bring an interesting contribution to the problem of initiation of diverging detonations. They demonstrate from simulation that existence of curved generalized CJ detonation wave needs a minimum radius of curvature R_c of the wave of amplitude, at least two or three order of magnitude larger than L_i, the only scale of the problem, in agreement with observations [11] given above.

5. CONCLUSIONS

Critical direct initiation of spherical gaseous detonations in different gaseous reactive systems has been investigated.

Two modes of initiation are studied :

1°) transmission into a large volume of a plane CJ or overdriven detonation wave propagating in a d i.d. tube and

2°) deposition of an energy E by an ideal strong point source of explosion.

As generally observed :

1°) The onset of spherical detonation occurs after a predetonation sphere of radius $R = R_c$ which appears to be an intrinsic parameter of the explosive mixture linked to the cell spacing λ_{CJ} by a large and constant factor (generally 20).

2°) as a consequence of 1):

a) the detonation wave which exists generally near the "source" cannot resist strong curvature effects, even in CJ conditions. So, the self-sustained CJ detonation wave needs a maximum curvature in comparison to λ_{CJ}. When radius of detonation takes the value R_c roughly, the detonation may ignore the rear expansion wave. This can be summarized by a competition between the rear expansion effects and the chemical production in the $R_c = 20\ \lambda_{CJ}$ relationship.

b) R_c may vary from few millimeters for common C_nH_m - H_2/O_2 reactive mixtures at ambiant conditions to few meters for less detonable mixtures as C_nH_m - H_2/Air mixtures.

c) the critical diameter of transmission d_c is linked to λ by the classical relationship $d_c = 13\ \lambda$, $\lambda = \lambda_{CJ}$ for the CJ wave and results from the $R_c = 20\ \lambda_{CJ}$ requirement.

d) the critical initiation energy E_c of the strong point source of explosion varies as :

$$E_c \sim R_c^3$$

and may be very large, owing to the fact that R_c contains a large number of cells λ_{CJ} (20), each cell includes itself generally a large number of chemical induction length L_i (generally 30 for C_nH_m/Air systems), i.e. $R_c \cong 600\ L_{iCJ}$.

Discrepancy from classical rules is observed in detonation presenting a very regular cellular systems. In these systems, the critical radius of curvature R_c of a detonation is larger if compared to λ_{CJ} (or L_{iCJ}) than in common reactive mixtures and propagation in rigid tubes more dependent on confinement. This emphasizes the fact that the three-dimensional structure of detonation plays a specific role in the propagation, the initiation and failure of the self-sustained detonation wave, which cannot be explained on the simple basis of the ZND structure of the wave.

References

[1] Zeldovich Ya. B., Kogarko S.M. and Simonov N.N., *J. Phys. Technol.* **26** (1956), 1744-1772.
[2] Mitrofanov V.V. and Soloukhin R.I., *Dokl. Akad. Nauk. SSSR.* **159** (1964), 1003-1006.
[3] Matsui H. and Lee J.H., Seventeenth International Symposium on Combustion (1978), 1269-1280.
[4] Edwards D.H., Thomas G.O., Nettleton M.A., *AIAA Progr. Astron. Aeronautics* **75** (1981), 341-357.
[5] Moen I.O. et al., Nineteenth International Symposium on Combustion (1982), 635-644.
[6] Desbordes D. and Vachon M., *AIAA Progr. Astron. Aeronautics* **106** (1986), 131-143.
[7] Lee J.H., Knystautas, R. and Bach G.G. Theory of explosions, MERL Report 69-10, Mc Gill University, Montreal, Canada.
[8] Klimkin, V.F., Soloukhin, R.I. and Wolanski, P., *Comb. and Flame* **21-1** (1973), 111-117.
[9] Kamel, M.M. and Oppenheim, A.K., *Aerotec. Missili Spazio*, **2**, 122-134.
[10] Edwards, D.H., Hooper, G., Morgan, J.M. and Thomas, G.O., *J. Phys.D. Al. Phys.*, **11** (1978), 2103-2117.
[11] Desbordes, D., *AIAA Progr. Astron. Aeronautics* **106** (1986), 166-180.
[12] Lafitte, P., *Ann. Phys.*, **10**(4) (1925), 623-634.
[13] Desbordes, D., Aspects stationnaires et transitoires de la détonation dans les gaz : Relation avec la structure cellulaire du front, Thesis n°498 of the University of Poitiers, France (1990).
[14] Desbordes, D., Brissot, D. et Guerraud, C., *Ann. Phys. Fr.*, **14** (1989), 629-635.
[15] Jouguet, E., La Mécanique des Explosifs (1917) DOIN, Paris.
[16] Taylor, G.I., *Proc. R. Soc.*, **A200** (1950), 235-247.
[17] Zeldovich Ya.B., *Zh.E.T.P.*, **12** (1942), 389-406.
[18] Taylor, G.I., *Proc. R. Soc.*, **A201** (1950), 159-174.
[19] Sedov, L.I., Similarity and Dimensional methods in mechanics (1959) Academic Press, Inc. NY.
[20] Moen, I.O., Sulmistras, A., Thomas, G.O., Bjerketvedt, D. and Thibault, P.A., *AIAA Progr. Astron. Aeronautics*, **106** (1986), 220-243.
[21] Desbordes, D., Guerraud, C., Hamada, L. and Presles, H.N., *AIAA Prog. Astron. Aeronautics*, **153** (1993), 347-359.
[22] Fickett, W.and Davis W.C., Detonation (University of California Press, Berkeley), (1979).
[23] Dupré, G., Peraldi, O., Lee, J.H. and Knystautas R. *AIAA Prog. Astron. Aeronautics*, **114** (1988), 248-263.
[24] Chue, R.S., Lee, J.H., Scarinci ,T., Papyrin, A. and Knystautas R. *AIAA Prog. Astron. Aeronautics*, **153** (1993), 270-282.
[25] Bull, D.C., Elsworth, J.E. and Hooper, G., *Acta Astron.*, **5** (1978), 997-1008.
[26] Vasiliev, A.A. and Grigoriev, V.V., *F.G.I.V.*, **16** (1980), 117-125.
[27] Lee, J.H., *Ann. Rev. Fl. Mech,*. **16** (1984), 311-336.
[28] Knystautas, R., Guirao, C., Lee, J.H. and Sulmistras, A., *AIAA Progr. Astron. Aeronautics*, **94** (1984), 23-37.
[29] Murray, S.B. and Lee, J.H., *AIAA Progr. Astron. Aeronautics,* **106** (1986), 329-355.
[30] He, L. and Clavin, P., *J. Fluid Mech.,* **277** (1994), 227-248.

JOURNAL DE PHYSIQUE IV
Colloque C4, supplément au Journal de Physique III, Volume 5, mai 1995

The Limits of Applicability of Usual Kinetic Relations to the Detonation Waves Chemistry. Homogeneous Explosives

B.N. Kondrikov

Mendeleev University of Chemical Technology, 9 Miusskaja Sq., Moscow 125047, Russia

Abstract: The report presented contains the brief description of some of the macrokinetic dependencies in field of detonation of homogeneous, preferably liquid, explosives. Chemical kinetics data and mechanisms of the detonation reactions of pure nitrocompounds at different initial temperature, and the mixtures of them with sulfuric acid are obtained. The data from both groups of measurements for TNT virtually coincide with results of kinetic calculations at which the frequency of spin-pulsating subsurface waves in lean TNT/RDX mixture was used as a source of macrokinetic information. A.N.Dremin theory of failure diameter, usually used for kinetic calculations, is supplemented in three directions. (1) Velocity of the dark wave, one of the most significant elements of the theory, is connected with energy of activation and in this way it is defined independently as an inherent part of the extinguishment process. (2) The gas bubbles formation and growth in the compressed reactive substance in the dark zone are included into consideration as important moments of the detonation wave initiation. (3) The new phenomenon, that has been observed in some of the modern molecular modeling investigations: separation and collection in groups of particles of different mass in shock and detonation waves, was applied in order to explain the strong influence of additives on detonation ability of nitromethane.

The usual approximation in physical chemistry of shock waves consists of the suggestion that the thermodynamic equilibria has enough time to establish during the period of the shock wave parameters measurement. If a chemical reaction or polymorph transformation behind the shock front take place, the equilibria can be delayed, and sometimes it should not be taken into consideration at all. Correspondingly kinetic relations have to be taken into account, considered usually however, if one may say so, in so called equilibria approximation: Maxwell-Boltzman energy and velocity distribution is supposed exists, and the relations at least as to the homogeneous systems is concerned do not differ significantly from the usual Arrhenius formulae. The strong acceleration of the chemical transformation in the wave is expected to be a result of the heat evolution, and consequently the heat explosion. A role of pressure, level of which in shock and detonation waves in condensed media is essentially (sometimes in hundreds of thousand, and million times) higher than it appears to be in the routine chemical kinetics investigations, in such a case practically is omitted.

If the heterogeneous chemical reaction in the wave takes place, in systems from the point of view of density or the phase composition nonhomogeneous, the reaction is originated in sites having the higher temperature or reaction ability level, and it develops from them in form of the relatively slow burning. Due to the high pressure influence it has been proceed mainly in gas phase, and correspondingly the pressure dependence of burning rate can be considered in frames of the usual u(p) law.

The most significant contradiction as to the heterogeneous systems detonation is concerned consists in that the reaction rate estimated by means of the extrapolated burning velocity data does not conform with reaction rate obtained by means of the modern theory of the curved detonation front calculations. As a rule the extrapolated velocity is about 3-6 times less than the data derived from the detonation experiments. It is necessary to introduce some additive suggestions, say influence of pressure oscillations in the reaction zone, the frequency of which is about several GHz. Another possible reason of the explosive fast burning is the fragmentation of bubbles in the incident shock wave.

One can say that the experimental facts and laws in field of the heterogeneous systems detonation that are related by the very complicated way to the real mechanisms of the chemical reaction can hardly give the essentially positive information about the chemical reaction kinetics. Correspondingly they might be only scarcely used as a tool for the problem formulated solution. The homogeneous detonation characteristics provide in this respect more favorable information because they are appeared to be connected with the mechanisms of the reaction at detonation more closely.

The abundant information about kinetics and mechanisms of the detonation reactions in homogeneous and heterogeneous systems was obtained in this Laboratory during the last two decades mainly using the failure diameter - initial temperature, or additives concentration relations, and detonation velocity - charge diameter dependencies. [1-7], and A.N.Dremin and J.Bdzil [8, 9] theories application, as well as by means of the shock wave pressure - induction period dependencies [10] treatment. R.Engelke and J.Bdzil [11] had derived kinetic data on nitromethane decomposition in detonation wave from the detonation front curvature measurements. Quite recently a group of investigators of Washington State University [12] using the modern spectroscopy instruments possibilities has obtained interesting data concerning kinetics of nitromethane/ethylenediamine mixture reactions in temperature and pressure region very close to the dark zone at extinguishment of detonation. All the more interesting perspective appears to be the application in the nearest future of pico-, and femtosecond spectroscopy measurements [13, 14].

In case of the homogeneous, mostly liquid explosives the D(d) relations as a rule may not be measured accurately due to strong temperature dependence of the reaction rate and the detonation instability influence. Correspondingly, the main source of information on chemistry in the detonation wave from the macroscopic point of view is the failure diameter, $d_f(T_0,C_{solv.})$ change, and the classic Dremin theory application. The most amusing fact in this respect is that namely instability in such a case provides the chemical kinetics from $d_f(T_0,C_{solv.})$ data extraction owing to the peculiar kind of the pulsating reactor formation, in the reaction zone of which the process has developed in the quasi steady state conditions suitable for the kinetic measurements.

We have obtained the initial temperature - failure diameter dependencies for nitromethane, nitroglycol, diethyleneglycoldinitrate, TNT/H_2SO_4 50/50 and nitromethane/H_2SO_4 50/50 mixtures [3, 5, 6], and have used the Belyaev and Kurbangalina data [15] for pure TNT and nitroglycerine. The most amazing result is the absence of difference in detonation ability of the liquid and crystal nitroglycol (Fig. 1). It is a check of the idea of possible influence of the crystallic structure of a substance on reaction rate at shock wave attack [16]. The calculations performed demonstrate in particular a good correlation between the data on

the adiabatic explosion period $\tau(p)$ dependence [10] and our data estimated from $d_f(T_0)$ line for NM [7]. The lines $\tau(p)$ obtained for pure NM at different initial temperatures intercept the curve calculated from $d_f(T_0)$ relation at approximately the same T_0 values (Fig.2).

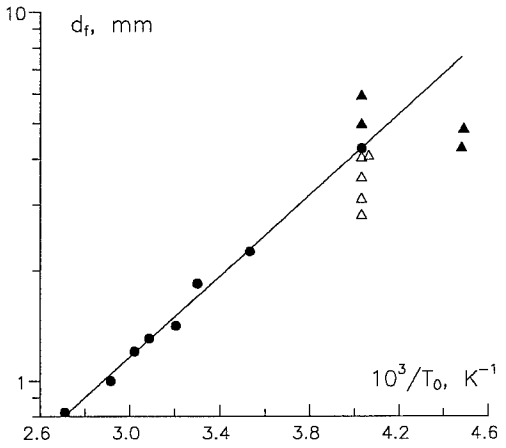

Fig.1. Data on the failure diameter - $1/T_0$ dependence obtained by G.D.Kozak and V.V.Kondratiev for liquid (●, in the conical glass tubes), and crystallic solid (Δ,Δ - detonation, failure detonation; in the cylinder glass tubes) nitroglycol.

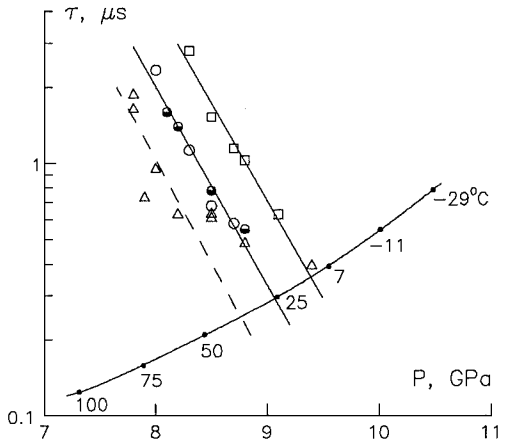

Fig.2. Adiabatic ignition period τ obtained at the different initial temperatures by the methods: the curve - $d_f(T_0)$ [5], the straight lines - $\tau(P)$ [10]. T_0: Δ 40^0C, ○○ 25^0C, □ 4-6^0C (gas chromatografically purified and spectral quality NM data only). This figure is taken from [7].

Several years ago a new phenomenon in field of detonation of homogeneous liquid and solid explosives and propellants was observed [4]. At detonation of the cylinder charge, diameter of which is a little bit more than the failure diameter of the substance the spin detonation wave can arise under and near the surface of the charge in a thin layer of the explosive compressed by the main coaxial detonation wave. The velocity of the spin wave may reach ~10 km/s, and the corresponding high pressure forms a flow of the detonation products and the original material particles which leave the deep spiral furrows on the metal witness plate. The subsurface layer can arise spontaneously owing to the extinguishment of the detonation reaction on the edge of the charge, or it may be formed coercively by cutting preliminary the thin spiral line on the cylinder surface. In case of the spontaneous spin wave formation the phenomenon is supposed to be described as the spin-pulsating process, frequency of which might be used for estimation of the adiabatic self-heating induction period, and correspondingly, the kinetic constants of leading chemical reaction. The thermodynamic conditions in the compressed subsurface layer can be estimated using relations of Dremin's dark wave theory. As a matter of fact the results for TNT demonstrate unity of all the values calculated by different methods, on base of experimental results measured by the quite different ways: $d_f(T_0)$ dependence [15], $d_f(C_{H2SO4})$ [5,6], and spin frequency - detonation rate relations give E_a=109-110 kJ/mol, $k_0=10^9$-10^{10} s^{-1}.

Two main uncertainties of Dremin theory should be taken into account before kinetic results might be obtained inherently on the one hand and independently of the more complicated measurements on the other.

The first of them is the uncertain value of the dark wave, or the dumping reaction wave velocity v, which in frames of the theory must be determined experimentally.

We have calculated [17] the dark wave velocity in the suggestion , that the detonation front, at least on the edge of the charge, has a form of a wave

$$y = A \cdot \sin(k \cdot x) \cdot \cos(\omega \cdot t),$$

where t is time, A is amplitude, $\omega = 2 \cdot \pi / \tau$ is cyclic frequency, τ is the period of the wave, $k = 2\,\pi/\lambda$ is the wave number, λ is the length of the wave. In this approximation $v = \lambda/\tau$.

One can suppose that the reaction extinguishment condition is reached, when temperature in the wave becomes less than $T_* = T - R \cdot T^2/E_a$ and $W_* = W/e$, where T and W are the steady-state detonation front temperature and reaction rate, T_* and W_* are critical values of the temperature and reaction rate, E_a is the energy of activation.

At $T \sim p \sim D^2$ we obtained

$$v^2 = (A^2 \cdot \omega^2 / RT) \cdot E_a,$$

or

$$v^2 = a \cdot E_a,$$

where a is a constant (mol/kg), which may be defined from the well known data for NM and TNT failure diameter vs. initial temperature relations:

$$a = 65 \text{ mol/kg}.$$

Using this value of a we calculated the more precise data of the overall kinetic constants of the reactions in the dark zone of the extinguishing detonation wave [17].

The second contradiction in Dremin theory consists in the fact that reaction in the dark zone develops in accordance with the adiabatic heat explosion laws: the explosion springs up in the end of the zone as a result of the reaction heat acceleration. However just near the zone a thick layer of the hot - up to 3000 K - gaseous products exists, which moreover is constantly mixing with the compressed initial substance owing to the turbulence stimulated by the difference (about 100 m/s) in velocities of the layers. The second circumstance that should be comprehended in this respect is the mechanisms of deflagration originated from the hot source, whether it be a selfignition or by the hot gas inflammation, to detonation transition.

One way or another, we came to conclusion, that the main process in the dark zone is formation of the gas bubbles, the presence of which was proved some twenty years ago by F.Walker and R.Wasley [18] and then confirmed by some others [19]. When the bubbles concentration and dimensions become high enough to provide the DDT process development in the zone, it will be obtained, originating from the every source which one can propose - the adiabatic selfignition, the inflammation by the hot gas, or due to the influence of the weak shock waves irradiated by the main detonation front oscillations. In any event, the point of the violent reaction initiation should be placed at the end of the dark zone, where the bubbles have enough time to grow to the dimensions necessary for the violent, explosive deflagration, and for the deflagration to detonation transition.

The process of the bubbles grow can be stipulated by the coalescence of small gas nucleus in the quickly moving turbulent flow, but it seems plausible that it can be connected also with burning of the initial substance after the dimension of the initial "germ" becomes sufficient for inflammation. This dimension is ~ æ/u, where æ is the thermodiffusivity coefficient and u is the linear burning rate.

At usual magnitudes of æ and u, about 10^{-7} m^2/s, and 1-10 m/s, correspondingly, we obtain the critical nucleus dimension ~ 10-100 nm. During induction period of about 0.1-1 μs the nucleus can grow up to $2 \cdot u \cdot \tau \sim$ (2-20) μm. These dimensions are quite sufficient for detonation at relatively low shock wave attack initiation, and for the DDT process development. The expansion of the explosive in the dark zone behind the oblique shock wave promotes the grow of the bubbles.

Fortunately, this addition to the model of A.N.Dremin virtually does not affect at least in the first approximation the calculation scheme existed. Formation of the necessary quantity ($\alpha \sim 10\%$ v/v) of the gas bubbles needs depending on the extent of expansion of 2-5% of the initial substance decomposition. It is only about two times more than the theory of adiabatic heat explosion utilized in Dremin model requires. The preignition development of the reaction requires about the same time as the burning of the explosive around the nucleus.

So the uncertainty of about two for the Arrhenius preexponential factor should be anticipated. In this respect the rather strange result of ours [20] concerning the influence of aeration of diglycoldinitrate on the failure diameter of the substance can be explained. Instead of more or less fast decrease of d_f at porosity rise as it traditionally is in case of all the other explosives studied, the DGDN`s d_f quickly enhances from about 15 mm at zero porosity up to at least 50 mm at porosity of about 5%. The most probable reason of this unusual behavior, strange as it may seem, is the high reactivity of DGDN as a nitric ester. Even a small concentration of bubbles in the liquid leads to the quick burning in the dark zone from the very beginning of the zone formation. The burning destroys the zone as the necessary element of the lateral detonation wave providing the main detonation front regeneration, and in such a strange manner leads to the failure diameter augmentation. The paradoxical character of this explanation consists in that the substance of higher reactivity can have under certain circumstances the higher failure diameter than the more inert one.

The results of our investigations of the "inert" solvent on d_f influence [1-3, 5] have demonstrated that almost no really inert solvent exists. Oppositely to the wide spread ideas of the past, all of the organic liquids used react intensively with the nitrocompounds or with the products of the decomposition thereof in detonation wave as if they were a part of a molecule of the explosive. Moreover, most of them accelerate the chemical reactions at detonation, consequently decreasing d_f. Bases, acids, unsaturated compounds, halogen containing substances, and even distilled water can accelerate the detonation wave reactions (at least in case of NM).

The most impressive of the results obtained is the strong enhancement of the detonation ability of nitrocompounds at mixing them with bases and acids. From the practical point of view especially significant is the unusually strong d_f of TNT decrease when adding of the concentrated or super-concentrated, containing excess of SO_3, sulfuric acid. The failure diameter of $TNT/H_2SO_4/SO_3$ mixture reaches approximately 2 mm, some thirty times less than the pure TNT d_f value. It is about the failure diameter that have been obtained for such dangerous nitric esters as nitroglycerin or nitroglycol. The theory of the process is proposed in the works [6, 7, 21].

From the theoretical point of view of course the most essential fact is the catalytic activity of small (up to 0.02%) admixture of amines or acids to nitromethane [1, 2].

The idea proposed at discussion the results with Ja.B.Zel'dovich was the chain reaction initiated by amine or acid. It is necessary to note that this idea needs the suggestion of 150-200 steps long chains in the reaction zone (sometimes during the period of time up to 10^{-6}-10^{-8}s). If we take into account that the chain reactions at the nitrocompounds decomposition or detonation in no single one case were definitely observed the idea as a whole becomes at least a very suspicious one. We still had developed it in many details [3, 22] in spite of the natural resistance of the authors to the ideas of others. This purely psychological opposition supposedly led us to the new model of the phenomena and to the more pronounced understanding of the processes proceed in the dark zone.

Of course the new concept needs in turn some additive proposals. One of them consists in the fact one could note at the reports of D.Robertson, P.Haskins, J.Boris, E.Oran and some others presented on the IVth Gordon Conference, June 26-30 1994, New Hampton, NH, USA and on the 2nd International Workshop on Microscopic and Macroscopic Approaches to Detonation, Saint Malo, France, October 2-7, 1994. At molecular modeling of detonation forming two different sorts of molecules in products, one has clearly seen that the products are separated: some of them combine the groups, meanwhile the others form a layer around them. This process, which could be called as coalescence in two-phase media, and is appeared to be a peculiar "antidiffusion" in case of the single-phase substance, probably is connected with the strong collisions between the molecules in shock wave. The molecules of the different masses acquire at collisions the different velocities, for instance the more light particles are rejected, thrown away, and the more heavy ones are collected together. Dr.A.A.Borisov has mentioned in private discussion that the process reminds him the well known fact of polarization in shock wave, i.e. separation of ions and electrons due to quick diffusion of electron gas [23]. One cannot exclude however that this is just superficial resemblance of two similar but in the essence still different effects.

If in the dark zone behind the shock wave, formed at initiation or at extinguishment of detonation, the molecules of nitromethane and an additive form a heavy intricate complex, they can combine together into ensemble the dimensions of which are enough to produce the hot spot from which burning of the substance may originate. Correspondingly the system can produce the number of bubbles which is sufficient for the DDT process occurrence at relatively small number of the molecules added.

The nucleus of about 10 nm in diameter can be formed by 10^2-10^3 of the sufficiently big molecules. In this respect, one could mention that the only heavy, big molecules of organic amines are the additives that usually are utilized as the catalysts (though may be mainly from the practical point of view due to involatility of the heavy amines). The concentration of the bubbles of the final dimension of ~ 10 μm originated from the nucleus at the gas relative volume in liquid of about 10% is ~ $2 \cdot 10^{14} m^{-3}$. It is quite reasonable value. If we propose that number of heavy complexes in one group is about 10^2-10^3, then the whole number of the molecules of the catalyst gathered in groups is $2 \cdot 10^{16}$-$2 \cdot 10^{17}$ m^{-3}. At the suggested content of amine molecules in nitromethane ~ 0.02 mole % the whole number of the catalyst particles is ~ $2 \cdot 10^{24}$ m^{-3}. So the part of the molecules gathered in the groups is only 10^{-5}-10^{-6}% of all the molecules of the additive in the mixture.

This may be rather complicated mechanism of the catalytic additive on nitrocompounds detonation influence has been confirmed however by the results obtained recently by the group of investigators [12] using the methods mentioned above. At essentially isentropic compression of nitromethane containing 0.1% ethylenediamine up to 13.7 GPa they could observe only first order consumption of ~ 0.1 % of nitromethane without any significant self-acceleration. Obviously, in absence of the shock-wave collection the amine-nitromethane complexes being not possible to combine in groups decompose separately without forming nucleus of self-ignition and subsequent burning.

This is very important experiment. It shows that 0.1% ethylenediamine in absence of the shock wave influence do not accelerate nitromethane decomposition process significantly, all the catalyst added

"burns out" without significant self-acceleration of the nitromethane reaction (although some enhancement of the nitromethane consumption at pressure from 9.8 to 13.7 GPa augmentation is still definitely observed). In any case the consumption of 0.1% of the explosive itself at the conditions of isentropic compression can give only the very confined, about 3-4 K, temperature rise, and may not lead to the adiabatic self-acceleration. It is necessary to add also that the results [12] actually show that the pressure itself is in no case the determining factor of the heat evolution at reaction in detonation wave.

One can see, that most of the rather unusual effects and dependencies related to the detonation reactions kinetics and mechanisms may be explained quite logically by means of the usual macrokinetic relations drawing the relatively small number of the additive suggestions. Again, one can see that the molecular dynamic calculations results and the modern spectroscopic measurements are extremely useful for understanding of some of the well-known but badly explained facts. It obviously is the main practical output of the heavy and expensive works, development of which is stipulated by the concentrated financial support of several highly qualified scientific groups, and the main purpose of which in turn is namely to use the modern theoretical and experimental methods possibilities for explanation of the great mass of information accumulated during the many decades of the energetic materials shock and detonation phenomena investigation.

REFERENCES

1. Kondrikov B.N., Kozak G.D., Raykova V.M. et al., *Dokl. Akad. Nauk SSSR*, **233** (1977) 402-405 (Russ.).
2. Kondrikov B.N., Chemical kinetics of detonation in some organic liquids. 8th ICOGER, Minsk 23-26 August 1981, Shock Waves, Explosions and Detonations, J.R.Bowen, N.Manson, A.K.Oppenheim, R.I.Soloukhin, Eds. (Vol. 87 of Progress in Astronautics and Aeronautics, 1983), pp. 426-441.
3. Starshinov A.V., Cand. Sci. (Ph.D.) Thesis, Mendeleev Institute of Chemical Technology, Moscow, 1979.
4. Kozak G.D., Kondrikov B.N., Oblomsky V.B., *Comb., Expl., Shock Waves*, **25** (1989) 459-465.
5. Khoroshev S.M., Cand. Sci. (Ph.D.) Thesis, Mendeleev Institute of Chemical Technology, Moscow, 1987.
6. Gamezo V.N., Kozak G.D., Kondrikov B.N. et al., *Explosive Materials and Pyrotechnics*, CNIINTIKPK (1992), N 3 (218), pp.3-9 (Russ.).
7. Gamezo V.N., Diploma (Master's Degree) Thesis, Mendeleev Institute of Chemical Technology, Moscow, 1988. Cand. Sci. (Ph.D.) Thesis, Mendeleev Institute of Chemical Technology, Moscow, 1992.
8. Dremin A.N., *Dokl. Akad. Nauk SSSR*, **147** (1962) 870-873 (Russ.).
9. Bdzil J.B., *J. Fluid. Mech.* **108** (1981) 195-226.
10. Berke J.G., Shaw R., Tegg D. et al., "Shock initiation of nitromethane, methylnitrate, and some bis-difluoramino-alcanes", V Symp. (Int.) on Detonation, Pasadena, Ca, 18-21 August, 1970 (ACR-184, Office of Naval Research, 1971) pp.237-246.
11. Engelke R., Bdzil J.B., *Phys. Fluids*, **26** (1983) 1210-1221.
12. Constantinou C.P., Winey J.M., Gupta Y.M., *J.Phys.Chem.* **98** (1994) 7767-7776.
13. Lee I.-Y.S., Hill J.R., Dlott D.D., *J. Appl. Phys.*, **75** (1994) 4975-4983.

14. Wang W., Weferss M.M., Nelson K.A., "Femtosecond spectroscopy of chemical reactive solids: a methodology", Structure and Properties of Energetic Materials, Boston, Ma, USA, 30 November - 2 December, 1992. D.H.Liebenberg, R.W.Armstrong and J.J.Gilman Eds. (MRS, Piltsburgh, Pa, 1993) pp.130-140.

15. Belyaev A.F., Kurbangalina R.H., *Journ. Fiz. Khim.*, **34** (1960) 603-610 (Russ.)

16. Kondrikov B.N., "The kinetics of chemical reactions in physico-chemical waves", Ya.B.Zel'dovich Memorial, Moscow 12-17 September, 1994, S.M.Frolov, Ed. (Russian Section of the Combustion Institute, Vol. 2, 1994) pp.36-38.

17. Gamezo V.N., Kondrikov B.N., *Khimicheskaya Fizika*, **13** (1993) 1502-1505 (Russ.).

18. Walker F.B., Wasley R.J., *Comb. Flame*, **22** (1974) 53-67.

19. Vorobjev N.A., Trofimov V.S., *Fizika Gorenija i Vzryva*, **14** (1978) 152-153.

20. Kondrikov B.N., Kozak G.D., Oblomsky V.B. et al., *Comb., Expl., Shock Waves*, **23** (1987) 195-202; "Peculiarities of detonation of porous liquid nitrocompounds", Fundamental Problems of Physics of Shock Waves, Azau, 18-21 May, 1987, (Acad. Sci. USSR, Vol. 1, part 1, 1987) pp. 34-36.

21. Gamezo V.N., Khoroshev S.M., Kondrikov B.N. et al., "Sulfuric acid influence on the nitrocompounds detonation reaction", 2nd Workshop on Macroscopic and Microscopic Approaches to Detonation, Saint Malo, France, 2-7 October, 1994.

22. Starshinov A.V., Kondrikov B.N., Kozak G.D. "Homogeneous catalysis at nitromethane detonation", I Vsesoyusnoye Sovestchaniye po Detonatsii, Chernogolovka, 1977. (Detonation, Akad. Sci. USSR, Chernogolovka, 1977), pp. 73-76.

23. Zel'dovich Ya.B., Raizer Yu.P., Physics of shock waves and high temperature hydrodynamic effects ("Nauka", Moscow, 1966), p.404.

2-3 Discussion

Moderator: Dr. Gabrielle Dupré, C.N.R.S., Laboratoire de Combustion des Systèmes Réactifs (LCSR), Orléans, France

In the session dedicated to detonation in liquids and gases, some new ideas, experiments and calculations have been presented, concerning the initiation and propagation of detonation in homogeneous media, the three-dimensional structure and its relationship to chemical kinetics, the energy release involved during the detonation process, the initiation of detonation in a liquid explosive. Then, statements from two laboratories gave some insight over the validity of the classical theories.

Afterwards, an interesting discussion took place between the audience and the speakers. Various questions have been posed or comments stated, as you can see below, concerning GZND theory, critical parameters for the initiation phase of detonation, wave curvature, strong initiation, properties of matter above the critical point, location of the onset of chemical reactions in liquid explosives, anisotropic properties and polarization effects within the shock front in liquid explosives...

In the following pages, I have tried to restitute the discussion as fair as I could, according to the cassette, with some slight modifications in order to take into account what the authors wrote afterwards.

A.N. Dremin A comment:

The CJ detonation theory has not proposed any mechanism of EMs transformation at detonation and therefore one should not expect from the theory the detonation limits (SDT, unstability, failure diameter) and interpretation. In regards to the ZND theory it has appeared in fact as some response to the need for the theory capable to interpret the limits. The notion of the finite chemical reaction zone at detonation is undoubtly the main point of the EMs transformation mechanism proposed by the ZND detonation theory.

The following experimental findings are inconsistent with the ZND detonation theory:

First: Very small change of liquid EMs detonation velocity D with charge diameter d near their rather big failure diameter d_f. Opposite to this finding, it follows from the theory that any EMs D(d) dependence and their d_f have to correlate; the smaller is the dependence -- the smaller d_f has to be.

Second: The fact that explosion induction time at shock initiation of detonation in homogeneous (gaseous and liquids) EMs becomes negligibly small at a shock pressure approximately equal to CJ pressure and not at the pressure of the shock of the CJ detonation velocity.

Third: Unstable detonation. Before the ZND detonation theory advent, one believed that one-head and many-headed spinning detonations were separate original phenomena different from normal detonation. Later on, one tried to interpret the instability as some small perturbations of the ZND detonation wave physical model. However, it turned out that the unstable detonation physical model and the ZND detonation model have nothing common in general. They differ fundamentally.

In essence the theory could not explain the unstable detonation origin mechanism. The nature elicitation has led to a new phenomenon discovery. The phenomenon has come to be known as chemical reaction breakdown. It has been revealed that all limits of detonation are governed by the phenomenon.

phenomenon has come to be known as chemical reaction breakdown. It has been revealed that all limits of detonation are governed by the phenomenon.

Clavin-Desbordes : *about critical length and critical energy*
Clavin : What are the mechanisms involved in the critical length and critical energy, in the initiation phase of detonation ? In few words, I would say that, as shown by Desbordes, there is a critical radius below which it is not possible to have a self-sustained detonation. This can be explained by non-linear dynamic effects that may occur. It is not surprising that there is a natural length scale which is the induction length. It is clear that below this length, you cannot have any spherical detonation. This was the argument of Zel'dovich, even in his papers. But what is surprising in the experiments is that the ratio between the critical radius Desbordes measured and the induction length is about 600 to 700. Now, if you go through the critical energy, that is $r_0\ D_{CJ}^2\ L_{iCJ}^3$, the number that we have to explain is no more 700 but 700^3, that gives a number which is between 10^6 and 10^8. This is a real question that we have to answer.
Desbordes : For me, the induction length L_i is just a concept derived from the model of detonation called ZND. This length remains nevertheless very instructive for the detonation point of view. The only relevant and real length, which is due to a more complex detonation structure than the ZND model, is the cell size λ, typical length of a three-dimensional structure, which is surprisingly proportional to L_i, which is a one-dimensional length. As a consequence, no conceptual reason forbids the existence of a detonation in a tube of diameter d, equal to or of the same order as L_i. Unfortunately, such a detonation is not observed. Detonation is only observed if $d = \lambda_{CJ}$. A similar observation is found for curved detonation where a criterion for the existence of detonation has to be discussed between the radius of curvature and the cellular structure, that is the more elementary micro-scale of detonation that can be found.

Oran : *about the improvement of reaction scheme and its influence on detonation cell size*
I would like to comment only the effects of the chemical reactions on the size of the detonation cells. Just recently, we have done a series of computations on H_2/O_2 reaction scheme. We went from a rather crude reaction scheme for H_2/O_2 which models just an induction time and an energy release to an improvement of the chemistry, using 2D calculations and a four chemical kinetic reaction-scheme. We found that, in fact, as we made this improvement of the chemistry, we got significant effects of the size of the detonation cell ; this is because of the distribution of the energy release.

Kondrikov-Desbordes : *about intense source of explosion*
Kondrikov : What did you say about the nature of the dark zone around the exploding wire ? Is it just a strong detonation and a reaction zone too narrow to irradiate light, or is it an effect of expansion of the evaporated metal ? Can you measure the velocity in this zone ? How big is it ?
Desbordes : The energy released by an intense source of explosion (as the exploding wire initiation source) creates in gases a very strong spherical expanding shock wave which decays as it expands. Generally, in a reactive medium, an overdriven spherical detonation is created and, if the characteristic chemical length (i.e. the post shock chemical induction length of the global reaction) is too large in comparison to the radius of curvature when the detonation approaches the CJ regime of the wave, then the

detonation vanishes completely. So, in a general way, a CJ self-sustained detonation cannot resist to a too strong curvature of the wave compared to its chemical induction length.

Melius-Presles, Desbordes, Dremin : *about properties of gases and liquid above the critical point*

Melius : My question is about gases and liquids both, because at high pressures and temperatures, above the critical point, we cannot anymore distinguish the gas from the liquid. So it seems to me that perhaps the differences are due to the density rather than to the properties of the liquid or the gas and, unfortunately, the issues arisen at high temperature and pressure may not be appropriate terms anymore and, if you find many similarities, it is perhaps because of the density that makes the difference.

Presles : I do not understand very well the question, you are talking about differences between what and what ?

Melius : We do not held the concept of a liquid or a gas anymore above the critical point, they are just the same fluid. So what are the differences between a liquid and a gas that we are trying to differentiate like in low an high density materials ? What effects of detonation of gases versus liquids might be attributable to differences in density rather than in phase characteristics ?

Presles : It is a large question.

Desbordes : Detonation in either gas or liquid phase gives detonation products above the critical point. For gases, the EOS of ideal gas can generally be applied. For liquid explosives, when pressure effects are very high because pressure in detonation products is proportional to initial density, we need an EOS of the detonation products that eventually takes into account some solid species. Chemical kinetics may be certainly be completely different, even if there are both homogeneous media.

Dremin : May I comment this question ? You know that even at a very high range of pressures, it is a real liquid. In all our shock experiments, we are under the critical point. If you put a text at the bottom of a vessel of a liquid explosive and run a shock in it, you can read the text through the shock compressed material. The transparency of shock compressed materials is extremely nice.

Dremin : *about rate of energy release and rate of adiabatic cooling*

I would like to continue with the following problem. As a matter of fact, whatever is the shape of the wave, a planar or a spherical one, it does not matter. The fact that the shock transforms into a detonation or not depends on two parameters : the rate of energy release and the rate of adiabatic cooling. If the adiabatic cooling cannot compensate the rate of energy release, then the shock turns into detonation. If the rate of adiabatic cooling can compensate completely the release of energy, then the shock cannot transform into detonation.

Boris-Dremin, Nelson, Gupta : *about anisotropic properties of liquid explosives*

Boris : My question is to all of you who have worked with liquid explosives. In the Navy, we deal a lot with water and it is understood that water can have very anisotropic properties on short time scales. We are talking about very fast shock and initiation of detonation in liquids. Do any of these liquids display some of the anisotropic properties that we have talked earlier, these structure-based anomalies usually associated with

solids, such as anisotropy, dislocations, holes, etc ? Or do liquids behave more homogeneously like dense gases ?
Dremin : In comparison with water that looses its transparency at some specific pressure, liquid explosives do not change their transparency under the shock pressures usually used for the initiation of detonation. That means that they change their chemical structure very slightly, in comparison to water. Liquid explosives behave like dense gases until shock intensities induce a critical pressure able to initiate a detonation.
Nelson : Anisotropy is another question that will go away from the liquid on a time scale of few picoseconds. It may last longer if there exist some cavitations or some macroscopic structures.
Gupta : You can have rotational molecules in a liquid, although it is believed that molecular rotation occurs very rapidly, at a 30-50 ps time scale. However, under a pressure of 50-60 kilobars, it is not clear that it can happen within picoseconds time scale. We have some spectroscopic observations which we have interpreted as to be due to the rotation of molecules under shock conditions.
Coming back to the issue about anisotropy, there is a very interesting paper of Tony Campillo where he looked at life-times, and it turns out that if we shock something, on the average we go very quickly to anisotropic conditions.

Dlott-Presles, Ramsay : *about relationship between beginning of chemistry and region of slight discoloration*
Dlott : You showed pictures of the initiation of liquid nitromethane. They show the dark regions and the light regions and, in between, there is a slight discoloration region and you pointed out and said : this is where the chemistry began. How do you know there was not lots of chemistry before that, which simply did not appear in your picture ?
Presles : You are right : on the picture, we see luminosity and we say that chemical reactions start at that time, but in any case, chemical reactions have begun earlier. It is because this is the only way to measure some induction time and it is why I propose (and not only me) to use an electrical method which may more precise.
Ramsay : In response to the question on the reaction in shocked liquids, basically the first reference to that was given in a conference which was held around 1963 ; also in the last Detonation Symposium, there are several papers that have addressed that question. There are reactions which starts relatively early, with an energetics apparently very low, because it is very low detectable in fact in the shock front. So we have argued basically for simplicity in saying that the reaction starts when we see the light. But in fact, there is some sort of reaction which occurs earlier. And the light is quite strong in liquid TNT and in other liquid explosives.

Dremin-Presles, Dremin, Presles : *about electrical polarization in the shock front*
Dremin : You are talking about electrical polarization in the shock front. What do you mean ? Are explosive molecules dipoles or is there a deformation of molecules in the shock discontinuity zone, then an interaction of the shock with the deformed molecule ?
Presles : I do not know exactly what happens inside the shock front, but I only refer to previous work on polarization effects in polar molecules, which says that this effect is due to the orientation of dipoles inside the medium. So whatever the medium, explosive or not, when it is submitted to a shock wave, we get this effect and, in this case, the medium seems to be anisotropic, because it appears that there is an orientation of some dipoles.

3 FINAL DISCUSSION

Chairman : Pr Louis Brun, Centre d'Etudes de Vaujours-Moronvilliers (CEA/DAM)

Considering the extreme diversity of energetic materials, any attempt to classify them according to whatever criterion can be highly clarifying. For instance we know that the distinction between homogeneous and heterogeneous EMs is meaningful with regard to the SDT process. Another often referred to distinction concerns the detonation itself : ideal or non-ideal.

This morning, Davis and Fauquignon reasserted the status of ideality already assigned by C.Fauquignon at Megève to the simplest theory of Fickett and Davis' Detonation. Several laboratories then provided us with examples of what might be perceived as an approximation to ideal behaviour in the realm of solid EMs.

Further statements from laboratories are next going to elaborate on definitely non-ideal behaviours such as are encountered in granular beds or composite explosives.

All these contributions take it for granted that the simplest theory is best qualified to embody the ideal behaviour. This option is questionable considering the simplest theory restricts the detonation wave front to be plane, while curvature is the common attribute of any wave front of finite extent.

Which are then the features a detonation model should possess in order to serve as a reference for assessing more realistic models and consequently be termed ideal ? Is the simplest theory not too ... simple or limiting for that ? A final exchange among the participants should help, I hope, further the question.

3-1 Statements from Laboratories on Non-ideal Behaviour of Energetic Materials

Characterization of High-explosive Initiation and Safety at Los Alamos ; J.M.McAfee

Research into the Detonation of Non-ideal versus Ideal Explosives ; **R.S. Miller** and J.M. Goldwasser

The Challenges of Non-ideal Detonation ; D.L.Kennedy

Williamsburg Equation of State for Modelling Non-ideal Detonation ; **W.Byers Brown,** Zhao Feng and M.Braithwaite

JOURNAL DE PHYSIQUE IV
Colloque C4, supplément au Journal de Physique III, Volume 5, mai 1995

Characterization of High-Explosive Initiation and Safety at Los Alamos

J.M. McAfee

Detonation Systems Group, DX-10, Los Alamos National Laboratory, Los Alamos, New Mexico, 87545, U.S.A.

Abstract

The Chapman-Jouget and ZND models of steady detonation have proved most useful for engineering estimation of the propagation of near-planar, steady detonation in short-reaction-zone explosives. However, even in well characterized systems, the purposeful initiation of detonation is not described by these models. The highly divergent and microscopic nature of point initiation require discerning experiments, modeling, and theoretical analysis.

Recently, safety considerations in complex or damaged systems, possibly containing long-reaction-zone (insensitive) high explosives, have dominated our thinking. These situations are rarely planar or steady, the physical state of the explosive may not be easily characterized, and there is a wide range of potential stimuli. The high-explosive reaction may range from none, to deflagration, to partial detonation, or to full detonation. Techniques and data applicable to estimating the level of response are needed.

The design and prediction of explosive systems have mostly been accomplished using the simple C-J model. In most cases considerable testing and incremental modification are necessary to produce the desired function for even moderately complex geometries. However, the precise and reproducible initiation of detonation has relied even more on the empirical approach.

The build-up to detonation from an initial stimulus is a transient phenomenon (Fig. 1). It involves an interplay of chemical kinetics, mechanics, hydrodynamics, and material properties. Historically, the first predictive correlation between stimulus and transition-to-detonation was discovered by Ramsay and Popolato[1]. They showed, for a one-dimensional promptly initiating system, that the logarithm of the shock input pressure was linearly proportional to the logarithm of either the distance- or time-from-impact to full detonation (Fig. 2). These relationships, named "Pop Plots", are a function of the density, temperature, phase, particle size, particle-size distribution, and almost any other physical variable. The Pop plot is widely used for the estimation of where and when a detonation will occur, given a specific shock strength.

The first successful continuum model to extract "microscopic" rate information from these measurements is the Forest Fire model[2]. Although based on the incorrect assumption of "single-curve build up," this model has had considerable use and success in calculations of resolved 1-, 2-, and 3-dimensional initiation problems. Because this and similar approaches do not account for the heterogeneous nature of solid explosives, the rates derived from this and similar models are only averaged properties that represent only the heat release. The details of the microscopic mechanics and chemistry are not predicted or accounted for.

The design of precision detonators and detonation systems is primarily based on comprehensive experience and testing. *A priori* prediction of the quantitative interactions of exploding bridge wires (EBWs, Fig. 3) with fine-grained initiating explosives has not been possible because of the strong coupling of divergence, kinetics, mechanics, and other phenomena. Only in the past few years has an empirically calibrated model of the slapper detonator (Fig. 4) proved useful. R. J. Yactor[3] has correlated hundreds of experimental measurements by fitting a multi-parameter model based on simple physical concepts. The SLAPPER model can predict values and trends for firing-set voltage thresholds for single and multi-point detonators.

We at Los Alamos are very interested in safety considerations for complex or damaged systems. Understanding and predicting the response of explosives to abnormal environments and accidents are important components of our program. Probable scenarios are rarely planar or steady, the physical state of the explosive is not easily characterized, and there are a wide range of potential stimuli and responses. An insult that will not normally produce a violent response in undisturbed explosive may produce high-explosive reaction ranging from none, to combustion, to deflagration, to partial detonation, to full detonation in a damaged system. Our goal is to develop experimental and computational tools that qualitatively and quantitatively predict the level of energy release.

Explosive systems, even when used as designed, have many space and time scales. The introductory papers by Fauquignon and Davis have described the wide range and interdependence of these scales for steady detonation. Accidents and abnormal environments introduce the additional factors of system size, configuration, confinement, altered material properties, and lengthened time scales. At Los Alamos, we have approached this complex and ill-defined problem by performing experiments on simplified systems. As examples, I will describe two projects: The initiation of a liquid explosive by hypervelocity metal jets, and our studies of the deflagration-to-detonation transition (DDT) in metal-confined granular explosive.

The planar shock initiation of nitromethane (NM) was first described by Los Alamos workers in the 1960s[4] (Fig. 6), and has been continued and refined more recently[5]. The behavior of this system is perhaps the simplest and best explained for common condensed explosives. However, when we initiate NM with an explosively-formed hypervelocity metal jet[6], some results are very complex. High-speed photographs (Fig. 6) show the formation of periodic three-dimensional structures. Analysis of the velocity of the leading wave shows cycles of detonation and failure (Fig. 7). Such complex behavior is not accounted for by the simplest theories.

The build-up to detonation from relatively weak thermal or mechanical insults involves a complex interaction of combustion, deflagration, and mechanics[7,8]. Our experimental system to simulate a damaged explosive system is a strong steel pipe filled with granular HMX (Fig. 8). Initial combustion in the HMX can be started by mechanical or thermal input. In either case, the initial energy and power are far below that necessary to initiate detonation. Figure 9 describes the Los Alamos model of the DDT in this system. Undoubtedly, the very early stages of combustion in ignited experiments are convective. The pressures, Reynolds numbers, and gas-evolution rates are small enough that gas can flow through the initial bed (60-70% of the Theoretical Maximum Density, TMD). However, the gas permeation velocity into the nascent bed is limited (10s of m/s). The HMX burning rate is high enough that gas is produced faster than it can flow away. Therefore, the gas pressure in the combustion region builds rapidly. The rising pressure eventually becomes greater than the strength of the granular bed, and a combustion-supported compaction wave is started.

The compaction wave velocity is significantly faster (100s of m/s) than the combustion. Behind the wave, the bed is compacted to approximately 90% TMD. Throughout this dynamic compaction, shear of and friction between the granules provide energy to start decomposition of the compacted material. After an induction time determined by the chemical kinetics, deflagration in the compacted HMX begins and proceeds at a velocity approximately equal to the compaction-wave velocity. The onset and propagation of this deflagration does not depend on the permeation of hot gasses, but rather on the length of time since the passage of the compaction wave. This "ignition wave" is merely the locus of a specified level of reaction or reaction rate. It defines the boundary between the slowly decomposing compact and the quickly deflagrating compact.

After the deflagration is established, a competition between gas pressure and mechanical stress in the region above the ignition locus and behind the compaction wave determines the next stage. The region below the ignition locus pressurizes rapidly because of the fast burning. The forces generated by this pressure are carried above the ignition locus as mechanical stress in the matrix of

solid particles. At the same time, the gas pressure between these solid particles is rising because of the slow decomposition started by the compaction wave. The mechanical stresses are trying to further compact the bed while the gas pressure is resisting. There is a point where the mechanical stress becomes much larger than the inter particle pressure, and the granular bed further compacts to near 100% TMD. We call this region of complete compaction the "plug" because on the time scale of interest (10s of μs) it behaves as inert material.

In the plug, the gas-phase and gas-producing reactions stop because there is essentially no free volume and the increase in thermal conduction rapidly cools the residual gas. Therefore, the ignition locus terminates when it intersects the plug.

If the mechanical confinement of the burning region is sufficient, the high gas pressures accelerate the plug into the compact. Mass balance arguments show that the top of the plug has a velocity approximately ten times faster than the bottom. At these high velocities, the top of the plug is a shock traveling in the compact. This shock will transit to detonation if the velocity is high enough and duration long enough. Failure of the mechanical confinement can slow the shock such that detonation does not occur. The combustion-deflagration process can begin again when the shock overtakes the compaction wave. We have strong evidence for such interrupted processes eventually leading to detonation (Fig. 10).

Computational modeling of this process is formidable. The space scales range from detonation reaction zone thickness to the full system size. The time scales range from fractions of nanoseconds to seconds. In the past two years J. Bdzil, B. Asay, and S. Son at Los Alamos and D. S. Stewart and A. Kapila from universities have developed a computational model that reproduces the observed phenomena starting with the compaction wave. However, accurate and physically-based chemical kinetic information is still needed.

Additional projects at Los Alamos are attempting to characterize the mechanical and chemical states of damaged explosives. We have a great need for appropriate diagnostics, well designed experiments, and convincing analysis.

REFERENCES

1. J. B. Ramsay and A. Popolato, "Analysis of Shock Wave and Initiation Data for Solid Explosives," Fourth Symposium (International) on Detonation, White Oak, Maryland (1965).

2. C. L. Mader and C. A. Forest, "Two-Dimensional Homogeneous and Heterogeneous Detonation Wave Propagation," Los Alamos Scientific Laboratory Report LA-6259 (1976).

3. R. J. Yactor, Unpublished results from the SLAPPER code (1994).

4. A. W. Campbell, W. C. Davis, and J. R. Travis, "Shock Initiation in Liquid Explosives," Physics of Fluids, **4**(4), p. 498, (1961).

5. S. A. Sheffield, R. Engleke, and R. R. Alcon, "In-Situ Study of the Chemically Driven Flow Fields in Initiating Homogeneous and Heterogeneous Nitromethane Explosives," Ninth Symposium (International) on Detonation, Portland, Oregon (1989).

6. B. W Asay, J. M. McAfee, and E. N. Ferm, "Nonsteady Detonation Driven by a Hypervelocity Jet in a Homogeneous Explosive," Physics of Fluids A, **4** (7), p. 1558, (1992).

7. J. M. McAfee, B. W Asay, A. W. Campbell, and J. B. Ramsay, "Deflagration to Detonation in Granular HMX," Ninth Symposium (International) on Detonation, Portland, Oregon, (1989).

8. J. M. McAfee, B. W Asay, and J. B. Bdzil, "Deflagration to Detonation in Granular HMX: Ignition, Kinetics, and Shock Formation," Tenth Symposium (International) on Detonation, Boston, Massachusetts (1993).

Shock Initiation of Heterogeneous Explosive

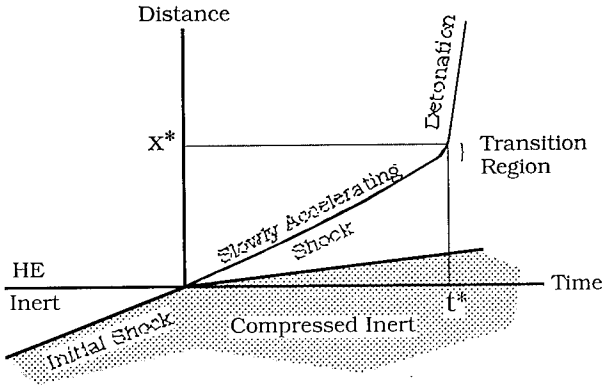

Induction distance (x*) and time (t*) are a function of Shock Pressure: x*= x*(P), and t* = t*(P)

The "Pop Plot" for Some High Explosives

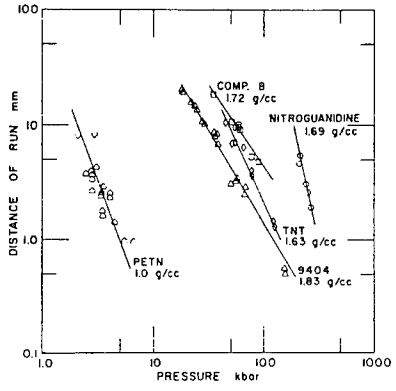

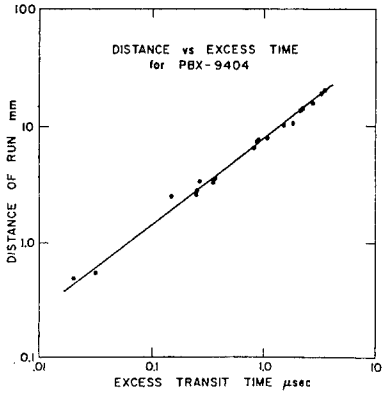

Correlations of Shock Initiation Data from J. B. Ramsay and A. Popolato (1965)

Exploding BridgeWire (EBW)

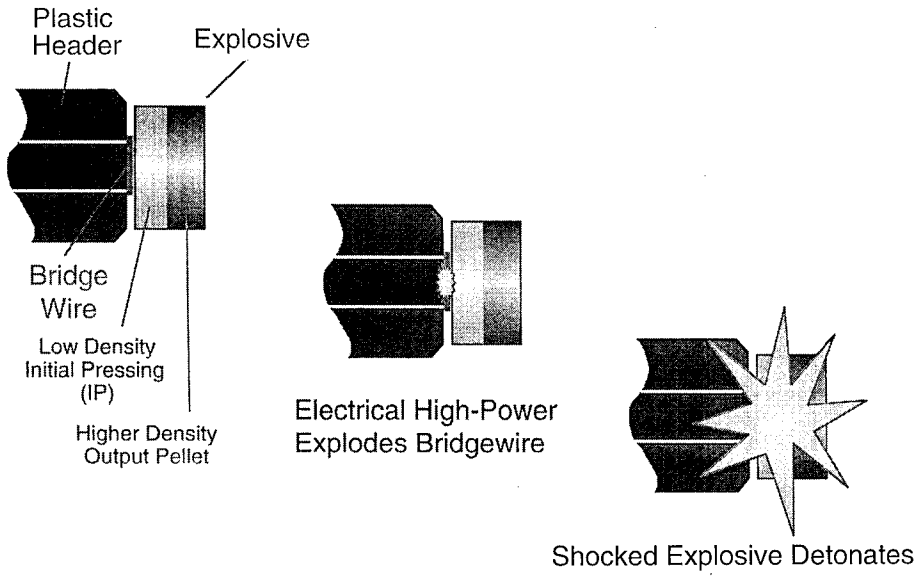

Slapper Detonator

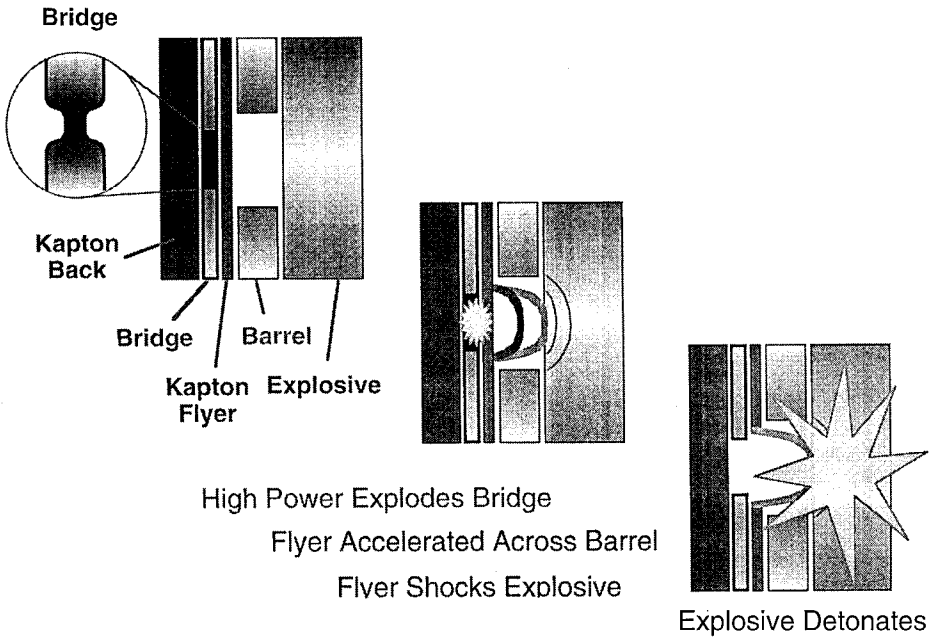

Shock Initiation of Homogeneous Explosives

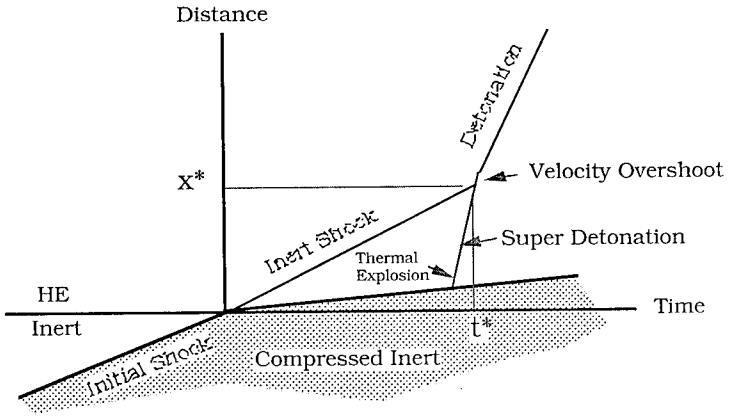

Induction distance (x*) and time (t*) are a function of Shock Pressure: x*= x*(P), t* = t*(P)

Photographs of a 6.5-mm/μs Jet in Nitromethane

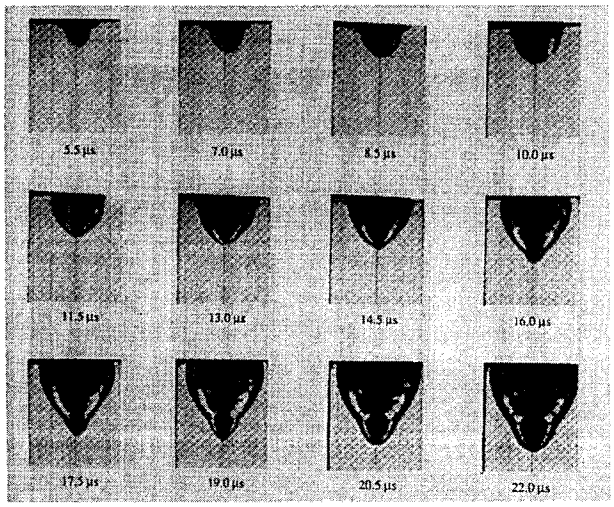

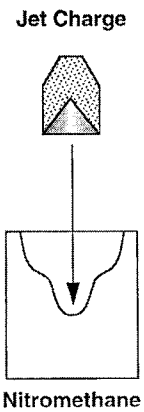

Tip Velocity of 6.5-mm/μs Jet in Nitromethane

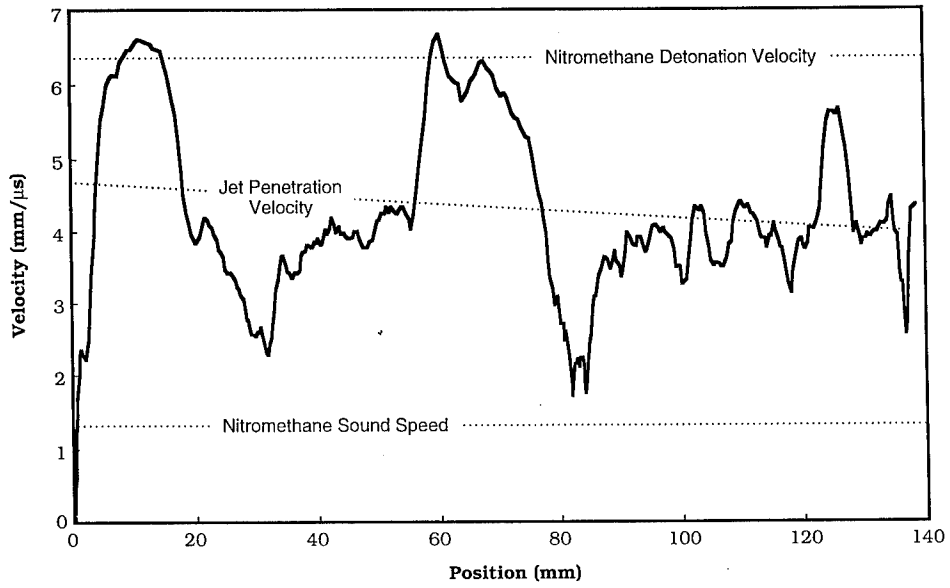

Los Alamos DDT Experiment and Diagnostics

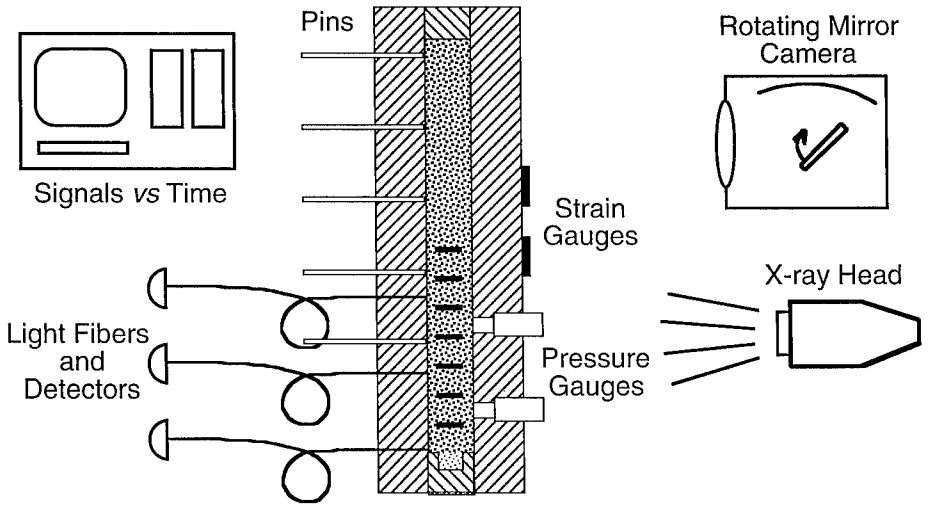

Time-Distance Description of DDT in HMX

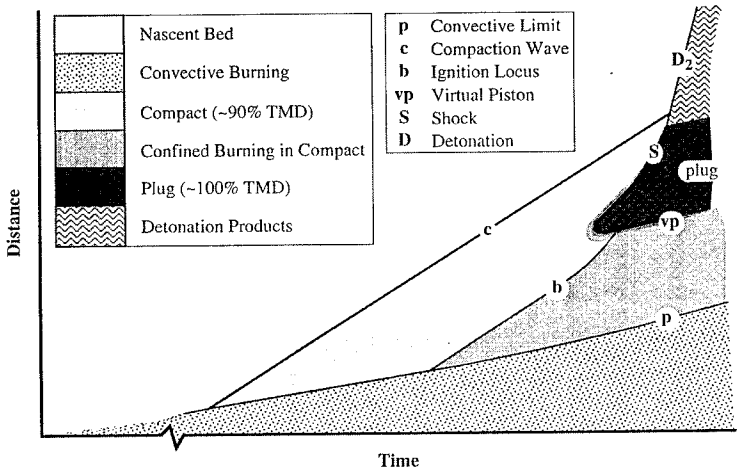

Radiography Data and Analysis

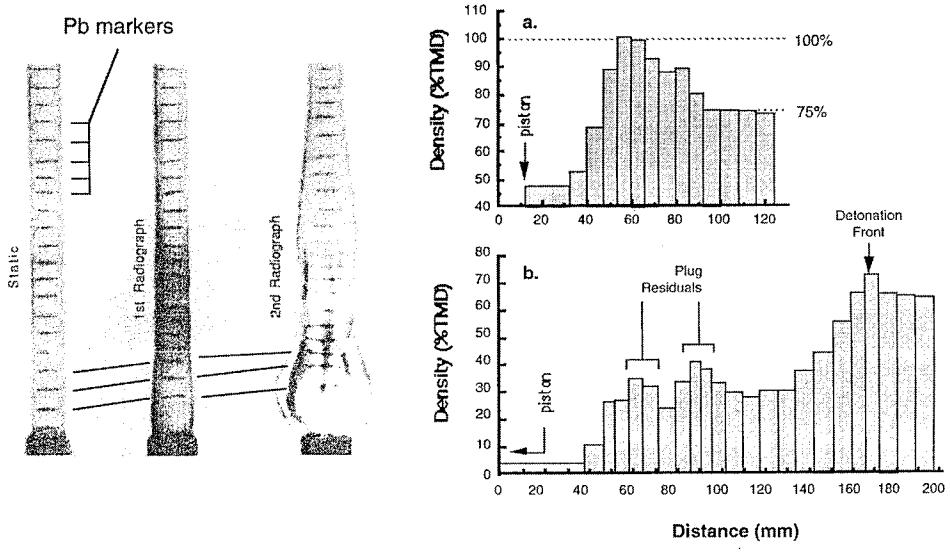

JOURNAL DE PHYSIQUE IV
Colloque C4, supplément au Journal de Physique III, Volume 5, mai 1995

Research into the Detonation of Non Ideal Versus Ideal Explosives

R.S. Miller and J.M. Goldwasser

Office of Naval Research, Mechanics and Energy Conversion Division, 800 North Quincy Street, Arlington, VA 22217-5660, U.S.A.

The objectives are to determine, understand, and control the mechanisms and the rates of energy release in metallized explosive compositions during the detonation state and in the post-detonation regime. The goals of the initiative are to: (i) account for the total energy and the rates of energy release in the underwater detonation of a composite metallized explosive, (ii) establish and demonstrate concepts which can be employed to "dial" the near field pressure/time profile in order to maximize the desired energy coupling to the target, and (iii) develop a laboratory scale underwater detonation experiment, which will be able to accurately characterize the performance of novel metallized composite explosives. Research will be conducted to: (i) characterize the detonation both inside the explosive medium and in the water column at near-field, (ii) understand the parameters in the microstructural transport processes which govern the reactions of metal fuels with oxidizer molecules at temperature and pressure extremes , and the rates with which these processes take place, and (iii) identify the mechanisms by which energy is added, lost, or modified as the detonation wave and subsequent gas expansion propagate from the explosive into the water.

Our overall objectives are to determine and understand: (a) the mechanisms of chemical energy release and transport of mass, momentum, and energy in the detonation of heterogeneous metallized explosive compositions and (b) the resultant coupling of the released energy to the surrounding water medium. Underwater explosive formulations are non-ideal explosives. Non-ideal explosives are microscopically heterogeneous, detonable mixtures of oxidizer particles in fuel matrices that are separated by distances comparable to the multi-micron particle sizes of the oxidizer particles. Underwater explosives are inherently very different from ideal explosives used in air and surface applications. Ideal explosives are detonable, molecular mixtures of oxidizers and fuels, which are separated only by covalent or ionic bonds at Ångstrom distances, and release their energy very quickly compared to non-ideal explosives. In ideal explosives, the mixing and chemical reaction of shock decomposed oxidizer and fuel fragments occur quickly. The diffusion and the chemical reaction rates between reactive shocked oxidizer and fuel fragments are very fast, and the accompanying exothermic energy release rates to the reaction products occur over extremely short, Ångstrom distances in contrast to the long, multi-micron distances for non-ideal explosives. The fundamental differences are not only in the degree of heterogeneity, mixing distances, diffusion rates, reaction times and energy release rates but also in the environment in which they

are employed. Large quantities of detonated ideal explosives work to rapidly accelerate and deform relatively small masses of metal in shaped charge and fragmenting warheads. In comparison, relatively small quantities of non-ideal explosives work to slowly accelerate relatively large masses of water. The inertial confinement of the environment of underwater explosives by the surrounding mass of water is, therefore, much greater than the inertial confinement of metal surrounding ideal explosives of shaped charges or fragmenting warheads. One of the consequences of the differences described above is in the failure diameter of composite explosives. Because of the heterogeneities of the explosive composition and relative slowness of reaction, the diameter of the explosive required to sustain a detonation is typically in the centimeter range as opposed to the millimeter range for ideal explosive compositions. The importance to science lies in understanding the microscopic kinetics of transport and chemical energy release processes of non-ideal detonations, and the time dependent coupling of these energy release processes to macroscopic hydrodynamic phenomena. As a result, the early time and near field chemistry and physical phenomena that govern the energy release mechanisms for these heterogeneous formulations are much slower than those of homogeneous explosives. However, they are much more complex, and have been very difficult to study and characterize. Of interest are the detonation wave and in the early post-detonation gas expansion. Our specific objectives are: (a) the characterization of the in-situ and near-field energy release profile of metallized composite explosives and the understanding of the energy losses and shock wave attenuation resulting from transition from the explosive medium through the interfacial layer into the water column, (b) the identification of the chemical reaction pathways; the micromechanical transport mechanisms responsible for mixing of metal/oxidizer fragments under shock loading; the characterization of the reaction kinetics as a function of temperature and pressure (up to 3000 K and 30 GPa); introduction of pressure dependent chemical reaction parameters into metal combustion models, and (c) the establishment of a laboratory scale 1D experiment to characterize the underwater detonations of novel metallized composite explosives and the introduction of the time dependent energy release parameters into equation of state predictions. Some specific research issues are: (a) How accurately can the in-situ and near-field pressure/time histories, positions, velocities, and curvatures of the shock and expanding bubble fronts be determined for metallized explosives using advanced diagnostic techniques? (b) What are the energy addition, loss, and shock wave attenuation processes which affect the pressure/time profile as the detonation wave proceeds from the explosive into the water medium through the interfacial layer? (c) How much can one probe in real time the chemical reactions in single particle and microdetonics experiments? (d) Are the spectroscopic signals strong enough and relaxation fast enough to use vibrational spectroscopy to accurately follow the reaction temperature during the detonation and early post-detonation regimes? (e) What is the regression mechanism of the metal fuel particles under detonation conditions and how would changing the detonation products from solids to gases affect the energy release rates and coupling efficiency to the medium? (f) Can shock initiated solid state reactions be successfully used to modify the reaction temperature and detonation kinetics? (g) Can a 1D laboratory scale underwater detonation experiment be implemented to accurately characterize novel metallized composite explosives in terms of pressure, temperature, velocity and shape of the shock wave, and rate of expansion of the compressed gas bubble in order to generate equations of state which account for the time-dependent events which will be valid to predict large scale characteristics and performances?

JOURNAL DE PHYSIQUE IV
Colloque C4, supplément au Journal de Physique III, Volume 5, mai 1995

The Challenge of Non-Ideal Detonation

D.L. Kennedy

ICI Australia Operations Pty. Ltd., P.O. Box 196, Kurri Kurri 2327, Australia

Abstract : This paper will compare and contrast detonation in ideal and in highly non-ideal explosives. Ideal explosives, represented here by a TATB / binder system, have relatively flat velocity of detonation (VoD) versus inverse charge diameter relationships, and fail at VoDs only slightly below their ideal CJ values. Highly non-ideal explosives, such as the physically heterogeneous composites used both in Naval and in mining applications, display more complex VoD relationships, and greater deficits at failure. Indeed, the example chosen here of an ANFO / emulsion blend has a bi-linear diameter effect curve, with the VoD at failure being only 30% of its CJ value. These behaviours are interpreted by examining their reaction rate surfaces (namely the 3D relationship between pressure, extent of reaction and reaction rate). Many of the experimental tests in common use, and many models of the detonation process, rely on particular features of the reaction rate surface that are specific to ideal explosives. Such features are modified or absent from the surfaces for highly non-ideal explosives, with the result that the experimental tests can become either misleading or irrelevant, while the theoretical models are inappropriate.

1. INTRODUCTION

A casual glance through the collected indexes [1] of the first eight Symposia (International) on Detonation is sufficient to show that detonics research over the last four decades has concentrated overwhelmingly on the behaviour of explosives developed for applications which demand the highest possible power generation. Together with the secondary criteria of stability and sensitivity [2], this has narrowed attention down to about half a dozen high density monomolecular explosives, and mixtures thereof, all of which exhibit fast reaction kinetics under detonation conditions. As a result of this concentration of effort, the majority of the experimental techniques and the theoretical models that have been developed and applied over this time period have implicitly assumed the "ideal" type of detonation behaviour that is exhibited by these explosives.

However, there are other applications that apply different selection criteria to the choice of explosive composition. Naval underwater explosives are formulated to provide moderate pressures of long pulse duration, often by the addition of aluminium. Energetic propellants (based on ammonium perchlorate) must deflagrate stably at low pressure without transiting to a detonation that they are also capable of supporting. Mining explosives must detonate at low pressure with long pulse duration to avoid excess

pulverisation but still provide sufficient fracture and movement of large rock masses : as such, modern compositions are usually based on ammonium nitrate. All of these different composite explosive types exhibit long reaction zones even under detonation conditions, resulting in pronounced "non-ideal" behaviour, where detonation is strongly influenced by the charge size and external confinement.

It is then essential to verify that any experimental technique or theoretical model proven with ideal explosives is still valid when applied to non-ideal explosives.

As an example, Kennedy and Jones [3] examined the detonics of the Naval explosive PBXN-111 (formerly PBXW-115), concluding that (i) the extraction of detonation zone lengths from shockfront curvature measurements, (ii) run distance to detonation data, and (iii) a small-sample technique [4] for measurement of infinite diameter detonation velocity, all required different interpretation for this non-ideal explosive, compared to what would be the case for an ideal one. However, this analysis was based on a CJ detonation velocity predicted by a chemical equilibrium code [5] to be 0.5 mm.μs^{-1} higher than the infinite diameter value inferred from a linear extrapolation of the experimental detonation velocity data [6]. This makes its diameter effect curve (the dependence of steady-state detonation velocity D on charge diameter d in cylindrical geometry) concave up when plotted in the D vs d^{-1} plane, unlike those of ideal explosives which are usually linear or concave down, as summarised by Campbell and Engelke [7].

This paper will examine the detonics of a highly non-ideal explosive which has a pronounced and well-defined concave up diameter effect curve. It is known in the mining industry as a heavy ANFO (henceforth called HANFO), being an ICI proprietary blend of porous ammonium nitrate (AN) prill plus fuel oil (FO) mixed with an AN/water-in-oil emulsion.

Its detonics will be contrasted to those of X-0219 (90/10 TATB/KelF 800) which displays essentially ideal behaviour. X-0219 was chosen partly because of the completeness of the necessary experimental data, but also partly because TATB-based explosives are believed to have the longest reaction zone lengths of any ideal composition.

2. REACTIVE EQUATION OF STATE MODEL

The reactive equation of state (EoS) has been modified slightly from that used previously by Kennedy and Jones [3] to model PBXW-115 (now renamed PBXN-111), and extended to incorporate the effects of initial porosity.

2.1 Unreacted explosive

The unreacted or explosive phase is described by a Mïe-Grüneisen EoS in the form

$$e_x = e_r + \frac{(p_x - p_r)}{\rho_{r0}\Gamma_{r0}} \tag{1}$$

where p is pressure, ρ is density, $v = \rho^{-1}$ is specific volume, e is specific internal energy, and Γ is the Grüneisen coefficient. The subscripts are: x for the (porous) unreacted explosive, 0 for the initial state, and r for the reference (non-porous) state. Formerly [3], the latter was represented by the principle isentrope for the non-porous condensed phase, given by the Birch-Murnaghan finite strain equation in the form described by Jeanloz [8]. This was found to work well with materials for which the slope s_r of the Hugoniot, given by :

$$U = C_{r0} + s_r u \tag{2}$$

where U is shock velocity and u particle velocity, is moderately low in value, say $s_r \leq 1.6$. This condition holds for the geophysical materials studied by Jeanloz [8]. However, for more compressible materials such as the AN / water based emulsions of interest here, the Hugoniot slope is greater, typically $s_r \geq 2.0$, and it was found that the Mïe-Grüneisen EoS centred on the Birch-Murnaghan principle isentrope was not consistent with equation (2) for physical values of the Grüneisen coefficient Γ_{r0}.

The reference state for equation (1) is now the shock Hugoniot of the condensed phase, so that

$$p_r = \frac{\rho_{r0} C_{r0}^2 \varphi}{(1 - s_r \varphi)^2} \quad \text{and} \quad e_r = \frac{p_r \varphi}{2\rho_{r0}} \quad \text{where} \quad \varphi = 1 - \rho_{r0} v_r \tag{3}$$

In order to treat initial porosity in the unreacted explosive, it is then necessary to relate v_r to v_x. This is performed here by assuming that the porosity is fully removed by compression at some low pressure to some specified specific volume, v_{comp} (where $v_{comp} < v_{x0}$). Then, under shock compression :

$$\left.\begin{aligned} v_r &= v_{comp} + \left(\frac{v_{r0} - v_{comp}}{v_{x0} - v_{comp}}\right)(v_x - v_{comp}) \quad \text{for } v_{comp} < v_x \le v_{x0} \\ v_r &= v_x \qquad\qquad\qquad\qquad\qquad\qquad\quad \text{for } v_x \le v_{comp} \end{aligned}\right\} \tag{4}$$

The pressures developed by detonating explosives are sufficient to always cause complete compaction, so that in all subsequent flow, $v_r = v_x$.

2.2 Reacted products

The reacted or product phase, denoted by the subscript p, is described by a polytropic EoS with a density-dependent index, namely

$$e_p = \frac{p_p v_p}{\gamma_p - 1} - q_p \qquad \text{where} \qquad \gamma_p = \gamma_0 + \gamma_1 \rho_p + \gamma_2 \rho_p^2 \tag{5}$$

and where q_p is the heat of reaction. The γ_i constants in equation (5) are determined by requiring that the correct values for $(\partial \ln p / \partial \ln v)_s$ are returned at the CJ state and at infinite expansion. These are taken from ICI's chemical equilibrium code IDeX (standing for Ideal Detonation of eXplosives), based on an intermolecular EOS [5] for the gaseous products and the Murnaghan EoS for the solid products

2.3 Mixture rules

The equation of state for the reacting mixture is then completed by invoking the simple mixture rules

$$p \equiv p_x \equiv p_p \,,\; v \equiv v_x \equiv v_p \,,\; e = (1 - \lambda) e_x + \lambda e_p \tag{6}$$

where λ is the extent of reaction, varying from 0 for the unreacted explosive to 1 for the detonation products. These rules will be discussed later.

2.4 Reaction rate law

The reaction rate law that controls the global energy release was originally developed for non-ideal composite porous explosives by Kirby and Leiper [9]. In order to describe the behaviour of ideal explosives such as X-0219, it has been necessary to increase the pressure dependency by allowing pressure exponents greater than unity, giving :

$$\dot{\lambda} = (1 - \lambda)\left\{ \frac{p_{hs}^{R_h} a_h}{\tau_h} + \frac{p^{R_i} a_i}{\tau_i} + \frac{p^{R_f} a_f}{\tau_f} \right\} \tag{7}$$

where

$$p_{hs} = \begin{cases} \dfrac{p}{4}\left(\dfrac{3p}{4p_{cr}}\right)^3 & \text{for } p < 4p_{cr}/3 \\ p - p_{cr} & \text{for } p \ge 4p_{cr}/3 \end{cases} \tag{8}$$

The subscripts are: h for hotspot, i for intermediate, and f for final stages of the reaction. Apart from the three power exponents R, there are four main adjustable parameters — three characteristic reaction times τ, and the critical pressure p_{cr} that inhibits the onset of the hotspot reaction.

The a factors in equation (7) describe the assumed geometry of the burn front, controlling the switching on and off of the hotspot, intermediate and final reaction rate terms. They are functions of λ, and are Gaussian in shape, namely

$$a_h = \exp\left\{-\left[(\lambda - C_i)/W_h\right]^2\right\}, a_i = 0, a_f = 0 \qquad \text{for } 0 \le \lambda \le C_i$$

$$a_h = \exp\left\{-\left[(\lambda - C_i)/W_i\right]^2\right\},\ a_i = 1 - a_h,\ a_f = 0 \qquad \text{for } C_i < \lambda \le C_f \quad (9)$$

$$a_h = \exp\left\{-\left[(\lambda - C_i)/W_i\right]^2\right\},\ a_i = \exp\left\{-\left[(\lambda - C_f)/W_f\right]^2\right\} - a_h,\ a_f = 1 - a_h - a_i \qquad \text{for } C_f < \lambda \le 1$$

where the Gaussian parameters are defined in terms of the mass fractions, Φ, of the three stages as:

$$\text{Centroids} \quad \begin{cases} C_i = \Phi_h^2 \\ C_f = (\Phi_h + \Phi_i)^2 \end{cases} \qquad \text{Half-widths} \quad \begin{cases} W_h = 2C_i/(1+C_i) \\ W_i = \Phi_h(1-\Phi_h) \\ W_f = \Phi_f(1-\Phi_f) \end{cases} \quad (10)$$

3. HYDRODYNAMIC MODELS

The above reactive equation of state was embedded into both the finite element hydrocode DYNA2D [10], and ICI's non-ideal detonation code CPeX (standing for Commercial Performance of eXplosives). The latter was developed to describe the detonics of non-ideal composite explosives by Kirby and Leiper [9], who extended the small divergent detonation theory of Wood and Kirkwood [11]. It describes the flow along the central streamtube between the detonation front and the sonic point (henceforth referred to as the WK point) for steady detonation in unconfined cylindrical geometry (henceforth referred to as WK detonation) by using the shooting method described by Braithwaite et al. [12] to solve the system of ordinary differential equations including the Euler equations of motion, the reactive equation of state, and the reaction rate law. Since the equations of motion have been restricted to the axis, the solution is incomplete, and requires an empirical relationship between the shock front curvature R_s and the charge diameter d. The following simple form has been found adequate for many types of explosives :

$$\frac{d}{R_s} = \alpha + \beta\frac{d_f}{d} \quad (11)$$

where α and β are empirical constants and d_f is the failure diameter. Chaissé et al. [13] have derived a similar expression from their transverse analysis of the physical variables at detonation fronts.

4. MODEL CALIBRATION

CPeX was calibrated for each explosive by varying the adjustable parameters in the reaction rate law, equation (7), until the predicted variation of detonation velocity with unconfined charge diameter matched the experimental measurements shown in Figure 1(a), constrained by the curvature relationships of equation (11) shown in Figure 1(b).

For HANFO, both the detonation velocities and the shockfront curvature data were measured by Sheahan [14], with the ideal detonation velocity D_{CJ} as predicted by IDeX [5]. Figure 1 also includes the results of DYNA2D simulations of the rate stick experiments. This diameter effect curve displays non-ideality on a larger scale than any previously published, with the detonation velocity at failure being only about 30% of the predicted CJ value. The inflection point at $d_f/d \approx 0.4$ is sharper than in the only other cases reported of upward curvature [14 and 15], dividing the diameter effect curve neatly into a small diameter and a large diameter branch. If the detonation velocity experiments had been performed only on the small diameter branch ($d_f < d < 2d_f$), the measurements would have displayed a linear dependence between D and d^{-1} with a correlation coefficient of $r^2 = 0.997$, though the extrapolated D_∞ would be lower than D_{CJ} by 1.65 mm.μs^{-1}. The large diameter branch is seen to extrapolate smoothly towards the predicted D_{CJ}, though the measured detonation velocity in the largest charge tested (250mm in diameter and 1500mm in length) is still 1.35 mm.μs^{-1} below D_{CJ}.

For X-0219, the detonation velocities are those tabulated by Gibbs and Popolato [16], with the shockfront radii of curvature from Campbell and Engelke [7]. The ideal detonation velocity predicted by IDeX [5] was 7.775 mm.μs^{-1}, slightly higher than the value of 7.630 mm.μs^{-1} from a linear extrapolation of the diameter effect curve. The latter was adopted for the fitting procedure. The reaction rate law for X-0219 was further constrained so that DYNA2D simulations of wedge tests reproduced the LASL Pop-plot

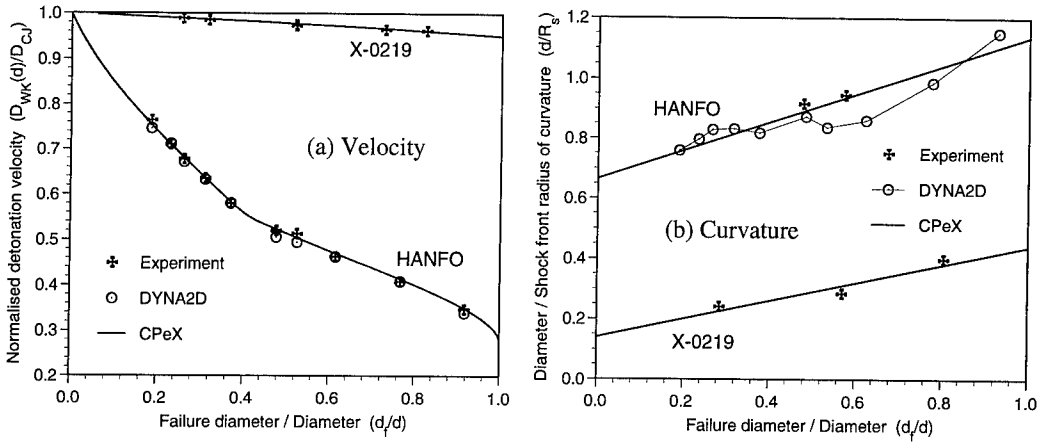

Figure 1. Fits to the experimental diameter effect data (left) constrained by the shockfront radii of curvature data (right) for X-0219 and HANFO. Both abscissa have been normalised by multiplying the inverse diameters by the respective failure diameters of 14mm and 46mm. For the diameter effect curve (left), the ordinate has been normalised by dividing the detonation velocities by the predicted CJ velocities of 7.630 mm.μs^{-1} and 5.807 mm.μs^{-1} respectively.

results [16] shown in Figure 2. For reasons to be discussed below, DYNA2D simulations could not be performed for rate stick experiments on X-0219.

In spite of the paucity of experimental shockfront radii of curvature for HANFO, it is evident that the shockfronts in HANFO are considerably more curved (i.e. smaller radii of curvature by a factor of roughly three) than their counterparts in X-0219 over the full range of charge diameters. The HANFO shockfronts are also more curved than those of the non-ideal explosive PBXN-111 [3], though are almost identical when normalised as in equation (11) to those of emulsion explosives with a range of initial densities and failure diameters [17].

5. FEATURES OF THE WK POINT

Figure 3 displays how the CPeX values of various flow variables at the WK point vary with charge diameter for X-0219 and for HANFO. In view of the dissimilar diameter effect curves and shockfront

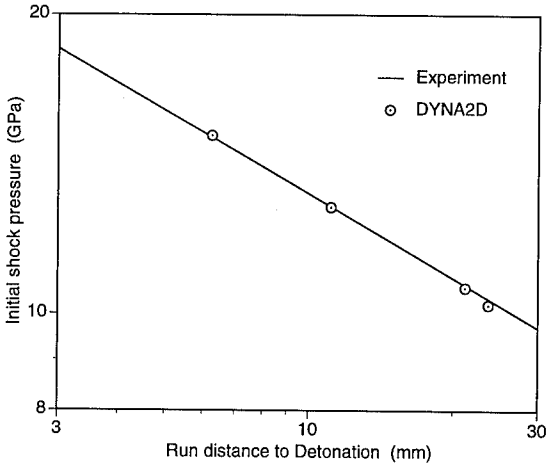

Figure 2. Comparison between the experimental Pop-plot [16] for X-0219 and the results of DYNA2D simulations using the reaction rate surface shown in Figure 8(a).

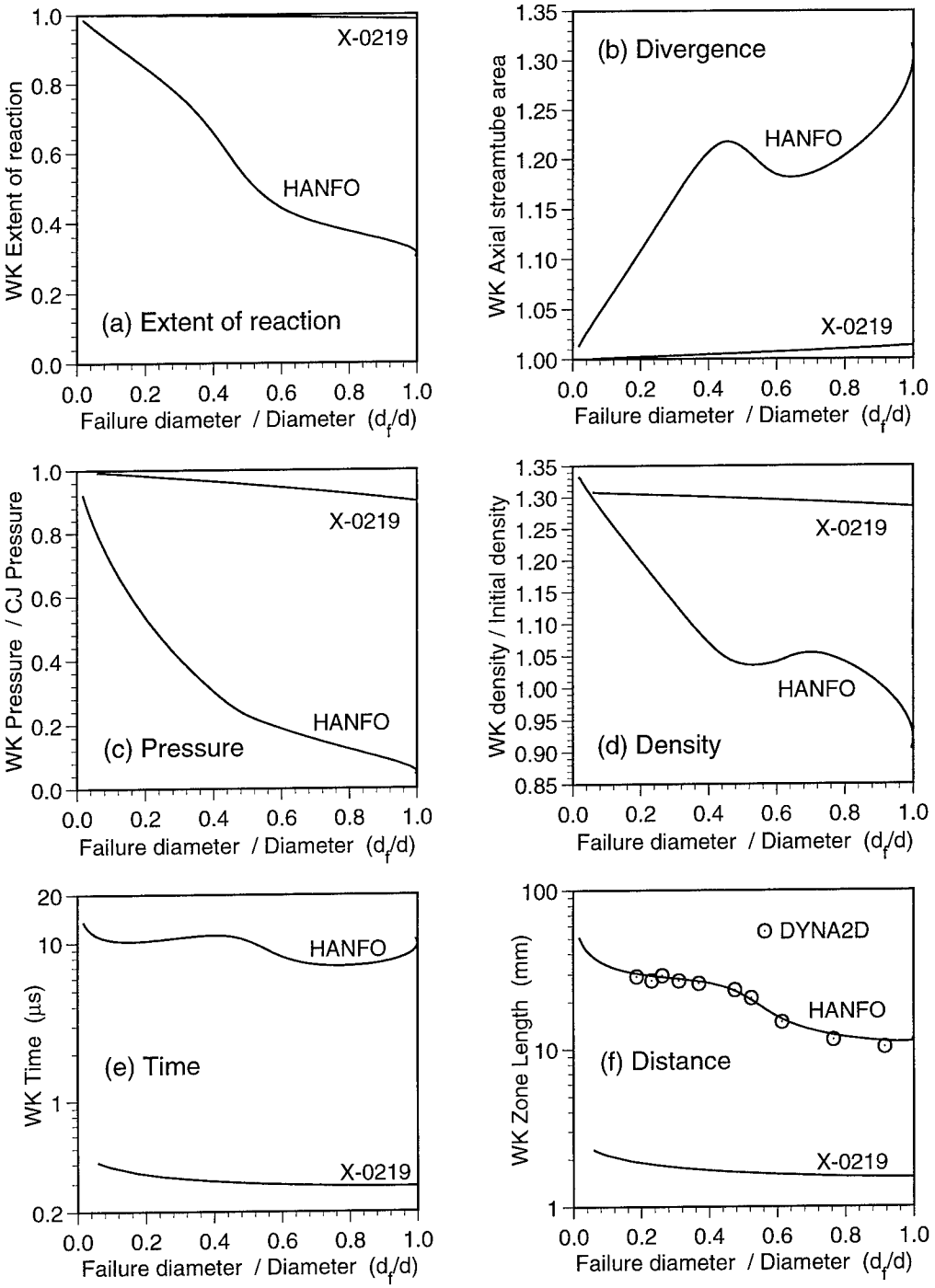

Figure 3. CPeX flow variables at the WK point of steady detonation in unconfined cylindrical charges of X-0219 and HANFO. The inverse diameters have been normalised by multiplying by the respective failure diameters of 14mm and 46mm. The pressures in 3(c) have been normalised by dividing by the CJ pressures of 26.3 and 8.87 GPa respectively, while the densities in 3(d) have been normalised by dividing by the initial densities of the explosives, which are 1.915 g.cm^{-3} and 1.04 g.cm^{-3} respectively.

curvatures, it is not surprising that the related flow variables for the two explosives also exhibit large and significant differences.

Figure 3(b) examines the expansion of the central streamtube, chosen to have unit area at the shock front. This expansion is small (< 2%) for the X-0219 but large (≈ 30%) for the HANFO close to the failure diameter. Since this streamtube expansion is directly related to w_r (the radial partial derivative of the radial particle velocity), and since Wood and Kirkwood [11] expanded their correction terms to the conservation equations only to first order in w_r, it is pertinent to examine the accuracy with which CPeX can treat HANFO.

6. ACCURACY OF CPEX AND COMPARISON WITH DYNA2D

6.1 HANFO

It can be seen that CPeX is able to accurately reproduce both diameter effect curves in Figure 1, even the complex shape exhibited by the HANFO. However, of course, this does not verify CPeX, since the reaction rate parameters were varied until these fits were achieved. Unfortunately, there is insufficient experimental data currently available to independently test the CPeX analysis of HANFO.

When CPeX was applied to the non-ideal explosive PBXN-111 [3], the derived reaction rate surface could be used in DYNA2D simulations to accurately reproduce a wide variety of experimental data probing both steady and non-steady flows. However, this success will not necessarily translate to the present situation, because the CPeX central streamtube expansion at the failure diameter of PBXN-111 was only 4%.

For the present purpose, the only recourse is to compare the CPeX analysis with the results of DYNA2D simulations. While not providing an independent test of the reactive equation of state model, any demonstrated agreement between CPeX and DYNA2D would help confirm at least the broad features of the CPeX flow divergence model.

In this context, the high degree of accuracy with which the DYNA2D simulations (included in Figure 1) reproduce the CPeX detonation velocities and assumed shockfront radii of curvature relationship for HANFO is gratifying. As well as reproducing these gross features of detonation in rate stick geometry, the DYNA2D simulations also confirmed the fine structure in the CPeX analysis, such as the complex dependence of WK detonation zone length on charge diameter shown in Figure 3(f).

A further example is illustrated in Figure 4(b), displaying the predicted pressure and extent of reaction profiles along the axis for steady detonation in a 61mm diameter unconfined charge of HANFO — similar

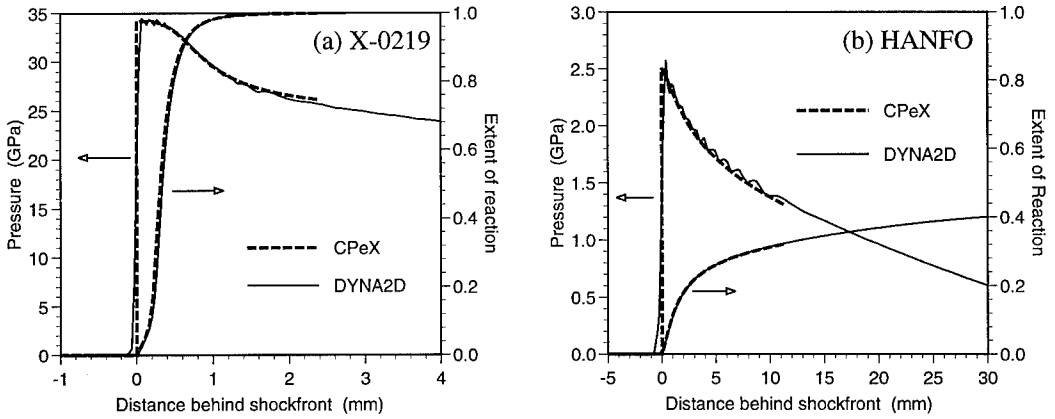

Figure 4. Pressure and extent of reaction profiles for steady detonation. For X-0219 (left), the DYNA2D profiles are after the detonation has run 150mm in planar 1D geometry, while the CPeX profiles are for WK detonation in a 220mm diameter rate stick. For HANFO (right), all profiles are for a 61mm diameter rate stick.

agreement between CPeX and DYNA2D occurred over the full range of diameters. The finite element simulation of Figure 4(b) used a uniform mesh with 0.5mm×0.5mm elements, which at first glance may appear very coarse but in fact gives 61 elements across the radius of the charge, and about 22 elements in the detonation zone within which only about 35% reaction occurs.

6.2 X-0219

Figure 4 includes a comparison of CPeX and DYNA2D results for detonation in X-0219. The CPeX profiles are for WK detonation in 220mm diameter, which was the largest diameter for which CPeX could find a solution — this is taken to represent WK(∞). The DYNA2D simulation was performed with boundary conditions which restricted the flow to planar 1D geometry. The simulation was started by a programmed burn (with a free rear boundary) through a 50mm slab of X-0219, followed by a resolved reactive flow calculation through a 125mm slab of X-0219. It can be seen that the two approaches are in excellent agreement with each other.

This finite element simulation employed a uniform mesh with 0.01mm×0.01mm elements. Roughly 60% of the reaction (namely from $\lambda \approx 0.1$ to $\lambda \approx 0.7$) is predicted to occur over a zone of about 0.2mm in length, necessitating this high spatial resolution. The simulation of the rate stick experiments (with a minimum charge size of say 16mm diameter by 100mm length) would require at least 7 million elements to properly resolve the reaction, and since this was not feasible during this study, no 2D simulations could be performed on X-0219.

7. ACCURACY OF THE EQUATION OF STATE

Figure 5 summarises steady detonation in the p-v plane for these explosives, with the solid lines pertaining to 1D and the dot-dash lines to 2D. As described by Wood and Kirkwood [11], the radial divergence in a 2D detonation perturbs the Rayleigh "line" away from its linear 1D form, so that in 2D, the von Neumann spike, the WK (sonic) point and the point representing the initial undisturbed explosive are no longer co-linear.

For X-0219, this perturbation is small, and indeed is not readily apparent on the scale of Figure 5(a). All of the WK points are close to the CJ point, and hence for example, using the CJ product isentrope

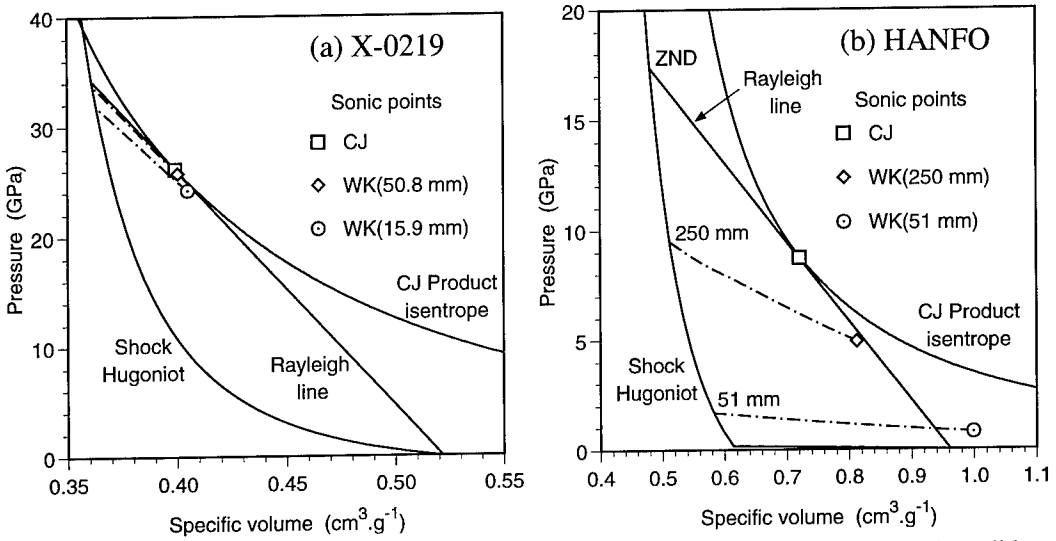

Figure 5. p-v diagrams for steady detonation in X-0219 (left) and HANFO (right). The solid lines show the shock Hugoniots, the Rayleigh lines and the CJ product isentropes for 1D ZND detonation in these explosives, while the dot-dash lines show the reactive paths followed by 2D WK detonation in the largest and smallest diameters investigated experimentally.

predicted by a chemical equilibrium code to describe the isentrope in a WK detonation should not introduce significant additional error. Conversely, the JWL product equation of state determined in a copper tube expansion test, thus notionally under WK conditions, can be used to provide a reasonable description of the CJ state for explosives like X-0219.

This is not the case for HANFO, where the perturbations are significant. Indeed, for detonation in diameters close to the failure diameter, the specific volume at the WK point is expanded relative to the initial specific volume of the unreacted explosive — Figure 3(d) displays this in more detail. Furthermore, it is obvious that the state (including entropy, internal energy and temperature) of the shocked explosive behind the WK detonation front of a 51mm diameter charge will be vastly different from that behind a ZND detonation front. This will lead to a different set of product chemical species, so that basing the reactive equation of state (as described in section 2) only on the CJ product isentrope calculated by a chemical equilibrium code must be appreciably in error.

Johnson et al. [18] recognised this problem during their study of the performance of non-ideal ANFO + aluminium systems in the aquarium test. They treated some fraction of the ammonium nitrate (AN) as inert in their chemical equilibrium calculations using BKW, varying this fraction until the resulting predicted CJ velocity matched the experimental WK velocity for the particular geometry of interest. The remaining AN was then assumed to react outside the detonation zone. This procedure should lead to a more relevant equation of state than is used in the present study, though is still not rigorous due to the arbitrary treatment of the reaction and to the extent by which the 2D WK points lie off their equivalent 1D Rayleigh lines.

The p-v relationships shown in Figure 5 for WK detonation refer to conditions along the axis of symmetry. The uncertainties in treating the reactive equation of state are magnified at the edges of the detonating charges. Figure 6 presents contour plots generated by a DYNA2D simulation of detonation in a 51mm diameter unconfined charge of HANFO, this being only marginally larger than the failure diameter of 46mm. Figure 6(b) illustrates that there is an outer zone of about 5mm in thickness where the extent of reaction remains frozen at 25% or less. As can be seen from the plot of relative volume $\rho_0 v$ in Figure 6(d), the shockfront fully compacts the initially porous explosive, and it is the compressibility of this compacted material that largely controls the expansion of the outer inert zone and hence ultimately the radial divergence of the whole flow. Thus it is the case that the DYNA2D simulations of detonations close to failure are more sensitive to the details of the release isentrope of an initially porous material than they are to the reacted product isentrope.

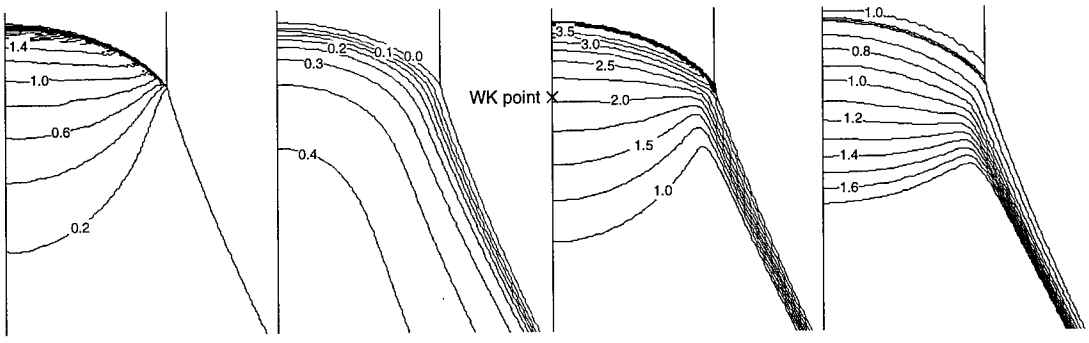

Figure 6. DYNA2D simulation of detonation in a 51mm diameter charge of HANFO. The displayed segments are 50mm in length, with the detonation having run 300mm from the plane wave initiator. Both radial and axial axes are plotted on the same scale. The numbers under each label denote the contour interval. The location of the WK point is identified on plot (c), being where $u+c=D$, with u being the axial component of the particle velocity and c the sound speed.

The discussion to date has assumed that a shock Hugoniot is well defined for HANFO, by treating it as a homogeneous continuum. This assumption turns out to be incorrect.

The ammonium nitrate prills manufactured for incorporation in heavy ANFOs are typically 2 to 3 mm in diameter, and contain sufficient voidage to reduce their bulk density from its crystal value of 1.73 g.cm^{-3} down to roughly 1.33 g.cm^{-3}. The density of the AN/water-in-oil emulsion is also roughly 1.33 g.cm^{-3}, but being non-porous has a different compressibility from the prills. This difference in compressibility on the macroscopic scale of the heavy ANFOs gives rise to considerable shock focussing and dispersion. This is illustrated in Figure 7, which shows a DYNA2D simulation of the instantaneous pressure field in a regular array of AN prills with the layers separated by emulsion. (Being a 2D simulation, the prills are represented as infinitely long cylinders rather than as spheres.) In this simulation, both components are treated as completely unreactive, in order to examine the approach to pressure equilibrium. The lower boundary is being driven at 1 mm.μs^{-1}, which in an intimate mixture of the two components would give rise to a pressure of 4.25 GPa following the treatment of Afanasenkov et al. [19], where it is assumed that the two components are in pressure equilibrium and with each compressed to its respective shock Hugoniot volume. The pressure versus distance profiles exhibit excursions of up to 50% away from the continuum model pressure. In true 3D geometry and in lower density heavy ANFO compositions where the extra voidage is present as macroscopic air bubbles in the emulsion phase, these excursions are expected to be magnified even further. The pressure oscillations persist over distance scales of 20 to 30 mm, which from Figure 3(f) is comparable to typical detonation zone lengths for these explosives.

Hence, it is the case that pressure equilibrium does not exist even between the components of the unreacted phase, and so the unreacted equation of state must be understood to apply only in a very average sense. The mixing rules of section 2.3 were adopted with this in mind. In particular, requiring that the specific volumes of the unreacted and product phases remain equal is nonphysical, but greatly

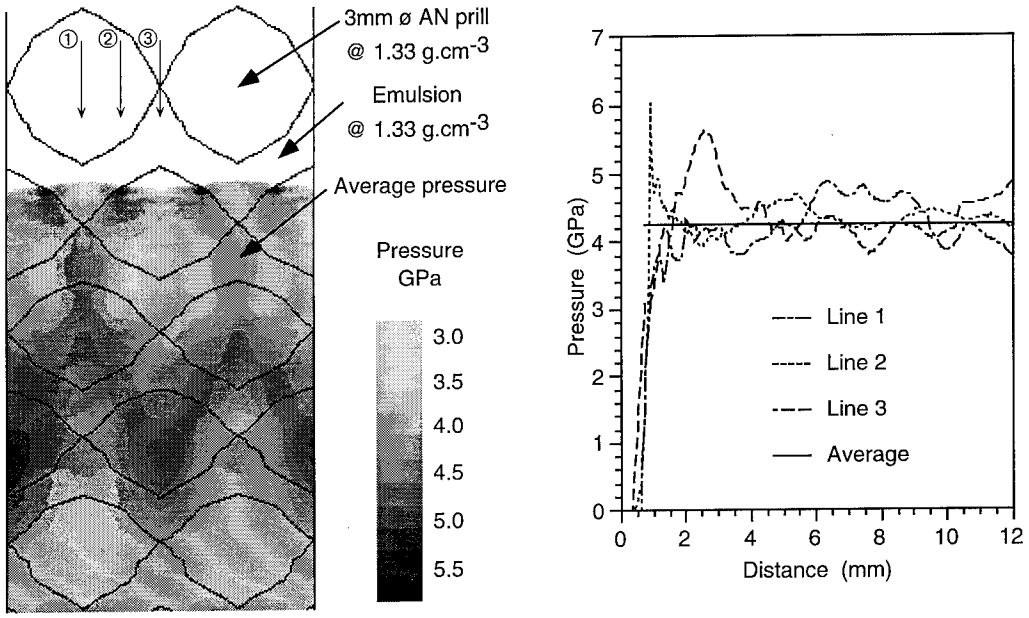

Figure 7. DYNA2D simulation of a shockwave propagating through a 63/37 mixture of inert porous AN prills and emulsion in slab geometry. The lower boundary is being driven upwards at 1mm.μs^{-1}, giving an average pressure of 4.25GPa. The left hand plot shows the pressure field in an area of 6mm×12mm in size, while the right hand plot records the pressure versus distance profiles at the indicated locations.

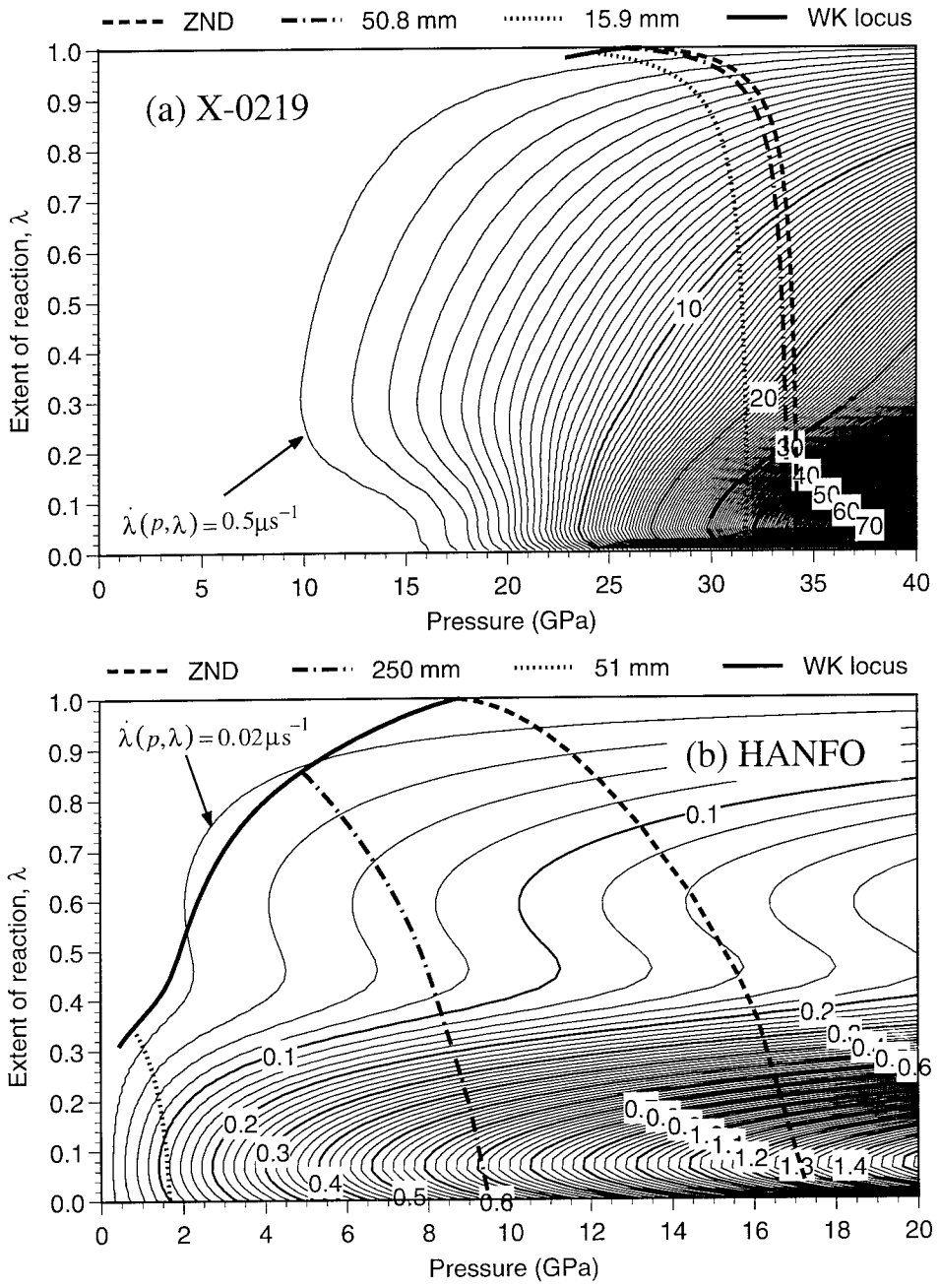

Figure 8. Reaction rate surfaces for X-0219 (upper) and HANFO (lower) determined from the CPeX fits to the diameter effect curves of Figure 1. The contour plots show lines of constant reaction rate, plotted at 0.5 μs^{-1} intervals for X-0219 and at 0.02 μs^{-1} intervals for HANFO. Superimposed over each contour surface are firstly the dashed line traced out by the $(p(t), \lambda(t))$ histories between the shock front and the CJ point of a ZND detonation, secondly its 2D analogues in the largest (dot-dash) and smallest (dot) diameters investigated experimentally, and finally the solid line traced out by the $(p(d), \lambda(d))$ pairs at the WK point as the diameter is increased from its critical value (left hand end) to infinite diameter (right hand end) for steady detonation in unconfined cylindrical charges.

simplifies the solution algorithms.

A full rigorous solution to the theoretical problems described in this section lies beyond the scope of this paper.

The scale of the physical heterogeneity indicated in Figure 7 also introduces significant challenges to the experimentalist. The irregularities in the shock front preclude accurate measurements of the radii of curvature in 2D detonations. Any embedded pressure or particle velocity gauge needs to be long enough to average across a representative sample of the explosive, but the resulting high shear generated during the differential collapse of the two phases would cause gauge breakup well before the 8 to 12μs timescale required to sample the end of the detonation zone as shown in Figure 3(e).

8. REACTION RATE SURFACE DIAGRAMS

Once the adjustable parameters in equation (7) have been fixed for a given explosive, it can be seen that this reaction rate law describes a unique 3D surface in $\left(p,\lambda,\dot{\lambda}\right)$ space. Such surfaces can be represented in a variety of graphical forms — it has been found most informative to display them as contour plots with pressure p and extent of reaction λ as the independent axes, and the contour lines representing the dependent $\dot{\lambda}$. Figure 8 presents the reaction rate surfaces necessary to reproduce the experimental diameter effect curves of Figure 1 using the CPeX reactive equation of state and divergent flow models. The pressure axis, for which $\lambda = 0$, corresponds to the conditions at the shock front.

Superimposed over these contour plots are line diagrams defining the regimes in which steady 1D and 2D detonation can occur.

Note that the contour interval for X-0219 is 25 times larger than that for HANFO.

8.1 X-0219

The reaction rate surface divides into four broad regimes along the pressure axis.

- Over the range $0 \le p < 8$ GPa, $\dot{\lambda} \approx 0$ and X-0219 is essentially inert.
- Over the range $8 \le p < 16$ GPa, $\dot{\lambda}(\lambda \approx 0)$ is small, and $\partial\dot{\lambda}/\partial\lambda > \partial\dot{\lambda}/\partial p$. Under these conditions, a sustained shockwave will propagate at steady or weakly accelerating velocity, until reaction at the rear boundary reaches $\lambda \approx 0.2$ and the reaction rate increases. This positive feedback situation generates a pressure excursion at the rear boundary, which eventually overtakes the initial shock taking it into the fourth regime discussed below. Hence, experimental wedge tests [16] conducted in this pressure regime would provide sharp shock to detonation transitions, with the traces of shock position versus

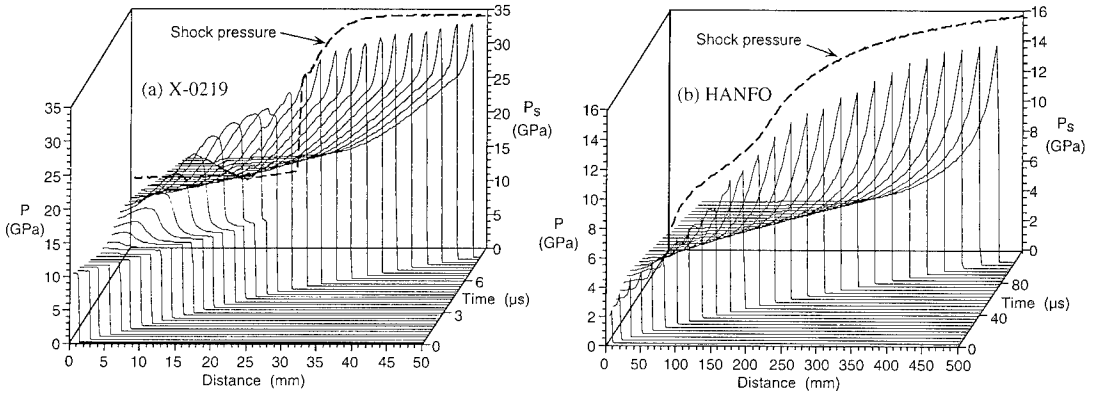

Figure 9. DYNA2D pressure profiles for sustained shock initiation in 1D planar geometry, following impact by a thick aluminium flyers at the left hand boundary. The profiles are shown at 0.25 μs intervals for X-0219, and at 4.0 μs intervals for HANFO. The dashed line on the back plane shows the shock pressure recorded at each distance.

time showing distinct low velocity and high (detonation) velocity regimes. Figure 9(a) exemplifies this.

- Over the range $16 \le p < 24$ GPa, $\dot{\lambda}(\lambda \approx 0)$ is moderate, and $\partial\dot{\lambda}/\partial p > \partial\dot{\lambda}/\partial\lambda$. Any shock in this regime will show strong acceleration at the front, and a rapid transfer into the next regime. The shock position versus time traces observed in a wedge test will be curved, so the transition to detonation is diffuse.
- For $p \ge 24$ GPa, both $\dot{\lambda}(\lambda \approx 0)$ and $\partial\dot{\lambda}/\partial p$ are large. Any shock will quickly accelerate as far to the right of the pressure axis as the energy balance will permit.

This surface may be interpreted physically in a qualitative fashion. Over the first pressure regime, hotspot creation is inefficient, and thermal diffusion quenches reaction. Over the second regime, a limited volume of the shocked explosive is ignited by the formation of a small number of hotspots — the overall reaction rate eventually increases as the burn fronts grow geometrically. In the fourth high pressure regime, a large volume of the explosive is ignited by an increased variety of different hotspot mechanisms, giving the peak reaction rates at or just behind the shock. The third regime is transitional.

It is the resulting strong state dependence of the reaction rate law (i.e. large $\partial\dot{\lambda}/\partial p$ gradients at detonation pressures) that restricts the 2D WK detonation histories to a narrow band of pressures close to the ZND history. It is the high reaction rates within this band (i.e. $\dot{\lambda}(p \approx 34\,\text{GPa})$ is large) that force the reaction almost to completion within the detonation zone.

It is the large difference, a factor of roughly 100 to 500 in the absolute reaction rates between the low pressure regime, $8 \le p < 16$ GPa, and the high pressure regime, $p \approx 34$ GPa, that makes it meaningful to ascribe shock initiation, with its associated Pop-plot [16], to the former and detonation to the latter.

8.2 HANFO

The reaction rate surface for HANFO shown in Figure 8(b) bears little resemblance to that discussed for X-0219. It does not divide into different pressure regimes, but instead, into different λ regimes. This is the result of control over the hotspot formation mechanisms (via the distribution of voidage) and the reliance on mass diffusion to limit reaction rates (via the physical separation between oxidiser and fuel phases).

Because of mass diffusion, the state dependence of the reaction rate law is weak (i.e. small $\partial\dot{\lambda}/\partial p$ gradients everywhere) and the absolute reaction rates are slow. The former makes it possible to sustain 2D detonation over a wide range of pressures. The latter allows the reaction to be incomplete within the WK detonation zone, since it becomes possible to satisfy the second WK condition [11], requiring the rate of energy production at the sonic point to match the radial expansion, at $\lambda << 1$.

Figure 9 compares initiation in HANFO to that in X-0219. The DYNA2D simulations were performed assuming planar 1D flow, starting at the time when a thick flyer plate impacts the left hand boundary. The flyer velocities were chosen so that the initial reaction rates for both explosives were equal, namely $\dot{\lambda} = 0.01\mu s^{-1}$. For the HANFO, $\partial\dot{\lambda}/\partial p > \partial\dot{\lambda}/\partial\lambda$, and so the pressure accelerates at the shock front. However, both the gradients $\partial\dot{\lambda}/\partial p, \partial\dot{\lambda}/\partial\lambda$ and the absolute rate $\dot{\lambda}$ are small everywhere, so the acceleration is weak. It may be noted that the detonation has not reached steady state even after 500mm of run. From his perturbation method study of a model explosive with a late slow reaction, Bdzil [20] concluded that detonation in such explosives would indeed exhibit only very slow approach to steady state in 1D planar geometry. To examine this further, a second simulation was performed replacing the flyer plate by 200mm of detonating Composition B, with the results shown in Figure 10. Even after the detonation in the HANFO has run 500mm, the DYNA2D pressure versus distance profile has still not reached the equivalent profile predicted by CPeX for a 25m diameter charge (taken to represent infinite diameter). It may confidently be concluded that no current facility in the world could perform a 1D experiment on a sufficient scale to probe the CJ state of HANFO.

There is some structure evident in the trace of the shock pressure versus distance of Figure 9(b) which would translate into similar structure in shock velocity versus distance, but to extract shock to detonation

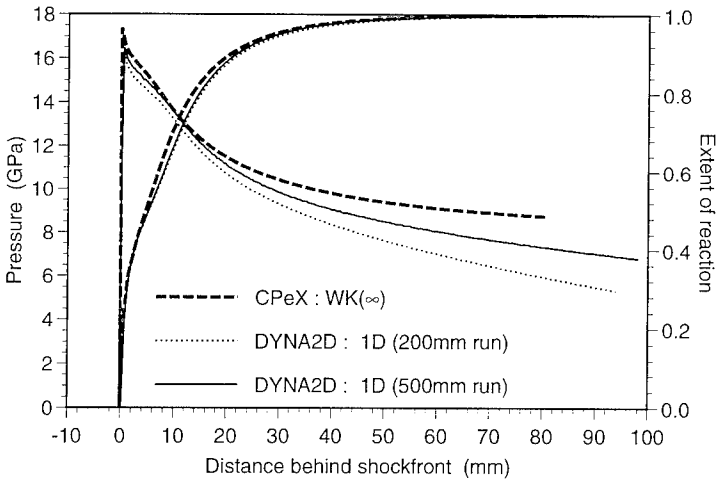

Figure 10. Pressure and extent of reaction profiles for HANFO. The DYNA2D profiles, for 1D planar geometry, are after the detonation has run 200mm and 500mm through the HANFO, following initiation by a programmed burn through 200mm of Composition B. The CPeX profiles are for WK detonation in 25m diameter (assumed to represent infinite diameter).

transitions from this structure would be inappropriate. Indeed, HANFO can detonate at this initial pressure provided its shockfront is sufficiently curved. In this type of non-ideal explosive, the difference between shock initiation and detonation lies in the geometry of the shockfront, not in its pressure. A Pop-plot cannot be defined for HANFO because the topography of its reaction rate surface does not provide the positive feedback mechanism that leads to shock-to-detonation transitions. The same is true of the emulsion investigated by Lee et al. [21], whilst PBXN-111 has a Pop-plot in the low pressure regime but not at intermediate pressures [3].

8.3 Accuracy of the reaction rate surface

The calibration procedure described in section 4 compensates to some degree for the errors in the divergent flow model discussed in sections 5 and 6, and for the errors in the reactive equation of state model discussed in section 7. This reduces the physical significance of the reaction rate law, making its fitted parameters strongly dependent on the models adopted.

Even with more rigorous models, there would remain uncertainties in the reaction rate surfaces that are inherent in the calibration procedure. When fitting a diameter effect curve, the solution is strongly dependent upon both the rate $\dot{\lambda}$ and its integral $\int_0^{WK} \dot{\lambda}\, dt = \lambda$ at the WK point, but only weakly dependent on its intermediate values between the shock front and the WK point. These zones of dependency are shown schematically in Figure 11.

8.3.1 X-0219

As a consequence, the CPeX reaction rate surface for X-0219 is very poorly specified, since the WK solution points lie within very tight bands in both pressure and extent of reaction. Indeed, the WK solutions here are more sensitive to the form of the geometrical depletion term, namely $(1-\lambda)$, than to the characteristic reaction time constants in the reaction rate law. In order to sensibly fix these time constants, it was necessary to supplement the detonation velocity measurements with DYNA2D simulations of the experimental Pop-plot. Thus, only the grey areas in Figure 11(a) are based on experimental data, while the remaining white areas are inferred by extrapolation using the functional forms assumed in the reaction rate law.

Furthermore, after all the calculations reported here had been completed, the papers by Campbell [14]

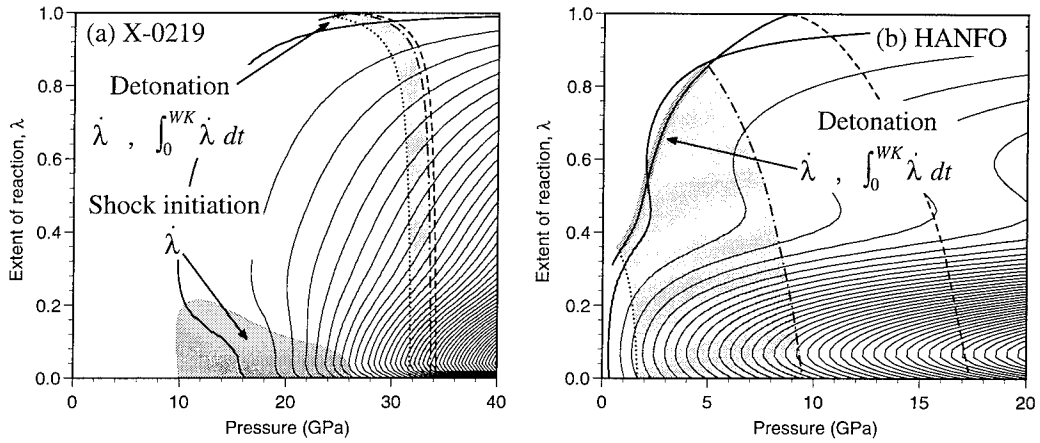

Figure 11. The areas shaded in grey define where the CPeX reaction rate surface is determined from experimental data. Dark grey signifies a strong sensitivity, while light grey signifies a weak sensitivity, to the data.

and by Chaissé [15] came to our attention, demonstrating that the diameter effect curves for the similar explosives PBX-9502 (95 / 5 TATB / KelF 800) and Composition T (96% TATB) respectively were not linear as previously described by Campbell and Engelke [7] and collated by Gibbs and Popolato [16] for X-0219 and PBX-9502, but instead was concave upwards in large diameter and concave downwards in small diameter. As mentioned in section 4, the chemical equilibrium calculations using IDeX [5] predicted an ideal detonation velocity for X-0219 that was higher than that based on a linear extrapolation of the diameter effect curve. If the diameter effect curve of X-0219 is in fact similar in shape to that of other TATB explosives (and hence incidentally also of HANFO), this would alter the shape of its reaction rate surface in the region $\lambda \approx 0.9$. Rather than the present surface for which $\partial\dot{\lambda}/\partial\lambda < 0$ and $\partial^2\dot{\lambda}/\partial\lambda^2 = 0$ in this region, the surface would need to be altered so that $\partial\dot{\lambda}/\partial\lambda < 0$ and $\partial^2\dot{\lambda}/\partial\lambda^2 > 0$. This would eliminate all reaction rate laws based on a $(1-\lambda)^n$ depletion term, where $n < 1$ to yield a finite reaction zone length.

Nonetheless, it is believed that the reaction rate surface plotted for X-0219 in Figure 8(a) is realistic away from this region. Sheffield et al. [22] inferred reaction rates in PBX-9502 from subnanosecond resolution particle velocity measurements. They estimated that the initial reaction rate immediately behind the detonation front was 80 μs^{-1}, and that this rate decreased as the reaction proceeded. This compares favourably with the peak rate of 50 μs^{-1} determined here for X-0219, remembering that the failure diameters of these explosives are 9mm for PBX-9502 and 14mm for X-0219.

The only direct experimental estimate of the ZND detonation zone length in X-0219 is 0.3mm from the plate push experiments of Craig (quoted by Campbell and Engelke [7]), based on the break point in a plot of plate velocity versus plate thickness. Measurements on similar TATB-based explosives have given longer values. From their particle velocity experiments, Sheffield et al. [22] estimated that the 1D reaction zone length for PBX-9502 was about 2mm. Davis [23] varied the charge length of PBX-9502 in a plate push experiment, seeking to discriminate between the steady and non-steady flow regimes behind the detonation front — this gave a detonation zone length of 3.3mm. The form of the depletion term, $(1-\lambda)$, adopted in CPeX gives infinite reaction zone lengths in the limit as $\lambda \to 1$. However, the CPeX detonation zone lengths summarised in Figure 3(f) would support values around 3mm.

8.3.2 HANFO

The diameter effect curve for HANFO covers a broad region of both the pressure and the extent of reaction space, mapping out the surface quite efficiently. Shock initiation experiments are not required in the conventional sense to probe reactivity in the *low* pressure regime. Instead, wedge tests could be used

to probe the *high* pressure regime, where it is not economical to perform detonation experiments. This is the exact opposite of the situation for X-0219.

In particular, the measurements have sampled through the local minimum in the reaction rate surface at $\lambda \approx 0.45$. Such a minimum has not previously been reported in the literature, and indeed, few published reaction rate schemes could accommodate such a minimum.

9. CONCLUDING REMARKS

The behaviour of X-0219 described here exemplifies the type of detonics for which the recent theories by Bdzil et al. [24], by Lambourn and Swift [25], and by Brun [26], have been developed. These theories, which can relate detonation velocity to wavefront curvature in rate stick geometry, all share the common assumption that the thickness of the detonation zone x_{WK} can either be neglected or is much smaller than the other distance scales in the problem (typically either the charge diameter or the shockfront radius of curvature R_S). This is the case for X-0219, where even close to the failure diameter, the ratio $x_{WK} / R_S \approx 0.035$. A short detonation zone necessarily limits the extent of radial divergence that can occur within it, leading directly to 2D detonation in rate stick geometry being only slightly perturbed from 1D detonation in planar geometry. In particular, the pressure, density, and extent of reaction at the WK point of a 2D detonation are all close to their CJ values. X-0219 can rightly be considered an ideal explosive.

This is not true of HANFO, where the differences between the 1D and 2D detonations are profound, and on a scale not previously reported. Here, the ratio $x_{WK} / R_S \approx 0.25$, so that the basic assumption of the wavefront curvature models is violated. The long detonation zones give time for appreciable radial divergence to occur, leading to significant deviations from CJ predictions. Hence, close to the failure diameter, the WK pressure for a 2D detonation is an order of magnitude lower than the CJ pressure of a 1D detonation. HANFO is a highly non-ideal explosive.

This non-ideality derives from the topography of the HANFO reaction rate surface, which in turn derives from the key role that mass diffusion is believed to play in limiting reaction rates in physically heterogeneous explosives. Such non-ideality and heterogeneity challenge both the theoretician and the experimentalist.

The features in the reaction rate surface for X-0219 that make shock initiation a distinct phenomenon from detonation are absent from the surface for HANFO. This must be clearly understood if the hazards of handling highly non-ideal explosives are to be properly assessed.

10. REFERENCES

[1] Crane S.L., Deal W.E., Ramsay J.B. and Takala B.E., "Indexes for the Proceedings of the Symposia (International) on Detonation — 1951 through 1985", Ninth Symposium (International) on Detonation, Portland 28 August - 1 September, 1989 (OCNR 113291-7), pp. 1543-1634.

[2] Brunauer S., Discussion at the conference on The Chemistry and Physics of Detonation, Washington 11-12 January 1951 (NSWC MP 87 - 194), p 111.

[3] Kennedy D.L. and Jones D.A., "Modelling shock initiation and detonation in the non-ideal explosive PBXW-115", Tenth Symposium (International) on Detonation, Boston 12-16 July, 1993, Preprint paper No. 102, pp. 36-39.

[4] Held M., *Propellants, Explosives and Pyrotechnics*, **17** (1992) pp. 275-277.

[5] Freeman T.L., Gladwell I., Braithwaite M., Byers-Brown W., Lynch P.L., and Parker I.B., *Math. Engng. Ind.*, **3** (1990) pp. 97-109.

[6] Forbes J.W., Lemar E.R. and Baker R.N., "Detonation Wave Propagation in PBXW-115", Ninth Symposium (International) on Detonation, Portland 28 August - 1 September, 1989 (OCNR 113291-7), pp. 806-815.

[7] Campbell A.W. and Engelke R., "The Diameter Effect in High-density Heterogeneous Explosives", Sixth Symposium (International) on Detonation, Coronado 24-27 August 1976 (ACR-221) pp. 642-652.

[8] Jeanloz R., *Journal of Geophysical Research*, **94** No B5 (1989) pp. 5873-5886.
[9] Kirby I.J. and Leiper G.A., "A small divergent detonation theory for intermolecular explosives", Eighth Symposium (International) on Detonation, Albuquerque 15-19 July, 1985 (NSWC MP 86-194), pp. 176-185.
[10] Hallquist J.O., "User's Manual for DYNA2D", UCID-18756, Rev. 3, March 1988, Lawrence Livermore National Laboratory, Livermore, CA.
[11] Wood W.W. and Kirkwood J.G., *Journal of Chemical Physics*, **22** (1954) pp. 1920-1924.
[12] Braithwaite M., Farran T., Gladwell I., Lynch P.M., Minchinton A., Parker I.B., and Thomas R.M., *Math. Engng. Ind.*, **3** No. 1 (1990) pp. 45-57.
[13] Chaissé F., Servas J.M., Aveillé J., Baconin J., Carion N. and Bongrain P., "A Theoretical Analysis of the Shape of a Steady Axisymmetrical Reactive Shockfront in Cylindrical Charges of High Explosive ; A Curvature — Diameter Relationship", Eighth Symposium (International) on Detonation, Albuquerque 15-19 July, 1985 (NSWC MP 86-194), pp. 159-167.
[14] Sheahan R.M., ICI Australia, unpublished data, 1992.
[15] Campbell A.W., Propellants, Explosives, Pyrotechnics **9** (1984) pp. 183-187.
[16] Gibbs T.R. and Popolato A., Editors, LASL Explosive Property Data (University of California Press, 1980).
[17] Leiper G.A., Kerr I.D. and Kennedy M., "Calculations and measurements of the flow in unconfined detonations", First MoD Detonics Conference, Royal Military College of Science, Shrivenham 23-24 September 1987.
[18] Johnson J.N., Mader C.L. and Goldstein S., *Propellants, Explosives, Pyrotechnics* **8** (1983) pp. 8-18.
[19] Afanasenkov A.N., Bolomolar V.M. and Voskoboinikov I.M., *Zhur. Prok. Mekh. Tekh. Fig.* **10** (1969) pp. 137-147.
[20] Bdzil J.B., "Perturbation Methods applied to problems in Detonation Physics", Sixth Symposium (International) on Detonation, Coronado 24-27 August 1976 (ACR-221) pp. 352-371.
[21] Lee J., Sandstrom F.W., Craig B.G. and Persson P.A., "Detonation and shock initiation properties of emulsion explosives", Ninth Symposium (International) on Detonation, Portland 28 August - 1 September, 1989 (OCNR 113291-7), pp. 573-584.
[22] Sheffield S.A., Bloomquist D.D. and Tarver C.M., *J. Chem. Phys.* **80** (1984) pp. 3831-3844.
[23] Davis W.C., "Magnetic probe measurements of particle velocity profiles", Sixth Symposium (International) on Detonation, Coronado 24-27 August 1976 (ACR-221) pp. 637-641.
[24] Bdzil J.B., Fickett W. and Davis W.C., "Detonation Shock Dynamics : A New Approach to Modelling Multi-Dimensional Detonation Waves", Ninth Symposium (International) on Detonation, Portland 28 August-1 September, 1989 (OCNR 113291-7), pp. 730-742.
[25] Lambourn B.D. and Swift D.C., "Application of Whitham's Shock Dynamics Theory to the Propagation of Divergent Detonation Waves", Ninth Symposium (International) on Detonation, Portland 28 August-1 September, 1989 (OCNR 113291-7), pp. 784-797.
[26] Brun L., "Un nouveau modèle macroscopique de la détonation non soutenue dans les explosifs condensés", Symposium International Hautes Pressions Dynamiques, la Grande Motte, June 1989, pp. 103-107.

JOURNAL DE PHYSIQUE IV
Colloque C4, supplément au Journal de Physique III, Volume 5, mai 1995

Williamsburg Equation of State for Modelling Non-Ideal Detonation

W. Byers Brown, Z. Feng* and M. Braithwaite**

Mass Action Research Consultancy, Devonshire House, 14 Corbar Road, Buxton SK17 6RQ, U.K.
** Department of Chemistry, University of Manchester, Manchester M13 9PL, U.K.*
*** ICI plc Explosives GTC, Ardeer Site, Stevenston, Ayrshire KA20 3LN, Scotland, U.K.*

ABSTRACT

The recently developed Williamsburg equation of state (EOS) for detonation products is used in the one-dimensional ZND model for the reaction zone of a condensed explosive. This appears to be the first time a realistic EOS, capable of describing entropy and temperature changes accurately, has been incorporated into the ZND model. The unreacted explosive is described by a new Parsafar-Mason-Vinet EOS so that both phases receive the best thermodynamic treatment currently available. Results for the two extreme inter-phase assumptions regarding the thermal interaction of the reactant and product phases are presented and discussed.

1. INTRODUCTION

The thermodynamic behaviour and interaction of the reactant explosive and its products within the reaction zone are of crucial importance to the detailed structure of a detonation wave, and to its propagation. The reacting material within the reaction zone should therefore be described by realistic thermodynamics. The traditional assumption is that the reacting material can be regarded as a mixture of two phases, one consisting of the as yet unreacted explosive and the other of the detonation products. The problem of the thermodynamics of the reacting material is thereby simplified into finding appropriate equations of state (EOS) for the separate phases.

Early treatments used the polytropic equation for both unreacted explosive and detonation product gases, often with the same polytropic index. This EOS is unsuitable for liquids and solids, and is not in agreement with experiment. The Jones-Wilkins-Lee (JWL) EOS is much more flexible, but assumes the Grüneisen gamma coefficient is constant, and is not a complete equation of state, so that temperature and entropy cannot be calculated without a subsidiary crude assumption, for example that the heat capacity is a constant, which is never true.

The new WILLIAMSBURG (WBG) EOS for detonation products, proposed by Byers Brown and Braithwaite [1,2,3,4,5], is unusual in giving the specific energy E as a function of the specific volume V and the specific entropy S, and is therefore a complete EOS, embracing both mechanical and thermal properties, particularly well suited for describing adiabats and shocks. The comparatively small number of parameters it involves can be found by fitting the principal adiabat calculated from an ideal detonation code, for example IDeX [6], incorporating a sophisticated EOS based on statistical mechanics and intermolecular potentials. The WBG fits of energy, pressure, temperature, adiabatic and Grüneisen gammas and heat capacity, are highly satisfactory for a wide range of explosives.

In this paper we solve the one dimensional conservation equations for the Zeldovich-von Neumann-Döring (ZND) steady state of the reaction zone as a function of the extent of reaction parameter λ, with the WBG and (where possible) the JWL EOSs for the detonation products, and a new EOS (dubbed PMV) combining features of the recently proposed Parsafar-Mason [7] and Vinet [8,9,10] EOSs to describe the unreacted explosive.

The inter-phase condition determining the thermal interaction between the reactant and products, and the increase of entropy in the reaction zone, are especially featured and discussed.

2. ZND MODEL

We start from the basic one-dimensional conservation equations [11] and the reactive EOS,

$$P - P_0 = (\rho_0 D)^2 (V_0 - V) \quad \text{(Rayleigh line)}, \tag{2.1}$$

$$E - E_0 = \frac{1}{2}(P + P_0)(V_0 - V) \quad \text{(Rankine-Hugoniot)}, \tag{2.1}$$

$$P = f(E, V, \lambda) \quad \text{(reactive EOS)}, \tag{2.3}$$

where $\rho=1/V$ is the density, D the detonation speed, P the pressure, E the specific energy, and the zero subscript indicates the initial state. For a given value of D, provided the EOS relations are given, the equations can been solved numerically. In our paper, standard NAG (Numerical Algorithms Group) Library subroutines are employed to solve them.

3. EOS IN REACTION ZONE

Typically, the reacting material in the reaction zone is taken to be an ideal mixture of unreacted explosive and reacted product. Therefore their EOS s determine the overall reactive EOS in the reaction zone according to an assumed mixing rule and the inter-phase conditions. The EOSs which are used in the calculations are as follows.

3.1 EOS for unreacted explosive

The PMV EOS [6] is a complete EOS, best defined in terms of Helmholz free energy A(T,V), which can be deduced from the following equations for the pressure

$$P = (\rho/\rho_0)^2 p_2 + (\rho/\rho_0)^3 p_3 + (\rho/\rho_0)^4 p_4 + \theta T, \tag{3.1.1}$$

and the specific heat capacity at constant volume,

$$C_v = C_\infty + C_1(T_0/T) + C_2(T_0/T)^2, \tag{3.1.2}$$

where the p_i, C_i, and θ (the thermal pressure coefficient) are constants. This basic form can be extended by the addition of further terms as required by the experimental data available.

3.2 EOS for reaction products

(a) WILLIAMSBURG (WBG)
This is a complete EOS with variables V, S which can be written in the simple form

$$E = \frac{PV}{g(v,\sigma) - 1}, \tag{3.2.1}$$

with

$$g(v,\sigma) = \gamma_0 + \sum_{j=1}^{M} \frac{\gamma_j}{1 + \beta_j v \sigma^{\overline{\alpha_j}}}, \tag{3.2.2}$$

where $v = V/V_0$ is the reduced volume and σ is a reduced entropy factor defined by

$$\sigma = \exp[(S - S_O)/nR], \tag{3.2.3}$$

with n the moles per unit mass, R the gas constant, and

$$\overline{\alpha_j} = \alpha_j + \delta_j \log \sigma, \tag{3.2.4}$$

$$\gamma_0 = 1 + \sum_{j=1}^{M} \alpha_j \gamma_j \ , \tag{3.2.5}$$

where α_j, β_j, γ_j, δ_j are constants, and usually the number of terms for an adequate fit is M=2.

(b) JONES-WILKINS-LEE (JWL)
This is an incomplete EOS which can be written either in the form P=P(E,V) or alternatively as

$$E = \frac{PV}{\gamma - 1} + \sum_{j=1}^{M} e_j \left(1 - \frac{\alpha_j v}{\gamma - 1}\right) \exp\left(-\alpha_j v\right) , \tag{3.2.6}$$

where again $v = V/V_0$, and α_j, e_j, γ are constants, and usually M = 2, although here also the equation has been extended to a larger number of terms. It is postulated to be valid over the whole PV-plane. The familiar JWL equation for the pressure along an isentrope can be recovered by integrating the adiabatic differential equation dE+PdV=0.

4. MIXING RULE AND INTER-PHASE CONDITIONS

4.1 Mixing Rule

As in the usual treatments, a linear phase mixing rule is assumed for all extensive properties, so that

$$V = (1-\lambda)V_x + \lambda V_g \ , \tag{4.1.1}$$

$$E = (1-\lambda)E_x + \lambda E_g , \tag{4.1.2}$$

where x and g denote the explosive and the gaseous products.

4.2 Inter-phase Conditions

To solve the equations, two further assumptions are needed to relate the two phases, which we call the inter-phase conditions. The first condition, as usual, is mechanical equilibrium:

$$P = P_x = P_g . \tag{4.2.1}$$

There are two alternative assumptions which lead to simple second inter-phase conditions.

(a) Thermal equilibrium:

$$T = T_x = T_g . \tag{4.2.2}$$

(b) Thermal isolation of the explosive phase:

$$S_x = const. \tag{4.2.3}$$

The two inter-phase conditions (a) and (b) are extreme cases. The first one indicates that the rate of heat conduction is infinite so that the two phases are always in thermal equilibrium. The second indicates there is no heat conduction between the unreacted explosive and the reaction products. Clearly, the actual situation will be somewhere in between these two extremes.

5. CALCULATION AND RESULTS

We use an ANFO explosive consisting of ammonium nitrate with 6% of a hydrocarbon (ρ_0 = 0.85 g/cc) as an example. The end-point of the reaction zone in ZND theory is the Chapman-Jouguet (CJ) state (λ=1), which according to the IDeX ideal detonation code [6] for this explosive has pressure P_{cj}=5.60 GPa, specific volume V_{cj}=0.864 cc/g, and detonation speed D=5.02 km/s. The WBG EOS for the products is constrained to have exactly the same CJ state, and the remaining parameters are fitted by a least squares procedure to the IDeX principal adiabat.

The PMV EOS for the unreacted explosiveis fitted to experimental shock and thermodynamic results for ammonium nitrate modified to allow for the presence of 6% of a hydrocarbon of known density. The starting-point of the reaction zone in ZND theory is the von Neumann spike, which is at the intersection of the unreacted Rankine-Hugoniot (λ=0), calculated from the PMV EOS, and the Rayleigh Line through the initial and CJ states, which depends only on the product WBG EOS. The von Neumann pressure is P_n=12.3 GPa and the specific volume is V_n=0.497 cc/g. The results of the calculations on the PV-plane are shown in Figs 1 and 2.

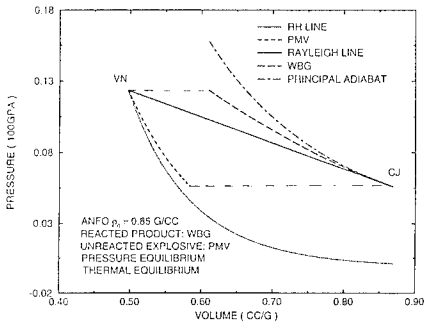

Fig 1 PV-diagram for ZND detonation of ANFO assuming thermal equilibrium.

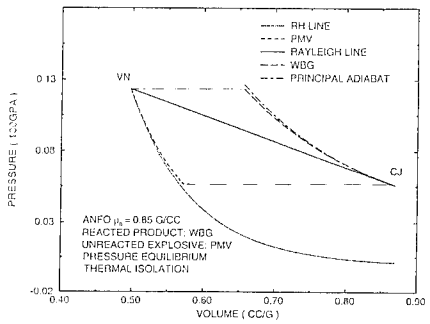

Fig 2 PV-diagram for ZND detonation of ANFO assuming thermal isolation.

Fig 1 is based on the assumption of thermal equilibrium between the explosive and product phases. The Rankine-Hugoniot of the unreacted explosive (described by the PMV EOS) is shown, ending at the von Neumann spike (VN), and also the straight Rayleigh Line between VN and the Chapman-Jouguet point (CJ). Also plotted, to the best of our knowledge for the first time, are the specific volumes of the individual explosive and product phases.

Fig2 is based on the assumption of the thermal isolation of the unreacted explosive phase, so the specific volume curve for the explosive is the adiabatic expansion from the Neumann point VN. It can be seen that the specific volume of the product phase is very close to the principal adiabat of the products which passes through the CJ point, so that unlike the thermal equilibrium case, very little additional entropy is created by the pre-CJ expansion.

It is not possible to use the JWL EOS for the gaseous products with the assumption of thermal equilibrium, since temperature is not defined. However, it can be used assuming thermal isolation of the explosive. It turns out that with JWL parameters chosen to make the CJ point agree exactly with that of the IDeX code (and therefore with that of the WBG EOS), there is no appreciable difference between the JWL and WBG individual specific volume curves.

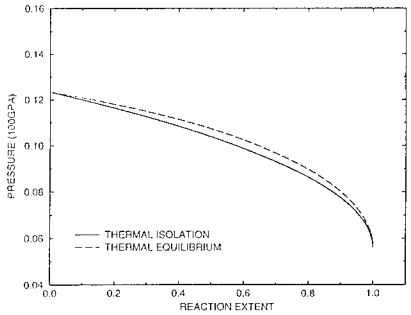

Fig 3 Pλ-plot for ZND detonation of ANFO.

The WBG EOS is used for the products in all the calculations on which the subsequent figures are based. The P -λ curves for the two assumptions are shown in Fig 3, and lie close together. Of greater interest and novelty, the specific volumes V_x and V_g , and also the total

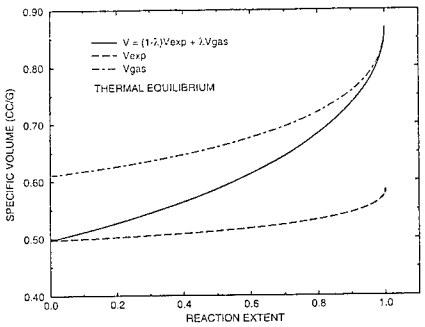

Fig 4 Vλ-plots for ZND detonation of ANFO assuming thermal equilibrium.

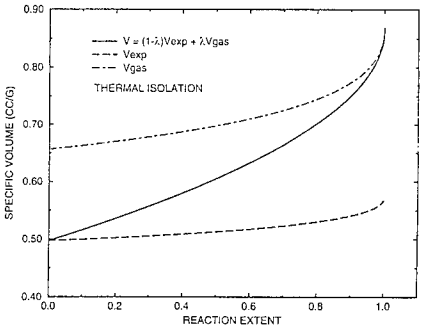

Fig 5 Vλ-plots for ZND detonation of ANFO assuming thermal isolation.

specific volume V, are shown as functions of the extent of reaction parameter λ in Figs 4 and 5 for the two alternative interphase assumptions. Qualitatively they are similar, but quantitatively the V_g curves differ considerably.

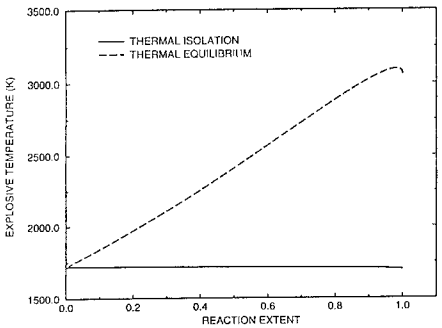

Fig 6 Tλ-plots for unreacted ANFO on ZND theory.

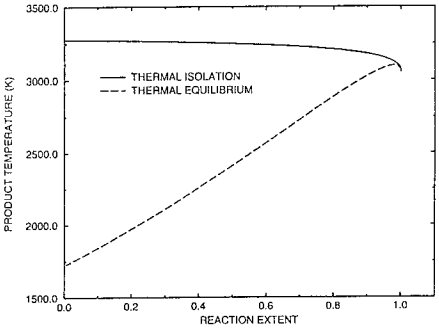

Fig 7 Tλ-plots for detonation products of ANFO on ZND theory.

Figs 6 and 7 show the corresponding temperatures T_x and T_g respectively for the two thermal assumptions; the thermal equilibrium curves are, of course, identical in both figures, and exhibit an almost linear increase of temperature with λ.

6. DISCUSSION

The WBG is a complete EOS. It allows the temperature and the change of entropy to be calculated. The results show that while there is always a large increase of specific entropy on going from the explosive to products, in the case of thermal isolation the subsequent production of entropy in the reacted phase is very small because there is no heat conduction between the two phases. On the other extreme assumption there is an increase of entropy due to heat transfer from the hot products to the unreacted explosive. Heat conduction is essential for initiation, as pointed by Nutt [12], and the actual situation must lie between the two extremes.

The JWL can only be employed assuming thermal isolation, as the temperature is not defined.In this case its predictions do not differ dramatically from the more accurate WBG EOS. However, it cannot be used in more sophisticated calculations, for example, one in which the entropy production is minimized to find the balance between the two extreme assumptions, or another in which the heat transfer equation is coupled to the one-dimensional conservation equations and solved simultaneously.

ACKNOWLEDGEMENT

One of us (ZF) is grateful for the financial support of ICI Explosives Group Technical Centre, Ardeer, and to the British Council for a Scholarship (SBFSS scheme) .

REFERENCES

[1] Byers Brown, W. and Braithwaite, M., "Analytical Representation of the Adiabatic Equation for Detonation Products based on Statistical Mechanics and Intermolecular Forces",*Shock Compression of Condensed Matter 1991*, Elsevier, 325-328 (1992).

[2] Byers Brown, W., "Analytical representation of the adiabatic equation for detonation products based on statistical mechanics and intermolecular forces" *Phil.Trans.Roy.Soc.A* **339,** 345-353 (1992).

[3] Byers Brown, W., and Braithwaite, M., "Williamsburg Equation of State for Detonation Product Fluid",*Shock Compression of Condensed Matter 1993,* Colorado Springs, June 1993, S.C. Schmidt et al. Eds. (American Institute of Physics Press, 1994) pp.73-76.

[4] Byers Brown, W., and Braithwaite, M., "Development of the Williamsburg Equation of State to model Non-ideal Detonation" *Proc. 10th Symposium (International) on Detonation,* Boston, Massachusetts, July 1993 (to be published)

[5] Byers Brown, W., "Williamsburg Equation of State for Fluids at Very High Density", Contract Report for ICI plc Explosives Group Technical Centre, Ardeer (February 1994)

[6] Freeman, T. L., Gladwell, I., Braithwaite, M., Byers Brown. W., Lynch, P.M., and Parker, I.B., "Modular Software for Modelling the Ideal Detonation of Explosives", *Math. Eng. Industry*, **3**, 97-109 (1991).

[7] Parsafar, G., and Mason, E. A., "Universal Equation of State for Compressed Solids" *Phys Rev B* **49** 3049-3060 (1994)

[8] Vinet, P., Ferrante, J., and Rose, J.H., "A Universal Equation of State for Solids", *J.Phys. C:Solid State Phys.* **19** L476-L473 (1986)

[9] Vinet, P., Ferrante, J., Rose, J.H., and Smith, J.R., *J.Geophys.Res.* **92** 9319 (1987)

[10] Vinet, P., Smith, J.R., Ferrante, J., and Rose, J.H., *Phys.Rev. B* **35** 1945-1953 (1987)

[11] Fickett, W., and Davis, W.C., "Detonation" (University of California Press, 1979)

[12] Nutt, G. L., "A Reactive Flow Model For A Monomolecular High Explosive", *J Appl Phys* **64** 1816-1826 (1988)

3-2 Discussion

Questions - Answers

Comment by David L. Kennedy : Proposed New Nomenclature for Steady Detonation

Final comment by Louis Brun : The Ideal Detonation

Questions - Answers

Brun - Fauquignon :

Q : Would you please go back over your conception of ideality ?

A : Ideality means that the sonic point and the point of ends of reactions coincide, and this is only possible when we have only one degree of extent of reactions. What Dick Miller has shown is that there is some correlation between non-ideality for the geometry and for the composition. By this I mean that a charge of sufficiently large diameter made of a non-ideal composition may behave as an ideal one. The degree of non-ideality is accordingly a function of the kinetics and of the geometry.

Veyrié - Clavin :

Q : What is the meaning of the CJ point when the flow is neither plane nor steady.

A : In my opinion, a good criterion for generalizing a CJ detonation to unsteady and multidimensional cases, is the existence of a sonic point (in the burning gases) that protects the leading shock from the perturbations (as rarefaction waves) coming from burned gases.

Melius - Davis and Fauquignon:

Q : Dr Fauquignon presented a figure this morning indicating strong and weak detonations. I have not heard any discussion of these points neither on the extent of non-ideality. Could someone please comment ?

Davis : Strong detonations can be sustained only when the wave is followed by a piston or some other support, which cannot usually be arranged in real experiments. If a strong detonation is formed, it will decay to a CJ detonation. Weak detonations can exist only under very special circumstances.

Strong, weak and CJ detonations are idealized constructs that do not really exist ; they are one-dimensional (infinite in two directions), laminar, and have steady reaction zones. Some experiments can be designed to approximate these conditions, but most applications of explosives detonate in forms far from them.

A detailed discussion of strong, weak, CJ, and other detonations, as well as an introduction to curved three-dimensional detonations, can be found in Fickett and Davis, "Detonation", University of California Press, 1979

Volk - Miller :

Q : *Ideal non ideal explosives.* If we compare TNT with nitroguanidine (NQ) we find a similar energy output but a higher detonation velocity of NQ. But a disadvantage of NQ is that a fairly high content of HCN is found in the detonation products which decreases the energy output dramatically

because of the metastable behavior of HCN. This product results from a typical nonequilibrium reaction.

How should we call this explosive (NQ) ? Ideal or non ideal ?

A : In this case of NQ, the formation of the HCN may be a kinetic effect in a nearly "ideal" explosive. Certainly NQ is closer relative to TNT or HMX than to the AP/AL/RDX/Binder system.

Kondrikov - Mc Affee :

Q : I would like to mention at first that no real difference exists between mechanisms of detonation near the failure diameter conditions between the liquid "homogeneous" and solid heterogeneous explosives as I tried to show including into consideration the results of detonation of the porous DEGDN, and I could explain it in more details, but now I have a question : could you explain the postconvective wave on your graph occurence and origination, and do you really need the chemical mechanism of the explosive burning ? may be the u(p) dependence would be enough ?

A : 1 - I think you do need the kinetics of the burning to understand the early parts of the process before any shock wave be formed.

2 - I will assume that the "post convective wave" you ask about is the leading edge of what we call the "plug" (the ≈100% TMD region). A detailed explanation of the origin of this wave is given in the proceeding of the 10th Detonation Symposium in a paper by McAfee, Asay ; "Deflagration to Detonation in granular HMX : Kinetics and Ignition in the predetonation region", p.411. I will try to summarize the conclusions of this paper.

The 100% TMD region comes into existence as a result of a competition between two processes : (1) Increasing stress in the solid matrix, caused by the pressurization in the region below the ignition locus ; (2) gas pressure in the interstices of the matrix caused by low levels of decomposition started by the compaction wave. The mechanical stresses are trying to further compact the matrix. The gas pressure is resisting this compaction. Eventually the mechanical stress (generated by pushing from the burning region) overcomes the intersticial gas pressure. The collapse to ≈100% TMD quenches any further "burning" reaction. The 100% TMD plug acts as a piston being pushed by combustion. Eventually, the "top" of the plug forms a shock which will initiate the HMX to detonation (figure 1).

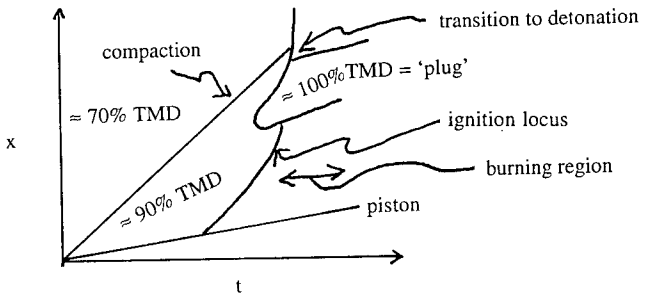

Knowledge of the explosive burning rate is important because the formation of the "post-convective wave" (plug) derives from competition of processes. The time between the compaction to the ignition locus is determined by the chemical kinetics on time scales of hundreds of μs.

Borisov - McAfee, Davis and Fauquignon

Comments : I would like to make a comment concerning the heat release kinetics during DDT. There are a few mechanisms providing progressive acceleration of the process and formation of the strong compression wave coupled with the energy release zone. These mechanisms are different in different combustion stages : a) convective burning due to hot gas penetration into the pores, b) adiabatic compression of the gas filled with the combustion products in the compression wave, c) ignition of the material due to collapse of the pores behind the compression wave. Also important in the transition is burning of the fractured material formed during all the stages (a, b and c). This burning is progressive because of two reasons : constant supply of the fragments from the reaction zone in the solid phase and further fracture of the fragments due to pressure growth inside the pores in the fragments. So heat release in these waves is governed mostly by physical phenomena.

The second comment concerns two vivid examples of good application of the ZND and hot spot models to essentially three-dimensional phenomena such as nonideal low-velocity detonation in gases and solids. The reaction is initiated there only in hot spots due to multiple reflections of the shock wave from obstacles in gases and collapse of pores in solids. That is why the heat is released in these waves due to flame propagation from the spots.

Inclusion of heat and momentum losses into the quasi-onedimensional ZND wave model enables one to nicely depict all the peculiarities of these waves.

Kondrikov - Miller :

Comment : Weak detonation is an usual thing for composite explosives. The simple example is RDX or HMX big up to 1-2 mm crystals in a matrix of paraffin. You can obtain the velocity 8.11 Km/s at ρ_0 = 1.0 g/cm^3, about 2 Km/s higher than the usual velocity at this density. It is a very interesting example of non-ideal detonation in a composite system. Besides, for such a system the dependence of detonation velocity upon diameter can be much more complicated than usual. In particular, the ideal detonation velocity may be practically out of reach.

A : The example cited by Professor Kondrikov belongs to the class of ideal explosives that is an explosive containing crystals which contain a balance of oxygen, carbon, hydrogen and nitrogen that yields upon detonation CO, H_2O, N_2 and perhaps carbon. The non-ideal explosives adressed here contain oxidizers crystals (NH_4 ClO_4) (NH_4^+ $^-N(NO_2)_2$) physically separated by binder films of a few microns from the fuel or aluminium powder.

The detonation of RDX or HMX large crystals in paraffin is fascinating indeed but I would argue nevertheless a peculiar class of ideal explosive behavior.

Borisov - Brun :

Comment : My comment concerns the question raised by Dr L.Brun about the differences in positions of the CJ plane and the plane where the reaction is over. This situation is often encountered in detonation waves both in gases and condensed media when lateral expansion of the reacting matter is allowed. Thus, we can assert that detonation waves with the reaction persisting behind the CJ plane (at least in part of the charge) are a rule rather than an exception. Here I would like to mention an example which manifests this difference most vividly. This is the two-front detonation in heterogeneous mixtures, e.g. a suspension of high explosive particles in air. If the size distribution of the particles is not single-modal, small particles are the first to ignite (because they are heated fast), and the larger particles serve as heat sinks at this stage. Thus, before the larger particles ignite, there could be a stage of energy absorption (instead of heat evolution). This latter fact gives rise to the second detonation wave which arises in the supersonic flow of the partially reacted explosive material (smaller particles) behind the first CJ (sonic) plane. This last sonic plane is positioned at the point where the rate of heat gain from burning of smaller particles equals the rate of heat absorption by larger particles. The second CJ plane is positioned at the point where the rate of external heat losses equals the rate of heat gain from burning of the larger particles.

The two-front detonations, where the two detonation waves propagated one after another at equal velocities, were observed in experiments with suspensions of RDX or HMX particles in air.

There are also some other systems that exhibit a similar peculiar behavior.

To conclude, I would like to emphasize that it is mandatory that at the sonic plane the overall heat evolution rate (which is the difference between the heat gain from the reaction and heat losses caused either by heat transfer or rarefaction waves) be equal to zero. Thus, the requirement that the reaction be finished at the CJ point applies only to ideal detonations, i.e.to the waves without losses.

Comment by David L. Kennedy
Proposed New Nomenclature for Steady Detonation

During the course of this workshop (and indeed, at previous meetings on detonics), there has been some unnecessary confusion and debate about the nature of the CJ point in a steady detonation. This comment is not new : in their discussion of eigenvalue detonations (examining the limits of the simple ZND theory), Fickett and Davis [1] bemoan : "... The results of the investigations of these steady solutions have unfortunately not received the attention they deserve. The rather formal mathematical arguments and the unfamiliar geometrical spaces in which the equations are most conveniently studied have left most experimentalists with a limited appreciation of the work and its implications..." This comment is not unique : other authors working with non-ideal explosives still see the need for lengthy introductory remarks about the difference between the CJ states of ideal and non-ideal detonations (see for example Guirguis [2]).

In my opinion, part of the reason for this is as follows. As newcomers to the field, we develop a conceptual model of detonation by reliving history — we start with the simple CJ theory, and then graduate to the ZND theory, of steady planar 1D detonation. We learn that the flow is steady between the detonation front and the CJ point, where the flow is sonic, the reaction is complete, with the resulting detonation velocity a minimum. Unfortunately, since we then use the same terminology to describe steady 2D detonations, it is too easy to transfer the 1D concepts to the 2D situation.

In particular, the expression "CJ reaction zone" is commonly misused in 2D — does it refer to the region between the shockfront and the sonic locus, or to the region in which reaction is occurring ? Brun [3] has already proposed that this region between the shockfront and the sonic surface be called instead the "detonation zone". Since this is clear, unambiguous, and has universal application, I would strongly endorse his proposal.

I would make a further proposal to fill a perceived gap in the terminology of detonation in condensed explosives. I will introduce it first, making the following justification easier to write. We should restrict the term *CJ point* (or *CJ plane*) to the sonic point, with its associated *CJ state*, of a steady 1D planar *CJ* or *ZND detonation* with a single exothermic irreversible reaction. In honour of Wood and Kirkwood [4], we should introduce the new terms *WK point* and *WK state* to their analogues on the axis of symmetry in steady 2D axisymmetric ("rate stick") detonation, which should henceforth be called *WK detonation*. For completeness, the sonic surface off axis becomes the *WK surface*. The region between the shock front and the sonic surface then becomes the *detonation zone* in each case, with the distance between the shockfront and the CJ or WK point becoming the *CJ* or *WK zone length* respectively. The subscripts *CJ* and *WK* can then be used unambiguously with associated flow variables (restricted to the axis of symmetry and for a quoted diameter in the case of a WK detonation).

There are two parts to this — why single out 2D axisymmetric geometry, and why Wood and Kirkwood ?

Firstly the geometry. Our *conceptual understanding* of detonation is based around the 1D planar CJ and ZND models. Our *numerical knowledge* of detonation (at least in condensed explosives) stems predominately from experimental measurements of WK detonations. This is due to the pivotal role that the ideal detonation velocity, D_{CJ}, plays in all our theories. Indeed, whenever a measured detonation velocity differs from D_{CJ}, we probe deeper to find out why, leading into non-steady or eigenvalue or multi-dimensional detonations..... Direct experimental measurements of detonation velocities in 1D planar geometry are limited to short run distances (say 100mm) before lateral rarefactions destroy the

planarity ; this is too short to ensure that the whole flow field has stabilised. Instead, the accepted values of ideal detonation velocities have generally come from extrapolations of rate stick experiments over different charge diameters, d. Thus we assume that $D_{CJ} = D_{WK}(\infty)$ in our compilations of explosive properties. We can of course predict D_{CJ} from chemical equilibrium codes, but their equations of state have all been either directly calibrated against, or checked for consistency with, $D_{WK}(\infty)$. Furthermore, most hydrocode simulations of shock initiation and detonation events in condensed explosives employ JWL equations of state for the detonation products, and these are calibrated against WK detonations in the copper tube expansion test.

Hence, it is the case that the limit process $D_{WK}(\infty) \equiv D_{WK}(d) \xrightarrow{d\to\infty} D_{CJ}$ is crucial in the understanding of condensed explosives. However, this limit is not always easy to achieve experimentally. As an example, the detonation velocity measurements on the TATB-based explosive PBX-9502 by Campbell and Engelke [5] indicated that it behaves like liquid explosives by having a linear diameter effect (i.e. $D_{WK}(d)$ versus d^{-1}), which is *simpler* in shape than the concave down shapes exhibited by other ideal explosives. However, subsequent detailed measurements by Campbell [6] eventually proved that it has a more *complex* shape than other ideal explosives, being concave up in large diameter, and concave down in small diameter.

As always, experiment and theory must proceed jointly. Eyring et al. [7] described a generalized Chapman-Jouguet condition for non-planar steady detonation, mentioning similar earlier work by Devonshire [8], though their quoted reference is obscure. The Eyring model of 2D axisymmetric detonation, based on approximating the curved detonation front by spherical segments, was not supported by subsequent experiments and has not been pursued. Instead, the classical paper to which most modern authors refer was by Wood and Kirkwood [4], who rigorously generalized the ZND model of 1D planar detonation to the 2D axisymmetric case, describing the necessary modifications to both the Chapman-Jouguet and the Rankine-Hugoniot conditions along the axis of symmetry, correct to first order in the radial divergence. It is of historical interest to note the unease suggested by the quotation marks used by Wood and Kirkwood in their paper, when they write '... Thus we obtain a generalized "Chapman-Jouguet condition" for detonation in a finite stick....' [4].

For some four decades, the Wood-Kirkwood approach has been treated as the yardstick against which any rigorous theory that seeks to resolve the detonation zone of a steady 2D axisymmetric detonation must be judged. A number of treatments have directly extended their approach, with a partial list of authors including Cowperthwaite [9], Bdzil [10], and Kirby and Leiper [11]. Others (including for example Thouvenin [12] and Matsui et al. [13]) have started from a different viewpoint, but then show compatibility with the Wood-Kirkwood conditions at the WK point.

Over the past decade, a number of authors have developed descriptions of generalised non-steady multi-dimensional detonation. Bdzil and Stewart [14] and Lambourn and Swift [15] cited their work as being extensions to reactive flow of Whitham's geometrical shock dynamics [16]. Brun [17] assumed the flow is sonic but the reaction incomplete on the downstream side of the shockfront. All three theories relate detonation velocity to shockfront curvature for WK detonation, and indeed when applicable, are much more efficient than Wood-Kirkwood approaches. However, their common assumption that the detonation zone can be neglected in comparison with other natural distance scales (e.g. charge diameter or shockfront radius of curvature) restricts their application to the subset of "ideal" explosives.

Within the last year, two new approaches offering complete solutions to WK detonation have been proposed by Cowperthwaite [18] and by Guirguis [19]. While showing promise for the future, to date

these approaches have been applied only to model explosives with simple equations of state and reaction rate laws.

Thus, I believe that the contributions made by Wood and Kirkwood to the detonics of condensed explosives are worth honouring.

Obviously, there are many forms of detonation not covered by this that will need additional qualifying descriptors. Thus, for example, the inclusion of multiple reactions or endothermic or dissipative processes in 1D planar geometry leads to *pathological* or *eigenvalue ZND detonation*. A strong coupling between the state variables (such as pressure or temperature) and the reaction rate leads to the *unsteady detonations* studied by Erpenbeck [20] for example. The existence of transverse waves gives rise to complex non-steady 3D detonations, ranging from the *spinning detonation* described by Voitsekhovskii et al. [21] and by Schott [22], through to Dremin's *microdetonations* [23] and to the *cellular detonations* reviewed by Strehlow [24].

In all of these cases, there will be a *sonic point* or *sonic surface* somewhere in the flow (though it may be difficult to identify), but the specific labels *CJ* or *WK* would be inappropriate. In such cases, Brun's proposed *Jouguet surface* seems fitting [25].

This change in nomenclature does not introduce any new concepts, nor does it imply that the model processes of either CJ detonation or WK detonation are physically attainable. Furthermore, it does not impose a preferred solution algorithm for the numerical description of either detonation.

New jargon should not be introduced casually. It has value only if it improves the transfer of concepts and information. The proposed nomenclature will probably prove to be of little benefit in written papers, where there is space to properly define the meaning of all symbols. However, it should improve the clarity of any information necessarily presented in concise form, such as in tables and figures (often copied out of context), in abstracts, and in short oral presentations at conferences. The paper presented at this workshop by Kennedy [26] is an example of this nomenclature in operation.

[1] Fickett W. and Davis W.C., Detonation (University of California Press), 1979, pp. 133 - 229.
[2] Guirguis R.H., "Relation between early and late energy release in non-ideal explosives', presented at the 1994 JANNAF PSHS, 1-5 August 1994, San Diego.
[3] Brun L., private communication October 1994, referencing an internal CEA-DAM report from April 1989.
[4] Wood W.W. and Kirkwood J.G., *J. Chem. Phys.*, **22** (1954) 1920 - 1924.
[5] Campbell A.W. and Engelke R., "The Diameter Effect in High-density Heterogeneous Explosives", Sixth Symposium (International) on Detonation, Coronada 24-27 August 1976 (ACR-221) pp. 642-652.
[6] Campbell A.W., *Propellants, Explosives, Pyrotechnics* **9** (1984) pp. 183-187.
[7] Eyring H., Powell R.E., Duffey G.H. and Parlin R.B., *Chem. Rev.*, **45** (1949) 69 - 181.
[8] Devonshire A.F., Theoretical Research Report No. 3/43. (As quoted by Eyring et al. [7])
[9] Cowperthwaite M., "Two-dimensional Steady-state Detonation Waves", Thirteenth Symposium (International) on Combustion, Salt Lake City 23 - 29 August, 1970, (Pittsburgh : The Combustion Institute, 1971) pp. 1111 - 1117.
[10] Bdzil J.B., *J. Fluid Mech.* **108** (1981) 195 - 226.
[11] Kirby I.J. and Leiper G.A., "A Small Divergent Detonation Theory for Intermolecular Explosives", Eighth Symposium (International) on Detonation, Albuquerque 15 - 19 July, 1985 (NSWC MP 86-194), pp. 176 - 186.

[12] Thouvenin J., "Influence of the reaction zone on the state of detonation in a steady axial wave", Seventh Symposium (International) on Detonation, Annapolis 16-19 June 1981 (NSWC MP 82-334) pp. 661-668.
[13] Matsui H., Moritani A., Yoneda K. and Asaba T., "A generalised CJ condition for simple axial flow with a spherical shock front : its application to the slurry explosives", Eighth Symposium (International) on Detonation, Albuquerque 15 - 19 July, 1985 (NSWC MP 86-194), pp. 168-175.
[14] Bdzil J.B. and Stewart D.S., *Phys. Fluids* **A1** (1989) 1261 - 1267.
[15] Lambourn B.D. and Swift D.C., "Application of Whitham's Shock Dynamics Theory to the propagation of divergent detonation waves", Ninth Symposium (International) on Detonation, Portland 28 August - 1 September, 1989 (OCNR 113291-7), pp. 784-797.
[16] Whitham G.B., *Linear and Non Linear Waves*, Wiley-Interscience (1974).
[17] Brun L., "Un nouveau modèle macroscopique de la détonation non soutenue dans les explosifs condensés", 3ème Symposium International Hautes Pressions Dynamiques, la Grande Motte, June 1989, pp. 103 - 107.
[18] Cowperthwaite M., *Phys. Fluids* **6** (1994) pp. 1357-1378.
[19] Guirguis R.H., "Streamline Dynamics Method for Highly Curved Detonation Waves", Tenth Symposium (International) on Detonation, Boston 12 - 16 July, 1993, Preprint paper No. 23, pp. 84 - 86.
[20] Erpenbeck J.J., *Phys. Fluids* **13** (1970) 2007-2026.
[21] Voitsekhovskii B.V., Mitrofanov V.V. and Topchian M.E., *Fiz. Goreniya Vzryva* **5** (1969) 385 - 395.
[22] Schott G.L., *Phys. Fluids* **8** (1965) 850 - 865.
[23] Dremin A.N., "Critical Phenomena in the Detonation of Liquid Explosives", Twelfth Symposium (International) on Combustion, (Pittsburgh : The Combustion Institute, 1968) pp. 691 - 698.
[24] Strehlow R.A., *Astronaut. Acta* **14** (1969) 539 - 548.
[25] Brun L., "Comment propager l'onde explosive ?" Chocs (revue scientifique et technique de la DAM), n° 5, 1992.
[26] Kennedy D.L., "The Challenge of Non-ideal Detonation", presented at this Workshop, 1994.

Comment — J. McAFEE

I think the idea of a nomenclature that clearly indicates the aspects of a detonation structure is a good one. Some of the concepts of a CJ wave do not translate to 2- or 3-D detonations. Therefore names that clearly remind us that we are not in 1-D may help us think and communicate more certainly.

Comment — C. FAUQUIGNON

Recalling the Monday presentation of the reactive flow of a 2D detonation, I would like to say again that the steady condition is satisfied by the radial gradient of the reaction rate and pressure.

Comment — B. N. KONDRIKOV

Dr. D. Kennedy told us about the famous Wood - Kirkwood theory and its relation to the usual theory of Chapman - Jouget. We have the results of calculations made by means of our elaboration of the Bdzil - Wood - Kirkwood theory performed mainly by my pupil Dr. V. Gamezo and by my graduate student Ya. Alymova. We obtained the rather good results concerning transformation of several $D(d)$ relations :

Eyring's linear dependence, our exponential $D(d)$ function, Campbell and Engelke function into $W(p)$ relations, where W is the relative heat evolution rate, p is the pressure behind the shock front. The main result of the calculations is the straight proportionality of the Bdzil reaction zone width Z^* to the arbitrary critical diameter d^* in our generalized $D(d)$ curve approximation, and to the tangent of the angle of inclination of the straight line to the abscissa axis in the Eyring's theory.

Comment — J. J. DICK

I agree to reserve "C-J" for 1-D steady detonation. But I see no need to add jargon such as "W-K" for 2-D steady detonation. Just use "sonic" surface.

Question — A. A. BORISOV

When defining the WK model of detonation, do you consider the wave as quasi-one-dimensional or truly two-dimensional ? If it is quasi-one-dimensional, I agree with the relations you wrote (particularly, the finite reaction rate at the sonic plane). If you consider it to be truly two-dimensional, the reaction rate is not necessarily finite at all the points, the sonic surface should be defined more precisely (whether it corresponds to the total velocity or to its component normal to the front), and sonic surfaces in this case have a meaning different from that in the CJ model. Two-dimensional detonation is not the only one in nature. There are plenty of wave shapes. In this context, do not you think that we should call them by individual names ? What you actually define as the WK detonation is simply non-ideal detonation.

Answer — D. L. KENNEDY

The 2-D detonations with which I routinely deal have the smallest shockfront radii of curvature (relative to charge diameter) of any explosives described in the literature. Hence, I attempt to approach them as truely two-dimensional. However, this is irrelevant. I am trying to label the conceptual features of steady 2-D axisymmetric detonation, rather than to prescribe how those features should be identified or treated mathematically.

While nature has indeed provided us with a multitude of detonation wave shapes to study, it has given us only a few geometries in which something approaching steady detonation is attainable experimentally. The obvious ones are planar 1-D, planar 2-D and axisymmetric 2-D geometry. In practice, the third of these predominates. For example, to the best of my knowledge, there were no cases at all in Australia throughout 1994 of explosive charges being fired to establish planar 1-D or planar 2-D detonation. Over the same period, there were at least 10 million explosive charges fired in axisymmetric 2-D geometry. A similar story would be told in any country that has a mining industry. I am simply trying to make it easier to talk about the most commonly realised form of detonation. In particular, "WK detonation" is a lot easier to say than "steady 2-D axisymmetric detonation", and it is far more specific than "non-ideal detonation".

Final Comment by Louis Brun
The Ideal Detonation

In view of the preceding presentations and discussions, everyone would probably agree calling a detonation a reactive flow that comprises a shock wave and a sonic surface.

Concerning the steady detonation, two circumstances were met according as the sonic surface is situated away from or adjoins the shock wave front. On account of the fact that the first type of detonation was systematically termed non-ideal, I plainly suggest to term ideal the second one.

The adjoining of the sonic surface to the shock-wave in the second circumstance turns out to result in a downstream sonic and reactive shock wave (namely a surface presenting a jump of chemical composition too). The suggested definition thus becomes more precisely :

An ideal detonation is a laminar flow headed by a reactive sonic shock wave.

In case of the steady regime, the concept of a detached sonic surface at stake in the first circumstance is not self-evident (see Q.-A. : Borisov-Kennedy). In case of the unsteady regime, it is even less evident and not likely to be soon unearthed, despite the comforting answer of P. Clavin to P. Veyrié. Conversely, the concept of a reactive sonic shock wave involved in the foregoing definition applies without more difficulty in the non-steady context.

The present suggestion is one possible answer to the question I asked in the introduction to this final discussion whether Davis and Fauquignon's definition of the ideal detonation could be extended to include diverging fronts. It provides a meaningful way of sizing up more or less classical models, theories and solutions related to detonation, as shown next.

- The *simplest theory* [1] (1D flow, Jouguet's assumptions [2] of total decomposition through the sonic shock wave), to which Davis and Fauquignon's 'ideal' detonation identifies, supplies an example of ideal detonation model.

- The *Zel'dovitch-Taylor* self-similar solution [4], [5] to the problem of the spherical detonation initiated at a point, still along Jouguet's assumptions [2], depicts an ideal detonation. Some noteworthy features attributable to these assumptions : Front uniformly propagates at $D = D_{CJ}$, pressure and material velocity downstream gradients are infinite (this holds for any curved wave front [6]). Besides, [6], the motion is necessarily non-converging, the self-similar solution to the piston problem for spherical detonation comprises an ordinary shock wave ...

- The *JR model* [7], which removes or "relaxes" (hence the R of JR) Jouguet's assumption of total decomposition, provides an example of an ideal detonation model allowing detonation velocities $D < D_{CJ}$. This same model would have been labelled 'non-ideal' by Cook [9]. Some noteworthy features : Gradients are here finite. Front motion locally obeys an acceleration-celerity-curvature relationship in the form $dD/dt = f(D,\kappa)$, with κ the mean curvature of the front surface (explicit form available in Chevalier's statement [9]). Model predicts a celerity-curvature relationship $f(D,\kappa)=0$ at the leading edge of an axisymmetric steady detonation. It introduces a transverse (or front wave) speed depending on the local D,

which governs the transient front shape evolution. It explains the observed trend in wave front motion of spherically diverging high explosive detonations [10]. Solution of the piston problem in a simple physical and geometrical setting is under way.

- The *Wood and Kirkwood theory* [11] affords the first example, as far as I know, of a theory intended to deal with non-ideal detonation in the axisymmetric steady context. Main outcome : a well-known celerity-curvature relationship on the axis. This relationship established following a procedure which, as discussed in [1], is not a rigorous one, necessarily differs from its counterpart associated to the JR model starting from the same constitutive assumptions (The definitions of sonicity actually cannot be matched outside the axis in the two theories : one is local and even applies to non-steady motions as aforesaid, the other involves the galilean frame with respect to which the motion is steady).

- The *celerity-curvature models* of Damamme [12], Stewart and Bdzil [13], Lambourn and Swift [14] result from more or less general analyses which amount to extending to the whole front the above WK celerity-curvature relationship. They accordingly relate to non-ideal detonation, contrary to Kennedy's assertion [15].

What of the ZND theory ? Why isn't it included in the above catalogue, next to the simplest theory for instance ? The reason is that, the ultimate goal of Detonics, an engineer's one, being to predict the motion imparted by detonation to adjacent media, one must compute the motion of detonation products at the same time. ZND theory is not useful for that, since it is meant to provide a detailed picture of the detonation wave front structure, much in the same way as an ordinary shock front is "resolved" *via* transport phenomena (A parallel reservation applies to some extent, for other reasons, to the celerity-curvature relationships above : up to now there is lacking a proper coupling of the downstream flow to the front motion).

Ideality pertains to continuum mechanics. ZND theory refers to what happens inside the detonation wave front and is instead closely tied up with micro physics issues. This somewhat controversial theory will best be discussed in the following chapter.

[1] Fickett W. and Davis W.C., *Detonation*, University of California Press, 1979.
[2] Jouguet E., *Mécanique des Explosifs*, Doin et Fils Eds, 1917.
[3] Davis W.C. and Fauquignon C., "Classical Theory of Detonation", this Workshop.
[4] Zel'dovitch Ya.B., "On the Distribution of Pressure and Material Velocity in Detonation Products. The Spherical Wave in Particular" *Zh. Eksp. Teor. Fiz*, 12 (1942) 389 -.
[5] Taylor G.I., "The Dynamics of the Combustion Products Behind Plane and Spherical Detonation Fronts in Explosives". *Proc. Roy. Soc.* London, Series A, 200 (1950) 235 - (declassified from "Detonation Waves", 1941).
[6] Brun L., "Sur l'Autonomie des Ondes de Choc à Etat Aval Sonique". Cas de la Détonation", *J. de Méc. Th. et App.* (1982) 623 -.
[7] Brun L., "Une Théorie de la Détonation dans les Explosifs Condensés Fondée sur l'Hypothèse de Jouguet", internal CEA-DAM report, April 1989 ;"Un Nouveau Modèle Macroscopique de la Détonation Non Soutenue dans les Explosifs Condensés", *Third International Symposium on High Dynamic Pressures*, La Grande Motte (1989) 103 - ; "Comment Propager l'Onde Explosive ?", *Chocs*, 5 (1992) 53 - (Translated in LACP-93-201, september 1993).
[8] Cook M.A., "Detonation Wave Fronts in Ideal and Non-Ideal Detonation", *Second Symposium (International) on Detonation*, Washington D.C., 1955.

[9] Chevalier J.-M., "On the Detonation Wave Propagation", this Workshop.

[10] Aveillé J., Baconin J. et al., "Experimental Study of Spherically Diverging Detonation Waves", *Eighth Symposium (International) on Detonation,* Albuquerque, N.M., 1985.

[11] Wood W.W. and Kirkwood J.-G., "Diameter Effect in Condensed Explosives. The Relation Between Velocity and the Radius of Curvature of the Detonation Wave", *J. Chem. Phys.*, 22, (1954) 1920 -.

[12] Damamme G., "Généralisation de la Notion d'Onde de Détonation Chapman et Jouguet" *Sc. et Tech. de l'Armement*, 61 (1987) 65 -.

[13] Stewart D.S. and Bdzil J.B., "The Shock Dynamics of Stable Multi-Dimensional Detonation", *Combustion and Flame*, 72 (1988) 311 -.

[14] Lambourn B. D. and Swift D.C., "Application of Whitham's Shock Dynamics Theory to the Propagation of Divergent Detonation Waves", *Ninth Symposium (International) on Detonation,* Portland (1989) 784 -.

[15] Kennedy D.L., "Proposed New Nomenclature for Steady Detonation", this Workshop.

II ALTERNATIVE VIEWS ON DETONATION

A Comparaison of the Classical and a Modern Theory of Detonation ; F.E.Walker

Towards Detonation Theory ; A.N. Dremin

JOURNAL DE PHYSIQUE IV
Colloque C4, supplément au Journal de Physique III, Volume 5, mai 1995

A Comparison of the Classical and a Modern Theory of Detonation

F.E. Walker

Interplay, Danville, California 94526, U.S.A.

ABSTRACT

A quite complete exposition of what has been called the classical theory of detonation is given in the Scientific American of May 1987 by W.C. Davis. However, Davis states in his report that, "In spite of the variety of modern applications of explosives, detonation science has not yet reached maturity . . .," and, "Scientists who study explosions are spurred on by being constantly reminded that the current detonation theory is incomplete." In this paper a comparison is made between the classical theory as expounded by Davis and a more modern theory based on the concepts that: (1) The energy in the very narrow shock or detonation front is highly nonergodic, and thermal equilibrium, particularly between the translational and vibrational energy modes, does not exist in the front; (2) No realistic temperature can be ascribed to this very narrow zone; and (3) A physical regulator which constrains shock and detonation velocities is directly related to the vibratory velocities of the atoms of the shocked materials.

The paper includes a short historical summary, a statement of some crucial deficiencies in the classical theory, and it contains the presentation and discussion of a number of experiments and mathematical arguments favoring the alternative theory. Among these are experimental observations made in the 1960s and 1970s and continuing to the present. Proposals of tribochemical or mechanical bond fracture in shock fronts in explosives were made as early as 1938, and they appeared occasionally in later years, but they were often ignored. Finally, results from more recent experiments and calculations are summarized, which appear to support forcefully the alternative theory.

INTRODUCTION

The early history of the study of the detonation of explosives was reviewed by W.C. Davis in the May 1987 issue of the Scientific American--from the synthesis and detonation of nitroglycerin by Ascanio Sobrero in 1846 through the development of the ZND theory by Yakov Zel'dovich, John von Neumann, and Werner Doering. He discussed the pioneering analysis done by David Chapman and Emile Jouguet that led to the C-J theory, from which most modern theoretical studies have been derived.

The concepts included in the ZND model provided useful hypotheses as to how detonation is structured and maintained. According to the model, a shock wave propagates into the unreacted explosive and compresses it instantly. This compression, modeled as a piston moving against the explosive, provides enough heat to initiate chemical reactions (in thermal equilibrium) behind the shock front which release the explosive energy. This chemical energy produces the high temperature and pressure which maintain the detonation. The expansion of the reactions' gases provides the forces that are observed as the useful work, or the destructive power, of the high explosive.

From this theory, a rather complex formalism with the associated mathematics was developed. Davis described this formalism, as shown graphically in Fig. 1. Briefly, a plot of all possible pressure values in a shocked material (the material behind a shock wave) for all possible values of the shock velocity in the material is called a Hugoniot curve (a). All the possible states (pressure and material velocity) of a shocked material for a given shock-wave velocity can be depicted in the Hugoniot-curve coordinate system as a straight line, a Rayleigh line, whose slope is proportional to the shock-wave velocity. The final state of a material under the influence of a shock wave with a given velocity is shown graphically as the point at which its Hugoniot curve intersects the specific Rayleigh line, as seen in Fig. 1(a).

The C-J theory maintains that the point at which the Rayleigh line is tangent to the Hugoniot for the completely reacted explosive (the C-J point) specifies the state from which the reaction products expand to do work. This point also determines the detonation velocity (D) from the slope of the Rayleigh line, as seen in Fig. 1(b). The ZND theory requires Hugoniot curves for the partially reacted explosive, as well

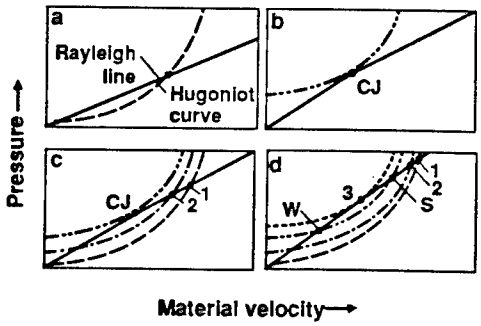

Figure 1. The Hugoniot and Rayleigh curves which represent the C-J and ZND models.

as for the unreacted and completely reacted material. The explosive will be at a higher pressure in its unreacted (1) and partially reacted (2) states, as seen in Fig. 1(c). A higher detonation velocity (a steeper Rayleigh line) denotes a "strong" detonation, as seen in Fig. 1(d). In some cases, a temporary state (3) is possible in which the Hugoniot curve lies above the curve for the completely reacted explosive. This state describes a "weak" detonation, which can reach a final state (W) that has a lower material velocity and pressure than in the C-J state.

This is a macroscopic theory that can be modeled with hydrodynamic and thermodynamic algorithms, but it denies the importance or even the necessity for kinetic inputs, and it provides no helpful microscopic insights. As Davis states (Ref. 1), "In spite of the variety of modern applications of explosives, detonation science has not reached maturity . . .", and, "Scientists who study explosions are spurred on by being constantly reminded that the current detonation theory is incomplete."

The C-J and ZND theories lead to the conclusion that the "constant" detonation shock waves observed for particular materials cause the explosive material to turn into gaseous products at a temperature sufficient to just exactly provide the correct pressure to maintain the correct detonation velocity. Therefore, the proponents of these theories have developed a number of equations of state (EOS) with some rather arbitrary coefficients and parameters to calculate the "correct" temperatures and pressures in the reaction products. Two quite recent statements on the failure or inaccuracy of EOSs are given and discussed in a later section.

The principal purpose of this report is to present for comparison a quite different theory, or hypothesis, which describes both initiation and detonation in a microscopic or molecular regime, includes new kinetic principles, and gives a physical explanation for the constancy of detonation velocities.

To direct attention to the significant aspects of the experiments and calculations to be reviewed in the following sections, here are the basic concepts of this modern theory:

1. The initiation of explosive reaction by shock waves in chemical explosives is determined by (a) the production by the the momentum transfer, shear, or energy gradient forces across the shock front of ions, free atoms and radicals, in addition to thermally-activated molecules, randomly distributed within the bulk of the shocked explosive; (b) the growth of reaction sites at the points where sufficient numbers of the free atoms, radicals, ions, and molecular fragments are formed to sustain the appropriate initiation reactions; and (c) the input of a critical quantity of energy fluence from the shock forces to the shock-compressed explosive to enable a minimum number of reaction sites to reach a self-sustaining exothermic reaction. (Ref. 2).

2. The exceedingly high kinetic energy of momentum transfer in the detonation front is sufficient to cause massive fracture of the covalent bonds of the explosives molecules at and near the front so that the large majority of the molecules are broken, as in the initiating shock, to individual atoms, radicals, molecular fragments, ions, and they are rearranged extensively. These particles can then react in about 10^{-14} to 10^{-12} s to provide the chemical energy which drives the detonation.(Ref. 3).

3. The energy in the very narrow shock or detonation front is nonergodic, and thermal equilibrium, particularly between the translational and vibrational energy modes, does not exist in the front. No realistic temperature can be ascribed to this zone (Ref 4).

4. A physical regulator constrains the shock and detonation velocities, and this regulator is directly related to the vibratory velocities of the atoms of the shocked material (Ref. 5). This concept of determining energy release rates or reaction rates through a nonequilibrium process based on the relative vibration velocities of the atom pairs and groups involved, is designated as physical kinetics.

A summary of comparisons of the classical and the modern theory is given in Table 1 to assist in the elucidation of the differences as they are presented in the following discussion.

EARLY SIGNIFICANT CLASSICAL STUDIES

Discussion of several early experiments and theoretical analyses may aid in understanding the departures of the new theory from what have been called the classical studies in shock initiation and detonation. Campbell et al.(Ref. 6) conducted some elaborate experiments in the early 1960s on the initiation to detonation of homogeneous (nitromethane) and heterogeneous (Ref. 7) (PBX-9404, a plastic-bonded HMX) explosives. Analysis of the experiments in which nitromethane (NM) was initiated with shocks of about 8 GPa and durations of about 1 μs led the experimenters to the conclusion that the shock wave compressed the NM; the compression heated the NM to some value at which significant thermal reaction began; and, after an induction period, the detonation wave originated at the NM face first impacted, traveled through the compressed liquid overtaking the shock front, and continued into the unshocked material. The entire process was considered to be a thermal equilibrium process. The activation energy presumed was about 59 kcal/mole, as in low temperature thermal decomposition.

The analysis of heterogeneous initiation was not so easily reached, because the bulk temperature in an explosive shocked strongly enough to cause initiation to detonation was believed not to be nearly high enough to produce sufficient

Table 1. Comparisons of the Classical and the Modern Theories

Classical Theory	Concepts, Principles and Observations	Modern Theory
The shock acts as a piston, compression heating, equilibrium thermal decomposition, Arrhenius kinetics, thermodynamic determination and control of detonation velocity, many different equations-of-state required.	Theory Concept	Shock energy carried in very narrow zone by momentum transfer, very high energy gradient forces cause mechanical fracture of covalent bonds, physical kinetics, detonation velocity determined and controlled by average relative vibrational velocities of atom pairs or in molecular fragments, equations-of-state not valid.
No good explanation.	Eyring's Starvation Kinetics	Corresponds well with mechanical fracture concept and reaction rates observed. Very different from Arrhenius kinetics.
Shock acts as piston for compression heating, requires various concepts of thermal heating to form hot spots.	Shock Initiation of Heterogeneous Explosives	Mechanical fracture of covalent bonds in shock front leads to hot spots, critical energy fluence required for initiation.
No good explanation.	Differences in Sensitivity in Various Sensitivity Tests	Explained by different fractions of thermal and shock input.
No good explanation, Violation of theory.	Time to Initiation of NM at Low Shock Pressures	Explained by physical kinetics.
No good explanation.	Acceleration of Shock Front with Non-Initiating Shocks	Mechanical fracture of bonds in and near the shock front.
No good explanation.	Initiation to Detonation by Free-Radical Gradient	The high energy gradient forms shock wave which initiates detonation.
No good explanation.	BTNEA Experiment	Explained by massive mechanical bond scission.
No explanation; violation of theory.	Increased Detonation Velocity of NM + DETA	Easily explained by physical kinetics, and it is calculated accurately from Hugoniot data and empirical formulae.
No good explanation.	Mechanical scission of Bonds in Plastics R.Graham, et al.	Corroboration of massive bond scission.
No good explanation.	Shock-Induced Chemistry, R. Graham et al.	Corroboration of massive bond scission.
Very little help.	Understanding of Microscopic Processes	Provides rational explanations.
No good explanation.	Isomer Pairs Differ in Thermal or Shock Sensitivity	It is probable that they would differ, since one decomposition is thermal, and the other is by mechanical bond fracture.
Difficult explanation.	Detonation at Low Velocity	Different kinetic rate due to lower level of bond fracture at lower initiation pressure.
With best equation-of-state, calculation in error by 14.5%	Calculated Detonation Velocity of E25 (PETN/Paraffin:75/25)	Calculated by Hugoniot values and empirical formula within 0.5%.

Note: There are still questions about how to explain deflagration-to-detonation transfer (DDT) and how to determine the temperature in a shock front. The modern theory proposes temperatures of about 10,000 to 30,000 K versus 3,000 to 5,000 K by the thermodynamic theory in the detonation front.

reaction to lead to a detonation in the time observed. Previously, Bowden, Gurton and Joffe (Refs. 8,9) proposed and observed that small centers of concentrated reaction did occur, and they then assumed that an energy-concentrating mechanism produced "hot spots" in the bulk explosive. Many explanations and processes have been proposed for this phenomenon:

(a) Gases in voids in the explosive were compressed and heated; this heat was transferred to the molecules around the voids; and the reaction started on the void surface.

(b) The shock waves collided or reinforced other waves when they moved through and around the explosives crystals, thus causing spots of higher pressure.

(c) The shock caused friction between the explosive grains, and this friction produced small areas of high temperature.

Other explanations were suggested, but none have been well quantified.

To check the concept of the gases in the voids being compressed and heated, experimenters compacted explosives in atmospheres of gases with different heat capacities. The idea was that the gases that were heated to higher temperatures by the shock compression would cause initiation in shorter times. This proposed correlation was not observed.

It has been assumed that there is compression of gases in voids, some friction between grains, and some shock interactions and reflections, but no very convincing arguments have been made that "proved" any of these concepts as the sources of effective hot spots. However, the hypothesis has persisted that some macroscopic process within the shock wave produces hot spots from which the initiating reaction develops.

A number of tests were developed in this earlier period to measure and compare the shock sensitivity of explosives then in use and under study. There were wedge tests, card-gap tests, drop-hammer tests, and gun tests. Analyses of these tests were generally based on a value of shock pressure at which the explosive would detonate, usually some 50% of the trials. Experimenters observed, but did not explain why, some explosives were more sensitive than others in one test and less sensitive in another. Several tests, such as the drop-hammer and skid tests, had components of heating that resulted from friction or material flow that also led to some confusion in the interpretation of the results, but they did provide useful information for rather specific situations.

A great strength of opinion had developed in the explosives literature and in the community studying initiation and detonation that shock pressure (compression) alone (or predominantly) was the determinant in shock initiation (very likely because of the piston model). As a result of this,

when a very precise set of some 60 experiments was later performed on the initiation of PBX-9404 (Ref. 10) by the impact of aluminum plates, the experimenter failed to analyze the data properly.

Henry Eyring and colleagues (Ref. 11) at the University of Utah in the 1940s, studied reaction rates in detonating explosives. One striking result from their observations and analyses in this early period is that the reaction rates, as calculated from the detonation velocities, are quite similar for all of the explosives they studied, even though the low-temperature decomposition rates and the thermodynamic energy content are quite different. Later, Eyring and other associates analyzed this disturbing observation again (Ref. 12). They studied materials as different as cyclopropane, tetryl, and mixed explosive compositions. In all cases, they found that the logarithms of the reaction rates for assumed first-order decompositions were about 6.0 ± 0.5 (Ref. 13). Eyring's analysis from reation-rate theory led to his concept of "starvation kinetics," in which he calculated that only 20 degrees of freedom in any of the explosives molecules he studied were contributing energy to the bond that was first to break, no matter how large the molecule might be. This was markedly different from Arrhenius kinetics or a thermal equilibrium process.

SIGNIFICANT EXPERIMENTS AND CALCULATIONS IN SUPPORT OF THE NEW THEORY

Some 25 years ago, Richard Wasley and I began a series of experiments on the initiation and detonation of explosives with the object of extending the data into some unexplored areas. In preparation for the early experiments, we reviewed some data (Ref. 10) obtained on the shock initiation of PBX-9404 with impacting aluminum plates. Our interpretation of the data was very different from that published, and it led to the derivation and publication of the critical energy fluence concept (Ref. 14) of shock initiation for heterogeneous explosives. The equation which describes the concept,

$$E_c = \frac{tP^2}{\rho U_s}, \qquad (1)$$

is easily derived from the kinetic energy and Hugoniot equations. It serves well to describe shock initiation in most of the generally-used explosives in the range of shock and detonation pressures from about 0.3 to 40 GPa.

In the equation, t is the time width of the initiating shock pulse, P is its pressure, ρ is the initial density of the explosive, and U_s is the shock velocity at the pressure P.

This concept and the equation provide the explanation for the previously observed sensitivity anomalies in the initiation of a specific explosive in various sensitivity tests.

Additionally, it was shown (Ref. 15) to provide a rational correlation for data from ten different sources and test methods, over nearly seven orders of magnitude in time and three in pressure, for PBX-9404 and other HMX-based explosives.

The reason this quite simple relationship was not discovered for so many years appears to be a result of the historical development of explosives theories based on the piston concept. Thus pressure, not energy fluence, was considered to be the determinant of initiation. The piston concept was both the genius and the demon of the C-J and ZND theories.

Low-Pressure Initiation of Nitromethane

The initiation data on nitromethane were meager in 1968. It had been observed that about 8 GPa of shock pressure was required to initiate NM to detonation. Here again, the old concept was held of pressure being the determinant of initiation, but it was found that the detonation was observable in about one microsecond.

In an effort (Ref. 16) to determine if the critical energy hypothesis might also apply in some degree to initiation in homogeneous systems, we used an experimental design (shown in Fig. 2) to provide nearly rectangular shock waves of about 5.0 to 6.5 GPa that persisted for more than 20 microseconds. According to the thermal-equilibrium concept, the time to initiation of NM at a pressure of 6.0 GPa should be near 0.1 s (Ref. 6), as seen in Fig. 3. What we observed most clearly in both framing-camera and streak-camera records (see for example Fig. 3) was that initiation at 6.0, 6.2 and 6.5 GPa occurred in approximately 20, 16 and 10 microseconds, respectively. This is some 4 orders of magnitude shorter in time (Fig. 3) than predicted by the thermal equilibrium theory.

This very short time to detonation was not the only curious result. It was also evident that the detonation had not started at the nitromethane face first put under pressure and heated, as the old theory required, but it appeared at some position very near the shock front. The film records show clearly that a retonation also proceeds from the initial detonation site back toward the face first impacted. In fact, if the detonation had started at this face first put under compression, the streak-camera film shows that initiation at 6.0 GPa would have occurred in an even shorter time--about 8 microseconds.

The criticism from the explosives community was that there must have been some defect in the five very consistent experiments. However, after more than 20 years, no defect has been found or reported.

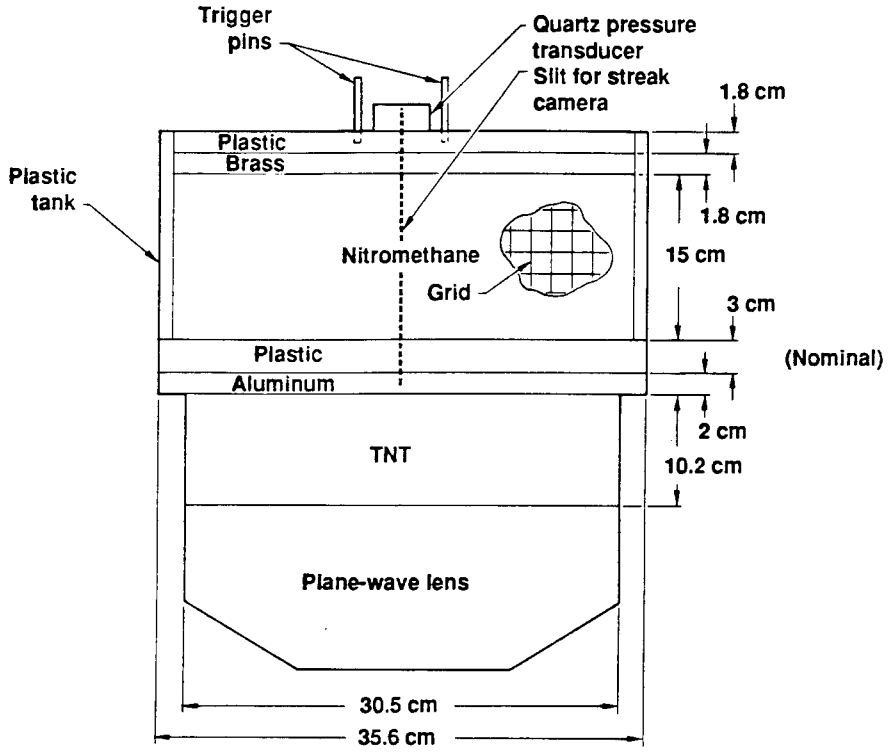

Figure 2. Design of the experiments used to study the lower pressure shock initiation of nitromethane.

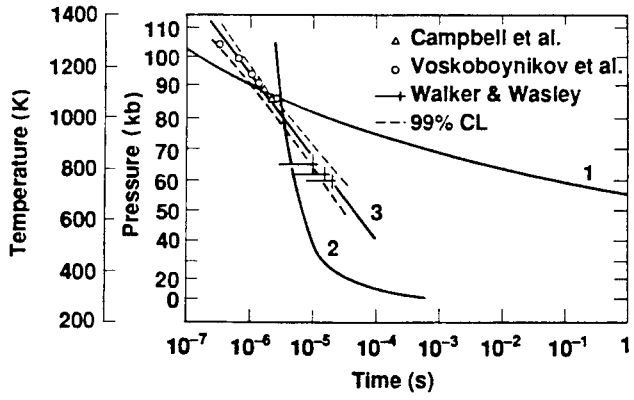

Figure 3. The calculated time to initiation as a function of shock pressure or shock temperature for a thermal equilibrium process (curve 1) compared with the initiation data for nitromethane.[38]

Acceleration of the Shock Front in Nitromethane with Non-Initiating Shocks

The results from the NM experiments just described brought into doubt the classical model of the initiation of homogeneous explosives. Strong evidence existed that some chemical reaction was started at or very near the shock front that grew rapidly close behind the front into a detonation. Also, streak-camera records provided evidence that before the detonation appeared, the shock front was being accelerated some small amount.

To explore this possibility further, we designed a series of experiments (Ref. 16) in which the velocity of non-initiating shock waves developed in ethylene glycol could be measured as the shocks passed through tanks of NM. Framing cameras showed that the shocks were accelerated above the expected hydrodynamic values as they passed through the NM and that the increased rate of acceleration was a direct function of the shock pressure profile. Additionally, a computer-calculated model of the experiment (Fig. 4) showed that the amount of nitromethane decomposition energy (about 1 to 4%) required to explain the experimental data, when included in the calculations, gave an excellent reproduction of the experimental results.

This is a key observation, because it indicates a level of reaction in or very near the shock front that is greater than a thermal-equilibrium process would produce. Furthermore, it shows that the shock-front acceleration occurs with no subsequent explosion or detonation in the NM to provide energy to the shock from behind it. More explicitly, it says the shock front is a very narrow, non-equilibrium zone.

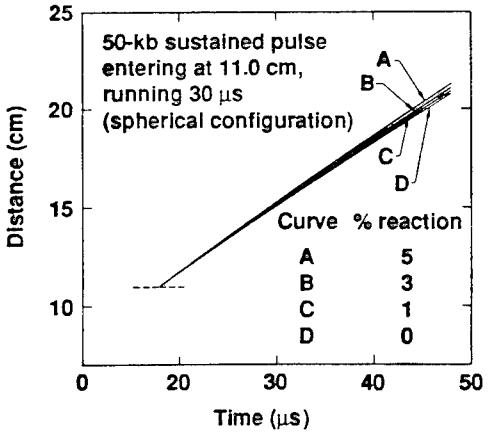

Figure 4. A computer calculation of experiments used to study acceleration of a shock front in shocked nitromethane.

Initiation Patterns Produced in Explosives by Low-Pressure Long-Duration Shock Waves

Following the previous experiment, it seemed important to investigate the shock front and the area near it more closely to study any observable processes there. In three new experiments with low-pressure shocks (4.0 to 6.0 GPa), we designed and fired long-duration (20 to 40 microseconds) shocks. The reason for working in the lower shock-pressure regime is that the initiation zone and time are lengthened. This allows more detailed and explicit framing-camera records to be obtained.

In the first experiment of this set (see Fig. 5), a spherical shock wave produced in a large tank of water passes over two disks of LX-10 (a plastic-bonded HMX explosive). The photo record obtained by the framing camera shows that the number of initiation sites is a direct function of the shock pressure and that the sites appear quite randomly in time and space. This work was corroborated in a similar experiment by L.G. Green at the Lawrence Livermore Laboratory.

In a following experiment, in which NM was shocked just below an initiation level (Ref. 17), random centers of reaction again appeared and coalesced behind the shock front, but ahead of the face first put in compression. In all of these experiments, absolutely no evidence existed for a detonation developing at the surface first impacted.

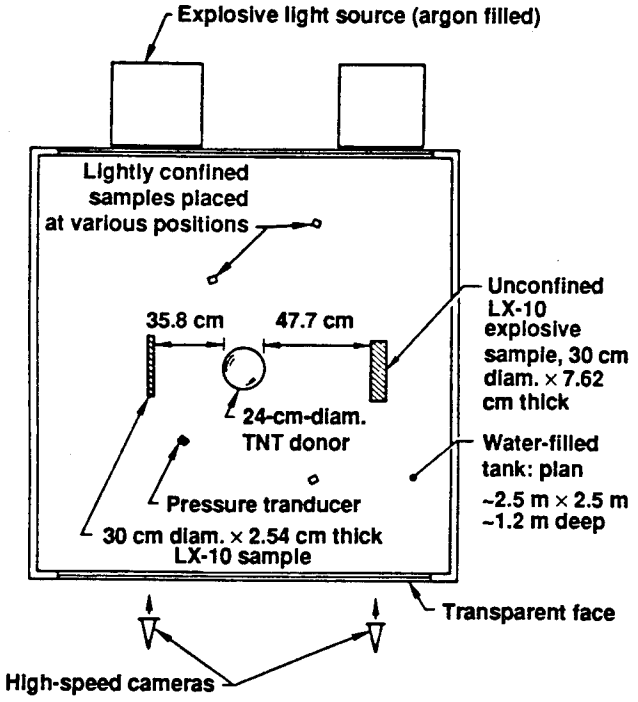

Figure 5. Design of experiment to observe effects of low-pressure shocks on LX-10.

Although the photos were so plain that no alternate explanations were seriously proposed, and although an experiment

conducted independently corroborated the results in the solid explosives, the data were generally simply ignored because they did not fit the historic model.

Forces and Temperature in the Shock Front

Analysis of our previously described experiments and other available data led to the consideration of the possibility that mechanical fracture of some of the covalent bonds did indeed occur in and near the shock front. Experiments had been (Ref. 18) and continued to be (Ref. 19) performed in which mechanical bond scission was proposed and supported by analysis. Calculation (Ref. 2) of the probable acceleration and shear forces in and near a shock front showed that mechanical forces on atomic dimensions were likely to be stronger than the covalent bonds (i.e., C-N, N-O, C-C) in organic explosives. It seemed probable that at free surfaces of the explosive crystals, or in voids or at crystal and lattice defects, mechanical bond fracture could occur that would produce free radicals and atoms, very energetic ions, and excited molecules and molecular fragments that could react very quickly (in ps to tens of fs), and essentially in place, to produce the chemical energy that would accelerate the shock front or detonation front and maintain it.

Another facet of this study of the shock forces in and near the front is that the microscopic lattice can be distorted, and the atoms right in the front must be accelerated for at least some small distance (about 1 to 4 angstroms) up to the velocity of the shock or detonation wave by the momentum from the atoms immediately behind them. As the shock front is, in reality, the motion of these atoms in the front, they are accelerated from some random thermal motion to the velocity and with the more nearly uniaxial motion of the shock. The magnitude of the average acceleration can be calculated easily from

$$a = \frac{v}{t} \quad . \qquad (2)$$

The force, $f = ma$, providing this acceleration can exceed the covalent bond strength (Ref. 2), so that the explosive material (or other organics) would be fragmented at open faces, voids, and some defects. This has been corroborated in many molecular dynamics (MD) calculations, with indications that at very high shock pressures, scission can occur within the lattice and within enclosed molecules.

One other significant fact that must be considered in this context is that at the front, the major motion of the atoms is directed in one dimension, along the axis of the shock, so that temperature, normally considered as random gaussian motion of the atoms, is not a viable concept within the shock front (Ref. 20). At some distance behind the front where thermal equilibrium is again approached (tens of ps to ns) a temperature may be measured. Great efforts to measure temperature in the front have been disappointing. Estimates

of the "one-dimensional" temperatures in various detonating explosives, based on the one-dimensional velocities along the shock axis, have ranged from 10,000 to 30,000 K (Ref. 20).

Free Radical Initiation of Gases

P. Urtiew, E. Lee and I conducted some experiments to study the hypothesis that concentrations of free radicals could lead to detonation. In a system of silane and tetrafluorohydrazine, in which radicals formed rapidly upon mixing of the two gases, we mixed a scavenger, cis-2-butene, in the silane in sufficient concentration to keep the reaction under control until the two gases were well mixed. Otherwise, reaction would have occurred immediately on contact at the gas-gas interface. We thus demonstrated (Ref. 21) that the well-mixed gases would detonate once the free-radical scavenger had been consumed.

This demonstration of the production of a detonation from a high concentration of free radicals without an impacting shock was supported in experiments by J. Lee et al. (Ref. 22) on xenon-irradiated mixtures of hydrogen and chlorine, hydrogen and oxygen, and acetylene and oxygen. The classical theory provides no explanation for these phenomena.

In another series of experiments (Ref. 4), several chemicals known to be able to supply or capture free radicals were added to TNT at the 5 weight percent level. The impact sensitivity of the TNT in a drop hammer study was changed dramatically by these additives. This work was continued by impacting samples of TNT and the additives with flying plates in an air gun. The results were consistent with the drop-hammer results.

Inert solids and liquids, very hard and grainy materials, and some very sensitive explosives were added to the TNT in separate control studies. However, the changes in sensitivity made by the free-radical donors and getters were much greater than with any of the control additives.

Initiation and Detonation of Nitromethane with Diethylene Triamine (DETA) Added

Although amines were known to sensitize NM to shock initiation, not much quantitative data relating to this observation existed. Therefore, Wasley and I conducted a series of experiments (Ref. 23) using the same geometry shown in Fig.2, but now small amounts (0.01 to 5.0 wt%) of DETA were added to the nitromethane just before the experiments were fired. The decrease in time to initiation as a function of DETA concentration is shown in Table 2. and Fig. 6a.

Table 2 and Fig. 6b also show that the detonation velocity of the nitromethane changed as a function of DETA concen-

Table 2. Results of initiation experiments in which DETA is added to nitromethane.

DETA Conc. (%)	Time to det. (μs)	Detonation velocity (mm/μs)
0.0 (control)	18 ± 2	6.40[a]
0.0 (control)	9[b]	6.34[a]
0.01	8.4[b]	6.45[a]
0.02	7.8[b]	6.47[a]
0.05	7.3[b]	6.76[a]
0.05	6.8[b]	6.70[a]
0.05	6.7[b]	6.45[a]
0.10	5.4[b]	6.52[a]
1.0	2.0 ± 0.5	6.41[a]
5.0	0.5 ± 0.3	6.22[a]

[a] ±0.07.
[b] ±1.

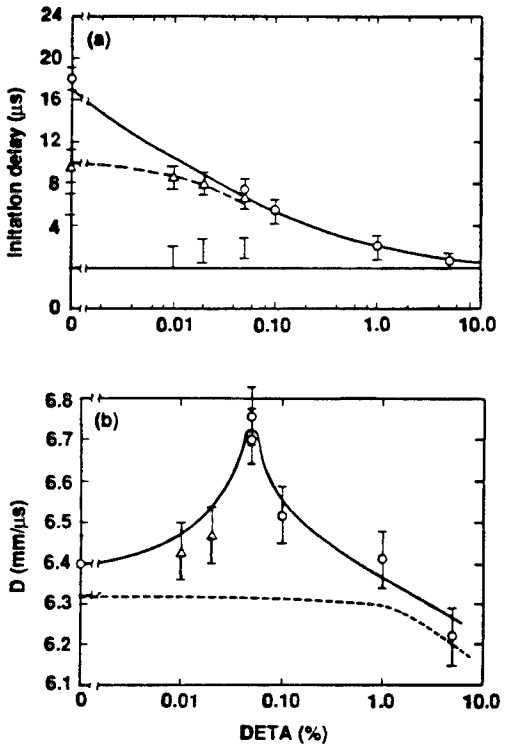

Figure 6. (a) Time to initiation of nitromethane at 6.0 GPa as a function of DETA concentration; (b) Detonation velocity of nitromethane as a function of DETA concentration.

tration. This was another specific violation of the C-J, ZND, and other classical concepts. Changes in reaction kinetics were not supposed to affect detonation velocities. Further, with the use of an equation derived by Skidmore and Hart (Ref. 24) that relates changes in detonation velocities to overdriving detonation pressures, the "C-J pressure" of the new nitromethane reaction with 0.05% of DETA added would appear to be near 19 GPa. This would require a dramatic change in reaction rate. At a level of 0.05% DETA, the measured detonation velocity in three separate experiments was about 6.72 km/s, compared to the normal value of 6.32. This would seem to require that free-radical mechanisms enhanced by the DETA be involved to give the results shown in Table 2 and Fig. 6b. The dashed line in Fig. 6b shows the detonation velocity that was calculated with the TIGER code (Ref. 25), using a selected EOS and the thermodynamic principles from the old model.

Several other interesting results were observed in this series of ten highly technical and costly experiments. As in the earlier work with neat NM, the origin of the detonation is at or very near the shock front in the experiments with 0.1% or less of added DETA. The retonation from the zone where the detonation originated is clearly evident. The red-brown color (probably from nitrogen dioxide), also seen by Cook (Ref. 25) in his NM initiation studies, is shown in the

framing-camera records to sweep backwards toward the face first impacted, in consanance with the retonation. In these experiments with the lower concentrations of DETA, some initiation sites appeared at separated points at the shock front and coalesced into the detonation front, as seen in our earlier experiments with low pressure shocks.

When the DETA concentrations were 1% and 5%, the detonation developed in about 2 and 0.5 microseconds, respectively. This is similar to the time to detonation in NM with no additives with shock pressures of about 7.5 to 9.0 GPa, compared to the 6.0 GPa in these experiments. An interesting phenomenon seen in the framing-camera photos of these two firings was that the initiation occurred in hundreds of small centers of reaction, which quickly coalesced into the detonation front. The small centers appeared first to be distributed quite randomly in time and space. The pattern was finer at the higher concentration. This is remiscent of the results seen previously in the initiation studies of heterogeneous explosives (Ref. 17), except that here the number of reaction sites is a function of increased DETA concentration rather than increased pressure. However, both increased DETA concentration and increased pressure lower the time to detonation.

Here is another observation of considerable interest. Now that the detonation occurs in about 1 microsecond, as in the earlier work (Ref. 6) at 8.0 GPa, the detonation appears in the streak-camera photos to originate at the nitromethane face first impacted. However, it can be seen easily in the framing-camera photos that the detonation is actually forming in the narrow band where the reaction sites are coalescing. Thus, in the old streak records (Ref. 6), the detonation would have appeared to come from the container-NM interface. In fact, in some of those early records, the reaction light seems to reach rather tenuously toward the interface. This same phenomenon would have made it difficult for Hardesty (Ref. 26) to observe the exact position of the detonation front in his initiation study. Recent experiments (Ref. 25) on the initiation of liquid nitric oxide support the contention that the detonation is formed in a narrow zone where the reaction sites are coalescing and not at the container-explosive interface.

The BTNEA Experiment

A homogeneous ideal explosive, bis-trinitroethyl adipate (BTNEA) was synthesized with the isotopic labels (carbon thirteen and oxygen eighteen) introduced into the positions indicated in Fig. 7. This explosive was chosen for this experiment, because it appeared that the CO and carbon dioxide molecules expected as detonation products were already formed, and the isotopic labels would be found in the CO and carbon dioxide products.

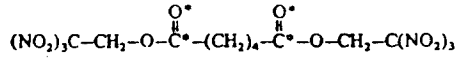

BTNEA

Figure 7. The structure of bis-trinitroethyl adipate. The asterisks indicate carbon atoms of isotope 13 and oxygen atoms of isotope 18.

The explosive was detonated in a bomb calorimeter in which the products were collected and then analyzed for the isotopic ratios (Ref. 27). The experimental results show that the ratios of C^{12}/C^{13} and O^{16}/O^{18} are essentially the same for all of the products containing C and/or O, and they are nearly equal to the isotopic ratios in the original BTNEA sample. The analytical values of the ratios were said to be well within the experimental precision of the determination. The conclusion that is obvious is that almost every covalent bond was broken, the atoms were scrambled, and they were randomly combined into the detonation products. Quoting from the paper, "We must conclude that, in the case of the homogeneous ideal explosive, all of the bonds of the original explosive molecules are, in effect, broken during the detonation process. These molecular fragments then must recombine in a statistically random fashion prior to the kinetic "freeze out" of products during the adiabatic expansion. Certainly, diffusion on a molecular level cannot be an important rate-controlling process."

Is Detonation Velocity Determined by Thermodynamics or Atomic Vibrational Velocities?

From the early days of the study of explosives, detonation velocities have been known to be relatively constant for a given explosive. In the ZND and other hydrodynamic models, the major velocity determinant is considered to be the thermodynamic content of the explosive, which provides a definitive pressure during the detonation. Reaction kinetics are considered to be irrelevant to the process.

The NM-DETA experiments previously discussed indicate that kinetics may affect detonation velocities. However, as seen in the DETA work (Ref. 23), even with an almost 50% increase in detonation pressure, the detonation velocity of NM increased only about 6%. It appears obvious that there is some large energy loss or some restraining factor. Is there some process that controls the detonation's reaction rate in a chemical or physical sense that was not previously considered?

Many recent quantum-mechanical and other (Ref. 25) kinetics studies have supported the contention that the shocked system is not in thermal ewuilibrium, principally

because the calculations show that the acoustic energy from shock waves is transferred too slowly to a thermally equilibrated state of the intramolecular vibrons. These results support the concept of the nonequilibrium nature of the shock-front processes (Ref. 4), but they do not help much to explain what is occurring at or very near the shock front to cause it to accelerate, what causes the reaction patterns seen, and what causes the appearance of the detonation at or very near the front; nor does it tell us why detonation velocities should have the values they do or why they should be relatively constant. These questions will be addressed below.

The scale of km/s in which shock or detonation velocities are usually given is the same scale as angstroms per s^{-13}. The significance of this observation is that during shock initiation or detonation, the front is moving across a covalent bond of an explosive in a period on the order of the vibrational frequency. When one calculates the relative velocity of the vibrating atoms in a C,H,O,N system by three different methods (Ref. 25), these velocities are found to fall in the same magnitude as the shock and detonation velocities. Could this be the key to the velocity restraint and the stabilization of detonation velocities?

In MD calculations of covalent systems (see Ref. 25 for the references to studies reported in this paragraph) related to organic explosives, John Hardy, Arnold Karo and I found a shock front to be quite narrow (about 10 to 100 angstroms). This same result was obtained in MD calculations by Dremin (Ref. 20) and Holian; in MD calculations of detonating systems by Peyrard et al., Lambrakos et al., and Elert et al.; in quantum mechanical (QM) calculations by Coffey and Toton, Dancz and Rice, Zerilli and others; in light-reflection experiments in NM and water by Harris and Presles, and Kormer, Campillo et al., and others. If this is so, then the shock front energy is held in a very narrow band, and the energy- or momentum-transfer rate is enormous, as was calculated by us previously (Ref. 5). This suggests that the acceleration and shear forces in the shock front are of the magnitude previously calculated (Ref. 2), which are of the order to mechanically scission covalent bonds, particularly at voids, surfaces, crystal defects, etc.

If the Hugoniot curves of a number of organic materials are compared for the pressure range of 0.2 to 30 GPa, the shock velocities all fall quite close, running from about 3 to 9 km/s. The unreactive Hugoniots (no chemical energy released) of the organic explosives are very nearly the same. Now, if the detonation pressures and velocities of most of the common explosives are plotted on the same graph with these other values, they fall very near this shock velocity curve of the inert or unreacted materials (Ref. 3 and Fig. 8).

If a small allowance (about 10%) is made for the addition to the shock velocities due to the much higher temperatures in the detonating explosives, all of the D values of these 15 commonly-used and studied explosives are enclosed in this small space between the Hugoniot shown for the inert materials, or the unreacted curve for triaminotrinitrobenzene (TATB), and the 10% increase line. This means that the extremely rapid release of the great quantities of chemical energy in the detonating explosives has only a relatively small effect on the shock or detonation velocity (D). The piston formalism denies the importance of and excludes kinetics from consideration. However, since the Ds are indeed relatively constant for a specific material, a physical or chemical explanation is required.

Remembering that shock fronts cross the interatomic bonds of organic materials in times of the same order as the vibration periods (Ref. 28), I attempted to calculate the relative vibrational velocities of the atoms of these bonds using three distinct methods: (1) infrared and x-ray crystallographic data (Ref. 28), (2) MD calculations (Ref. 25), and (3) the Hulburt-Hirschfelder equations (Ref. 25). It was seen that the detonation velocities for all of the organic explosives lie in the band of vibration velocities characteristic of the C,H,O,N atom pairs (Ref. 28). Additionally, we found that the relative vibrational velocities rise slowly to moderate maxima even at extremely high temperatures.

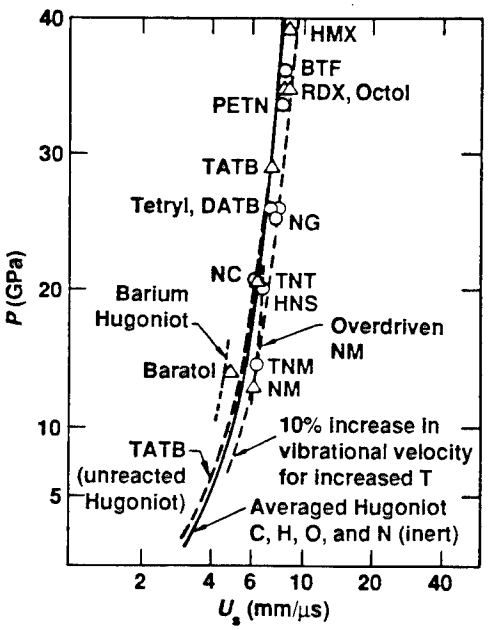

Figure 8. Comparison of Hugoniot curves for organic materials with the detonation velocities of common explosives.

A rather simple physical explanation exists, then, for a near constancy of detonation velocities. The vibrational motion that carries the principal bond-scission activating energy can proceed through the detonating explosive, even at very high temperatures, only at or near the relative vibrational velocities. That is why greatly increased levels of shock pressure and high temperatures add little to detonation velocities.

Thus, as shown in Ref. 23, kinetics is important and can change detonation velocities, but a large increase in reaction rate (or energy release rate) and high additional pressure (Ref. 24) make only a small increase in the D. This does not mean that thermodynamic energy content does not influence detonation velocities or explosive power output. It does mean, however, that it is not the thermodynamic energy content that restrains the velocities to a range of about 5 to 9 km/s.

Another observation (Ref. 29) on detonation that adds concern about a purely thermodynamic constraint is that Ds measured along different crystal axes in single crystals of RDX and PETN have different values. This can be explained in the new theory as a result of different kinetics due to different free radicals and molecular fragments and ion species formed by the mechanical forces on the different molecular orientations in the crystal lattices.

SIGNIFICANT MOLECULAR DYNAMICS CALCULATIONS

Two-Dimensional Calculations of the Effects of Lattice Defects

The macroscopic effects of the increase in sensitivity to shock initiation caused by crystal defects such as voids or cracks or very irregular crystal structure or the inclusion of heavy particles in an explosive had been experimentally observed. However, no calculations on the atomic scale had been found that simulated these conditions. Therefore, we completed a series of two-dimensional (2D) MD calculations to study these conditions. In every case, the defect studied showed a substantial increase in the number of bond scissions and energy concentrations at the sites of the defects (Ref. 25).

We next introduced a mathematical concept by which an amount of energy equal to approximately the heat of detonation per bond was added to the calculation along a reaction coordinate where bond scission had occurred. The idea considered was that the radicals formed from the endothermic bond fracture would react in about 10^{-13}s, thereby adding exothermic reaction energy to the system not far from where the scission occurred, when the radicals reacted. We made a number of calculations in different geometries and at different initial temperatures using this "reactive" potential. The effect was dramatic (Ref. 3). This study illuminated another factor--the time scales involved in the different initiation models that had been proposed. The mechanical bond scission could lead to exothermic reaction at times on the order of 10^{-13}s, and this could, therefore, influence the shock velocity by providing significant reaction energy at or very near the shock front. On the other hand, the equilibrium thermal processes proposed (gas compression, friction heating, etc.) all require much longer times (on the order of nanoseconds

to microseconds) to provide significant exothermic response. The shock front in these cases would be far downstream by such times.

The shock energy in both the 1-D and 2-D calculations did not couple well with the thermal or vibrational energy in the lattices. This supported the conclusion stated earlier that "the energy in the shock front is highly nonergodic and that thermal equilibrium, particularly between the translational and vibrational energy modes, does not exist in the front."

We completed several series of 2-D and some 3-D MD calculations to explore the factors involved in shock rise times and the associated shock-front widths. In both the 2-D and 3-D studies, the shock energy stayed localized in some small number of layers (4 to 15) of atoms. In calculations with the initial vibrational motion of the lattice atoms simulating conditions near the melting point or cold (with no initial thermal motion), the net results as to the shock-front widths and thus the rise times were similar (Ref. 25).

If one considers the case in which the shock front stays coherent in 12 layers of atoms (about 24 angstroms) and an initiating shock was proceeding into the material at 4 angstroms in 10^{-13}s (4 km/s) the microscopic rise time would be 6×10^{-13}s. In the case of a detonation front moving at 8 angstroms in 10^{-13}s, the microscopic rise time is 3×10^{-13}s. Allowing for some lattice irregularities and slightly increased intermolecular distances in real systems, rise times could be near picoseconds, and the shock width would be close to the span of 15 water molecules, as proposed by Harris and Presles (Ref. 30).

Calculations of Shock-Induced Chemistry

A new field that combines physics and chemistry has come into prominence in the past decade. This research and development involves the synthesis and fabrication of new compounds, alloys, and other materials through shock-induced chemical and physical reaction (Ref. 25). The chemistry and physics in these processes are directly related to the shock-induced reaction proposed in the new theory.

To add more realism to the MD calculations, we made two diatomic studies in which nitric oxide and sulfur nitride lattices were simulated: in the first case we calculated the effect of the impact of an aluminum plate on a model face-centered-cubic nitric oxide lattice containing a void; and in the second case, a similar geometry was used in which the aluminum plate impacted a model face-centered-cubic sulfur nitride lattice. The calculations were made in each case with the initial random motion of the atoms representative of room

temperature and again when the systems were "cold," with no initial thermal motion.

These four sets of calculations were compared with those of an earlier, more general, covalent system. The same qualitative results were obtained of bond scission, with atoms and molecular fragments flying across the void to impact the opposite walls and cause further scission. When the reactive potential was used in a similar geometry in a more general lattice, the initial "spall" from the inner surface of the void and the impact on the opposite void face led to activity of the atoms that was very suggestive of hot spot formation through free-radical chemistry. These motions and simulated reactions are all nonergodic, nonequilibrium processes.

SUMMARY OF MORE RECENT SUPPORTIVE EVIDENCE

Sharma et al. reported (Ref. 31) studies of initiation sites found in TATB shocked to near-initiation levels. They found the sites, by scanning electron microscopy (SEM), to be tiny holes on the surfaces and edges of the explosive grains. They showed, by x-ray photoelectron spectroscopy (XPS), that deposits of acetone-soluble reaction products in the holes were furoxan and furazan derivatives of TATB. Their analysis suggested that the furoxan product could react with adjacent TATB molecules in an exothermic chain reaction to give a water molecule and a new furoxan. Thus the shock=formed furoxan could immediately (i.e., in 10^{-13} to 10^{-12}s) provide reaction energy very near the shock front. Sharma suggested that this reaction could be involved in the initiation of TNT as well.

Tanaka et al. provide a strong defense of the new theory. They report (Ref. 32) that an explosive designated as E25 (75% PETN/25% paraffin) at a density of 1.265 g/cc has a measured D of 7.230 km/s, whereas pure PETN (pentaerythritol tetranitrate) at the same density has a measured D of 6.60 km/s. However, the calculation using shock velocities and the empirical formula gave a value of 7.267 km/s, within o.51% of the measured value. This is well within the precision of D measurements. The classical theory calculation missed the measured value by 14.24%. The author of the paper who reported the E25 data stated that, "All equations-of-state available to us cannot reproduce these results."

In 1992, Brenner, Robertson et al. published results of their MD studies in which they use many-body interatomic potentials to provide more realism to their calculations. Their excellent graphics show in unmistakable detail (Fig. 9) the narrow shock and detonation zones, the massive mechanical fracture of the covalent bonds, the free atoms and molecular fragments, and the free-radical chemistry in and very near the front. These processes are nonequilibrium and nonthermal.

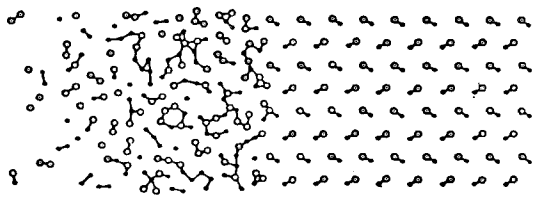

Snapshot from a simulation of a detonating film. The length of the system shown is ≈ 80Å.

Figure 9. Molecular dynamics calculation of a model detonating solid with two types of atoms and with exothermic reactivity incorporated into the dynamics.

Simpson, Helm and Kury (Ref. 34) studied the nonreactive Hugoniot for HMX/water mixtures, and they reported that with shocks of 5.17 to 5.99 GPa there was no evidence of HMX reaction. However, they showed by comparison with these results that in solvent-pressed HMX in wedge tests about 3 to 7% of the HMX had reacted in less than about 100 ns. They report, "The observed higher shock velocities in the solvent-pressed data we attribute to a reaction-supported shock front." Other pertinent comments from this paper are: "Implicit in the use of a detonation product EOS is the assumption that chemical reactions occurring under the shock loading conditions of the wedge tests go to completion. Therefore, since early time reactions may only proceed to intermediate states, the extent of reaction inferred through reactive modeling will be conservative." "The greatest uncertainty in determination of state behavior of HMX from measurements on a mixture is the assumption of a one-dimensional shock wave passing through a homogeneous medium."

The information in these four references explicitly adds strong support for the new Walker, Wasley, Karo (WWK) theory.

NEW EQUATIONS USED TO CALCULATE DETONATION VELOCITIES

In 1968, Kamlet and Jacobs (Ref. 35) reported the development of two empirical equations for calculating detonation pressures and velocities. With some simplification of their concept and an algebraic derivation, a simple equation for calculating D = f(P) was obtained:

$$D = 2.45 + \frac{P^{\frac{1}{2}}}{3} \quad . \qquad (3)$$

When the detonation data for 14 very different explosives are compared by means of this relationship, two interesting results appear:

(1) The aliphatic compounds are all on one side of an averaged curve, and the aromatics (plus sterically-hindered PETN) are all on the other side.

(2) With a small positive correction for hydrogen and nitrogen content (to compensate for their relatively higher shock velocities at a given pressure) and a small offset for aromaticity, an equation was formulated that reproduces the data for the 14 explosives within +1.57 and -1.03%. That equation follows:

$$D = \left(\frac{P^{\frac{1}{2}}}{3} + 2.0 + 0.25a\right) + 0.05\ \left(H_p + \frac{N_p}{20}\right), \qquad (4)$$

where a = 0 if the compound is aromatic and a = 1 if it is aliphatic, and H_p and N_p are the weight percents of hydrogen and nitrogen, respectively.

The concept underlying the equation is that detonation velocity is principally a rather simple Hugoniot relationship, D = f(P). More explicitly, thermodynamic factors, the EOSs, and even reaction rates have limited influence on the actual values of D.

Kamlet's empirical equation for calculating detonation pressures is probably as useful as the TIGER thermodynamic code with the complex EOSs that are used, and we have shown that the Ds for 48 very different explosives can be calculated accurately (well within the experimental error of the better measured values) from the Hugoniot values of the elements that make up the explosives. The equation used is as follows:

$$D = T_c\left(\sum U_{si} f_i\right), \qquad (5)$$

where U_{si} is the shock velocity of the elements at $P_{C\text{-}J}$, f_i is the atomic weight fraction of the element, and T_c is a small correction (about 3 to 8%)(Ref. 25) required because the detonation temperatures are considered to be about 2500 to 5000 K, whereas the Hugoniot values of the elements are usually measured between about 70 and 950 K. The Ds for 21 of the best-characterized explosives were calculated with Eq. 5, and the correlation coefficient obtained for these values is 0.976. D values were calculated for 25 other explosives for which less data were available, and the correlation coefficient for this set is 0.932, (Ref. 36).

CONCLUSIONS

It is concluded: (1) That the new concept of physical kinetics is a valid concept for determining reaction rates in detonations and in highly shocked systems. Shock and detonation velocities are related directly to the average relative vibrational velocities of the atom pairs in C,H,O,N materials.

(2) That the exceedingly high kinetic energy in the detonation front is sufficient to cause massive fracture of the covalent bonds of the molecules of explosives (and other organics) at and near the front, so that the large majority of the molecules are broken to individual atoms or radicals and are rearranged extensively, and that the rates of the subsequent very rapid chemical reactions can be influenced by the addition in the explosives of chemicals providing enhancing or inhibiting reactions.

(3) That the simple Eq. 5 is a rational equation, based on appropriate Hugoniot principles, which provides for very accurate calculation of detonation velocities from the shock velocities of the elements in the empirical formulae of the explosives.

(4) That the concepts of physical kinetics and the small increase in vibrational velocities with increasing temperature provide the earlier missing pieces that now explain the relative constancy of detonation velocities.

(5) That the comparison presented herein shows that this new modern theory (the WWK theory) of the initiation and detonation of explosives provides a realistic microscopic description of and significant utility in understanding and calculating explosives phenomena.

REFERENCES

1. W.C. Davis, Sci. Am. 256(5), 106 (1987).
2. F.E. Walker and R.J. Wasley, Propellants and Explosives 1, 73 (1976).
3. F.E. Walker, Proceedings of the 19th International Pyrotechnics Seminar, 20-25 February 1994, pp. 297-318, South Pacific Inform. Services Ltd, Christchurch, N.Z. (1994).
4. F.E. Walker, Propellants, Explosives, Pyrotechnics 7, 2 (1982).
5. F.E. Walker, J. Appl. Phys. 63(11), 5548-5554 (1988).
6. A.W. Campbell, W.C. Davis, and J.R. Travis, Phys. Fluids 4, 498 (1961).
7. A.W. Campbell, W.C. Davis, J.B. Ramsay, and J.R. Travis, Physics Fluids 4, 511 (1961).
8. F.P. Bowden and O.A Gurton, Nature 161, 348 (1948).
9. A. Joffe, Nature 161, 349 (1948).
10. E.F. Gittings, Fourth Symposium on Detonation (Preprints) Vol. II, C-15 (U.S. GPO, Washington, D.C., 1965).
11. H. Eyring, R.E. Powell, G.E. Duffey, and R.B. Parlin, Chem. Rev. 45, 69 (1949).
12. H. Eyring and An-Lu Leu, Proc. Nat. Acad. Sci. USA 72(5), 1717 (1975).
13. H. Eyring, Science 199, 740 (1978).
14. F.E. Walker and R.J. Wasley, Explosivstoffe 17, 9 (1969).

15. H. Cheung, A. Weston, L. Green, and E. James, Explosive Initiation, Lawrence Livermore National Laboratory, Livermore, CA, UCRL-76578 (1975).
16. F.E. Walker and R.J. Wasley, Combust. Flame 15, 233 (1970).
17. F.E. Walker and R.J. Wasley, Combust. Flame 22, 53 (1974).
18. W. Taylor and A. Weale, Trans. Faraday Soc. 34, 995 (1938).
19. M. Held, Explosivstoffe 11/12, 241 (1969).
20. A.N. Dremin and V. Yu. Klimenko, Progress in Astronautics and Aeronautics 75, J. Ray Bowen, N. Manson, A.K. Oppenheim, and R.I. Soloukhin, Eds. (AIAA, New York, NY, 1981). pp.153-168.
21. P.A. Urtiew, E.L. Lee, and F.E. Walker, Arch. Thermodyn. Combust. 9, 259 (1978).
22. J.H. Lee, R. Knystautos, and N. Yoshikawa, Acta Astronaut. 5, 971 (1978).
23. F.E. Walker, Acta Astronaut. 6, 807 (1979).
24. I.C. Skidmore and S. Hart, Proc. 4th Symp. (Internat.) Detonation, U.S. Naval Ordnance Laboratory, White Oak, MD, 12-15 October 1965 (U.S. GPO, Washington, D.C.) p.47.
25. F.E. Walker, Initiation and Detonation of Explosives--an Alternative Concept, Lawrence Livermore National Laboratory, Livermore, CA, UCRL-53860, 11 January 1988.
26. D.R. Hardesty, Combust. Flame 27, 229 (1976).
27. R.R. McGuire and D.L. Ornellas, Propellants and Explosives 4, 23 (1979).
28. F.E. Walker, Propellants and Explosives 6, 15 (1981).
29. H.W. Koch and Ch. Baras, Institut Franco-Allemand de Recherches de Saint-Louis, France, Rapport 28/71 (1971).
30. P. Harris and H.-N. Presles, J. Chem. Phys. 80(1), 524 (1984).
31. J. Sharma, J.W. Forbes, C.S. Coffey, and T.P. Liddiard, J. Phys. Chem. 91, 5139 (1987).
32. K. Tanaka, S. Oinuma, et al., Shock Compression of Condensed Matter 1989, S.C. Schmidt, J.N. Johnson, L.W. Davison, (editors), Elsevier Science Publishers B.V., (1990).
33. D.W. Brenner, D.H. Robertson, et al., Microscopic Simulations of Complex Hydrodynamic Phenomena, Edited by M. Mareschal and B.L. Holian, Plenum Press, New York, NY, pp. 111-123 (1992).
34. R.L. Simpson, F.H. Helm, and J.W. Kury, Propellants, Explosives, Pyrotechnics 18, 150-154 (1993).
35. M.J. Kamlet and S. Jacobs, J. Chem. Phys. 48(1), 23 (1968).
36. F.E. Walker, Propellants, Explosives, Pyrotechnics 15, 157-160 (1990).

Table 3. Correlations Between Reaction Dynamics Experiments and Detonation Energy and Time Characteristics.

Property	Reaction Dynamics	Detonation
Velocities of atoms and molecules		
Center of mass (I···CN)*	2 km/s	
Translation of H atoms	20 km/s	
Velocities of atoms and molecules in detonation front		6 to 9 km/s
"C" and "H" atoms from MD calcs.		1 to 20 km/s
Vibrational velocities of atom pairs as f(T) at second vib. level--from QM calculations**	HH	13.7 km/s
	CH,NH,OH	8.1 to 9.6 km/s
	CC,NN,OO	2.0 to 2.7 km/s
H atoms from detonating charge		15 km/s
Energy of atoms and molecules		
For the reaction:		
(I-CN) —— (I···CN)* —— I + CN (Energy available for reaction)	0.883 eV	
H + OCO —— (H···OCO)* —— OH + CO (H kinetic energy)	2.07 eV	
Energy of PES barrier to TS	105 kJ/mol	
Kinetic energy of atoms at 8 km/s		
N		4.72 eV
O		5.34 eV
Bond energies in RDX		
C-N		2.30 eV
N-N		1.06 eV
Times to reaction		
Lifetime of TS		
(I···CN)*	0.2 ps	
(H...OCO)*	5.0 ps	

Table 3. (cont.)

From MD calculations	
"Time to reaction"	
C-H in "CH_2"	0.06 to 0.24 ps
C-H in "PETN" interior	0.6 to 1.0 ps
N-O in "PETN" interior	0.4 to 1.0 ps
C-C in "C" matrix	0.06 to 0.3 ps
Estimate of time to reaction in detonation at 8 km/s	
In 20 angstrom zone	0.25 ps
In 40 angstrom zone	0.5 ps

** From Hulbert-Hirschfelder calculations

JOURNAL DE PHYSIQUE IV
Colloque C4, supplément au Journal de Physique III, Volume 5, mai 1995

Towards Detonation Theory

A.N. Dremin

Institute of Chemical Physics (Chernogolovka), Russian Academy of Sciences, Moscow region, Chernogolovka 142432, Russia

ABSTRACT: Experimental findings inconsistent with both the CJ and the ZND detonation theories are discussed. These are the unstable detonation and the weak dependence on charge diameter of liquid explosives detonation velocity at sizable value of their failure diameter. The investigations have resulted in the discovery and introduction into detonation theory of two new theoretical notions: chemical reaction breakdown (BD) and shock discontinuity zone (SDZ). It is shown that the BD governs the limits of the following phenomena: the shock-to-detonation transition, the detonation stability, and the detonation failure diameter, whereas the SDZ governs the regularities of EMs change at detonation.

1. INTRODUCTION

Detonation phenomenon is known since the previous century. The phenomenon thermodynamic analysis performed by Michelson [1], Chapman [2] and Jouguet [3] has resulted in the shock wave theory generalization. Detonation wave has been represented as a shock wave with energy evolution inside the wave front. It was the most prominent step in detonation theory progress. However,it is a well-known fact that the CJ hydrodynamic theory of detonation has not been fully developed. It has formulated some principle for detonation velocity choice. But the principle has not been substantiated enough, namely the impossibility of self - sustaining weak detonation has not been proved in general.

In essence the CJ theory deals only with energetic characteristic of detonation waves. The theory has not taken into account chemical reaction kinetics. Moreover the theory followers believed that explosives at detonation transform into detonation products practically instantaneously. The idea seemed to be justified once it had been revealed that for all gaseous mixtures investigated shock wave pressure initiating chemical reaction with a vanishing small time delay characteristic of detonation practically coincide with the CJ pressure, the shock wave velocity being considerably smaller than the mixtures detonation velocities (see for example [4] and references in). It was because of this experimental finding that the CJ theory followers thought that explosive at detonation transform into detonation products during the process of their compression within detonation wave shock front. Therefore the CJ detonation wave model was sometimes called the "Zero-reaction zone" model. The definition of the detonation model employed was in apparent contradiction with the usual concept of chemical reaction process. The matter is that shock wave front width totals only some free paths of molecules (see [5] and references in)and according to the concept reagents need many thousands collisions to reach the process final product.

Apart from the above-mentioned contradiction the CJ detonation theory has other shortcomings. Since the theory had not taken into account the finite zone of chemical reaction and any perturbations

originating behind the zone can not reach the front of self-sustained detonation wave it failed to give any interpretation of the detonation failure diameter d_f [6] (the smallest diameter of explosive charge which can detonate without any outside support). It failed to interpret the so-called spinning detonation [7] as well.

In 1940 Zeldovich substantiated theoretically detonation wave physical model with finite reaction zone [8]. Since von Neuman [9] and Döring [10] obtained independently related resuls the new theory was named the ZND theory.

According to the ZND theory the detonation wave front has become complicated. Really, at the CJ detonation, explosive transforms into detonation products completely during its compression inside the wave shock front and at the ZND detonation, quite the reverse, explosive does not change chemically at all within the shock front, it is only compressed inside the front and its decomposition sets in behind the front in the shock-compressed state under the effect of the high temperature due to the shock compression. In essence detonation has changed into deflagration moving behind the shock front with the front velocity. The zone consisting of the shock-compressed explosive and its transformation into detonation products is characterized by high pressure and has been called the chemical spike. The spike time t_{cs} is the time of the explosive transformation at detonation.

Correct way to the d_f phenomenon understanding was directed by Rosing and Chariton [6]. According to Rosing and Chariton explosive detonation capability is governed by some equilibrium between, heat evolution due to explosive chemical transformation into detonation products, on the one hand, and, on the other hand, explosive energy loss due to its scattering from the zone. The equilibrium is disturbed at the d_f,so that at smaller diameters detonation can not travel at all. Thus, it results from the above-said that according to Rosing and Chariton any substance can detonate if its decomposition reaction is exothermal and charge diameter is larger than the d_f.

Taking into account that explosive scattering is in fact some rarefaction which proceeds with sound velocity c, Chariton advanced [11] some formula to estimate failure diameter value: $d_f \simeq 2ct_{cs}$. Experimental data gained in a number of year [12-15] lend support to the validity of the d_f qualitative concept [6,11] and the ZND detonation theory [8,10]. However, it should be noted that they failed to interpret some contradiction between rather weak dependence of liquid explosives detonation velocity on charge diameter, on the one hand, and finite value of the explosives d_f, on the other. Indeed, according to the d_f theories developed on the basis of the concept (see, for example, [6,11,16-20]) the d_f value is proportional to explosive detonation chemical transformation time t_{cs}, the larger being the time, at the larger charge diameter detonation velocity depending on the diameter value. And on the contrary, the smaller is the time, at the smaller charge diameter detonation velocity depends on the diameter value. So that at the time approaching zero detonation velocity dependence on charge diameter has to vanish. Naturally as this takes place the d_f value has also to approach zero. However, in the case of liquid explosives the detonation velocities of which as a rule do not practically depend on charge diameter, the d_f by contrast are not equal to zero and amount to considerable values. For example, nitromethane detonation velocity at room temperature is equal to 6.3 km/s and changes insignificantly near by its d_f. Nevertheless nitromethane d_f is rather sizable $\approx$ 15 mm at room temperature [21]).

The spinning detonation phenomenon was discovered by Campbell and Woodhead in 1926 [7]. The appearance of some spot of bright luminosity on detonation wave front at inner side of tube containing gaseous explosive mixture and the spot spin around the tube axis were found to be basic features of the phenomenon [22-24]. It was later revealed that the spinning detonation always originated nearby any limits of detonation propagation [25-30].

For a long time the spinning detonation was considered as an original phenomenon. Shchelkin was the first who had realized and declared that the spinning detonation was in fact some limit of unstable so-called pulsating detonation [31,32]. By now the pulsating detonation as well as the spinning detonation have been investigated in considerable detail [32,33]. Shchelkin starting from the ZND detonation wave model [8-10] was of the opinion that close to the detonation propagation limits chemical reaction proceeds slowly at the shock-compressed state in the detonation wave plane

smooth front and therefore spin originates. According to Shchelkin spin is conducted by some oblique detonation wave appearing on the basic detonation wave shock front and being sustained by the ZND chemical spike high pressure [32,34]. The idea was substantiated theoretically by Zeldovich who called attention to the fact that the oblique detonation wave was a strong detonation [35]. The oblique detonation wave origin was explained by Shchelkin in the framework of his notion of detonation waves kinetic instability [31]. According to the notion some casual perturbations of the detonation wave ignition plane can overcome the detonation wave shock front and bend it bringing the oblique detonation wave into being.

Thus according to Shchelkin the oblique strong detonation wave is the principal element of spinning detonation structure. In contrast to Shchelkin siberian scientists Voicekhovsky, Mitrofanov, and Toptshijan, have proposed and elaborated in detail the spinning detonation with some transverse detonation wave as the principal element of the spinning structure [33,36,37]. They also start from the ZND detonation theory. In accordance with the theory they believe that at gaseous detonation the shock-compressed and heated substance without chemical reaction appears between the detonation wave shock front and its combustion plane, the appearance being conditioned by a large value of the substance ignition delay time. Furthermore, they consider that owing to some casual reason a perturbation can arise inside the heated zone and it will lead to the transverse detonation wave origin. As far as the oblique wave is concerned it appears in their view on the basic detonation wave shock front under the effect of the transverse detonation wave high pressure. It should be mentioned that siberian scientists have also shown that even far from the detonation propagation limits the transverse waves exist and the waves are not distinct in nature from that of the spinning detonation [34].

It should be mentioned that Manson [38,39], Fay [40] have succeeded to explain some features of the instable detonation wave by the effect of burned gas acoustic vibrations. They have clearly demonstrated that the unstable detonation front perturbations and the burned gas acoustic vibrations are interrelated. However, the problem needs some further investigations. It is unlikely that the unstable pulsating detonations appear owing to the burned gas acoustic vibration. Conversely, more likely the burned gas acoustic vibration are governed by the unstable detonation front perturbations [33].

So, there results from the foregoing that there are some experimental findings which are consistent neither with the CJ nor with the ZND detonation theories. The findings are the following:

- The spinning and the pulsating detonations; the question - how does the unstable detonation originate? - is still open.

- The fact that the dependence of liquid explosives detonation velocity on their charge diameter is very weak at a sizable value of the explosives d_f.

In the paper the interpretation of the findings founded on the notion of the chemical reaction breakdown phenomenon (BD) [21] are presented. Some considerations based on the notion of the shock discontinuity zone (SDZ) effect [41] on the mechanism of ideal explosives (these explosives contain fuel and oxidizer in their molecules) transformation at detonation are discussed as well.

2. BREAKDOWN PHENOMENON

The BD phenomenon has come to light in the course of the investigation of liquid explosive detonation processes [21]. Exactly speaking it was discovered in the course of the elucidation of the second above-mentioned experimental finding inconsistent with the available detonation theories.

The greater part of the investigations have been performed with nitromethane and its mixture with acetone. The explosives detonation front is unstable. Clearly the most feasible approach was to use the unstable detonation decomposition mechanism concept in order to look for the finding cause. By this was meant that the unstable detonation failure diameter theory had to be developed. The theory had been elaborated on the basis of decomposition mechanism concept worked out by Shchelkin and Troshin [32] in the early sixties for gas unstable detonation.

Shchelkin's and Troshin's explosive detonation transformation mechanism dissimilarity from that of the ZND detonation theory consists in the following. The ZND detonation front is stable; explosive transformation reaction originates behind the detonation wave shock front in the explosive shock-compressed state simultaneously over the wave front. In Shchelkin's and Troshin's case detonation front is unstable; explosive transformation reaction originates non-simultaneously over the detonation wave shock front but at discrete spots of double collisions of the contrary-moving triple-shock configurations (TSCs) [32]. According to Shchelkin and Troshin the explosive transformation reaction spots will not appear over the detonation wave shock front if the double collisions do not take place. In their view the TSCs originated exist then in the detonation wave shock front owing exclusively to the configurations repeated collisions with each other or with gas containing tube walls; each separate configurations passing away inevitably. However, the collisions give rise to new explosive spots which lead to new TSCs origin. The TSCs originated collide again and so on. Taking into account the mechanism one could imply that the sequence of the events never ceases at the stationary detonation wave front except at the front edge of the charge lateral free surface. In the case the last TSCs moving to the charge free surface at the detonation front edge have no contrary partners to collide with. Due to the reason the explosion spots can not appear close by the surface. It follows from this that new TSCs can not origin too and in one's turn it has to result in the impossibility for neighbor explosive spots located more distant to the surface to appear. So the charge free surface presence has to lead to explosive spots nonoriginating successively in the direction from the surface, that is to the appearance of some reaction-quenching wave moving from the charge free surface towards its axis.

The reaction-quenching waves have been really found by specially arranged experiments. In the experiments the explosives detonation wave moving inside some metal tube transits through a sudden enlargement of the tube diameter. The detonation wave front occupies the first tube cross section entirely. In accordance with the foregoing in means that the TSCs collisions with the tube wall result in the explosive spots appearance in the same manner as at their collisions between themselves. Owing to the fact the reaction-quenching waves do not originate during the detonation wave motion inside metal tubes. (It stands to reason that the contention is valid only in the case when the tube's inner surface is smooth). Also in accordance with the foregoing considerations on the reaction-quenching wave origin cause it has been implied that the last TSCs round the unstable detonation wave front edge will have nothing to collide with at the first tube end and it will bring the reaction-quenching wave appearance and the detonation death.

It has been verified in the experiments that the reaction-quenching waves really appear at the first tube end. However, it turns out that they spread over the detonation wave front towards the charge axis only to some depth. Moreover, it has been found that the detonation wave moves along the charge axis without change its velocity if the first tube radius is larger than the depth and the detonation wave generally ceases if the reaction-quenching waves shut down the tube cross-section entirely. It has been shown that for liquid explosives unstable detonation the depth coincides with the explosives detonation failure radii [42]. The failure diameter theory developed [42,43] was founded on the experimental finding.

The fact that the reaction-quenching wave can penetrate from the charge lateral free surface towards its axis only to some depth is a convincing explanation of the liquid explosives detonation wave velocity independence on the charge diameter. It goes from the finding that the explosive detonation wave moves along the charge axis and it "knows" nothing about the events which take place in neighbor parts located some distant apart the charge axis at the charge diameter larger than the failure one.

The important feature of the above-presented considerations on the nature of liquid explosives unstable detonation failure diameter is the reaction-quenching wave. It was predicted on the basis of Shchelkin's and Troshin's spot mechanism developed for explosives transformation in the unstable detonation. However, it turns out that the reaction-quenching waves originate as well in the case of liquid explosives stable detonation [21]. The finding has lead to the perception that the reaction-

quenching waves appear in fact not owing to the explosion spots successive death concept given above but due to some general phenomenon which is an inherent characteristic of all energetic materials (gaseous, liquid, solid) explosion processes. In essence it was the discovery of the chemical reaction break-down (BD) phenomenon which governs the limiting conditions of shock-to-detonation transition (SDT) process, the detonation stability , and detonation failure diameter as well [44].

What is the BD phenomenon main point? When does it take place? To begin with the questions one needs to discuss the process of shock wave motion through some energetic material, that is to discuss the SDT process. It is well known that the shock wave intensity decreases during its motion through any inert material if it has no outside support. Behind the front of the shock wave without support there is rarefaction wave which leads to the material adiabatic cooling. However, the effect of the shock wave of any intensity results in EM energy evolution just behind the shock wave front, the evolution favoring the wave support. It should be mentioned that the initial rate of the evolution depends on some factors: on EM type (different materials can release their energy with different rate), on EM charge structural features (on EM particle size and structure - single crystals or fragments of broken cast, on the nature of the filler in the charge pores, on EM state - liquid or solid, density, and so on), and on the shock wave intensity as well (the larger the intensity, the larger the initial rate).

So, the change of the shock wave intensity in any EM is governed by two processes: explosion energy evolution, on the one hand, and the EM adiabatic cooling due to the rarefaction wave effect, on the other. It is obvious that the wave intensity will increase and it results in the initiation of detonation if the initial rate of the EM energy evolution is larger than that of the adiabatic cooling, and vice versa, the wave intensity will decrease if the initial rate of the adiabatic cooling is larger than that of the energy evolution.

The decrease of the shock wave intensity is necessary condition for the BD phenomenon manifestation. However, the condition is not sufficient to provoke the BD. The matter is that the BD can occur only when the dependence of EM transformation time on shock wave intensity is strong. It is really strong at low shock pressures but the dependence falls down with the pressure increase. It follows that the BD does not need to be if the intensities of the shock during its attenuation are sufficiently high. Naturally the question arises - what level of shock intensity is "sufficiently high" to prevent the BD? It seems likely that a shock is sufficiently strong if the shock - induced EM energy evolution rate is maximum just behind the shock wave front, that is if the initial rate of the EM energy evolution is fast. To the contrary it is believed that the shock is weak as soon as the maximum is displaced from the front, which is to say that some induction time of the EM fast transformation appears behind the shock front. In other words, the shock is weak if the initial rate of the shock-induced EM energy evolution rate is slow. The BD is very probable in the EM under the weak shock effect since the induction time is usually strong function of the material state, that is of the shock wave intensity.

3. SDT AND DETONATION INSTABILITY PHENOMENA

It is well known that the response of heterogeneous and homogeneous EMs to the shock effect is very different (see Proceedings of some last Symposium (Int.) on Detonation which contain many papers of the "Shock-to-Detonation" sessions). The differences are the following. First, shock wave critical intensities to initiate detonation at the same experimental conditions differ significantly; in the case of heterogeneous EMs it is considerably smaller than in homogeneous ones. It turns out that rather weak shock of some kbar intensity can initiate detonation in heterogeneous EMs, whereas one needs shock of 5-10 GPa to initiate detonation in homogeneous explosives.

The difference of heterogeneous and homogeneous EMs shock sensitivities is conditioned by marked difference in initial rates of their energy evolution just behind initiating shock waves fronts. In the case of heterogeneous EMs it is usually fast and it leads to the shock gradual transition to detonation if the shock intensity is larger than that of the critical one. In contrast the initial rate of homogeneous EMs energy evolution is usually very slow under the effect of the shock approximating critical intensity, so that the bulk of their energy is evolved at some distance behind the shock wave

front.

The slow rate of EMs energy evolution is the cause why the CJ detonation of homogeneous EMs always originates from strong detonation (SD). It is obvious if the initiating shock pressure is higher than the CJ pressure. However, it turns out that the SD also originates in homogeneous EMs at any initiating shock pressure larger than the critical one, that is at pressures lower than the CJ pressure as well. The matter is that some layer of shock-compressed explosive (SCE) appears (exactly speaking, a layer of partially decomposed SCE, the decomposition scale depending on its decomposition initial rate) and the SCE detonation arises first at the piston-SCE interface in the SCE explosion induction time [21,45,46]. The SCE detonation arises at the interface due to extremely fast energy evolution in the induction time. The SCE detonation pressure exceeds considerably the pressure of initial homogeneous EM CJ detonation. Therefore, the SD appears in the initial EM just as the SCE detonation overtakes the initiating shock wave front. So the CJ detonation appears from the SD at any way of it's initiation.

As mentioned above, the mechanism of unstable detonation origin and its structure are governed by the BD phenomenon. It is well known that initiating shock wave transforms into detonation gradually in all heterogeneous EMs. Usually their CJ detonation is reached asymptotically, that is without the SD appearance during the SDT process. Maximum rate of their energy evolution just behind the shock wave front is the very cause of the feature. Homogeneous EMs are another matter; their CJ detonation always originates from the SD. However, it turns out that the energy evolution proceeds with maximum rate in power homogeneous EMs just behind the SD wave front. Due to this reason the BD does not take place during the SDT process and the CJ detonation is stable in the power homogeneous EMs.

As an example of power homogeneous EM one can give liquid nitroglycerine (NG). Its CJ detonation pressure is equal to $\approx$ 27 GPa, critical intensity of the shock to initiate detonation at laboratory experiments - 12 GPa, and detonation pressure of NG compressed by $\approx$ 12 GPa intensity shock $\approx$ 50 GPa [21]. It was shown experimentally that NG SD generated by the SCE detonation attenuates to the CJ detonation without the BD appearance, so that its CJ detonation is stable.

So it was shown experimentally that power homogeneous EM detonation is stable since the BD does not occur during the SDT process [21]. Weak homogeneous EM detonation quite the reverse has usually unstable front since the BD occurs easily during the process of their SD transition to the CJ detonation. It happens for their SD wave front becomes weak and consequently the initial rate of their energy evolution becomes slow under the rarefaction wave effect. In the case adiabatic cooling due to the rarefaction wave effect compensates completely the explosive heating due to its chemical transformation and it leads to the BD appearance. The BD behind the SD results in the wave chemical spike disappearance. After that the following process resembles the SDT process [21,46]. As in the case a layer of SCE appears. It appears under the effect of high pressure just detonated explosive. The SCE state parameters (pressure and pressure gradients) change in such a way that in some time characteristic of the state the SCE detonation originates in the immediate vicinity of the detonation products-SCE interface. (It should be mentioned that for a strong but short duration initiating shock wave the detonation may not originate again after the first BD, however, this case is of no interest for the present discussion). Since the SCE detonation pressure exceeds considerably the CJ detonation pressure the SD will originate again in the initial undisturbed explosive as soon as the SCE detonation overcomes the shock wave front, that is as soon as it consumes the SCE layer. After that the BD and the SCE detonation origin will repeat.

So it follows from the afore-said that the pulsating detonation is a property of those explosives which energy evolution rate at detonation conditions is slow [47]. For the Arhenius kinetics it corresponds to a high value of the EMs transformation activation energy, on the one hand, and relatively low explosive temperature, on the other [48,49]. The list of the EMs consists of practically all gas explosive mixtures [32,33] as well as some weak liquid explosives [21]. As an example of weak liquid explosive one can give nitromethane (NM). At room temperature NM CJ detonation pressure is equal to $\approx$ 13 GPa, critical intensity of the shock to initiate detonation at laboratory experiments

$\approx$ 8 GPa, and detonation pressure of NM compressed by 8 GPa intensity shock - 25 GPa [21].

It also follows from the afore-said that one would have to observe so-called one-dimensional instability at weak homogeneous EM detonation since the sequence: the BD during the SD transition to the CJ detonation - the SCE layer appearance after the BD - the SCE detonation origin in some induction time - and finally the SD appearance again will repeat continuously. However, the one-dimensional instability is not observed in spite of the fact that the sequence does repeat continuously. The point is that for some casual reasons the BD and subsequent SCE detonation in reality do not take place simultaneously over the whole detonation front, but do occur at randomly distributed individual spots [21,50].

The SCE detonation from each spot spreads hemispherically in the SCE. Each individual detonation overcomes the shock front and causes the SD diverging in the initial undisturbed explosive. The rarefaction rate behind these detonation fronts is larger in comparison with that behind the plane front and therefore the reaction breaks down easily again. After the BD in some strong divergent detonation the SCE detonation spreads over the SCE layer like a ring, some islet of a new SCE appearing in the ring center. The ring cross-section represents the TSC. The TSC consists of the straight shock wave, the principal element of the configuration - the transverse wave representing the SCE detonation, and the oblique wave which is undisturbed explosive SD. The straight shock wave pressure is on average equal to the CJ pressure, the transverse detonation wave spreading over the SCE of the CJ pressure. The oblique SD wave pressure decreases rapidly away from the TSC triple point and finally reaches the straight wave pressure. Due to the reason the unstable detonation front surface irregularity is not considerable; the relation of average inhomogeneity size over the front surface to the average size of the front departure from the plane is as large as ten [21].

The ring detonation progress over the detonation wave front is accompanied by the increase of the ring islet, new SCE local explosions originating in the center of some islets (at the detonation products - SCE interface) before the islets merging if the SCE life time exceeds its explosion induction time. In the other case the islets merge all together with the SCE continuous layer origin as the TSC exits only until the meeting with each other in the course of non-steady process of the SD transition to the CJ detonation. However, since the SCE local explosions originate at the beginning chaotically at randomly distributed spots, the SCE continuous layer is not a constant thickness. Therefore new SCE explosions arise again nonsimultaneously. It should be noted that the average induction time of the local explosions in each next subsequently appearing SCE layer increases in comparison with that of the previous one as the SD attenuates during its transition to the CJ detonation.Due to the reason the SCE ring detonations corresponding to each new explosion spread over the detonation wave front surface and consume adjacent parts of the SCE layer with the result that the explosions have no time to occur in the parts. Just for this reason the explosions number in the detonation front decreases during the process of the strong detonation transition to the CJ detonation or to some final stationary detonation characteristic of explosive composition and charge diameter. The number decrease looks superficially as the increase of the detonation front non-homogeneity scale. The reason seems likely to be also responsible for the regularity of the unstable detonation front non-homogeneity.

It should be noted that the same mechanism of the local explosions number change governs steady scale of the spherical unstable detonation non-homogeneity. Indeed, since the spherical detonation front surface increases the free path of each ring detonation as well as their SCE islet size increases too. The process leads inevitably to the appearance of the new SCE local explosions in the center of those islets which SCE life time exceeds its explosion induction time.

So it follows from the foregoing that the mechanism of the SCE local explosion origin governs any change of the explosions number: the number decrease at the process of the SD transition to the CJ detonation and the explosion number increase in the spherical unstable detonation front. The mechanism can be also employed to interpret the second experimental finding inconsistent with the CJ and the ZND detonation theories. The finding consists in the fact that in gaseous as well as in liquid explosive unstable detonation [21] the decomposition time at the CJ detonation velocity

corresponds to the shock of the CJ pressure. In accordance with the above-presented considerations the fact means that the SCE pressure in the center of the islets on average is equal to the CJ pressure. For gaseous detonation it is easy to show that the velocity of the shock of the CJ pressure is of $\sqrt{2}$ times smaller than the CJ detonation velocity.

It follows from the foregoing that the unstable detonation front with its SCE local explosions is rather complicated. However, the front in fact can be even more complex. The matter is that there are SCE local explosions of different orders. Those which have been discussed above are the first order local explosions. The explosions are basic and they originate at the SCE-detonation products interface at the pressure level which is equal on average to the CJ pressure. The maximum amplitude of the unstable detonation front pulsations is governed by the explosions. Moreover, the existence (macrostability) of the unstable detonation wave is governed by the first order local explosions as well; if the explosions do not appear the detonation will cease.

The next order local explosions in essence govern fine (superfine and so forth) structure of the unstable detonation front [47,50]. Their origin is some manifestation of oblique wave instability: the second order local explosions - the instability of the oblique waves of the TSCs originating under the effect of the first order (basic) local explosions, the third order local explosions - the instability of the oblique wave of the TSCs originating under the effect of the second order local explosions and so forth.

Maximum order of the local explosions along with all other peculiarities of the unstable detonation wave is governed by the BD phenomena. It follows from the fact that the local explosions follow the BD since the SCE in which they originate appears only after the BD. So, as soon as the BD does not take place the local explosions will not appear.

The oblique shock waves of the TSCs in the unstable detonation front are the SDs and their pressure is larger than that in front of the transverse waves of the same TSCs, the pressure of each next order oblique SDs and consequently the initial rate of explosive energy evolution just behind of its front being larger than these of the previous order. Due to the reason the BD probability in the front of each next order oblique SD becomes smaller in comparison with that of the previous one, so that eventually the oblique SD of some higher order will be stable.

It should be mentioned that the local explosion induction times in each unstable oblique SD waves increase away from the TSC triple point since the wave pressure decreases in the direction. Usually the dependence is very strong, so that the BD and the reinitiation cease at some distance from the triple point, the new local explosion appearing in the center of the islet if the islet size is sufficiently large. In that case one can consider a sequence of the BDs and reinitions with the beginning nearby the triple point and the end in the islet center as the single sequence.

At gaseous detonation in a strong tube the stationary detonation regime is governed by the tube diameter. The point is that the wave loses its energy at the expense of its interaction with the tube walls (friction and thermoconductivity), the wave energy loss increasing with the tube diameter decrease . It was shown experimentally that the wave inhomogeneity scale increases with the tube diameter decrease [33]. In accordance with the above-presented concept of the unstable detonation origin it means that the induction time of the SCE explosion in the wave front increases and the number of the local explosions decreases, so that at some tube diameter proper for each gaseous mixture the spinning detonation originates. It originates during the SD transition to the final stationary regime. Since the SD attenuates faster at the tube walls its front bends and chemical reaction breaks down first in the front at the wall. After the BD the unstable detonation wave front changes into the ordinary shock wave, the SCE layer originating behind its front. Some double-shocked substance has to appear owing to the inclined shock wave reflection from the wall. It is not improbable that the local explosions occur at the walls just within the double-shocked substance.

It seems likely that random local explosions appear at the walls just before the spinning detonation origin. Each explosion gives rise to a strong local divergent detonation in the initial substance. However, as noted above chemical reaction ceases in the strong divergent detonation front. From this point onwards the SCE detonation (that is the transverse detonation) spreads over the SCE-

detonation products interface in approximately a half-ring from. It is well-known that the spin head occupies only part of a tube radius [32,33]. In accordance with the foregoing concept of the detonation instability nature it means that the transverse detonation is discontinued at this distance from the wall. Specific reasons of the detonation cessation are not known. However, it stands to reason that it is also due to the chemical reaction breakdown in its front.

So the SCE transverse detonations originated at the wall are discontinued at some distance from it. However, the detonations run along the SCE layer edge around the tube diameter to meet each other. Let's assume that an explosion from the number of random local explosions appearing at the walls just before the spinning detonation origin takes place some time prior to the others and the transverse detonation waves originated by reason of the explosion break into run in both directions. Let's also assume that some local explosions appear in front one of these detonations. As it has been above-mentioned transverse detonation waves exits only until the meeting with each other during the basic SD transition to its final stationary regime. It means that all contrary transverse detonation waves of these local explosions will disappear, in this instance, except the most distant one which will continue its motion till the meeting with the other transverse detonation wave generated by the first local explosion.

Obviously the strength of the TSCs originated at different times is different. Therefore, their collisions will look as though the stronger TSC sweeps off the weaker one, that is the stronger TSC as if absorbs (eats up) the weaker one. By and large the collision process appears as the stronger TSC continuous motion and the weaker TSC death. At this very instant the spinning detonation will come into being if the explosion induction time of the SCE just in front of the SCE transverse detonation wave of the remaining TSC is larger than the time of the transverse detonation wave motion around the tube diameter.

Thus, it follows from the foregoing that the transverse wave is the principal element of the triple-shock spin configuration. It should be noted that Voitsekhovsky, Mitrofanov and Topchiyan have shown experimentally that the wave front is unstable, spinning detonation fine structure experimentally observed being the wave kinetic instability manifestation. However, it is evident that this wave instability has in all appearance a little to do with the stability of spinning detonation as a whole. It is likely that the existence of actually spinning (that is one-headed) detonation is governed by two circumstances. In the first place, SCE explosion induction time in front of the transverse wave has apparently to be larger than the time of the wave motion about the tube axis. Secondly, it is the oblique wave instability. The matter is that, local explosions can originate behind the oblique detonation wave front and it leads to the appearance of the second order TSCs which try to travel in all directions (like ring detonations of shock-compressed explosive). However, spinning detonation can come into being only under such conditions (initial pressure of gaseous mixture, tube diameter) when the second order TSCs suffer loss of their capability of traveling in the direction from the triple point of the first order TSC (as it is often observed in the case of liquid explosives). The fact means that chemical reactions cease (that is BD takes place) behind their transverse waves. The reverse statement regarding the second order TSCs motion is also valid: as soon as the TSCs regain their capability of traveling in all directions, spinning detonation will immediately transform into pulsating one.

It should be mentioned that the spinning detonation is not the limit of gaseous detonations as it was believed earlier [25-30]. Later so-called galloping detonation was discovered [51-53]. Along with the pulsating and the spinning detonations it originates from the SD, however, at smaller tube diameters than the spinning detonation. During the SD attenuation process the BD and reinitiation take place, the number of the local explosions decreasing to zero in the course of the process at the tube diameter proper for the galloping detonation. After that a cylinder of the SCE appears inside the tube under the effect of the detonation products high pressure, the cylinder length being considerably larger than its diameter. In some induction time characteristic of the SCE state the SCE detonation originates at the SCE-detonation products interface all over the tube cross-section. It means that the detonation appeared in one or some local explosions at the interface spends far

less time to spread all over the interface than it needs to overcome the shock wave of the SCE cylinder. So the SCE detonation front occupies all cross-section of the tube and when it consumes the SCE cylinder the SD in undisturbed explosive will appear again. After that the sequence of the above-mentioned events will repeat. From that point of view the sequence looks as though it were the detonation wave one-dimensional kinetic instability.

The spinning as well as the pulsating detonations differ fundamentally from the ZND detonation. The mechanism of initial substances transformation into their detonation products at the unstable detonation is of a radically different kind from the mechanism characteristic of the stable detonation waves which is implied to be described by the ZND theory. It is absolutely wrong to treat the instability as the manifestation of some fine structure of the ZND detonation wave model [32, 33]; it is absolutely wrong to consider that the TSCs of the unstable detonation front exits on the ZND detonation chemical spike level, that is to consider that the pressure of the straight waves of the unstable detonation front TSCs is equal to the ZND detonation chemical spike pressure. In reality chemical spike, in the ZND detonation theory sense, does not exists at all in the unstable detonation; it disappears as soon as the BD takes place during the SD transition to some final steady-state detonation regime. At the unstable detonation initial substance transformation into detonation products is largely brought about by the transverse detonation waves inside the SCE, the pressure of the straight shock waves of the TSCs in the unstable detonation front being approximately equal to the CJ pressure. The BD and reinitiation of chemical reaction were shown above to be the chief causes of the SCE and the transverse detonation waves origin in the unstable detonation wave front.

The followers of the CJ theory believed that explosive at the detonation changes into detonation products during its compression inside the detonation wave shock discontinuity zone (see [4] and references in). It should be noted that the followers know nothing at that time about the detonation instability. The matter is that there is no in fact any reaction at all in the shock discontinuity zone; initial substance is only compressed inside the zone. It changes into detonation products behind the zone at shock compressed state, the state pressure being equal approximately to the CJ pressure in spite of the fact that the detonation wave travels with the CJ velocity [33,21]. The finding seems to be absolutely impossible from the standpoint of the ZND detonation theory [8-10] since the theory implies that initial substance is at first compressed without any chemical change inside the front of the shock wave of detonation velocity, the detonation wave being beyond question stable. But gas detonations to which the CJ theory was applied at first are always unstable. The unstable detonation front pulsates, that is its CJ velocity is in fact average. The characteristic time of the pulsation is equal to the average space size of the front inhomogeneity over its surface divided by the SCE transverse detonation wave velocity. During this time different part of the front pulsate non-simultaneously. Nevertheless each part of the front changes its velocity from the velocity of the strong attenuating detonation till down (after the BD) the velocity of the shock of pressure somewhat smaller than the CJ pressure in the initial undisturbed explosive.

It is well-known that at liquid explosives detonation the SCE layer appears at lateral free parts of the detonation front of any uncovered cylinder charge [21,54]. The layer originates due to the BD in the detonation front under the lateral rarefaction waves effect. It is also known that the SCE detonation can originate in the layer and reestablish the detonation wave front over the whole charge diameter. However, the question whether the SCE detonation can rotate around the charge axis or not is still open. There was some informations that the spinning detonation in some liquid explosives had been observed [54]. However, in the light of the above-stated it seems unlikely. Most likely had been observed some pattern of the process of the detonation front restoration rather than the SCE detonation rotation around the charge axis.

There are some observations which are interpreted as manifestations of the spinning detonation in solid explosives (see, for example, [55] and references in). But the data are very restricted and the problem needs to be investigated further.

4. EM SHOCK WAVE CHEMISTRY

It follows from the foregoing that the limits of the SDT, the detonation kinetic stability as well as the d_f phenomena are governed by the BD, and the BD, in turn, is governed by the regularities of EMs explosion energy evolution. A long-standing investigations of the SDT process lead to the conclusion that condensed EMs change proceeds in the course of the process through so-called "hot spots" mechanism [21,56,57]. The conclusion was shared by many investigators (see the Proceedings of every Symposiums (Int) on Detonation) and the hot spots mechanism was intensively employed for numerical modeling of detonation processes (see, for example [58-62]) over a wide range of shock pressures from a few kbar to several tens of GPa.

Two experimental lines of attack were employed in the Department search of data on the regularities of EMs explosion energy evolution: first - the investigations of the SDT process and, second - the investigations of the detonation chemical reaction zone (chemical spike time t_{cs}) both versus EMs charge properties (initial density, particle size and their structure - single crystals or fragments of broken cast, nature of fillers in pores, EMs' structure - solid or liquid,...). It has been found out that there exists some shock wave pressure P^* characteristic of each EM charge such that EMs charge properties influence their explosion energy evolution rate under the shock effect of lesser intensity than the P^*, and vice versa EMs charge properties don't influence the regularities of their energy evolution at all under the shock effect of larger intensity than the P^* [63]. It means that surroundings influences on the regularities of EMs explosion energy evolution are dominant under the shock of lesser intensity than the P^*, that is EMs transformation proceeds through the hot spots mechanism at low shock pressures. It follows from the well-known fact that the mechanism is strongly governed by EMs charge structure. On the other hand, it means that the regularities are some properties of explosive molecules in themselves under the shock effect of larger intensity than the P^*, that is EMs molecules structure rather than their charge properties governs their energy evolution regularities.

It should be mentioned that the P^* value of each EM charge turns out to be smaller than the charge CJ pressure, that is the regularities of EMs explosion energy evolution at detonation are the properties of their molecules as well. In accordance with the inference it has been found out that the detonation chemical spike time t_{cs} does not practically depend on EMs charge properties; it depends only on the detonation wave pressure, the dependence being rather weak [64]. For example, t_{cs} for the detonation of TNT changes from $\approx$ 1.5 mks to $\approx$ 0.2 mks while the detonation wave pressure changes from 5 GPa to $\approx$ 20 GPa. It is obvious that the temperature of the explosive changes considerably in this same pressure interval. If the shock decomposition mechanism were the same as the mechanism under ambient conditions, the change in t_{cs} would be much greater.

In searching for an explanation for the $t_{cs}(P)$ weak dependence, a surmise on the possible break-up of explosive molecules in the course of explosive compression within the detonation wave shock front has come to mind; that is a suspicion has appeared that the ZND detonation theory concept regarding explosive molecules invariability during the compression process is invalid, the sequence of considerations being the following. It has been assumed after the ZND detonation theory founders that detonation reactions proceed in a similar way to thermal explosions. (The considerations proposed below are also valid for chain explosion regularities). It is known that during the explosion induction period (activation-stage time), which is the main part of the entire reaction time, only a small portion of the explosive decomposes but, the reaction later becomes of an explosive nature. It follows also from the theory that the activation-stage time of the explosive is a strong function of the explosive state and, on the contrary, the time for the final stages depends only weakly on the initial chemical state [48]. Logically the surmise - whether the reaction tail is only registered at detonation - is based on understanding various features of the explosion, which are that only a small part of the explosive decomposes during the explosion activation stage, and that the final stage of the explosion only depends weakly on the initial state. If this is so, it means that the process activation stage does take place during the explosive's compression within the shock front. In essence it means the following. Events which occur during the induction period of a thermal explosion take up most of the time of explosion. However, in a detonation the events proceed some orders of magnitude faster within the extremely narrow shock front zone. The final stages of both processes proceed rapidly

with times which depend only weakly on the initial state of the explosive.

It should be mentioned that it has since become clear that some experimental results testify in favour of the surmise. The point is that an induction period for detonation has not yet been observed in any of the explosives investigated. One has always registered a very sharp decrease of pressure (or particle velocity) within the chemical spike [21,65,66]. It corresponds to the maximum rate of the EMs energy evolution just behind the detonation wave shock front. Therefore, one could infer that the progress of the reaction had been conditioned by some preparatory process inside the shock front which is still beyond the reach of observation by present techniques. However, the possibility of the destruction of complex polyatomic molecules inside the shock front has been substantiated by special experiments in which samples of aromatic compounds (benzene, naphthalene, antracene) have been recovered and investigated after shock of $1.1 - 1.5$ GPa ($100 - 200°$C) intensity. It was found that the compounds partly decomposed ($\approx 1\%$), the destruction corresponding to the rupture of bonds of the benzene ring (see [67] and references therein). It should be noted that at the same static pressure and temperature the compounds investigated never decompose entirely [68]. At normal pressure and high temperature they decompose without breaking the benzene ring. Chemical ring condensation and hydrogen elimination happen during the process. Complete graphitization occurs when the temperature reaches $\approx 2000°$C [69]. Taking the above facts into account, one can assume that the data testify in favour of the specific action of the shock wave front, that is, the shock front effect is responsible for the unusual destruction products of the aromatic compounds observed in the experiments.

Many explosives are complex organic compounds. Therefore, the decomposition of the explosives molecules inside the shock wave front seems to be a highly probable process. The portion decomposed is not known at present. Obviously it is some function of the wave intensity and can be significant at the detonation of powerful explosives in which the chemical spike pressure amounts to ten or more GPas.

Naturally the question arises: What is the mechanism of the intrafront destruction of complex explosive molecules? There are some papers devoted to the problem [63,70-74]. The accumulation mechanism has been introduced for polyatomic molecules [71]. The gist of the accumulation mechanism is as follows. Because of a tremendous rate of material loading inside the SDZ ($\approx 10^{-13}$ s [75,76]), an excessively high translational temperature (overheat) appears at the beginning, and it is followed by the other-excitation of certain bonds. The overheat effect means a higher temperature level than the equilibrium one behind the front. The over-equilibrium translational temperature arises due to the fact that the kinetic part of the shock compression energy, which behind the shock front, is equally distributed among all the translational, vibrational and rotational degrees of freedom of the polyatomic molecules, is absorbed only by the translational degrees of freedom within the shock discontinuity zone. The maximum translational temperature overheat value is $T_{oh} = 2(n-1)(T-T_o)$ [73], where n is the number of atoms in a molecule, and T_o and T are equilibrium temperatures in front of and behind the shock wave front. It is obvious that due to the translational-vibrational relaxation process the energy of the transitional degrees of freedom is redistributed to the vibrational degrees of freedom. At first, the energy flow will be directed towards those vibrational degrees of freedom which are most easily excited. If the energy flow towards these degrees of freedom exceeds the loss owing to the vibrational-vibrational relaxation process, they will over-excite and decompose faster in the shock front than behind it, where the state is one of equilibrium.

The considerations presented above regarding the T_{oh} origin are phenomenological, however, they have been verified by direct simulation of the process of excitation of polyatomic molecules inside the shock front [73].

The origin of the translational temperature overheat is of great significance for understanding the mechanisms of the shock compression of complex molecules. The translational temperature overheat for molecules consisting of tens of atoms can be tens of thousands of degrees for shock wave intensities characteristic of the detonation of powerful explosives. At such temperatures the process of electronic excitation (activation energy $2-5$ eV [77]) and even the thermal ionization process (activation energy

$6 - 10$ eV [78]) become possible inside the overheat zone.

Thus the non-equilibrium dissociation of polyatomic molecules inside the detonation wave shock front can proceed in three ways: through the accumulation mechanism, through electronic excitation as well as by thermal ionization. The accumulation mechanism has been developed before [71,72,79]. The decomposition mechanism through thermal ionization has not been investigated so far. As far as decomposition by electronic excitation is concerned, there are some experimental data supporting the mechanism. For example, hexogen (RDX, cyclotrimethylene trinitramine) sample recovered in special ampoules after the effect of shocks of 2.0-4.0 GPa have been investigated by X-ray photoelectron spectroscopy and paramagnetic resonance methods [80]. It has been found that shock decomposition products of hexogen differ from those of its thermal decomposition, and are identical to those of the photochemical decomposition. The data testify in favour of decomposition by electronic excitation under the shock, because it is well known that the photochemical decomposition proceeds through the electronic excitation.

Besides the aforesaid, the significant assumption of some preliminary electronic excitation of the molecules, introduced to explain the experimentally observed correlation between the electronic structure of the molecules and their detonation ability should also be noted [81]. However, the assumption has been introduced without any reliable and convincing interpretation of the excitation. But from the results obtained by us it follows that it is just the high-energy molecular collisions inside the translational temperature overheat zone that are responsible for the excitation.

It is obvious that owing to the three aforementioned ways in which polyatomic molecules can be destroyed inside the detonation wave shock front, some active particle (radicals, ions and so on) will originate. The particles behave as if they had been injected into the compressed and heated explosive. Naturally, they influence the subsequent decomposition of the explosive behind the shock front (that is, during the second afterfront stage) in a state of chemical second afterfront stage) in a state of chemical and thermodynamic equilibrium when the translational temperature overheat and overexcitation of certain bonds disappear. The interaction of the explosive molecules with the active particles originating inside the front (that is, during the first intrafront stage) is the main process behind the front. As a rule, the activation energy for this interaction is low (5-15 kcal·mole^{-1}) [78]. Because of the low value of the activation energy the decomposition proceeds extremely fast and is almost independent of the temperature change.

Thus, in accordance with the above-presented conception of the detonation decomposition mechanism of condensed explosives reaction is homogeneous rather than by the hot spot mechanism. The mechanism regularities are the explosives characteristics. The decomposition process does not depend on the initial physical state of the explosive charge (powder, pressed, cast or liquid). The process consists of two stages. The principal stage is the first intrafront stage. Its duration is equal to the time necessary for the most slowly excited bonds of complex polyatomic explosive molecules to be excited ($\approx 10^{-10}$ s). The stage begins with the SDZ of $\approx 10^{-13}$ s time duration [71,75]. The activation and non-equilibrium destruction of some explosive molecules takes place during the first stage and it leads to the fast transformation of the explosive into the final detonation products during the second stage. Since the activation and destruction are endothermic processes the pressure has to increase inside the shock front of the steady-stationary detonation wave, and conversely the pressure decreases during the second afterfront stage for the total exothermic character of the stage chemical reactions.

So, the first stage largely governs the detonation decomposition regularities of condensed explosives. Unfortunately this stage has not been investigated yet. Some Raman spectroscopy techniques have been developed by French (see [82] and references therein) and American scientists (see [83,84] and references therein) for the investigation of shock processes. However, the spectral and time resolution of the techniques is for the present still insufficient. Indeed the spectral resolution of $10 - 20\%$ and the time resolution of about 1 ns have been achieved. It is evidently too low a resolution for the study of the problem discussed since the entire time of the intrafront stage is even smaller. Therefore, one now needs elaboration of theoretical and experimental methods of at least picosecond resolving

power. In that case one will have the possibility of studying the stage in detail. Obviously, until the problem is solved the chemical pathway controlling explosive energy release will be unknown. In this connection the femtosecond spectroscopy [85] is noteworthy; the matter is that the first mention was already made of its use for the problem study [86].

In spite of the fact that the detonation decomposition mechanism of condensed explosives presented above is still mostly qualitative, it is possible even now to advance a certain hypothesis: the highest detonation ability corresponds to the explosive, the electronic structure of which changes at compression in such a way that it favours the explosive molecules electron excitation, as well as explosives in which molecule bonds excitation times differ considerably from each other. However, the problem needs some further investigation. Probably it will be solved when the chemical pathways of molecules inside the detonation wave shock front are studied from the very beginning of explosive loading.

5. CONCLUSIONS

1. Thus, four novelties have been introduced into the detonation phenomenon investigations during last 50 years since the ZND theory advent. Two of them are experimental: first - the unstable detonation discovery; second - the elucidation of the cause of liquid explosives unstable detonation velocity weak dependence on charge diameter at considerable value of their failure diameter. These experimental findings have resulted in the discovery and introduction into detonation theory two new theoretical notions. One of them was named the breakdown (BD) of chemical reaction; the other - the shock discontinuity zone (SDZ). The SDZ denotes the whole process of complex polyatomic molecules excitation and destruction within shock wave front (10^{-10} s). In spite of the SDZ width (10^{-13} s) is considerable smaller than that of the shock front, the whole process was named the SDZ since the process main cause is explosive molecules translational temperature overheat originated just inside the SDZ owing to tremendous rate of substance loading within the zone.

The BD and the SDZ are interrelated in all detonation phenomena; the BD as if follows the SDZ. The SDZ is characterized by the endothermic processes of complex polyatomic molecules excitation and destruction inside the detonation wave shock front and the BD manifests itself behind the front where the exothermic processes of interaction of excited explosive molecules and active particles originated within the front proceed. As this takes place, the larger is the wave intensity, the larger number of the active particles originate inside the detonation wave shock front and at the same time the higher explosive shock compression equilibrium temperature is. It means that the larger is the wave intensity, the higher the explosive energy evolution initial rate is behind the detonation wave shock front and therefore the less probable the BD is. In the contrary, the weaker is the wave intensity, the lower the explosive shock compression temperature is and the smaller number of active particles originate inside the detonation wave shock front. It means that the weaker is the wave intensity, the slower the explosive energy evolution initial rate is behind the shock front and therefore the more probable the BD is. Thus, the more the SDZ manifests itself, the less probable the BD is. And in contrast, the less the SDZ works, the more probable the BD is.

The foregoing means that the BD can occur the most easily in the explosive which energy evolution rate behind the shock wave front is slow (these are usually weak homogeneous explosives - practically all gaseous mixtures as well as some liquid explosives) and the most difficult in the explosive which energy evolution rate behind the shock wave front is fast (these are usually power explosives).

Detonation waves in homogeneous weak explosives are usually unstable, chemical reaction ceasing and appearing continuously and nonsimultaneously over their detonation wave fronts [21,17,50]. The explosives detonation failure diameter theory has been elaborated [12,13]. According to the theory the failure diameter is governed by the depth till which the BD wave originating at the charge lateral free surface can spread over the detonation front to the charge axis.

Detonation wave front in power homogeneous explosives is stable; the BD does not take place in their detonation waves fronts during their strong detonation transition to the CJ detonation at the SDT process. However it happens at the charge lateral free surface. It has been shown experimentally

that the BD governs the failure diameter nature of both power and weak homogeneous explosives with stable detonation fronts [21]. However, these explosives detonation failure diameter theories have not been developed yet.

Detonation front in solid heterogeneous explosives (cast, pressed, ...) has to be stable (in the kinetic instability concept sense) since the BD does not usually take place over the detonation wave front. However, it should be mentioned that chemical reaction ceasing and reinvitation in the detonation wave front at the charge lateral surface have been observed in the case of some cast explosive charges [54,55,87].

2. The problem of a detailed mechanism of detonation is still a central point in the explosion science. To describe sufficiently enough various detonation processes some models of condensed explosives detonation are used. The models are based on different explosive shock decomposition mechanisms. Common short- comings of the model are the fact that each of them uses the same mechanism to describe explosive response to the shock effect within a wide region of pressure from units up to tens of GPa. It is in this way that the hot spots decomposition mechanism in its various versions is used most widely at present [58-62].However, from the foregoing follows that shock decomposition processes at low and high pressures proceed qualitatively differently. For instance, detonation decomposition of any explosive proceeds equally in both liquid and solid states at pressures larger than the P^* characteristic of each explosive [63]. (P^* is smaller than Chapman-Jouguet detonation pressure.) This means that the hot spots mechanism governed by the solid explosive's initial state does not work at high pressures. It works at low pressures ($P < P^*$, region I). In high pressure regions ($P > P^*$, region II) explosive decomposition is not influenced by the initial state; in the region the regularities of EMs explosion energy evolution are some properties of explosive molecules in themselves.

Thus, it is not correct to describe any explosive shock decomposition in wide pressure regions by only one mechanism. On the other hand, it is also incorrect to develop individual models for different pressures because the transition from the first pressure region to the second one often takes place at some detonation process progress. For instance, it occurs at the most frequently modeling process of detonation initiation by shocks of various intensity and time. Hence, one needs some joint model comprising explosive decomposition features characteristic of each pressure region.

In order to develop a detonation computation model with great predictive power, it is required that the physical model include all physical and chemical processes in explosive under the shock effect. A model of this kind has been elaborated [74,88].

ACKNOWLEDGEMENTS

The author is pleased to thank Prof. John H. Lee, Prof. Yojendra M. Gupta, and Prs. Simone Odiot for numerous fruitful discussions on condensed EMs detonation problems and the strong advise to write the paper.

REFERENCES

1. Michelson V.G., *Utshenie Zapiski Imperatorskogo Moskovskogo Universiteta, Moskva ISSUE 10*, (1891) 1-92.

2. Chapman D.L., *Philos. Mag*, 47 (1899) 90-104.

3. Jouguet E., *Mathem J.*, 6 (1904) 5.

4. Sokolik A.S., Self Ignition, Flame and Detonation in Gases (Academija Nauk SSSR, Moskva,1960)

5. Zeldovich Ya.B., Shock Wave Theory and Introduction to Gasdynamics. (Academija Nauk SSSR, Moskva, 1946)

6. Rosing V.O. and Chariton Yu.B., *Doklady Akademii Nauk SSSR*, 26 (1940) 360-361.

7. Campbell C. and Woodhead D.W., *J.Chem.Soc.*, (1926) 3010-3021.

8. Zeldovich Ya.B., *Zurnal Experimentalnoi i Teoretitsheaskoi Fiziki*, 10 (1940) 542-568.

9. Von Neuman J., Report on "Theory of Detonation Waves" (OD-02). National Defence Rosearch Committee of the Office of Scientific Research and Development (1942). Division B, Section B-1, Serial N 238.

10. Döring W., *Ann.Phys.*, 43 (1943) 421-436.

11. Chariton Yu.B., "On explosives detonation capability". Voprosi Teorii Vzrivtshatich Veshestv (1947), No 1, Academija Nauk SSSR, Moskva-Leningrad, pp.7-28

12. Apin A.Ya., Bobolev V.K., *Dokladi Akademii Nauk SSSR*, 58 (1947) 241-

13. Stesik Z.N., Akimova Z.N., *Zurnal Fizitsheskoi Khimii (Russ)*, 33 (1959) 1762 -

14. Beljaev A.F., Kurbangalina P.Kh., *Zurnal Fizitsheskoi Khimii (Russ)* 34 (1960) 603-

15. Apin A.Ya., Bobolev V.K., *Zurnal Fizitsheskoi Khimii (Russ)*, 20 (1946) 1367 -

16. Eyring H., Powelb R.E., Duffet G.H., and Paril R.B., *Chem.Rev.*, 45 (1949) 69-181.

17. Dubnov L.V., *Zurnal Fizitsheskoi Khimii (Russ)* 34 (1960) 2367-2372.

18. Evans M.W., *J.Chem.Phys.*, 36 (1962) 193-200.

19. Rempel G.G., *Vzrivnoe Delo, (Russ)* (1963) 39-56.

20. Bolkhovitinov L.G., *Vzrivnoe Delo (Russ)* (1976) 150-164.

21. Dremin A.N., Sawrov S.D., Trofimov V.S., and Shvedov K.K., Detonacionnie volni v kondensirovannich sredakh (Nauka, Moskva 1970); Detonation waves in condensed media (Translated from Russian by Foreign Technology Division, Wright-Patterson Air Force Base, O.H., Aug.1972).

22. Campbell C., and Woodhead D.W., *J.Chem.Soc.*, (1927) 1577-1578.

23. Campbell C., and Finch A.C., *J.Chem.Soc.*, (1928) 2094-2106.

24. Bone W.A., and Fraser R.P., *Philop., Trans., Roy.Soc. London*, 230 (1931) 363-385.

25. Rivin M.A., and Sokolik A.S., *Zurnal Fizitsheskoi Khimii (Russ)*, 18 (1936) 767-773.

26. Rakipova H.A., Troshin Ya.K., and Shchelkin K.I., *Zurnal Technisheskoi Fiziki (Russ)*, 17 (1947) 1409-1414.

27. Kogarko S.M., and Zeldovitsh Ya.B., *Dokladi Akademii Nauk SSSR* , 63 (1948) 553-556.

28. Mooradian A.J., and Gordon W.E., *J.Chem.Phys.*, 19 (1951) 1166-1172.

29. Kogarko S.M., *Zurnal Technitsheskoi Fiziki (Russ)* 28 (1958) 2072-2083.

30. Gordon W.E., Mooradian A.J., and Hasper S.A., *7th Symposium (International) on Combustion, London*, (1959) 752-759.

31. Shchelkin K.I., *Zurnal Experimentalnoi i Teoretsheskoi Fiziki (Russ)* 36 (1959) 600-606.

32. Shchelkin K.I., and Troshin Ya.K., Gasodinamika Gorenija (Akademija Nauk SSSR, Moskva 1963).

33. Voicekhovsky B.V., Mitrofanov V.V., and Toptshijan M.E., Detonation Front Structure in Gases (Sibirskoe Otdelenie Academii Nauk SSSR, Novosibirsk, 1963)

34. Shchelkin K.I., *Dokladi Academii Nauk SSSR* 47 (1945) 501-503.

35. Zeldovich Ya.B., *Dokladi Akademii Nauk SSSR* 52 (1946) 147-150.

36. Voicekhovsky B.V., *Dokladi Akademii Nauk SSSR* , 114 (1957) 717-720.

37. Voicekhovsky B.V., Mitrifanov V.V., and Toptshijan M.E., *Zurnal Prikladnoi Mechaniki i Technitsheskoi Fiziki (Russ)* 3 (1962) 27-30.

38. Manson N., *L'Office National d'Etudes des Recherches Detonautique, Paris* (1947).
39. Manson N., *Compt. Rend.* 222 (1954) 46-48.
40. Fay J.A., *J.Chem.Phys.* 20(1954) 942-950.
41. Dremin A.N., *Phil. Trans. R. Soc. Lond.* 339 (1992) 355-364.
42. Dremin A.N., *Dokladi Akademii Nauk SSSR*, 147 (1962) 870-873.
43. Dremin A.N., and Trofimov V.S., *Proceedings of the Tenth Symposium (Int) on Combustion, The Combustion Institute, Pittsburg* (1965), 839-843.
44. Dremin A.N., *Proceedings of the 12th Symposium (Int) on Combustion. Poiters, France,* (1968) 691-699.
45. Compbell A.W., Davis W.L., and Travis J.R., *Physics of Fluids* , 4 (1961) 498-510.
46. Chaiken R.F., *Journal Chemical Physics*, 33 (1960) 760-768.
47. Dremin A.N., *Fizika Gorenija i Vzriva (Russ)*, 4 (1983) 159-169.
48. Frank-Kamenetckij D.A., Diffusion and Heat Transfer in Chemical Kinetics (Nauka, Moskva, 1987).
49. Merzanov A.G., Zelikman E.G., and Abramov V.G., *Dokladi Akademii Nauk SSSR* , 180 (1968) 639-642.
50. Dremin A.N., *Progress in Astronatics and Aeronautics (Ed.-in-chief A.Richard Seebass)*, 153(1993) 105-111.
51. Meoradian A.J., and Gordon W.E., *J.Chem.Phys.* 19 (1951) 1166-1172
52. Manson N., Brochet C., Brossard J. and Pujol Y., "Vibratory Phenomena and Instability of Self-Sustained Detonations in Gases" 9th Symp. (Int) on Combustion, New York, Academic Press, (1963), pp.461-469.
53. Saint-Cloud J.P., Guerraud C., Brochet C., and Manson N., *Acta. Astr.*,17 (1972) 487-498.
54. Kozak G.D., Kondrikov B.N. and Oblomsky V.B., *Fizika Gorenija i Vzriva (Russ)* (1992) 93-98.
55. Kozak G.D., Kondrikov B.N. and Oblomsky V.B., *Fizika Gorenija i Vzriva (Russ)* 4 (1989) 86-91
56. Campbell A.W., Davis W.L., Ramsay J.B., Travis J.R., *Phys. of Fluids* 4 (1961) 511-521.
57. Dremin A.N., "On condensed explosives detonation decomposition mechanism" Symp. Int. on High Dynamic Pressure, Paris (1978), pp.175-182.
58. Lee E.L., Tarver C.M., *Phys. of Fluids* 23 (1980) 2362-2372.
59. Tarver C.M., Hallquist J.O., Erickson L.M., "Modeling Short Pulse Duration Shock Initiation of Solid Explosives" Proceedings of the 8th Symp. (Int) on Detonation, USA, Albuguerque, NM, (1985), pp.951-961.
60. Lobanov V.F., *Fizika Gorenija i Vzriva (Russ)* 16 (1980) 113-
61. Tang P.K., Johnson J.N., Forest C.A., "Modeling Heterogeneous High Explosive Burn With an Explicit Hot-Spot Process" Proceedings of the 8th Symp. (Int) on Detonation, USA, Albuguerque, NM, (1985), pp.52-61
62. Kim R., Sohn C.H., "Modeling of Reaction Buildup Processes in Shocked Porous Explosives" Ibid, pp.926-933.
63. Dremin A.N., Shvedov K.K., "On Shock Wave Explosive Decomposition" Proceedings of the 6th Symp. (Int) on Detonation (1976), USA, NSWC, White Oak, pp.29-35.
64. Shvedov K.K., Koldunov S.A., *Combustion and Explosions, Moscow, Nauka* (1972), 439-443.
65. Seitz W.L., Stacy H.L., Engelke R., Tang P.K., and Wackerle J., "Detonation reaction zone structure for PBX 9502". Ninth Symp (Int) on Detonation. Office of Naval Research, USA, (1989), pp.657-669.
66. Green L.G., Tarver C.M., and Erscine D.J., "Reaction zone structure in supra compressed detonating explosive" Ibid, pp.670-682
67. Dremin A.N., Babare L.V., "The shock wave chemistry of organic substances" Shock wave in Condensed Matter (ed W.J.Nellis, L.Seamar, and R.A.Graham), New York: American Institute of Physics, (1982), pp.363-381.

68. Block S., Weir C.E., and Piermarini P.J., *Science, Wash.* 169 (1970) 586-587

69. Magaril R.Z., Mechanism and kinetics of homogeneous transformation of hydrocarbons (Moscow: Khimija 1970).

70. Dremin A.N., "Modern problems of condensed explosives detonation study" Scientific Transactions of the Institute of Mechanics of Moscow State University, Moscow (1973), No 21, pp.150-157.

71. Klimenko V.Yu., And Dremin A.N., "On the Decomposition Reaction Kinetics in the Shock Wave Front" In Detonation, chemical physics of combustion and explosion processes. Chernogolovka: Institute Of Chemical Physics (1980), pp.69-73. (English Translation in Sandia National Laboratories, Rep.RS 3180 (81/38, Feb. 1981)).

72. Dremin A.N., "On the physical model of condensed explosives detonation wave" In Proc. Int. Symp. on Pyrotechnics and Explosives (ed J.Ding), Blijing: China Academic Publishers (1987), pp.497-505.

73. Dremin A.N., Klimenko V.Yu., Davidiva O.N., and Zoludeva T.A., "Multiprocess detonation model" In Proc. Ninth Symp. (Int) on Detonation. Office of Naval Rescarch, USA (1989), pp.725-728.

74. Dremin A.N., *Phil. Trans. R. Soc. Lond.* 339 (1992) 355-364.

75. Klimenko V.Yu., Dremin A.N., "The Structure of the Shock Wave Front in Liquids" In Detonation, Critical Phenomena, Physico- Chemical Transformation in Shock Waves (Russ) (ed. O.N.Breusov), Chernogolovka: Nauka (1978), pp.79-84.

76. Klimenko V.Yu., Dremin A.N., *Dokl. Akad. Nauk SSSR*, 251 (1979) 1379-1381.

77. Baltrop J.A., and Coyle J.D., Excited states in organic chemistry (London: John Wiley 1975).

78. Kondratiev V.N., Gas-phase reactions rate constant (Moscow: Nauka. 1971).

79. Dremin A.N., Klimenko V.Yu., Mikhailyuk K.M., and Trofimov V.S., "On decomposition reaction kinetics in shock wave front" In Proc.Seventh Symp.(Int) on Detonation (ed.J.M.Short), Naval Surface Weapon Center, USA (1981), pp.789-794.

80. Owens F.J., and Sharma J., *J.Appl.Phys.*, 51 (1979), 1494-1497

81. Odiot S., Peyrard M., Schnur J., and Oran E., *Int J.Quantum Chim.* 29(1986) 1625-1634.

82. Delpuech A.E., "The use of time-resolved spectroscopies in the study of initiation of explosive at molecular level" In Proc. Ninth Symp. (Int) on Detonation. Office of Naval Research. USA (1989), pp.172-179.

83. Schmidt S.C., Moore D.S., Shaner S.W., Shampine D.L., and Holt W.T., *Physics*, 1-3 (1986) 139-1954.

84. Schmidt S.C., Moore D.S., Shaner S.W., Shampine D.L., and Holt W.T., Coherent and spontaneous Raman spectroscopy in shocked and unshoched liquids (In "Advances in chemical reaction dynamics" (ed. R.M.Rentzepis and C.Capellos), New York: D.Reidel 1986) pp.425-454.

85. Lowin R., *Science* 238 (1987) 1512-1513.

86. Tarver C.M., Ruggerio A.J., Fried L.E., and Calef D.F., "Energy transfer in detonation of solid explosives" In Paper Summaries of Tenth Int. Detonation Symp., USA, Boston (1993), pp.95-97.

87. Howe Ph., Frey R., and Melan G., *Combustion Science and Tecnology*, 14 (1976) 63-74.

88. Klimenko V.Yu., Yakoventcev M.A., and Dremin A.N., *Chemical Physics (Russ)* 12 (1993) 671-680.

III ENERGY TRANSFER IN CONDENSED ENERGETIC MATERIALS (EMs) THEORIES AND EXPERIMENTS

1 GENERAL LECTURES

2 MOLECULAR MECHANISMS OF ENERGY TRANSFER IN EMs

3 SHOCK RESPONSE OF CONDENSED EMs - EXPERIMENTS

4 GENERAL DISCUSSION

4-1 Statements from Laboratories on the Experimental Assessment of the Molecular Mechanisms

4-2 Discussion

1 GENERAL LECTURES

Chairman : Roger Chéret, Inspecteur technique de la Direction des Applications Militaires

Phonon Lifetimes in Molecular Crystals with Isotopic Impurities ; S.Califano

Energy Transfer in Molecular Liquids ; S.Bratos

Single-Shot Femtosecond Spectroscopy of Reactive Organic Molecular Crystals ; Weining Wang, Dutch D.Chung, John T.Fourkas, Lisa Dhar and **Keith A.Nelson**

Discussion

JOURNAL DE PHYSIQUE IV
Colloque C4, supplément au Journal de Physique III, Volume 5, mai 1995

Phonon Lifetimes in Molecular Crystals with Isotopic Impurities

S. Califano

European Laboratory for Non Linear Spectroscopy, University of Florence, Largo E. Fermi, 50125 Florence, Italy

The subject of phonon relaxation is the study of the processes which contribute to the finite lifetime of phonon states in a crystal. Phonons are collective crystal excitations, coupled together through anharmonic terms of the crystal Hamiltonian. These phonon-phonon interactions are responsible of the finite phonon lifetime. In molecular crystals phonon lifetimes typically range from few picoseconds to some hundred picoseconds at the liquid He temperature. For very isolated phonon levels, lifetimes can even reach higher values, up to several nanoseconds. As the temperature increases the lifetime decreases, since the number of decay channels increases with temperature.

The anharmonic phonon-phonon coupling terms of the crystal Hamiltonian give rise to two basically different relaxation processes. The first involves the simple loss of phase of the collective excitation due to scattering processes with thermal bath phonons. The second process is due to the decay of the phonon energy into the thermal bath, i.e. to a depopulation of the phonon state. In addition crystal defects and impurities, in particular isotopic impurities, give further contributions to the lifetime.

For molecular solids a convenient theoretical approach to the dynamics of anharmonic crystal vibrations is the perturbative expansion of the hamiltonian in terms of phonon normal coordinates. The perturbation expansion can be carried out in principle to any order in the Van Hove expansion parameter, although in practice the inclusion of fourth order terms is already a major task. In order to investigate the convergence of the perturbative expansion, we have compared the lattice dynamics calculations with a computer simulation of bandwidths and anharmonic shifts for some simple molecular systems. These calculations show that the bandwidths converge already at the fourth order of perturbation whereas shifts converge at much higher orders.

The interpretation of the experimental results has been thus made in terms of elementary relaxation processes involving third and fourth order phonon-phonon coupling mechanisms. If only third order processes are present, the inverse lifetime must show a linear variation with temperature in the classical regime. The occurrence of fourth order processes produces instead a T_2 dependence of the inverse lifetime.

Lifetime measurements can be made either in the time domain

by ps time-resolved CARS spectroscopy or in the frequency domain by high resolution Raman and IR spectroscopy. The two types of experiments are equivalent in principle, since the Fourier transform of the time domain relaxation curves gives the band profile in the frequency domain.

We have investigated in details the effect of isotopic impurities on the phonon lifetimes. Experimental data were collected for isotopically pure $^{35}Cl_2$ and $^{32}S_8$ as well as for the corresponding natural crystals.

In the case of chlorine we have measured the Raman spectrum of natural and 99% isotopically pure $^{35}Cl_2$ crystals, in the lattice and in the internal mode regions, using a high resolution Raman spectrometer. Measurements were made on a wide temperature range to obtain the temperature dependence of the linewidth for both the lattice and the internal vibrational modes. The data were analyzed in terms of anharmonic interactions and contributions from the isotopic disorder. The lattice phonons are little affected by the isotopic disorder, while the internal vibrons are extremely sensitive to the presence of isotopic impurities. In the latter case the linewidths of the A_g and B_{3g} internal vibrons are about one and two orders of magnitude, respectively, larger in the natural than in the isotopically pure sample. The Raman spectrum of natural chlorine in the internal region is correctly reproduced by an harmonic lattice dynamics calculation weighted over the statistical distribution of the isotopic species in the lattice.

We have also measured the bandwidths of several phonons and vibrons in single crystals of isotopically pure ^{32}S, grown in our laboratory. For most of the bands a linear variation of the inverse lifetime with temperature was observed in the classical regime. For some others, however, a strongly non-linear variation was instead obtained. We have also measured the bandwidth of the same phonons and vibrons in crystals of natural sulfur containing 4.22 % of ^{34}S isotopic impurities. The bandwidths are in most of the cases much larger when the impurities are present and in addition the difference with the isotopically pure crystal is temperature dependent.

Using the formalism of the retarded Green's functions we have developed a theory of the influence of isotopic impurities on phonon and vibron frequencies and linewidths. The theory takes into account both harmonic and anharmonic processes in the crystal and yields a proper self-energy, developped up to the second order, that includes impurity-activated contributions depending on the concentration of impurities and on the ratio of the masses of the isotopic species. Central to the theory is a technique of averaging the anharmonic phonon propagators over the ensamble of impurity configurations. The most important result is that the imaginary part of the proper self-energy includes two different contributions to the bandwidth, one which is temperature independent due to harmonic scattering processes and one which depends on T, due to anharmonic scattering processes. These theoretical predictions are correctly verified by experiments.

References
(1) P. Procacci, G. Cardini, R. Righini and S. Califano
Phys. Rev. B, 45, 2113 (1992)
(2) L. Bussotti, M. Becucci, S. Califano, E. Castellucci and D. A. Dows
j. chem Phys, 1995 in press
(3) M. Becucci, E. Castellucci, P. Foggi, S. Califano and D. A. Dows
J. Chem. Phys. 96, 98 (1992)
(4) A. A. Maradudin and S. Califano Phys. Rev. b. 48, 12628 (1993)

JOURNAL DE PHYSIQUE IV
Colloque C4, supplément au Journal de Physique III, Volume 5, mai 1995

Energy Transfer in Molecular Liquids

S. Bratos

Laboratoire de Physique Théorique des Liquides, Université Pierre et Marie Curie, Case Courrier 121, 4 Place Jussieu, 75252 Paris cedex 05, France

Abstract : The existing information on the energy exchanges in molecular liquids is briefly reviewed. Main experimental methods are enumerated, and a phenomenological description of the observed material is given. The effects of various competing processes such as bond scission, conformational changes, twist-induced charge transfer, etc, are commented. Theoretical methods employed is this field, as well as difficulties inherent to them, are sketchily presented at the end.

1. INTRODUCTION

The purpose of the present paper is to review briefly the information on the energy exchanges in molecular liquids, and to transfer it from the liquid state physics to detonics. This task is difficult, experimental conditions being very different in the two fields. There is no similarity between the structure, at the atomic level, of a liquid sample in thermal equilibrium, and of a shock wave. The difficulty is further increased by the limited size of this review. It is then impossible to treat the problems in any comprehensive way ; only the most basic information can be given. Though, the resulting picture will hopefully be representative of the state of the art in the field.

2. EXPERIMENTAL METHODS

Early work on the energy transfer in molecular liquids was based on the use of classical spectroscopic techniques such as fluorescence or ultrasonic attenuation. For example, the average decay period, τ, of fluorescing material indicates that this is the order of magnitude of the lifetime of excited molecules. Various modes of deactivation of the electronically excited molecules may be studied in this way. From the other side, when absorbing an ultrasonic wave, the molecules of the liquid sample are vibrationally excited. As the absorption spectra depend on the energy relaxation rates, the latter are deducible from the experiment. A significative information has been collected in this way. Nevertheless, the real expansion of this field did not occur until the development of sensitive laser techniques. The time domain from the nano- to the femtosecond has been explored in this way.

The basic principles are as follows [1]. The system submitted to the investigation is a pure liquid, or a liquid mixture, in thermal equilibrium. A short and intense pump pulse is focused on the sample, bringing molecules to an excited vibrational or electronic level ; the saturation conditions are generally avoided. A nonequilibrium situation results ; the return of the system to the equilibrium is then monitored as a function of time. A number of methods have been invented for that purpose. (i) In a time resolved fluorescence experiment, the emitted radiation is analysed by employing devices for wave length selection, and a detection system including signal recording and data processing. Streak cameras and time-correlated single photon counting systems are of current use. (ii) In a pump-probe absorption experiment, a weak probe pulse monitors the changes in transmission, reflection or polarization after a variable delay time τ (Fig.1). For other experimental techniques, see Ref. [1].

The characteristics of the initial, pump-prepared state are as follows. The majority of degrees of freedom remain in, or close to, thermal equilibrium at room temperatures and pressures. Only some of

them are selectively excited to energies corresponding to high temperatures. For example, a 1eV electronic excitation corresponds to 11605°K, and a 1000 cm^{-1} vibrational excitation to 1440°K. The states representative of detonics are very different. A large number of degrees of freedom are exited to high temperatures. Moreover, statistical characteristics of the matter in the shock wave front are only poorly understood. Any attempt of transferring data from molecular physics to detonics thus requires much care.

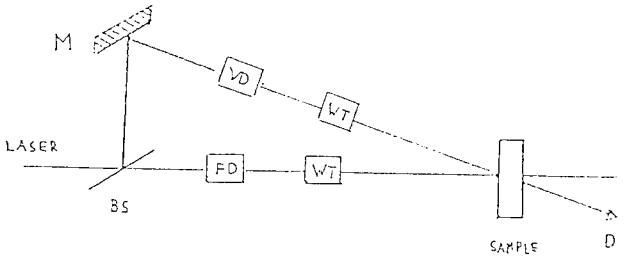

Fig.1 Picosecond pump-probe spectrometer (BS is a beam splitter, M a mirror, VD a variable delay device, FD a fixed delay device, WT a wavelength tuner and D a detector).

3. PHENOMENOLOGICAL DESCRIPTION

3.1 Generalities

Transitions between different molecular states, radiative or radiationless, are governed by selection rules. Those expressing the conservation of angular momentum, are particularly important. The overwhelming majority of liquids are formed by molecules which exist in a singlet ground state. Moreover, as spin and orbital momenta are only weakly coupled to each other, the rule of spin conservation is independently valid. Only singlet states are thus available for the absorption of light. The absorption process does not generate any significative distortion of molecular geometry (Franck-Condon principle).

3.2 Deactivation channels.

The subsequent discussion [1] is greatly facilitated by the use of the well known Jablonski diagram (Fig.2). According to the Franck-Condon principle, some vibrational excitation usually accompagnies electronic excitation. The primary relaxation process is then vibrational relaxation (VR) ; this process is very fast and is accomplished in few picosecond or less. It leads to a distribution of vibrational energy to other modes, or to a descent down the vibrational ladder of a given mode.

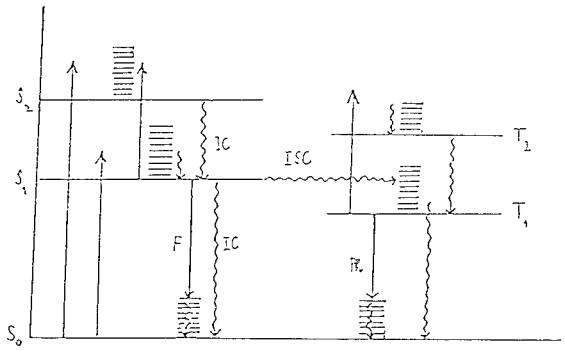

Fig.2 Jablonski diagram (S_0, S_1, S_2, T_1, T_2 are the singlet and triplet electronic states, IC indicates the internal conversion, ISC the intersystem crossing, F the fluorescence and Ph the phosphorescence). Straight lines represent the radiative, and wavy lines the radiationless transitions.

Once the vibrational relaxation is accomplished, the excited molecule may convert its electronic energy to vibrational energy of a lower electronic state of the same multiplicity, a process called internal conversion (IC). It is much faster for higher excited states than for the lowest excited singlet state. This fact is expressed by the Kasha rule according to which various conversion processes usually start from the vibrationally relaxed lowest excited state of a given multiplicity.

One of these processes is the radiationless transition from the lowest excited singlet to the corresponding triplet state, a process called intersystem crossing (ISC). Since it is forbidden, comparatively low rates are usually observed. Other processes are fluorescence, a radiative transition between two singlet states, and phosphorescence, a radiationless depopulation of the lowest triplet to the ground state. Characteristic relaxation times of all those processes are collected in Table I.

3.3 Competing processes

3.3.1 Bond scission.
Energy exchanges between molecules are often complicated by the presence of various competing processes. One of them is the rupture of a chemical bond A-B, producing either two oppositely charged ions $A^+ + B^-$, or two neutral radicals A +B. In favorable conditions, this process may be studied in real time conditions. For example, the reaction I - CN $\rightarrow$ I + CN was examined by setting up an experiment, in which ICN was first excited from the ground to the first excited repulsive state and next, after a time delay τ, from this state to another repulsive state (Fig.3). Knowing the R-dependence of the energy of the two repulsive states, the τ dependent separation of the fragments I and CN may be examined. This experiment was realized in the gas phase [2], but data are also available for liquids.

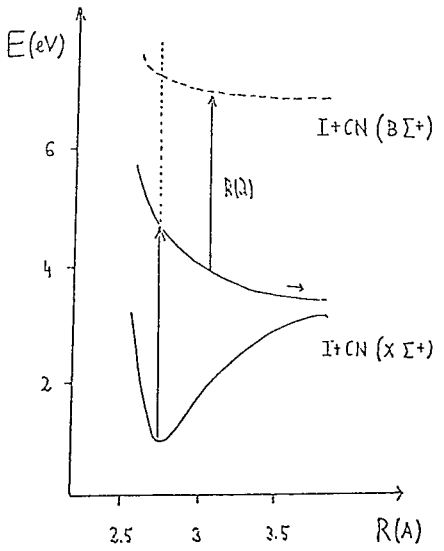

Fig. 3 Schematic presentation of the experiment permitting a real time study of dynamics of the ICN dissociation.

3.3.2 Conformational changes.
Geometrical changes may occur via rotation of a part of a molecule with respect to the remaining part. The spectral effect depends on the viscosity of the solvent [1]. If the isomerisation barrier height and the solvent viscosity are both low, a multiexponential decay of fluorescence is observed. Another observation is the conversion of the molecule, excited by the light absorption to a Franck-Condon state, to a local energy minimum of the first excited singlet state. Other spectral effects are described in the same reference.

3.3.3 Photoejection of electrons.
First reported in 1942, this process has frequently been observed in rigid solutions, but is also present in the liquid phase [3]. Photoionisation takes place either immediately after absorption, or after some delay ; there may be a barrier to the electron loss due to the resonance effects. Photoionisation can be monophotonic, biphotonic, or involve intermediate states between successive ionisations. Typical questions to be answered concern the rate of autoionisation, the nature of the intermediate states and the final fate of the resulting radical cation and of the electron. A number of systems have been investigated from this point of view.

3.3.4 Twist-induced charge transfer (TICT).
Subsequent to an electronic excitation, the TICT occurs in molecules composed of electron donor and acceptor subgroups. It is favored by appropriate conformation changes [4]. For example, a twisted configuration in which the two parts of the bichromophoric molecule are orbitally decoupled, is often representative. Arguments for the existence of the twisted configuration come mainly from the characteristic solvent dependence of the fluorescence, and from theoretical considerations. Although extensively studied, the detailed mechanism of the TICT is not yet entirely understood.

3.3.5 Solvatochromism
Solutions submitted to pico-or femtosecond light pulses often exhibit a time dependent fluorescence [5]. The origin of this effect is the variation of the electronic distribution of the dissolved molecule when it is electronically excited, and the subsequent reorganisation of the solvent around it. The experimentally measured quantity is the spectral response function

$$S(t) = \frac{\omega_p(\tau) - \omega_p(\infty)}{\omega_p(0) - \omega_p(\infty)} \qquad (1)$$

where $\omega_p(0)$, $\omega_p(\tau)$ and $\omega_p(\infty)$ indicate the peak frequencies of the fluorescent light immediately after the excitation, τ seconds after excitation and at very long times, respectively. In practice, some care must be exercised in determining $\omega_p(0)$ and $\omega_p(\infty)$. This experiment permits to explore the poorly known excited state charge distributions.

Table I
Representative lifetimes

Vibrational relaxation	$1 - 10^3$ ps
Internal conversion	$10^1 - 10^5$ ps
Intersystem crossing	10^6 ps
Fluorescence	$10^2 - 10^6$ ps
Phosphorescence	$1 - 10^2$ sec

4. THEORY

4.1 Semi-classical approach

Any theory of the energy transfer in liquids requires the knowledge of the electronic distributions inside a molecule, as well as that of molecules in the liquid sample. It thus associates two disciplines of a very different origin. Quantum chemistry permits the study of the electronic structure of molecules as well as that of intermolecular forces. The latter are most often considered to be pair additive, which reduces the N-molecule electronic problem to its 2-molecule analogue. Statistical mechanics, in its classical form, permits to study the motions of N molecules of the liquid sample, coupled under the influence of these forces. According to a well known rule, the classical approach is valid whenever the inequality $\hbar\omega/k_BT << 1$, where $\hbar\omega$ is a representative molecular energy, holds true.

The electronic problem is generally treated in the clamped nuclei, or Born-Oppenheimer, approximation. The currently employed methods are the self-consistent field (SCF) and configuration interaction (CI) methods [6]. The maximal size of the basic set of atomic orbitals is of the order of a few thousands, whatever method is used. If a precise determination of molecular properties is required, the molecule should not contain more than 15 atoms of the second row of the periodic system. In other cases, compromises are necessary ; a number of semi-empirical methods have been invented for that purpose. As far as the density functional method is concerned, see below.

The statistical part of calculation may conveniently be realized by applying the molecular dynamics or Monte Carlo methods [7]. The procedure consists in substituting to the real system a system of reduced dimensions. The latter contains, typically, 10^2 to 10^3 molecules. In the molecular dynamics method, the Newton equations of motion are solved numerically, by the help of a computer. Alternatively, in the Monte Carlo method, the configuration integral is calculated by a judicious choice of configurations representative of the system ; here again, a computer must be employed. The calculations are often large-scale calculations, and parallel computors may be necessary.

4.2 Quantum mechanical approach

The semi-classical theory just described is inappropriate whenever some nonelectronic degrees of freedom are quantum mechanical, e.g. the proton degrees of freedom in a proton transfer reaction. Even if this is not the case, fully quantum mechanical simulations may be preferable, e.g. in calculating intermolecular potentials in thermally inaccessible regions. Quantum numerical methods are actually under development, following the initial work by Car and Parinello [8]. The procedure is based on the density functional theory, and involves energy minimization procedures such as simulated annealing. Several versions of this method exist at the present time. Although not yet applied to problems covered in this paper, quantum simulations will certainly play a major role in the future of this field.

4.3 Applications

Theoretical methods sketched above permit, in principle, to study energy exchanges in liquids. At first sight, the situation seems much alike that currently encountered in the liquid state physics. Unfortunately, the present problem is in reality much more difficult. The first difficulty is that several electronic states, both singlet and triplet, are involved in calculations. Energies, charge distributions and intermolecular forces must thus be evaluated for each of them. As they are much less known than for the ground electronic state, the experimental control is fragmentary. The second problem is that energy transfer processes are often relatively long ; compare with Table I. As it is difficult, at the present time, to perform molecular simulation runs much longer than 10^3ps, it is impossible to follow an internal conversion process over a time interval as long as 10^5ps ! Brownian dynamics, in which the true intermolecular forces are replaced by an effective stochastic force, permits to prolongate the calculations to a certain extent, but not as much as desirable. Another possibility is to consider the Heller theory of the internal conversion in free molecules [9] ; this theory employs the overlap correlation functions. In spite of these difficulties, a number of problems have been treated successfully by the existing theory. Two of them are illustrated below.

The first example of a succesful application of the theory is the calculation of the vibrational relaxation time T in liquids. The starting point is the well known Landau-Teller formula for the transition rates

$$T_{ij}^{-1} = \frac{2\hbar^2}{1+\exp(-\beta\hbar\omega_{ij})} \int_{-\infty}^{\infty} dt \ \exp(i\omega_{ij}t) \ < V_{ij}(0)V_{ji}(t) > \qquad (2)$$

where $\hbar\omega_{ij}$ is the energy separation of the vibrational states i,j and $V_{ij}(t)$ the matrix element of the intermolecular potential between them. The latter is calculated, in principle, by employing quantum chemical methods, but empirical potentials are used too. The correlation function $<V_{ij}(0)V_{ji}(t)>$ is then evaluated by performing a classical molecular dynamics simulation of the liquid sample. A number of systems have recently been treated in this way [10], e.g. the mixtures CH_3Cl/H_2O, I^-_2/H_2O and the pure water.

The second, and the last, example concerns the solvatochromic effect. One generally assumes a linear solvation response, which permits to replace the spectral response function $S(\tau)$ by a simpler objet, the classical time correlation function

$$C(\tau) = \frac{\langle (\omega(\tau) - <\omega>) \ (\omega(0) - <\omega>) \rangle}{\langle (\omega(0) - <\omega>) \ (\omega(0) - <\omega>) \rangle} \qquad (3)$$

where $\hbar\omega(\tau)$ is the fluctuating energy difference of the two electronic states ; the average is taken over the ground electronic state distributions [11]. The above simplification, which makes the calculation of averages in the excited electronic state unnecessary, has been controlled by several authors. It was found satisfactory even for jump as large as a full electronic charge on the solute molecule. A good agreement between theory and experiment has been reported.

5. DISCUSSION

It results from the above discussion, that a large body of information is actually available on the energy exchanges in molecular liquids. Experimental techniques exist to study the underlying molecular dynamics up to the femtosecond time scales. Moreover, theoretical methods are powerful enough to analyse an important fraction of the experimental material. Unfortunately, the number of theoreticians working in the field is relatively limited ; this field certainly merits more attention.

The situation is more uncertain as far as direct numerical simulations of detonations are concerned ; see e.g. Ref.[12]. As the structure of the shock wave is virtually unknown at the atomic level, numerical simulations are highly desirable. In fact, a significative progress has been accomplished in this domain the last decade. New computer architectures and new numerical algorithms have been developped ; the systems submitted to the investigation are more realistic and include more spatial dimensions and chemical complexity. Nevertheless, a computer simulation always remains, to a certain extent, an experiment. The experience has convinced the liquid state physicsts that a long time is necessary before the quality of simulations can be assessed with certainty. This will no doubt be the conclusion of experts in this field too!

References

[1] V. Brückner, K.H. Feller and U.W. Grummt, Application of time-resolved spectroscopy (Elsevier, Amsterdam, 1990).
[2] M. Dantus, M.J. Rosker and A.H. Zewail, J. Chem. Phys. 87 (1987), 2395.
[3] J. C. Mialocq, J. Chimie Physique 85 (1988), 31.
[4] Z.R. Grabowski and J. Dobrowski, Pure and Appl. Chem. 55 (1983), 245.
[5] P.F. Barbara and W. Jarzeba, Adv. Photochem. 15 (1990), 1.
[6] A. Szabo and N.S. Ostlund, Modern Quantum Chemistry (Mac Graw Hill, New York, 1989).
[7] J.P. Hansen and I.R. Mc Donald, Theory of Simple Liquids (Academic Press, London, 1986).
[8] R. Car and M. Parrinello, Phys. Rev. Letters 55 (1985), 2471.
[9] E.J. Heller, J. Chem. Phys. 68 (1978), 2066.
[10] R.M. Whitnell, K.R. Wilson and J.T. Hynes, J. Chem. Phys. 96 (1992), 5354.
[11] M. Maroncelli and G.R. Fleming, J. Chem. Phys. 89 (1988), 5044.
[12] E.S. Oran and J. Boris, this book.

JOURNAL DE PHYSIQUE IV
Colloque C4, supplément au Journal de Physique III, Volume 5, mai 1995

Single-Shot Femtosecond Spectroscopy of Reactive Organic Molecular Crystals

W. Wang, D.D. Chung, J.T. Fourkas, L. Dhar and K.A. Nelson

Department of Chemistry, Massachusetts Institute of Technology, Cambridge, MA 02139, U.S.A.

Abstract

Recent progress in single-shot femtosecond spectroscopy is described. This methodology is necessary for ultrafast time-resolved observation of solid-state chemical reactions, since the build-up of reaction products which cannot be flowed away or otherwise conveniently removed causes spectroscopic signals to change (and samples to undergo deterioration) as a particular region of the sample is irradiated many times. The first single-shot femtosecond observations of molecular vibrations and of short-time response in a photoreactive crystal are discussed.

1. INTRODUCTION

The mechanisms of chemical reactions in energetic solids have come under intense study in recent years. Advances in theory and simulation have provided models for the dynamics of reaction initiation, propagation, and termination, with important insights into the disposition of energy among collective and molecular vibrations and electronic degrees of freedom. Unfortunately, there is scant direct experimental guidance for and testing of the models. Most spectroscopy of real energetic materials and their chemical intermediates is done at very low temperatures [1], where the lifetimes of metastable species may become long, on nanosecond or slower time scales [2]. However, under ordinary conditions, many of the initial energy transfer and chemical events which may lead to detonation take place on femtosecond and picosecond time scales. According to differing models [3], these fast events may include transfer ("up-pumping") of lattice vibrational energy to molecular vibrational or electronic degrees of freedom and early chemical events such as breaking (and in some cases forming) of covalent molecular bonds.

The experimental capabilities for femtosecond time-resolved spectroscopy of chemical reactions in gas and liquid phases are now well developed. Several femtosecond time-resolved measurements of reversible solid-state reactions, such as excimer formation in organic molecular crystals, have been reported. However, irreversible solid-state chemistry of the type occurring in energetic materials and many other reactive solids has never before been examined directly in the time domain. This has led to a dearth of experimental information about solid-state chemical reaction dynamics.

The experimental difficulty presented by solid-state photochemistry is the buildup of reaction products which cannot be flowed or otherwise conveniently removed from the region of optical observation. In contrast, gases and liquids can be easily flowed so that there is a continual replenishing of the irradiated volume with fresh sample material. As a result, the reaction products produced by the excitation pulse do not remain present to contribute to signal after successive excitations. In photoreactive crystals, the

accumulation of reaction products can significantly influence measurements even after only a few excitations (sometimes just one excitation shot), and in many cases the irradiated region of the crystal cracks and even decomposes after a modest number of shots.

To circumvent these problems, we have developed an experimental methodology which permits femtosecond time-resolved measurements to be completed in a single laser shot. This capability is acquired easily on slower time scales, where an excitation pulse can be followed by a cw or quasi-cw probe beam whose time-dependent transmission through the sample may be resolved by a streak camera (picosecond time scales) or a wide-bandwidth oscilloscope (nanosecond time scales). There are no electronic components or data acquisition devices which can operate on femtosecond time scales, and so the method we have developed is all optical in nature. Here we present a description of the method and preliminary data from a molecular liquid and a photoreactive organic molecular crystal.

2. SINGLE-SHOT FEMTOSECOND PUMP-PROBE SPECTROSCOPY

In conventional pump-probe spectroscopy, two focussed laser beams are crossed in a sample; one beam acts as the excitation ("pump") pulse and the other as the probe pulse. In order to scan the temporal response of the sample, the time at which the probe pulse arrives at the sample can be varied with respect to the pump pulse by varying the distance the probe pulse must travel before arriving at the sample. This method, though, requires multiple pump-probe cycles in order to acquire a complete set of data points covering the desired temporal range. Each pump-probe cycle provides only one point on the time axis.This is clearly unacceptable when examining an irreversibly photoreactive solid.

Our single-shot technique, in contrast to the conventional pump-probe experiment which retrieves the array of temporal data points with an array of variably delayed probe pulses, each of which follows a different excitation pulse, retrieves the temporal information with a single cylindrically focussed probe pulse. The approach [4] is illustrated in Fig. 1. In this method, both the pump and probe beams are cylindrically focussed such that they overlap with each other along a line at the sample. In addition, the beams are arranged such that they overlap at a substantial angle (typically about 25°) relative to each other. As illustrated in the Fig. 1, the pump pulse wavefront may arrive normal to the sample so that the entire irradiated region is excited simultaneously. Since the probe pulse is incident on the sample at a substantial angle away from the normal, different regions of the probe pulse arrive at the sample at different delay times relative to the excitation pulse. Consequently, the different parts of the probe beam are able to retrieve information about the sample's temporal response at different times. A CCD array detector is then used to measure the spatially encoded temporal response by measuring the intensity of the transmitted probe pulse along the cylindrically focussed line. Figuratively, the CCD array spatially resolves the single beam into an apparent array of probe pulses. Each element in the CCD array conveys a data point at a distinct time delay relative to the excitation pulse, and all the elements in the array together describe the response of the sample over an extended temporal range.

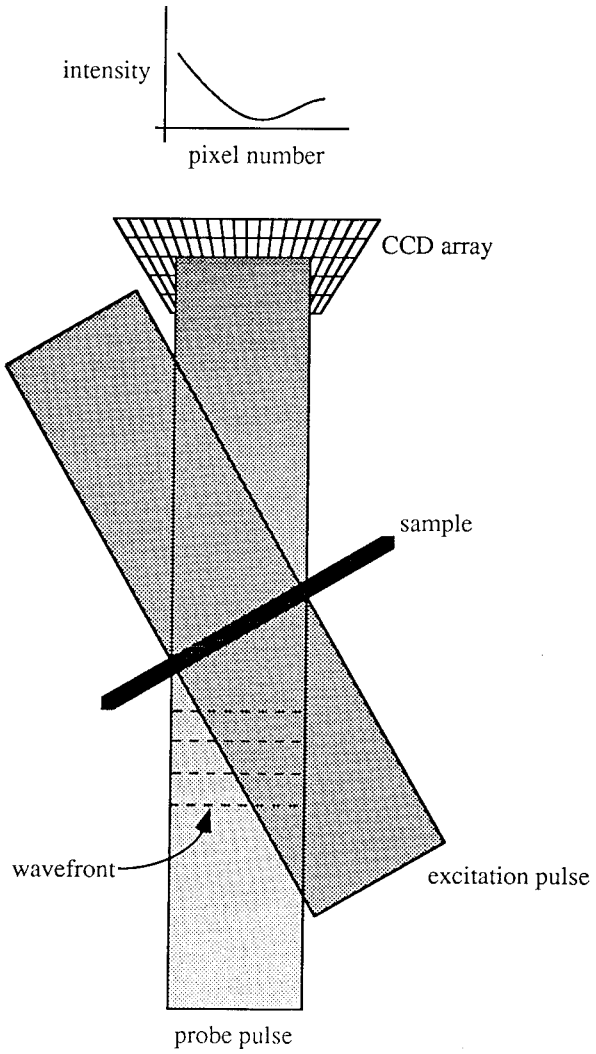

Figure 1: Schematic illustration of the single-shot technique

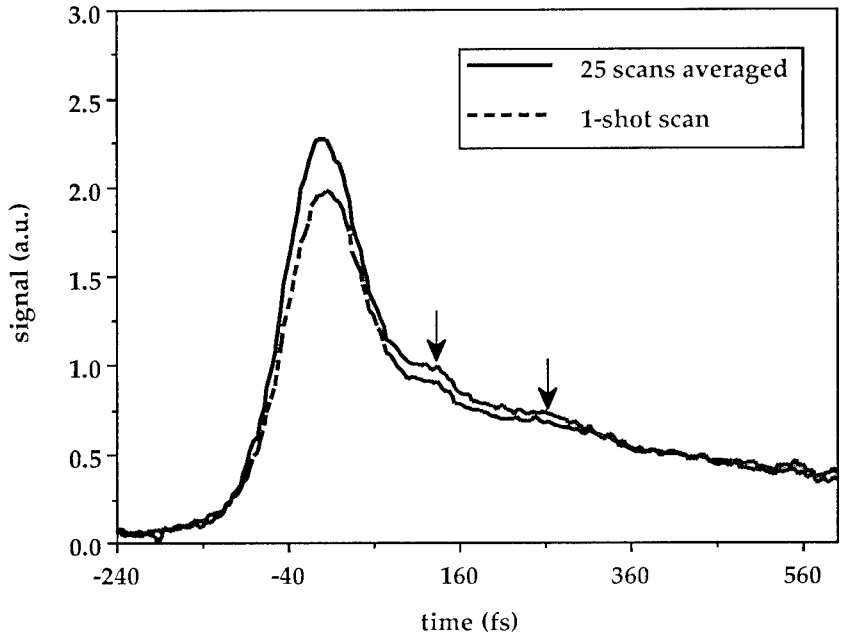

Figure 2: A transient absorption single-shot scan of ethyl violet in methanol compared to a 25-shot scan. The arrows indicate where the oscillations can be seen.

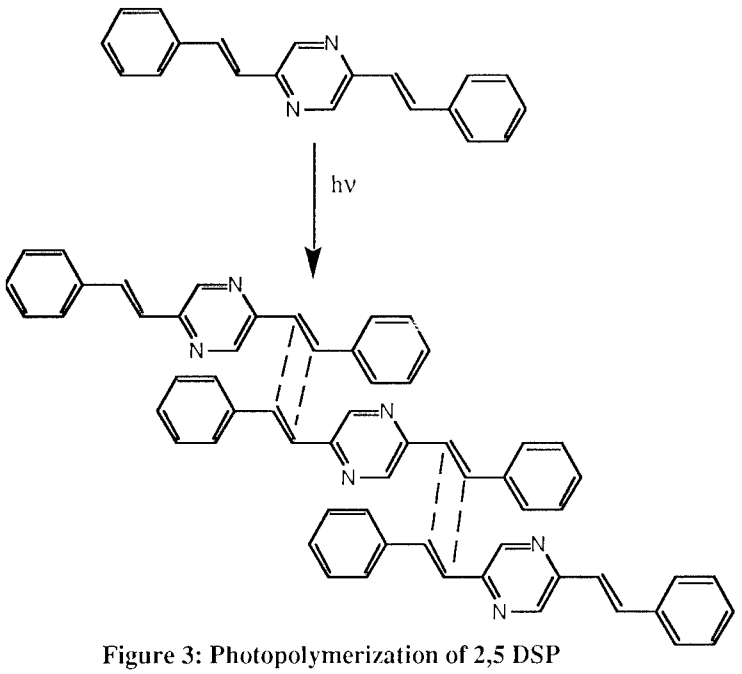

Figure 3: Photopolymerization of 2,5 DSP

3. REAL-TIME OBSERVATIONS OF MOLECULAR VIBRATIONS IN LIQUID SOLUTIONS

To demonstrate the single-shot technique, we first examined the relaxation dynamics of ethyl violet in methanol which has been already studied by conventional pump-probe spectroscopy [5]. The laser system used to conduct this experiment has been described in detail in an earlier publication [6]. Briefly, the femtosecond excitation and probe pulses at 620nm were generated by a sync pumped antiresonant ring dye laser which was pumped by the frequency-doubled output of a mode-locked Nd:YAG laser. The dye laser output was amplified in a three-stage amplifier chain which was pumped by a Nd:YAG regenerative amplifier. A mechanical chopper was used to reduce the pulse repetition such that the shutter on the CCD was able to sample only one pulse. The pulse width of the pump and probe was measured to be 72fs.

From the earlier study done by conventional pump-probe spectroscopy, it was found that with a sufficiently short pulse, ethyl violet dye exhibits a 155-fs oscillation. When the dye molecule is excited, the phenyl groups in the dye molecule rotate to a new conformation in the excited state. It is believed that the observed oscillations reflect coherent vibrational motion of the dye molecules which occurs in the electronic excited state reached through optical absorption. Encouragingly, the oscillations in Fig. 2 were found to match the vibrational period measured by conventional femtosecond pump-probe spectroscopy. Furthermore, the signal-to-noise ratio between scans from a single-shot data set and from a 25-shot data set were not significantly different.

4. PRELIMINARY RESULTS FROM A PHOTOREACTIVE CRYSTALLINE SOLID

Encouraged by the liquid-state results, we began a study of the photoreactivity of a molecular crystal, 2,5-distyrylpyrazine (DSP). DSP is a diolefin which undergoes [2+2] photoaddition at both olefinic positions when irradiated with UV light (Fig. 3) [7,8]. DSP crystal structure plays an important role in dictating its reactivity. It is known that DSP crystallizes in two crystallographic forms, one is photoreactive while the other is photostable. The reactivity difference was attributed to the different molecular packing in the two polymorphs. When the photoreactive DSP crystal is irradiated with light of wavelength longer than about 400nm, it forms oligomers with an average length of three monomer units. When it is further irradiated with light below 400 nm, the oligomers will polymerize.

While extensive studies have been done on DSP in the crystalline state [8], no ultrafast time-resolved study has been performed. In our experiment, we used a mode-locked titanium:sapphire laser (Coherent) pumped by an argon-ion laser (Coherent). The pulses from that laser were amplified through chirped-pulse amplification by a home-built regenerative amplifier [9] pumped by a home-built Q-switched intracavity-frequency-doubled Nd:YAG laser. The amplified output at 810nm was used as the probe pulse, and the frequency-doubled light at 405nm was used as the excitation pulse. The pulsewidth was typically 150fs.

The data collected from DSP in solution (chloroform) using the single-shot technique were found to be congruent to the data collected using the conventional pump-probe technique (Fig. 4). In the crystal, the almost parallel plane-to-plane stacking of the molecules should predispose it toward faster reaction than in solution. Surprisingly, it was found (Fig. 5) that the temporal response of DSP in crystalline form was identical to the temporal response of the molecule in solution in the 2-ps temporal range examined. In view of the high photochemical quantum yield of DSP [10], the primary pathway for population decay from the excited state should come from photoaddition and not from radiative or non-radiative energy transfer. Assuming the signal decay is proportional to the decay of the excited-state population from reaction, it appears, from the absence of any signal decay, that DSP does not react within the first 2ps of irradiation.

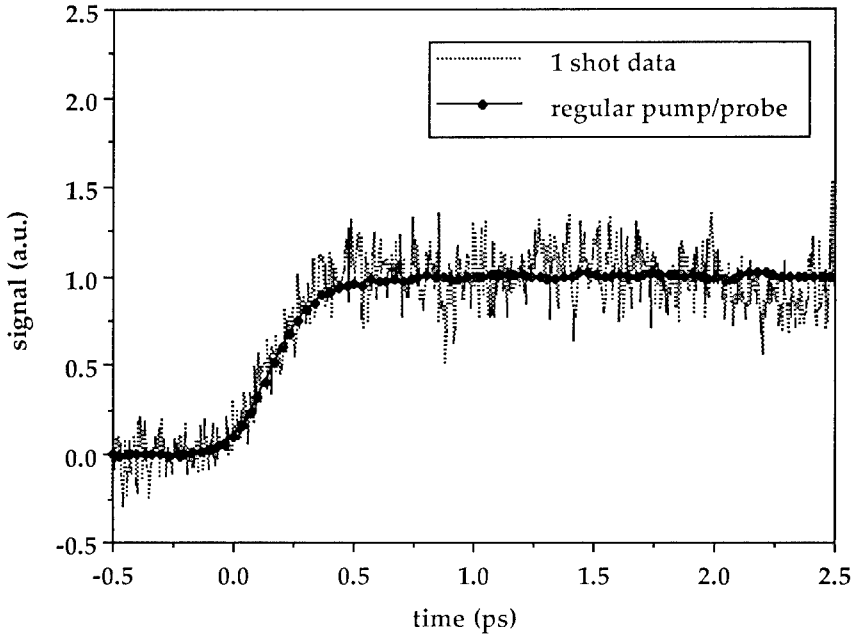

Figure 4: Single shot scan compared to a conventional pump-probe scan of 2,5 DSP in solution

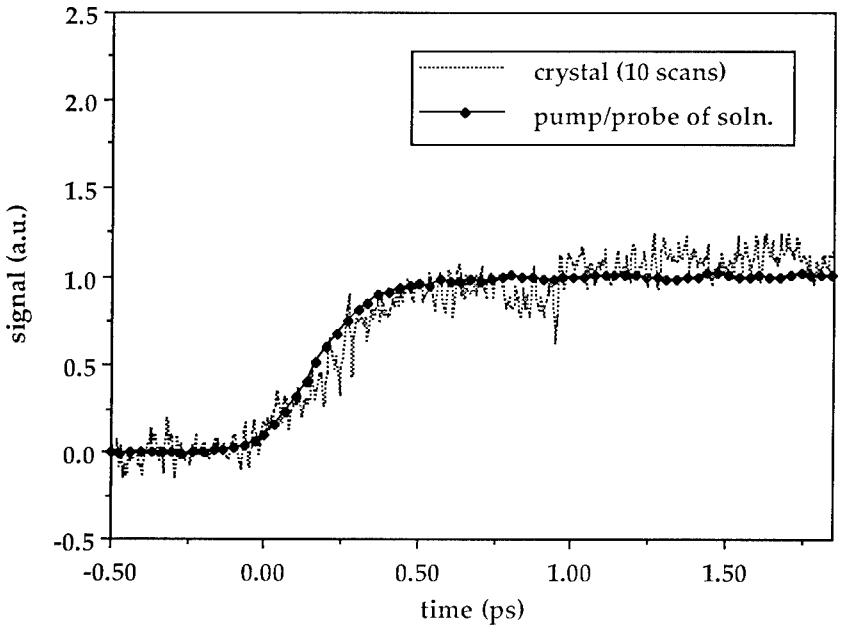

Figure 5: 10 averaged single shot scans of a 2,5 DSP crystal compared to conventional pump-probe data of 2,5 DSP in chloroform

When crystalline DSP is excited by light of wavelengths longer than 400nm, two transitions, $\pi^* \leftarrow \pi$ and $\pi^* \leftarrow$ n, are both excited. The non-bonding electron in the nitrogen from the pyrazine ring is excited in the $\pi^* \leftarrow$ n transition while the electron in the highest occupied π molecular obital is excited by the $\pi^* \leftarrow \pi$ transition. It is believed that the exciton formed from the $\pi^* \leftarrow$ n transition, which is localized and shows strong exciton-phonon coupling, helps to trap the delocalized exciton from the $\pi^* \leftarrow \pi$ transition and thereby facilitate the photoaddition at the double bonds on the styryl moiety [11]. In solution, photodimerization is expected to be slow since monomers must encounter each other to react. In the crystal, reaction might have been expected to occur on a faster time scale. There are at least two possible reasons why this reaction doesn't happen on a femtosecond time scale. First, localization of the initially excited exciton state may take longer than 2 ps. Second, even if the trapping process does occur quickly, it is possible that there is a potential energy barrier to molecular motion along the reaction pathway from the initial configuration to a higher-energy transition state and finally to the product.

Further experiments are under way to gain a deeper understanding of the DSP system. It is noteworthy as a demonstration of experimental capabilities that the irradiated regions of this material not only have a buildup of reaction product but undergo mechanical shattering and decomposition after just a few seconds of irradition at a 1-KHz repetition rate. This illustrates graphically the need for a single-shot experimental approach.

5. OUTLOOK

The study of ultrafast reaction dynamics in energetic solids requires single-shot experimental methods. We have demonstrated a suitable approach through measurements of liquid-state molecular vibrations and preliminary measurements of the short-time behavior of a photoreactive solid. Experiments on energetic materials are now in preparation. Measurements of solid-state chemical reaction dynamics promise to offer fundamental insight into the effects of the nonreactive surroundings in any phase. In energetic materials, the crucial effects of the surroundings in mediating energy exchange among reactive and nonreactive channels will be opened up for study through direct time-resolved observation of reaction dynamics and energy relaxation processes.

This work was supported in part by ONR Grant No. N00014-90-J-4070. DDC thanks the National Science Foundation for a predoctoral fellowship in chemistry. We thank N.M. Peachey (Los Alamos National Laboratory) and C.J. Eckhardt (University of Nebraska-Lincoln) for providing us the DSP crystals used in this study. We thank Yongqin Chen (University of California-Berkeley) for providing us a design of the Q-switched intracavity doubled Nd:YAG laser and Jeff Squier (University of Michigan) for help on the Ti:Sapphire amplifier.

6. REFERENCES

1. J.M. McBride and J.P. Toscano. *ONR/LANL Workshop Fund. Phys. and Chem. of Combustion, Initation, and Detonation of Energetic Materials.* (CPIA Publ. 589, March 1992), 71.

2. Y.M. Gupta. In *Shock Compression in Condensed Matter 1991*. S.C. Schmidt, Ed. North-Holland: Amsterdam, Netherlands, (1991), 15.

3. S.Chen, W.A. Tolbert, and D.D. Dlott. *J. Phys. Chem.* **98** (1994) 7759; L.E. Fried and A.J. Ruggiero. *J. Phys. Chem.* **98** (1994) 9786.; A. Tokmakoff, M.D. Fayer, and D.D. Dlott. *J. Phys. Chem.* **97** (1993) 1901; G. Gao, R. Pandey, and A.B. Kunz. In *Structures and Properties of Energetic Materials*. D.H. Liebenberg, R.W. Armstrong, and J.J. Gilman, Eds. Materal Research Society: Pennsylvania, (1993), 149. J.J. Gilman. *Philos. Mag. B.* **67** (1993) 207. T. Luty and R. Fouret. *J. Chem. Phys.* **90** (1989) 5697. F.J. Zerilli and E.T. Toton. *Phys. Rev. B.* **29** (1984) 5891.

4. L. Dhar, J.T. Fourkas, and K.A. Nelson. *Optics Letters.* **19** (1994) 1.

5. F.W. Wise, M.J. Rosker, and C.L. Tang. *J. Chem. Phys.* **86** (1987) 2827.

6. S. Ruhman, A.G. Joly, B. Kohler, L.R. Williams, and K.A. Nelson. *Revu de Phys. Appl.* **22** (1987) 1717.

7. M. Haswegawa, in Advances in Polymer Science, Volume 42, Springer-Verlag Berlin, Heidelberg, 1982. p.1.

8. H. Nakanishi, Y. Suzuki, F. Suzuki, and M. Hasegawa. *J. Polym. Sci. A-1*, **7** (1969) 753; J. Swiatkiewicz, G. Eisenhardt, P.N. Prasad, J.M. Thomas, W. Jones, and C.R. Theocaris. *J. Phys. Chem.* **86** (1982) 1764; E.M. Ebeid, and S.E. Morsi. *J. Chem. Soc. Faraday Trans. I.* **79** (1983) 1183.; E.M. Ebeid and N.J. Bridge. *J. Chem. Soc. Faraday Trans. I.* **80** (1984) 1113; J. Swiatkiewicz and P.N. Prasad. *J. Polym. Sci: Polym. Phys. Ed.* **22** (1984) 1417; N.M. Peachey and C.J. Eckhardt. *Chem. Phys. Lett.* **188** (1992) 462; N.M. Peachey and C.J. Eckhardt. *J. Phys. Chem.* **98** (1994) 7106.

9. F. Salin, J. Squier, G. Mourou, and G. Vaillancourt, *Opt. Lett.* **16**, 1964(1993).

10. E.M. Ebeid, M.H. Abdel-Kader, and S.E. Morsi. *J. Chem. Soc. Faraday Trans. I.* **78** (1982) 3213.

11. N.M. Peachey and C.J. Eckhardt. *J. Am. Chem. Soc.*, **115** (1993) 3519.

Questions - Answers, Comments

Dlott - Califano :

Q : How can your formalism be extended to consider localized phenomena such as the passage of a sharp shock front through a crystal ?

A : The scattering process is localized at every site where are impurities. What is delocalized is the concept of phonons.This concept of phonons is non localized because in the theory one develops any local transition in terms of phonons of the original crystal, as a basis functions. But the process is localized.

Rullière - Nelson :

Q : Gaussian beam shape leads to an inhomogeneous repartition of the excited state population. In single shot technics, this inhomogeneous repartition can lead to under/overestimation of the measured rates. How do you manage this problem ?

A : We examine the probe beam spatial profile very carefully on a single-shot basis, using a "reference" beam which reaches our CCD detector just like the transmitted "probe" beam. Separately, we examine the excitation pulse spatial profile - usually averaged over several shots. In practize we can now work with precision of about 0.1%. Ultimately our ability to measure small changes in the sample's absorption (i.e. small changes in probe transmission) is limited by how precisely we can characterize the beam profiles.

Q : With large spectral range probe beams it is very difficult to avoid the "chirp" problem. It means that along the beam diameter of the excitation beam, you will not have, for a given position, the same time reference for all wavelengths. How do you take into account this problem ?

A : In proposed experiments we will resolve both time and frequency, yielding a broadband absorption spectrum as a function of time in a simple shot. In this case "chirp", in which for example the redder part of the pulse arrives at the sample before the bluer part, presents a problem. Of course, as much as possible we'll eliminate chirp so that each part of the pulse has the same spectrum. But in any event, we must still use a "reference" pulse which, like the transmitted probe pulses is displayed in two dimensions (one for time and one for wavelength) on the CCD. In this manner we can correct for any chirp. As in the current 1-dimensional case (a "line" is displayed on the CCD, different points corresponding to different times), our precision will depend on how well we can characterize the reference beam and normalize the signal beam.

Melius - Nelson :

Q : Is it possible to use your multi-pulse Raman pumping to do state-selected intramolecular vibrational excitation (e.g. a C-H stretch or an O-H stretch) ?

A : Using ISRS as the excitation mechanism, no - because the frequency is too high. The pulse duration has to be short compared to one vibrational cycles and that would mean just a few

femtosecond in this case. But it is possible to convert visible fs pulses to IR fs pulses. These can drive polar modes directly, an IR pulse sequences can be made. In this way it may be possible to drive large OH amplitudes, for example.

Dufort - Nelson :

Q :What are the devices used to achieve wavelength conversion in your IR experiments ?

A : A difference-frequency mixing crystal can be used to convert a visible femtosecond pulse to an IR femtosecond pulse. If the IR pulse duration is too long then another (sum) frequency mixing crystal can be used to go back to the visible. This mixer can be gated by an ultrashort visible pulse to preserve good time resolution.

Q : What are the methods today - on a theoretical point of view - to investigate what will be the shifts of the vibration modes of the molecules under extreme conditions of pressure or (and) temperature of the detonation processes ?

A : At static pressure, not in real shock wave, it requires expertise but it is doable. To do it under shock loading requires extraordinary expertise and experimental apparatus that Dr Gupta would be able to do.

Q : In the reactive zone to analyse process of decomposition, among different patterns knowledge of the evolution of vibrational molecules is needed. How to do ?

A : Real spectroscopy in the reaction zone, we have not already a good solution.

Bratos : *Comment* In extreme conditions of high temperature and pression, the vibrational normal mode is no more a useful concept. Moreover, the distribution of vibrational modes is quasi continuous. In these conditions, the analytical treatments are particularly difficult, and numerical methods seem appropriate.

Dremin : We study shock energy transfer to molecules. Shock excitation is not the same process than laser excitation.

Under compression, even through a weak shock, EMs behaves like a liquid, and from an energetic point of view like a chaos. Is it possible to use the phonon concept for this state of the material ?

About chemical reactions, we are interested with the very very beginning of chemical change, shock mechanical energy transfer to EM. How does it proceed ?

Kondrikov - Nelson :

Q : Using one shot excitation you obtain a vibrational mode of a bond in the molecule, and the amplitude of the vibration is about 1-100 fm, essentially harmonic approximation. When you use your mechanism of multisteps excitation, the amplitude enhences in 10^3-10^4 times, and consequently you can include into the move all the neighboring molecules, so you transfer another vibrational, and breaking process. Am I right ?

A : First a clarification. Our "single-shot" method is for detection, not excitation. It allows us to do

experiments on irreversible events in crystals without warrying about the effects of permanent change on the "next" laser shot, which never comes. It's separate from ISRS excitation of lattice phonons, using single or mutiple pulses.

Concerning ISRS excitation, if we can reach large amplitudes we will certainly reach the anharmonic region with increased mode-mode coupling. The issue isn't coupling between one molecule and the others, since we are mainly concerned with collective (optic phonon) modes anyway, but coupling among different optic phonon and also molecular (vibron) modes. There are important non linear lattice dynamics effects that need to be considered, so that our optimum pulse sequence probably will not consist simply of evenly spaced pulses as in the harmonic limit. I think that pulse sequences will provide a factor of more than 10 on vibrational amplitude in many cases (resonance enhancement and higher pulse intensities that are possible on a single-shot basis will also help). With all this we should reach the 0.1-0.5 Angstrom vibrational amplitude regime in some cases.

When a rest is needed

Dufort - Nelson

Q : Pr Nelson, what is your opinion of the french school of Saussure, Foucault, Lacan, Derrida et al ?

Going back farther, could you comment on Rousseau versus Sade ?

A : Thank you for this opportunity. Rousseau was the father of modern Romantism, what essentially defines modern-day personality in the west. Unfortunately, he is also remembered for his proposal that man is inherently good and evil acts are due only to corrupting influences of society. This neglects deep-rooted anxiety and turbulence inherent in human character, in my view. The Marquis de Sade opposed this view by celebrating man's darker nature - the inevitable progression from Romantism to Decadence.

Foucault, Lacan et al. built on Rousseau's weak premises adding the central idea that all experience is constituted by language. This further disregards the complexity, turbulence and possibility for heroic struggle against the self that pervades human subconscious and conscious in my view.

2 MOLECULAR MECHANISMS OF ENERGY TRANSFER IN EMs

Chairman : Jacques Boileau, Expert DRET

I am in charge to introduce the lectures about mechanisms of energy transfers and molecular responses in energetic materials.

Generally speaking, the goal is to find a high explosive with high performances, associated with a high degree of safety and a reasonable cost. It must detonate under a programmated and strong enough initiation, but also remain quiet and without severe reactions under untimely stimuli. A way is to understand the SDT mechanisms of energetic materials.

1. General remarks

11. In the mechanisms, it is necessary to distinguish initiation and propagation of detonation : it is not always clear in the theories.

The initiation may occur by shock, and also by laser.

- It is necessary to define what is a shock : pressure, duration, eventually the delay to obtain the pressure. Then, what is the signification of a shock at a molecular size ? What is a shock on a crystal or on a liquid ?

- The effect of a laser pulse to initiate an energetic material can be a direct interaction with the molecules, or an intermediate initiation of a slapper. The mechanisms may perhaps be different, but it could exist a synchronization problem for the observation.

12. The sequence of successive events delays is important : subpico, pico, nano, microseconds. Do not forget these time scales in a range of 10 power 6 or 7 (the same ratio than between 1 second and 3 months). In this frame, some observations may be optical (laser) and/or electrical ones, e.g. emission or absorption of light...

Theories must be compatible or coherent with the observations and the experiments results. It is absolutely necessary, when a theory is presented, to imagine the simple, and, if possible, cheap and easy to build, experiments that may ascertain or invalidate the theory. The theory has to be able to explain the observations. Don't forget that theories may be correct in some domains and not in others. Sometimes, or often, some theories are simultaneously valuable.

2. Theories on detonation for macroscopically homogeneous explosives

They may be divided into two groups of mechanisms.

- Heterogeneous mechanisms : hot spots generated by voids and cavities, by shearing, by crystal defects, by steric hindrance effects (Armstrong, Coffey, Dick ..).

- Homogeneous mechanisms.

The discussion is : how the shock energy goes into the molecules and the crystalline lattice ?

The beginning mechanism is totally out of equilibrium. Molecules and atoms motions are quantified. Some theories (Fayer, Dlott, Tarver...) suppose a transfer to vibration modes without push of the molecules into excited electronic states.

Some other mechanisms suppose transitions to electronic states (e.g. predissociative) (Delpuech, Odiot, Sharma...)

The role of free radicals in the shock front has been emphasized by F.Walker.

An effect of bond breaking by shock has been proposed by Gilman ; he supposes also that the electrons ejected by this break form a plasma that plays a role.

Tang proposes a mechanism where the shock creates inhomogeneities similar to hot spots.

Dremin distinguishes domains for both heterogeneous and homogeneous mechanisms, giving an explanation about the energy transfer phases.

You will find successively the explanations given by S.Dufort, F.Walker, D.Dlott and A.Dremin.

I hope that the discussion allows to explain some observations :
For instance :

- The results described in the thesis of Spitzer on PETN monocrystals, for instance the light emission during the detonation process

- Why is it no evident correlation between sensitivity and critical diameter (e.g. HNS) ?

- Why some high explosives are more sensitive in a liquid than in a solid state (e.g. hydrazine nitrate, perhaps TNT) and the reverse for others (HNF_2, perhaps nitroglycerine) ?

- Other questions : are the mechanisms different for the same product in solid and in liquid phase ?

Don't forget also that sensitivity is a macroscopic observation which includes the measurement methods together with the characteristics of the crystals.

Les méthodes prédictives pour le développement de nouvelles molécules explosives ; S.Dufort

A new Kinetics and the Simplicity of Detonation ; F.E.Walker

Molecular Mechanical Energy Transfer behind the Shock Front - see 3-1 paper, Theoretical Model ; D.D.Dlott

EM Shock Wave Chemistry, see paper, Towards Detonation Theory, § 4 ; A.N.Dremin

JOURNAL DE PHYSIQUE IV
Colloque C4, supplément au Journal de Physique III, Volume 5, mai 1995

Les Méthodes Prédictives pour le Développement de Nouvelles Molécules Explosives

S. Dufort

Commissariat à l'Energie Atomique, Centre d'Etudes du Ripault, BP. 16, 37260 Monts, France

L'utilisation de méthodes prédictives permettant de juger, avant synthèse, des performances et de la sécurité d'un nouvel explosif constitue aujourd'hui un élément important dans l'organisation des travaux des laboratoires de chimie des matériaux énergétiques. L'emploi de telles méthodes est rendu d'autant plus nécessaire que les cahiers des charges apparaissent de plus en plus exigeants, tant sur le plan des propriétés physiques du matériau que sur celui du coût de la molécule. Dans ces conditions, la mise au point d'un nouvel explosif satisfaisant l'ensemble des contraintes ne peut plus résulter du seul talent du chimiste organicien, mais doit s'appuyer sur une véritable démarche d'ingénierie moléculaire intégrant les paramètres physiques, chimiques et économiques du problème.

Les études conduisant à l'établissement d'un outil prédictif peuvent se classer en deux grandes catégories :

- les méthodes fondées sur la recherche de corrélations empiriques par l'analyse statistique de molécules connues : c'est le cas, par exemple, de la méthode de Rothstein et Petersen pour l'estimation des pression et vitesse de détonation d'un explosif à partir de sa seule formule moléculaire brute,

- les méthodes issues de l'étude physique du comportement de la molécule soumise à une sollicitation, dans le but de comprendre les relations entre la structure du motif chimique et ses propriétés expérimentales.

C'est cette seconde voie qui a été développée, depuis près de vingt ans, par le Commissariat à l' Energie Atomique. Ce choix ambitieux est étayé par la mauvaise fiabilité des méthodes empiriques lorsqu'elles s'adressent à des molécules autres que celles qui ont servi à leur établissement. Nous présentons dans cet exposé le principe des travaux effectués, leur retombée en termes de conception de nouveaux explosifs et les perspectives offertes par les progrès des techniques théoriques et expérimentales.

I - Les bases physiques des méthodes prédictives développées au C.E.A.

a) *Structure chimique et caractéristiques de sécurité des explosifs (sensibilité au choc et stabilité thermique)*

Afin d'approcher à l'échelle moléculaire le comportement de l'explosif soumis à une sollicitation par choc, nous nous sommes intéressés, du double point de vue expérimental et théorique, aux modifications d'ordre structural subies par la molécule juste derrière le passage du front de choc et avant décomposition. Le recueil de ces informations, sans perturber le milieu observé, a nécessité la mise au point d'un montage de spectrométrie à haute résolution temporelle. Ce montage utilise la diffusion Raman de la lumière ; il permet, en un point bien localisé de l'explosif et dans un intervalle de temps très bref (10 ns), d'enregistrer les spectres de vibration caractéristiques de l'état de la molécule à l'instant de l'analyse. La comparaison des spectres obtenus au repos et derrière l'onde de choc renseigne sur la nature et l'ampleur des modifications apportées à la structure chimique de l'explosif. La figure ci-dessous illustre, à titre d'exemple, un résultat-type relatif aux bandes de vibration $N\text{-}NO_2$ de l'hexogène :

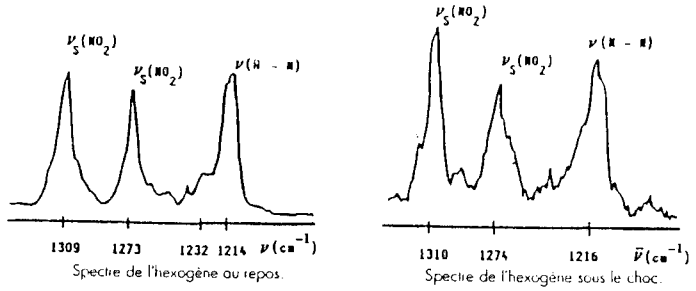

Spectre de l'hexogène au repos. Spectre de l'hexogène sous le choc.

De façon générale, et durant les 50 ns séparant le passage du choc du début de la décomposition chimique, les spectres obtenus se caractérisent par :

- des fréquences de raies peu perturbées, montrant que la géométrie de la molécule reste identique sous choc,
- d'importantes fluctuations de l'intensité des bandes, traduisant une profonde modification de la structure électronique de l'explosif.

Ces observations sont à la base des développements théoriques menés en parallèle autour de l'analyse de l'influence de la structure électronique d'une molécule explosive sur sa sensibilité au choc. Il s'agissait :

- d'une part, de comprendre et de modéliser les mécanismes d'interaction onde de choc - molécule,
- d'autre part, de dégager les paramètres caractéristiques de la structure électronique d'un explosif représentatifs de sa sensibilité au choc expérimentale.

Les méthodes de la Chimie Théorique nous ont permis d'amener des réponses à ces interrogations. Tout d'abord en assimilant le choc, à l'échelle microscopique, à une onde de compression entraînant sur son passage une diminution des distances inter - moléculaires et, par suite, une brusque variation des potentiels électrostatiques entre molécules. Le modèle d'interaction onde de choc - molécule se ramène alors à la perturbation d'un objet quantique (la molécule) par un front de potentiel voyageant à la vitesse du choc. Le développement par la Mécanique Quantique de ce principe a montré l'existence d'un processus non uniforme d'excitation à des énergies élevées, de l'ordre de quelques eV. Ce résultat, tout à fait original, conforte l'idée d'un mécanisme d'excitation conduisant à des niveaux électroniques spécialisés de la molécule.

D'autre part, l'analyse détaillée des états électroniques d'une soixantaine d'explosifs organiques a montré l'existence d'une forte corrélation entre l'évolution de la polarité de la liaison explosophore au cours de l'excitation et l'échelle expérimentale des sensibilités au choc. Cette relation, proposée par A. DELPUECH dès 1977, est à la base des calculs prédictifs effectués aujourd'hui afin d'évaluer la sensibilité des explosifs étudiés.

Une approche similaire a également été mise en oeuvre afin d'interpréter la réponse moléculaire aux sollicitations d'origine thermique. Dans ce cas, ce sont des mécanismes faisant intervenir l'état électronique fondamental qui sont pris en compte ; la plus faible énergie d'activation de dissociation d'une liaison chimique associée à cet état permet d'apprécier *a priori* la température de décomposition d'une nouvelle molécule.

b) Caractéristiques énergétiques des explosifs.

Le deuxième grand volet de notre méthodologie prédictive se situe au niveau des propriétés énergétiques de la molécule. L'évaluation de ces propriétés a nécessité la mise au point d'un outil numérique performant, le code ETARC (**E**quilibre **T**hermodynamique **A**vec **R**éactions **C**himiques). Ce code permet de proposer une description physique des produits de détonation à partir de la seule connaissance de la composition chimique de la molécule, de sa densité et de son enthalpie de formation. L'utilisation de ce logiciel a pour objectif de prévoir, outre les paramètres classiques pression et vitesse de détonation, l'énergie transmise au milieu connexe par l'expansion des produits de détonation.

II - Du prédictif à l'ingénierie moléculaire

L'ensemble de la démarche prédictive mise en oeuvre au CEA est rassemblée dans l'encadré 1. On remarquera, en plus des méthodes associées aux caractéristiques physiques de l'explosif (énergie et sécurité), le recours à un système expert de synthèse assistée par ordinateur (SESAME) chargé d'appréhender les grandes voies chimiques applicables à la synthèse d'une nouvelle molécule, compte tenu de sa structure. Ces informations, préliminaires à la décision de développement du nouvel explosif, constituent un élément fondamental pour juger de la complexité du procédé de synthèse (donc de son coût) et de sa capacité à supporter un parcours ultérieur d'industrialisation.

Quelle que soit l'efficacité des méthodes prédictives, la question importante reste malgré tout de savoir concevoir sur le papier un motif moléculaire en mesure de satisfaire les exigences de cahiers des charges très contraignants. La disponibilité de modèles établis par l'analyse approfondie du comportement des explosifs et l'expérience de l'application des outils qui en découlent à un grand nombre de molécules, débouche sur la compréhension du rôle joué par les différents groupements chimiques composant un édifice moléculaire. Il en résulte de véritables "règles de construction", que nous illustrerons par l'exemple du DANTNP. Cette molécule devait répondre à trois objectifs :

- un objectif de thermostatibilité (température de décomposition > 300°C),
- un objectif de sensibilité au choc ($H_{50\,\%}$ (5 kg) > 60 cm),
- un objectif énergétique : gain de 20 % par rapport au TATB.

La conception du DANTNP repose sur deux étapes d'ingénierie moléculaire :

1. Mise en évidence par les études de Mécanique Quantique de l'intérêt du motif amino-nitro-triazole (ANT) comme générateur d'insensibilité,

2. Greffage de deux de ces motifs sur un cycle thermostable afin d'assurer l'énergie et la tenue thermique du matériau.

La synthèse du DANTNP a été réalisée et une composition explosive élaborée. Ses propriétés, prévisionnelles et expérimentales, sont regroupées dans l'encadré 2.

III - Perspectives

Cette présentation dresse l'état des connaissances acquises dans nos laboratoires; si elles se sont d'ores et déjà traduites par de grands progrès dans la rationalisation de nos recherches, des points particuliers doivent encore être éclaircis :

- au niveau de la densité, dont la prédiction par des méthodes empiriques conduit bien souvent à des valeurs éloignées de la réalité. Les progrès observés dans le domaine de la **M**écanique **M**oléculaire devraient permettre d'améliorer les choses, grâce à une capacité accrue à prendre en compte des systèmes polymoléculaires simulant l'état solide.

- au niveau de la manière dont l'explosif délivre son énergie dans le temps, paramètre sans doute plus important que la vitesse de détonation pour le dimensionnement des édifices pyrotechniques. Le développement de nouvelles méthodes spectrométriques aptes à identifier les mécanismes chimiques accompagnant la décomposition est un maillon essentiel pour la modélisation du processus de détente des produits de détonation.

Ces deux points font actuellement l'objet de recherches actives au CEA

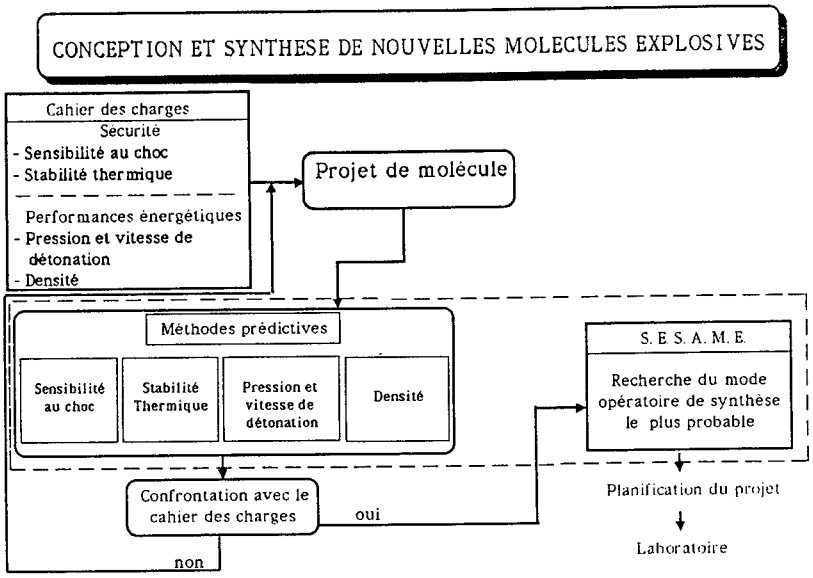

	Objectif	Prédictif	Expérimental
Sensibilité au choc (5 kg) - cm	> 60	60 - 70	70
Thermostabilité	> 300	> 300	350
P_{CJ}	> 330	330	327
Densité		1,85	1,865
Vitesse de détonation (m/s)		8100 - 8200	8200
W / W TATB	+ 20 %	+ 18 %	+ 15 %

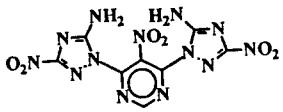

JOURNAL DE PHYSIQUE IV
Colloque C4, supplément au Journal de Physique III, Volume 5, mai 1995

A New Kinetics and the Simplicity of Detonation

F.E. Walker

Interplay, Danville, California, U.S.A.

ABSTRACT

The results are presented from three experiments, as well as a number of molecular dynamics and quantum mechanics calculations, which cast in serious doubt the validity of some concepts and theories of detonation. This doubt led to numerous studies in search of more satisfying concepts, and the quite surprising results of several of those studies are given. Particularly, a new concept of the kinetics of shock-induced chemical reaction is presented. This process, designated as physical kinetics, is described as a nonequilibrium, nonthermal process in which chemical reaction rates are determined and regulated by the averaged vibrational velocities of the bonded atoms in condensed systems under the influence of high velocity shock waves. These velocities limit the advance of the kinetic energy which leads to the very high impact velocities of the atoms and molecules which cause massive bond fracture in the molecules in extremely short times. The majority of the free atoms and radicals and other highly activated species formed then react in very short times (10^{-14} to 10^{-12} s), often in chain reactions, to provide the chemical energy which maintains the enormous level of kinetic energy at the detonation front. These high levels ensure that many reaction pathways are available--not only those with the lower activation energies or barrier potentials. It is in this regime of the detonation process that the more normal chemistry begins and then continues in other subsequent reactions to produce the adiabatic expansion forces and the final product mixtures. It is shown that this detonation model based on the new kinetics model, with the major initial reactions occurring in times of the order of tenths of picoseconds and in distances on the order of tens of angstroms--in the shock or detonation front--can provide a precise and satisfying mathematical and physical description of detonation phenomena.

INTRODUCTION

There are a number of experiments and calculations from molecular dynamics, MD, and quantum mechanics, QM, which cast in serious doubt the validity of what have been called the classical concepts and theories of detonation. (Ref. 1)

Presented here are a new concept of kinetics (Ref. 2), applicable particularly to shock-induced chemical reactions, but also in many other very fast reactions, and a very different theory of detonation, with a simpler rationale that contributes to the confidence in and the utility of its application. The principal elementary physical principles used as the basis for the kinetics are the Hugoniot relationship ($P-P_o = \rho U_s U_p$), a concept of the momentum transfer of the shock energy, and a consideration of the efficacy of the kinetic energy of the atoms and molecules in a shock front in the mechanical fracture of covalent bonds in extremely short times. It will be shown that a detonation model based on this kinetics model, with the major initial reactions occurring in times of the order of tenths of picoseconds and in distances on the order of tens of angstroms--in the shock or detonation front, can provide a precise and satisfying mathematical and physical description of detonation phenomena.

Particularly, strong phenomenological evidence and data will be presented supporting the proposals that the kinetic energy from the shock forces, with the addition in a few tenths of a ps of a large fraction of the available chemical energy to the atoms in and near the front, can fracture serially a major portion of the covalent bonds of an explosive. The detonation velocity can now be calculated from the weight-averaged shock velocities of the component elements of the explosive. This method of calculation demonstrates that a minimal contribution to the detonation velocity is made by equilibrium thermal processes or thermodynamic factors, and that a key factor is simply the Hugoniot relationship (shock velocity versus pressure) of the elements of the empirical formulae of the explosives.

BACKGROUND

The microscopic details of the chemical and physical phenomena by which a few grams of a seemingly quiescent and stable organic material can be converted in one or two microseconds into a mainly gaseous product, at temperatures of 2500-5000 K and pressures up to nearly 400,000 atmospheres, have eluded explosives scientists for more than a century. It will be shown herein that two very simple empirical equations and one other physically-meaningful equation can provide values of detonation velocities as well as or better than complex computer codes (Ref. 3), and that the new physical kinetics provides a rational explanation of the microscopic details of the phenomena.

If we review the data on 14 commonly-used explosives, we find they have, as measured and calculated, detonation pressures, P_d, covering a range of 13.0 to 39.0 GPa and detonation velocities, D, from about 6.32 to 9.11 km/s. It is seen now that a three-fold increase in P_d increased D by only 44%. It is important to consider also that a velocity of 9.11 km/s is also 9.11 angstroms/10^{-13} s. This means that the atoms in the detonation front are being accelerated by momentum transfer on a ps time scale to energies near 5 eV, and the front is crossing the covalent bonds of these organic compounds in one to a few vibration periods. This indicates that there is sufficient energy to break most of the bonds in the explosives molecules to provide many reaction pathway options,* not simply the ones with the lowest energy barriers or activation energies, and that this fracture can occur in time scales near 10^{-14} s. (Ref. 3)

Experiments and molecular dynamics calculations (Ref. 1) give strong evidence that the width of the shock front is on the order of 50 angstroms, with a rise time in the ps range.

*This consideration also provides a rationale for low velocity detonation in an explosive initiated at a lower shock pressure, as well as for the increase in D for nitromethane with diethylenetriamine. It is feasible that a stable reaction regime could be established with less massive bond fracture, leading to a lower level of chemical reaction in and near the detonation front and thus a lower P_d and detonation velocity.

The MD studies further show that a major (about 80%) part of the energy of momentum transfer in the front, which begins to flow into the vibrational component in the molecular bonds in a few femtoseconds, has risen to levels near 4 eV in about 80 fs. MD studies also show that this violent energy fluence or flux (about 5 eV/ps) causes scission of covalent bonds by impact, compression or shear forces to produce very energetic free atoms and radicals in excited states. (Ref. 1,2,3)

In a momentum transfer involving an N atom at 8 km/s with 4.72 eV of kinetic energy to a surface N-N couple with a bond strength of 1.06 eV, there is a high probability the bond would be broken and the exterior N atom would be given translational energy of about 3.5 eV and a velocity of 6.5 km/s. (Ref. 3)

Three of the reasons it is important to have a new detonation theory are now discussed. (See Ref. 1) We completed a series of experiments on the low-pressure (5.1 to 6.5 GPa) initiation of nitrometnane, NM, (Ref. 4) and found (1) that the time to initiation was about 4 orders of magnitude shorter than predicted by the thermodynamic theory, and also (2) the pattern of the initiation process was much different from the classical model. (Ref. 4) We also carried out a series of initiation experiments in which diethylenetriamine, DETA, was added to NM. (Ref. 5) One observation from this series was (Reason 3) that the detonation velocity of the NM was increased to about 6.72 km/s from the nominal measured value of 6.32 km/s for neat NM, by the addition of only 0.05% of DETA. This would not be explainable with the thermodynamic concepts, but it is easily defended under the new theory presented herein. In fact, we proposed that the DETA would provide NH radicals and free N and H atoms which could provide new chain reaction pathways to increase the energy release rate. A calculation using the Skidmore-Hart equation (Ref. 1) for overdriven detonations showed a probable very high P_d of about 19 GPa had been attained. Using the new equation given later (based only on the elemental Hugoniots) for calculating D's, we see that the new D should have been near 6.7 km/s for the NM with o.o5% DETA, as we measured. (Ref. 1)

DEFINITIONS

Physical Kinetics. In detonations and some other very fast and shock-induced reactions, the rates of reaction are determined by the physical limitations of the advance of the activating energy of bond fracture through the reacting materials. This is essentially a nonthermal, nonequilibrium process related to the shock velocities, U_S, of the individual elements of the reactive materials.

Detonation. The new detonation theory, based on the concept of physical kinetics, includes the experimental and calculational observations that nearly all of the covalent bonds of the explosives molecules are broken or rearranged within the detonation shock front (about 20-100 angstroms) by impact, compression and shear forces, and that the majority of the free atoms and radicals and other highly activated species formed then react in very short times (10^{-14} to 10^{-12}s) to release chemical energy which maintains the enormous levels of kinetic energy at the detonation front. Other subsequent more normal reactions provide the adiabatic expansion forces and the final product mixtures. Since the molecules are essentially broken down to their elements in the shock front, the detonation velocities are determined by the weight-averaged shock velocities of the elements of the empirical formulae. It follows that thermodynamics has only a secondary role, and there is probably insufficient time in this initial phase for the anharmonic coupling of excited phonon modes with the low frequency molecular vibrations.

NEW CONSIDERATIONS OF SHOCK VELOCITY

The basic equation for shock velocity calculations is the Hugoniot relationship, $P-P_o = \rho U_S U_p$, where P is shock pressure, ρ is density, and U_S and U_p are shock and particle velocity, respectively. However, it appeared, from some information from MD calculations, that one might be able to calculate shock velocities of the condensed elements from simply the data in the periodic chart--atomic weight, atomic radius and density. Studies in this regard led to the equation,

$$U_s = \left(\frac{r_a}{w_a}\right)^{\frac{1}{4}} \rho^{-0.1} f(P) \qquad (1)$$

where $f(P) = (0.42P + 10.3P^{\frac{1}{2}} + 12)$ for most of the elements, and only a slightly modified f(P) gives excellent results for those elements with relatively large atomic radii. The attainable accuracy is shown in Fig. 1 (Ref. 6) This accuracy corresponds well with the precision of the data.

The next step in this line of investigation was to determine if the Hugoniots of organic compounds could be calculated from the U_s versus P information calculated for the elements. Again, a quite simple equation was derived,

$$U_{sc} = \sum(U_{si} f_i) \qquad (2)$$

in which U_{sc} is the shock velocity of the compound, the U_{si}'s are the shock velocities of the elements of the compound at a given P, and the f_i's are the weight fractions of the elements obtained from the empirical formulae of the compounds examined. (Ref. 7) This equation also gives very good results.

A Hugoniot "experiment" was conducted with a series of MD calculations in which the velocity of an impacting plate was increased in increments, and the resultant shock velocities in a representative covalently-bonded lattice were measured. (Ref. 1) The shock velocity values obtained, using two covalent potentials spanning the normal range found in organic compounds, are given in Fig. 2. Also given are the measured shock velocities for a number of organic plastics and explosives. It can be seen that the MD calculations compare favorably with the data. This fact adds confidence to the MD study of shock processes.

It was determined that the average relative vibrational velocities, ARVV's, of the covalent atomic pairs (C-H, N-H, O-H, C-N, etc.) could be calculated from thermal motion measureable in x-ray crystallographic data and, also, from the infrared spectrographic frequency data for specific bonds. (Ref. 8) A somewhat surprising and interesting correlation of these results with other shock phenomena is given in Fig. 3, where it is seen that all of the detonation velocities lie in the cross-hatched

area which includes the shock velocities and the ARVV's of the C-H, O-H, and N-H couples. (Ref. 9)

To obtain more precise values of the ARVV's, a series of QM calculations of the values for 10 selected atom pairs found in organic explosives was calculated using the least-squares fit of the diatomic potentials to Hulbert-Hirschfelder functions. (Ref. 10) The plot of these values versus energy levels for the 10 atom pairs is given as Fig. 4. The calculations show values of the ARVV's comparable to those calculated from the infrared and x-ray crystallographic data. These values all correspond closely to the shock velocities we calculated for the C, N, O elements and pairs with H and for the organic compounds examined. These considerations will be shown to be key factors in the new kinetics and detonation concepts.

KINETICS DISCUSSION

In 1975, Henry Eyring (Ref. 11) showed that the ordinary concepts of chemical kinetics must be modified significantly to explain observed reaction rates in some shocked hydrocarbons and explosives. He proposed a concept which he designated as "starvation kinetics" to help explain why the high temperature (more than 1200 K) decomposition of the different materials in his studies had nearly the same reaction rate, even though the low temperature (less than 500 K) rates were rational, different from each other, and described quite well by Arrhenius principles. If the decomposition is assumed to obey first-order kinetics, then the logarithms of the rate constants at high temperature for all the materials Eyring studied were nearly equal and in the rather narrow range of 5.5 to 6.5.

Even when one makes the obvious comments that first-order kinetics is probably not the only order involved and that both decomposition mechanisms and rates probably would change significantly over such a wide range of temperatures, this should in no way lead to the conclusion that all of the high temperature rates presented (see Fig. 5) should be nearly equal nor should they be approximately equal to first-order Arrhenius rate constant

logarithms of 5.5 to 6.5. However, in the concept of physical kinetics, and with reference to the observations and calculations of shock velocities and the ARVV's, these rates should be about equal, and they should coincide with pseudo-first-order Arrhenius rates, as measured and observed. The rates for the detonation reactions fall in this range. (Ref. 9)

The alternative kinetics concept presented herein is that there is a physical regulator of the rate of transfer of the decomposition energy (principally, the atomic vibrational energy) from one molecule to the adjoining molecules or from one vibrating bond to others in its immediate vicinity. This regulator is the effective ARVV's of the vibrating atoms in the material while it is under shock loading. This nonthermal, nonequilibrium reaction kinetics, regulated by this energy transfer process, is designated as physical kinetics.

Early indicators for the requirement for a new kinetics hypothesis were these two observations: (1) Shock and detonation waves are moving past the atoms in condensed materials on the same time scales as the vibrational frequencies of the organic bonds; and (2) there is enough energy in a moderate shock front (about 7 GPa) to mechanically fracture a C-N or N-O bond in a representative chemical explosive, RDX (hexahydro-1,3,5-trinitro-1.3.5-triazine). (Refs 3,12) The nominal energy of a C-N bond in RDX is 0.37 aJ (10^{-18}J), and for an N-N bond it is 0.17 aJ. The kinetic energy of an O atom or an N atom moving at 8 km/s would be 0.86 aJ or 0.76 aJ, respectively. Thus, through momemtum transfer the impact of an O or an N atom of these energies on an exterior C-N or N-N couple could mechanically fracture the bond. (Refs. 3,13)

The vibrational velocities of the atoms in an organic molecule are of the same velocity scales (km/s or angstroms/10^{-13}s) as shock and detonation velocities. They can be calculated with a simple equation from infrared spectroscopic data, $V = \nu cu$, where V is the vibrational velocity, ν is the infrared-derived vibrational frequency in cm^{-1} of a specific bond (i.e., C-H, N-H,

O-H), c is the velocity of light, and u is the nominal distance relative to each other the specific vibrating atoms move in one vibration.

A key argument in support of physical kinetics and the importance of shock velocities in determining detonation velocities is given in Fig. 6. (Refs. 2,13) Here the averaged Hugoniot measurements for a number of organic compounds and the elements C, O, and N are plotted in comparison with the unreacted Hugoniot for TATB (s-triaminotrinitrobenzene), ρ = 1.876 g/cm^3. These two curves are very nearly congruent. Also plotted in Fig. 6 are the D's and P_d's of 15 common, but both chemically and energetically diverse, condensed explosives.

What is clearly evident is that the detonating explosives have velocities at their detonation pressures only slightly higher than the shock velocities of the inert materials. A curve representing a 10% increase to the shock velocities of the nonexplosive elements and compounds was added to the graph to compensate for the higher temperature in detonation, and all of the explosives, except NM which is only slightly outside, are included within this parameter. (Refs. 2,13) Thus, it appears that any thermodynamic factors can have only a minimal effect in determining detonation velocities.

The chemistry immediately following the initial bond fracture (about 10^{-13} to 10^{-12} s) is extremely important. By adding sources of new free radicals and thus new reaction chains, the rate of energy release can be increased, and higher pressures can be attained. This can lead to higher detonation velocities and to smaller critical diameters, as seen in the NM-DETA experiments. It has been demonstrated that very low levels of additive (less than 0.1%) have large effects. (Refs. 5,13,14,15)

The addition of 0.08% DETA to NM-acetone mixtures yields a decrease of 80% of the mean cell size in the detonation. Addition of 0.1% DETA increased the acceptable dilution for detonation by 35.7%. Finally, 0.03% of DETA in NM reduced the critical diameter by 43%. (Ref. 13) These data support our observed increase in the D of NM with 0.05% added DETA.

MASSIVE BOND FRACTURE

The BTNEA Experiment. A homogeneous ideal explosive, bis-trinitroethyl adipate (BTNEA) was synthesized with isotopic labels (C^{13} and O^{18}) introduced into the positions indicated in Fig. 7. This explosive was chosen for this experiment, because it appeared that the CO and CO_2 molecules expected as detonation products were already formed, and the isotopic labels would be found in the CO and CO_2 products.

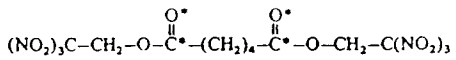

BTNEA

Figure 7. The structure of bis-trinitroethyl adipate. The asterisks indicate carbon atoms of isotope 13 and oxygen atoms of isotope 18.

The explosive was detonated in a bomb calorimeter in which the products were collected and then analyzed for the isotopic ratios. (Ref. 16) The experimental results, in Table 1, show that the ratios of C^{12}/C^{13} and O^{16}/O^{18} are essentially the same for all of the product species containing C and/or O, and they are nearly equal to the isotopic ratios in the initial BTNEA sample. The analytical values of the ratios were said to be well within the experimental error of the determination. The conclusion that is obvious is that almost every covalent bond was broken, the atoms were scrambled, and they were randomly combined into the detonation products. Quoting from the paper, "We must conclude that, in the case of the homogeneous ideal explosive, all of the bonds of the original explosive molecule are, in effect, broken during the detonation process. These molecular fragments then must recombine in a statistically random fashion prior to the kinetic "freeze out" of products during the adiabatic expansion. Certainly, diffusion on a molecular level cannot be an important rate controlling process." (Ref. 16)

Comparative results of massive fracture of covalent bonds in and near a shock front in simulated organic matrices have been observed in the MD calculations of many workers and in our studies. (See Refs. 1,9,10,17,18-21) In many other experimental

studies the mechanical scission of chemical bonds has been observed or proposed (Refs. 2,10,22-25), and it has been demonstrated in numerous shock-induced chemistry experiments. (Ref. 22) (See Figs. 8a,8b)

Data and information reported from reaction dynamics experiments appear to correlate very well with data and calculations from the study of detonation. The development of femtosecond lasers and their combination in experimental systems with the molecular beam technique, for monitoring energy states immediately before and after a chemical reaction, have provided an effective method for observing the transient state, TS, in a reaction as it forms and divides into products. (Refs. 26-28)

The results of reaction dynamics, RD, studies of a system in which a van der Waals molecule, IH···OCO, undergoes UV photolysis which accelerates the H atom to about 20 km/s toward the OCO molecule, thus forming the TS, show the appearance of an OH signal in about 5 to 15 picoseconds after the deconvolution of the TS. In another experiment involving the decomposition of ICN, it was reported that the TS has a lifetime of about 200 fs and a translational velocity of about 2 km/s. This shows that this TS exists for about four vibrations of the IC-N bond, and that the ICN molecule rotates about only 7^{o} during this period. The energy reported to be available for this reaction is about 0.87 eV, or near 7000 cm^{-1}. (Refs. 27,28)

This experimentally-derived information appears to be directly related to data and calculations (MD and QM) seen in the study of detonation (and initiation) of chemical explosives. There appear to be many fundamental correlations in these two chemical physics regimes--molecular and atomic velocities in km/s and reaction times in the ps range. (See Ref. 3)

CALCULATION OF DETONATION VELOCITIES

From the foregoing data and discussion we can now present the perceived simplicity of this theory of detonation. For more than 100 years scientists around the world have struggled to obtain or derive equations, computer programs, sophisticated

theories, and erudite and exotic equations-of-state, EOS, to use to calculate accurately detonation velocities. This has been accomplished, but in an often complex and complicated manner, with large computer codes.

Following are three amazingly simple equations that are used successfully to calculate detonation velocities with a high degree of accuracy. (Refs. 1,7,29) The results from the second and third show correlation coefficients with large sets of data of 0.971 and 0.954, respectively. For sets involving the explosives which are best characterized, the coefficients are 0.991 and 0.976.

$$D = 2.45 + \frac{P^{\frac{1}{2}}}{3} \qquad (3)$$

$$D = \left(\frac{P^{\frac{1}{2}}}{3} + 2.0 + 0.25a\right) + 0.05\left(H_p + \frac{N_p}{20}\right) \qquad (4)$$

$$D = T_c \sum (U_{si} f_i) \qquad (5)$$

Eq. 3 was developed algebraically from two empirical equations derived before 1969 to calculate detonation pressures and velocities. (Refs. 1,30) The use of this very elementary equation provided some evidence that detonation velocity was a rather weak function of pressure and that detonation was probably a much less complicated process than had been believed. Eq, 4 was developed from observations of the results from Eq. 3. Specifically, it was easily seen that the aromatic molecules had about 0.25 km/s lower D's for given P_d's, which could reflect the additional energy required to break up the aromatic rings and some of the more complex molecular structures. Additionally, compounds with relatively higher H and N content appeared to have slightly higher D's.

Calculations with Eq. 4 showed excellent correlations to the data. This observation, along with the new concepts of physical kinetics--that shock velocities and the ARVV's were related and similar (as proposed herein) and that massive kinetic fracture of the covalent bonds of an explosive in the shock front was probable, led to the development of Eq. 5. (Ref. 29) Here,

T_c is a small (about 2 to 6%) correction to the shock velocity based on the fact that the temperatures of detonation are much higher than those at which Hugoniot values are usually measured. The correction curve is taken from the Hulbert-Hirschfelder calculations of U_s versus T. (Ref. 29) The U_{si} and f_i functions are simply the shock velocities of the elements of the empirical formula of an explosive at P_d and the weight fraction of each element, respectively. The excellent correlation to the data obtained with Eq. 5 (See Table 2) is a validation of the concepts presented earlier in this paper, which are summarized below:

1. Physical kinetics applies in determining D.*
2. Shock velocities of the component elements are key factors.
3. The kinetic energy in the detonation front leads to massive fracture of the covalent bonds in and near the front, by impact, compression and shear.

Thus, thermodynamics, excited atomic and molecular states, the transfer of energy from shock produced phonons to the internal vibrations of the molecules, electronic transitions, and some other often considered factors, although certainly involved at some level, have a relatively minor influence on detonation velocity.

If the molecules were not broken into their component atoms at or very near the front, Eq. 5 probably would not represent a rational concept, and it is highly improbable that it would provide any correct calculations of D--certainly not a set of 47 with a correlation coefficient of 0.954.

*There may be some intrinsic regulation of detonation velocities involving velocities of impact of atomic and molecular species, orientation of impacted molecules or bonded couples, and resonance relationships between impact velocity and vibrational frequency of impacted molecular bonds, but these factors do not appear to be required considerations for the detonation velocity determination.

Additionally, in a more recent report (Ref. 31), an explosive designated as E25 (75% PETN/25% paraffin) at a density of 1.265 g/cm^3 has a measured D of 7.230 km/s, whereas pure PETN (pentaerythritol tetranitrate) at the same density has a measured D of 6.60 km/s. Using the thermodynamic codes, E25 showed a calculated D of 6.20 km/s. However, the calculation with Eq. 5 gave a value of 7.267 km/s, within 0.51% of the measured value. This is well within the precision of D measurements. The classical theory calculation missed the measured value by -14.24%. The author of the paper who reported the E25 data (Ref. 31) stated that, "All equations-of-state available to us cannot reproduce these results." This relatively recent observation is compelling support for the concepts described herein.

ADDITIONAL CONSIDERATIONS

Analysis of a set of data on the shock initiation of PBX-9404 (an HMX-based, plastic-bonded explosive) led to the derivation of the critical energy fluence equation which provides the criteria for the shock initiation of explosives. This equation is:

$$E_c = \frac{tP^2}{\rho U_s} \qquad (6)$$

where t is the time-width of an initiating shock of velocity U_s providing a pressure P in the shocked explosive. The initial density of the explosive is ρ. The equation is derived from simple basic physics equations involving kinetic energy and shock velocity, showing the importance of those factors in initiation as well as in detonation. This critical energy equation has been used successfully for about two decades in numerous shock initiation studies (Refs. 32,33), for designing explosives-activated escape systems for aerospace applications, and for many other purposes. (Ref. 34)

Another interesting factor appears in our work and the work of A.N. Dremin. (Refs. 9,35) The one-dimensional translational "temperature" of the atoms in the shock front of a nominal 5 GPa shock is calculated to be greater that 12,000 K, and for N and O

atoms, accelerated by momentum transfer in the detonation front to 8 km/s, these translational pseudo-temperatures would be about 20,000 K or higher.

For many years, since at least 1974, we have maintained that the very high levels of kinetic energy in the detonation front provide levels of impact, compression, and shear forces sufficient to cause mechanical fracture of a major portion of the covalent bonds. (Refs. 1,2,3,12,36,37) Much recent work in molecular mechanics, particularly by J. Gilman (Ref. 39) provides a quantitative mathematical and chemical description of the mechanical (nonthermal) bond fracture mechanisms, which may apply in shock-induced reactions and detonation.

We have proposed that the chemistry immediately following the initial bond fracture (about 10^{-13} to 10^{-12} s) is extremely important. By adding sources of new free radicals, and thus new reaction chains, the rates of energy release could be increased and higher reaction pressures could be attained. This can lead to higher detonation velocities and to smaller critical diameters, as has been observed in many NM-DETA experiments. (Refs. 5,14, 15,36) These additional considerations add credence to our experimental observations and calculations.

CONCLUSIONS

It is concluded: (1) That the new concept of physical kinetics is a valid concept for determining reaction rates in detonations and in highly shocked systems, and that the methods given for the calculation of shock velocities for the elements and compounds and explosives mixtures are based on proper physical principles. These shock velocities are related directly to the ARVV's and to detonation velocities.

(2) That the exceedingly high kinetic energy in the detonation front is sufficient to cause massive fracture of the covalent bonds of the molecules of the explosives at and near the front, so that the large majority of the molecules are broken to individual atoms or radicals and rearranged extensively, and that the subsequent very rapid chemistry can be influenced by the

addition in the explosives of chemicals providing enhancing or inhibiting reactions or other chemicals which could influence sensitivity.

(3) That the simple equation, $D = T_c \sum (U_{si} f_i)$, is a rational equation, based on appropriate Hugoniot principles, which provides for the very accurate calculation of detonation velocities from the shock velocities of the elements in the empirical formulae of the explosives.

ACKNOWLEDGMENTS

I wish to acknowledge helpful conversations regarding this paper with R.J. Wasley, A.N. Dremin, H.N. Presles, S. Odiot, J.J. Gilman, and D.D. Dlott.

TABLE 1. ISOTOPIC RATIOS IN BTNEA AND ITS DETONATION PRODUCTS

		C^{12}/C^{13}	O^{16}/O^{18}
Labeled BTNEA		4.8	11.7
Products	H_2O	-	16.6
	CO_2	4.7	11.4
	CO	4.8	11.2
	CH_4	4.5	-
	C	4.6	-

TABLE 2. DETONATION VELOCITIES CALCULATED FROM EQUATION 5

Explosive*	DATA P(GPa)	D(km/s)	CALCULATION D_c(km/s)	D	% Dev.
BTF	36.0	8.49	8.50	0.01+	0.12+
DATB	25.9	7.52	7.62	0.10+	1.33+
HMX	39.0	9.11	9.09	0.02-	0.22-
HNS	20.0	6.80	6.83	0.03+	0.44+
PETN	33.5	8.26	8.21	0.05-	0.61-
RDX	33.8	8.70	8.59	0.11-	1.26-
TATB	29.1	7.87	7.98	0.11+	1.40+
Tetryl	26.0	7.50	7.55	0.05+	0.67+
TNT	21.0	6.94	7.01	0.07+	1.01+

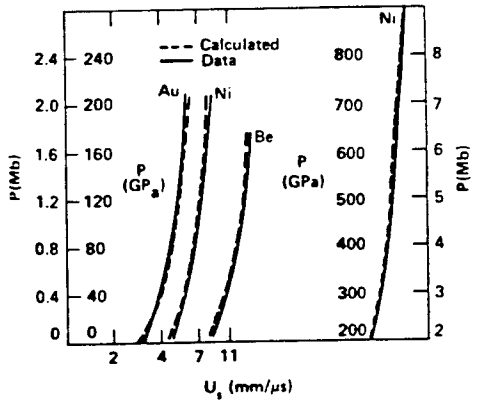

Figure 1. U_S versus P curves for beryllium, nickel, and gold calculated with Equation (1).

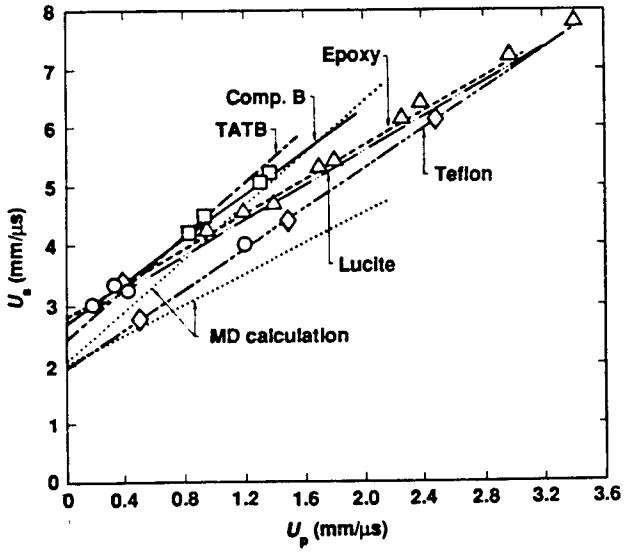

Figure 2. The Hugoniot plot of common organic plastics and explosives compared with the MD Hugoniot calculations.

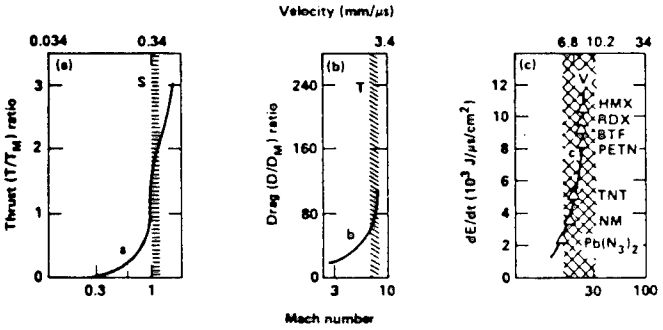

Figure 3. Representation of sonic (S), thermal (T) and shock (V) "barriers" as related to (a) sonic flow, (b) hypersonic flow, and (c) detonation velocity.

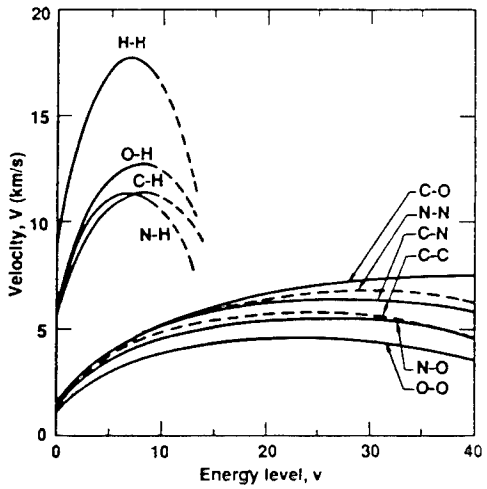

Figure 4. Plot of average vibrational velocity vs energy level for the ten atom pairs considered here.

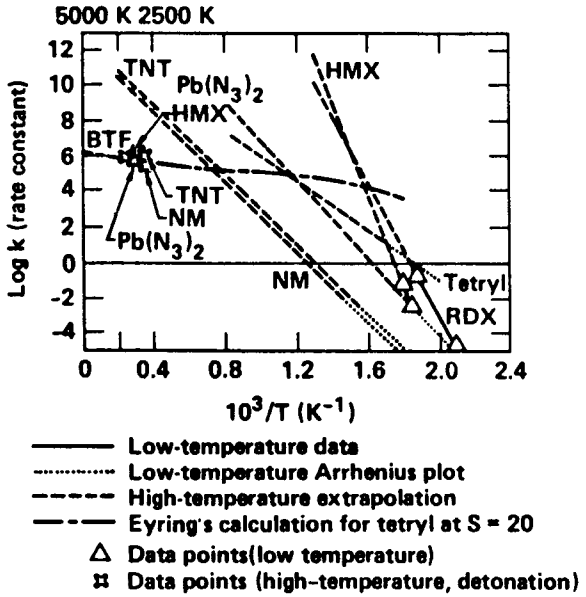

Figure 5. Thermal decomposition data for 7 explosives showing that the high temperature decomposition rates all appear to be nearly equal--log of the rate constant is about 6.

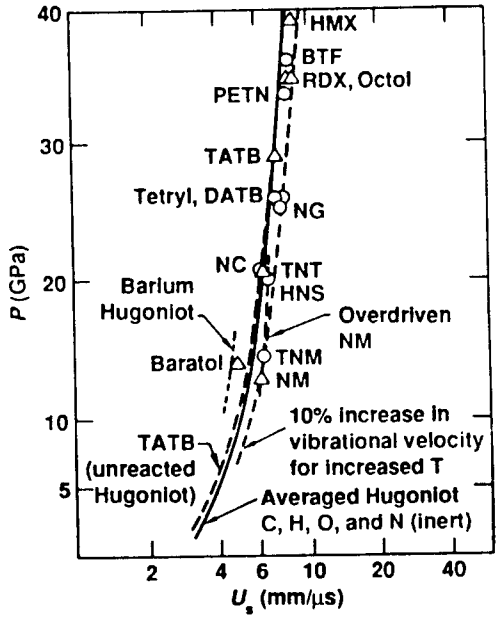

Figure 6. Comparison of averaged Hugoniot plots for the elements in organic explosives and common organic materials with the unreacted Hugoniot for TATB. Also shown are the D's for 15 common explosives with the P_d's.

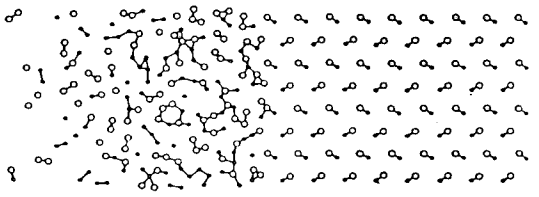

Snapshot from a simulation of a detonating film. The length of the system shown is ≈ 80Å.

Figure 8a. Molecular dynamics calculation of a model detonating solid with two types of atoms and with exothermic reactivity incorporated into the dynamics.

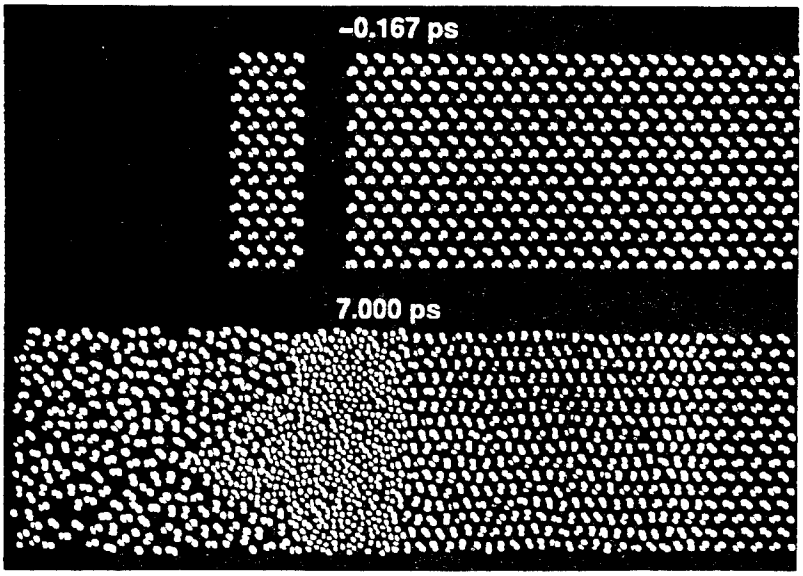

Figure 8b. Molecular dynamics calculation with Tersoff-like potentials used to simulate the detonation of an energetic two dimensional semi-infinite molecular solid.

REFERENCES

1. F.E. Walker, Lawrence Livermore National Laboratory, CA Report No. UCRL-53860, 11 January 1988.
2. F.E. Walker, J. Appl. Phys. 63, 5548 (1988).
3. F.E. Walker, Propell., Explo., Pyrotech. 15, 190 (1990).
4. F.E. Walker and R.J. Wasley, Combustion and Flame 15, 233 (1970).
5. F.E. Walker, Acta Astronautica 6, 807, Pergamon Press Ltd. (1979).
6. F.E. Walker, F.G. Walker and J.B. Walker, J. Appl. Phys. 60, 3876 (1986).
7. F.E. Walker, Evidence of a Physical and Kinetics Basis for Detonation Velocity and Stability, Naval Research Lab., Tech. Report, 17 August 1988.
8. A.M. Karo and F.E. Walker, Proceedings of the APS 1981 Topical Conference on Shock Waves in Condensed Matter, Menlo Park, CA, 23-25 June 1981.
9. F.E. Walker, Propellants and Explosives 6, 15 (1981).
10. F.E. Walker and A.M. Karo, Shock Waves in Condensed Matter 1987, S.C. Schmidt, N.C. Holmes (editors) Elsevier Science Publishers B.V., p. 543 (1988).
11. H. Eyring, Chem. Eng. News 53, 27 (1975).
12. F.E. Walker, Lawrence Livermore National Laboratory, CA Report No. UCRL-75722, Rev. 1, 21 April 1975.
13. F.E. Walker, Proceedings of the International Conference on High Energy Rate Fabrication (HERF), Ljubljana, Slovenia, 18-22 September 1989.
14. H.N. Presles and D. Desbordes, Revue Scientifique et Technique de la Defense-4^{o} Trimestre 1991, pp. 11-15.
15. F.E. Walker and R.J. Wasley, Combust. and Flame 22, 53 (1974).
16. R.R. McGuire and D.L. Ornellas, Propell. and Explo. 4, 23 (1979).
17. D.W. Brenner, F.E. Walker, et al, Int. J. of Quantum Chem., Quantum Chemistry Symposium 23, 1989. John Wiley and Sons, Inc. (1989)
18. A.M. Karo and J.R. Hardy, Fast Reactions in Energetic Systems, pp. 611-643, C.Capellos and R.F. Walker (editors) D. Reidel Publishing Co. (1981) NATO Advanced Study Institute, Series C: Mathematics and Physical Sciences.
19. D.H. Robertson, D.W. Brenner, et al, Shock Compression of Condensed Matter 1991, S.C. Schmidt, R.D. Dick, J.W. Forbes, D.G. Tasker (editors) 1992, Elsevier Science Publishers B.V., pp. 123-126 (1992).

20. D.W. Brenner, D.H. Robertson, et al, Microscopic Simulations of Complex Hydrodynamic Phenomena, Edited by M. Mareschal and B.L. Holian, Plenum Press, New York, pp.111-123 (1992).

21. M. Peyrard, S. Odiot, et al, J. Appl. Phys. 57, 2626 (1985).

22. R.A. Graham, J. Phys. Chem. 83, 3048 (1979).

23. A.N. Dremin and O.N. Breusov, Priroda 12, 10 (1971).

24. B.W. Dodson, E.L. Venturini and J.E. Rogers, Proceedings of the 4th Annual Topical Conf. on Shock Waves in Condensed Matter, Spokane, WA 1985, edited by Y.M. Gupta, Plenum Press, New York, 1986.

25. F.J. Owens and J. Sharma, J. Appl. Phys. 51, 1494 (1980).

26. R. Lewin, A New Window Onto the Chemists' Big Bang, Science 238, 1512 (1987).

27. N.F. Scherer, A.H. Zewail, et al, J. Chem. Phys. 87, 2395 (1987).

28. M. Dantus, M.J. Rosen and A.H. Zewail, J. Chem. Phys. 87, 2395 (1987).

29. F.E. Walker, Propellants and Explosives 15, 157 (1990).

30. M.J. Kamlet and S.J. Jacobs, J. Chem. Phys. 48, 23 (1968).

31. K. Tanaka, S. Oinuma, et al, Shock Compression of Condensed Matter 1989, S.C. Schmidt, J.N. Johnson, L.W. Davison (editors) Elsevier Science Publishers B.V., 1990.

32. J.L. Austing and A.J. Tulis, Proceedings of the 14th Int. Pyrotechnics Seminar, Jersey, Channel Islands, UK, 18-22 September 1989, pp. 583-601.

33. J.L. Austing and A.J. Tulis, et al, Proceedings of the 16th Int. Pyrotechnics Seminar, Jönköping, Sweden, 24-28 June 1991, pp.274-288.

34. F.E. Walker and R.J. Wasley, Explosivstoffe 17, 9 (1969).

35. A.N. Dremin and V.Yu. Klimenko, Progress in Aeronautics and Astronautics, edited by J.R. Bowen, N. Manson, A.K. Oppenheim and R.I. Soloukhin, Vol. 75, 253 (1981) New York.

36. F.E. Walker and R.J. Wasley, et al, Lawrence Livermore National Laboratory, CA Report No. UCRL-75339, 1974.

37. F.E. Walker, Propell., Explo., Pyrotech. 7, 2 (1982).

38. J.J. Gilman, Shock Compression of Condensed Matter 1989 S.C. Schmidt, J.N. Johnson and L.W. Davison (editors) Elsevier Science Publishers B.V., p. 267 (1990).

Questions - Answers, Comments

Shackelford - Dlott :

Q : Take for example, a normal molecule like HMX and a deuterated molecule like HMX-d8. How might this deuterium substitution affect this model in terms of chemical reaction initiation, especially in terms of energy transfer rates and time to chemical reaction initiation ?

A : Experiments by Dlott, Califano, Hochstrasser and Chronister show molecular energy transfer is faster in deuterated non-energetic molecules. In our model this reduces the possibility of hot-spot formation in up-pumping zone.

Califano : *a comment* I like very much the idea of hot spots presented by Dana. I would like to suggest that a hot spot is not only a trap for energy but also a center of scattering processes which can open new channels to the up conversion process.

Nelson : *a comment to Dremin*

You are correct that femtosecond spectroscopy of real shocked materials will be impossible if it requires synchronization of light pulses with shock loading at femtosecond accuracy. But other methods are possible.

For example, Yogi Gupta has suggested femtosecond pump-probe spectroscopy of a material with a shock wave passing through it. For example there is a narrow zone of endothermic reaction products they could be detected and characterized.

Dana Dlott has taken a different approach, building very small spatial structures into the sample to permit a kind of synchronization which could be done on subpicosecond time scales

Delpuech - Dlott : *a comment* :

A complement about a remark of Dr Dlott. The value of the temperature considerated in the proposition of excited state is not an average value.

Is the value that we can obtain, at the molecular scale, in the crossing under energy loading, of dislocations in the crystal ? In this case this value is compatible with few electron-volts.

Of course at the begining we have excited states only in localised zones and not in the bulk of the explosive.

The question is not how the phonons give the energy of the shock at the molecule, but how an excited molecule gives with the phonon its energy to the other molecules in order to obtain a cooperative mode of decomposition.

Boris - Dlott :

Q : What are the effects of energy transport from the sea of excited phonons into the hot spot ? Can this focusing of energy enhance the sensitivity enough to account for observed explosive behavior?

A : Mechanical energy must flow to the hot spots in order for them to overheat. In unpublished work by us, we found the transport of energy to a hot spot by acoustic phonons did not have a substantial effect, although this work is not complete. One interesting effect we have discussed in our J.Chem.Phys. article involved hot spots formed in small grains of material. The (extensive) heat capacity of small grains is limited, so hot spots cannot become as hot. This led to our prediction of size effects in defect-assisted shock-induced chemistry.

Odiot - Dlott :

Q : I should agree with your model if you could explain to me how a shock may excite phonons through Gruneisen parameter in such a non equilibrium state of a shocked material.

A : The Grüneisen parameter $\Gamma = \Sigma_i \gamma_i c_i / \Sigma_i c_i$ where γ_i are mode grüneisen parameters and c_i are mode heat capacities. Upon a change in volume, the change of a mode's internal energy E_i is proportional to $\gamma_i = -\, d\ln E_i / d\ln v$. For phonons, γ_i is typically 10^2 bigger than for vibrations. Thus the initial transfer of energy from a shock is principally to the phonons.

Ramsay - Dlott :

Q : Can your model of phonon pumping around a discontinuity (bubble) be compared with the data available in the pictures presented by Dr Presles on monday ?

A : I don't know.

Rullière - Dlott :

Q : You showed multi steps absorption of phonons to reach vibrational excited state. Are the lifetimes of involved vibration and the probability to meet a phonon compatible to get a high probability for this process to occur efficiently ?

A : In diatomic molecules, energy transfer from phonons to vibrations (multiphonon up-pumping) is quite inefficient. It involves a high-order anharmonic process with simultaneous absorption of n-phonons (e.g. n>20 for N_2). In large molecules, up-pumping involves a lower-order process where n = 3-4. This lower-order process is much more efficient. Up-pumping occurs by a sequence of many of these lower order steps. For example, it is possible for a larger molecule to absorb thousands of cm^{-1} on a 100 ps scale.

Walker *to workshop on what a shock really is, a comment* :

Let's no forget what a detonation really is. As Prof Eyring explained many years ago, it is a momentum transfer process - $m_1v_1 = m_2v_2$. It is the momentum of one layer of atoms accelerating and displacing the next layer - in a simplified view. The detonation velocity in HMX is 9.11 Å in 10^{-13} s. This means that the detonation front on the atomic scale is crossing the original position of each layer of atoms in 10^{-14} s. Any chemical energy that would be released in 10 ps would be 1000 layers of atoms behind the front with no understandable way of catching up to the

front. In a μs, it would be 100,000 layers too late. Energy strong enough to drive the detonation front must be available very near the front.

The ingenious spectroscopic instruments and devices discussed today would certainly be useful in studying shock initiation, but a laser beam burning a spot in an explosive sample or even making an impacting shock of a high velocity is not forming a detonation.

My concept of the extremly high kinetic energy from the extremly high momentum transfer producing enough force to fracture covalent bonds or cause very high velocity impacts on an atomic and molecular level to ensure chemical reaction and energy release within a time of 10^{-14} to 10^{-12} seems to be required. The kinetic energy in the detonation front is in the level of several ev.

Dlott *to workshop in general about Walker's presentation. Comment*

Dr Walker considers very intense shock waves characteristic of detonation (e.g. 40 GPa). In this regime, the kinetic energy of atoms is much greater than the energy of all covalent bonds. In this regime, his suggestion of efficient bond scission at the front seems reasonable.

In our model, we consider chemistry induced by weak shock waves. Then chemistry is not likely at the front but instead less efficient thermochemical bond cleavage will occur farther behind the front. Keep in mind these two models describe different situations.

3 SHOCK RESPONSE OF CONDENSED EMs - EXPERIMENTS

Chairman : Pr Boris Kondrikov, Mendeleev University of Chemical Technology

Mesdames et Messieurs, Ladies and Gentlemen

I appreciate very much all the organizers of this exclusively important meeting for the opportunity to visit France, and in the first time in my life to have honor to be a Chairman of a session of one of the international Conference I was not be able to take part in during more than two decades.

The first day of our workshop was devoted mostly to the macroscopic aspects of the detonation processes. It was absolutely necessary to begin our discussion namely with these macroscopic approaches which were elaborated during about a century, having in mind the great experience accumulated at these investigations is a ground for all the future understanding of thin structure of matter. Now we have to discuss some of them, I would say probably the best of them. It was the wonderful lecture here given by Dr.K.Nelson on femtosecond measurements we had possibility to hear just now, and the reports of Dr.Y.Gupta and Dr.Dlott on pico- and nano-second measurements that should be presented in this session.

I would like to note that I had opportunity to discuss all three of the reports this year on Gordon Conference New Hampshire USA, and Dr.Gupta's paper also on Zel'dovich Conference in Moscow. I believe it is a very good idea to present them in different meetings and for the broad audience, because all of these works are absolutely new word in field of shock and detonation transformations, and correspondingly they need much attention and one could say the deep penetration into the essence of the new results obtained in the course of the very hard work (as well as the very big expenditures). In this connection I would like to mention here about a role of Office Naval Research and personally Dr.R.Miller, who have partly supported these programs, having in mind first of all the obvious necessity of these investigations for the fundamental science of developments as a natural base for all the future practical applications. I have to note also that though strickly speaking not all of the data obtained are concerned literally with behavior of high explosives at very strong shock stress during the very short period of time, the field of science we have been penetrating into at these investigations is so much more complicated than any other, in this part of physics and chemistry, that we need to use all the possible ways to reach the positive and definitive results.

It should be also taken into account that as a matter of fact we have now instead of the single classical theory of detonation the many kinds of detonation-alike processes for solid and liquid

compounds, for composite explosives (some potentially very interesting lectures will be given later), at relatively low, and at very high pressures and temperatures. Everyone of the processes needs special examination and employment of all possible means to expose the essence of them, and to use it in science and technology.

Recent Developments to understand Molecular Changes in Shocked Energetic Materials ; D.D. Dlott

Picosecond Dynamics behind the Shock Front ; Y.M. Gupta

JOURNAL DE PHYSIQUE IV
Colloque C4, supplément au Journal de Physique III, Volume 5, mai 1995

Picosecond Dynamics Behind the Shock Front

D.D. Dlott

School of Chemical Sciences, University of Illinois at Urbana Champaign, Box 37-1 Noyes Lab, 505 S. Mathews Ave., Urbana, IL 61801, U.S.A.

Abstract: Understanding the microscopic details of shock-wave initiation of energetic materials requires a realistic picture of picosecond time scale processes occurring in large molecules located in an ~100 nanometer thin layer just behind the front. In this paper, I discuss a theoretical model for shock wave induced chemistry which highlights the role of molecular mechanical energy transfer processes, especially multiphonon up-pumping. Picosecond laser measurements of multiphonon up-pumping in a high explosive, nitromethane, are presented. Up-pumping occurs on the ~100 picosecond time scale in nitromethane. The fundamental problem in direct measurement of the states of molecules just behind a shock front is simultaneously achieving picosecond time resolution and nanometer space resolution. A new method for probing dynamics immediately behind a shock front using optical nanogauges is described, and some preliminary results are presented.

1. INTRODUCTION

Little is known about the very first events occurring just behind the shock front during shock-induced initiation of condensed phase explosives. Because typical velocities for initiating shock waves are on the order of 3-6 km/s, and 1 km/s = 1 nm/ps, material within 100 ps of the shock front is present in a very thin layer whose thickness is a few hundred nanometers. In this paper, I will discuss theoretical models and experimental measurements of condensed matter molecular dynamics in this layer. Both the theoretical and experimental investigations face daunting obstacles. To develop an adequate theory, one has to know much about the detailed microscopic dynamics of rather large and complicated molecules under harsh, extreme conditions which are evolving on the picosecond or even femtosecond time scales. To investigate these phenomena experimentally, one needs to use spectroscopic techniques with good time resolution, which is straightforward today, but one must also combine extremely high spatial resolution, ideally much better than a wavelength of visible light.

In this paper, I will concentrate on the problem of molecular mechanical energy transfer behind the shock front [1]. As shown in Fig. 1, in the long term a shock wave produces a jump in the temperature and pressure. But in the short term, the molecules just behind the shock front are far from mechanical and thermal equilibrium [1,2]. The motivation for studying picosecond dynamics behind a shock front is to learn more about the behavior of molecules far from equilibrium, to relate this behavior to the sensitivity of energetic materials to shock excitation, and to attempt to develop a detailed picture of the first few nanoseconds of the initiation process.

The paper is divided into three parts. In the first part, I discuss the elements of a theoretical model developed in collaboration with Prof. M. D. Fayer and Dr. A. Tokmakoff of Stanford University. In the second part, I discuss experimental measurements of picosecond time scale energy transfer dynamics in a high explosive. The third part describes some new techniques which use optical shock nanogauges to probe the behavior of molecules in the nanometer-thick layer just behind the shock front.

2. THEORETICAL MODEL

The details of this model have been described in two recent publications [1], so only the basic elements are given here. The model is intended to describe how the passage of a shock wave through an elastic solid causes chemical reactions to occur in energetic materials which, for widely used secondary explosives, are crystals consisting of relatively large molecules. The restriction to elastic solids means that hydrodynamic phenomena such as shear or moving edge dislocations are not considered. Although these phenomena may be quite important in many circumstances, the intent of the model is to understand chemistry caused by the weakest shock waves possible, because the critical issues in sensitivity involve weak shock waves characteristic of accidents.

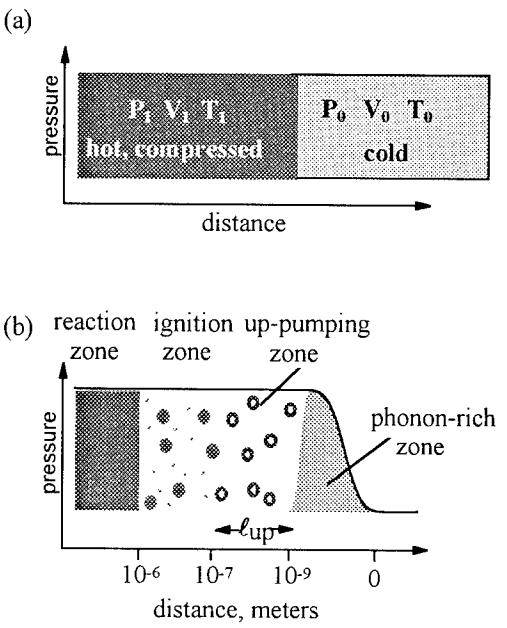

Figure 1. (a) A shock wave ultimately causes a jump in T, P. (b) Immediately behind the front, the material is not in thermal equilibrium. Reproduced from ref. 1.

The fundamental idea is that shock waves do not instantaneously produce Boltzmann equilibrium. Instead the shock front preferentially excites phonons (see Fig. 2). Subsequently these phonons excite intramolecular vibrations by the process termed *multiphonon up-pumping* [1,3]. The vibrational states must be excited before thermochemical reactions can occur [1]. Immediately behind the shock front is a thin layer which is phonon-rich and vibration-starved. Arrhenius kinetics are not valid in this up-pumping zone (Fig. 1b). The up-pumping problem is handled using a simplification termed the quasitemperature model [1]. In this model, the phonon excitation level is characterized by a time-dependent phonon quasitemperature $\theta_p(t)$, and the vibrational excitation by a time-dependent vibrational quasitemperature $\theta_{vib}(t)$.

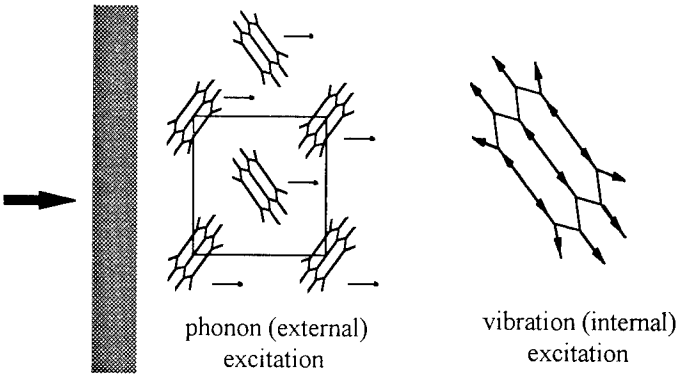

Figure 2. The shock first excites phonons, which are states which couple efficiently to volume perturbations. Molecular vibrations are excited later by multiphonon up-pumping.

For a given thin layer of energetic material, we denote the zero of time to occur when the shock front reaches the layer. For a shock which ultimately heats the material from T_0 to T_1, the initial conditions are $\theta_{vib}(t) = T_0$ and $\theta_p(t) >> T_1$. In other words, efficient shock-to-phonon transfer results in an

instantaneous zero-time value of $\theta_p(t)$ which is *much greater* than T_1. This temporarily massive phonon overheating is a central feature of our model [1].

Phonons up-pump vibrations via anharmonic coupling [1,3]. In a large molecule, there are many different pathways for up-pumping, and in order to have a tractable model, we need to know which pathways dominate. Experimental studies of picosecond time scale vibrational energy transfer [4] show the principal mechanism of up-pumping involves the lowest-order or cubic anharmonic coupling. In the cubic coupling mechanism, the lowest energy vibrations, termed doorway states, are excited by simultaneously absorbing two phonons. Subsequently, molecules with excited doorway states can be pumped to higher vibrational levels in many steps, each involving absorption of a single phonon [1].

By using reasonable values for anharmonic coupling and density of states parameters, we have computed the rate of up-pumping, and the width of the up-pumping zone behind the shock front (Fig. 1b), as a function of the compression ratio, as shown in Fig. 3 [1]. We estimated the width of this zone to be ~100 nm, and the up-pumping time constant to be 30-100 ps [1].

We have also investigated how energy transfer can affect the sensitivity of energetic materials. There is no *a priori* reason why up-pumping alone should directly affect sensitivity. With up-pumping there is simply a brief delay time of ~100 ps between the passage of the shock front and the onset of activation of the molecular vibrations. Nevertheless, recent calculations by Fried and Ruggerio [5] led them to suggest that the most insensitive energetic materials have the slowest up-pumping processes and the most sensitive materials have the fastest up-pumping. Although that work is still in its early stages, the initial result is certainly intriguing. Two quite different ways in which up-pumping can affect sensitivity have been suggested. L. Fried has pointed out that more efficient up-pumping is a sign that the molecular vibrations are more efficiently coupled to the bath [6]. In Kramer's theory of condensed phase reaction dynamics, there exists a weak-coupling limit where increased coupling to the bath increases the rates of chemical reactions.

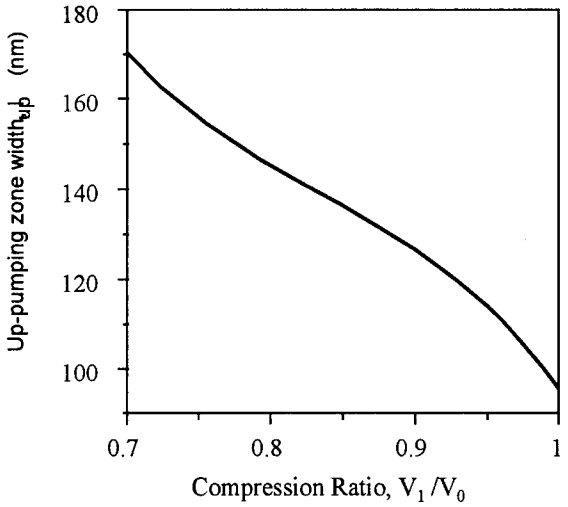

Figure 3. Computed width of the up-pumping zone. Reproduced from reference 1.

Dlott and Fayer proposed that the magnitudes of anharmonic couplings near defect-perturbed domains (DPD) in an imperfect solid might differ from couplings in the bulk [1]. The parameter ξ is the magnitude of the anharmonic coupling enhancement. For DPD's where $\xi > 1$, the local anharmonic coupling exceeds the bulk coupling. In these DPD's, localized temporary hot spots can be produced. Hot spots are produced because the phonons pump these DPD's faster than they pump the bulk vibrations. Because chemical reactions are highly sensitive to temperature, the reactivity of these hot spots can be much greater than the bulk reactivity. Using chemical reaction rate laws for typical energetic materials, we calculated Fig. 4. In Fig. 4, we assumed a 4.7 GPa shock wave. The heating caused by this shock wave causes a bulk reaction probability of $\sim 10^{-10}$. This means one molecule in 10^{10} reacts, which is hardly enough to initiate widespread reactions. But just a small amount of anharmonic enhancement, e.g. $\xi = 2$ in Fig. 4 can cause the defect reaction probability to increase by eight orders of magnitude [1].

When these theoretical models were proposed, we pointed out the need for experimental measurements of up-pumping time constants, and a better understanding of the role of DPD's in energy transfer, specifically the relationships between DPD structure and anharmonic coupling [1]. Such experiments are quite difficult and they require the development of new techniques, especially using time-resolved nonlinear optical phenomena.

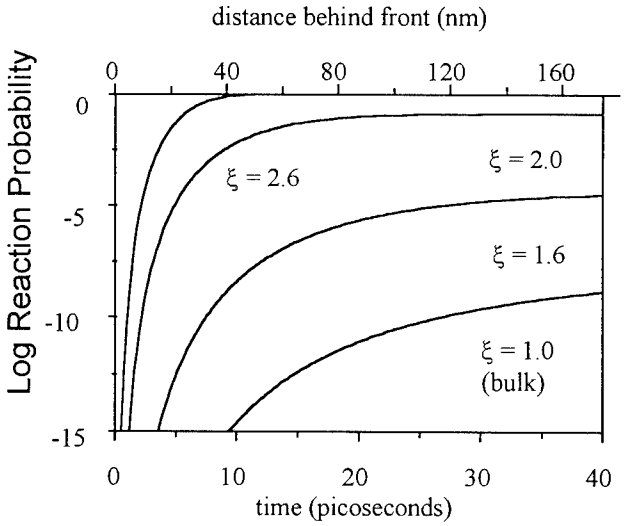

Figure 4. Computed reaction probability for different values of ξ, the anharmonic enhancement factor in the defect-perturbed domain (DPD). The reaction probability can be increased by orders of magnitude in DPD's with a small increase in anharmonic coupling.

3. DIRECT OPTICAL MEASUREMENT OF UP-PUMPING IN HIGH EXPLOSIVES

Although many different techniques have been developed for studying vibrational relaxation and vibrational cooling in molecular systems, measurements of up-pumping are more problematic. In a vibrational relaxation measurement, a higher energy vibration is excited by a short laser pulse. The decay of energy (or coherence) of this state is then relatively easy to monitor because the laser-induced excitation is far greater than the equilibrium level of excitation [4]. In up-pumping studies, a method must be found for instantaneously producing a huge excess of phonons. The phonon excess must be sufficient to drive a substantial number of the molecule's vibrations to an excitation level which can be readily detected.

We have solved the phonon excitation problem by using a unique molecular dye [7] termed IR-165. This near-IR dye is useful because: (1) its maximum absorption is near $\lambda = 1$ μm, which is the wavelength of the most efficient solid state laser systems, Nd:YAG and Nd:YLF; (2) after absorbing a near-IR photon, efficient internal conversion and vibrational cooling processes result in a nearly total conversion of the optical energy into heat on the 4 ps time scale [8]; and (3) the mechanical energy lost by this dye excites mainly phonons in the surroundings [7,8].

In our experiments [9], we dissolved a small amount (~1%) of IR-165 dye in nitromethane (NM). A 1 mJ, 1.053 μm pulse of 75 ps duration pumps the dye, producing a burst of phonons. The pumping process deposits enough energy into a uniformly heated volume to ultimately produce a temperature jump of $\Delta T \sim 25$ degrees. A visible, 0.527 μm pulse then probes the excited volume. This pulse produces incoherent anti-Stokes Raman emission, which is collected and analyzed with a spectrometer and a photodetector. The anti-Stokes emission from a given vibration is proportional to the instantaneous occupation number of the state. Thus anti-Stokes probing is mode specific, and it allows us to quantitatively measure the change in occupation number $\Delta n_\omega(t)$ for a particular NM vibration. For convenience, we mathematically converted this occupation number into a time-dependent vibrational quasitemperature increase $\Delta\theta_\omega(t)$, using the relation, $\Delta n_\omega(t) = [\exp(\hbar\omega/k\Delta\theta_\omega)-1)^{-1}$. Figure 5 shows our results on NM [9].

In our experiments we probed two states of NM, the 657 cm^{-1} vibration, which is assigned to a symmetric bending vibration of the NO_2 group, and the 918 cm^{-1} vibration, assigned to a C-N stretching motion [9]. The latter vibration is of much interest, since many theoretical models of NM ignition focus on the process of phonon-activation of the C-N stretching vibration, followed by cleavage of the C-N bond.

There are two interesting features in Fig. 5. The duration of the up-pumping period is about 100 ps, and vibrations are excited sequentially; we observed an ~30 ps delay between the excitation of the lower energy vibration and the excitation of the higher energy vibration. This experiment [9] provides the first direct measurement of multiphonon up-pumping in high explosives. The results are generally consistent with the theoretical model described in the previous section, namely that up-pumping occurs on the ~100 ps time scale, and it is the result of phonons first pumping doorway modes, and then later pumping higher energy vibrations.

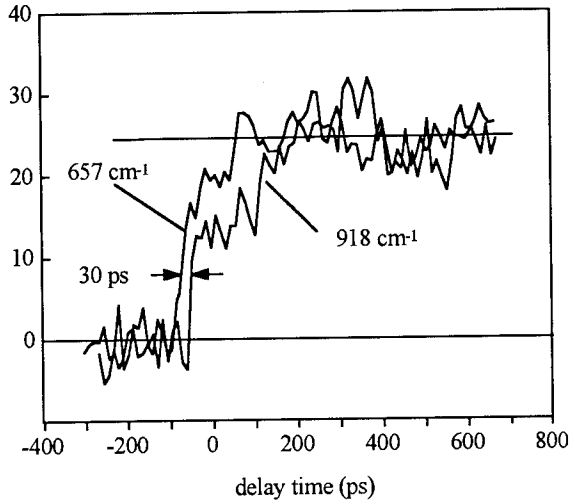

Figure 5. Multiphonon up-pumping in nitromethane (NM). Up-pumping occurs on the 100 ps time scale. Higher energy vibrations become excited later. The y-axis is the increase in quasitemperature of each vibration.

4. PICOSECOND DYNAMICS BEHIND THE SHOCK FRONT

There are many technical obstacles to studying picosecond energy transfer dynamics behind a shock front. The principle problems are: (1) generating reproducible solid-state shock waves at a reasonable repetition rate; (2) probing the shocked material with a method which provides detailed information about energy transfer and chemical reactivity, and (3) localizing the probe measurement to a nanometer-scale region behind the front, and accurately synchronizing the measurement to the arrival of the shock front at this layer.

There are many options to deal with problems (1) and (2), but until just recently problem (3) seemed insoluble. The principle obstacle is that time-resolved optical measurements are limited in principle by diffraction to regions of micron thickness, and in practice, depth-of-field considerations and edge effects give even worse spatial resolution. Our novel approach to this problem involves the use of shock target arrays with optical nanogauges. The nanogauge system is shown in Fig. 6.

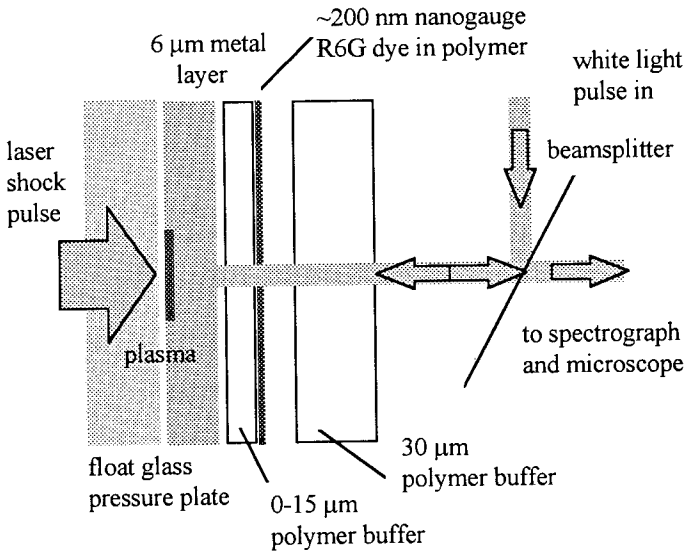

Figure 6. Schematic drawing (not to scale) of one element of a shock target array. Rapid expansion of the laser-driven plasma drives a shock wave into the polymer layers. A picosecond white-light pulse observes the instantaneous absorption spectrum of the optical nanogauge, consisting of a dye in a polymer thin film.

In our experiments, a picosecond near-IR pulse produces shock waves at a repetition rate of 10 shocks/s, using an exploding confined foil generator developed by workers at the Naval Research Laboratory [10]. The pulse travels

through a glass pressure plate, and it is weakly absorbed by a thin metal layer. When the surface of this layer is hot enough to form a strongly absorbing plasma, the remainder of the pulse intensely heats the plasma. Rapid expansion of the plasma drives a shock wave through the metal layer into the sample region [10], which is a multilayer polymer thin film [11]. After traveling a few μm through polymer, the shock front hits the ~200 nm thick optical nanogauge. In our initial experiments [11], the nanogauge consisted of an absorbing dye, R6G. Energy transfer in R6G, occurring as a result of the shock excitation, is monitored using a ps-duration white light pulse. This white probe pulse does a double-pass through the nanogauge, reflecting once off the metal layer. The probe is then sent to an optical microscope, or to a multichannel spectrograph. The large-area array target has about 10^5 individually adressible shock pixels. A motorized positioner is used to translate the sample through the axis of the laser pulses, so a fresh target region is used for every shot. The details of this technique are reported in ref. 11.

With the microscopy apparatus, we can detect the arrival of the shock wave at the metal-polymer interface, and the arrival of the shock at the optical nanogauge. By knowing the thickness of the polymer buffer layer in Fig. 6, we accurately determined the shock velocity, which was 5.5 km/s, giving a shock pressure of ~15 GPa [11]. Because the white probe pulse is seeing only effects attributed to the absorption of the R6G dye, we have, by microfabrication of this array, limited the region of observation to a nanometer thick volume.

Figure 7 shows an unshifted, and shock-shifted spectrum of R6G, taken with our apparatus [12]. Shock-induced spectroscopy of dye molecules is not new [13], but there is a critical difference in our experiments: the risetime of the shift is <50 ps, which is several orders of magnitude better than anything observed previously. Besides the shift, there are subtle changes in the red-edge of the optical absorption which can be used to investigate the redistribution of vibrational energy in the dye molecules during shock-induced up-pumping [14].

5. CONCLUDING REMARKS

Now that we have found experimental solutions to the fundamental problems of studying picosecond time scale energy transfer behind a shock front, we intend to extend these methods to study energetic materials under conditions typical of shock initiation processes. Most interesting energetic materials do not have the intense visible absorption of R6G, so a different probing technique is needed. We have recently been able to show that picosecond time-resolved coherent Raman scattering (ps CARS) can be used to study the vibrational dynamics and chemical reactions of colorless materials just behind a shock front [15], We have considerable optimism that direct ultrafast time scale measurements of energetic materials behind a

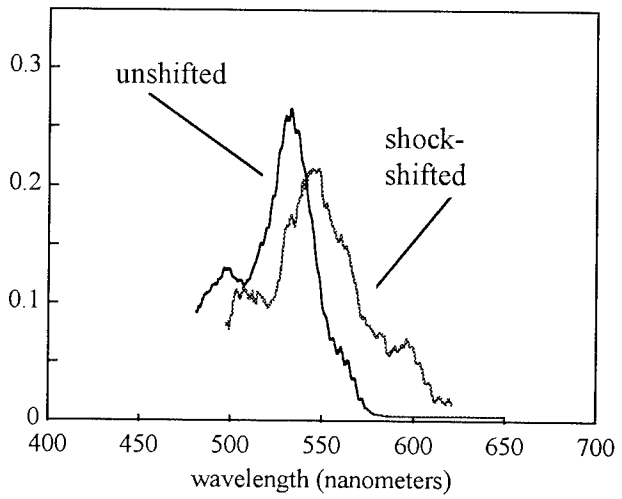

Figure 7. Spectrum of R6G optical nanogauge, taken using the apparatus in Fig. 6. The unshifted spectrum was taken a few tens of ps before the shock front reached the nanogauge. The red-shifted spectrum was taken about 100 ps after the front reached the nanogauge. The red shift is consistent with the ~15 GPa pressure of the shock wave.

shock front will be accomplished in the near future. These measurements promise to open a new window onto the picosecond dynamics behind the shock front, which we believe will be key in understanding the initiation of energetic materials at the molecular level.

6. ACKNOWLEDGMENT

This research was supported by US Air Force Office of Scientific Research grant F49620-94-0108, US Army Research Office grant DAAH04-93-G-0016, and National Science Foundation grant DMR-9404806. The work would not have been possible without the efforts of many valued collaborators. The shock-induced chemistry model was developed with Prof. Michael D. Fayer and Dr. Andrei Tokmakoff of Stanford University. The nitromethane measurements were performed by Dr. Sheah Chen and Dr. Xiaoyu Hong at Illinois and Dr. William Tolbert, presently at 3M Corporation. The shock measurements were made by Dr. I-Yin Sandy Lee and Dr. Jeffrey R. Hill at Illinois.

7. REFERENCES

[1] D. D. Dlott and M. D. Fayer, J. Chem. Phys. **92** (1990) 3798; A. Tokmakoff, M. D. Fayer and D. D. Dlott, J. Phys. Chem. **97** (1993) 1901.

[2] C. S. Coffey and E. T. Toton, J. Chem. Phys. **76** (1982) 949; F. J. Zerilli and E. T. Toton, Phys. Rev. B **29** (1984) 5891; R. D. Bardo, Int. J. Quantum Chem. **20** (1986) 455.

[3] H. Kim and D. D. Dlott, J. Chem. Phys. **93** (1990) 1695.

[4] D. D. Dlott, in Laser Spectroscopy of Solids II; Topics in Applied Physics, vol. 65, W. Yen, ed. (Springer Verlag: Berlin; 1989), Chapter 5.

[5] L. Fried and A. Ruggerio, J. Phys. Chem. **98** (1994) 9786.

[6] L. Fried, personal communication.

[7] S. Chen, I-Y. S. Lee, W. A. Tolbert, X. Wen and D. D. Dlott, J. Phys. Chem. **96** (1992) 7178.

[8] X. Wen, W. A. Tolbert and D. D. Dlott, J. Chem. Phys. **99** (1993) 4140.

[9] S. Chen, W. A. Tolbert and D. D. Dlott, J. Phys. Chem. **98** (1994) 7759.

[10] A. L. Huston, B. L. Justus and A. J. Campillo, Chem. Phys. Lett. **118** (1985) 267; B. L. Justus, A. L. Huston and A. J. Campillo, *ibid*, **128** (1986) 274; B. L. Justus, C. D. Merritt and A. J. Campillo, *ibid*, **156** (1989) 64; B. L. Justus, A. L. Huston, and A. J. Campillo, Appl. Phys. Lett. **47** (1986) 1159.

[11] I-Y. S. Lee, J. R. Hill, and D. D. Dlott, J. Appl. Phys. **75**, (1994) 2975.

[12] I-Y. S. Lee, J. R. Hill, and D. D. Dlott, (unpublished work).

[13] X. A. Shen and Y. M. Gupta, J. Appl. Phys. **70** (1991) 7549.

[14] X. Wen, W. A. Tolbert and D. D. Dlott, Chem. Phys. Lett. **192** (1992) 315.

[15] D. E. Hare and D. D. Dlott, Appl. Phys. Lett. **64** (1994) 715; D. E. Hare, J. Franken, D. D. Dlott, E. L. Chronister and J. J. Flores, Appl. Phys. Lett. (in press, 1994).

JOURNAL DE PHYSIQUE IV
Colloque C4, supplément au Journal de Physique III, Volume 5, mai 1995

Recent Developments to Understand Molecular Changes in Shocked Energetic Materials

Y.M. Gupta

Shock Dynamics Center and Department of Physics, Washington State University, Pullman, Washington 99164-2814, U.S.A.

Comment:

First of all I would like to thank Professor S. Odiot and her colleagues for organizing a productive and enjoyable workshop. The presentations at the workshop covered a broad range of topics which reflects the interdisciplinary character of the field. Given my current interests, I shall confine my comments to fundamental issues related to the shock initiation problem. I believe that examination of the shock front remains an important challenge. Without this knowledge, it is difficult to address the question of how the energy is transferred to the molecules. The "up pumping" mechanism proposed by Dlott and Fayer is an interesting hypothesis and one that needs to be examined more carefully. Jerry Dick's ideas about the role of steric hindrance for chemical decomposition merit further study. How fast can this mechanism occur? If a detailed understanding of molecular mechanisms is the need, which it should be, then experiments on single crystals and liquids are essential. These are also the materials for which theoretical calculations can provide insight and, hence, aid experimental analysis. I believe that concerted and sustained efforts on a few selected materials will be most useful. Both experiments and theoretical calculations are needed to understand the role of atomic/molecular defects on a fundamental level. Regarding the onset of chemical reactions, is the problem completely thermal in nature or is it possible to obtain direct electronic excitations? While the latter may not seem energetically favorable at first glance, we need to keep in mind that the shock front represents major disruption of the crystal lattice. These are interesting and difficult questions which will keep us busy for some time.

Once the reaction has been initiated, it is important to follow the various intermediate steps to provide a good link to the reactive flow or the hydrodynamic problem. Experimentally, this is again a very difficult task and anybody who can contribute to this problem should be encouraged to do so. I believe this is an area where high pressure and high temperature studies may provide useful insight.

In closing I make two observations: (i) Understanding the shock response of condensed explosives is a challenging, interdisciplinary problem that will require interactions among experts from several different disciplines. However, care is needed to ensure that scientific convergence will be achieved. (ii) I am very encouraged by the emphasis on fundamental research on energetic materials in France. Thank you for a valuable interaction.

I. INTRODUCTION

A good understanding of molecular mechanisms governing shock induced chemical decomposition in condensed explosives is important to studies of shock sensitivity and the development of new energetic materials. While the need for achieving this understanding has long been recognized, progress has been slow because of the inherent complexity of the scientific issues and the difficulty in conducting the desired shock compression experiments on explosives [1,2]. Historically, the development and use of energetic materials in ordnance applications has relied on advances in formulation and synthesis of energetic materials and correlating these to data from tests designed to measure performance and sensitivity for applications of interest. On the analytic side, studies have focused mainly on the mathematical modeling of phenomena related to the generation, propagation, and stability of detonation waves [1-4].

Plane shock wave experiments provide a well controlled method to examine shock initiation (defined as the onset of measurable chemical decomposition) in condensed energetic materials [5]. Because the loading times in these experiments are comparable to the characteristic times associated with structural and chemical changes, they provide a unique opportunity to examine time dependent microscopic processes associated with these changes. Experimental developments in the United States, the Former Soviet Union, and France in the late sixties and seventies have resulted in time resolved continuum measurements on a large number of explosives [5,6]. These data have provided considerable information on the properties of unreacted and reacted explosives. Phenomenological models have been developed to infer details regarding reaction kinetics and energy release rates from stress and/or particle velocity histories. A good account of the macroscopic or continuum mechanisms governing shock sensitivity and the subsequent coupling of chemical decomposition to hydrodynamic flow may be seen in Part Three of Reference 2. In contrast to the considerable progress in continuum measurements and analyses, a good understanding of molecular mechanisms remains a challenging problem primarily due to the lack of real time spectroscopy data in shocked condensed explosives. Some representative examples of the theoretical work on molecular mechanisms governing decomposition and experimental measurements on recovered samples are summarized in Part Two of Reference 2.

The remainder of this paper reviews some recent developments associated with shock induced chemical decomposition by defining the key scientific issues, indicating experimental approaches to time resolved optical spectroscopy, and summarizing some results from our ongoing work on liquid nitromethane. Current limitations of such studies and future directions are indicated. As requested by the workshop organizers, the paper is intended to provide an overview of the developments. More details may be seen in the cited literature.

II. SCIENTIFIC ISSUES

Because of the emphasis on microscopic mechanisms, the present discussion is restricted to energetic materials that are macroscopically homogenous. We consider the propagation of a plane shock

wave in a homogenous explosive and the subsequent build up of pressure due to the initiation of a chemical reaction and the release of chemical energy. It is convenient to consider this problem in three sequential stages:

1. Transfer of energy from the shock wave to the energetic material, that is, "excitation" of the molecules.
2. Initial and subsequent molecular changes associated with chemical decomposition of the "excited" molecules.
3. Significant energy release and coupling of this energy to the propagating shock wave resulting in macroscopically observable pressure increase.

The stages indicated above are an idealization and there will likely be an overlap between these stages depending on the characteristic times associated with each stage. The incorporation of macroscopically heterogeneous materials does not change the problem conceptually; it does introduce an extra complexity at the continuum level because of inhomogenous deformation in the material.

Almost all of the shock wave research on condensed explosives has concentrated on the third stage or the reactive flow problem [1-4]. This emphasis is due primarily to the close relationship of such studies to practical considerations of performance, stability, and safety in various applications. While the benefits of continuum studies on shocked energetic materials are well recognized, it is not possible to get information about the first two stages from the continuum data alone.

Regarding the question of energy transfer, the rise time of the shock front and the nature of atomic/molecular changes at the front are central to understanding this aspect of the problem. As Dremin has pointed out [7], the creators of the ZND model likely envisioned the shock front to be equal to the mean free path of a few molecules and thus their assumption of no reaction in the front seemed reasonable. However, the tremendous rates of loading at the front can significantly alter the material state which in turn influences the subsequent chemical decomposition [7]. For a mechanical disturbance involving the motion of ions or atoms, rise times are expected to be 100fs or larger. Hence, an examination of how the energy is transferred from the shock wave to molecules in a condensed material requires fast diagnostics. While several competing hypotheses have been put forward [8-10], the energy transfer mechanism remains an open question because of a lack of experimental data. The mechanisms proposed by Faust, and Dlott and Fayer represent a start on this challenging problem [9,10]. Although molecular dynamics calculations are expected to be quite beneficial [11], high time resolution data (ps time scales) are needed to address this issue.

Most of the experimental effort on examining molecular changes has concentrated on the second part, that is, spectroscopic measurements behind the shock front. This is the principal theme of the remainder of this paper.

III. OPTICAL SPECTROSCOPY EXPERIMENTS

The need to understand the shock response of condensed materials at the atomic/molecular level led to the development of optical spectroscopy methods, during the eighties, at several organizations: CEA (France), Livermore, Los Alamos, NRL (Washington, D.C.), Sandia, and our laboratory at Washington State University. These measurements can be divided into two categories: electronic spectroscopy (absorption emission, fluorescence, and reflection) and vibrational spectroscopy (CARS, TRISP, Spontaneous Raman) [12-14]. A noteworthy aspect of the work at Washington State University has been the development of time resolved measurements for both electronic and vibrational spectroscopies. Although time resolved measurements are inherently more difficult, such data are essential for understanding the mechanisms and kinetics that govern time dependent processes such as shock induced chemical decomposition.

During the last fifteen years, time resolved absorption, reflection, fluorescence, and Raman measurements have been obtained on both liquids and solids at Washington State University. Details of our work and spectroscopy efforts by others may be seen in published articles and reviews [12-16]. Here we briefly summarize how the optical spectroscopy experiments are conducted and the current limitations of such measurements.

Optical spectroscopy under shock loading can be considered as a "pump and probe" experiment where the pump is the propagating shock wave. Although there exist many techniques for producing shock waves, flyer plate impact methods provide the best control for producing pulses of known amplitude and duration. Because of the single event nature of the experiment and because the pump is a large amplitude mechanical shock wave produced by impact, these experiments are quite challenging. Figure 1 shows a typical experimental setup that is used for our time resolved spectroscopy measurements in shocked liquid nitromethane [17-19]. In our impact experiments, thin liquid samples (ranging from 10 to 250 μm depending on the spectroscopic method) are subjected to step-wise-loading (SWL) due to shock reverberation between two optical windows (typically, sapphire crystals); for a solid sample the front window can be eliminated. By varying the impactor velocity and thickness, shock wave amplitudes and durations can be controlled precisely.

Raman measurements are obtained continuously at pre-determined time intervals (few ns to 50 ns) while the sample is being subjected to shock wave, uniaxial strain loading. Light from a pulsed laser is sent to the sample and scattered light is dispersed in frequency by the spectrometer, temporally dispersed by the electronic streak camera and recorded on a two-dimensional CCD detector; the data consist of intensity-frequency-time output. Other optical components are indicated in the figure; all light transmission to and from the sample is carried out using optical fibers. For destructive experiments, this is an important feature. Using appropriate trigger pins, the pulsed laser and the streak camera are carefully synchronized with both the impact event and the arrival of a the shock wave at the sample. For high time resolution, time synchronization becomes an increasingly difficult and important problem.

The electronic spectroscopy experiments, particularly reflection and luminescence experiments, are quite similar in setup because both of them utilize a back scattering geometry. The absorption experiment utilizes a single pass transmission measurement and, as such, the impactor arrangement has to be modified to permit light to come from the impactor side [18]. Further details on all of these experimental methods may be seen elsewhere [18-20]. It is worth emphasizing that despite the sophistication of the optical spectroscopy measurements, such data are of limited value unless the continuum parameters (stress amplitude, pulse duration, and temperature when applicable) are precisely known. Hence, the optical measurements compliment the continuum data but are not a substitute for these data. In all of our work, a careful attempt is made to correlate the optical spectroscopy data with continuum results.

Before concluding the brief discussion on optical spectroscopy experiments, a non-trivial issue associated with these measurements needs to be mentioned. Because a shock wave is a propagating disturbance, both spatial and temporal variations need to be considered for the physical quantities of interest. It is for this reason that time resolved continuum measurements using Lagrangian probes (stress and/or particle velocity histories at a fixed material location) have proven immensely beneficial to reactive flow studies [21]. Ideally, one would want the highest spatial and temporal resolution to be achieved simultaneously in the spectroscopy experiments. It is not obvious how such data can be obtained with existing detector technology. In our experiments, we have attempted to meet this requirement by using thin samples (~10-100 μm) and recording the spectra with ns resolution. The price we pay is that the sample reaches the peak state through step-wise-loading (SWL) and not through a single shock. By using very thin samples, the total time for shocking up may be reduced considerably but it will still take several steps to reach the peak stress. Alternatively, experiments can be carried out on thick samples to achieve single shock loading but it is not clear that very high spatial and temporal resolution can be achieved for a time-dependent process. Examination of the propagating shock front remains an important challenge.

IV. SHOCK RESPONSE OF NITROMETHANE

To date, the most comprehensive optical spectroscopy work on a shocked condensed energetic material is the effort on liquid nitromethane at Washington State University [17-19, 22]. Although it is not possible to summarize all aspects of our nitromethane work in a few pages, some features of this work that are important to this workshop are indicated here. Two other examples of comprehensive spectroscopic investigations of shock induced molecular changes may be seen in the Los Alamos work on liquid diatomics [23] (particularly nitrogen) and the work on liquid CS_2 at Washington State University [24].

Nitromethane is an insensitive high explosive that is well suited for investigation at an academic institution. It has served as a good prototype material for investigating chemical decomposition in nitrocompounds. Because of these reasons, it is one of the best studied energetic materials and there is a

large body of spectroscopic data at ambient pressures [25], static high pressure data [26], and continuum data under shock loading [27]. There existed some shock wave spectroscopy data prior to our work but most of these data constituted exploratory efforts and the results were not always in agreement [28-30]. Nitromethane has the additional advantage that it can be sensitized by very small amounts of amines [25]. Potential mechanisms for chemical decomposition in pure and sensitized nitromethane have been considered by Engelke [31], Bardo [32], Constantinou [25], and Cook and Haskins [33]. The Ph.D thesis by Constantinou presents a comprehensive account of thermal decomposition studies in pure and sensitized nitromethane at ambient pressures, and provides an excellent background to the present work [25]. Our objectives in this work were to address the following broad issues:

1. What are the molecular changes associated with shock induced decomposition in nitromethane?
2. Are the differences in pure and sensitized nitromethane response merely differences in threshold pressure and temperature or are the molecular mechanisms themselves different?
3. How are the spectroscopic and continuum studies related?
4. Is the initiation of chemical reaction in nitromethane controlled by pressure or by temperature?

In addition to these issues, there were a number of other needs that were addressed in this work. Among the most prominent of these tasks was the development of an equation of state for liquid nitromethane for use at different initial temperatures. The experimental work on sensitized nitromethane was carried out by G. Pangilinan and C. Constantinou while the pure nitromethane work has comprised the Ph. D thesis of J.M. Winey. Extensive studies [17-19, 22] using both electronic and vibrational spectroscopy on pure and sensitized nitromethane (addition of 0.1 wt. percent of ethylenediamine) were conducted. To establish that the data corresponded to irreversible chemical changes, a number of unloading experiments were carried out; in these experiments, the shock pressure is unloaded to very small values while maintaining the sample in a state of uniaxial strain.

The electronic spectroscopy experiments are simpler to carry out and are valuable in establishing threshold conditions for irreversible changes and for examining the kinetics of the decomposition. Winey's measurements on pure nitromethane at different initial temperatures have been very useful in inferring induction times, defined as the time delay between the shock first arriving at the sample and the occurrence of an irreversible change in the electronic spectra [22]. In thermal explosion models, the induction time is related to the reciprocal of the reaction rate. Winey's results demonstrate that, as expected, the absorption data provide a more sensitive probe of the reaction process. This inference is based on the smaller induction time observed in the spectroscopy experiments in contrast to the continuum data. The absorption data from experiments conducted at different initial temperatures show a strong correlation with the calculated peak temperatures and minimal dependence on pressure [22].

While the electronic spectroscopy measurements are very useful as indicated above, they are difficult to analyze to obtain detailed information about the molecular changes. Hence, we have invested

a considerable effort in obtaining good time resolved Raman measurements in shocked nitromethane. A recent paper has presented the first evidence of the ability to continuously monitor molecular changes associated with the onset of a chemical reaction in a shocked explosive [19]. In the following paragraphs, we summarize some of the important findings from our Raman measurements [17, 19, 22]. Further details will be presented elsewhere [22, 34].

In shocked nitromethane, we are able to monitor several of the intramolecular modes: CN stretch (917 cm^{-1}), superposed NO_2 stretch/CH_3 bend (1400 cm^{-1}/1377 cm^{-1}), and the CH_3 stretch (2968 cm^{-1}). Studies of unreacted shocked nitromethane showed hardening of different modes and a relative enhancement of the NO_2 stretch/CH_3 bend [17]. A representative example of the changes in the Raman spectra in pure nitromethane shocked to 14 GPa is presented in Figure 2. For clarity, not all of the spectra are shown. These data clearly reveal the mode hardening with pressure. As discussed elsewhere [17,18], the response of pure nitromethane is completely reversible to a peak pressure of 14 GPa under step-wise-loading (SWL). As shown in Winey's work, pure nitromethane undergoes irreversible changes at 16-17 GPa and higher pressures, and at higher initial temperatures [22]. The higher peak pressure threshold under SWL, in contrast to single shock loading, is a consequence of the lower peak temperature attained under SWL loading [22].

In contrast to pure nitromethane, our electronic spectroscopy results had shown that sensitized nitromethane (0.1 wt. percent ethylenediamine) undergoes an irreversible change at peak pressures in the vicinity of 10 GPa (the exact threshold pressure has not been determined) [18]. To investigate the molecular changes associated with the chemical decomposition in sensitized nitromethane, a series of Raman measurements were carried out in sensitized nitromethane [19,34]. Representative spectra of sensitized nitromethane shocked to 14 GPa are presented in Figure 3. Initially, mode hardening and some broadening can be observed in the spectra. The most dramatic result is the difference between the last two spectra which show the complete disappearance of the CN bond while the other modes, though broadened, are clearly present. These results have been confirmed by higher resolution experiments. Unlike the pure nitromethane spectra at the same shock pressure, the major changes observed in sensitized nitromethane are irreversible.

Our data is consistent with the hypothesis of Cook and Haskins [33] that CN bond scission is important in the shock induced decomposition of amine sensitized nitromethane. They carried out ab-initio molecular orbital calculations to show that the activation energy for breaking the CN bond is lowered significantly because of the interaction of the amino group with the nitromethane molecule. We conclude by pointing out that Winey's results demonstrate that not only is the threshold shock pressure (and temperature) higher for a chemical reaction in pure nitromethane but the reaction mechanism is different [22]. Unlike sensitized nitromethane, CN bond scission is not the first step in the chemical decomposition of pure nitromethane. To summarize, the presence of amine is not merely a catalyst for the nitromethane reaction; instead, it changes the mechanism of decomposition in shocked nitromethane.

V. DISCUSSION AND CONCLUDING REMARKS

The nitromethane work has demonstrated clearly the ability to monitor molecular changes associated with shock induced chemical decomposition in condensed energetic materials. Despite this exciting development, numerous challenging problems remain both in experimental and theoretical work. Using the nitromethane work as a representative example, some specific issues are discussed first. Next, some broader issues and future needs are commented upon.

Some of the unresolved issues pertaining to the nitromethane work are: temperature measurements in the unreacted material to better define the threshold pressure and temperature conditions and to permit comparisons with more conventional decomposition studies; determining the specific cause of the large background increase (intensity change) and identifying the subsequent reactions and products beyond the initial onset of decomposition; further details about the molecular processes that lead to the lowering of the CN bond energy because of the presence of the amine. Cook and Haskins [33], and Constantinou [25] have put forward conflicting suggestions as to how this occurs. Resolution to these ideas will require experiments designed to evaluate the different suggestions.

Issues indicated in the preceding paragraph are also expected to arise in similar studies on other materials. Resolution to these issues will require the ability to obtain and analyze intensity measurements with high precision. This is not a simple matter and we are currently conducting an in-depth examination of the response of various components used for signal detection and recording. Given the inherently weak Raman signals, improvements in signal-to-noise ratio remain an ongoing challenge.

At a broader level, we emphasize the need for parallel theoretical studies that can provide guidance to the experimental effort. Given the complexity, cost, and time associated with shock wave experiments, it is not possible to resolve scientific issues by gathering vast amounts of data. Unlike conventional spectroscopy experiments, the spectral and temporal windows have to be pre-determined and current limitations on detectors necessitate a compromise between spectral coverage and spectral resolution. In most of our experiments, we obtain low dispersion measurements (similar to Figures 2 and 3) followed by higher dispersion measurements. Theoretical calculations can significantly increase the efficiency of the experimental work.

An obvious extension of the present work is to examine energetic solids. Dick and coworkers at Los Alamos have drawn interesting correlations between their continuum measurements and optical emission data and suggested a potential micromechanism for shock initiation based on the idea of steric hindrance [35]. Dick has also put forward ideas as to how such a mechanism might work for crystalline nitromethane [36]. We expect to start work in the near future on energetic solids using the electronic and vibrational spectroscopy techniques reported here.

The question of how a shock wave imparts energy to energetic materials is an important one. Dremin has pointed out the need for examining the shock front; this is a problem of long standing both in energetic and non-energetic materials. Given the temporal resolution needs, there is not a simple or

obvious way to carry out such measurements. We are currently investigating potential experimental approaches that may permit sub-nanosecond time resolution. With regards to the energy transfer problem, molecular dynamics calculations on a realistic system (including incorporation of atomic defects) are expected to be valuable. As stated earlier, the work by Dlott and Fayer provides a comprehensive description of a potential mechanism [10]. Although their hypothesis appears attractive for many situations, it is not clear how their mechanism can explain the observations of Dick and coworkers on crystalline solids [35].

In conclusion, we point out that the subject of shock induced chemical reactions in condensed energetic materials is at an exciting stage. Experimental and theoretical developments have made it possible to address issues that could not be addressed even a few years ago. There exists now the potential for linking molecular mechanisms to continuum and hydrodynamic phenomena. However, the scientific issues of interest are exceedingly complex. In our opinion, careful selection of a limited number of materials and sustained studies on these materials by different groups will be needed to achieve success. Interactions similar to those that took place at this workshop are most beneficial.

ACKNOWLEDGMENTS

It is a pleasure to acknowledge the hard work and dedication of Gerry Pangilinan, Mike Winey, and Dinos Constantinou who have carried out much of the nitromethane work reported here. George Duvall is sincerely thanked for his work on the nitromethane equation of state and for many helpful discussions. Dave Savage and Kurt Zimmerman contributed to the impact experiments. Finally, this work would not have been possible without the sustained support of the Office of Naval Research; Dr. R.S. Miller is sincerely thanked for his vision, enthusiastic support, and periodic reminders to work on a real explosive.

REFERENCES

[1] Fickett Ward Davis W.C., Detonation (University of California Press, Los Angeles, 1979).

[2] Cheret R., Detonation of Condensed Explosives (Springer-Verlag, New York, 1993).

[3] Mader C.L., Numerical Modeling of Detonations (University of California Press, Los Angeles, 1979).

[4] Dremin A.N., Lectures on Detonation and Shock Compression of Condensed Materials (Shock Dynamics Center, Washington State University, Pullman, WA 99164-2814, 1993).

[5] Chapter IX of Reference [2].

[6] Proceedings of Sixth through Tenth Symposia (International) on Detonation (Office of the Chief of Naval Research, Arlington, VA. 22217-5000).

[7] Page 59 of Reference [4].

[8] Page 68 of Reference [4].

[9] Faust W.L., Science **247** (1989) 37.

[10] Dlott D.D. and Fayer M.D., *J. Phys. Chem.* **92** (1990) 3798; Tokmakoff A., Fayer M.D., and Dlott D.D., *J. Phys. Chem.* **97** (1993) 1901.

[11] Brenner D.W., Robertson D.H., Elert M.L., and White C.T., *Phys. Rev. Lett.* **70** (1993) 2174.

[12] Gupta, Y.M. Shock Compression of Condensed Matter-1991, S.C. Schmidt, R.D. Dick, J.W. Forbes, and D.G. Tasker, Editors (North-Holland, Amsterdam, 1992), 15.

[13] Moore D.S. and Schmidt S.C., Shock Waves in Condensed Matter-1987 (North-Holland, Amsterdam, 1988), 35.

[14] Renlund A.M. and Trott W.M., Shock Waves in Condensed Matter-1987 (North-Holland, Amsterdam, 1988) 547.

[15] Gupta Y.M., *High Pressure Research* **10** (1992) 713.

[16] Boteler J.M. and Gupta Y.M., *Phys. Rev. Lett.* **71** (1993) 3497.

[17] Pangilinan G.I. and Gupta Y.M., *J. Phys. Chem.* **98** (1994) 4522.

[18] Constantinou C.P., Winey J.M., and Gupta Y.M., *J. Phys. Chem.* **98**, (1994) 7767.

[19] Gupta Y.M., Pangilinan G.I., Winey J.M., and Constantinou C.P., *Chem. Phys. Lett.* **232** (1995) 341.

[20] Gustavsen R. and Gupta Y.M., *J. Phys. Chem.* **95** (1991) 451.

[21] Cowperthwaite M.C. and Rosenberg J.T., Proceedings of the Sixth Symposium on Detonation (OCNR, Arlington VA, 1976) 786.

[22] Winey J.M., Ph.D. thesis, work in progress.

[23] Schmidt S.C., Moore D.S., and Shaw M.S., *Phys. Rev. B* **35** (1987) 493.

[24] Yoo C.S., Gupta Y.M., and Duvall G.E., in Shock Compression of Condensed Matter-1989 [North-Holland, Amsterdam, 1990] 675.

[25] Constantinou C.P., The Nitromethane-Amine Interaction, Ph.D. thesis, Cambridge University (1992).

[26] Miller P.J., Black S., and Piermarini G.J., *J. Phys. Chem.* **93** (1989) 462.

[27] Hardesty D.R., *Combust. Flame* **27** (1976) 229.

[28] Delpeuch A. and Menil A., Shock Waves in Condensed Matter-1983 (Elsevier Publishing, New York, 1984) 309.

[29] Renlund A.M. and Trott W.M., Shock Compression of Condensed Matter-1989 (Elsevier Publishing, New York, 1990) 875.

[30] Schmidt S.C., Moore D.S., Shaner J.W., Shampine D.L., and Holt W.T., *Physica* **139 & 140B** (1986) 587.

[31] Engelke R., Schiferl D., Storm C.B., and earl W.L., *J. Phys. Chem.* **92** (1988) 6815.

[32] Bardo R.D., *Int. J. Quantum Chem.* **20** (1986) 455.

[33] Cook M.D. and Haskins P.J., Proceedings of the Ninth Symposium (International) on Detonation (OCNR, Arlington, VA. 1989) 1027.

[34] Pangilinan G.I., Constantinou C.P., and Gupta Y.M., manuscript in preparation.

[35] Dick J.J., Mulford R.N., Spencer W.J., Pettit D.R., and Shaw D.C., *J. Appl. Phys.* **70** (1991) 3572.

[36] Dick J.J., *J. Phys. Chem.* **97** (1993) 6193.

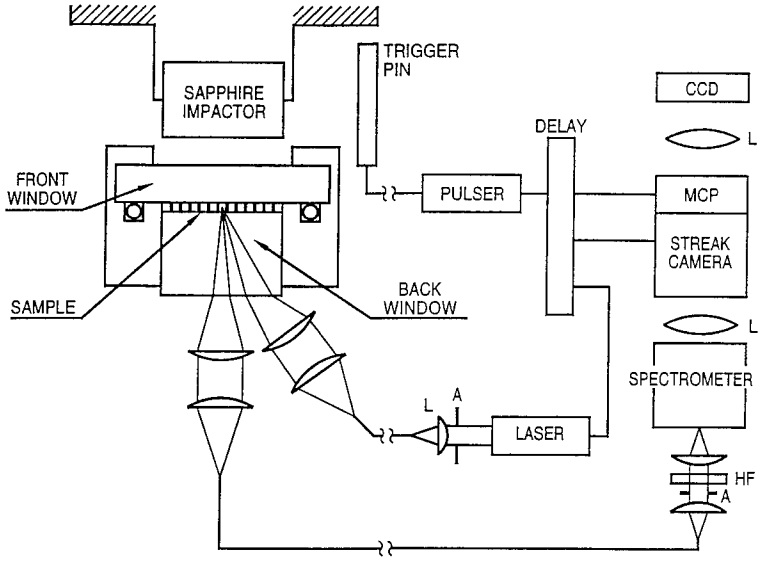

Figure 1. Experimental configuration for obtaining time resolved Raman measurements in shocked nitromethane. L-lens; A-aperture; HF-holographic laser line filter; MCP-microchannel plate intensifier; CCD-charge coupled device detector. Light transmission to and from the sample is carried out using optical fibers. (Ref. 19)

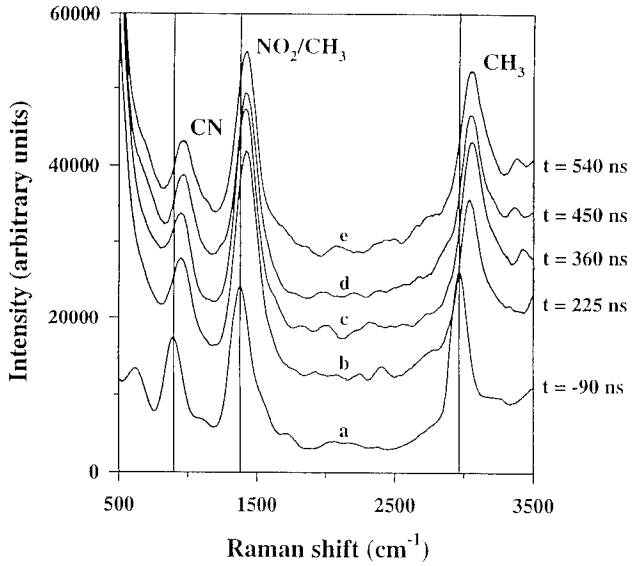

Figure 2. Representative Raman spectra of nitromethane shocked to 14 GPa, obtained at (a) ambient pressure; (b) during shock up; (c), (d) and (e) after peak pressure has been reached. t=0 corresponds to the time when the shock wave initially enters the sample. Vertical lines mark the frequency positions of the various modes at ambient pressure. For clarity, spectra (b) to (e) are vertically offset successively to 5000 units. (Ref. 19)

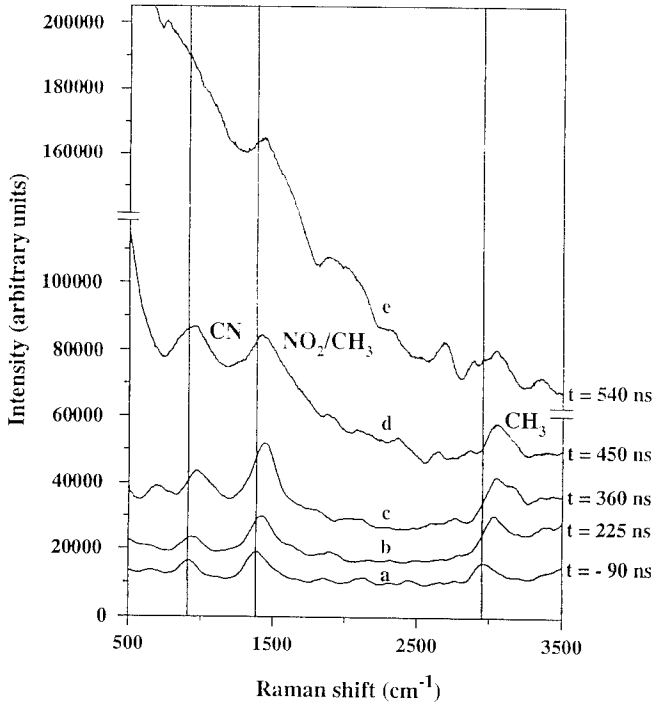

Figure 3. Representative Raman spectra of a solution of nitromethane with ethylenediamine additive (0.1 weight %) shocked to 14 GPa, obtained at times similar to those in Figure 2. Vertical lines mark the frequency positions of the various modes at ambient pressure. Spectra (b) to (e) are vertically offset successively by 5000 units. The CN vibration softens in spectrum (d) and then disappears in spectrum (e). An increase in the background, due to weak broad features and elastic scattering, is observed after peak pressure is attained. (Ref. 19)

4 GENERAL DISCUSSION

Chairman : Alain Delpuech, Centre d'Etudes du Ripault (CEA/DAM)

Après une première partie consacrée à une approche macroscopique de la détonation, un ensemble de travaux présentés dans cette partie et les suivantes se préoccupent de l'échelle microscopique.

Ces travaux ont souvent pour dénominateur commun un souci de proposer à l'échelle moléculaire une approche qui permette de rendre compte des grandeurs et propriétés caractéristiques de la substance (vitesse de détonation, sensibilité, thermostabilité, ...). Et dans tous les cas ils se concluent par la proposition d'un modèle plus ou moins élaboré faisant appel à un certain nombre de propositions bâties au moyen de théories souvent originales, toujours complexes mais parfois éloignées de la réalité physique des phénomènes mis en cause dans le cas de l'explosif.

La question majeure est de valider ces modèles, de les compléter ou de les infirmer sur la base de résultats expérimentaux.

L'objet de cette table ronde est de confronter les mécanismes de décomposition envisagés d'un point de vue théorique, aux résultats de l'expérience.

Sachant que nous avons tous à l'esprit que ces expériences sont difficiles compte-tenu des contraintes de temps (phénomènes mis en jeu dans des plages de 10^{-12} à 10^{-9}s), des contraintes de température (plusieurs centaines à milliers de degrés) et de pression (plusiers centaines de kilobars), nous verrons en particulier combien en raison de ces contraintes, le développement de ces expériences doit être spécifique au sujet traité.

Nous nous poserons sans doute la question de savoir si les résultats obtenus à l'aide des techniques spectroscopiques les plus sophistiquées et les plus récentes (picosecondes) sont représentatifs de ce qui se passe dans un front de choc et dans quelle mesure l'utilisation ou l'évolution de ces techniques doivent être analysées.

Ayons bien conscience que cette évolution sera, si elle est possible, très longue, et qu'il serait très dangereux de prendre pour argent comptant les résultats obtenus dans des conditions "tranquilles" et de s'en servir mal à propos pour étayer des modèles rendant compte de phénomènes survenus au moment de la décomposition explosive.

4-1 Statements from Laboratories on the Experimental Assessment of the Molecular Mechanisms

A Raman Spectroscopy Study of Nitromethane up to 350°C and 35 GPa ; **S.Courtecuisse**, F.Cansell, D.Fabre and J.P.Petitet

Sub-Picosecond Time-Resolved Spectroscopy of Energetic Materials ; The Nitromethane and Nitro-Stilbenes; C.Rajchenbach, G.Jonusauskas and **C.Rullière**

Experimental Study of Photon-Phonon Interactions in an Explosive by Laser Probe Mass Spectrography ; J.F.Eloy and **A.Delpuech**

Influence of Initiation Strength, Ambient Inert Gas, Al-Content and Polymeric Binder on the Detonation Products of High Explosives ; F.Volk

Sulphuric Acid Influence on the Nitrocompounds Detonation Reactions ; **V.N.Gamezo**, B.N.Kondrikov, G.D.Kozac and S.M.Khoroshev

Carbon in Detonation products. A "Three-Phase" Modelisation ; **M.L.Turkel** and F.Charlet

Rearrangements of Ammonium Nitrate Cluster Ions with High Internal Energy ; **R.J. Doyle** and Brett I. Dunlap

JOURNAL DE PHYSIQUE IV
Colloque C4, supplément au Journal de Physique III, Volume 5, mai 1995

A Raman Spectroscopic Study of Nitromethane up to 350 °C and 35 GPa

S. Courtecuisse, F. Cansell*, D. Fabre* and J.-P. Petitet*

Centre d'Etudes de Vaujours-Moronvilliers, CEA, 77181 Courtry, France
** Laboratoire d'Ingénierie des Matériaux et des Hautes Pressions, CNRS, Institut Galilée, Université Paris-Nord, 93430 Villetaneuse, France*

Abstract: Nitromethane has been studied as a model of the energetic nitro materials. The liquid - transition line has been established by Piermarini [1] and a first solid - solid transition corresponding to the methyl group rotation locking has been evidenced by Cromer [2]. In order to precise the phase diagram of nitromethane, a study has been performed by Raman scattering in the pressure and temperature range of 0 - 35 GPa and 20 - 350°C respectively. From these experimental results three new solid phases of nitromethane called III, IV, V and their stability domain have been located. A first chemical transformation line has been detected by the disappearance of nitromethane Raman modes and by the irreversible formation of a transparent solid (CI). A second chemical transformation (CI - CII), at higher temperature, is observed by the sudden darkening of the sample.

1. INTRODUCTION

The nitromethane, the simplest energetic nitro-compound, has been choosen as a model. Since the study of the phase diagram of the nitromethane appears to be a preliminary stage to deal with a study of the violent decomposition phenomena, we report in this communication results of Raman spectroscopy up to 35 GPa and 350°C. At ambiant pressure and at low temperature the crystal structure of solid nitromethane was determined by Trevino *et al.* [3]. The structure is orthorhombic with four molecules per cell. At pressures between 0.3 and 6.0 GPa at ambiant temperature the structure is the same as the low temperature structure except for a rotation of the methyl group [2]. From the experimental results two chemical transformation have been determined. The first transformed compound CI is obtained from nitromethane with a low transformation rate (several hours). The second compound (CII) at higher temperature is obtained with a higher tranformation rate than CI (some minutes). Moreover three new phase transitions are reported in the *P-T* diagram.

2. EXPERIMENTAL METHOD

The experiments have been performed in a high pressure membrane type diamond anvil cell [4] made of refractory alloy. The pressure was monitored by a pneumatic ram connected to a pressure generator through a high pressure flexible capillary. The stainless steel gasket had an aperture of 0.15 mm in diameter and 0.15 mm in depth. Heating is performed by a coil surrounding the cell and monitored by a thermocouple in contact with the diamond anvils. The pressure was determined by the pressure shift of the $^5D_0$-$^7F_0$ singlet (685.4 nm at 0.1 MPa) of $SrB_4O_7:Sm^{2+}$ chips set inside the high pressure chamber [5]. Raman experiments were carried out in backscattering configuration with an argon ion laser at 514.5 nm wavelength. The laser power was 50 mW in order to avoid any thermal or photochemical effect. The frequencies were measured with a multichanel spectrometer DILOR XY. Plasma lines were used for the frequency calibration. Measurements have been performed at constant temperature and variable pressure for the localization of the solid - solid transitions and at variable temperature for the determination of the irreversible transformations. Nitromethane samples were from commercial purchase (ALDRICH 99+%) and were used without further purification.

3. RESULTS AND DISCUSSION

The *P-T* diagram of nitromethane has been determined (Fig. 1) by the study of the shift of different Raman modes versus static pressure and temperature: $A_1\nu(CN)$ (Fig. 2). $A_1\nu_S(CH_3)$. $A_1\nu_S(NO_2)$ and $B_1\nu_a(NO_2)$ (Fig. 3). Four solid - solid transitions and two irreversible transformations have been determined.

The solid I - solid II transition is located at 3 ± 0.2 GPa at 20°C. It is detected by breaks or discontinuities in the behaviour of the different studied Raman modes. The discontinuity of the linewidth (Γ_{NO}) (Fig. 4) of the B_1 $\nu_a(NO_2)$ mode versus pressure confirms unambiguously the transition. The solid I - solid II transition line does not run parallel to the temperature axis (Fig. 1). The solid I - solid II transition is reported by Cromer *et al.* [2] at 3.5 GPa at ambiant temperature. But these works were made with too large pressure increments to precisely locate the transition.

The solid II - solid III transition is located at 7.5 ± 0.5 GPa at ambiant temperature. It is particularly detected by the appearance of new bands. The behaviour of Γ_{NO} and of the linewidth (Γ_{CH}) of the $A_1\nu_S(CH_3)$ mode versus pressure confirms the transition. This transition is probably a first order transition with an increase of the molecule number per cell. The solid II - solid III transition is independent of the temperature.

The solid III - solid IV is located at 13.2 ± 1 GPa at ambiant temperature. It is observed by discontinuities or breaks in the slope of the different Raman modes versus pressure and confirmed by the behaviour of Γ_{NO} and Γ_{CH}. This solid III - solid IV transition is dependent of the temperature and the pressure.

The solid IV - solid V is located at 25 ± 1 GPa at ambient pressure. This transition has not been studied at higher temperature since nitromethane is transformed as soon as about 55°C are reached.

The transformation nitromethane - CI compound is irreversible and slow. Since CI is an amorphous

compound its Raman peak is not distinguishable from the ground.

The CI - CII transformation is irreversible and more rapid than the nitromethane - CI transformation. CII did not give any Raman signal.

From these results, a specific behavior of the nitromethane has been observed. First the stability domain increases with the pressure up to 17 GPa (Fig 1). Second, the unusual negative jump of the wavenumber versus pressure of the $B_1\nu_a(NO_2)$ mode is particulary interesting (Fig 3). The same study performed with deuteried nitromethane does not show such a jump of wavenumber of the $B_1\nu_a(NO_2)$ mode.

4. CONCLUSION

The pressure and temperature dependence of the more intense vibrational Raman modes of solid nitromethane has been studied for the purpose of establish its phase diagram. The nitromethane compression up to 35 GPa at ambiant temperature allowed to show up four solid - solid transitions and two chemical transformations. Some of the reported results show an unusual behavior of nitromethane vs. pressure and temperature.

REFERENCES

[1]: G.J.Piermarini, S.Block and P.J.Miller, *J. Phys.Chem.*, **93**, 457 (1989)

[2]: D.T.Cromer, R.R.Ryan and D.Schiferl, *J. Phys.Chem.*, **89**, 2315 (1985)

[3]: S.F.Trevino, E.Prince and C.R.Hubbard, *J. Chem. Phys.*, **73**, 2996 (1980)

[4]: R.Letoullec, J.P.Pinceaux and P.Loubeyre, *High Pressure Res.*, **1**, 77 (1988)

[5]: A. Lacam and C. Chateau, *J. Appl. Phys.*, **66**, 366 (1989)

[6]: F. Cansell, D. Fabre and J.P. Petitet, *J. Chem. Phys.*, **99**, 7300 (1993)

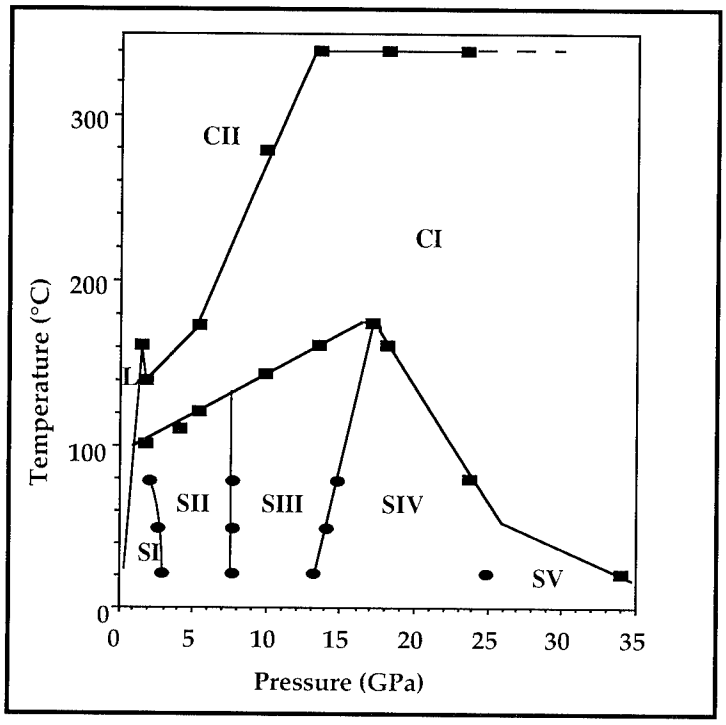

Figure 1: Phase diagram of nitromethane versus static pressure and temperature. The liquid - solid transition is from [1].

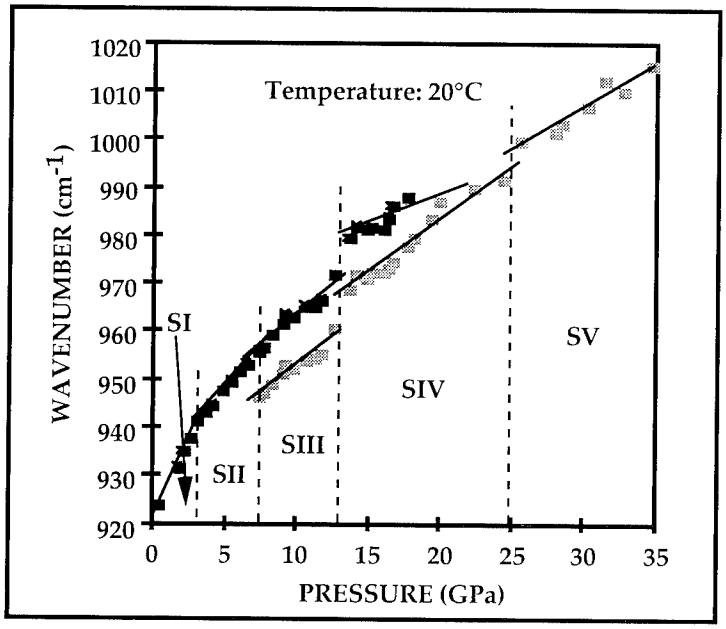

Figure 2: Effect of pressure on the $A_1\nu$(CN) mode of nitromethane at ambient temperature.

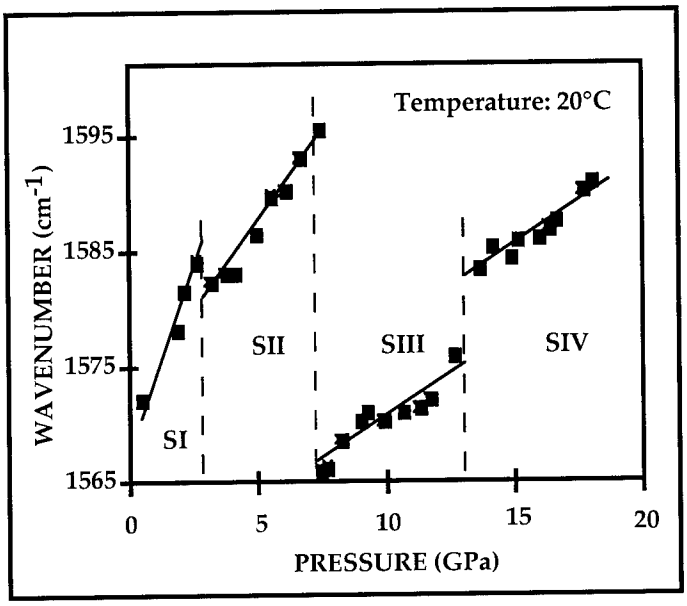

Figure 3: Effect of pressure on the $B_1\nu_a(NO_2)$ mode of nitromethane at ambient temperature.

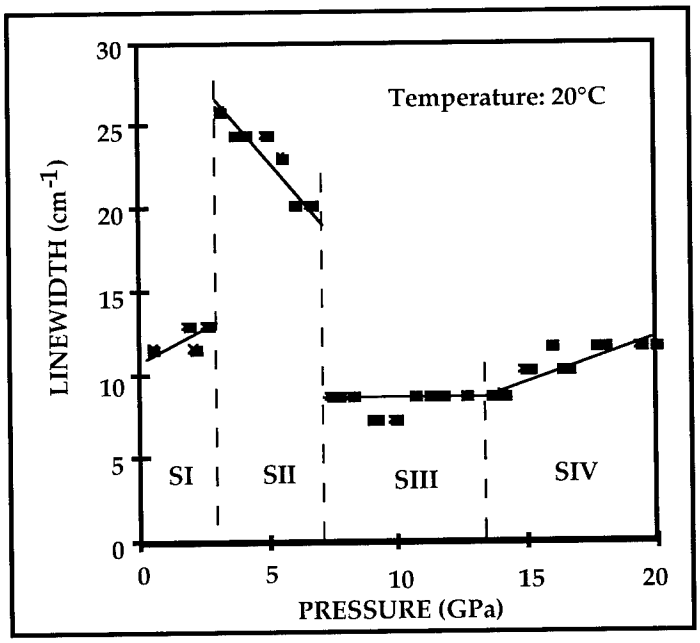

Figure 4: Evolution of the linewidth (Γ_{NO}) of the nitromethane $B_1\nu_a(NO_2)$ mode at ambient temperature. The spectral resolution is 7 cm^{-1}.

JOURNAL DE PHYSIQUE IV
Colloque C4, supplément au Journal de Physique III, Volume 5, mai 1995

Sub-Picosecond Time-Resolved Spectroscopy of Energetic Materials: the Nitromethane and Nitro-Stilbenes

C. Rajchenbach, G. Jonusauskas and C. Rulliere

Centre de Physique Moléculaire Optique et Hertzienne (CPMOH), UA 283 du CNRS, Université de Bordeaux I, 351 Cours de la Libération, 33405 Talence cedex, France

Abstract: Using sub-picosecond CARS experiment we observed direct photolysis of liquid nitromethane after pulse excitation at 299 nm. We measured the dynamic behaviour under excitation of three main ground state Raman lines at 917 cm^{-1}, 1400 cm^{-1} and 2968 cm^{-1}. We deduced an excited state lifetime of 1.1 ±0.3 ps and we measured a photolysis quantum yield at 299 nm of 24% ± 5%. Using "pump-probe" experiments we observed the evolution of excited states of eight nitro-stilbene derivatives including 2,4,6,2',4',6'-hexanitro-stilbene (HNS). In the studied compounds important non-radiative desexcitation channels have been observed and their possible role on explosive process is discussed.

1. INTRODUCTION:

It has been already suggested [1] that molecular excited states may play a decisive role in ignition of detonation. It is then very important to observe the characteristics and the behaviour of molecular excited states. Comparison of excited state properties of explosive and non-explosive molecules may indeed allow to understand the specificity of explosive molecules and, finally, the key of the ignition of explosion and detonation processes. However, excited state lifetimes may be very short and these states, after excitation, may evolve and be transformed on a sub-picosecond time-scale. It is then necessary to observe these excited states with a sub-picosecond time-resolution.

To observe the behaviour of molecular excited states with sub-picosecond time-resolution two main techniques are available. The first one is "pump-probe" experiments in which one excites the sample with a UV pulse and observes its behaviour, after excitation, by means of a probe pulse. This method mainly involves electronic transitions between excited states. At certain wavelengths, corresponding to electronic transitions between excited states, the probe pulse can be absorbed by the different excited species present in the sample after excitation. The transmission characteristics (dynamic and spectral) of the probe pulse through the excited sample give information on the behaviour of the excited sample.

Rather than observe the behaviour of a sample under excitation through changes of electronic transitions, another way is to use a spectroscopic method to study the behaviour of certain vibrational modes of the sample. When a molecule is excited, we may expect to observe for example the disappearance or the evolution of its vibrational characteristics.

From this point of view, spontaneous and coherent Raman spectroscopies are powerful tools because it is well known that the Raman spectra of complex molecules give more detailed information and are more sensitive to structural changes in the molecules than other conventional spectroscopic methods such as absorption or fluorescence spectroscopy. In comparison with spontaneous Raman spectroscopy, coherent

+ Direction des Recherches et Etudes Techniques (DRET) fellowship

anti-Stokes Raman scattering (CARS) offers two main advantages: The CARS signal is much stronger than the spontaneous Raman signal, and furthermore it is collimated in a well known and precise direction. Taking advantage of this, a CARS signal can be observed even in the presence of a strong luminescent or ambient light background and with high spectral resolution [2, 3]. In this paper we describe applications of these two technics ("pump-probe" and CARS spectroscopy) to the study of excited states properties of explosive molecules: liquid nitromethane and nitro-stilbene derivatives.

Considerable experimental and theoretical work has been done on nitromethane in order to understand its photochemical and spectroscopic properties after UV excitation. Indeed, this rather small molecule, with well defined and intense Raman lines, is a unique model for testing and developing theoretical models, without involving large computations. Moreover nitromethane is the simplest of a series of explosive molecules. A better understanding of the explosion mechanism requires a detailed knowledge of the molecular properties under normal conditions before extrapolation to "explosive" conditions (high pressure and temperature) after shock initiation. It was then interesting to study this molecule under UV excitation. In this paper we describe, using sub-picosecond time-resolved CARS experiment, the observation of the decomposition of liquid nitromethane, after UV excitation, and measure the decomposition rate and the excited state lifetime.

HNS (2,4,6,2',4',6'-hexanitro-stilbene) is also a well known explosive and a member of the stilbene family. However trans-stilbene is not an explosive molecule. It is then interesting to progressively add nitro groups to this molecule and to transform trans-stilbene in mononitro, dinitro, tetranitro and finally hexanitro-stilbene (HNS). Comparison between the excited state properties of these different compounds could reveal some specificity related to the explosive characteristics of HNS for example. The possible existence of specificity could greatly improve the general understanding of ignition of detonation. In this paper we present some preliminary results concerning nitro-stilbene derivatives, including HNS, studied by "pump-probe" spectroscopy technics.

2. EXPERIMENTAL SECTION:

2.1 CARS experimental set-up:

The main part of this experimental set-up has been described elsewhere [4, 8]. In the present work we used the degenerate (two-colour) CARS method which requires two beams: the pump beam at fixed frequency ω_p and the Stokes beam at variable frequency ω_S such that $\omega_P - \omega_S = \Omega$, the molecular vibration frequency to be observed. In such a situation the CARS signal is generated at frequency $\omega_{CARS} = \omega_P + \Omega = 2\omega_P - \omega_S$ in a different and well defined propagation direction with respect to the beams at frequencies ω_p and ω_S. The propagation directions of the three beams (ω_S, ω_p, ω_{CARS}) are in fact fixed by the phase matching condition imposed by the conservation of momentum. To excite the sample in the UV a third beam is necessary at frequency ω_{UV}, which creates the excited population.

Our experiments were carried out using the following experimental set-up shown in figure 1. Our laser system employs a hybridly mode-locked dye laser (Coherent 702) which is synchronously pumped by the second harmonic of an actively mode-locked cw-pumped Nd^{3+}:YAG laser (Coherent "Antares-76"). An active stabiliser (AS) (Coherent 7670 Active Amplitude and Position Stabiliser) improved the stability of the "Antares" output. The dye laser operates with rhodamine 6G solution as an amplifier medium and pinacyanol chloride in solution as a saturable absorber [5]. The dye laser output, centred at 598 nm, (0.5 W CW, pulse duration ≤500 fs fwhm) is amplified by a dye amplifier ("Continuum PTA 60" with Kiton Red 620 as amplifier dye) pumped by the frequency doubled output (532 nm, 10 Hz, 70 ps, 25 mJ) of the Nd:YAG regenerative amplifier ("Continuum RGA 10"). The dye amplifier delivers pulses with an energy up to 1.5 mJ at a 10 Hz repetition rate. Dye amplifier output pulse parameters were controlled with a home-made single shot autocorrelator.

The dye amplifier output was frequency doubled in a KDP crystal to deliver the ultraviolet radiation at frequency ω_{UV} (299 nm, $\tau \leq 500$ fs) used to excite the sample under study. The remaining part of the 598 nm beam, after the KDP crystal, was separated from the UV beam by means of a beam splitter. It is this beam which is used to create the beams at frequencies ω_p and ω_S and to generate the CARS signal.

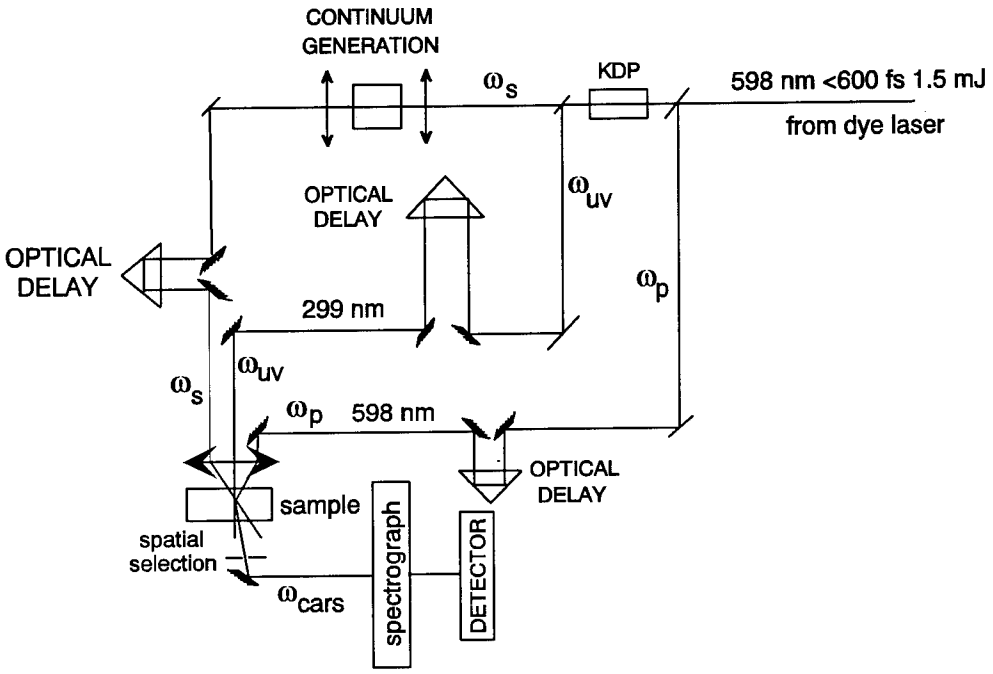

Fig.1: Experimental set-up of the time-resolved CARS experiments (see text).

Less than 10% of this 598 nm beam is used as the ω_p beam in the CARS generation process. The rest is focused by a 10 cm focal lens into a rotating quartz disk or a D_2O cell to produce a light continuum extending from 320 nm to 900 nm. It is this continuum light which forms the Stokes beam at frequency ω_s, necessary for the CARS signal generation at frequency $\omega_{CARS}=2\omega_p-\omega_s$. Taking advantage of the large spectral width of this pulse, we were able to obtain the CARS spectrum over a wide spectral range (up to 2000 cm^{-1}) and thus to observe simultaneously several Raman lines. The polarizations of the various incoming beams were adjusted in order to obtain maximum signal for the different vibration modes studied below.

The ω_{UV} ,ω_p and ω_s beams were focused into a nitromethane sample by a 15 cm focal length lens. The maximum energies were 5 μJ/pulse (ω_p beam), 10 μJ/pulse (ω_s beam in a 2500 cm^{-1} spectral range) and up to 50 μJ for the UV pump pulse (ω_{UV} pulse). The focused beam diameters at the sample were not more than 100 μm.

After spatial separation using an aperture, the CARS beam ω_{CARS} was focused on the slit of a spectrograph (Chromex 5001S). Signal detection was achieved by an intensified photodiode-array (Princeton Instruments IRY 512 S/R) system connected to a computer for spectrum analysis.

Cross-correlation measurements of the pump and probe pulses are made using the optical Kerr effect in the nitromethane sample [6]. Using these procedures, the cross-correlation of the UV pump pulse and other pulses are measured to be shorter than 500 fs. Cross-correlation data also have been measured to ensure the synchronisation of all laser pulses to a zero delay at the sample with a maximum error of 60 fs. Delays between the UV pump and CARS generating pulses at the sample are achieved with an automatic translation stage (MT120 "Micro-Controle" with a 60 fs step unit). A second optical delay line allows control of the delay between the ω_p and ω_s beams and ensures perfect coincidence between these two pulses in the sample.

The experiments were then performed according to the following procedure. Without UV excitation of the sample, we optimised the CARS signal by adjusting positions and delays of the ω_p and ω_s beams and

then recorded the CARS signal corresponding to the unexcited sample by accumulating 500 laser shots. Without any changes we sent the UV beam, and then recorded the CARS signal corresponding to the excited sample for a given time Δt after excitation (Δt is determined by the respective positions of the different optical delay lines). Then we moved the optical delay line of the UV beam in order to change Δt and again recorded the CARS signals corresponding to the unexcited and the excited sample. We made these series of experiments for different delay times Δt and for different spectral ranges in order to study the behaviour of different Raman lines of the sample.

2.2 Sub-picosecond "pump-probe" experiments:
The main part of this experimental set-up has been described elsewhere [7, 8] and the laser system is the same as described above: hybridly modelocked dye laser (Coherent 702) synchronously pumped by the second harmonic of an actively mode-locked cw-pumped Nd^{3+}:YAG laser (Coherent "Antares-76") associated to regenerative amplifier (Continuum RGA 10) and dye amplifier (Continuum PTA 60).

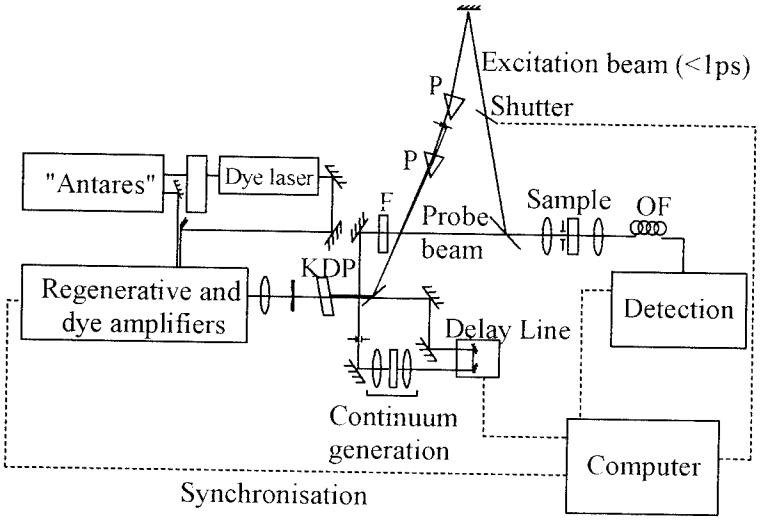

Fig.2: Experimental "pump-probe" set-up.

The pulses at 300 nm and 600 nm are separated by a beam splitter. The UV pulse (300 nm) is sent on the sample in order to excite the molecules to be studied. The 600 nm pulse, after passing through an optical delay line (60 fs steps) is focused on a rotating quartz plate to generate a continuum of light which extends from 320 nm to 900 nm. This continuum is sent through the sample as the probe beam and analysed by means of a spectrograph (Chromex 500I S) and an intensified photodiode array (Princeton IRY 512 S/R) controlled by a computer. Measuring the spectral distribution of the continuum transmitted by the sample in presence and in absence of the UV pulse allows determination of transient absorption spectra of the sample. Changing the position of the optical delay line make possible observation of the time-evolution of the transient spectra (spectral shape and absorbance as a function of time) on a picosecond time-scale.
The UV pump pulse and the probe pulse were linearly polarised. By means of polarisers we adjusted to 54°7 (the "magic angle") the angle between polarisation directions of these beams to ensure kinetics free from reorientational effects.

2.3 Samples:
Commercially available nitromethane (Aldrich Chem., spectrophotometric grade) was used without further purification. A free flowing jet for the sample was used instead of a cell to avoid the accumulation of the photochemical products due to intense photo-irradiation and parasite signals from the windows. Moreover the small thickness of the jet (≈200 μm) makes possible CARS signal generation in a large spectral range (up to 2000 cm^{-1}) since in these conditions phase-matching conditions are not critical.
Nitro-stilbene derivatives used for these experiments are described below (see fig. 3) and the syntheses and purification will be described elsewhere [9-11]. Solvent was propylene carbonate (Aldrich Chemie, spectroscopic grade) and the concentrations of the order of 10^{-3} M/l.

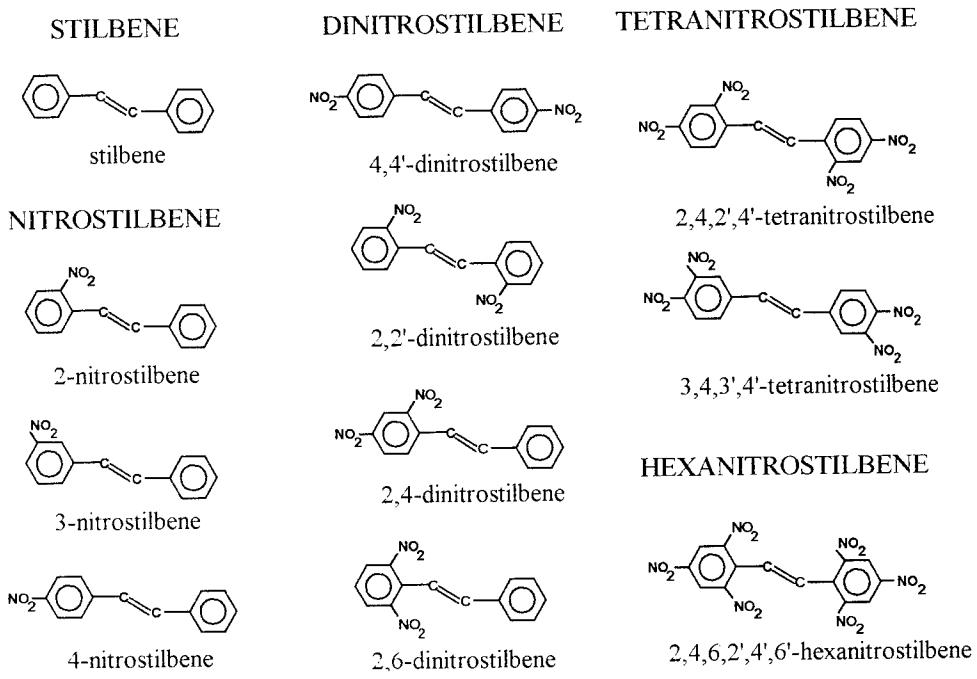

Fig.3: Studied stilbene and nitro-stilbene derivatives

3. EXPERIMENTAL RESULTS AND DISCUSSION:
3.1 Nitromethane study by CARS technics:
Some typical spectra recorded in the experimental conditions described above are shown in figure 4. We observe that the CARS spectra are quite similar with and without UV excitation, with peaks centred near the following Raman lines of ground state nitromethane: the ν (CN) mode at 917 cm^{-1}, the ν_s (NO_2) and δ_s (CH_3) modes near 1400 cm^{-1} and the ν_s (CH_3) mode at 2968 cm^{-1}. Intensity changes are observed under UV excitation, but there are no new Raman lines which could be attributed to excited states of nitromethane. To summarise, with our experimental sensitivity only ground state Raman lines are observed. This point deserves some comment. It is indeed possible to observe Raman lines from excited states, as has been shown for various molecular species [11-16] and as we observed for example in t-stilbene [8]. However we should note that observation of excited state Raman lines was possible until now only when the Raman resonance conditions are fulfilled for the excited states to be studied but not for the ground state Raman lines. In other words the frequencies ω_p and ω_s should correspond to strong electronic transitions between excited states. In this case, Raman lines of the excited states are strongly enhanced with respect to those of the ground state, even if the excited state population is small compared to ground state population. In these conditions the CARS signal is a superposition of both the ground

and the excited state Raman lines, the latter being strongly enhanced and quite obvious in the resultant CARS signal.

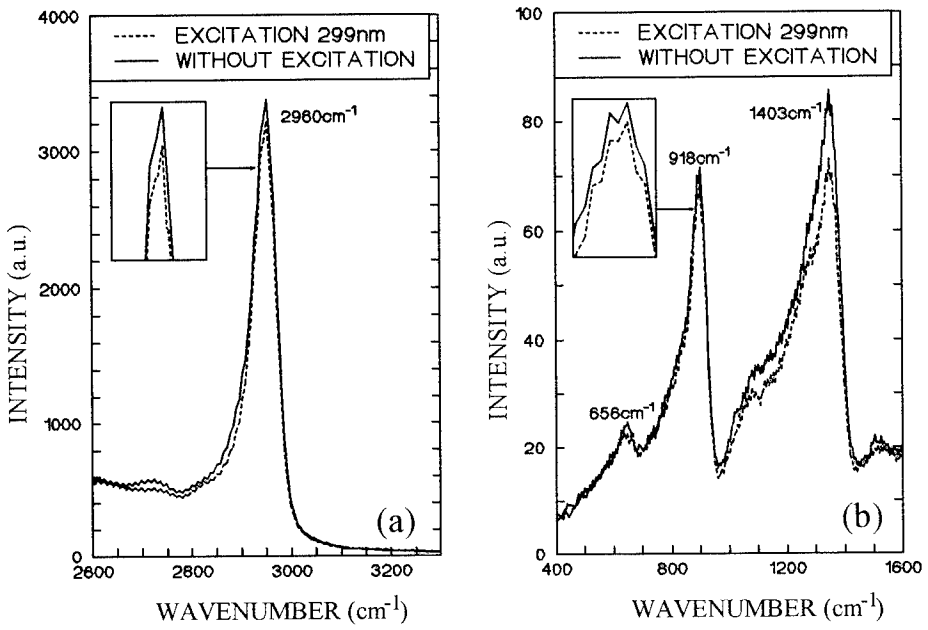

Fig. 4: Typical CARS spectra illustrating the observed changes under UV excitation. a) spectral range corresponding to the $\nu_S(CH_3)$ vibration mode near 2960 cm^{-1}.The dotted spectrum (- - -) was obtained at time Δt=6 ps after UV excitation. b) spectral range corresponding to the $\delta(NO_2)$, $\nu(CN)$, $\delta_S(CH_3)$ and $\nu_S(NO_2)$ vibration modes. The dotted spectra (- - -) has been obtained at time Δt=32 ps after UV excitation.

To observe whether or not the resonance conditions was fulfilled in our experimental conditions, we made, as described in the introduction, "pump-probe" experiments using the experimental set-up described above. We did not detect any electronic transitions or absorbing transient species of excited nitromethane in the spectral range ω_p and ω_S. That can be explained if we take into account that, due to the small size of nitromethane, electronic absorption bands are strongly shifted to the UV [17] in comparison with large size molecules (large size means at least ten carbon atoms). Such transitions should appear at larger frequencies than ω_p and ω_S. We can thus deduce that our experimental conditions did not fulfil the resonance conditions for the excited states Raman lines. Due to these experimental conditions, Raman lines from the excited states did not appear on the CARS spectra. As a consequence the CARS spectra have to be considered as due to the Raman lines of the ground state molecules. Their evolution will thus give information about the evolution of the ground state population under UV excitation.

UV photo-excitation can perturb the ground state Raman lines in two ways. The first may involve some spectral changes (peak position, bandwidth) which can appear because of some changes affecting the ground state population under UV photo-excitation. Obviously figure 4 shows that no strong spectral changes are observed. Any spectral changes are smaller than the experimental error. The second way is a intensity change of the Raman lines which can be connected to variation of the ground state population. Under UV photo-excitation, the ground state can be depopulated (by transition from ground to excited states or photo-decomposition) or repopulated by electronic transitions (radiative or non-radiative) from excited to ground states. The intensity variations of the ground state Raman lines can thus be related to excited and ground state populations as described in detail in [18], after taking into account the non-

resonant contribution to the CARS signal. It is possible, from the intensity of the Raman lines, to measure the kinetics of the ground state population. Some typical results are shown in figure 5 a,b and deserve some comments.

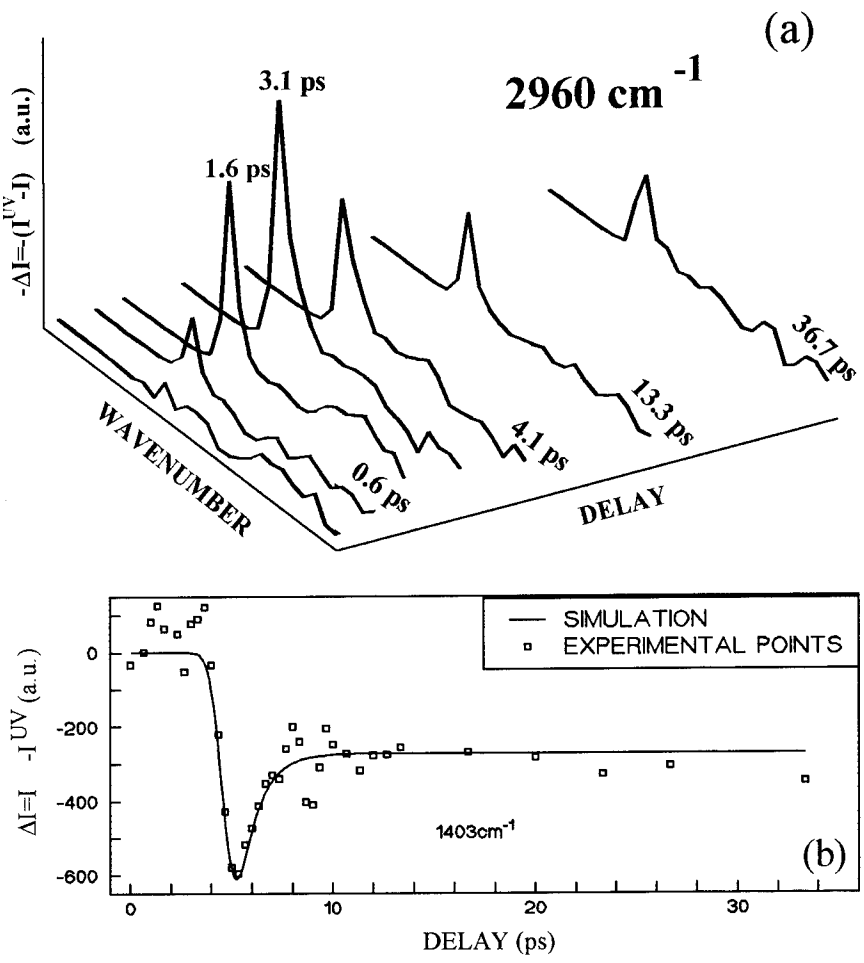

Fig. 5: a) $\nu_s(CH_3)$ vibrational mode intensity as a function of the time after UV excitation. Note that ΔI values are negative and correspond to a decrease of the band intensity.

b) Difference of the integrated intensity of vibrational bands with and without UV excitation, ΔI, as a function of delay after the UV pulse for the Raman lines near 1400 cm^{-1} ($\delta_s(CH_3)$ and $\nu_s(NO_2)$).

The full line (—) is the simulated curve. The results of the simulation are given in the text.

We observe that under excitation the CARS signal from the ground state of nitromethane sample immediately decreases, due to the depopulation of the ground state by the excitation pulse. A minimum intensity is reached corresponding to a maximum depopulation of the ground state. After this maximum has been reached, we observe a fast decay indicating that the ground state is repopulated from the excited state. Then the signal reaches a plateau which extends without change to 1 ns, the longest time we could observe with our experimental set-up. The fast decay is an indication that the ground state population is

quickly repopulated from the excited state. But the plateau indicates that after excitation the ground state population does not recover its initial value. In other words ground state nitromethane molecules have disappeared.

From these results we can infer that we observed the time-resolved decomposition of nitromethane. These results can be interpreted in the following way. During excitation a certain part of the ground state molecules is transformed in excited molecules. This creates a hole in the ground state population and a corresponding decreases of the CARS signal. After that, a part of the excited state population returns, by non-radiative transition to the ground state. This process is illustrated by the fast decay observed on the kinetics of figure 5. The other part of the excited state population will evolve on the photo-decomposition energy surface pathway to new species. This part of the excited state population will never return to the ground state population, in agreement with the experimental lowering of the final CARS signal.

Taking into account these different processes we can model this behaviour to obtain the rate constants of the different processes by fitting the kinetic curves. The kinetic scheme can be illustrated as following:

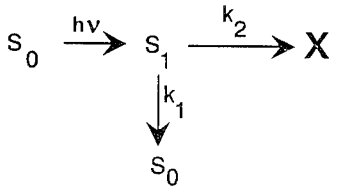

Scheme 1

where S_0 is the ground state, S_1 the excited state and X the decomposition products. According to this scheme we were able to simulate these experimental curve [18] and to determine unambiguously the rate parameters k_1 and k_2 ($1/k_1$=1.5±0.3 ps and $1/k_2$=4.7±0.3 ps). From these values we calculated an excited state lifetime of 1.1±0.3 ps and a quantum yield of photo-decomposition ($k_2/(k_1+k_2)$) of 24±5% at 299 nm. The results of the simulations are shown in figures 5a and b for the Raman lines at 1403 cm^{-1} and 2960 cm^{-1}.

From these results some comments are in order with ignition of detonation. We observe that a fast decay channel from excited states to the ground state is observed. This channel is a non-radiative channel since the radiative lifetime, taking into account the absorption cross-section of the $S_0 \rightarrow S_1$ transition and the nature of the excited state (n-π^*) [19], is much longer than 10 ns. This non-radiative channel may have some importance in the photo-decomposition of liquid nitromethane and more generally for decomposition under shock.

Indeed our results show that practically 76% of the energy deposited in the sample is evacuated non-radiatively. Excitation to the electronic state S_1 generates vibrationally hot ground state molecules by fast internal conversion of the photon excitation energy at 33445 cm^{-1} (λ=299 nm). It has been shown that in this case temperature over 1000°K are reached by the molecules in their ground state [20, 21]. In liquid nitromethane, taking into account the specific heat (C_p=106.6 J/mol K [22]) and the excitation energy (33444 cm^{-1}), a vibrational temperature of 3500 K can be theoretically reached. After that, the excess thermal energy is evacuated to the bath by collision with the neighbouring molecules of the first shell around the hot molecule. It has been shown [20, 21] that the molecules of the first shell also attain a very high temperature in some picoseconds, the rate of this thermalization process being controlled by the thermal conduction of the liquid. That means strong gradient temperature which will heat very fastly the different molecules after excitation. As a result a strong and fast local heating occurs by non-radiative transitions which can activate the decomposition. Since it has been shown that excited states are very important in the explosive process [1], we suggest that this process has to be taken into account for a microscopic description of the explosion mechanism on a microscopic scale. We will develop this point later and let us now present our results on nitro-stilbene derivatives.

3.2 Study of nitro-stilbene derivatives:

Figure 3 shows the studied compounds and figures 6 to 12 some typical transient absorption spectra recorded at different times after UV photoexcitation. The presented spectra are corrected for the influence of the chirp which appears between the spectral components of the probe continuum beam. In

regard of the large number of studied compounds, it is difficult to explain in details the results obtained for each compound. That will be made in a forthcoming publication [23] and in this paper we will focus on the main important aspects of the photophysical behaviour of these compounds.

As explained in the introduction, the goal of this study is to try to observe a logical evolution of the photophysical properties of nitro-stilbenes, starting from t-stilbene and going to mono, di, tetra and finally hexanitro derivatives, in order to understand the specificity of nitro-stilbenes in relation with explosive ability. Let us then summarise the main tendencies deduced from our study.

First of all, in t-stilbene we did not observe any special behaviour from the observation of transient absorption spectra. A single absorption band was observed, centred near 580 nm and we did not note strong evolution of this band as a function of time. It was attributed to a single excited state, populated by excitation and decaying with a lifetime in the range of some tenths of picosecond. This is the classical behaviour of t-stilbene, already observed elsewhere [24].

If only one nitro group in introduced on the molecular skeleton of t-stilbene, the behaviour of t-stilbene becomes immediately different as shown in fig.6 for 4-nitro-stilbene.

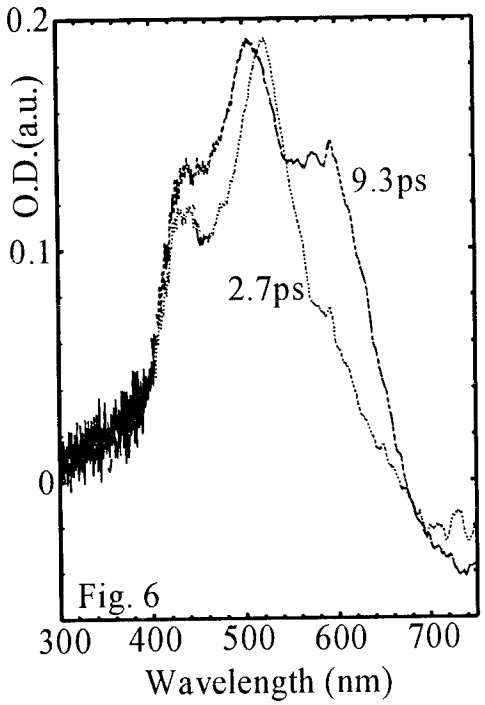

Fig. 6: Absorption spectra of 4-nitro-stilbene at different delay times after excitation. Dotted line: 2.7ps; dashed line: 9.3ps.

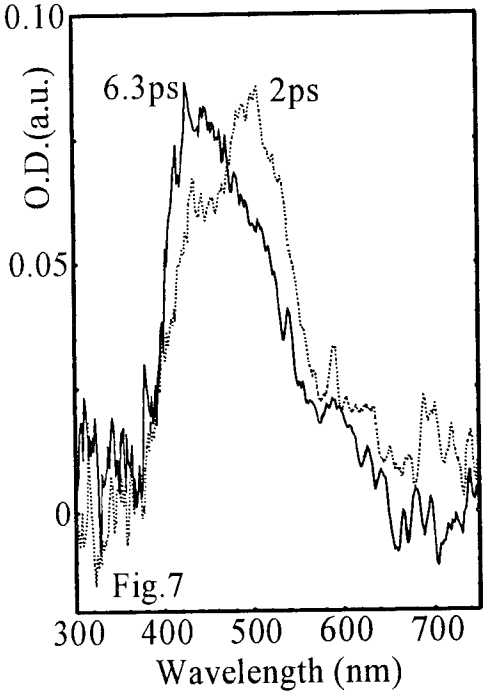

Fig. 7: Absorption spectra of 2-nitro-stilbene at different delay times after excitation. Full line: 6.3ps; dotted line: 2.0ps.

We may observe that three absorption bands can be observed developing on different time scales. These three different bands may be attributed to the presence at different times of at least three different excited species. Obviously the introduction of only one nitro group completely changes the photophysical behaviour of t-stilbene. It is interesting to observe how evolves this behaviour with the position of the nitro groups or with the introduction of more than one nitro group. Fig.7 to 12 show some typical results. We may observe for example that the introduction at the ortho position of a nitro group changes the behaviour compared to introduction at the para position. In 2-nitro-stilbene (see fig. 7) only two absorption bands may be observed. One band (with maximum at 505 nm) which appears with the excitation and a second band (with maximum at 440 nm) which appears later. Obviously in this compound two excited states (related to absorption bands centred at 440 nm and at 505 nm) are present, the first one being directly populated from the UV excitation pulse and the second one being populated

from the first one in approximately 5 ps. At longer times (t> 5ps) the populations of these two states are in equilibrium. The comparison between 4-nitro-stilbene and 2-nitro-stilbene then shows that the position of the substitution may also change strongly the photophysical behaviour of these derivatives.
The influence of the introduction of more than one nitro group also changes drastically the photophysical properties of nitro-stilbenes as illustrated on the next figures.

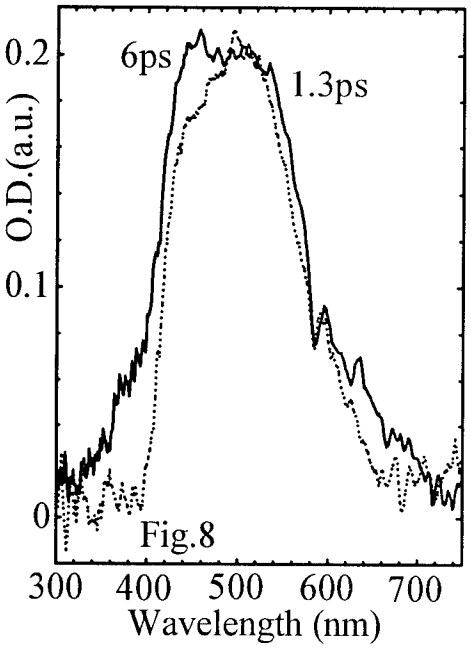

Fig.8: Absorption spectra of 2,4-dinitro-stilbene at different delay times after excitation. Full line: 6.0ps; dotted line: 1.3ps.

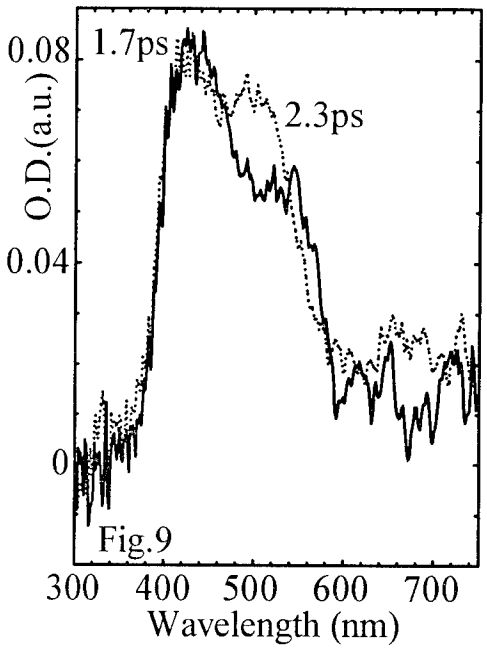

Fig.9: Absorption spectra of 2,2'-dinitro-stilbene at different delay times after excitation. Full line: 1.7ps; dotted line: 2.3ps.

For example, in di-nitro derivatives we observed in all the studied compounds, the presence of two excited states (revealed by the presence of two absorption bands as shown in fig. 8 and 9). The populations of these two states are in equilibrium.
In tetra-nitro derivatives, as shown in fig. 10 and 11, at least two states are still present but the equilibrium between their populations is strongly displaced in favour of last formed state. In 3,4,3',4'-tetra-nitrostilbene, for example, at longer times than 5 ps, only the second excited state is populated and decays on a nanosecond time scale. The first created excited state is no longer populated.

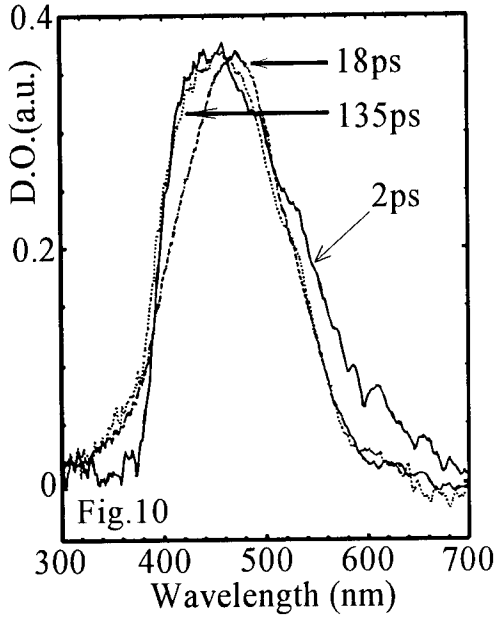

Fig.10: Absorption spectra of 2,4,2',4'-tetranitrostilbene at different delay times after excitation. Full line: 2.0ps; dotted line: 135ps; dash line: 18ps.

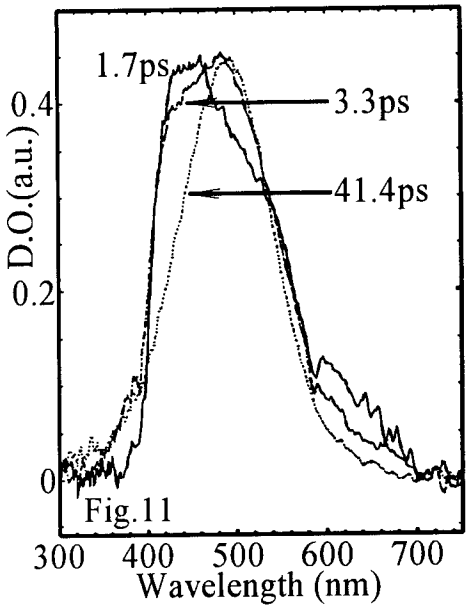

Fig.11: Absorption spectra of 3,4,3',4'-tetranitrostilbene at different delay times after excitation. Full line: 1.7ps; dotted line: 41.4ps; dash line: 3.3ps

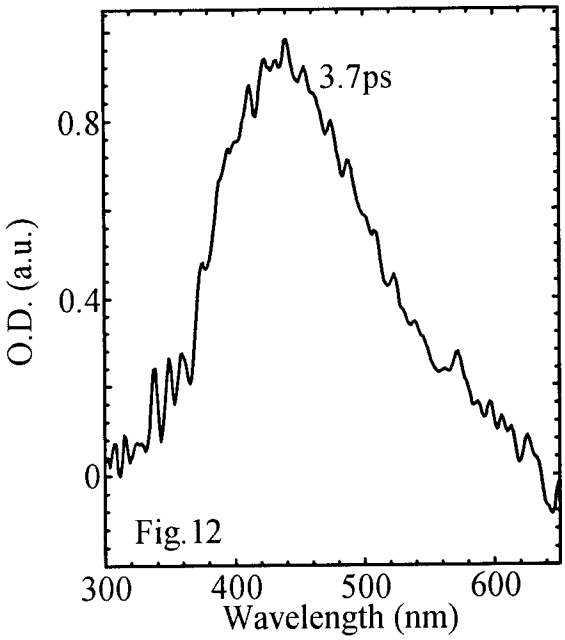

Fig.12: Absorption spectra of 2,4,6,2',4',6'-hexanitro-stilbene at different delay times after excitation. Full line: 3.7ps.

In 2,4,6,2',4',6'-hexanitro-stilbene, the first band is practically absent and not observed even at very short times after excitation. The second band appears fastly, is very broad and structureless and decays with a lifetime in the nanosecond time scale. No equilibrium is present in this compound.

Let us now summarise these different results. Introduction of nitro groups completely modifies the photophysical behaviour of t-stilbene with the appearance of several excited species which are not present in t-stilbene. In 4-nitro-stilbene, three absorption bands are observed, the second one shifting to the blue as a function of time in polar solvents. This shift is an indication of a relaxation process which may involve a molecular conformation change or a cage relaxation process. In any case this state is further stabilised by interaction with environment. It can be a possible indication that charge transfer exists in this compound. In fact comparison of the behaviour of 4-nitro-stilbene in polar and non-polar solvents [24] supports strongly this hypothesis.

If the number of nitro groups is greater than one there exist two excited species (excepted in 2,4,2',4'-tetra-nitro-stilbene) revealed by the observation of two different absorption bands evolving with different characteristic times. In any compounds the first state is immediately populated by the excitation pulse. This state is the franck-condon state accessible from the ground state configuration. From this first populated excited state, a second excited state is fastly populated with characteristic rise times in the range of 1-10 ps. Depending on the compound an equilibrium, more or less important, may exist between the populations of these states. This second state has a lifetime in the range of 1-5 nanosecond. When the number of nitro groups is equal or larger than four, the equilibrium practically does not exist. In HNS, this second excited state is very fastly populated after excitation.

Let us now discuss the specificity of HNS in regard of explosive ability taking into account these results. It seems reasonable to assert the explosive ability to the presence of the second excited state. This excited state seems to be the key of the explosive ability. Indeed, as the number of nitro groups is increasing this state is more and more populated after excitation. The equilibrium existing between the populations of the two observed excited states is strongly moved in favour of the second excited state. Moreover as the number of nitro groups increases this state is fastly populated, particularly in HNS, where the presence of the first excited state is difficult to detect with our available time-resolution.

If we accept that strong charge transfer exists in this state, it is reasonable to consider that charges are strongly localised on electron acceptor nitro groups. So the explosive ability can be correlated to this charge localisation. It's exactly the same conclusion that obtain Delpuech [1] on a theoretical basis. However before to conclude about the validity of this hypothesis other experiments are necessary. Let us however discuss and propose a possible mechanism for ignition of explosion under shock, in the light of our results.

It is well known that under shock, excited states can be populated in certain materials. This process is well known and called "mechano luminescence" [25-28]. To our knowledge this process has not been observed in nitromethane and nitro-stilbenes or more generally in explosives. But we have to take into account that, due to fast non-radiative channels, fluorescence quantum yield are very small and luminescence will be difficult to detect. It is then well possible that after shock excited states are formed. After excitation molecules may be decomposed as in nitromethane, the decomposition rate being increased by the local heating due to fast non-radiative transitions which create large gradient temperature. After these preliminary decompositions chain chemical reaction will be initiated opening the door to the detonation and explosion. In the case of nitro-stilbenes, it seems that it is the second excited state formed after excitation that is responsible for this process. In the case of these molecules we have to take into account the presence of fast non-radiative channels. For example the formation of the second excited state from the first one is very fast (in the range 1-10ps) and is also non-radiative and heat dissipative. Like in nitromethane we may imagine that fast local heating occurs and accelerates the decomposition reaction.

Naturally this proposed model is hardly speculative but it is quite possible to verify the validity of the developed points above.

1/ The spectra of excited states being now known, it is possible to envisage to check the presence of such states under shock and detonation conditions, for example by time-resolved absorption methods. These spectra are indeed the signature of these particular excited states: the observation or the non-observation of these spectra under shock could allow to test the validity of the proposed model.

2/ Fast non-radiative transitions seem still present in all the studied molecules in the present work. Nevertheless it will be also interesting to observe, like in nitromethane, if fast non-radiative transitions

spectra are indeed the signature of these particular excited states: the observation or the non-observation of these spectra under shock could allow to test the validity of the proposed model.
2/ Fast non-radiative transitions seem still present in all the studied molecules in the present work. Nevertheless it will be also interesting to observe, like in nitromethane, if fast non-radiative transitions exist too in nitro-stilbenes as direct desexcitation channel between excited and ground state. Indeed we observed only fast non-radiative channel between excited states in nitro-stilbenes. We planify experiments to observe direct and fast non-radiative channel between excited and ground states. If such a channel really exists in these compounds, this fact could be one of the keys explaining explosive ability of such compounds.

CONCLUSION:

Use of time-resolved CARS and "pump-probe" experiments provides the first time-resolved data on the excited state behaviour of liquid nitromethane and nitro-stilbene derivatives. Very fast photochemical and photophysical channels have been revealed in the range of 1-10ps, depending on the compounds. These experiments have also shown for the first time the presence, in nitromethane molecule, of a very important and fast non-radiative channel between the excited and the ground states. The presence of this channel means that most times that a molecule is excited, a strong and fast local heating occurs for the neighbouring molecules. The presence of this non-radiative channel has to be taken into account to explain the first steps of explosion on a microscopic level.
From these different data we proposed a hardly speculative model to explain the mechanism of detonation and explosion ignition on a microscopic level. We proposed some experiments to test the validity of this speculative model. Some of the proposed experiments are currently in progress in the lab.

Acknowledgements: This work was financially supported by Direction des Recherches et Etudes Techniques (DRET contract N° 940045) which is gratefully acknowledged. One of us (C. Rajchenbach) wants also to thank DRET for the attribution of a grant fellowship.

REFERENCES

[1] Delpuech A., *J. de Physique*, **C34-48** (1987) 353.
Odiot S., *J. de Physique*, **C34-48** (1987) 225.
[2] Akhmanov S.A. and. Koroteev N.I, Methods of Nonlinear Optics in Light Scattering Spectroscopy (Nauka, Moscow, 1981, in Russian).
[3] Shen Y.R., The Principles of Non-linear Optics, (Wiley, New York 1984).
[4] Shkurinov A. P., Jonusauskas G., Rullière C., *J. Ram. Spectroscopy*, **25** (1994) 359.
[5] Hébert P., Marguet S., Gustavsson T., Mialocq J.C., *Opt. Comm.*, **90** (1992) 85.
[6] Cataliotti R. S., Foggi P., Giorgini M. G., Mariani L., Morresi A. and Paliani G., *J. Chem. Phys.*, **98** (1993) 4372.
[7] Létard J. F., Dumon P., Jonusauskas G., Dupuy F., Pée Ph., Rullière C., Lapouyade R., *J. Phys. Chem.* **98** (1994) 10391.
[8] Shkurinov A. P., Koroteev K., Jonusauskas G., Rullière C., *Chem. Phys. Lett.*, **223** (1994) 573.
[9] Shipp K. G., *J.Org.Chem.*, **29** (1964) 2620.
[10] Mc Gookin A., *J. Soc. Chem. Ind.*, **68** (1949) 195.
[11] Lau A., Werncke W., Pfeiffer M., *Spectrochimica Acta Rev.*, **13** (1990) 191.
[12] Goldberg L. S., Picosecond Phenomena III, Editors K. B. Eisenthal, R. M. Hochstrasser, W. Kaiser, A. Laubereau, (Springer Berlin, 1982) p.94.
[13] Chikishev A. Yu., Kamalov V. F., Koroteev N. I., Kvach V. V., Shkurinov A. P., Toleutaev B. N., *Chem. Phys. Lett.*, **144** (1988) 90.
[14] Matsunuma S., Akamatsu N., Kamisuki T., Adachi Y., Maeda S., Hirose C., *J. Chem. Phys.*, **88** (1988) 2956.
[15] Werncke W., Lau A., Pfeiffer M., Weigmann H. J., Freyer W., Tschö J. T., Kim M. B., *Chem. Phys.*, **118** (1987) 133.
[16] Kamalov V. F., Koroteev N. I., Toleutaev B. N. in Time Resolved Spectroscopy, Editors R. J. Clarck, R. E. Hester, (John Wiley and Sons Ltd, New York) 1989 p. 255.
[17] Nagakura S., *Mol. Phys.* **3** (1960) 152.

[18] Rajchenbach C., Jonusauskas G., Rullière C., *Chem. Phys. Lett.* (in press).
[19] Schoen P. E., Marrone M. J., Schnur J. M., Goldberg L. S., *Chem. Phys. Lett.*, **90** (1982) 272.
[20] Sukowski U., Seilmeier A., Elsaesser T., Fischer S. F., *J. Chem. Phys.*, **93** (1990) 4094.
[21] Elsaesser T., Kaiser W., *Annu. Rev. Phys. Chem.*, **42** (1991) 83.
[22] in Handbook of Chemistry and Physic, CRC Press, Ed. D.R. Lide, (1992-1993) 73rd edition.
[23] Rajchenbach C., Jonusauskas G., Dumon P.,Rullière C., (in preparation for J. Energ. Mat.).
[24] Greene B. I., Hochstrasser R.M., Weisman R. B., *J. Chem. Phys.* **70** (1979) 1247.
[25] Chandra B. P., Ramrakhiani M., Ansari M. H., Tiwari S., *Pramana J. Phys.* **36** (1991) 407.
[26] Chandra B. P., Rahangdale Y., Ramrakhiani M., *Phys. Stat. Solid. A* **121** (1990) 281.
[27] Chandra B. P., Rahangdale Y., *Cryst. Res. Technol.* **25** (1990) 197.
[28] Tokhmetov A. T, Vettegren' V. I., *Sov. Phys. Solid. State* **31** (1989) 2125.

JOURNAL DE PHYSIQUE IV
Colloque C4, supplément au Journal de Physique III, Volume 5, mai 1995

Experimental Study of Photon-Phonon Interactions in an Explosive by Laser Probe Mass Spectrography

J.F. Eloy and A. Delpuech

Commissariat à l'Energie Atomique

ABSTRACT

We have shown in a series of previous papers the part of the molecular electronic structure played in the decomposition process of an explosive submitted to a shock wave. This part is important especially as regards energy transfer properties.

This work is intented to investigate the process of these transfers by the study of photon-phonon interactions in this type of material. The experimental technique used for this purpose is laser probe mass spectrography. The first tested explosives are RDX and HMX studied in the shape of single crystals.

1. INTRODUCTION

In previous discussions, we have stated that the conditions for the birth of detonating regime were directly dependent on the properties of energy transfer between molecules. In the proposed model, these properties take account of preferable nitrated groups. These initiation conditions suppose both mechanisms of molecular excitation under shock, similar to those observed under radiation, and de-excitation processes by means of lattice's phonons.

In order to confirm and analyse the fundamental behaviour of the NO_2 groups involved in such mechanism, we intended to study the photon-phonon interactions in the case of nitrated secondary explosives. The primary difficulty was in the choice of an experimental technique which allowed investigation of both decomposition fragments and their mechanism of generation. We considered the time of flight (T.O.F.) laser probe mass spectrograph (L.P.M.S.) was the one appropriate technique to reach this dual purpose.

I present here the results of the RDX and HMX study (in single crystal form) by the T.O.F. laser probe mass spectrograph.

The results are analysed with regard to a non-linear approach of the laser explosive interaction.

2. INSTRUMENTATION AND METHODS

The vaporization and ionization of the explosive single crystal are induced by laser beam bombardment of one crystal face. The (Nd/YAG) laser head used delivers a tripled frequency (λ = 0,355 μm) of a TEM_{00} laser beam. The total energy of the laser impulse is between 10 and 30 μJ and focused on a surface of about 400 μm^2 with gaussian spatio-temporal profiles. The laser time duration is 3 - 4 ns and the shot repetition rate is 1 Hz.

The so-created laser micro-plasma is released in an equipotential expansion box without electric and magnetic fields. The positive ionic species are then extracted and accelerated by an electrostatic field corresponding to a difference of potential of 8 kV. These ions are analysed by a spatio-temporal mass-separator combining both magnetic field action and time of flight separation. They are detected by an electro-optic panoramic device and their masses identified by time of flight measurements.

The instrument is equipped with a sample viewing system witch provides a high power observations (G : 300-420 X).

3. RESULTS

In brief, the study of the RDX and HMX single crystals behaviour under laser bombardment reveals the emission of three types of mass spectra. Two types correspond to "classic" mass spectra of organic compound fragmentation by laser pyrolysis. One type (characterised by very energetic ionic species, very high ionized plasma and very high electronic density and temperature) is distinctive of the explosive. Its appearance is likely due to the "explosive" feature of this material.

The study of the crystalline faces considers a mechanism of non-linear interaction.

The study of the crater shapes by optical microscopy (binocular) reveals that the laser beam effect induces physical transformations (appearance of a "white zone" area) of the crystal around the distances between 30 to 80 μm. The observations of the craters by scanning electron microscopy (SEM) reveals :

- the formation of cracks a long way from the crater (> 50 μm) as a consequence of structure collapse,

- a truncated shape of these craters witch results from a sudden vaporisation initiated "in volume".

Now, we intend to consider the physical phenomena wich can explain at once this non-linear effect and "white zone" area creation (ϕ = 30-80 μm) around the crater.

4. PROPOSAL OF A MODEL FOR THE LASER EXPLOSIVE INTERACTION

Taking only the phonons (created by the laser beam in surface and in volume) into account is insufficient to explain our experimental results. The energy carried by the phonons is insufficient to generate the observed craterization effect ; and the appearance of the "white zone" suppose a speed of propagation for the particles twice the speed of phonons. In fact, a non-negligible probability of interaction exists between photons and phonons in the crystalline medium. These interactions generate a process of "chain reaction". Each centre of interaction becomes the spot where an energy liberation can produce dislocations and energetic chain reactions by bond breakings. In this case, the laser decomposition is initiated in volume (and not in surface) in opposition to the general case of organic and metallic materials.

The coupling of the vibration waves (or phonons) of the lattice with an electro-magnetic wave causes a polarization wave (or polariton) to appear. This P-wave propagates itself in the material and induces the application of a force on the bond dipole. This force will be all the stronger as the dipolar moment is strong. In the case of RDX and HMX, the $N\text{-}NO_2$ groups will be the more strongly activated.

Three facts are in keeping with the model proposed :

- the initiation of the laser decomposition by such a process leads to a large proportion of NO^+ ions. Our mass spectra reveal systematically this effect,
- the middle extinction curve of polarization wave (P-wave) is compatible with the size of the sensitive "white zone",
- the observation of an interaction especially efficient with the crystalline axis which offers a higher density of nitrated bonds.

5. CONCLUSION

The first results of this work is to confirm the original contribution of the laser probe mass spectrograph for the study of photon-explosive interactions mechanism.

The results obtained as a whole permit the conclusion that the behaviour of this explosive material is different in regard to all the organic products previously studied with this technique. We proved that this material is a medium which induces non-linear phenomena.

Our experimental results also demonstrate an appropriate decomposition model by taking non-linear effects into account. This approach is supported by three kinds of processes :

- phonons generations by photon absorption,

- photon and phonon propagation is the volume of material,

- creation of hot centers by polarization wave (P-wave) interaction with the $N\text{-}NO_2$ dipoles.

The fundamental part played by the nitrated bonds in the initiation mechanism of the explosive decomposition is like that confirmed.

REFERENCES

[1] S. DUFORT, A. DELPUECH

The 8th Symposium on Detonation - ALBUQUERQUE (USA) - 1985

[2] A. CHAME, J.F. ELOY

Scanning Electron Microsc. - 1983/II p. 841 - 851

[3] J.F. ELOY, A. DELPUCEH

APS Topical Conference - Shock Waves in Condensed Matter - MONTEREY (USA) - 1987

JOURNAL DE PHYSIQUE IV
Colloque C4, supplément au Journal de Physique III, Volume 5, mai 1995

Influence of Initiation Strength, Ambient Inert Gas, Al-Content and Polymeric Binder on the Detonation Products of High Explosives

F. Volk

Fraunhofer-Institut für Chemische Technologie (ICT), 76327 Pfinztal, Germany

1. Introduction

The knowledge of the reaction products of detonation processes is important for different reasons:

- in order to learn more in the field of kinetics of fast reaction processes, especially with regard to equilibrium or non-equilibrium reactions
- in order to evaluate the completeness of detonation reactions of energetic organic substances or of metallic ingredients such as aluminium (Al), especially as a function of the confinement and the oxygen balance of the explosive charge
- In all of these cases, the detonation products together with the heat output are capable of qualifying the reaction under different conditions.

It is the aim of this investigation to analyze the detonation products of different explosive charges, which were initiated with different initiation stimuli and under different confinements. Confinement influences reaction in so far as it adds resistances to the expansion of the gaseous detonation products and maintains high pressures and temperatures for a longer period of time before lateral rarefactions quench reaction [1)]

In addition, the following points have been investigated:

- the influence of ambient gas and of glass confinement
- and the influence of the Al content and of different polymeric binder systems on the detonation products.

3. Experiments

The experiments were conducted in a stainless steel containment with a volume of 1.5 m^3. The cylindrical high explosive charge had a mass of about 300 g with 50 mm in diameter and 80 to 90 mm in length.[2)] For the initiation, different boosters were used:

1) A booster with a weak initiation strength which consisted of 10 g RDX (Type I). The cylindrical shape of this booster had a diameter of 20 mm and a length of also 20 mm.

2) The second booster type consisted of 18 g explosive sheets (Type II) with the same diameter as the main explosive charge. It is expected that both boosters, type I together with type II, give rise to a more complete detonation reaction resulting in complete detonation products in such a way that no more explosive components can be identified in the post-blast residue. [4)]

4. Results

4.1 Different Initiation Stimuli

The results of the examination of the initiation strength of the two different boosters (type I and type I + type II) can be seen in table 1.

Table 1: Influence of a different booster strength on the initiation reaction

Initiating Booster		High Explosive Charge	TNT in Residue (wt%)
Type I 10 g RDX	Type II 18 g Expl. Sheets		
+	-	40% TNT/60% RDX (Compound B)	-
+	-	60% TNT/40% NQ	1.5
+	-	50% TNT/30% NQ/20% Mg	6.0
+	-	50% TNT/50% AN	2.0
+	+	60% TNT/40% NQ	-
+	+	50% TNT/50% NQ	-
+	+	50% TNT/50% TATB	-

w51.doc

In table 1 it is shown that compound B, which is much more easily to be initiated, reacts completely also by using booster type I alone. On the contrary, nitroguanidine (NQ) and ammonium nitrate (AN) containing high explosive charges, which need a stronger initiation stimulus, leave unreacted TNT in the post blast residue, which was analyzed by High Performance Liquid Chromatography (HPLC). The same holds for the charge containing magnesium (Mg). On the other side, a complete detonation reaction is shown by using both types of boosters together: No more TNT could be analyzed.

4.2 Influence of Ambient Gas and Glass Confinement on the Detonation Products

When detonating high explosives in different atmospheric conditions, it is of interest to know if the detonation products or the energy out-put will change. In order to investigate this behavior, charges containing 45 % TNT and 55 % Nitroguanidine (NQ) were initiated in the containment under different pressures of argon and in vacuum. In addition, the same charges were conducted which had a glass confinement. In this case, the glass tube exhibited a wall thickness of 9 mm. The results of the unconfined and the glass-tube confined charges are in table 2 and 3.

Table 2: Influence of vacuum and of different argon pressures on the detonation products

Sample No.		1450/1c	1450/2c	1450/3c
Ar pressure [MPa]		Vac.	0.05	0.1
Composition		45% TNT/55% NQ		
O_2-Balance [%]		-47.6		
Charge Weight [g]		331	332	331
ΔH_f [kJ/kg]		-661	-662	-657
Products [mol %]	H_2	20.7	8.3	5.0
	CH_4	0.04	0.1	0.24
	CO	32.1	17.9	14.3
	CO_2	3.7	7.9	10.3
	N_2	27.5	26.1	25.6
	NO	0.1	0.1	0.13
	HCN	0.3	3.2	3.6
	NH_3	0.5	3.0	4.9
	C_2H_2	0.02	0.03	0.1
	H_2O	10.7	19.6	20.0
	C_s	4.4	13.8	15.9
ΔH_{det} [kJ/kg]		2999	3653	3763
C in Residue [% of total C]		10.8	32.2	35.7
Gas formation [mol/kg]		44.5	37.9	35.7

Table 3: Influence of glass confinement on the detonation products

Composition	45% TNT / 55% NQ		
Sample No.	1451/1	1451/2	1451/3
Ar pressure (Mpa)	Vacuum	0.05	0.1
Oxygen balance (%)	-47.6	-47.6	-47.6
Charge weight (g)	332	335	332
ΔH_f (kJ/kg)	-656	-658	-658
Products (mol%)			
H_2	8.7	4.2	3.1
CH_4	0.2	0.4	0.44
CO	15.9	10.2	9.3
CO2	7.9	11.9	12.7
N_2	27.3	26.0	25.6
NO	0.06	0.05	0.14
HCN	1.35	2.4	1.1
NH_3	1.15	4.7	5.3
C_2H_2	0.07	0.1	0.13
H_2O	20.5	20.7	21.0
Cs	16.8	19.2	21.3
ΔH_{det} (kJ/kg)	3779	3960	4003
C in residue (% of total C)	39.8	43.3	47.2
Gas formation (mol/kg)	37.1	34.4	33.0

w55.doc

From table 2 we see that the detonation products change strongly when going from vacuum to 1,0 bar argon (0.1 MPa) of the unconfined charge. The concentration of H_2 und CO decrease, whereas CO_2, H_2O and carbon formation increase in the same manner as the detonation heat increases. This means that a detonation under a pressure of 1 bar is much more powerful with regard to the energy output than in vacuum.[2)]

On the other hand, the glass confined charge exhibits already in vacuum detonation products which are similar to those at 0.1 MPa argon of the unconfined charge, as we see comparing table 2 with 3. But the heat output increases also with higher ambient pressure of 0.05 and 0.1 MPa, but not in the same magnitude as before regarding the unconfined charges. As a conclusion we can say that ambient argon of one bar behaves as a confinement. Experiments conducted with 2,0 und 3,0 bar argon exhibited nearly no more further improvement of the confinement.[2)]

Composite explosives consisting of polybutadien binder and RDX have shown the same behavior as TNT/NQ when using different ambient pressures of argon as we see in table 4.

Also here increases the heat of detonation very strongly from vacuum to 0.05 MPA argon, because of the increase of H_2O and CO_2 and of carbon via the exothermal Boudouard-reaction

$$2\ CO \rightleftharpoons CO_2 + C; \quad \Delta H = -\ 127{,}7\ kJ/kg$$

Table 4: Detonation products of PBX - charges

Sample No.		HX 72/1	HX 72/2	HX 72/3
Ar pressure [MPa]		Vacuum	0.05	0.1
Composition		20% PB/80% RDX (10 µm)		
O_2-Balance [%]			-73.3	
Charge Weight [g]		329	328	330
ΔH_f [kJ/kg]		-94	-90	-95
Products [mol %]	H_2	33.5	15.0	12.3
	CH_4	0.1	0.7	2.9
	CO	34.4	17.3	13.1
	CO_2	1.2	3.5	6.6
	N_2	18.8	18.0	18.8
	NO	0.05	0.03	0.02
	HCN	0.1	0.8	0.9
	NH_3	0.5	2.9	2.8
	C_2H_2	—	0.06	0.5
	H_2O	4.8	19.6	19.9
	C_s	6.6	22.2	22.2
ΔH_{det} [kJ/kg]		2949	4214	4440
C in Residue [% of total C]		15.7	49.9	47.3
Gas formation [mol/kg]		52.1	42.0	39.7

4.3 Influence of Al Content on the Detonation Products

It is very interesting that the detonation of Al containing PBX-charges with Polybutadiene (PB) binders exhibit a different detonation behavior as to be seen in table 5. In this PBX-charge, consisting of 15 % PB, 15 % Al and 70 % RDX, we cannot more find the strong influence of vacuum on the detonation products compared with one bar argon (0.1 MPa). The same holds also for the detonation enthalpy, which is not very different for the vacuum shot compared with that of one bar argon.

Table 5: Detonation products of Al - containing PBX - charges

Sample No.		HXA 123/1	HXA 123/3
Ar pressure [MPa]		Vacuum	0.1
Composition		15% PB/15% Al Alcan 400	
		56% RDX Class C/14% RDX (10 µm)	
O_2-Balance [%]			-69.3
Charge Weight [g]		331	331
ΔH_f [kJ/kg]		-73	-71
Products [mol %]	H_2	29.5	25.8
	CH_4	0.04	1.1
	CO	26.1	20.1
	CO_2	0.01	2.7
	N_2	16.9	18.1
	NO	0.07	0.05
	HCN	0.1	2.35
	NH_3	2.2	0.9
	C_2H_2	0.04	0.3
	C_2H_4	0.03	0.2
	H_2O	4.2	7.2
	Al_2O_3	4.6	3.9
	Al	1.6	3.0
	C_s	14.6	14.3
$K_p(T)$		?	2.018
Freeze out Temp. [K]			1365
ΔH_{det} [kJ/kg]		5143	5066
C in Residue [% of total C]		35.6	34.5
Unreacted Al [%]		15.0	28.0
Gas formation [mol/kg]		38.6	37.0

Table 6: Detonation products of HMX / Al / PIB charges with different Al - content

Sample No.:	PHXA-81	PHXA-82
Composition, %	65 HMX/25 Al/10 PIB	60 HMX/30 Al/10 PIB
Ar pressure (MPa)	0.1	0.1
Oxygen balance (%)	-63.45	-66.05
Charge mass (g)	220.0	221.5
ΔH_f (kJ/kg)	-96.2	-119.7
Products (mol%)		
H_2	26.1	28.9
CH_4	1.7	1.4
CO	21.3	22.3
CO_2	3.2	2.5
N_2	20.1	18.9
HCN	3.2	2.6
C_2H_4	1.7	1.4
H_2O	3.6	2.6
C_s	7.1	6.9
Al_2O_3	7.9	9.4
Al	4.1	4.9
ΔH_{det} (kJ/kg)	6583	7027
Al in residue (% of total Al)	20.8	20.6
C in residue (% of total C)	17.7	18.0
Gas formation (mol/kg)	31.3	29.8

Table 7: Detonation products of charges with different binders

Composition, %	65 HMX/25 Al/10 PIB	60 HMX/25 Al/15 GAP
Ar pressure (MPa)	0.1	0.1
Oxygen balance (%)	-63.45	-54.40
Charge mass (g)	220.0	328.7
ΔH_f (kJ/kg)	-96.2	-141.8
Products (mol%)		
H_2	26.1	30.0
CH_4	1.7	0.1
CO	21.3	26.5
CO_2	3.2	0.2
N_2	20.1	21.6
NO	?	0.1
HCN	3.2	1.9
C_2H_4	1.7	0.05
H_2O	3.6	1.0
C_s	7.1	7.7
Al_2O_3	7.9	10.7
Al	4.1	0.12
ΔH_{det} (kJ/kg)	6583	7481
Al in residue (% of total Al)	20.8	0.6
C in residue (% of total C)	17.7	21.2
Gas formation (mol/kg)	31.3	30.1

w54.doc

We assume that an increase of CO_2 and H_2O with increased pressure is prevented by the reaction of these components with Al. This can be explained by the fact that especially H_2O decreases dramatically with increase of Al, as we see in table 6, where the detonation products of two plastic bonded explosive charges containing 25 % and 30 % Al are described. In this case HMX as explosive component and polyisobutylen (PIB) as a polymeric binder have been used.

4.4 Influence of the Polymeric Binder on the Detonation Products

In order to evaluate the influence of different binder systems on the detonation reaction, we investigated two explosive charges containing polyisobutylene (PIB) on the one side, and Glycidylazide polymer (GAP) on the other side. [3)]

The two compositions were as follows:

Charge A: 65 % HMX, 25 % Al, 10 % PIB

Charge B: 60 % HMX, 25 % Al, 15 % GAP

The main difference between the two charges is the oxygen balance, which is better in the GAP-containing charge (- 54,4 %) compared with - 63,45 % in the PIB containing charge, see table 7.

Although the enthalpy of formation is less negative and therefore more energetic in Charge A because of the higher HMX content, the better O_2-balance of Charge B is responsible for a more complete reaction of Al.

In Charge B with the energetic binder we found only 0,6 % of unreacted Al, compared with 20,8 % in Charge A.

The more complete Al-reaction leads to a much higher energy output:

Charge B: 7481 kJ/kg
Charge A: 6583 kJ/kg

This means that the O_2-balance is very important especially for Al-containing high explosives.

This behavior of different binder systems is easily to understand when we compare the O_2-balances of HMX with GAP, Polybutadien (HTPB) and Polyisobutylen (PIB) as to be seen in table 8.

Table 8: Oxygen balance and enthalpy of formation of different binder systems

	Oxygen balance (%)	ΔH_f (kJ/kg)
GAP	-121.1	1179
R 45M (HTPB)	-323.0	-380
PIB	-342.2	-1568
80 RDX / 20 GAP	-41.5	457.4
80 HMX / 20 GAP	-41.5	438.5
80 HMX / 20 HTPB	-81.9	126.9
80 HMX / 20 PIB	-85.7	-110.8

w52.doc

5. Conclusion

The influence of different boosters on the initiation of explosive charges containing TNT and nitroguanidine has been investigated. It was found, that a complete detonation was only observed after placing an additional booster sheet with the same diameter as the explosive charge on the front side of the cylindrical charge.

The investigation of Al-containing charges exhibited a very different behavior compared with the charges without Al. No more influence of vacuum or of different ambient gas pressure could be observed.

By comparing two charges with different oxygen balances it was found a great influence on the reaction of Al. The PBX charge with the better O_2-balance containing the energetic GAP-binder reacted nearly complete with the Al, opposite to the charge containing the Polyisobutylene (PIB) binder system.

References

1) Donna Price and Frank J. Zerill:
Notes from lectures on detonation physics, Naval Surface Weapons Center,
White Oak, Oct. 1981, NSWC MP 81-399

2) F. Volk and F. Schedlbauer:
Detonation Products of Less Sensitive High Explosives Formed under
Different Pressures of Argon and in Vacuum
9th Sympos.(International) on Detonation
August 28 to September 1, 1989, Portland, Oregon, USA

3) F. Volk and F. Schedlbauer:
Products of Al containing explosives detonated in argon and underwater
10th International detonation Symposium, July 12-16, 1993,
Boston, Mass., USA

4) M. Held:
Corner-Turning Distance and Retonation Radius
Propellants, Explosives, Pyrotechnics
14 (1989) 153-161

JOURNAL DE PHYSIQUE IV
Colloque C4, supplément au Journal de Physique III, Volume 5, mai 1995

Sulfuric Acid Influence on the Nitrocompounds Detonation Reactions

V.N. Gamezo, S.M. Khoroshev, B.N. Kondrikov and G.D. Kozak

Mendeleev University of Chemical Technology, 9 Miusskaja Sq., 125047 Moscow, Russia

Abstract: The detonation failure diameter d_f and detonation velocity D of mixtures of nitromethane, trinitrotoluene, dinitrotoluene, and trinitrobenzene with sulfuric acid and oleum have been measured in the wide range of concentrations. It was shown that the detonation ability of the nitrocompounds depends significantly on the sulfuric acid content. The minimum value of d_f for the mixture TNT/oleum is about 2 mm, i.e., 30 times less, than that for pure melted TNT, and practically equal to d_f of nitroglycerine. In some cases, the temperature dependencies of failure diameter have been determined. Dremin theory of detonation failure diameter was used to treat quantitatively the results of experiments with the NM and TNT solutions in the frameworks of the Arrhenius chemical kinetics.

1. INTRODUCTION

The strong sensibilizing effect of small quantity of the inorganic acids on the nitrocompounds detonation was observed earlier [1]. Nitromethane was used as a model. There was shown that the nitromethane detonation is greatly influenced by small concentration of additives. Of course it would be interesting to find out how it is affected by the large ones.

In this paper the sulfuric acid influence on the detonation ability of mixtures of sulfuric acid or oleum with nitromethane (NM), trinitrotoluene(TNT), dinitrotoluene(DNT), and trinitrobenzene(TNB) was studied in a wide range of the components concentrations[1] (from 93 to 108% H_2SO_4 in the concentrated sulfuric acid and oleum, and up to 64% of the acid in the mixture with nitrocompound). Dremin theory of detonation failure diameter [2-4] was used to treat quantitatively the results of experiments with NM and TNT solutions.

The work was mainly implemented during 1986-1990 as a constituent part of investigations were to reveal and to remove causes of accidents being arisen under the TNT production on the third stage of DNT to TNT nitration.

[1] Concentration of oleum and acid is expressed by percentage of sulfuric acid S. Content of suitable sulfuric ingredient in mixture with explosive is denioted by C_S.

2. EXPERIMENTAL

The experiments were carried out using the commercial grade TNT (solidification temperature, S.T.=80.2^{0}C) and 2,4-DNT (S.T.=68.9-69.2^{0}C). TNB was produced in the laboratory and purified by recrystallyzation from nitric acid (S.T. of TNB recrystallyzed was 122.8^{0}C). The commercial-grade NM was distilled at atmospheric pressure over P_2O_5. The main fraction 100.7-101.3^{0}C was taken for the experiments. The detonation failure diameter of this fraction of NM measured repeatedly every 1-2 months during about two years was 13±0.5 mm. The commercial-grade sulfuric acid (94% concentration) and oleum containing 60% "free" sulfuric anhydride were used to prepare the solutions containing up to 108.2% H_2SO_4. The H_2SO_4 concentration was determined by titration.

The detonation failure diameter d_f was measured in glass tubes (the wall thickness is ~1.5 mm) by the method go-no-go. Dark, open, and half-dark points (Fig.1,3,5) correspondingly designate detonation, failure of detonation immediately after initiation, and detonation extinguishment after more or less prolonged (up to several d in length) path of the detonation process. The tubes had the smooth widening in the upper part for initiator or booster setting, and for the continuous transition to the steady-state detonation. A pellet of pressed phlegmatized RDX (d=12 mm, m=2 g, ρ=1.66 g/cm^3) used as the booster was protected by the thin film of fluoropolymer to avoid the strong acid action on the booster. The result of the experiment was determined by means of the metal witness-plate attached directly to the tube wall.

The experiments at high temperature were carried out in the glass tubes inserted in tubes of higher diameter and isolated by the layer of cotton wool placed between the tubes walls. The assembly was heated to temperature 5^{0}C higher the proposed experiment temperature. After that the liquid investigated heated to the same temperature was quickly poured into the central glass tube, all the setting was placed into the explosion chamber, and after some delay monitored by means of the preliminary estimated cooling curve the detonation was initiated.

The detonation velocity D was measured in the steel tubes (d=10 mm, δ=13 mm, l=180-250 mm). The detonation process luminosity was registred by the Russian streak camera SFR-2 through the radial holes (d=1.5-2.0 mm), drilled in the wall of the tube at distance of 15 mm one from another. The holes as well as the bottom of the tube were closed by the glass plates, adhered by the acid persistent glue.

The measurements were made mainly under the initial temperature T_0=18.5^{0}C for NM solutions, 85-86^{0}C for TNT and DNT solutions, and 110^{0}C for TNB solutions (except the cases where the effect of initial temperature was estimated).

3. RESULTS

NM: The results of experiments with the solutions of NM in H_2SO_4 concentration of 93% and 100.5% are represented in Figs.1 and 2. The sulfuric acid addition leads to the failure diameter quick decrease, after that the flat minimum (about 1.5 mm) is reached, and progressive grow of the d_f value follows. The detonation velocity at $C_S \leq 20\%$ (S=100.5%) is practically constant, and equal to that of the neat NM (6.34 mm/μs at T =18.5^{0}C). For S=93% the D(C_S) dependence was not measured.

TNT: Oleum of concentration 100.6, 101.7, 103.8 and 108.2% H_2SO_4 was used to obtain TNT solutions. The results of the measurements of failure diameter of the solutions are represented in the Figures 3 and 4. Curves received at different oleum concentrations are similar to each other: as the oleum content C_S in mixture increases, detonation failure diameter reduces down to the minimum value and then rises. Minimum critical diameter d_f^{min} (mm) depends on S:

$$\log_{10} d_f^{min} = 1.2 \cdot 10^7 \cdot \exp(-0.1619 \cdot S)$$

The content of oleum in the mixture corresponding to the minimum of the curve is about 40-50% and tends to rise in these limits, when S grows. The minimum value of d_f for TNT diluted by oleum, S=108.2%, is about 2 mm, i.e. 30 times less, than that for pure melted TNT. It is practically equal to the detonation failure diameter of nitroglycerine.

The influence of oleum content on detonation velocity of TNT is shown in Fig.2. The velocity of detonation is almost constant up to C_S=50%. Further growth of oleum content results in the considerable decrease of the D value leading to extinguishment of detonation.

Influence of nitric acid on detonation of TNT solutions in oleum is of the obvious practical interest. Solubility of nitrocompounds in the sulfuric-nitric acids mixture is far less, than in oleum or sulfuric acid alone. One can introduce without loss of solubility to the mixture containing 40/60 TNT/oleum (S=103.8%) no more than 4% of nitric acid. Experiments carried out with such solution at concentration of nitric acid 2.5 and 4%, show that, regardless of wide-spread opinion, d_f of TNT solution in oleum does not grow. It remains constant and equal to 11-12 mm. Introducing of extra quantity of nitric acid results in emulsion formation, and experiments in this concentration region were not carried out.

DNT: The detonation failure diameter of pure melted DNT up to now is not estimated. Using some approximation, we can appraise it at 80-90^{0}C as about 0.5 m. In the steel tubes (d=10 mm, δ=13 mm) the detonation extinguished even at 190^{0}C. However, the steady-state detonation of the DNT solutions in oleum at S=103.8%, C_S=50% and 60% (T_0=85^{0}C) was observed. The mean detonation velocity of the solutions was equal to 5.5 mm/μs (Fig.2). At C_S=40% the detonation of the solution after considerable (110-130 mm) propagation failed, at C_S=70% the detonation was not observed. It is quite obviously that oleum reacts with DNT sensibilizing its detonation.

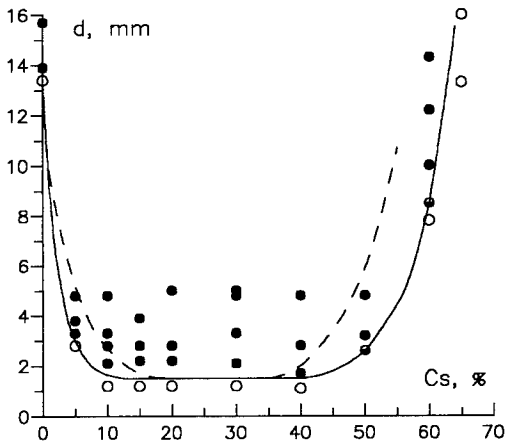

Fig.1. Influence of sulfuric acid on detonation failure diameter of NM. Dark, open, and half-dark points correspondingly designate detonation, failure of detonation, and detonation extinguishment. The points and the solid line (which separates the detonation region from the region of detonation failure) represent the results for S=100.5%. The dashed line corresponds to S=93%.

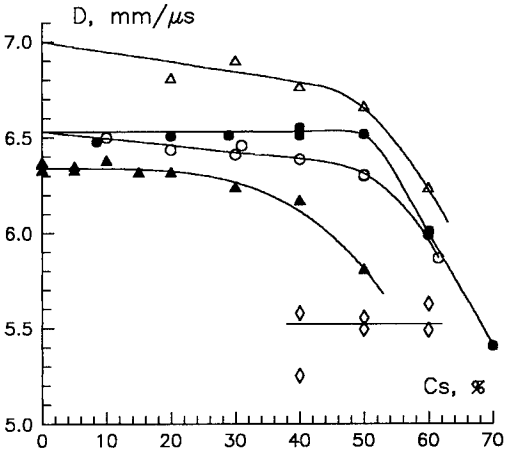

Fig.2. The results of detonation velocity measurements of the mixtures of nitrocompounds and oleum:

Δ - TNB/oleum (S=103.5%, T_0=110^{0}C),
● - TNT/oleum (S=103.8%, T_0=85-86^{0}C),
○ - TNT/oleum (S=101.6%, T_0=85-86^{0}C),
◊ - DNT/oleum (S=103.8%, T_0=85^{0}C),
▲ - NM/oleum (S=100.5%, T_0=18.5^{0}C).

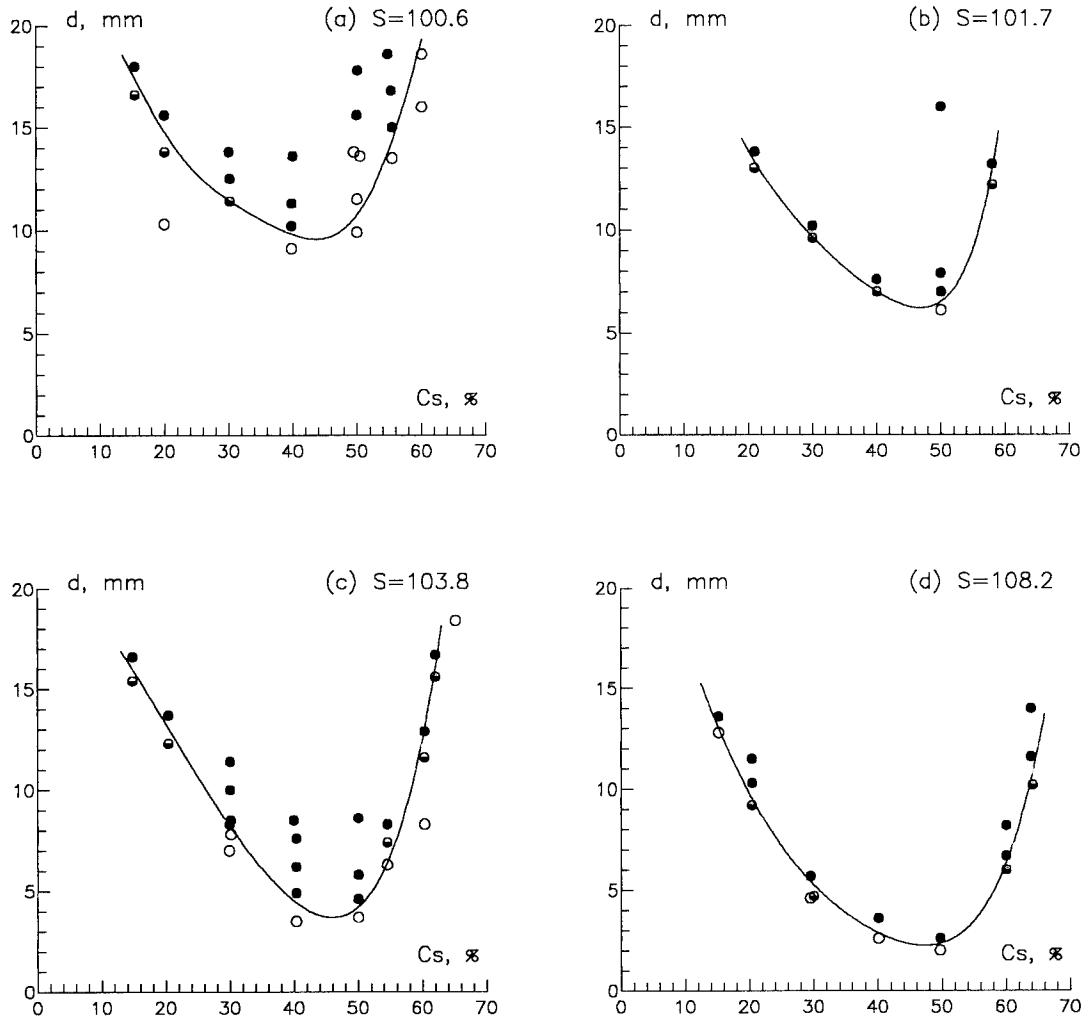

Fig.3. The results of detonation failure diameter measurements in the TNT/oleum mixtures. T_0=85-86^{0}C. Dark, open, and half-dark points correspondingly designate detonation, failure of detonation, and detonation extinguishment. The curve separates the detonation region from the region of detonation failure.

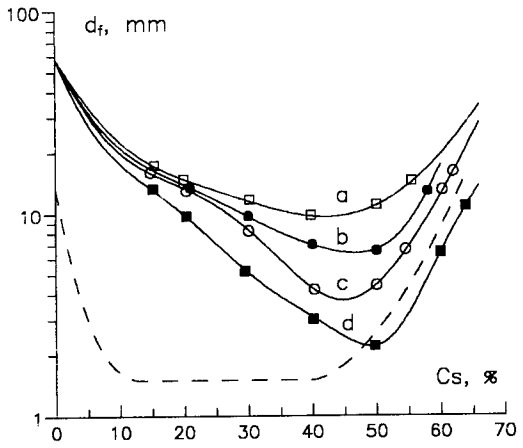

Fig.4. The detonation failure diameter of the mixtures of TNT (a-d) and NM (dashed line) with oleum versus its content in the solution. Oleum concentration S,%: a - 100.6%, b - 101.7%, c - 103.8%, d - 108.2%, and 100.5% for the mixtures of NM. The points are the mean experimental values; the solid lines are calculated for TNT mixtures using the kinetic scheme suggested.

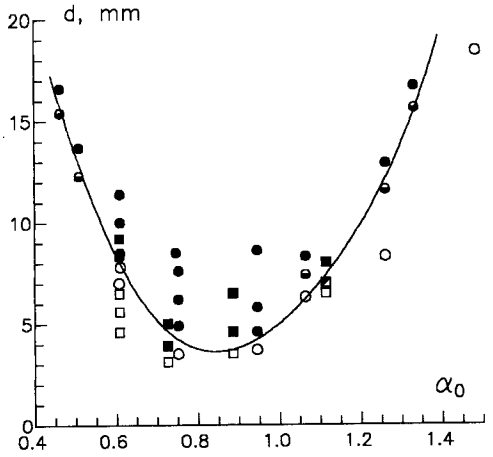

Fig.5. The detonation failure diameter versus inverse equivalent ratio α_0 for TNT/oleum (S=103.8%, T_0=85^{0}C, circles) and TNB/oleum (S=103.5%, T_0=110^{0}C, quadrangles) mixtures. Dark, open, and half-dark points correspondingly designate detonation, failure of detonation, and detonation extinguishment. The curve is common for two mixtures, and separates the detonation region from the region of detonation failure.

TNB: The experiments with TNB solutions were carried out at the oleum concentration S=103.5%. At 110^0 C one can get the solutions, containing up to 80% of TNB. The results of the detonation velocity measurements and the detonation failure diameter of the TNB solutions in oleum estimations are shown in Figs.2 and 5. Comparing these data with the results observed for TNT in oleum solutions (S=103.8%, Fig.3), one can conclude, that the curves are not only similar to each other, but even the values of d_f^{min} for TNT and TNB are almost exactly the same. However, to reach the same d_f values in case of TNB the higher temperature is required. In coordinates of d_f versus $1/\alpha_0$ the data for TNT and TNB coincide with each other (Fig.5).Here α_0 is the equivalent ratio of the mixture

$$\alpha_0 = (O) / [2(C) + (H)/2 - (S)]$$

where (O), (C), (H), and (S) are the molecular fractions of the elements in the mixture.

Effect of initial temperature: The $d_f(T_0)$ dependencies were determined for 50/50 mixtures of H_2SO_4 with NM (at S=93.0%), TNT (at S=103.0%), and TNB (S=103.5%). As for number of other explosives, the straight lines $\log_{10} d_f = A+B/T_0$ were obtained. Constants A and B together with the data [5] for neat TNT and NM are represented in the Table 1.

Table 1. The constants A and B of the straight lines $\log_{10} d_f = A+B/T_0$.

Explosive	T_0, K	A	B	d_f (353 K), mm (calculation)
TNT/oleum 50/50 (S=103.0%)	336-370	-2.176	1041	5.9
TNB/oleum 50/50 (S=103.5%)	358-383	-0.898	675	10.3
NM/H_2SO_4 50/50 (S=93.0%)	253-338	-1.194	585	2.9
TNT	357-513	-1.667	1231	66.1
NM	273-358	-0.866	581	6.0

4. DISCUSSION

The quantitative treatment of results in this paper is represented only for mixtures on base of NM and TNT, because the information on d_f dependencies for DNT and TNB mixtures is not sufficient for calculation. Dremin theory of detonation failure diameter [2-4] was used to treat the results. According to this theory based on conception of pulsating reaction zone we can calculate the adiabatic induction period τ_3 in this zone near the limit of detonation propagation at temperature of shock-compressed substance T_3. The calculation procedure in all details is given in [6]. The same velocity of the reaction failure wave $v = 3.8$ mm/μs for all the mixtures of NM as well as for neat NM [7] was accepted. Similarly, the value $v = 2.76$ mm/μs, reported in [3] for liquid TNT, was used for all TNT mixtures. The generalized Hugoniot of liquids $D = C_0+0.29+1.63u$ [8] was used for oleum. The sound velocity C_0 was determined in paper [9]. The Hugoniot adiabat of the mixture was defined supposing the components specific volume additivity.

4.1. NM solutions.

The polytropic exponent of detonation products γ for the NM solutions is assumed to be the same function of initial density ρ_0 as for pure nitromethane [7]: $\gamma=(0.656/\rho_0)+0.703+1.105\rho_0$ (ρ_0 in g/cm^3). The shock temperature of the solutions was calculated by the method [8]. These data were used to calculate the temperature T_3, and the corresponding ignition delays τ_3 along the solid curve on Fig.1.

The decomposition rate constant of pure nitromethane [5] is

$$k_1=k_{01}\exp(-E_1/RT), \qquad (1)$$

where $k_{01}=8\cdot10^{14}$ s^{-1}, $E_1=210$ kJ/mol. The activation energy is close to the values reported in [4], and obtained for thermal decomposition of NM at pressure of order of 10^4-10^5 Pa (see compilation [10]).

The decomposition rate on addition of sulfuric acid increases, obviously due to CH_3NO_2 - H_2SO_4 interaction. It is known [11], that this interaction gives $CH_3NO_2H^+$ ion, which is allowed to be named the nitromethonium ion by analogy with $H_2O{\cdot}H^+$ hydroxonium ion. The possible complexes of this ion with sulfuric acid are the nitromethonium bisulfate $CH_3NO_2H^+{\cdot}HSO_4^-$, and the nitromethonium sulfate $[CH_3NO_2H^+]_2{\cdot}SO_4^{2-}$. Our analysis shows that the sulfate ion formation is more essential source of the detonation reaction acceleration. When sulfuric acid content in the mixture is large enough (more than 30-35%), one can suppose that this complex is formed quantitatively, and nitromethane in the shock wave reacts quickly with sulfuric acid according to reaction

$$2CH_3NO_2+H_2SO_4 \xrightarrow{K_C} [CH_3NO_2H^+]_2{\cdot}SO_4^{2-} \quad (K_C\to\infty) \qquad (2)$$

The complex formed is decomposed. The decomposition rate constant supposedly is

$$k_2=k_{02}\exp(-E_2/RT)\,, \qquad (3)$$

and $k_2(T_3)>>k_1(T_3)$. Our estimation shows that $E_2 \cong E_1/2$. In this case to compute the constants ratio, one can use the expression

$$\tau_3 N/(\tau^0{}_3 N_0) = 2Y[1-Y\ln(1+1/Y)], \quad Y=(k_1 N/k_2 a C_2) \qquad (4)$$

being integral of the differential equation of adiabatic self-heating for two parallel reactions of the first order at the fixed (time-independent) reagents concentrations. In Eq.(4) N_0 and N are the initial and the current molar concentration of nitromethane, C is the molar concentration of the complex. For bisulfate $a = 1$, for sulfate $a = 2$. $\tau^0{}_3$ is the hypothetical period of induction in the system, where the complex is not formed, nitromethane concentration remains equal to N_0, and the heat release rate is not influenced by sulfuric acid:

$$\tau^0{}_3 = C_V \rho R T_3{}^2/(N_0 Q_V E_1 k_{01})\cdot\exp(E_1/RT_3) \qquad (5)$$

Here Q_V is the heat of NM decomposition, C_V and ρ are the heat capacity and density of mixture. As the sulfuric acid is added to the system $\tau^0{}_3$ increases rapidly. For example, $\tau^0{}_3/\tau_3=570$ when $C_S=60\%$.

If the proposed model is true, the straight line must be obtained in $1/T_3$-$\log_{10}(k_1/k_2)$ coordinates. The slope and intercept of this line give the difference of the activation energies E_1-E_2, and the ratio of the pre-exponential factors k_{01}/k_{02}.

By assuming that nitromethonium sulfate is formed, the experimental results allow to obtain the constants k_{02} and E_2 directly: when $C_S>44.5\%$ there is no free nitromethane in the system, and the self-heating equation reduces to the usual relation of the type (5) for $k(T)=k_2(T)$.

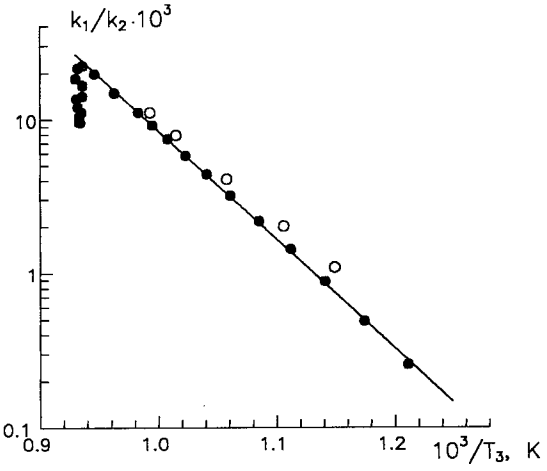

Fig.6. The k_1/k_2 ratio calculated by the formula (4) versus $1/T_3$ for mixtures NM/H_2SO_4: ● - on the basis of $d_f(C_S)$ for S=100.5%, O - using $d_f(T_0)$ for S=93%.

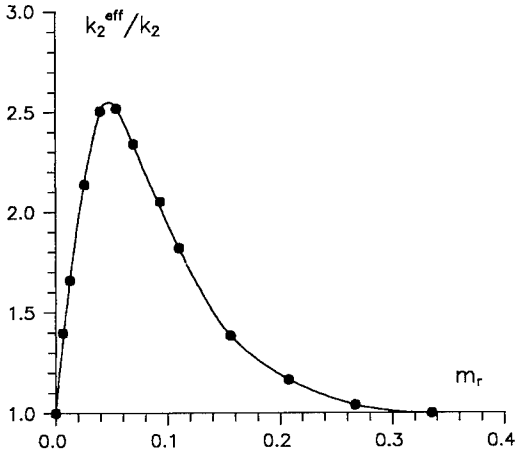

Fig.7. The ratio of the effective rate constant k_2^{eff} given by Eq.(4), to the decomposition rate constant of the nitromethonium sulfate k_2 as a function of the molar ratio of sulfuric acid to nitromethane.

The dependence of the $\log_{10}(k_1/k_2)$ versus $1/T_3$ calculated by the formula (4) (Fig.6) gives the line $\log_{10}(k_1/k_2) = 4.89\text{-}6970/T_3$ obtained in the range of $30\% \le C_S \le 64\%$, from which $E_2\text{-}E_1 = 133$ kJ/mol, and $k_{01}/k_{02} = 7.7\cdot10^4$. This corresponds to $E_2 = 77$ kJ/mol for $E_1 = 210$ kJ/mol. In the range of $44\% \le C_S \le 64\%$, where under the assumption $K_C \to \infty$ all nitromethane is turned to the nitromethonium sulfate, the dependence $\log_{10} k_2(1/T_3)$ results in $E_2 = 79$ kJ/mol, and $k_{02} = 1.7\cdot10^{10}s^{-1}$.

When sulfuric acid content is less than 30% the points (Fig.6) tend to fall down, tracing out a loop with a minimum at C_S=6-8%, then tend to line again. The initial part of the dependence is demonstrated in Fig.7, where the relation of the effective rate constant k_2^{eff} to the value of k_2, which is approximately constant in the concentration range considered, is plotted as a function of the molar ratio of sulfuric acid to nitromethane. Obviously, it does mean that the third group of reactions at low H_2SO_4 content takes place, probably connected with the aci-ion [12] formation under the acid influence. As sulfuric acid content increases, the conversion velocity of NM to aci-ion rises, but in the strong acid medium at high concentration of H_2SO_4, aci-form does not exist. So, for the large enough concentration of the acid the reaction reduces to the formation and decomposition of the nitromethonium sulfate, the overall decomposition rate decreases, k_2^{eff}/k_2 ratio tends to 1.

Dependence $d_f(T_0)$ measured for the mixture 50/50 of nitromethane and sulfuric acid (S=93%) was also processed in framework of Dremin theory. To do this it is required to know the experimental values of detonation velocity if only at any one value of initial temperature. The effect of T_0 on D was found using the coefficient of heat expansion. T_0 on T_3 influence was determined by the method proposed in [8].

The results of the calculations (for D_{298}=5.75 mm/μs) are shown in Fig.6 (open circles). The dependence $d_f(T_0)$ gives practically the same values of k_2, as the dependence $d_f(C_S)$. The variation of the initial temperature is no effect on the main result: the interaction of nitromethane with sulfuric acid leads, with the qualitative yield, to the formation of nitromethonium sulfate, the decomposition rate of which under the conditions considered is two orders of magnitude greater than that of nitromethane.

4.2. TNT solutions

The values of τ_3 and T_3 calculated for mixture (50/50) TNT/H_2SO_4 (S=103.0%) at different initial temperature are placed on the line:

$$\log_{10}(\tau_3/T_3^2) = -a + b/T_3 \qquad (6)$$

The values of a and b depend on equations of state of original components and explosion products, mainly, on polytropic exponent of detonation products γ. For mixtures of TNT and sulfuric acid this value is not determined as yet. Changing γ in the range of 2.8-3.2, one can get the a and b constants to be equal to 18±1 and $(15.7\pm0.5)\cdot10^3$, respectively. The activation energy of the reaction is changed correspondingly in the range of 100-120 kJ/mol. The activation energy of TNT detonation reaction calculated in [4], is equal to 109 kJ/mol, i.e. it corresponds to the middle of the interval obtained here. To simplify further calculations, the suggestion is proposed that the activation energies of the reactions determining d_f of the H_2SO_4 solutions, are equal to each other and close to the value of 109 kJ/mol.

The sequence of kinetic equations of the main reactions taken place at detonation of TNT/ H_2SO_4/SO_3 mixtures is

$$W_1 = k_1[TNT], \qquad (7)$$

TNT decomposition, where [TNT] is TNT molar concentration.

$$W_2 = k_2[TNT\cdot nH_2SO_4], \qquad (8)$$

decomposition of TNT and sulfuric acid complex. The possibility of the formation of such complex follows from the data on solubility of TNT in sulfuric acid [13]. It is quite possible, that, as well as in the case of NM, this complex included the ionized TNT molecule. The relative number of H_2SO_4 molecules in the complex n has to be determined from the best correlation of the calculation results with the experimental data.

The considerable influence of "free" SO_3 shows, that a reaction with sulfuric anhydride is also essential. One can suppose, that this reaction proceeds between the complex and SO_3

$$W_3 = k_3[TNT \cdot nH_2SO_4] \cdot [SO_3] \qquad (9)$$

One can suggest also, that the intermediate stage of transition of the reagents, entering into reaction (9), to its products is the formation of a complex with pyrosulfuric acid ($H_2S_2O_7$):

$$TNT \cdot nH_2SO_4 + SO_3 \xrightarrow{k_3} TNT \cdot (n\text{-}1)H_2SO_4 \cdot H_2S_2O_7 \xrightarrow{k_4} \text{products},$$

where $k_4 >> k_3[SO_3]$.

Taking into account the reactions (7-9), the value of k_0 in the equation for the quasi first order reaction rate ($W=k_0[TNT]_0 \cdot \exp(-E_a/RT)$) can be represented in the form of

$$k_0 = \frac{k_{01}[TNT] + k_{02}[TNT \cdot nH_2SO_4] + k_{03}[TNT \cdot nH_2SO_4] \cdot [SO_3]}{[TNT]_0} \qquad (10)$$

The values of the pre-exponential factors k_{01}, k_{02}, and k_{03} for the reactions (7), (8), and (9), as well as the coefficient n have to be defined from the experimental data.

The calculations were carried out at E_a=109 kJ/mol, $\gamma=2.027+0.7429\rho_0$ (taken from [5]). Using the obtained ignition delay τ_3, the value of k_0 was calculated as

$$k_0 = C_V \rho R T_3^2 / (Q_V M_{TNT} [TNT]_0 E_a \tau_3) \cdot \exp(E_a/RT_3) \qquad (11)$$

where C_V is the heat capacity of the mixture, Q_V is the heat of TNT decomposition. The concentrations (mol/m^3) are defined by the relations:

$$[TNT]_0 = (1\text{-}C_S/100) \cdot \rho / M_{TNT};$$
$$[SO_3] = S_{SO3}/100 \cdot C_S/100 \cdot \rho / M_{SO3};$$
$$[H_2SO_4] = (1\text{-}S_{SO3}/100) \cdot C_S/100 \cdot \rho / M_S;$$
$$S_{SO3} = M_{SO3}/M_{H2O} \cdot (S\text{-}100),$$

where M_{SO3}, M_{H2O}, M_{TNT}, and M_S are molecular weights of SO_3, water, TNT, and sulfuric acid, correspondingly; ρ is the mixture density; S_{SO3} is the mass concentration of "free" SO_3 in oleum. The pre-exponential factor k_{01} corresponds to the decomposition of TNT, remained after interaction with sulfuric acid:

$$[TNT] = [TNT]_0 - [TNT \cdot nH_2SO_4]$$

The value of k_{02} is responsible for $TNT \cdot nH_2SO_4$ complex decomposition rate, where n molecules of sulfuric acid are needed for one TNT molecule. At TNT surplus the concentration is defined by equality $[TNT \cdot nH_2SO_4]=[TNT]_0/n$, at sulfuric acid surplus it is found as $[TNT \cdot nH_2SO_4]=[TNT]_0$ (we suppose that the equilibrium is entirely moved to the complex formation). The value of k_{03} is connected with formation and decomposition under the action of sulfuric anhydride of still more reactive TNT form. The point

$[TNT]_0=[H_2SO_4]/n$ corresponds to the transition from quadratic to linear plot. It allows us to determine the n value. It proved to be equal 2. The values of k_{01}, k_{02} and k_{03} obtained by optimization, are equal to $1.42\cdot10^{10}$ s^{-1}, $2.2\cdot10^{11}$ s^{-1}, and $1.2\cdot10^{11}$ $l\cdot mol^{-1}\cdot s^{-1}$, respectively. The values of k_0 calculated using these constants are represented by curves in Fig.8.

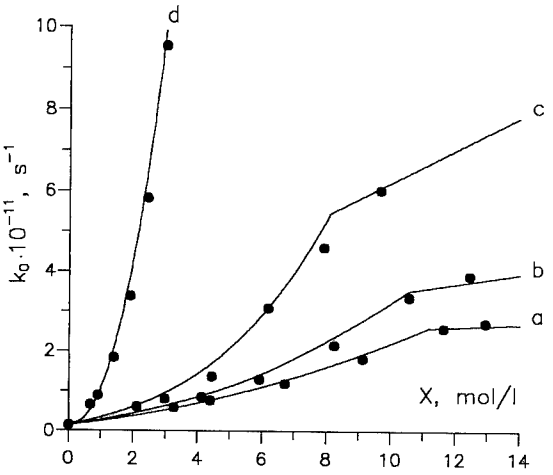

Fig.8. Influence of sulfuric acid ($X=[H_2SO_4]-[SO_3]$, mol/l) on decomposition rate of mixtures of TNT and oleum. The points represent the values of k_0 calculated on the basis of Dremin theory and the measurements of d_f; the curves are obtained using the kinetic scheme suggested at $E_a=109$ kJ/mol, $k_{01}=1.42\cdot10^{10}$ s^{-1}, $k_{02}=2.20\cdot10^{11}$ s^{-1}, $k_{03}=1.20\cdot10^{11}$ $l\cdot mol^{-1}\cdot s^{-1}$). Oleum concentration (S, %): a - 100.6, b - 101.7, c - 103.8, d - 108.2.

In Fig.4 the points are experimental data, the curves a-d are the results of the calculations carried out using the Eqs. (7-11). Having in mind the model used, they are extended to the region of low acid content. The dashed curve represents the results for mixtures of NM and sulfuric acid (S=100.5%). It is the same curve as the solid line on Fig.1. One can see, that the detonation failure diameter of TNT-based mixtures decreases less abruptly, than for the NM solutions, when acid is added to the system. It can be explained by the ability of nitromethane to form the aci-ion, which being quickly decomposed makes a supplementary contribution to the heat release rate.

5. CONCLUSIONS

The results obtained on detonation failure diameter prove a formation in the NM/H_2SO_4 and TNT/oleum mixtures of the complexes of the nitrocompounds with sulfuric acid having the composition of $[(CH_3NO_2)_2\cdot H_2SO_4]$ and $[TNT\cdot 2H_2SO_4]$. The decomposition rate of the nitromethonium sulfate is two orders of magnitude greater than that of nitromethane under the conditions considered (P~10 GPa, T~1000 K). The TNT complex decomposes 15 times faster than the pure TNT. It is said about considerable change of TNT molecule in this complex, may be associated with ionization. This complex reacts with SO_3 in oleum. The reaction rate at the maximum concentration of SO_3 (C_S=64%, S=108.2%) is 4 times higher, than the decomposition rate of the complex, and, hence, 60 times higher, than the decomposition rate of TNT itself.

REFERENCES

1. Kondrikov B.N., Kozak G.D., Raykova V.M., Starshinov A.V. *DAN SSSR* **233** (1977) 402-405.

2. Dremin A.N. *DAN SSSR* **147** (1962) 870-873.

3. Dremin A.N., Trofimov V.S. *PMTF* (1964) No 1, 126-131.

4. Enig J.W., Petrone F.J. "The failure diameter theory of Dremin". 5th Symposium (Int.) on Detonation, Pasadena, Ca, Aug. 18-21, 1970, Office of Naval Research, Arlington, Va. ACR-184, pp. 99-104.

5. Gamezo V.N., Kondrikov B.N. "Calculations of the kinetic constants for decomposition of nitromethane and TNT from the data on dependence of failure diameter on initial temperature". Proc. of IV Conference (USSR) on Detonation, Telavi, 1988, vol. 1, pp. 111-117.

6. Gamezo V.N. The heat release kinetics in the reaction zone of detonation wave. Cand. Sci. (Ph.D.) Thesis (Mendeleev University of Chemical Technology, Moscow, 1992).

7. Tarver C.M., Shaw R., Cowperthwaite M. Detonation failure diameter studies of four liquid nitroalkanes. *J.Chem.Phys.*, **64** (1976) 2665-2673.

8. Kondrikov B.N., Raykova V.M. Thermodynamics of combustion and explosion. (Mendeleev University of Chemical Technology, Moscow, 1981).

9. Briger G.I., Romanov Yu.L., Skotnikov V.A., Smirnov V.N. *J.Fiz.Khim.*, **54** (1980) 628-632.

10. Makovky A., Lenji L. *Chem. Revs.* **58** (1958) 627-644.

11. Brand J.C., Horning B.C., Thornley M.B. *J.Chem.Soc. (London)* (1952) No 4, 1374-1383.

12. Melius C.F. *Phil.Trans.R.Soc.(London)* A 339 (1992) 365-376.

13. Khoroshev S.M., Kondrikov B.N., Kozak G.D., et al. On the solubility of trinitrotoluene, trinitrobenzene and dinitrotoluene in sulfuric acid. Explosive materials and pyrotechnics. Problems of explosive safety of chemical workshops. (Ed. by B.N.Kondrikov. CNIINTIKPK, Moscow, 1992) 3(218) pp.14-20.

JOURNAL DE PHYSIQUE IV
Colloque C4, supplément au Journal de Physique III, Volume 5, mai 1995

Carbon in Detonation Products. A "Three-Phase" Modelisation

M.-L. Turkel and F. Charlet*

Commissariat à l'Energie Atomique, Centre d'Etudes de Vaujours-Moronvilliers, BP. 7, 77181 Courtry, France
** CISI, Centre de Saclay, BP. 28, 91192 Gif-sur-Yvette, France*

Abstract : Condensed carbon is a common and rather abundant component in reactive mixtures formed in shock compressed energetic materials. However, there still remain some questions about its molecular forms in these mixtures. The choice of an accurate model to be used in high pressure, high temperature simulations is essential to ensure better prediction of energetic substances performances and constitutes a major difficulty. We describe the main theoretical features of a three-phase equation of state used in the thermochemical code CARTE to represent the graphite-diamond-liquid system. Sensitivity of different characteristics (detonation velocity, energy release) to carbon equation of state is investigated for a large range of energetic materials.

1. INTRODUCTION

Predictive calculations of explosives performances turns out to be essential to reduce the stages that lead to the conception and the selection of a new energetic molecule. It can be done with thermochemical codes like BKW [1], TIGER [2], ETARC[3], CHEQ [4] and some others, developed all over the world. Fluid phases present in the dense and hot mixture of detonation products can now be accurately described with equations of state based on statistical mechanical considerations or more empirical equations. It is not always the case for condensed phases of carbon appearing in oxygen-deficient environment that are rather poorly described in these codes. Some of the deviations observed between thermochemical calculations and experimental data could be explained by the poor description of these condensed phases or more simply by phase changes in carbon. An extensive effort was made over the last years to improve the description of carbon in detonation products.

A "three-phase" equation of state model was proposed by M. Van Thiel and F. H. Ree [5] to describe the graphite-diamond-liquid system and is used in CHEQ. This model is consistent with shock and thermal data and also with the latest results concerning the phase diagram of carbon. It was introduced in the new thermochemical code developed at the CEA (CARTE) and used to calculate the characteristics of the Chapman Jouguet state and the energy released during the isentropic expansion of detonation products. After a rapid presentation of the thermochemical code and a brief description of the "3 phase" model, we compare the results obtained with this new model to those obtained with a Cowan Fickett equation of state [6] for a large range of high explosives.

2. THE THERMOCHEMICAL CODE CARTE

Thermochemical calculations of energetic performances are based on physical hypotheses for the thermodynamic description of detonation products and numerical algorithms for the solving of the

resulting equations. The different stages that arise in these predictive calculations are summarized in figure 1.

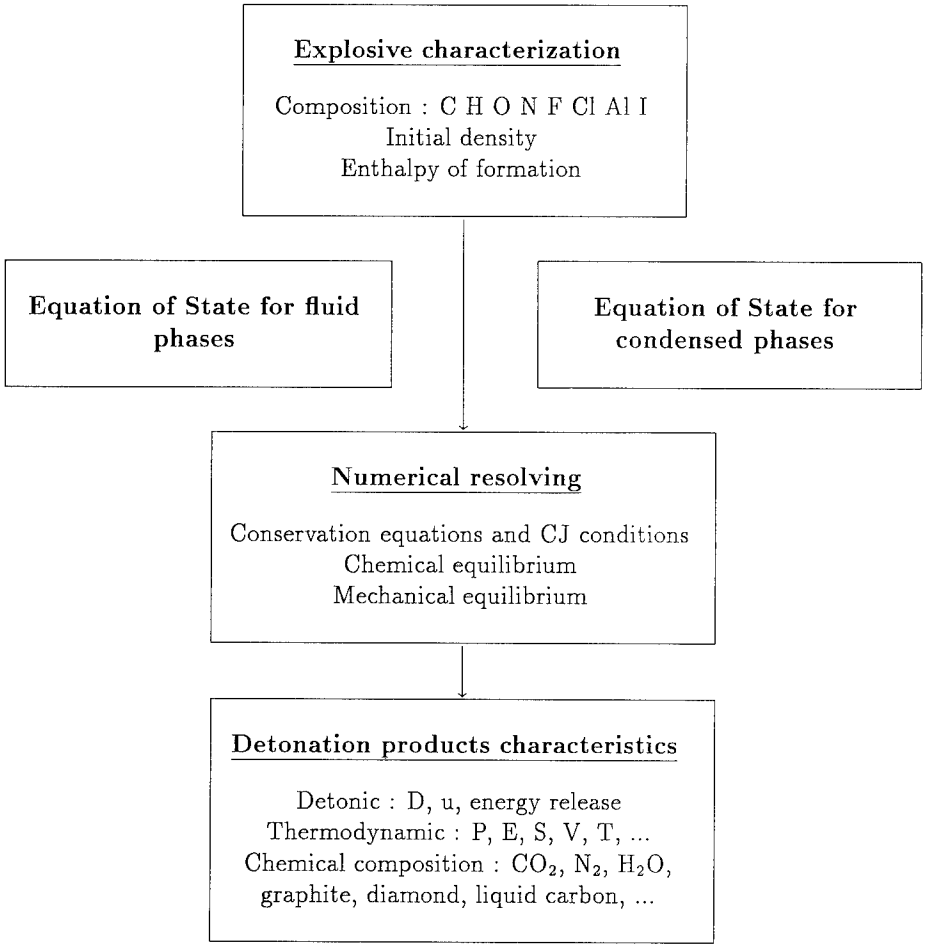

Figure 1: Organization of thermochemical calculations in the CARTE code.

The main properties of the CARTE code are:

-A large range of equations of state describing solid and fluid phases.
-Efficiency of numerical algorithms for the calculation of chemical equilibrium.
-Rapidity of calculations.

Equations of State

Several Equations of state are proposed to describe detonation products in a fluid phase:

* **WCA** : (4 different versions [3]) ; equations of state based on perturbation theory and used in the ETARC code.
* **MCRSR** : variational method developed by Ross [7] and used in CHEQ.
* **THEOSTAR** : accurate analytical equation developed by Byers-Brown [8], fitted on Monte Carlo data and WCA results (Ree version) ; used in the QUARTET code [9].
* **BKW** : empirical equation.
* **JCZ** : equation developed by Cowperthwaite [2] and used in TIGER.

The equations of state for condensed phases are:

* **Cowan-Fickett** EOS [10] : empirical equation used in ETARC to describe graphite and diamond properties.
* **Debye-Murnaghan** EOS : used for graphite, diamond, solid aluminium and alumine.
* **Three-phase** EOS : used for the graphite-diamond-liquid system.
* **Grover** EOS [11] : used for liquid aluminium.
* **Cowan** EOS [12] : empirical equation used for liquid alumine.

Numerical Performances

Resolving of chemical equilibrium represents the main numerical difficulty in thermochemical calculations. Given P and T, the equilibrium composition is determined by the minimum of the Gibbs free energy of the mixture. To illustrate the efficiency of numerical algorithms used in CARTE, we give, in table 1, a few comparisons of computation times for the determination of CJ isentropic expansions. The number of points calculated for each case is reported in brackets.

Table 1 : Calculation time comparisons.

Explosive	ETARC CRAY YMP	CARTE Sparc 10	Explosive	CHEQ Sparc 10	CARTE Sparc 10
NM	72mn (11 pts)	39s (50 pts)	HMX	18348s (50 pts)	175s (50 pts)
HMX compo.	135mn (35 pts)	48s (50 pts)			

Equations of State used in the first calculations are WCA for the fluid phase and Cowan Fickett for the solid phase (graphite). For the second set, 2 fluid phases are considered and represented with the MCRSR equation of state ; condensed phases of carbon are described with the "Three-phase" model.

3. THE "THREE-PHASE" EQUATION OF STATE

The model proposed by M. Van Thiel anf F. H. Ree takes into account two solid phases and one liquid phase. This liquid phase is represented by the mixture of two different liquid structures.

3.1 Solid phases description

A Mie-Grüneisen formulation is used to represent solid phases properties. The pressure is defined by the sum of three contributions:

$$P(V,T) = P_{0K}(V) + P_{v,th}(V,T) + P_{e,th}(V,T) \tag{1}$$

* The first term corresponding to the 0 kelvin isotherm is given by a modified Birch expansion.

$$P_{0K}(V) = \frac{3}{2}B_0\left[-B_K\eta^3 + (1+2B_K)\eta^{\frac{7}{3}} - (1+B_K)\eta^{\frac{5}{3}}\right]F(\eta) \tag{2}$$

with

$$F(\eta = V_{0K}/V) = \left\{ \begin{array}{ll} \frac{1}{2}(\eta^2+\eta^{-2}) & \text{in expansion } (\eta < 1) \\ 1 & \text{in compression } (\eta > 1) \end{array} \right\}$$

B_0 is the bulk modulus at $T = 0$ and $P = 0$. $B_K = 0.75(4 - B_0')$ and B_0' is the pressure derivative of the bulk modulus.

* The lattice thermal effects are approximated by the Einstein model:

$$E_{v,th}(V,T) = 3R\frac{\Theta_E}{e^{\frac{\Theta_E}{T}} - 1} \tag{3}$$

In the Grüneisen approximation, the thermal pressure is related to the corresponding energy by:

$$P_{v,th} = \frac{\Gamma_v}{V} E_{v,th} \tag{4}$$

where the Grüneisen coefficient Γ_v is related to the Einstein temperature Θ_E by:

$$\Gamma_v = -\frac{\partial \ln \Theta_E}{\partial \ln V} \tag{5}$$

An hyperbolic correction is used in the volume dependence of Γ_v [13]:

$$\frac{\Gamma_v(V)}{V} = \frac{\Gamma_{v_0}}{V_0}\left[1 + \delta_\gamma(1 + \tanh Z)\right] \qquad \text{where} \qquad Z = \frac{(V_\gamma - V)}{\delta V_\gamma} \tag{6}$$

* The electronic thermal effects are represented by:

$$P_{e,th}(V,T) = \frac{\Gamma_e(V)}{2V} g_e T^2 \tag{7}$$

with

$$\Gamma_e(V) = \frac{d \ln g_e(V)}{d \ln V} \qquad \text{and} \qquad \frac{\Gamma_e(V)}{V} = C^{st} \tag{8}$$

Integration of equation 2 leads to the 0K energy contribution. The integration constant $E_{0K}(V_0)$ is given in table 2. A correction to the entropy (δS_{298}) is used to yield the proper value at 1 atmosphere and $298K$ (it is a result of the imperfections of the Einstein approximation at low temperatures).

Graphite and diamond Hugoniots calculated with CARTE are represented on figures 2.a and 2.b. Graphite results are compared to the shock data of McQueen [14], Doran [15] and Coleburn [16]. Calculated diamond Hugoniot is compared to Pavlovski data [17]. The graphite-to-diamond transition is determined by the condition between the Gibbs free energies of the solids $G_{S_g}(P,T) = G_{S_d}(P,T)$ and compared to the experimental data of Berman [18] (figure 3).

Table 2 : Parameters of the "Three-phase" model for solid phases.

Parameters	Graphite	Diamond	Parameters	Graphite	Diamond
$V_0(m^3/mole)$	$5.27383\ 10^{-6}$	$3.4151\ 10^{-6}$	$B_0\ (GPa)$	51.10	439.7
$E_0/R(K)$	$(-0.0643)^a$	$(243.7503)^a$	B_0'	$7.1(5.0)^b$	3.65
Γ_{v_0}	0.35	1.15	$\delta S_{298}/R$	0.464	0.1331
Γ_{e_0}	0.24	1.10	δ_γ	3.0	0.0
$\Theta_{E_0}\ (K)$	1280	1411	$\delta V_\gamma\ (cm^3/g)$	0.065	1.0
$g_{e_0}/R\ (K)$	$1.156\ 10^{-6}$	0.0	$V_\gamma\ (cm^3/g)$	0.22	0.0

()[a] The reference state (zero enthalpy for graphite) is 0 Kelvin.
()[b] This value is used for expanded states.

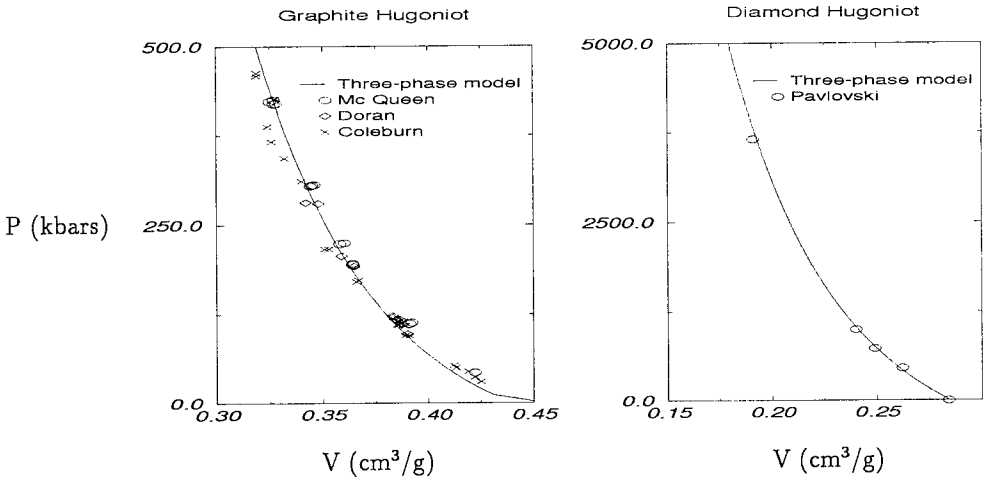

Figure 2: Comparison between calculated Hugoniot and shock data.

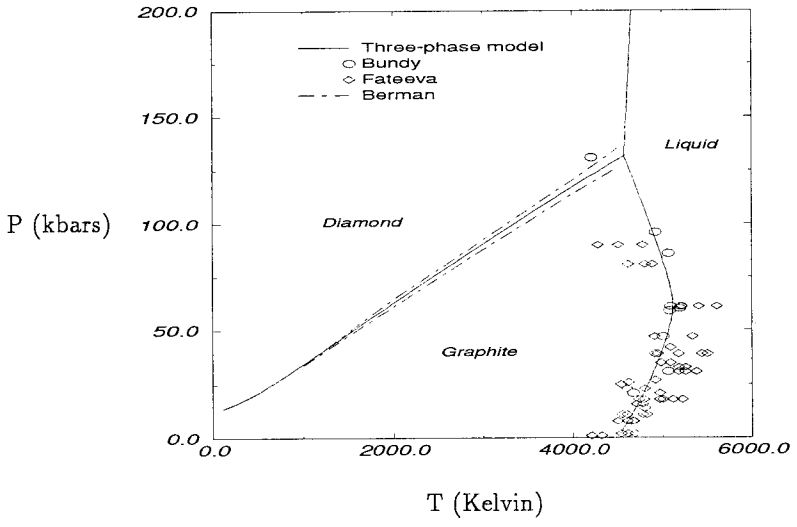

Figure 3: Comparison between the carbon phase-diagram calculated with the "Three-phase" equation of state model and experimental data.

3.2 Liquid phase description

The liquid phase consists of a mixture of two liquid structures, a graphitic one and a diamond-like one. The thermodynamic properties of these liquid states are calculated from the corresponding solid states properties by the scaling model of Grover [11]. The liquid heat capacity is deduced from the solid one by:

$$C_{V_L} = C^*_{V_S} - \frac{3}{2}R\frac{\alpha\tau}{1+\alpha\tau} \tag{9}$$

where:

$$C^*_{V_S} = C_{V_{S,v}} + g_{e_L}T \tag{10}$$

and

$$\tau = \frac{T}{T_m} \tag{11}$$

T_m, the melting temperature is represented by a Lindemann law. The formulation used for the diamond case is:

$$T_m = const.\ M\Theta_E{}^2 V_m{}^{\frac{2}{3}} \tag{12}$$

where M is the molar weight and V_m the molar volume in solid state. For the anisotropic case of graphite, an anharmonic correction is needed [19, 20]:

$$T_m = const.\ M\Theta_E{}^2 V_m{}^{\frac{2}{3}} (\frac{a}{c}(V_m))^{\frac{2}{3}} \left[(1 - f(V_m)) + f(V_m)(\frac{c}{a}(V_m))\right]^2 \tag{13}$$

with

$$\frac{c}{a}(V_m) = 0.2488 + 0.2109 V_m \quad (V_m \text{ is given in } cm^3/mole) \tag{14}$$

and

$$f(V_m) = 0.35/V_m^{\frac{1}{2}} \quad (V_m \text{ is given in } cm^3/mole) \tag{15}$$

Integration of equation 9 leads to the following entropy:

$$S_L(V,T) = S_S(V,T) + \Delta S_m + \Delta S_e(V,T) - \frac{3}{2}R\ln(\frac{1+\alpha\tau}{1+\alpha}) \tag{16}$$

where ΔS_e is a correction due to the modification of electronic properties between solid and liquid states (through a modification of the g_e parameter). ΔS_m is a melting entropy.

The Gibbs free energies of the two liquid states are then calculated and the free energy of the mixture is given by the mixing law:

$$G_L(P,T,x) = xG_{L_g}(P,T) + (1-x)G_{L_d}(P,T) + RT\left[x\ln x + (1-x)\ln(1-x)\right] + A_s(T,P,x) \tag{17}$$

where

$$A_s(T,P,x) = RT\left[\frac{A_{S,0}}{1 + (\frac{P}{P'_0})^{\frac{3}{2}}}\right] x(1-x) \tag{18}$$

The liquid phase is completely characterised by the molar fraction x of graphite-like liquid in the mixture. This can be done, for a given (P,T) state, by minimizing the Gibbs free energy of the mixture with respect to x.

The parameters used to calculate liquid states properties, differing slightly from those proposed by Van Thiel and Ree [21], are given in table 3.

Table 3 : Parameters of the "Three-phase" model for liquid states.

Parameters	graphite-like liquid	diamond-like liquid	Mixture
$\Gamma_{e_0,L}$	0.24	1.10	
$g_{e_0,L}/R\ (K)$	$1.156\ 10^{-6}$	$6.038\ 10^{-5}$	
$T_{m,0}\ (K)$	6000	5900	
$\Delta S_m/R$	2.557	1.007	
$A_{S,0}$			2.2
$P_0'\ (GPa)$			22

The melting line of graphite, determined by the condition $G_L(P,T) = G_{S_g}(P,T)$, is represented on figure 3 and compared to experimental data of Bundy [22] and Fateeva [23]. The data of Fateeva corresponding to a graphite-liquid-gas triple point temperature of 4000K have been corrected by adding the same ΔT to all values, according to the new estimation of this triple point temperatue (4500K). The curvature of the calculated graphite melting line seems to be smaller than the experimental ones. A better agreement could be obtained by increasing the parameter $A_{S,0}$, but the result would be a liquid-liquid phase transition in carbon which should need an experimental confirmation.

In the same way, the diamond melting line can be determined by $G_L(P,T) = G_{S_d}(P,T)$. Results are consistent with the last experimental data indicating a positive diamond-melting-line slope.

4. THERMOCHEMICAL CALCULATIONS

CJ characteristics and energetic performances were calculated for a large range of explosives. This means various chemical compositions and a large range of density, enthalpy of formation and oxygen-balance (negative in all cases). In these calculations, the fluid phase properties were described with a WCA equation of state.

4.1 CJ properties

The Chapman Jouguet characteristics calculated with the Cowan Fickett equation of state (CF) and with the "Three-phase" model (3P) for carbon are given in table 4.

In CJ conditions, for most explosives, both equations of state predict diamond as the stable phase. In this case, the new equation of state seems to give better predictions of detonation velocities. For the last 3 explosives designated by M2, M3 and M5, the "Three-phase" equation of state predicts liquid carbon (L). Calculated CJ characteristics are then very different. Unfortunately, there are no experimental data concerning these new molecules, not synthetised at this time and for which the uncertainty on the determination of density and enthalpy of formation is relatively important.

The CJ temperatures and pressures of these explosives have been reported on the phase diagram of carbon calculated with the "Three-phase" model and given in figure 4.

Table 4 : Comparison of CJ characteristics and energetic performances.

Explosive	$P_{CJ}{}^{CF}$ (kbars)	$D_{CJ}{}^{CF}$ (m/s)	$W_{10}{}^{CF}$ (MJ/kg)			$P_{CJ}{}^{3P}$ (kbars)	$D_{CJ}{}^{3P}$ (m/s)	$W_{10}{}^{3P}$ (MJ/kg)	D_{exp} (m/s)
HMX	401	8832	7.09			405	8969	7.09	9110
LX09	365	8621	6.79			372	8788	6.82	8840
TNT	162	6410	3.51	D	D	179	6813	3.72	6930
HNS	172	6440	3.72	I	I	193	6925	3.96	7030
NM	116	6184	3.53	A	A	119	6353	3.51	6287
COMPB	271	7883	5.59	M	M	290	8202	5.78	7980
LX04	327	8317	5.82	O		336	8480	5.88	8470
TATB	246	7564	4.22	N		255	7749	4.33	7580
M2	280	7276	5.97	D		314	7747	6.39	
M3	505	8666	8.97		L	400	9106	7.18	
M5	466	8323	9.33			493	8688	9.44	

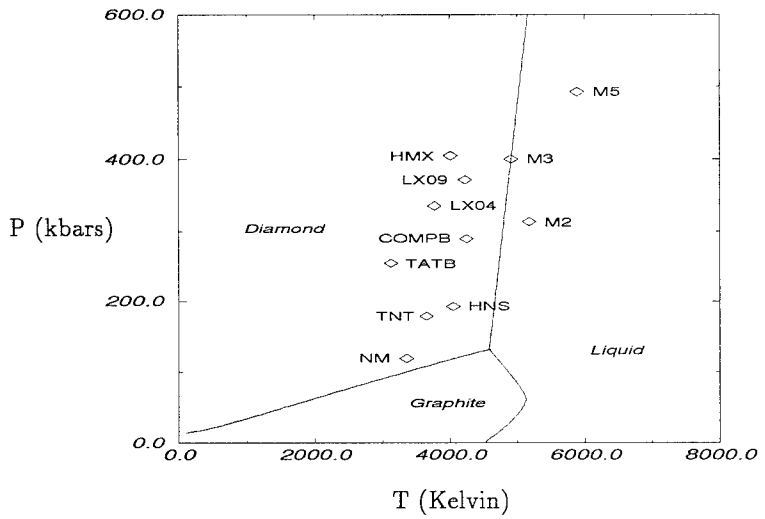

Figure 4: Chapman-Jouguet characteristics and carbon phase-diagram.

4.2 Energetic considerations

The energetic contents of these explosives can be represented by the work provided by detonation products during their isentropic expansion. The (P,V) curves calculated with the CARTE code are then integrated from the CJ point to 10 kbars ($\int_{10kbars}^{P_{CJ}} PdV$). Results are listed in table 4. The energy released greatly differs when carbon appears in liquid phase. An illustration of these calculations is given in figure 5 for the particular case of TNT. The phase transition between graphite and diamond appens for different pressures, depending on the carbon equation of state used.

Cylinder-expansion experiments are the usual test to evaluate energetic performances of new molecules and compositions. The (P,V) curves calculated with CARTE can be transformed with a simple model,

to give expansion velocity as a function of cylinder expansion. Results obtained for TNT (copper cylinder : $r_i = 12.7$ mm, $r_e = 15.306$ mm) are compared on figure 6 to LLNL experimental data.

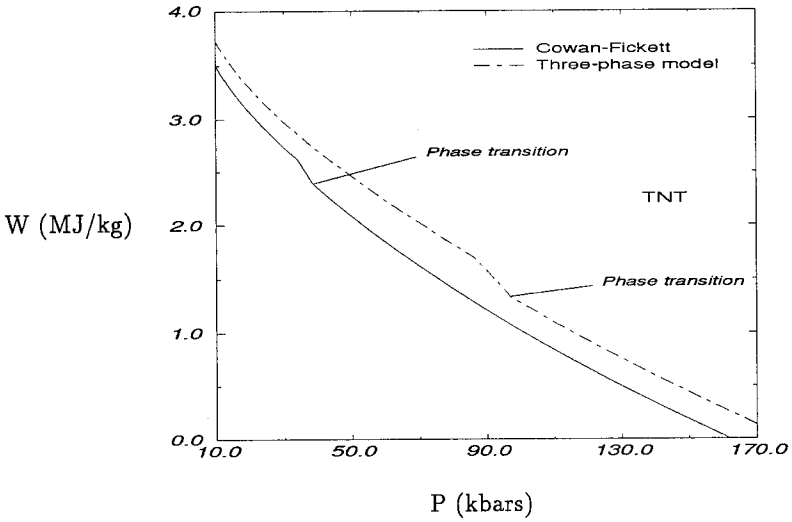

Figure 5: Work of TNT detonation products during their isentropic expansion from the CJ point to 10 kbars.

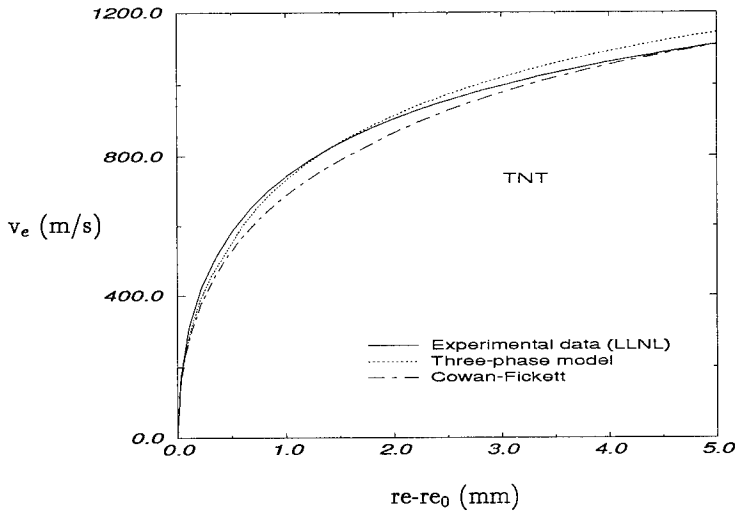

Figure 6: TNT expansion velocity function of external radius variation.

5. CONCLUSION

Some theoretical features of a Three-phase Equation of State model for carbon have been described. This model is rapid enough to be used in chemical equilibrium theory and sufficiently accurate to fit the latest results on carbon phase diagram. The influence of the carbon equation of state on detonation characteristics calculated with the thermochemical code CARTE is obvious. Introduction of a liquid phase in these calculations can considerably modify predicted performances.

References

[1] Mader C. L., "Numerical modeling of detonation", (University of California, Los Angeles, 1979).

[2] Cowperthwaite M., Zwisler W. H., VI symposium on Detonation, White Oak 24-27 August 1976, (Office of Naval Research, Arlington, Virginia, 1976) pp. 162-170.

[3] Chirat R., Pittion-Rossillon G., J. Chem. Phys. **74**(8) (1981) 4634.

[4] Ree F. H., J. Chem. Phys. **81** (1984) 1251-1263.

[5] Van Thiel M., Ree F. H., J. Appl. Phys. **62** (1987) 1761.

[6] Cowan R. D., Fickett W. J., J. Chem. Phys. **24**(5) (1956) 932.

[7] Ross M., J. Chem. Phys. **71** (1979) 1567.

[8] Byers Brown W., J. Chem. Phys. **87** (1987) 566-577.

[9] Heuzé O., "QUARTET ; Système de Calcul et de Simulation Thermochimique", (Softworld, Paris, 1991)

[10] Baute J., Chirat R., Eighth International Symposium on Detonation, Albuquerque 15-19 July 1985, (Naval Surface Weapons Center, Maryland, USA, 1985) pp. 521-530.

[11] Grover R., Proc. of the 7^{th} Symp. of Thermophysical Properties, (1977) p 67.

[12] Jones H. D., Gray M. V., Comb. and Flame **64** (1986) 185.

[13] Van Thiel M., Ree F. H., Int. J. of Thermophysics **10**(1) (1989) 227.

[14] Mc Queen R. G., Marsh S. P., Symposium on High Dynamic Pressures, (Paris, France, 1967).

[15] Doran D. G., J. Appl. Phys. **34**(4) (1964) 844.

[16] Coleburn N. L., J. Chem. Phys. **40**(1) (1964) 71.

[17] Pavlovski M. N., Soviet Physics - Solid State **13**(3) (1971) 741.

[18] Berman R., Simon F., Z. Electrochem. **59** (1955) 333.

[19] Van Thiel M., Ree F. H., Phys. Review B **48**(6) (1993) 3591.

[20] Van Thiel M., Ree F. H., High Pressure Research **10** (1992) 607.

[21] Van Thiel M., Ree F. H., High Temp. High Press. **24** (1992) 195.

[22] Bundy F. P., Proc. of the XI AIRAPT Int. Conf. (Kiev, USSR, july 1987).

[23] Fateeva N. S., Vereshchagin L. F., ZhETF Pis. Red. **13**(3) (1971) 157.

JOURNAL DE PHYSIQUE IV
Colloque C4, supplément au Journal de Physique III, Volume 5, mai 1995

Rearrangements of Ammonium Nitrate Cluster Ions with High Internal Energy

R.J. Doyle and B.I. Dunlap

Chemistry Division, Naval Research Laboratory, Washington, DC 20375, U.S.A.

Abstract: Sputtering of condensed-phase ammonium nitrate yields an extensive distribution of negative cluster ions of the form $[(NH_4NO_3)_nNO_3]^-$, $n \geq 3$. Collision-induced dissociation of mass-selected cluster ions suggests that the first two members of the series, $n = 1$ and $n = 2$, are missing because the ions rearrange to lose one or more ammonia molecules. Gradient-corrected density-functional calculations show that NH_4NO_3 is strongly hydrogen bonded and that $[(NH_4NO_3)NO_3]^-$ has no hydrogen bonds, consistent with this ion rearranging to lose NH_3 to form the strongly hydrogen-bonded ion $[H(NO_3)_2]^-$.

1. INTRODUCTION

As its name implies, ammonium nitrate (AN) can be viewed as an ionic solid made up of ammonium cations and nitrate anions. If this were a complete description of the solid, then sputtering would be expected to yield all ions of the form $[(NH_4NO_3)_nNH_4]^+$ as the only singly-charged ions in the positive-ion spectrum and all ions of the form $[(NH_4NO_3)NO_3]^-$ as the only singly-charged ions in the negative-ion spectrum. Such a positive-ion mass spectrum, for n from 1 to 43, is indeed seen upon sputtering AN [1,2]. The sputtered negative-ion spectrum is not as expected based on this ionic model, however. Instead, only $[(NH_4NO_3)NO_3]^-$, $n \geq 3$, negative ions are seen [3]. Two negative cluster ions ($n = 1$ and 2) are observed in trace amounts only. The absence of the $n = 1$ ion is all the more surprising because all the larger clusters would be expected to have this ion as their core.

The key to understanding why the first two members of the negative ion series are missing requires considering the effect of hydrogen-bonding on the structure of AN. If a proton were transferred from the ammonium cation to the nitrate anion in a formula unit, then the formula unit could be viewed as an ammonia molecule complexing through its lone-pair orbital to nitric acid. The resonance between the ionic and molecular interactions is hydrogen bonding, and the strength of the hydrogen bond is correlated with how far a proton is separated from each ammonium cation.

In either the positive or negative AN clusters, one or more of the ammonia-nitric acid bonds can cleave. An overall charge-dependent imbalance between ammonia or nitric acid fragments that escape during the formation of ions in the sputtering process rationally gives rise to the other relatively abundant cluster ions in the positive and negative mass spectra. The delicate balance between ionic and molecular bonding explains the absence of the $n = 1$ and 2 ions in the sputtered negative ion spectrum.

2. EXPERIMENT

In this work, the AN mass spectra were obtained using a ZAB-2F (VG Analytical Ltd.) reverse-geometry, double-focusing mass spectrometer operated with an accelerating potential of 8 kV. Samples were prepared by pressing ammonium nitrate into indium foil affixed to the tip of a fast-atom bombardment probe. Xenon atoms with an average kinetic energy of 6.5 keV were generated using a saddle-field gun operating at 8 kV with an ion current of 1.5 mA. The xenon neutral current equivalent was approximately 7 μA applied to a target area of 4 mm^2.

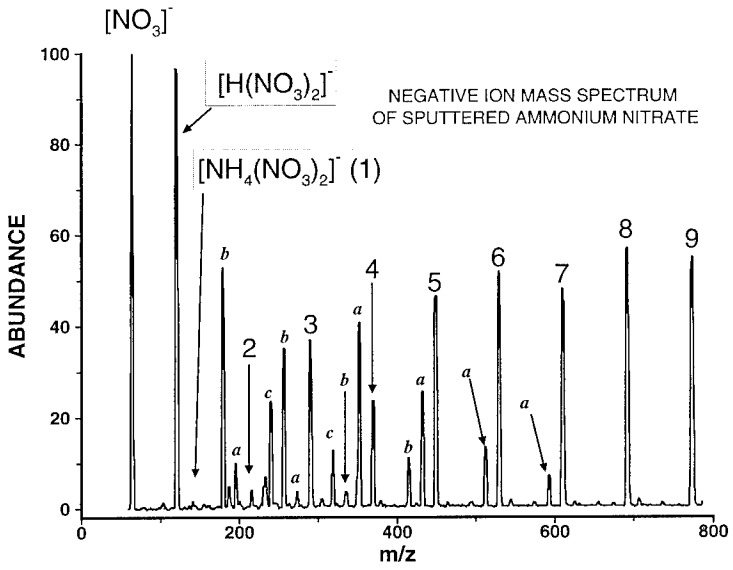

Figure 1. Partial negative-ion mass spectrum of sputtered ammonium nitrate.

Figure 1 shows the negative-ion mass spectrum of sputtered ammonium nitrate. Clusters with the general formula $[(NH_4NO_3)_nNO_3]^-$ are indicated by the numbers 1-9. Cluster ions with $n = 3 - 40$ are observed in relatively high abundance; the $n = 1$ ion is almost lost in the noise, and the $n = 2$ ion is far less abundant than the more massive members of the series. For smaller cluster sizes, the abundance of species apparently formed by losses of single and multiple NH_3 from $[(NH_4NO_3)_nNO_3]^-$ ions becomes pronounced. These are designated a, b, and c, corresponding to losses of 1, 2, and 3 ammonia molecules, respectively. Loss of NH_3 from $[NH_4(NO_3)_2]^-$ (the $n = 1$ negative ion) would result in $[H(NO_3)_2]^-$, which is the second most abundant ion after $[NO_3]^-$ in the spectrum.

To further test our hypothesis that the lack of the $n = 1$ and 2 negative ions results from these species rearranging and fragmenting, collision-induced-dissociation (CID) experiments were performed. The negative ions that are fairly abundant in the sputtered spectrum can be mass-selected by the magnetic sector of the instrument. These mass-selected species are then collided with a collision gas (helium in these experiments) in a field-free region of the instrument and the resultant fragment ions detected and identified[4,5]. The $n = 1$ cluster is found in very low abundance in the CID spectra of all AN clusters examined ($n = 3 - 15$). Figure 2 shows the negative-ion CID spectrum of $[(NH_4NO_3)_7NO_3]^-$. As in Figure 1, the numbers indicate $[(NH_4NO_3)_nNO_3]^-$ ions, and subsequent fragmentation of these ions leads to ions designated a, b, and c, which correspond to losses of 1, 2 and 3, ammonia molecules, respectively. The relative abundances of ions in the CID spectra are similar to those seen in the directly sputtered mass spectrum. For all parent

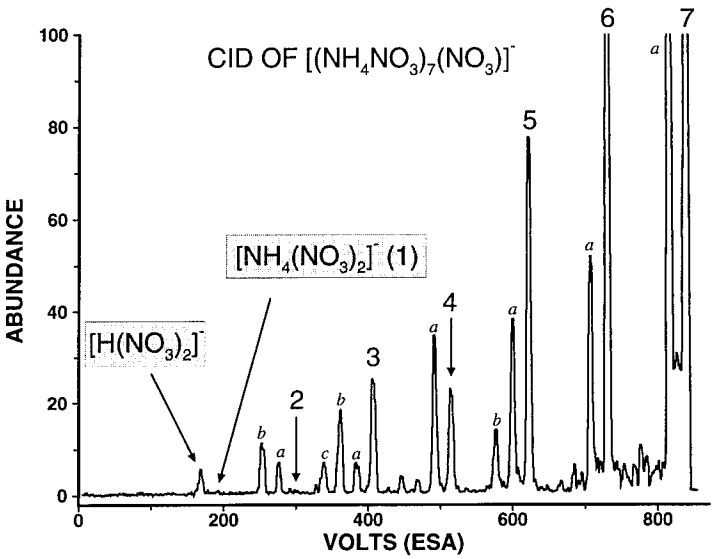

Figure 2. CID spectrum of $[(NH_4)_7NO_3]^-$.

cluster ions examined, $[NH_4(NO_3)_2]^-$ was observed in very low abundance. The spectra suggest that $[NH_4(NO_3)_2]^-$ dissociates rapidly to form $[H(NO_3)_2]^-$ by loss of NH_3.

Both the positive-ion and the negative-ion mass spectra of sputtered ammonium nitrate are more complicated than a simple ionic model would suggest. Previous work on positively charged ammonium nitrate clusters, under the same experimental conditions, identified the cluster-ion series, $[(NH_4NO_3)_nNH_4]^+$, where $n = 1$ to > 43 inclusive[3]. This is as expected from a simple ionic model. On the other hand, studies of the positive ions show that these ions can also rearrange and dissociate by the loss of a single HNO_3 molecule. As discussed above, the negative-ion clusters dissociate by losses of one to three NH_3 molecules and the $n = 1$ and 2 species are missing from the corresponding negative-ion series.

These experimental results are insufficient to answer the question of why the $n = 1$ species is not observed in the negative-ion spectra, while the corresponding $n = 1$ species is always abundant in the positive-ion spectra. The lack of thermodynamic data for many of these species suggests a purely theoretical approach to the question.

3. THEORY

Density-functional theory [7] is an appropriate method to use to study AN clusters where both ionic and hydrogen bonding compete in determining structures and energetics. Gradient-corrected functionals are very important because of the hydrogen bonding and the fact that relative total energies are important [8]. The deMon [9,10] computer code was employed, which uses three different Gaussian basis sets [11]: one to fit the one-electron orbitals, one to fit the exchange-correlation part of the electronic potential, and one to variationally fit [12] the density to obtain the Coulomb part of the electronic potential. The default double-zeta plus polarization-on-heavy-atoms basis set was used with the Becke exchange [13] and Perdew correlation [14] potentials. The geometries of selected clusters were optimized, and their total energies were evaluated are listed in Table 1.

Studying the optimized equilibrium structures of these molecules and ions is a good way to understand the energetics. Figure 3 shows the optimized structure of the ammonium nitrate molecule,

TABLE 1. The Becke-Perdew density-functional total molecular energies in Hartree atomic units.

Molecule	Energy	Positive Ion	Energy	Negative Ion	Energy
NH_3	-56.5703	$[NH_4]^+$	-56.9104	$[NO_3]^-$	-280.4672
HNO_3	-280.9928	$[(NH_4)_2NO_3]^+$	-394.5503	$[H(NO_3)_2]^-$	-561.5085
NH_4NO_3	-337.5876			$[NH_4(NO_3)_2]^-$	-618.1067

$[NH_4NO_3]$. In the upper part of the figure, the molecule is depicted in space-filling form. In the lower part of the figure the bond distances and bond angles are given. The atoms, from darkest to lightest are nitrogen, oxygen, and hydrogen. The fourth hydrogen atom of the NH_4 group is pulled away by 0.6 Å by the NO_3 group. This structure agrees very well with that obtained at the Hartree-Fock level of theory using a 4-31G Gaussian basis set [15]. Viewed as a molecule formed from ammonia and nitric acid components, the gradient-corrected density-functional bonding energy of AN is 15.4 kcal/mol. This binding energy is somewhat less than 21.7 kcal/mol obtained in the Hartree-Fock calculation, but the density-functional calculations also support the conclusion that AN contains one of the strongest known hydrogen bonds [15]. Viewed as a molecule formed from an ammonium cation and a nitrate anion its binding energy would be 132 kcal/mol.

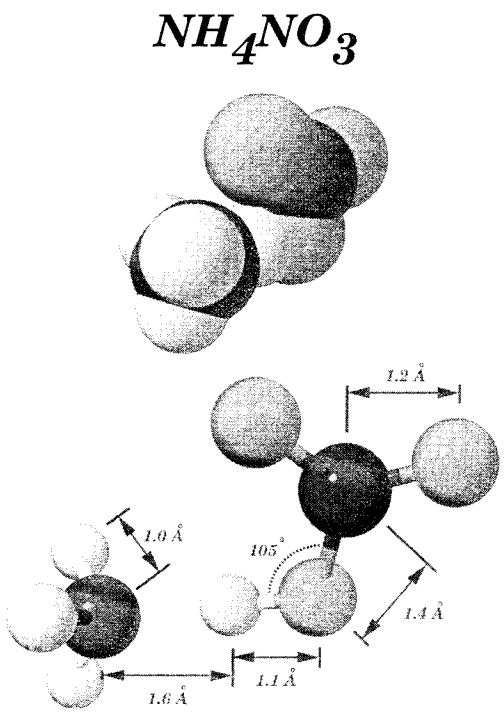

Figure 3. Structure of $[NH_4NO_3]$.

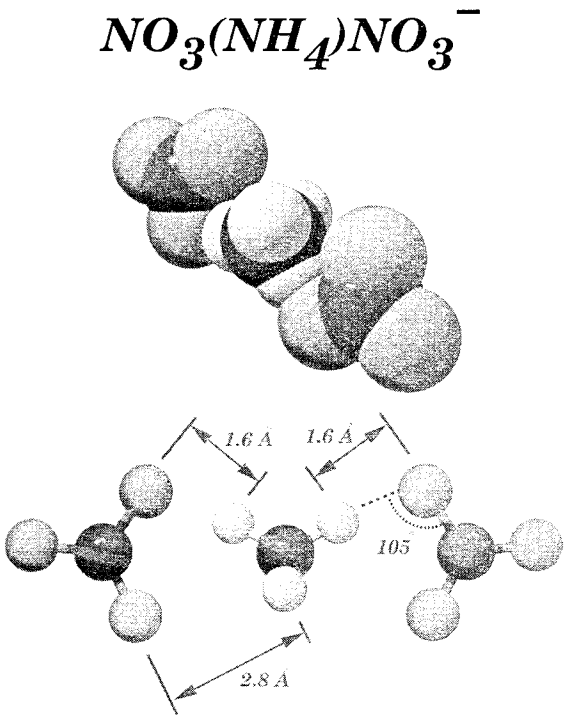

Figure 4. Structure of $[NH_4(NO_3)_2]^-$.

Figure 4 gives space-filling and ball-and-stick depictions of the geometry of $[NH_4(NO_3)_2]^-$. The 1.6 Å distance between oxygen and hydrogen atoms shows that there is essentially no hydrogen bonding in this ion. Viewed as being formed from AN and $[NO_3]^-$, its density-functional binding energy is only 32.6 kcal/mol [3].

Figure 5 gives space-filling and ball-and-stick depictions of the geometry of $[(NH_4)_2NO_3]^+$. The 1.5 Å distance between the oxygen and hydrogen atoms shows that there are two weak hydrogen bonds. These bonds are slightly stronger than in the corresponding negative ion of Figure 4. Viewed

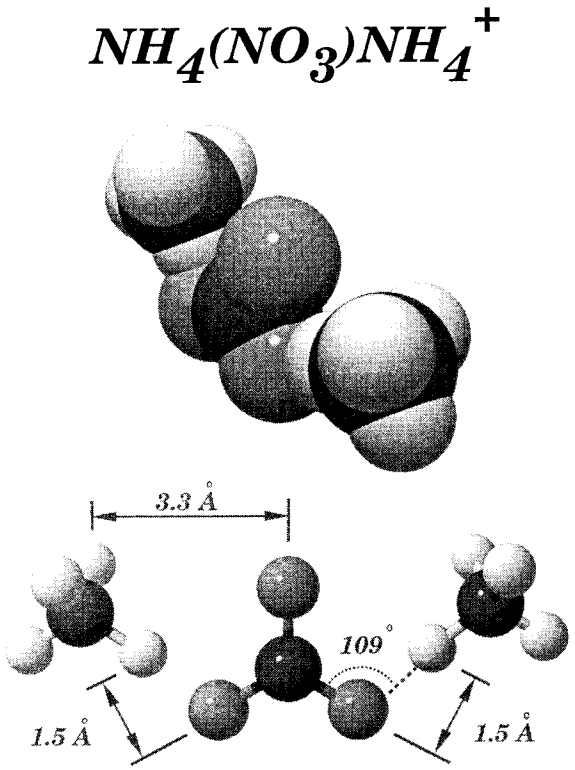

Figure 5. Structure of $[(NH_4)_2NO_3]^+$.

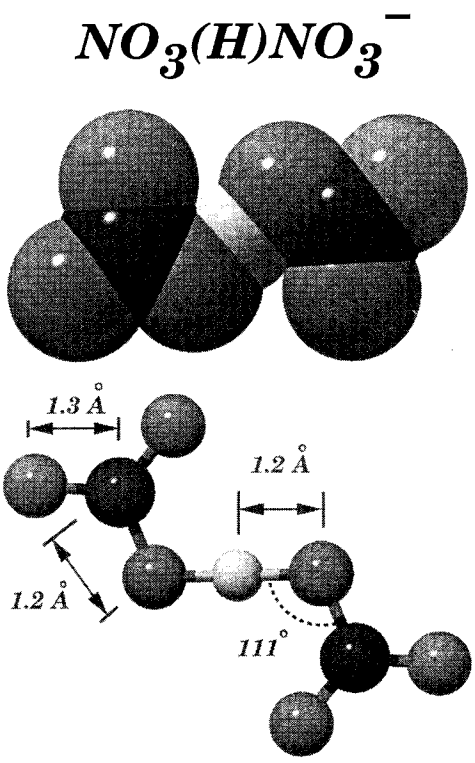

Figure 6. Structure of $[H(NO_3)_2]^-$.

as being formed from AN and $[NH_4]^+$, the $[(NH_4)_2NO_3]^+$ density-functional binding energy is 32.8 kcal/mol, somewhat larger than the binding energy of the corresponding negative ion.

The main difference between the positive and negative $n = 1$ ions is the level of hydrogen bonding that remains after rearrangement if the AN molecule of either ion is fragmented. $[NH_4NH_3]^+$, formed by the loss of HNO_3 from $[(NH_4)_2NO_3]^+$, has less hydrogen bonding than $[H(NO_3)_2]^-$, formed by the loss of NH_3 from $[NH_4(NO_3)_2]^-$. The later ion is depicted in Figure 6. The O-H bond distances of 1.2 Å are in agreement with an analysis of X-ray diffraction data [16]. Viewed as being formed from nitric acid and $[NO_3]^-$, its density-functional binding energy is 30.4 kcal/mol.

The density-functional energetics of the $n = 1$ negative ion rearrangement and fragmentation are shown in Figure 7. If $[NH_4(NO_3)_2]^-$ is created with a small amount of internal energy, as little as 18 kcal/mol, if there is no reverse activation energy, then it should be possible for it to rearrange to lose ammonia and form the very stable hydrogen dinitrate ion that is the second most abundant ion in the sputtered mass spectra of AN (Figure 1).

4. CONCLUSIONS

The absence, or low abundance, of $[(NH_4NO_3)NO_3]^-$ (n=1) is a consequence of the fact that this ion has essentially no hydrogen bond stabilization and that the ion is created with significant internal energy by the sputtering process. Two dissociation pathways are accessible, loss of NH_3 and loss of NO_3^-, which are only 18 kcal/mol and 33 kcal/mol, respectively, above the ground state of the n=1 ion. Both exit channels lead to products with strong hydrogen bonds. More ammonium nitrate molecules surrounding the n=1 ion increase the solvation energy to stabilize the larger clusters.

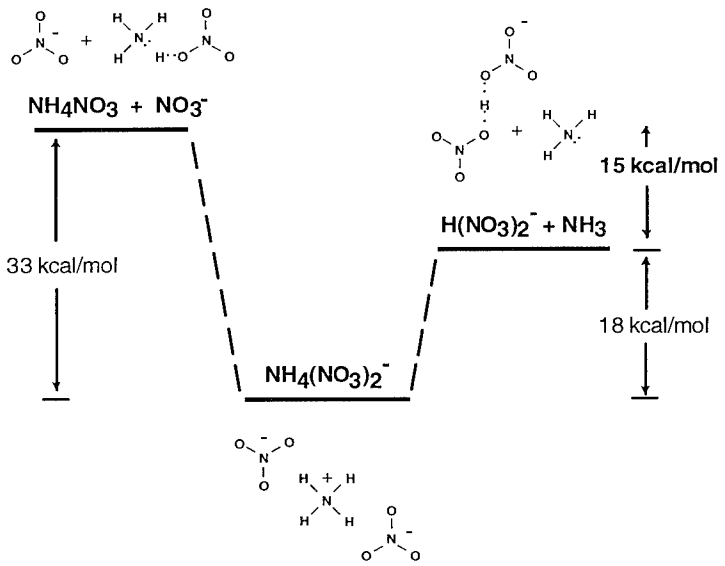

Figure 7. Density-functional energetics of $[NO_3)_2NH_4]^-$ association and dissociation pathways.

Acknowledgement

BID thanks Dennis Salahub for inclusion in the deMon collaboration. This work was supported by the Propulsion and Energetic Materials Program of the Mechanics Division of the Office of Naval Research, the Physics Division (Contract #N0001494WX23009) of the Office of Naval Research, and the Naval Research Laboratory Energetic Materials Accelerated Research Initiative.

References

[1] Doyle R.J., Jr., *J. Am. Chem. Soc.* **115** (1993) 5300-5301.

[2] Doyle R.J., Jr., *J. Am. Chem. Soc.* **116** (1994) 3005-3011.

[3] Doyle R.J., Jr., and Dunlap B.I., *J. Phys. Chem.* **98** (1994) 8261-8263.

[4] Doyle R.J., Jr., *J. Am. Chem. Soc.* **110** (1988) 8261-8263.

[5] Doyle R.J., Jr., *J. Org. Mass Spectrom.* **28** (1993) 83-91.

[6] Parr R.G., Yang W., Density Functional Theory of Atoms and Molecules (Oxford Univ. Press, Oxford, 1989).

[7] Andzelm J.; Wimmer E., *J. Chem. Phys.* **96** , (1992), 1280-1303.

[8] Salahub D.R., Fournier R., Młynarski P., Papai I., St.-Amant A., Ushio J., "Gaussian-based Density Functional Methodology, Software, and Applications", Density Functional Methods in Chemistry, Columbus 7-9 May 1990, J. Labanowski and J. Andzelm Eds. (Springer, New York, 1991) pp. 77-100.

[9] St-Amant A., Salahub D.R., Chem. Phys. Lett. **169** (1990) 387-392.

[10] Sambe H., Felton R.H., J. Chem. Phys. **62** (1975) 1122-1126.

[11] Dunlap B.I., Connolly J.W.D., and Sabin J.R., *J. Chem. Phys.* **71**, 3396-3402; 4993-4999 (1979).

[12] Becke A.D., Phys. Rev. A **38** (1988) 3098-3100.

[13] Perdew, J.P., Phys. Rev. B **33** (1986) 8822-8824.

[14] Latajka Z., Szczęśniak M.M., Ratajczak H., Orville-Thomas W.J., J. Comp. Chem. **1** (1980) 417-419.

[15] Barlič B., Hadži D., Orel B., Spectrochim. Acta **37A** (1981) 1047-1048.

4-2 Discussion

Questions - Answers, Comments

Rullière - Gupta :

Q : You observed disappearance of the C-N vibration mode but not for the other modes (CH_3, etc). You interpreted CN mode disappearing as the image of the nitromethane breaking. But in this case, $CH_3\cdot$ and $NO_2\cdot$ fragments are formed with different vibration mode not related to CH_3NO_2 modes. As a consequence nitromethane modes should disappear, not only CN mode. How do you explain this intriguing fact ?

A : You have asked an excellent question, and at the moment, I do not have an answer. It is a very important issue and one that we are thinking about. Because our results are very recent, we have not analyzed or understood them completely. Any suggestion you may have are welcome and will be acknowledged appropriately.

Q : Sensitization by small amount of amine is very interesting but opens some questions.

1) is this sensitization process related to electron donor ability of amines and what is the mechanism ?

2) how to explain that such a small amount can perturb all the sample taking into account this small concentration ?

A : Regarding the first part of your question, the mechanism for sensitization has not been resolved. Cook and Haskin have proposed a mechanism based on hydrogen bonding (see the latest International Detonation Symposium). In contrast, Constantinon and Chandhri have proposed a mechanism based on the formation of a charge transfer complex. I am hoping, we can clarify this issue in the future.

Regarding the second part of your question, I believe that the small amount of amine initiates the reaction and very quickly there is an auto-catalytic reaction (as suggested by Constantinon) takes over. Once the reaction is initiated, the subsequent reactions may be very complicated.

Boileau - Gupta :

Q : *a comment - Suggestion*

Using a tertiary amine instead of the DETA or EDA, are the shifts the same ?

Is it possible to add before shock a product that picks up a $CH_3\cdot$ or adds to C=N ?

Q : To study ethylnitrate (usable and not very dangerous liquid) under shock, (is it a shift of Raman lines ?) without and with some traces of amine (verification by Presles if amine is a sensitizer, I think no but it is to be verified) and after, put in ethylnitrate some nitromethane, without and with amine to see if the shifts in the nitromethane bands are modified. Is it possible by this way, to see if there are clusters in nitromethane ?

A : I think that these suggestions are interesting and address a question. Shock-business is a hard business and we have to work in a well defined direction and choose and concentrate on well defined sample with precise experimental conditions.

Melius - Gupta :

Q : The disappearance of the C-N bond frequency does not necessarily mean that the C-N bond is breaking. It is possible that a >C=N- bond or a -C≡N is being formed, such as in HCNO, HNCO or HCN. Is it possible for you to look for such new bond formations ?

A : In principle, the answer is yes. In practice, it will depend on the concentration. As you are aware, Raman scattering is a weak process.

Mialocq - Gupta :

Q : What is the physical origin of the shift of the nitromethane UV absorption spectrum under the pressure increase ? Is it some increase of the molar extinction coefficient or a real shift due to some Onsager cavity type effect ?

A : Because our interest was in the large shift due to chemical reactions, we have not thought in detail about the pressure induced shift. However, this latter issue has been addressed in our work on CS_2 (J.Chem.Phys. 95, 451 (1991) ; J.Phys.Chem. 94, 2857 (1990))

Dremin - Gupta

Q : I am afraid about the influence of the interface between the sample and the target. I mean heat conductivity, roughness of the surface, etc. Can you comment the reproductibility of the results ?

A : We know very well this problem and took great care about the experimental conditions. For example we subject sample to many laser shots to check that, we used stainless materials to avoid contaminations. Concerning nitromethane we used only fresh materials to avoid contaminations with metal and also sapphire windows. We checked eveything was possible to check.

Nelson - Delpuech

Q : May have some precision about the excitation mechanism that you suggested ? Is it a photon-polariton or a phonon-polariton, or an I.R. photon-polariton ?

A : The mechanism is a coupling between phonon and photon and it is a phonon-polariton.

Melius - Dufort

Q : Concerning the possible role of electronic excited states I have two remarks. The first one is concerned with time scale. If necessary time to break a bond is several hundred nanoseconds, excited state is not necessary, but if it is 100 ps it is necessary and I can consider excited state as a necessary mean. The second point is that you showed photon correlation with repulsive curve. A repulsive curve leads to radiationless process not involving photons. Can you comment ?

A : I presented a correlation between excited state characteristics and shock-sensitivity. The excited state was dissociative, but these correlations are not concerned with the photons emitted by the laser.

Gupta - Dufort

Q : You showed quantum mechanical calculations using harmonic oscillator solution, you put a shock-wave and calculating the population density. Can you give details about these correlations ?

A : Yes, it is a pure analytic calculation using Hermitte polynomes for eigen functions of the harmonic oscillator. That shows the evolution of the excitation probability as a function of the speed of the detonation velocity. The shock is simulated by a Heavy-side perturbation function.

Mialocq - Kondrikov :

Q : Do you have any spectroscopic evidence for the existence of a complex between sulfuric acid and nitromethane (or TNT) since you explain the strong sensibilizing effect of inorganic acids on the nitrocompounds detonation by the formation of a nitromethonium sulfate ?

A : Very good question and very short answer : no.

Odiot - Kondrikov

Comment : Calculations show that when 1me is added to the C and N atoms of the C-N bond, the strength of the bond increases by 1kcal/mole. It decreases in the opposite case. If you have nitromethane in a bath of H_2SO_4, it is surrounded by many protons, and the electronic charge on C and N will decrease, thus the bond strength decreases strongly. You have to take account of this effect when you study the sensitivity of nitromethane in a bath of protons.

Melius : There are two separate effects which are occuring. One is the environment of charge species which can help weaken bonds as you mention. The other thing that happens is say a proton charge can go on to the molecule and make a new molecule which now makes extremely different chemistry. Thus we must consider both effects.

Mialocq - Dlott :

Q : In your picosecond time scale transfer measurements in nitromethane, you made use of dye heaters absorbing at 1 μm. What is the energy transfer mechanism involved, considering the very short lifetime of IR absorbing dyes (probably polymethinecyanine dyes) ? What are the characteristic time constants ? Do you take into account the polar solvent relaxation around the dye solute and the vibrational cooling which both occur below 10 picoseconds according to the current litterature findings ?

A : The dye heater we use is called IR-165. We have studied it in detail (J.Phys.Chem., 1992). The vibrational cooling time is about 4 ps. That is sufficiently faster than our laser pulses that its vibrational cooling and other photophysical processes do not play a significant role in our multiphonon up-pumping measurements.

Q : Electronic relaxation is 1ps but vibrational relaxation in ground state is 4 ps for dyes. What do you observed in nitromethane ?

A : For nitromethane we used time-resolved incoherent Anti-Stokes Raman Scattering technics. We observed that the build-up of energy was on a two hundred picosecond time-scale. Since the

energy of the dye is not immediately transferred to nitromethane vibration, we imagine that there is collisional degree of freedom that we called "phonons" and explain this delay.

Rullière - Dlott :

Q : For energy transfer processes you showed two kinetics curves have the same rise-time but delayed in respect to each other. What is the mechanism explaining this delay while the rise-times look similar ?

A : The details of vibrational energy transfer mechanisms are complicated. They have been discussed by Hill and Dlott (J.Chem.Phys.) in 1988 and also in a recent J.Phys.Chem. article on nitromethane by Chen, Tolbert and Dlott. In the regime under study, a higher energy vibration $h\Omega$ transfers energy only to lower energy vibrations whose energies are within $h\Omega_{max}$, where Ω_{max} is the phonon cut-off frequency. The delay time is the time required to make a few steps in energy. For a few steps, the rise time is not increased so much.

Dremin *to Workshop* : Once again I'd like to turn our discussion to the problem we were going to discuss, namely to the problem of shock mechanical energy transfer to EM's molecules. At present some ideas on the problem have been already developed ; Gilman's idea of electronic excitation through metallization, our idea of electronic excitation, dissociation and nonequilibrium decomposition of EM's molecules in the detonation shock wave front, and others. My proposal is to spend more time to discuss on (to my opinion) the most important problem for the present for the further progress of the detonation physical model - the problem of shock mechanical energy transfer to EM's molecules.

Kondrikov - Volk :

Q : How big was the containment you filled with Argon ?

A : 1.5 m^3.

Kondrikov : So you had about 1.5 Kg of Ar and 0.33 Kg of explosive. Then cooling of the mixture by big volume of Ar stopped the reaction at relatively high temperature and pressure and lets you to preserve carbon in products.

IV THEORETICAL ASPECTS OF NON-LINEAR DYNAMICS OF DETONATION

Chairman : Marcel Barrère, Haut Conseiller de l'ONERA

Je remercie Madame Odiot pour son aimable invitation à présider cette Session. Je pense que, dans le domaine complexe de la détonation, de larges discussions sont nécessaires pour affirmer et affiner nos points de vue. Je voudrais souligner trois points qui me paraissent essentiels concernant :

- le sujet fondamental de l'Atelier "Approches microscopique et macroscopique des détonations",

- le rôle de la thermodynamique dans l'étude des détonations,

- l'importance du temps dans l'analyse de ces phénomènes.

L'ensemble de ces trois points se situe dans le développement moderne de la mécanique non-linéaire.

a) La compréhension de la coexistence d'une onde de choc et d'une onde de combustion n'est possible que si l'on dispose d'une analyse fine locale performante, à la fois dans l'espace (10^{-6}mm) et dans le temps (10^{-14}s), c'est l'approche microscopique, et si l'on dispose de l'analyse des répercussions globales, c'est l'approche macroscopique. Ces deux manières sont nécessaires et sont d'un même poids. Elles ne peuvent être dissociées car elles sont complémentaires et s'enrichissent mutuellement.
C'est la démarche d'Hadamard et Duhem, Poincaré insiste sur l'importance du passage du local au global, en particulier en topologie (Analysis situs).

b) Le deuxième point souligne, en particulier dans l'analyse de la détonation, l'importance de la thermodynamique. Dans le passé, ce rôle a été primordial pour la détermination de la vitesse de détonation, importance de la production d'entropie, qui est minimale en aval de l'onde. Nous pensons que ce rôle n'est pas terminé, notamment dans la partie irreversible à laquelle est consacrée une théorie nouvelle. La thermodynamique est la science de base des systèmes complexes car elle est multidisciplinaire, comme l'est l'onde de détonation, où physique et chimie coexistent. Nous pensons que le conseil de H.Poincaré faisant de cette science la base de la physique mathématique, est toujours d'actualité et reste toujours valable. Nous souhaitons que toute la partie non-linéaire de la physique et de la chimie ayant trait à la détonation utilise un peu plus la démarche thermodynamique qui me parait à l'heure actuelle quelque peu délaissée.

c) Le troisième point met l'accent sur le paramètre temps, si souvent difficile à maîtriser. Je

renvoie encore au travail de pionnier de H.Poincaré dans l'étude des phénomènes instationnaires non-linéaires. Ce travail relance, sur de nouvelles bases, les réflexions concernant le déterminisme et la prédictibilité ; il joue un rôle essentiel dans la théorie moderne des systèmes dynamiques. La France a la chance de posséder d'excellents physiciens comme Bergé, Chabert, Pomeau, ... qui ont apporté beaucoup dans l'étude de la dynamique des systèmes. Paul Clavin est de ceux-là. Il peut faire progresser l'étude des phénomènes transitoires relatifs à la détonation.

Iwould like to thank Mrs Odiot for her kind invitation to chair this session . I believe much discussion is necessary in the complex field of detonation to explain and clarify our positions. I would like to stress three points I feel to be essential.

- The fundamental topic of the "Microscopic and Macroscopic Approaches to Detonation" workshop.

- The role of thermodynamics in the study of detonation.

- The importance of the time factor in analyzing these phenomena.

These three points are part of the modern development of nonlinear mechanics.

a) It is not possible to understand the coexistence of a shock wave and combustion wave without both a detailed local analysis performing in space (10^{-7} cm) and time (10^{-14} s), i.e. the "microscopic approach", and an anlysis of the overall repercussions, i.e. the "macroscopic approach". These two approaches are necessary and equally important. They cannot be dissociated, since they are complementary and interrelated. This is the approach adopted by Hadamard and Duhem. Poincaré insists on the importance of the transition from local to general, in particular in topology (analysis situs).

b) The second point stresses the importance of thermodynamics, in particular in analysis of the detonation. In the past, this role was crucial for determination of the velocity of detonation (importance of the production of entropy, which is a minimum downstream of the wave). We believe this role is still important, especially in the irreversible part which gives rise to a new theory. Thermodynamics is the basis science of complex systems, since it is multidisciplinary as is the detonation wave, in which physics and chemistry coexist. We feel that the recommendation of H.Poincaré, to make this science the basis of mathematical physics, is still valid today. We would like the thermodynamic approach, which appears somewhat neglected today, to be used more in the nonlinear part of the physics and chemistry of detonation.

c) The third point emphasizes the time parameter, often so difficult to control. I would again like to mention the pioneering work of H.Poincaré in the analysis of unsteady nonlinear phenomena. This work spurs new reflections on determinism and predictability on new bases. It plays an essential role in modern theory of dynamic systems. France is fortunate to have excellent physicists, such as Bergé, Chabert, Pomeau, who contributed enormously to research on system dynamics. Paul Clavin is another such physicist. He can help us progress in the study of transient phenomena relative to detonation.

LECTURES

Direct Initiation of Gaseous Detonation ; **P. Clavin** and L. He

Analysis of Accelerating Detonation using Large Activation Energy Asymptoties

R. Klein

Spontaneous Localization of Vibrational Energy ; **D.W. Brown** and L. Bernstein

JOURNAL DE PHYSIQUE IV
Colloque C4, supplément au Journal de Physique III, Volume 5, mai 1995

Direct Initiation of Gaseous Detonations

P. Clavin and L. He

Institut de Recherche sur les Phénomènes Hors Equilibre, Unité Mixte de Recherche n° 138, CNRS & Université d'Aix-Marseille I & II, Service 252, Centre St-Jérôme, 13397 Marseille cedex 20, France

Abstract: A theoretical analysis of the direct initiation of gaseous detonations by an energy source has been published recently, the results are recalled here. Nonlinear curvature effects are proved to be essential mechanisms controlling the critical condition. These effects are first studied in a quasi-steady (q-s) state approximation valid for a characteristic time scale much larger than the reaction time scale. Two branches of q-s solutions are exhibited with a C-shaped curve and a critical radius below which generalised Chapman-Jouguet (CJ) solutions cannot exist. At ordinary conditions this critical radius is much larger than the thickness of the plane CJ detonation front (typically 300 to 500 times larger). Direct numerical simulations show that the upper branch of q-s solutions, acts as an attractor of the unsteady blast waves originating from a sufficiently strong energy source. The criterion of initiation derived here works to a good approximation and exhibits the huge numerical factor (10^6 - 10^8) which is observed in the experimental data of the critical energy source and which was not explained up to now. Transient may induce additional failure mechanisms close to the critical condition.

1. INTRODUCTION

Direct initiation of gaseous detonation by an energy source is an old problem which has been reviewed by Lee in 1977 and 1984 [1], [2]. For a subcritical level of the total energy of the igniter E_S, $E_S < E_C$, the shock wave decays continuously, the reaction front separates from the inert shock, and a premixed flame is finally ignited. With an energy larger than the critical value E_C, $E_S > E_C$, the shock wave and the reaction layer remain always coupled; the strong overdriven detonation originating from the source relaxes to a CJ detonation wave propagating at a constant velocity, D_{CJ}. The onset of this CJ detonation occurs at a distance from the point source increasing with the energy of the igniter E_S , $R^*(E_S) \approx (E_S/\rho_0 Q)^{1/3}$, where Q is the heat release per unit mass. A critical radius $R_C = R^*(E_C)$ has been identified experimentally at the critical condition. No CJ detonation can be observed with a front radius R_S smaller than R_C which is about twenty times larger than the cell spacing size which is itself ten to fifty times larger than the thickness of the reaction zone of a planar detonation (see Desbordes [3]). The existing theoretical models for the critical conditions were essentially phenomenological. Zeldovich et al. [4] provided the first criterion: a successful initiation occurs when the time necessary for the blast wave to decay to the level of the leading shock of a planar CJ detonation is larger than the chemical induction time τ_i at the Neuman spike of a CJ detonation. The kinetics data available at that time were too inaccurate for providing a meaningful experimental check of this criterion. The corresponding critical conditions are wrong by many orders of magnitude indeed. They may be estimated from the self-similar solution of Taylor [5] and Sedov [6] for strong adiabatic blast waves generated by an instantaneous deposition of energy at a point,

$$E_S = k_j [(j+3)/2]^{j+1} \rho_0 D^{j+3} \tau^{j+1} \iff E_S = k_j \rho_0 D^2 R_S^{j+1} \quad (1)$$

where j = 0, 1, 2 in the planar, cylindrical and spherical geometry respectively, ρ_0 is the gas density of the initial mixture, D and R_S are the shock velocity and the radius of the shock wave at any instant of time τ, E_S is the energy of the point source and k_j is a dimensionless constant of order unity. The critical energy and radius are evaluated from (1) by replacing D by D_{CJ} and τ by τ_i. This criterion yields a critical radius of the same order of magnitude as the thickness of the detonation $R_c \approx l_{iCJ} \approx D_{CJ}\tau_i$, in contradiction with the experiments of Desbordes [3] $R_c \approx 300\ l_{iCJ}$. When the relation $R_c \approx l_{iCJ}$ is used, the critical energy obtained from (1), $E_c \approx \rho_0 D_{CJ}^2 l_{iCJ}^{j+1}$, is roughly speaking the chemical energy available in a sphere of radius the detonation thickness (for a large Mach number, $D_{CJ}^2 \approx 2(\gamma^2-1)Q$). As shown later by Edwards et al. [7] who used accurate data for l_{iCJ}, the natural energy scale $\rho_0 D_{CJ}^2 l_{iCJ}^{j+1}$ is much smaller than the experimental data of critical energy for a detonation initiation by many orders of magnitude 10^6-10^8. Other phenomenological criteria have been derived later in a similar way but by replacing l_{iCJ} by much larger lengthscales as theses obtained from measurements of cell sizes or critical tube diameters, see Lee [1-2]. The best phenomenological fits have been obtained with a "magic ratio" 13/4 the cell size. Correlations with the cell size seem fortuitous; the initiation conditions are the same for mixtures in which detonation fronts have no cell structure, as is more likely the case for warm hydrogen mixtures encountered in safety problems of some nuclear plans.

In a recent theoretical work [8] we have shown that the critical conditions for a direct initiation of a gaseous detonations by a point source are governed by a nonlinear curvature effect presenting some analogies with a quenching phenomenon. The main steps of this analysis are briefly reported at this conference. The point source approximation is valid when the characteristic size of the igniter is much smaller than R_c and when the deposition time of energy is much smaller than the induction time τ_i. Then, when multi-dimensional effects such as those governing the cell structures, are neglected, a successful initiation may be viewed as a transition between two self-similar regimes:

i) At early times, the total heat released by the chemical reactions is negligibly small compared to E_S, the self-similar solution of Taylor and Sedov for strong adiabatic blast waves hold.

ii) At sufficiently long times after a successful initiation, E_S becomes negligibly small compared to the energy released by the chemical reactions. And, in the case of a stable detonation, the solution is well approximated by the self-sustained wave of Zeldovich [9] and Taylor [10] constituted by a smooth detonation front expanding at a constant CJ velocity and followed by a self-similar rarefaction wave.

Numerical solutions of a "detonation-wave model" were carried out by Korobeinikov [12] to describe such a transition in the limit of an infinitely fast chemical rate ($\tau_i \to 0$). The detonation front was considered as a discontinuity with Rankine-Hugoniot jump conditions. No critical condition of initiation is observed in this work; the onset of the CJ detonation occurs in spherical geometry at $R^*(E_S) = (1.3\ E_S/\rho_0 Q)^{1/3}$ for a specific heat ratio of 1.3, whatever be E_S. This shows clearly that the physical mechanisms governing the critical conditions are associated with those involved inside the inner detonation structure and characterised by a finite chemical time (length) scale τ_i (detonation thickness $l_i \approx \tau_i D_{CJ}$). The interesting question to answer is how such small effects may induce so strong effects as those responsible for critical conditions which involve a so large critical radius, typically 300 the CJ detonation thickness ? As for flames quenching [13-14], the answer lies on an amplification by a large sensitivity to temperature of the reaction rate. A small curvature of the detonation front may have a drastic effect upon the inner structure of the detonation wave in a way similar to quenching of planar detonations by momentum losses which was described by Zeldovich [15] for representing detonations propagating in rough tubes. A difficulty for solving analytically the initiation problem is its strong unsteady character. It turns out that a quasi-steady approximation of the detonation structure allows to capture the essential physical mechanisms

including the right order of magnitude determined from experiments.

2. THE BASIC EQUATIONS

When the molecular transport are neglected and when the chemical reaction is modelled by an exothermic irreversible one-step reaction, the unsteady and one-dimensional conservation equations are

$$\frac{\partial \rho}{\partial t} + \frac{\partial(\rho u)}{\partial r} + \frac{j}{r}(\rho u) = 0 \tag{2.1a}$$

$$\frac{\partial(\rho u)}{\partial t} + \frac{\partial(\rho u^2 + p)}{\partial r} + \frac{j}{r}(\rho u^2) = 0 \tag{2.1b}$$

$$\frac{\partial E}{\partial t} + \frac{\partial[(E + p)u]}{\partial r} + \frac{j}{r}(E + p)u = 0 \tag{2.1c}$$

$$\frac{\partial(\rho y)}{\partial t} + \frac{\partial(\rho u y)}{\partial r} + \frac{j}{r}(\rho u y) = -\rho\omega \tag{2.1d}$$

with $j = 0$, 1 and 2 in the planar, cylindrical and spherical geometry and with

$$p = \rho T \tag{2.1e}$$

$$E = \rho\left(\frac{1}{\gamma - 1}T + \frac{1}{2}u^2 + yQ\right) \tag{2.1f}$$

for a polytropic gas. In these equations p, ρ, T, E and y are respectively the pressure, density, temperature, specific energy and reactant mass fraction. These variables have been dimensionless by reference to the preshock state; $p/p_0 \rightarrow p$, $\rho/\rho_0 \rightarrow \rho$, $T/T_0 \rightarrow T$, $E/p_0 \rightarrow E$. The velocity is denoted u after non-dimensionalization through division by $c_0/\sqrt{\gamma}$ where c_0 is the sound speed at the preshock state and γ is the specific heat ratio. The non-dimensional time and space variables t and r are based on the chemical induction time τ_{iCJ} of the planar CJ detonation and on the reference length scale $(\tau_{iCJ}\ c_0)/\sqrt{\gamma}$ which is typically of the same order of magnitude as the thickness of the detonation front. When the reaction is governed by an Arrhenius law, the reduced chemical reaction rate takes the following form,

$$\omega = y\, B \tau_{iCJ}\, e^{-E_a/T} \tag{2.1g}$$

where B is the frequency factor and E_a the reduced activation energy. And the reference time scale is defined by

$$\tau_{iCJ} = \frac{T_{NCJ}^2}{B\,(\gamma-1)\,Q\,E_a}\, e^{E_a/T_{NCJ}} \tag{2.2}$$

where T_{NCJ} is the reduced temperature at the Neumann spike of the planar CJ detonation and Q the reduced heat release parameter, $Q/(C_p - C_v)T_0 \rightarrow Q$. In the moving frame attached to the shock, Eqs.(2.1a-d) can be written as

$$\frac{\partial \rho}{\partial \tau} + \frac{\partial(\rho v)}{\partial \xi} + \frac{j}{R_s - \xi}\rho(D - v) = 0 \tag{2.3a}$$

$$\frac{\partial(\rho v)}{\partial \tau} + \frac{\partial(\rho v^2 + p)}{\partial \xi} + \frac{j}{R_s - \xi}\rho(D - v)v - \rho\frac{dD}{d\tau} = 0 \tag{2.3b}$$

$$\frac{\partial h}{\partial \tau} + v\frac{\partial h}{\partial \xi} - \frac{1}{\rho}\frac{\partial p}{\partial \tau} = 0 \tag{2.3c}$$

$$\frac{\partial y}{\partial \tau} + v\frac{\partial y}{\partial \xi} = -\omega \tag{2.3d}$$

with reduced space and time coordinates

$$\xi = R_s - r \ , \quad \tau = t \tag{2.4a}$$

$$R_s = \int_0^t D\,(t')\,dt' \tag{2.4b}$$

where D and R_s are respectively the velocity and the position of the shock at any instant of time t, $v = D - u$ is the flow velocity relative to the leading shock wave, and the total enthalpy is

$$h = \frac{\gamma}{\gamma-1} T + \frac{1}{2} v^2 + yQ \tag{2.5}$$

Three types of term appear in (2.3): i) unsteady terms, ii) three conserved scalars in plane and steady detonations (ρv, $\rho v^2 + p$, h), iii) curvature terms.

3 NONLINEAR CURVATURE EFFECT

In the study of detonation structures with a radius of front curvature much larger than the detonation thickness, $R_s >> 1$, ξ may be neglected in $(R_s - \xi)$. The reference time scale which has been used is of the same order of magnitude as the intrinsic reaction time characterising the internal detonation structure. In the quasi-steady state approximation when the characteristic time of evolution is much longer than this reaction time, unsteady terms may be neglected. Then, in the framework of such multiple scales assumptions, the governing equations for the structure of a curved detonation reduce at the leading order to the following system of first order ordinary differential equations,

$$\frac{d(\rho v)}{d\xi} = - \frac{j}{R_s} \rho (D - v) \tag{3.1a}$$

$$\frac{d(\rho v^2 + p)}{d\xi} = - \frac{j}{R_s} \rho (D - v) v \tag{3.1b}$$

$$\frac{dh}{d\xi} = 0 \tag{3.1c}$$

$$v \frac{dy}{d\xi} = - \omega \tag{3.1d}$$

This quasi-steady approximation is meaningful whenever the unsteady terms are smaller than the perturbative curvature effects. The additional curvature term on the r.h.s. of (3.1a-b) are to be considered as perturbations, $R_s >> 1$. When they are omitted, eqs.(3.1a-c) reduce to the ordinary conservative system describing planar detonations. But even small, the curvature terms change the phase portrait. After elimination of p and ρ, eqs.(3.1a-d) may be written in the following form, suitable for the analysis of the detonation structure in the phase space v^2-y [15],

$$\frac{dv}{dy} = - \frac{v \, \psi(y,v,D)}{\omega(y,v,D) \, \varphi(y,v,D)} \tag{3.2a}$$

with $$\psi \equiv \frac{(\gamma-1)Q\omega}{c^2} - \frac{j}{R_s}(D - v) \quad \text{and} \quad \varphi \equiv 1 - \frac{v^2}{c^2} \tag{3.2b}$$

where ω, the reduced reaction rate (2.1g), c, the reduced local sound speed, and the reduced temperature T are expressed in terms of y, v, D by the total enthalpy conservation as

$$c^2 = \gamma T = \gamma + (\gamma-1) \left[\frac{1}{2} (D^2 - v^2) + (1 - y) Q \right] \tag{3.2c}$$

3.1 Weak curvature effects

System of equations (3.2a-c) has been used with a reaction rate ω represented by a regular function, to study the detonation structure in slightly divergent flows [16] or with weak curvature effects of the front

[17]. For a given value of R_s there is a one-parameter family of solutions labelled by D. A marginal solution corresponding to a local minimum of D, called "generalised CJ solution" and referred by $D_+(R_s)$ in this paper, has been pointed out, with a sonic condition $v = c$ occurring at $y = y^* > 0$, before the completion of the reaction. This marginal solution is qualitatively different from the CJ solution of the plane case, the condition $v = c$ corresponds to saddle point in the phase space v^2-y, $\psi = 0$, $\varphi = 0$ but $dv^2/dy \neq \infty$ while in the plane case $v = c$ at $y = 0$ with $dv^2/dy = \infty$. Solutions exist for larger detonation velocities, $D>D_+$, and they all correspond to overdriven detonations with a subsonic flow ($v < c$) everywhere ($0 \leq y \leq 1$). The trajectory of the marginal solution, $D=D_+$, passes through the saddle critical point ($y = y^*$) into the supersonic region and, as a consequence, this solution is qualitatively different from all the overdriven ones, the flow is subsonic in a first part behind the shock wave, $1 \geq y > y^*$, and supersonic in the last part of the combustion process $y^* > y \geq 0$. For slightly smaller detonation velocities, $D < D_+$, the sonic condition $v = c$ corresponds to a turning point ($dv^2/dy = \infty$) which appears at $y > 0$ as in the plane case for $D < D_{CJ}$, and no solution exists any longer because $y = 0$ cannot be attained. The relation between D and R_s referred below as $D(R_s)$, has been obtained from the marginal solution D_+[17].

Our analysis [8] shows that there exists indeed another branch of marginal solutions $D_-(R_s)$ ($D_- < D_+$) with solutions for $D < D_-$. Due to nonlinear effects the $D(R_s)$ curve has a C-shaped form with a critical radius R_c. An analytical solution of (3.1a-c) has been obtained in ref [8] for describing the nonlinear curvature effects in the framework of a square-wave model yielding a nonlinear relation for $D(R_s)$. For $R_s > R_c$, the velocity spectrum of quasi steady detonations is unbounded but presents two extrema. One, D_+, is a local minimum and the other D_- a local maximum, with a forbidden band $[D_+, D_-]$. An analytical expression for the critical radius R_c below which no generalised CJ solution exists, is obtained. When compared with numerical solutions of (3.1a-c) for an Arrhenius law, these analytical results show a good accuracy. They yield also an analytical determination of the critical energy of direct initiation.These result are briefly recalled below.

3.2 Square-wave model

The square-wave model is defined in a phenomenological way as follows. The chemical reaction is assumed to proceed in two sequential steps. The heat is released during a reaction time τ_r after a time delay called the induction time τ_i. The square-wave model corresponds to the limit $\tau_r / \tau_i \rightarrow 0$. The reaction rate ω becomes singular, and the heat release is localised within a thin exothermic layer considered as a discontinuity following the shock wave at a distance l_i defined as

$$l_i \equiv v_N \tau_i, \qquad (3.3a)$$

where by definition of the reference length scale used in (2.1a-d), $l_{iCJ} = O(1)$. The induction time is highly sensitive to the temperature fluctuations of the shocked gas just downstream the shock wave, δT_N. Let β be the large nondimensional reduced activation energy, $(\delta\tau_i/\tau_i) / (\delta T_N/T_N) = O(\beta)$, with $\beta >> 1$, then,

$$l_i/l_{iCJ} = \exp\{-\beta (T_N - T_{NCJ})/T_{NCJ}\} \text{ valid for } \beta >> 1, \qquad (3.3b)$$

where subscripts N and CJ denote the state at the shock and the planar CJ case respectively. Relation (3.3b) may be obtained from an Arrhenius law at the leading order of an asymptotic expansion in the limit $\beta \rightarrow +\infty$ (see Appendix of ref. [8]). This simplified model is sufficient to pick up the essential phenomena as well as the right orders of magnitude. Such a singular model is known from a long time to introduce spurious singularities when it is used for describing the intrinsic dynamics of a detonation front which develops on a characteristic time scale τ_i [18-19]. These problems, including the nonlinear dynamics of galloping detonations, have been very recently solved also analytically [20-21] . However the square-wave model has been proved already to be very powerful to describe critical conditions associated with quasi-steady mechanisms developing on a time scale longer than τ_i and which are stressed by a high sensitivity of the induction time [22]. When the attention is focused on cases where $\beta >> 1$ and $R_s = O(\beta)$, the curvature terms in the r.h.s. of (3.1 a-b) being small, of the same order of magnitude as $1/\beta$, the variations of the

shocked gas temperature from its value in the planar case are also small, $\delta T_N/T_N = O(1/\beta)$. But strong nonlinear effects are included at the leading order of the limit $\beta \to +\infty$; according to the high sensitivity to T_N in (3.3), one has $(\delta\tau_i/\tau_i) = O(1)$ and $(\delta l_i/l_i) = O(1)$. In the square-wave model, the thickness of the reaction zone is negligible and the curvature effects modify only the induction zone which does not consume the reactant, y = 1. The $1/R_s$ terms being negligible in the thin exothermic zone, this last one is described in the phase plane by the same equations as in the planar case, but with a different initial condition at y = 1, $v^2 \neq v_N^2(D)$ resulting from the curvature induced modifications across the induction zone. As for the planar case, the marginal solutions of the square wave model may be obtained directly from the conservation laws across the detonation structure without investigating the phase space. These conservation laws are readily obtained by a ξ-integration of (3.1a-c) across the detonation structure and may be written in a dimensionless form as:

$$\rho_b v_b = D - D\Gamma_1 \tag{3.4a}$$

$$(\rho_b v_b^2 + p_b) = (D^2 + 1) - D^2\Gamma_2 \tag{3.4b}$$

$$[\gamma/(\gamma-1)]\, p_b/\rho_b + (1/2)\, v_b^2 = \gamma/(\gamma-1) + (1/2)\, D^2 + Q \tag{3.4c}$$

where the subscript b denotes the burned gases (y = 0). The source terms of (3.4a-b), defined as

$$\Gamma_1 = \frac{1}{D}\frac{j}{R_s}\int_0^{l_i} \rho\,(D - v)\, d\xi \tag{3.5a}$$

$$\Gamma_2 = \frac{1}{D^2}\frac{j}{R_s}\int_0^{l_i} \rho\,(D - v)\, v\, d\xi \tag{3.5b}$$

represent the curvature induced modifications of mass and momentum fluxes across the detonation structure. They are both small perturbation terms; when they are neglected, (3.4a-c) reduce to the ordinary Hugoniot relations. Using $1/R_s = O(1/\beta)$, the leading order of Γ_1 and Γ_2 in the asymptotic limit $\beta \to \infty$ can be easily computed from (3.5a-b) with the square wave model by using the values at the Neumann spike of the CJ solution for D, v and ρ,

$$\Gamma_1 = j\,(\rho_{NCJ} - 1)\,\frac{l_i}{R_s} = O\left(\frac{1}{\beta}\right) \tag{3.6a}$$

$$\Gamma_2 = j\,\left(1 - \frac{1}{\rho_{NCJ}}\right)\frac{l_i}{R_s} = \frac{1}{\rho_{NCJ}}\Gamma_1 \tag{3.6b}$$

where the thickness of the induction zone is given by (3.3) and may be expressed in terms of the modification of detonation velocity $(D-D_{CJ})/D_{CJ}$ by using the Hugoniot relation of the leading shock in the fresh mixture,

$$\frac{T_N - T_{NCJ}}{T_{NCJ}} = -\frac{2}{1 + D_{CJ}^{-2}\gamma/(\gamma-1)}\,\frac{D-D_{CJ}}{D_{CJ}} \approx -\,2\,\frac{D-D_{CJ}}{D_{CJ}}$$

where the last approximation is valid for a sufficiently strong shock wave, $(\gamma-1)D^2_{CJ} >> 1$, yielding according to (3.3),

$$\frac{l_i}{l_{iCJ}} \approx \exp\left\{-\,2\beta\,\frac{D-D_{CJ}}{D_{CJ}}\right\}. \tag{3.6c}$$

According to (3.6a-c),

$$\delta\Gamma_{1,2} \approx -\,\frac{\delta D}{D_{CJ}}\,(2\beta\Gamma_{1,2}) \tag{3.6d}$$

then, a variation around the marginal solution of (3.4a-c) which is defined by an extremum condition $\delta D = 0$, confirms that such a solution is still determined in curved fronts by the same sonic condition in the burned gases as in the plane case: $v_b = c_b = (\gamma p_b/\rho_b)^{1/2}$. Then, introducing $v_b = (\gamma p_b/\rho_b)^{1/2}$ in (3.4a-c), a

pertubative analysis around the planar CJ detonation yields the curvature-induced modification of the detonation velocity ($D-D_{CJ}$) as a linear function of $\Gamma_1 = O(1/\beta)$ and $\Gamma_2 = O(1/\beta)$,

$$\{-\frac{2}{\gamma^2}\frac{\gamma(\gamma+1)+(\gamma^2-1)Q}{1+D_{CJ}^2}+\frac{2}{D_{CJ}^2}\}\frac{(D-D_{CJ})}{D_{CJ}} = (1+\frac{1}{D_{CJ}^2})\Gamma_1-\Gamma_2 \qquad (3.7)$$

which, by using a nonlinear expression obtained for Γ_1 from (3.6a-c),

$$\Gamma_1 = j\,(\rho_{NCJ}-1)\frac{l_{iCJ}}{R_s}\exp\{-2\beta\frac{D-D_{CJ}}{D_{CJ}}\}$$

provides a nonlinear equation for the velocity D of the marginal detonations,

$$(2\beta\frac{D_{CJ}-D}{D_{CJ}})\exp(-2\beta\frac{D_{CJ}-D}{D_{CJ}}) = \frac{8j}{1-\gamma^{-2}}(\beta\frac{l_{iCJ}}{R_s}) \qquad (3.8)$$

where the simplified forms of the coefficients corresponding to a strong detonations, $(\gamma-1)D^2_{CJ} > 1$, have been used for simplicity, $D_{CJ}^2 \approx 2(\gamma^2-1)Q$, $(\rho_{NCJ}-1)^2/\rho_{NCJ} \approx 4/(\gamma^2-1)$. Eq.(3.8) yields a nonlinear velocity-radius relation, $D(R_s)$, valid in the distinguished limit $\beta\to\infty$, $\beta l_{iCJ}/R_s = O(1)$, $\beta(D_{CJ}-D)/D_{CJ} = O(1)$, corresponding to a relatively small curvature intensity. This result exhibits a critical radius R_c

$$\frac{R_c}{l_{iCJ}} = \frac{8ej}{1-\gamma^{-2}}\beta \qquad (3.9a)$$

below which no solution exits, and a critical detonation velocity D_c given by

$$\frac{D_{CJ}-D_c}{D_{CJ}} = \frac{1}{2\beta} \qquad (3.9b)$$

For $R_s > R_c$, (3.8) yields two branches of solutions $D_+(R_s) > D_-(R_s)$. The physical one is the upper one which reaches the CJ planar solution from below when $R_s\to\infty$, $D_+(R_s)\to D_{CJ}$. The second branch of solution $D_-(R_s)$ is not physical: in the limit $R_s\to\infty$ one gets $\beta(D_{CJ}-D)/D_{CJ}\to\infty$ which does not correspond to the domain of validity of (3.8), $\beta(D_{CJ}-D)/D_{CJ} = O(1)$ for $\beta\to\infty$. We will discuss later the nature of this second branch of solutions. The critical condition (3.9a-b) is within the validity domain of the limit $\beta\to\infty$. For weak curvature effects, $\beta l_{iCJ}/R_s \to 0$, one gets the following linear relation for the upper branch,

$$(D_{CJ}-D_+)/D_{CJ} = [\,4\gamma^2/(\gamma^2-1)\,]\,j\,(l_{iCJ}/R_s) \qquad (3.9c)$$

which corresponds to a linear result obtained in the particular case of a one-step first-order reaction governed by an Arrhenius law at the limit of an infinitely large activation energy [17]. Finally, notice that the numerical factor in the r.h.s. of (3.9a) which is of order unity in the asymptotic limit $\beta\to\infty$ and which controls the numerical value of the critical radius, is a larger number $8ej/(1-\gamma^2) \approx 90$ for $\gamma=1.4$ and $j=2$ (spherical detonation). Thus, for ordinary values of the reduced activation energy based on the temperature at the Neumann spike, $\beta = E_a/T_{NCJ} = 5$ to 10, the critical radius is 400 to 900 times larger than the detonation thickness while the corresponding relative modification of the detonation velocity (3.9b) is small, 10^{-1} to $5\ 10^{-2}$. Thus, the origin of the large value of R_c/l_{iCJ} is clearly exhibited by the analytical results of the square wave model. These results are confirmed by those obtained by a numerical integration in the phase space of (3.1-2) with an Arrhenius law [8]. The critical value is well approximated by (3.9a). For a given R_S larger than the critical value R_c there are two trajectories corresponding to two different marginal detonation velocities D_+ and D_-. The trajectories associated with intermediate velocities of detonation, $D_- < D < D_+$, are the only one for which there is no solution linking the initial state $y=1$ to the final one $y = 0$; a turning point appears at at $y > O$. The set of solutions corresponds to two disconnected

ranges of detonation velocities, an upper one (D_+, $+\infty$) with a lower bound D_+ (local minimum) and another one with an upper bound D_-. In solutions corresponding to $D > D_+$ or $D < D_-$ the flow behind the leading shock is subsonic everywhere relatively to the shock. The marginal solutions D_+ and D_- are the only ones presenting a sonic condition in the burned gases. When R_S deceases D_+ decreases while D_- increases so that the two trajectories of the marginal solutions (D_+ , D_-) in the phase space v^2-y become closer and closer and collapse at $R_S = R_C$ (see fig. 1). When $R_S < R_C$ there is no more local extrema, a solution does exist for every value of D and the flow behind the leading shock is subsonic everywhere. Similar results with same order of magnitude as predicted by the square-wave model are also obtained with a complex chemistry for H2-O2 mixtures [23].

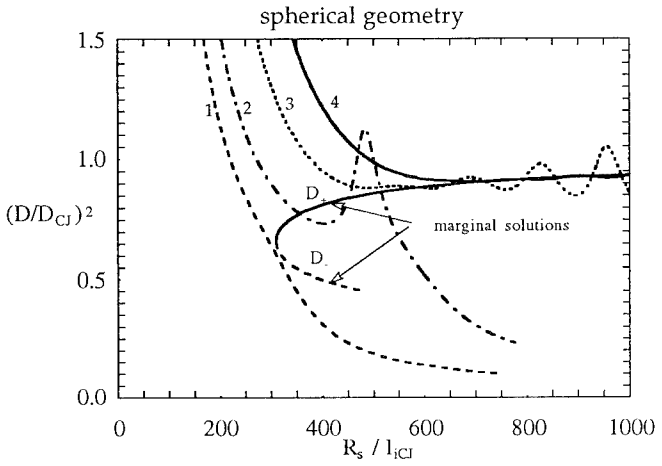

Fig.1 Numerical results of the initiation of spherical detonations. The front velocity is plotted as a function of the front radius and is compared with the corresponding marginal solutions for a reactive mixture characterised by $\gamma = 1.4$, $\beta = 5.33$, $Q = 12.5$ and for four values of the nondimensional source energy $E_s/(\rho_0 D_{CJ}^2 l_{CJ}^3)$
1.) 3.30×10^7, 2.) 5.69×10^7, 3.) 1.34×10^8, 4.) 2.64×10^8

4. DIRECT INITIATION

The selection mechanism of the CJ solution is worth recalling at this stage (see for example Landau and Lifchitz, [11]). Faster detonations waves are associated with a subsonic flow in the referential frame of the leading shock. Thus, the shock intensity is continuously weakened (down to CJ) by the rarefaction wave which has a leading weak discontinuity travelling at a sonic velocity relatively to the burned gases. This damping effect is screened only at the marginal CJ regime of propagation by a sonic condition of the flow at the end of the chemical reaction. Following the same idea, a selection mechanism may be predicted in the presence of curvature effects. Due to the rarefaction wave in the burned gas of an expanding overdriven detonation ($D(t) > D_+$) which are initially generated by a point source explosion, the upper branch D_+ of marginal solutions (minimum velocity) is naturally selected from above. The shock velocity of the solutions of the other set ($D < D_-$) is continuously decreased; the marginal D_- solution (local maximum) can never be

selected. Thus the upper branch of marginal solutions D_+ is predicted to act as an attractor for the unsteady blast waves generated by a sufficiently strong energy source. But this D_+branch is not always caught; in such circumstances the detonation wave dies out. Consider the direct initiation of a detonation by an energy source E_s. As discussed in the introduction, the initial stages correspond to the self-similar solution of a strong adiabatic blast wave (1.1) which is represented by a curve in the D-R_s plane,

$$E_s = k_j \rho_0 R_s^{j+1} D^2. \qquad (4.1)$$

Ignition failures may be predicted for source energies E_s for which the D-R_s curve do not cross the upper branch D_+ (see case 1 in Fig. 1). Successful initiations are expected in the opposite case (see case 3 and 4 in Fig. 1). As a result, a critical energy E_c may be evaluated from (4.1) by replacing R_s by R_c and D by D_c ($\approx D_{CJ}$), yielding the following approximate criterion when (3.9a-b) is used,

$$E_c = k_j \left(\frac{8ej\beta}{1 - 1/\gamma^2} \right)^{j+1} \rho_0 D_{CJ}^2 l_{iCJ}^{j+1} \qquad (4.2)$$

Equation (4.2) defines the critical energy which exhibits a huge factor $(R_c/l_{iCJ})^{j+1} = (8ej\beta\gamma^2/(\gamma^2 -1))^{j+1}$ with an order of magnitude ranging from 10^7 to 10^9 in the spherical case. The numerical simulations of a direct detonation initiation by an energy source confirm these predictions [8] [23]. Solutions corresponding to four values of the energy source are shown in figure 1 where the two branches of marginal quasi-steady solutions, D_+ and D_-, are also plotted for comparison.

5 DISCUSSION OF THE RESULTS

The results presented in this paper show clearly that the criterion for a direct detonation initiation by an energy source in cylindrical and spherical geometry is directly controlled by nonlinear curvature effects of the detonation front, at least in the range of parameters where the planar detonation is not strongly unstable. Considering the unsteady effects one must first discuss the validity of the quasi-steady state approximation used in (3.1a-d). The characteristic evolution rate on the D_+ branch, $1/t_e \equiv dD_+/dR_s$, is given far enough from the turning point by (3.9c), yielding $1/t_e = 4j\gamma^2(\gamma^2 -1)^{-1}(l_{iCJ}/R_s)^2(D_{CJ}/l_{iCJ})$. The neglected unsteady terms $\partial/\partial\tau$ in (3.1a-d), are effectively of the following order in the large radius expansion $\tau_i/t_e = O((l_{iCJ}/R_s)^2)$. Such an approximation does not hold close to the critical point where $dD_+/dR_s \rightarrow \infty$ but this does not change the final results because the divergence affects only a small vicinity of the critical point. More important are the unsteady effects related to the intrinsic dynamics of detonations (see ref. [20-21] for recent theoretical results). The detonation is known to become unstable for a sufficiently high activation energy and the instability mechanism is reinforced when approaching the critical point. Another problem is the dynamics of the selection mechanism of the D_+ branch which is unknown. The corresponding unsteady effects are enlightened by a comparative numerical study of the ignition problem in planar geometry. For the same set of parameters the critical size is much smaller than the critical radius in spherical geometry. This points out that the curvature effects are dominant in spherical and cylindrical geometries. Good order of magnitudes are obtained with our simple theory. But the unsteady effects cannot be ignored for an accurate prediction of the critical conditions and more specially for strongly unstable detonations. The multidimensional effects remain an open question.

REFERENCES

[1] Lee, J. H., *Ann. Rev. Phys. Chem.* **28** (1977) 75-104.
[2] Lee, J. H., *Ann. Rev. Fluid. Mech.* **16** (1984) 311-336.
[3] Desbordes, D., *Prog. Astronaut. Aeronaut.* **106** (1986) 166.

[4] Zeldovich, Ya.B., Kogarko, S. M., and Simonov, N. N., *Sov. Phys. Tech. Phys.* **1** (8) (1956) 1689-1731.
[5] Taylor, G. I., *Proc. R. Soc. Lond. A* **200** (1950) 235-247.
[6] Sedov, L. I., *Prikl. Mat. Mech.* **10** (1946) 241-250.
[7] Edwards, D. H., Thomas, G. O. and Nettleton, M. A., *J. Fluid Mech.* **95** (1979) 79-96.
[8] He, L. and Clavin, P. *J. Fluid Mech.* **277** (1994) 227-248.
[9] Zeldovich, Ya. B., *J. Exp. Theor. Phys.* (USSR) **12** (1942) 389-406.
[10] Taylor, G. I., *Proc. R. Soc. Lond. A* **200** (1950) 235-247.
[11] Landau, L. and Lifchitz, E. *Mecanique des fluids*, (MIR, 2nd Edition 1989).
[12] Korobeinikov, V. P., *Ann. Rev. Fluid. Mech* **3** (1971) 317-346.
[13] Linan , A., *Acta Astronautica* **1**(1974) 1007-1039.
[14] Joulin, G., and Clavin, P., *Acta Astronautica*, **3** (1976) 223-240.
[15] Zeldovich, Ya. B. 1940 On the theory of detonation propagation in gaseous systems. In Ostriker, J. P., Barenblatt, G. I. and Sunyaev, R. A. (Ed.) *Selected Works of Yakov Borisvich Zeldovich, Volume I Chemical Physics and Hydrodynamics*, 1992, Princeton University Press. pp. 411-451.
[16] Fickett, W. and Davis, W. C. Detonation (University of California press, Berkeley, 1979).
[17] Klein, R. and Stewart, D. S., *SIAM J. Appl. Math.* 54 (1993) 1401.
[18] Erpenbeck, J. J., *Phys. Fluids* **5** (1962) 604-614.
[19] Erpenbeck, J. J., *9th Symposium (International) on Combustion* (Academic Press Inc., New York, 1963) pp. 442-453.
[20] Clavin, P. and He, L., "Stability and nonlinear dynamics of one-dimensional detonations," To appear in *J. Fluid Mech.* (1995).
[21] He, L. and Clavin, P., "Dynamics of planar overdriven detonations," to appear in *C. R. Acad. Sci. Paris (1995).*
[22] He, L., "Theoretical determination of the critical conditions for the direct initiation of detonations in hydrogen-oxygen mixtures," To appear in *Combust. Flame.*

Discussion

Questions - Answers, Comments

Desbordes - Clavin :

Q : What change if one considers cellular structure as the "natural" size of the problem of initiation in comparison to R_c ?

A : The link between the size of cellular structure and the characteristics of the inner detonation structure is not yet clear for me. So I cannot answer this question presently.

Q : Can your model which ignores the three-dimensional structure of the gaseous detonation, but linked the dependence of $\Delta L_i/L_i$ to $2\beta(D_{CJ} - D)/ D_{CJ}$, explain the large variation (factor of 2) of k ($k = R_c/ L_i$) when β changes from 5.5 to 5 ?

A : The objective of our analysis is to explain the large difference in order of magnitude between R_c and L_i^{CJ}. One gets $R_c / L_i^{CJ} \simeq 500$ in spherical geometry for H_2 - O_2 mixture and R_c / L_i^{CJ} is predicted to vary linearly with β . But when compared with experiments, one has to be careful about the variation of L_i^{CJ} with β.

Brun - Clavin :

Q : If I remember well, Fickett and Davis do not explicitly refer to the initiation problem in their book. Is that true ?

If yes, how is it then that you refer to Fickett and Davis' analysis to deal with the initiation problem?

A : It is true. What I have tried to explain is that the critical conditions of the direct initiation problem is controlled (at least to explain order of magnitude, 10^8 factor in the reduced critical energy) by non linear curvature effects. Works reported in the book of Fickett and Davis concern linear curvature effects. I have shown how the non linear relation reduces to the linear one in the limiting case of weak effects.

Odiot - Clavin :

Q : Pourriez vous étendre vos résultats aux composés énergétiques en phase condensée ?

A : Les résultats que j'ai présentés reposent sur une grande sensibilité des réactions chimiques (qui se développent derrière le choc non réactif) aux conditions thermodynamiques des gaz juste derrière le choc. C'est le cas pour les détonations dans les mélanges gazeux H_2 - O_2 à travers la température.

Je ne sais pas ce qu'il en est pour les solides. Peut être que la pression est un paramètre mieux

adapté pour les solides.

Borisov - Clavin :

Q : Consistency of estimated critical diameters with experimental results is highly dependent on how you define the chemical reaction time. If in the Zeldovich approach we take the distance between the lead shock front and the final CJ plane instead of the induction period (the difference between these two distances may attain one or even two orders of magnitude) there will be no a big misfit of the theoretical and experimental data.

I would like to emphasize once again that when anybody wants to simulate a real detonation wave by an one-dimensional flow pattern he should use the effective kinetics of energy transformation rather than that depending only on the reaction scheme.

A : - A simular discussion occured for the definition of flame thickness ...

- The induction length and the thickness of reaction zone in a detonation propagating in H_2-O_2 gaseous mixture are now well defined without any ambiguity.The kinetics data used by Zeldovich et al. (1956) were wrong by 2 orders of magnitude (see Edwards 1978.)

The Zeldovich criterion is indeed wrong by many orders of magnitude, essentially because of the large reduced activation energy.

- The onedimensional effects (planar, cylindrical, spherical) are sufficient to recover the correct order of magnitude of the critical energy.

Van Tiggelen - Clavin :

Q : What about two chemical times, for instance induction time and heat release time ?

A : Nothing new if these two times are of the same order of magnitude.

When they are different, the problem is much more complex and two cases have to be considered and one may roughly say that :

- i) If the heat release time is much shorter than the induction time, strong instability phenomena occur on this short time.

- ii) In the opposite case, the intrinsic dynamic is controlled by the more sensitive time to the Neumann temperature variation.

Q : So, the condition for CJ plane is the sonic condition in the flow and not necessarily the full chemical equilibrium. Is this oversimplification correct in connection with your theoretical analysis?

A : I agree. For unsteady or curved detonation fronts, the sonic condition (when it appears) is not at the end of the chemical reaction. This does not affect the final results.

JOURNAL DE PHYSIQUE IV
Colloque C4, supplément au Journal de Physique III, Volume 5, mai 1995

Analysis of Accelerating Detonation Using Large Activation Energy Asymptotics

R. Klein[1]

Institut für Technische Mechanik, RWTH Aachen, Templergraben 64, 52056 Aachen, Germany

Galloping one-dimensional detonations exhibit a pulsating nonlinear instability characterized by rapid bursts of the detonation velocity followed by a slow-down and a longer re-acceleration. This has been observed experimentally as well as in numerical simulations, but to date there is no satisfactory theoretical description of this phenomenon that includes large amplitude deviations of the lead shock velocity. The present paper summarizes an extension of a recent analysis of the author based on large activation energy asymptotics. This earlier work exhibited a nonlinear slow-time instability for near-CJ detonations which leads to either an irreversible decomposition of the shock–reaction-zone complex or to a nonlinear continous acceleration, driving the wave speed away from the CJ-regime at an ever exceeding rate. Even though this analysis is based on an assumption of a slow characteristic evolution time scale, the insight gained seems to be worth a closer examination of the large amplitude regime that follows the above-mentioned acceleration stage. The present analysis, as well as the earlier study for the near-CJ regime, are in many respects close to the work by Buckmaster (1988), but they are not identical and seem to yield some new insight.

1. INTRODUCTION

One observes unsteady longitudinal oscillations experimentally as well as in one- and multi-dimensional direct numerical simulations based on Arrhenius one-step chemistry (Abuseif and Toong [1], Bourlioux and Majda [2]).

For highly overdriven fronts, an intriguing asymptotic theory, involving a modified Arrhenius reaction rate law, the limit of a specific heat ratio close to unity, low Mach number approximations in the shocked gas and small oscillation amplitudes of the detonation velocity has recently been presented by He and Clavin [3]. Here we are interested, in contrast, in order one overdrive and large amplitude excursions of the lead shock velocity.

The author has recently derived, via large activation energy asymptotics, a new inherently unsteady detonation front propagation law (Klein [4]). Let d, κ denote the scaled detonation speed perturbation ($d = \theta(D' - D'_{\rm CJ})/D'_{\rm CJ} = O(1)$) and the scaled lead shock curvature ($\kappa = \theta \ell'^{\rm CJ}_I \kappa'$), respectively. Here primes denote dimensional quantities, D' is the lead shock velocity of the detonation, $\ell'^{\rm CJ}_I$ the induction length of the associated CJ-wave, κ' the mean front curvature and $\theta = E_a/RT_{\rm sh}$ the nondimensional activation energy scaled with the post-shock state. Then the

(1) Currently at: Laboratoire de Recherche en Combustion, Université de Provence, Centre St. Jerôme, Service 252, 13013 Marseille cedex 20, France

new front evolution equation reads

$$\frac{\partial h(d,\kappa)}{\partial t} = g(d,\kappa)\,, \tag{1.1}$$

where $h(d,\kappa) = \ell_I/\ell_I^{CJ}$ is the nondimensional induction length whose functional relation to d,κ is a result of the asymptotic analysis. In the steady limit the relation

$$g(d,k) = 0\,. \tag{1.2}$$

defines a detonation speed – curvature relation which has been derived recently independently by Yao and Stewart [5], He and Clavin [3] and Klein et al. [6]. Even though changes of the relevant dependent variables are assumed in this theory to occur on a time scale much longer than the induction time for a shocked particle, equation (1.1) is nevertheless an inherently unsteady front propagation law as it includes, in contrast to its steady limit version (1.2), the time derivatives of both the curvature and the detonation speed perturbation. For a discussion of the applicability of (1.1) and (1.2) as unsteady front evolution equations see Klein [4].

In the same paper the author addresses the stability problem for the steady limit solution in (1.2) based on the unsteady evolution equation (1.1). Even though this ansatz involves a neglection of all time scales comparable to the induction time, the result seems interesting:

> *For curved fronts, the upper branch of the D-κ - curve is time unstable, while the lower branch is temporally stable.*
>
> *In the plane wave limit, the unsteady propagation law from (1.1) reveals a nonlinear long time instability, governed by the ODE*
>
> $$\frac{dh}{dt} = \mathcal{F}\,\ln h\,, \qquad \mathcal{F} = \text{const.} > 0\,, \tag{1.3}$$
>
> *for the time evolution of the induction length.*

Klein [4] discusses the implications of the first of these statements regarding the behavior of curved fronts. Here we focus on the plane wave limit and observe that a wave which commences as a slightly perturbed CJ-detonation with $h(0) = 1 + \delta h_0$ must either collapse ($h \to 0$ for $\delta h_0 < 0$) or fall apart ($h \to \infty$ for $\delta h_0 > 0$) as time evolves. This collapse is associated with an ever increasing acceleration of the front and here we try to describe systematically what happens when the wave leaves the CJ regime.

Buckmaster [7] considers practically the same asymptotic regime discussed in the following. The principal idea of a collapsing shock-fire structure with an imbalance of energy release and shock dissipation leading to a rapid front acceleration on progressively shortening time scales has already been expressed clearly in his paper. Yet, in his analysis a secularity of one of the first order perturbation functions (T^1) appears, which can be avoided. The consequence is a different detonation speed evolution equation.

2. FORMULATION AND EARLIER RESULTS

We consider the system of one-dimensional reactive Euler equations

$$\begin{aligned} \rho_t + (\rho\tilde{u})_x &= 0 \\ (\rho\tilde{u})_t + (\rho\tilde{u}^2 + p)_x &= 0 \\ (\rho e)_t + (\tilde{u}\,[\rho e + p])_x &= 0 \end{aligned} \tag{2.1}$$

for mass, momentum and total energy, supplemented by one reaction progress equation

$$(\rho\lambda)_t + (\rho\tilde{u}\lambda)_x = \rho w = \frac{1}{\theta}B(1-\lambda)\exp(\frac{\theta}{T}), \tag{2.2}$$

in case of a single-step reaction model. Here $\rho, \tilde{u}, e, \lambda$ and θ are the density, velocity in a laboratory frame, total specific energy, the burnt gas mass fraction and the non-dimensional activation energy, respectively. The source term ρw represents the chemical species conversion.

Equations (2.1), (2.2) are closed with respect ot the pressure p by specifying an equation of state. Here we chose the ideal gas equation,

$$\rho e = \frac{p}{\gamma - 1} + \frac{1}{2}\,\rho\tilde{u}^2 + Q\,\rho(1-\lambda)\,, \tag{2.3}$$

with constant values for the isentropic exponent γ and the specific heat of reaction Q.

The system (2.1) – (2.3) is in nondimensional form and we have assumed the following reference quantities for the scaling:

Primary reference quantities :

velocity	:	$D'_{\rm CJ}$	
density	:	ρ'_0	(unshocked gas density)
length	:	$\ell'^{\rm CJ}_I$	(unperturbed induction length)

Derived reference quantities :

pressure	:	$\rho'_0 D'^2_{\rm CJ}$
time	:	$\ell'^{\rm CJ}_I / D_{\rm CJ}$

According to the Zel'dovič - von Neumann - Döring theory, we seek solutions that consist of a leading shock wave followed by a narrow zone of chemical activity. Thus, given the detonation speed D, the solution has to satisfy the Rankine-Hugoniot jump conditions at $x = x_{\rm sh}(t)$, i.e., at the current location of the shock:

$$\begin{aligned} (\rho[\tilde{u} - D])_{\rm sh} &= -\rho_0 D \\ (\rho[\tilde{u} - D]^2 + p)^+ &= \rho_0 D^2 + p_0 \\ ([\tilde{u} - D]\,[\rho e^* + p])^+ &= -D\,[\rho e^* + p]_0 \end{aligned} \tag{2.4}$$

where e^* is the total energy per unit mass in a shock-attached frame (replace $\tilde{u}$ in (2.3) with $u = \tilde{u} - D$!). Also, the lead shock is non-reactive, so that

$$(\rho\lambda)_{\rm sh} = (\rho\lambda)_0 = 0. \tag{2.5}$$

In (2.4), (2.5), the superscript "$_{\rm sh}$" denotes post-shock conditions, while the subscript "$_0$" indicates conditions in the unshocked gas and the signs in $(2.4)_{1,3}$ indicate that the flow is from right to left in the front attached frame.

2.1 The near-CJ regime

In this section we summarize the analysis by Klein [4] for detonations that travel at close-to-CJ velocities. In the original analysis curvature effects were accounted for, but here we concentrate on plane waves in order to streamline the discussion. The underlying scaling assumptions for the following are:

i) Deviations of the lead shock velocity from the Chapman-Jouguet speed are small and comparable to the inverse of the activation energy

$$\frac{D - D_{\mathrm{CJ}}}{D_{\mathrm{CJ}}} = O\left(\frac{1}{\theta}\right) \qquad \text{with} \qquad \theta =\gg 1\,, \tag{2.6}$$

ii) The detonation structure is acoustically decoupled from the burnt gas flow so that, at the end of the reaction zone, the flow is sonic in the frame of reference attached to the "fire".

From Klein and Stewart [8], who presented a general set of front-attached coordinates suitable for the investigation of curved detonations, we extract the relevant system of governing equations here by specializing for one space dimension and keeping the terms indicating the time dependence of the detonation structure. The result is the following system of equations, which is equivalent to (2.1), but valid in the moving frame of reference:

$$\begin{aligned} \frac{\partial \rho}{\partial \tau} + \frac{\partial(\rho u)}{\partial n} &= 0 \\ \frac{\partial}{\partial \tau}(u + D) + u\,\frac{\partial u}{\partial n} + \frac{1}{\rho}\,\frac{\partial p}{\partial n} &= 0 \\ \frac{\partial E}{\partial \tau} + u\,\frac{\partial E}{\partial n} - \frac{p}{\rho^2}\left(\frac{\partial \rho}{\partial \tau} + u\,\frac{\partial \rho}{\partial n}\right) &= 0 \\ \frac{\partial \rho\lambda}{\partial \tau} + \frac{\partial(\rho\lambda u)}{\partial n} &= \rho w \end{aligned} \tag{2.7}$$

Here E is the the sum of thermal and chemical energy per unit mass of the gas mixture. The variables n and τ denote a spatial coordinate measuring the distance from the lead shock and the time variable, respectively.

For the following it is convenient to introduce the "Master Equation" (Klein and Stewart [8]) that may be used to replace the energy equation in (2.7):

$$\frac{1}{\rho}\,\frac{\partial p}{\partial \tau} - u\,\frac{\partial(u + D)}{\partial \tau} + (c^2 - u^2)\,\frac{\partial u}{\partial n} - c^2\,\sigma w = 0. \tag{2.8}$$

Here c is the local speed of sound and the thermicity parameter $c^2\sigma$ is related to the chemical energy Q via

$$c^2\sigma = (\gamma - 1)\,Q. \tag{2.9}$$

2.1.1 Induction zone analysis

Following standard procedures in large activation energy asymptotics for ignition type problems we first consider the solution in the induction region that immediately follows the leading shock front and introduce the expansions

$$D = D_{\mathrm{CJ}}\left(1 + \frac{1}{\theta}\,d^{\star}(\tau)\right) \tag{2.10}$$

for the lead shock velocity and

$$\underline{u} = \underline{u}_{\mathrm{VN}}^{CJ} + \frac{1}{\theta}\,\underline{u}^{(1)}(\xi, \tau) + O\left(\frac{1}{\theta^2}\right), \tag{2.11}$$

where

$$\underline{u} = (\rho, u, p, \lambda) \tag{2.12}$$

is the solution vector and

$$\xi = \theta\, n \tag{2.13}$$

is a stretched normal coordinate that resolves the induction zone. The scripts $^{CJ}_{VN}$ denote unperturbed post shock conditions.

Inserting this perturbation ansatz into the governing equations (2.7) – (2.9) we first find that all the time derivatives are negligible to leading and first order. Thus the system reduces to the steady state flow equations. As the explicit time dependence of the solution is now purely parametrical, one may use the reaction progress equation

$$\frac{\partial \lambda}{\partial \xi} = \frac{\hat{w}}{u} \tag{2.14}$$

in order to replace the normal coordinate ξ. Notice that

$$\hat{w} = w/\theta = O(1) \tag{2.15}$$

throughout the reaction zone in the present asymptotic large activation energy regime. Then the Master equation (Klein, Stewart [8]) reads

$$\frac{du^2}{d\lambda} = \frac{2(c^2\sigma)u^2}{c^2 - u^2}\,, \tag{2.16}$$

This is a closed form equation for either c^2 or u^2, provided one finds a functional dependence between u^2, c^2 and λ. For the quasi-onedimensional nozzle flow equations it is known that the total enthalpy is constant (see also Klein, Stewart [8]), i.e.,

$$H = \frac{c^2}{\gamma - 1} + \frac{u^2}{2} + Q\,(1 - \lambda) = \text{const} = \frac{\mathrm{D}^2}{2} + \mathrm{Q} \tag{2.17}$$

throughout the induction zone. Here we have used the fact that it is also constant across the lead shock and that $c^2 \approx 0, u^2 = D^2$ in the preshock state under the strong shock approximation. It is convenient (Klein et al. [6]) to solve for the perturbation C of c^2 in the induction zone in terms of the stretched progress variable

$$\Lambda = \theta\lambda. \tag{2.18}$$

One introduces

$$c^2 = c^{2\,\mathrm{CJ}}_{\mathrm{VN}} \left(1 + \frac{1}{\theta}\, C(\Lambda)\right), \tag{2.19}$$

and finds the following ODE for $C(\Lambda)$:

$$\frac{dC}{d\Lambda} = \alpha\,, \tag{2.20}$$

where

$$\alpha(\gamma) = \frac{3 - \gamma}{4(\gamma - 1)}\,. \tag{2.21}$$

The asymptotic expansion of the lead shock jump conditions yields

$$C(\Lambda = 0) = 2d^* \tag{2.22}$$

and the exact solution for $C(\Lambda)$ reads

$$C(\Lambda) = 2d^\star + \alpha\,\Lambda\,. \tag{2.23}$$

With $C(\Lambda)$ depending explicitly on the shock speed perturbation $d^\star$, we expect the induction length to vary nontrivially with time. The motion of the fire relative to the leading shock will introduce an inherently unsteady effect in the asymptotic solution of our problem and to determine its influence, we need to determine the induction length as a function of $d^\star$.

2.1.2 The induction length:
The induction length is the distance travelled by a mass element after it has been hit by the lead shock until it ignites and thus

$$l_I = \left| \int_{t_{sh}}^{t_{ign}} u\,dt \right|. \tag{2.24}$$

Using the expansion for the flow velocity u in the shock-attached frame from (2.11) and noticing that along a particle path one has

$$dt = \frac{d\lambda}{w} \tag{2.25}$$

according to the reaction progress equation $(2.7)_4$, we rewrite (2.24) as

$$l_I = |u_{VN}^{CJ}| \int_0^\infty \frac{d\Lambda}{\theta B\,(\exp(-\theta)\,\exp(C(\Lambda))}\,. \tag{2.26}$$

Inserting the exact solution for $C(\Lambda)$ from (2.23) one obtains

$$h(d^\star) = \frac{l_I}{l_I^{CJ}} = e^{-2d^\star}\,, \tag{2.27}$$

where the induction length for the undisturbed wave

$$l_I^{CJ} = \frac{u_{VN}^{CJ}}{\alpha\,\theta\,B\,\exp(-\theta)} \tag{2.28}$$

has been introduced.

Notice that the induction length depends on the detonation speed perturbation $d^\star$, which is varying nontrivially on the time scale considered. As a consequence, the induction length is changing too. In fact the order of magnitude of the velocity of the fire relative to the lead shock can be assessed to be

$$\dot{l}_I = l_I^{CJ}\,\frac{\partial h}{\partial d^\star}\,\dot{d}^\star = O\!\left(\frac{1}{\theta}\,D_{CJ}\right). \tag{2.29}$$

The estimate relies on the fact that we assume the time scale for changes of $d^\star$ to be given by $\theta l_I/D_{CJ}$. Thus we find that the motion of the fire in the shock frame corresponds to a first order velocity in terms of $1/\theta$ and we conclude that this motion will affect the asymptotic solution for the fire.

The induction zone solution exhibits a runaway as $\Lambda \to \infty$, since then $C(\Lambda)$ grows unboundedly and hence the perturbation expansion about the constant Chapman-Jouguet-von Neumann state becomes invalid. In the next subsection we will analyse the subsequent main reaction layer that is located in the immediate vicinity of the time dependent end of the induction zone. We will find that this main reaction region is quasisteady and that its structure is that of a weak deflagration. Assuming an acoustic decoupling of the reaction zone flow from the burnt gases, we impose sonic outflow from the fire to uniquely determine the solution.

2.1.3 The main reaction layer (fire)
In the main reaction layer the reaction rate becomes exponentially large in comparison with its magnitude in the induction zone. It is thus even more justified to seek a steady-state – or quasisteady – solution in a suitable reference frame. The onset of the rapid heat release occurs at the end of the induction zone, so that we may seek a quasisteady solution of the form

$$\underline{u} = \underline{u}^{(0)}(\theta(n + l_I)) + \frac{1}{\theta}\,\underline{u}^{(1)}(\theta(n + l_I)) + o(\frac{1}{\theta}) \tag{2.30}$$

with $\underline{u}$ as defined in (2.21). We expect the leading order solution not to depend on time, since the leading order induction zone solution is constant as well. The main reaction layer solution then satisfies the structure equation

$$\frac{d\tilde{u}^2}{d\lambda} = \frac{(c^2\,\sigma)\,\tilde{u}^2}{c^2 - \tilde{u}^2}\,, \tag{2.31}$$

where $\tilde{u}$ is the flow velocity in the fire frame. This is the master equation from (2.15) except for this change of the frame of reference. The exact leading order solution reads (Klein & Stewart [8]):

$$\tilde{u}^{(0)}(\ell) = -\frac{\gamma - \ell}{\gamma + 1}\,D_{\rm CJ} \qquad \text{where} \qquad \ell = \sqrt{1 - \lambda} \tag{2.32}$$

and one has

$$c^{2(0)}(\ell) = \frac{\gamma\,(1 + \ell)(\gamma - \ell)}{(\gamma + 1)^2}\,D_{\rm CJ}^2\,. \tag{2.33}$$

At first order one finds the perturbation equation for the velocity

$$\frac{du^{(1)}}{d\ell} = -2\ell\frac{c^2\sigma}{(c^2 - u^2)^{(0)}}\,u^{(1)} + \frac{2\ell}{D_{\rm CJ}}\,\frac{(c^2\sigma)\,u^{2(0)}}{(c^2 - u^2)^{(0)}}(c^2 - u^2)^{(1)}\,. \tag{2.34}$$

Now we seek the correct relation between $(c^2)^{(1)}$ and $(u^2)^{(1)}$, which should follow from the conservation of total enthalpy in the fire-frame: The total enthalpy (with respect to the fire frame) is defined by

$$\tilde{H} = \frac{c^2}{\gamma - 1} + \frac{\tilde{u}^2}{2} + Q\,(1 - \lambda) \tag{2.35}$$

and we have

$$\tilde{u} = u + \dot{l}_I\,. \tag{2.36}$$

Thus up to, but excluding, the second order in $1/\theta$ we have

$$\tilde{H} = \left[\frac{c^2}{\gamma - 1} + \frac{u^2}{2} + Q\,(1 - \lambda)\right] + \frac{1}{\theta}(u_{\rm VN}^{\rm CJ}\,\theta\dot{l}_I) = \frac{D^2}{2} + Q + \frac{1}{\theta}\,(u_{\rm VN}^{\rm CJ}\,\theta\dot{l}_I)\,. \tag{2.37}$$

where we use explicitly the constancy of the total enthalpy across the shock in the *shock-attached frame*. It follows that

$$(c^2 - \tilde{u}^2)^{(1)} = D_{\rm CJ}^2(\gamma - 1)\,\Delta c - (\gamma + 1)\,\tilde{u}^{(0)}\,\tilde{u}^{(1)}, \tag{2.38}$$

where

$$\Delta c = d^\star + \frac{u_{\rm VN}^{\rm CJ}\,\theta\,\dot{l}_I}{D_{\rm CJ}^2}. \tag{2.39}$$

We insert this in the perturbation equation for $\tilde{u}^{(1)}$ in (2.34) and find

$$\frac{d\tilde{u}^{(1)}}{d\ell} + \frac{\gamma}{\ell\,(\gamma - \ell)}\,\tilde{u}^{(1)} = -\frac{\gamma - 1}{\ell\,(\gamma - \ell)}\,\Delta c. \tag{2.40}$$

Next we impose the sonic boundary condition at the end of the reaction zone by requiring that $(c^2-u^2)^{(0)} = (c^2-u^2)^{(1)} = 0$ at $\ell = 0$. For the leading order solution, which corresponds to the plane wave Chapman-Jouguet solution, this is already satisfied. At first order we obtain

$$\tilde{u}^{(1)}\Big|_{(\ell=0)} = -\frac{\gamma-1}{\gamma}\Delta c\,, \tag{2.41}$$

where we have used that $\tilde{u}^{(0)}(0) = -\gamma/(\gamma+1)$. The exact solution is

$$\tilde{u}^{(1)} \equiv -\frac{\gamma-1}{\gamma}\,\Delta c = \text{const}\,. \tag{2.42}$$

This completes the computation of the first order main reaction layer solution.

Up to this point we have derived separate solution representations for the induction and main reaction regions and we are left with forcing these solutions to coincide in a suitable overlap region where the coordinate $\Lambda = \theta\lambda$ (from the induction zone) is large, while $\ell = \sqrt{1-\lambda}$ is close to unity. We will find that this overlap condition determines the correct value of the time derivative $\dot{l}_I$ of the induction length.

2.1.4 Matching and the wave speed evolution equation

The large $-\Lambda-$ representation of the flow velocity in the *shock frame* derived from the induction zone solution in section 2.1.2 is

$$\frac{u}{D_{\rm CJ}}\bigg|_{\rm ind}(\Lambda\to\infty) = -\frac{\gamma-1}{\gamma+1} - \frac{1}{\theta}\left\{\frac{\Lambda}{2(\gamma+1)} - \frac{2\gamma}{\gamma^2-1}\,2d^\star + \frac{\gamma+1}{\gamma-1}\,d^\star\right\}. \tag{2.43}$$

On the other hand, the main reaction layer solution for $\ell = \sqrt{1-\lambda} = 1 - 1/(2\theta)\ \Lambda + \ldots$ in an expansion for $\theta \gg 1$ reads, taking into account the change of reference frames,

$$\frac{u}{D_{\rm CJ}}\bigg|_{\rm MRL} = \frac{\gamma-1}{\gamma+1} + \frac{1}{\theta}\left\{-\frac{\Lambda}{2(\gamma+1)} - \frac{\gamma-1}{\gamma}\,\Delta c + \frac{\theta\,\dot{l}_I}{D_{\rm CJ}}\right\}. \tag{2.44}$$

Comparison of (2.43) and (2.44) yields the desired matching condition:

$$\frac{2\gamma}{\gamma^2-1}\left\{2d^\star - \chi d^\star\right\} = \frac{3\gamma-1}{\gamma(\gamma+1)}\,\frac{\theta\,\dot{l}_I}{D_{\rm CJ}}. \tag{2.45}$$

Using the explicit representation for $l_I(d^\star)$ in (2.27), we find

$$\frac{dh}{dt} = -\frac{2-\chi}{\psi(\gamma)}d^\star = -\frac{2-\chi}{2\psi(\gamma)}\ln h\,, \tag{2.46}$$

where

$$\psi(\gamma) = \frac{2\gamma^2}{(\gamma-1)(3\gamma-1)}\,. \tag{2.47}$$

This is the evolution equation announced in the introduction in (1.1) when curvature effects are absent, i.e., for $\kappa \to 0$. As discussed there, this equation describes either a collapse ($h \to 0$ in finite time) or a decomposition of the wave structure ($h \to \infty$ as $t \to \infty$ monotonously).

Here we have described the behavior of the detonation in the near-CJ regime and we have found that the wave will leave that regime as time evolves. Hence, the evolution equation found here is not closed in the sense that the solution leaves its regime of validity. In the collapsing mode the fire accelerates continously relative to the lead shock, while keeping its CJ-deflagration

structure. This acceleration leads to unbounded growth of the detonation speed perturbation function d^*. In the next section we consider the large amplitude continuation of this process and we will find that indeed there exists such a collapsing solution consisting of shock - induction zone - fire that evolves on a persistently shrinking time scale proportional to the ever shrinking induction length. We sketch the derivation of a nonlinear second order differential equation that describes this behavior.

3. LARGE AMPLITUDE ACCELERATIONS

In this section we derive an asymptotic solution to the unsteady equations in (2.1) – (2.3) for the reaction rate law

$$w = B\,(1-\lambda)\,\exp\!\left(-\frac{E_a}{RT}\right). \tag{3.1}$$

We assume that:

i) The detonation structure is acoustically decoupled from the burnt gas flow so that, at the end of the reaction zone, the flow is sonic in the frame of reference attached to the "fire",

and we consider a regime, where:

ii) Deviations of the lead shock velocity from the Chapman-Jouguet speed are large, so that

$$\frac{D - D_{CJ}}{D_{CJ}} = O(1)\,, \tag{3.2}$$

iii) time variations of the detonation speed are systematically slow measured on the *instantaneous* induction time scale,

$$t_I = (\ell_I/D)(\tau)\,,$$

where τ is a suitable, dynamically rescaled slow time variable defined by

$$\frac{\theta \ell_I}{D}(\tau)d\tau = dt \qquad \text{with} \qquad \theta(\tau) = \frac{E_a}{RT_{sh}(\tau)}\,. \tag{3.3}$$

The key idea will be to find detonation solutions that are inherently unsteady and consist of a coupled shock - fire structure, which itself is decoupled from the burnt gas flow through a sonic point at the end of the fire. Now, relaxing the requirement that the mass fluxes through fire and shock are identical (as in a stationary solution) one can construct unsteady accelerating solutions in which the mass burning rate in the fire exceeds the mass flux through the shock. In this situation only part of the heat release is used up to overcome the shock dissipation. The excess chemical power is available to accelerate the detonation. Hence, we seek solutions characterized by

1) A slowly accelerating (or decelerating) lead shock,
2) an induction zone whose length depends on the instantaneous shock strength and the unsteady changes induced by the acceleration,
3) a Chapman-Jouguet deflagration that burns the gas at the end of the reaction zone.

We outline in the rest of this paper the construction of these solutions by systematic matched asymptotics for large activation energy kinetics.

Using front-attached coordinates with the dynamic time rescaling from (3.3) and a distance coordinate that scales with the *current*, yet unknown induction length

$$\ell_I(\tau)\eta = x - x_{sh}(t)\,, \tag{3.4}$$

we are faced with the following system of balance equations:

$$\begin{aligned}
\frac{D}{\theta}\,\rho_\tau + (u - D\dot{\mathcal{L}}\eta)\,\rho_\eta + \rho\,u_\eta &= 0\\
\frac{D}{\theta}\,(u_\tau + \dot{D}(\tau)) + (u - D\dot{\mathcal{L}}\eta)\,u_\eta + \frac{1}{\rho}\,p_\eta &= 0\\
\frac{D}{\theta}\,(E_\tau - \frac{p}{\rho^2}\rho_\tau) + (u - D\dot{\mathcal{L}}\eta)\,(E_\eta - \frac{p}{\rho^2}\rho_\eta) &= 0\\
\frac{D}{\theta}\,\lambda_\tau + (u - D\dot{\mathcal{L}}\eta)\,\lambda_\eta &= \ell_{\rm I}(\tau)\,w
\end{aligned} \tag{3.5}$$

Here

$$\begin{aligned}
E &= \frac{1}{\gamma-1}\frac{p}{\rho} + Q(1-\lambda)\,,\\
u &= \tilde{u} - D\,,\\
\dot{\mathcal{L}} &= \frac{1}{\theta(\tau)}\,\frac{\dot{\ell}_{\rm I}}{\ell_{\rm I}}(\tau) = O(1)\,.
\end{aligned} \tag{3.6}$$

Before going into the details of the analysis, we outline the key idea of how to derive a detonation speed evolution equation: Having in mind the structure of a CJ-ZND detonation for large activation energy kinetics, which consists of a lead shock, an induction zone and a CJ-"fire", we seek dynamical solution with the same principal features. The lead shock velocity, however, is assumed to evolve on the instantaneous long time scale indicated in (3.3). It is followed by an induction zone, whose structure and length $\ell_{\rm I}$ remain to be determined and the structure is terminated by a CJ-deflagation that travels over the compressed post-shock state. The evolution equation for the lead shock velocity is obtained through the following steps:

1) Compute the post-shock state $[\rho_0, \tilde{u}_0, p_0](D(\tau))$ as a function of the instantaneous lead shock velocity $D(\tau)$, using the shock Hugoniot relations. (Recall that $\tilde{u}$ is the flow velocity in the laboratory frame!)
2) Compute the mass flux $\dot{m}_{\rm fire}$ through a CJ-deflagration that burns this compressed post-shock gas. This mass flux is then also a function of D. The velocity of this fire in the laboratory frame is
$$\dot{x}_{\rm fire}(D) = (\tilde{u}_0 + \dot{m}_{\rm fire}/\rho_{\rm sh})(D)\,. \tag{A}$$
3) Notice that the time change of the induction length obeys
$$\dot{\ell}_{\rm I} = D - \dot{x}_{\rm fire}(D) := \delta\ell(D) \tag{B}$$
and hence it can be expressed as a function of $D(\tau)$, too.
4) Compute, by activation energy asymptotics, the instantaneous induction length. The result, as we show in the next section, will be a relation
$$F(\ell_{\rm I}, \dot{\ell}_{\rm I}, D, \dot{D}) = 0\,. \tag{C}$$
5) Combine (B) and (C) to get first $F(\ell_{\rm I}, \delta\ell(D), D, \dot{D}) = 0$, but this is effectively an equation for the induction length as a function of D and $\dot{D}$:
$$\ell_{\rm I} = h(D, \dot{D})\,. \tag{D}$$
It follows, after time differentiation, that $D_0(\tau)$ satisfies the nonlinear second order differential equation (dropping the subscript for convenience)
$$\frac{\partial h}{\partial \dot{D}}(D,\dot{D})\,\ddot{D} + \frac{\partial h}{\partial D}(D,\dot{D})\,\dot{D} = \frac{d\delta\ell}{dD}(D)\,\dot{D}\,. \tag{E}$$

In the next sections we provide the key ingredients of the above calculations, but an evaluation of all the formulae and an analysis and solutions of the resulting equation in (E) will be left for a future publication.

3.1 Induction zone analysis

Following standard procedures in large activation energy asymptotics for ignition type problems we first consider the solution in the induction region that immediately follows the leading shock front. To this end, we introduce the expansions

$$\underline{U} = \underline{U}_{\rm sh}(D_0(\tau)) + \frac{1}{\theta}\,\underline{U}^{(1)}(\eta,\tau) + O\Big(\frac{1}{\theta^2}\Big), \tag{3.7}$$

for the flow variables

$$\underline{U} = (\rho, u, p, \lambda)\,. \tag{3.8}$$

In the expansion of the lead shock velocity,

$$D = D_0(\tau) + \frac{1}{\theta^2} D^{(2)} + \dots\,, \tag{3.9}$$

we suppress the first order term. The time evolution of the detonation velocity will be adjusted such that that a $D^{(1)}$ never occurs.

Inserting this perturbation ansatz into the governing equations in (3.5) we find that the leading order equations are satisfied automatically, while at first order the perturbations have to satisfy

$$\begin{aligned}
(u_{\rm sh} - D\dot{\mathcal{L}}\eta)\;\rho_\eta^{(1)} + \rho_{\rm sh}\;u_\eta^{(1)} &= -D\;\dot\rho_{\rm sh}(\tau)\\
(u_{\rm sh} - D\dot{\mathcal{L}}\eta)\;u_\eta^{(1)} + \frac{1}{\rho_{\rm sh}}\;p_\eta^{(1)} &= -D\;(\dot u_{\rm sh} + \dot D)(\tau)\\
(u_{\rm sh} - D\dot{\mathcal{L}}\eta)\;(E_\eta^{(1)} - \frac{p_{\rm sh}}{\rho_{\rm sh}^2}\rho_\eta^{(1)}) &= -D\;(\dot E_0 - \frac{p_{\rm sh}}{\rho_{\rm sh}^2}\dot\rho_0)\\
(u_{\rm sh} - D\dot{\mathcal{L}}\eta)\;\lambda_\eta^{(1)} &= \theta\ell_{\rm I}(\tau)\;w
\end{aligned} \tag{3.10}$$

where we have suppressed the subscript on D_0 for simplicity of notation and where the right hand side of the last equation must, by definition of the coordinates η and τ be of order unity (see below). Also notice that the lead shock is non-reactive, so that $\lambda_{\rm sh} \equiv 1$ and $\dot\lambda_{\rm sh} \equiv 0$.

The Arrhenius reaction rate law introduced in (3.1) involves the temperature as the major determining variable. Hence it is convenient to introduce the nondimensional temperature

$$T = \frac{p}{\rho} = T_{\rm sh}(\tau) + \frac{1}{\theta} T^{(1)}(\eta,\tau) + \dots \tag{3.11}$$

where obviously $T_{\rm sh} \equiv p_{\rm sh}/\rho_{\rm sh}$ and

$$T^{(1)} = \frac{1}{\rho_{\rm sh}}\,p^{(1)} - \frac{p_{\rm sh}}{\rho_{\rm sh}^2}\,\rho^{(1)}\,. \tag{3.12}$$

A lengthy elimination procedure based on (3.10) and (3.12) leads to the following single equation for $T^{(1)}$:

$$f_1(\eta;\tau)\;T_\eta^{(1)} - f_2(\eta;\tau)\;\big[\theta\ell_{\rm I}(\tau)\;Q\;w\big] = f_3(\eta;\tau)\,, \tag{3.13}$$

where the functions $f_i(\eta;\tau)$ are given by

$$\begin{aligned} f_1(\eta;\tau) &= \frac{1}{T_{sh}\,(\gamma-1)}\left\{u_*^2-\gamma\,T_{sh}\right\} \\ f_2(\eta;\tau) &= \frac{1}{T_{sh}}\left\{u_*^2-T_{sh}\right\} \\ f_3(\eta;\tau) &= D(\tau)\,\left[(\dot{u}_{sh}+\dot{D})-u_*\,\frac{\dot{\rho}_{sh}}{\rho_{sh}}-\frac{f_2}{u_*}\,(\dot{E}_{sh}-\frac{p_{sh}}{\rho_{sh}^2}\dot{\rho}_{sh})\right] \end{aligned} \tag{3.14}$$

where

$$u_*(\eta;\tau) = u_{sh}(\tau) - (D\dot{\mathcal{L}})(\tau)\,\eta\,. \tag{3.15}$$

The square bracket in (3.13) still contains the reaction source term which is now expanded in the following fashion:

$$\theta\,\ell_1\,Q\,w = \Lambda\exp(\frac{T^{(1)}}{T_{sh}})\,. \tag{3.16}$$

Here

$$\Lambda(\tau) = \theta(\tau)\,\ell_1(\tau)\,Q\,B\,\exp(-\theta(\tau)) \tag{3.17}$$

now appears as a parameter, which must be adjusted in such a way that the usual ignition thermal runaway of $T^{(1)}$ occurs at $\eta=-1$. This is to be required according to the definition of the induction zone coordinate η in (3.4) and will actually lead to the desired relation between $\ell_1, \dot{\ell}_1, D$ and $\dot{D}$ as announced above.

By inserting the expansion for the reaction term in (3.13) and reformulating for

$$\Phi = \exp(-\frac{T^{(1)}}{T_{sh}})\,, \tag{3.18}$$

as the unknown, we find the linear first order ODE problem in η

$$\Phi' + g_1(\eta)\,\Phi + \Lambda\,g_2(\eta) = 0\,, \qquad \text{with} \qquad \Phi(0;\tau) = 1\,, \tag{3.19}$$

where

$$\begin{aligned} g_1 &= \frac{f_3}{f_1}\,, \\ g_2 &= \frac{f_2}{f_1}\,, \end{aligned} \tag{3.20}$$

and where we have suppressed the τ-dependence for simplicity of notation. The initial condition for Φ follows from the expansion of the detonation velocity D in (3.9), which implies that there be no first order perturbations right behind the lead shock.

Formally, exact solutions to (3.19) can readily be written down and, given a solution family parametrized by Λ, one has to select the very value of this parameter that guarantees that $\Phi(1;\tau)=0$, which corresponds to a runaway of $T^{(1)}$ according to the definition of Φ in (3.18). This "eigenvalue" for Λ will depend on $D, \dot{D}$ and $\dot{\mathcal{L}}$ via (3.14) and (3.15), the latter being a function of $\dot{\ell}_1$, ℓ_1 and D according to $(3.6)_3$. This, combined with the definition of Λ in (3.17), yields the relation between $\ell_1, \dot{\ell}_1, D, \dot{D}$ as announced in statement (C) above.

What is left to do is to discuss the structure of the main reaction layer and show that its representation as a CJ deflagration running over the post-shock state is appropriate to the current order of approximation. Secondly, we will have to evaluate the shock and fire Hugoniot relations in order to manifest the function $\delta\ell(D)$ statement (B).

3.3 The main reaction layer (fire)

In the main reaction layer the reaction rate becomes exponentially large in comparison with its magnitude in the induction zone. It is thus even more justified to seek a steady-state – or quasisteady – solution in a suitable reference frame. The onset of the rapid heat release occurs in an extremely narrow layer near the end of the induction zone, where $\eta = -1$. The time scale for changes of the fire structure is dictated here by the slow time scaling introduced in (3.3), so that after introduction of a suitable rescaled space coordinate

$$\xi = \frac{1}{H(\theta)}(\eta + 1)\,, \tag{3.21}$$

with $H(\theta)$ being exponentially large in θ, the leading order solution in the fire is determined by the one-dimensional plane wave structure equations

$$\begin{aligned} (\hat{u}^{(0)}\rho^{(0)})_\xi &= 0 \\ \hat{u}^{(0)}\,\hat{u}^{(0)}_\xi + \frac{1}{\rho^{(0)}}\,p^{(0)}{}_\xi &= 0 \\ E^{(0)}_\xi - \frac{p^{(0)}}{(\rho^{(0)})^2}\rho_\xi &= 0 \\ \hat{u}^{(0)}\,\lambda^{(0)}_\xi &= \ell_1(\tau)\,w\,. \end{aligned} \tag{3.22}$$

Hence, the leading order solution does correspond to a plane steady deflagration in the "fire"-frame, characterized by $\eta \equiv -1$. The solution is uniquely determined be (i) the pre-deflagration pressure, temperature and fuel composition and (ii) by an additional constraint on the mass flux through the fire. Here we *assume* that this deflagration sees sonic outflow of the burnt gases in its own reference frame, so that it is a CJ-deflagration and guarantees that the shock - induction zone - fire structure decouples from the background flow.

Hence, as pointed out above, in order to describe the influence of the fire on the solution, we need to formulate in detail the CJ-deflagration Hugoniot-conditions to find the mass burning rate as a function of the post-shock state, or equivalently, as a function of the lead shock velocity.

3.4 Shock- and fire Hugoniot relations

The shock Hugoniot conditions can be extracted form any standard text book on gasdynamics. We recount them here, nevertheless, because the non-dimensionalisation introduced in section 2 is not usually used in text books and thus we prepare the jump relations for use in the present notation.

Let primes denote dimensional quantities and consider the dimensionless shock density and shock pressure

$$\begin{aligned} \rho^* &= \frac{\rho'_{\rm sh}}{\rho'_0}\,, \\ p^* &= \frac{p'_{\rm sh}}{p'_0}\,. \end{aligned} \tag{3.23}$$

Furthermore let

$$M^2 = \frac{D^2}{c_0^2} \qquad \text{with} \qquad c_0^2 = \gamma\frac{p_0}{\rho_0}\,, \tag{3.24}$$

be the shock Mach number. Then the standard text-book Hugoniot jump relations read

$$\begin{aligned} \rho^* &= \frac{(\gamma+1)M^2}{2+(\gamma-1)M^2}\,. \\ p^* &= \frac{2\gamma M^2}{\gamma+1} - \frac{\gamma-1}{\gamma+1}\,, \end{aligned} \tag{3.25}$$

These relations are re-written in the present non-dimensionalization as follows: First we have the scaled pre-shock pressure

$$\hat{p}_0 = \frac{p_0'}{\rho_0' {D_{\rm CJ}'}^2}\,, \tag{3.26}$$

and then

$$\begin{aligned} \rho_{\rm sh} &= \frac{(\gamma+1)}{(\gamma-1)+2\gamma\hat{p}_0/D^2}\,, \\ p_{\rm sh} &= D^2\left(\frac{2}{\gamma+1}-\frac{\gamma-1}{\gamma+1}\frac{\hat{p}_0}{D^2}\right)\,, \\ u_{\rm sh} &= -\frac{D}{\rho_{\rm sh}}\,. \end{aligned} \tag{3.27}$$

The post-shock velocity in the front-attached frame of reference has been derived by using the conservation of mass. This finishes the formulation of the shock Hugoniot conditions.

Now we consider the CJ-deflagration running over the state given by the shock conditions in (3.27). The mass flux through this flame, or rather the relative velocity between the fire and the mass elements in the post-shock state, can be expressed by a straight-forward, but very tedious calculation in the following fashion:

$$u_{\rm defl} := \frac{\dot{m}_{\rm defl}}{\rho_{\rm sh}} = \frac{\gamma-1+2\gamma\pi}{(\gamma+1)(1-\gamma\pi)}\,\sqrt{2(\gamma^2-1)Q} \tag{3.28}$$

where

$$\pi = \frac{2\gamma+(4\gamma-(\gamma-1)^2)q^*-(\gamma+1)\sqrt{q^*(4\gamma+(\gamma+1)^2q^*)}}{2(\gamma^2+2\gamma(\gamma-1)q^*)} \tag{3.29}$$

with

$$q^* = 2\frac{\gamma-1}{\gamma+1}\frac{Q}{p_{\rm sh}/\rho_{\rm sh}}\,. \tag{3.30}$$

The relations in (3.28) – (3.30) yield readily the desired fire velocity in the laboratory frame as expressed in statement (A) above as a function of $\rho_{\rm sh}(D), p_{\rm sh}(D)$ and the heat release parameter Q. In fact,

$$\dot{x}_{\rm fire} = D + u_{\rm sh}(D) + u_{\rm defl}(\rho_{\rm sh}(D), p_{\rm sh}(D), Q)\,. \tag{3.31}$$

or

$$\dot{\ell}_{\rm I}(D) = D - \dot{x}_{\rm fire} = -(u_{\rm sh}(D) + u_{\rm defl}(\rho_{\rm sh}(D), p_{\rm sh}(D); Q))\,. \tag{3.32}$$

This finishes the collection of formulae that are the ingredients of the second order nonlinear detonation dynamics equation as discussed at the beginning of this section.

Detailed evaluations of these formulas, suitable limit considerations for the near-CJ limit, for the passage through CJ conditions and for turning points in the evolution of $D(\tau)$, i.e., the analysis of acceleration - deceleration transitions and vice versa, will follow in a forthcoming publication. Here we have achieved our goal of outlining the construction of a detonation dynamics equation that relies on no mre and no less than a large activation energy limit analysis and the assumption of slow evolution on the instantaneous ignition delay time scale as expressed in (3.3).

4. SUMMARY AND CONCLUSION

In this paper we propose a large amplitude theory for the dynamics of detonation waves based on large activation energy asymptotics. Assuming the detonation structure to evolve on a timescale that is systematically by one order larger, in terms of the activation energy, than the instantaneous induction time, we arrive at a nonlinear second order evolution equation for the detonation shock velocity D:

$$\frac{\partial h}{\partial \dot{D}}(D,\dot{D})\,\ddot{D} + \frac{\partial h}{\partial D}(D,\dot{D})\,\dot{D} = \frac{d\delta\ell}{dD}(D)\,\dot{D}\,. \tag{4.1}$$

Here $h(D, \dot{D})$ is essentially the instantaneous induction length and a dot indicates a derivative with respect to the scaled time variable τ defined by the differential relation

$$\frac{\theta \ell_I}{D}(\tau) d\tau = dt \qquad \text{with} \qquad \theta(\tau) = \frac{E_a}{R T_{sh}(\tau)} . \tag{4.2}$$

Here E_a, T_{sh}, R, ℓ_I are the activation energy of the Arrhenius reaction rate law considered, the instantaneous post-shock temperature, the instantaneous induction length and the gas constant, respectively. We have outlined here the key ideas in deriving this equation. Detailed analyses of the function $h(D, \dot{D})$, which is the result of an involved induction zone analysis, and of the associated features of the equation in (4.1) will be reserved for future work.

We are aware that the assumption of a slow time evolution is a severe one, considering the chaotic instability of large activation energy detonations. Nevertheless, we believe that the present considerations should be taken seriously, because of the following fact: Any fast time stability theory based on a *steady state* solution might be erroneous, because the true background long time behavior may follow the slow-time dynamics described here. It would be interesting to study fast time perturbations that evolve *on top of* the large amplitude dynamical modes obtained here.

Also, we emphasize that in the present theory the "fire" moves relative to the lead shock of the detonation with a speed comparable to the detonation speed itself! Hence, the time of collapse is comparable to the passage time of a particle through the induction zone. We conclude that the present dynamical modes, due to the strong nonlinearity of the induction chemistry, override any evolution that would rely on a single time scale based on the induction length for a specific detonation strength. In fact, the evolution described here involves a highly nonlinear dynamical time rescaling so that the true characteristic time of evolution shrinks rapidly as the wave accelerates.

REFERENCES

[1] Abuseif G.E., Toong T.Y., "Theory of Unstable Onedimensional Detonations", *Comb. & Flame* **45** (1982) 67–94

[2] Bourlioux A., Majda A.J., "Theoretical and numerical structure of twodimensional detonations", *Comb. & Flame* **90** (1992) 211–229

[3] He L., Clavin P., "Stability and Nonlinear Dynamics of One-Dimensional Overdriven Detonations in Gases", submitted to *J. Fluid Mech.* January (1995)

[4] Klein R., "Curved Detonations in Explosive Gas Mixtures with High Temperature Sensitivity ", Intl. Conf. on Combustion, 80th Birthday Memorial for Ya.B. Zeld'dovic, Moskau, June 1994

[5] Yao J., Stewart D.S., "On the normal shock velocity-curvature relationship for materials with large activation energy", *Comb. & Flame* (1994) to appear

[6] Klein R., Krok , Shepherd J.E., "Investigation of Curved Quasisteady Detonations Using Asymptotic Analysis and Detailed Chemical Kinetics", to be submitted (1995)

[7] Buckmaster J., "Pressure Transients and the Genesis of Transverse Shocks in Unstable Detonations", *Comb. Sci. & Technol.* **61** (1988) 1–20

[8] Klein R., Stewart D.S., "The relation between curvature, rate state dependence and detonation velocity", *SIAM J.Appl.Math.* **53** (1993) 1401–1435

Questions - Answers, Comments

Borisov - Klein *Comment*

I would like to comment the calculation results as an experimentalist. The detonation arises in a shocked gas as an essentially three-dimensional process, that is due to self-ignition of a region with an ignition delay gradient. The ignition delay gradient is a prerequisite of fast development of detonation. In most cases this transition does not show overdrive (at least as the velocity measurements demonstrate), the overdriven wave arises only when the detonation wave catches up with the lead shock wave. The behaviour of the overdriven wave formed at this instance should depend on the prehistory of the reactive wave which reaches the leading shock wave, because it is not necessarily a well developed steady-state detonation wave and may have different profiles of the parameters behind its front. This means, depending on the various factors, the overdriven wave either decays from the beginning or may move at a rising velocity until the effect of the rear rarefaction wave (due to the finite size of the exploding volume) becomes dominant and kills the detonation wave (due to losses).

A : I agree with almost all of your comments. Let me reiterate that I consider the galloping detonation as a 3-stage process : 1) Built-up of a strong spike near the end of the reaction zone, which forms a detonation in the shocked gas. This phase, I have not discussed in the lecture due to a lack of time. I called it, "Recovery Phase", and it corresponds to the scenario you are describing.
2) Acceleration phase, which establishes after the "detonation in the shocked gas" has caught up with the lead shock and generates a wave with $D>D_{CJ}$. From here on, the accelerating collapsing mode of my lecture is active.
3) Slow down of the acceleration and achievement of a maximum of the shock speed and final decay of the lead shock due to the action of the expansion in the burnt gases.
4) back to 1).

You state that the behavior of the "overdriven" wave after the detonation in the precompressed gas has caught up with the lead shock should depend on the prehistory. - I claim that that is not necessaryly so, if the wave locks on to the collapsing - decoupled - mode I was describing. In fact, it will then be independent of the prehistory ! (at least until the acceleration phase is over again).

Clavin - Klein :

Q : When you start your unsteady analysis around the CJ solution you assume a large ratio of the intrinsic evolution time to the induction time, of the order of magnitude of the large reduced activation energy. In our recent unsteady analysis this ratio is found to be of order unity and the obtained results are very different than yours at least close to the CJ solution. When the time goes on your non linear solution experiences evolution on a much shorter time scale. Could you comment this ?

A : Yes, I first discovered the collapsing mode with a shock-induction zone - fire complex that is acoustically decoupled from the burnt gas flow in a near - CJ analysis. Near the Chapman - Jouguet regime, the lead shock and the "fire" move at speeds sastisfying $D_{fire} = D_{CJ} + \mathbf{O(\Theta^{-1})}$, so that the shock - fire distance changes very slowly on the time scale of $\Theta\ l_I^{CJ} / D_{CJ}$. In this regime, the theory neglects, indeed, the dynamics on the shorter time scale l_I^{CJ} / D_{CJ}. - Yet, at larger amplitudes, when $(D - D_{CJ}) / D_{CJ} = O(1)$, the fire velocity satisfies $(D_{fire} - D) / D = O(1)$, so that changes of the induction length occur on the time scale $l_I / (D_{fire} - D) = O(l_I / D)$. This is the same time scale that you observe in your analysis.

Importantly, I emphasize that the theory presented is valid only for very large differences between the induction length and the main reaction layer (fire) thickness and that I consider the galloping detonation as a 3 - stage - process that I repeat here :

1) Formation of a pressure spike near the end of the induction zone, which catches up with the lead shock and produces a wave with $D > D_{CJ}$.

2) Acceleration phase, described by the theory presented in this lecture. (collapsing mode, decoupled from the burnt gas flow).

3) Stopping / Slowing-down of the collapse by new effects due to the fact (most likely), that the main reaction layer is often times not as sensitive to temperature as the induction length, so that for D large enough, $l_{MRL} \backsimeq l_I$ and unsteady effects in the main reaction layer must be accounted for.

---> slow-down and decay of the lead shock due to the effect of the strong expansion in the burnt gases.

4) Back to 1). Thus, I do not claim that the theory presented here describes correctly the phenomena when $D \simeq D_{CJ}$. It is appropriate only during the acceleration stage, where $D > D_{CJ}$.

Davis - Klein :

Q : Does your approach explain the return to stability in overdriven detonation ?

A : The approach is based on a square-wave model with an infinity thin reaction zone. This model is always unstable. To find out the stability limit given by the direct numerical simulations for overdriven detonation[1], the thickness of the reaction zone must be taken into account. Our recent theoretical analysis[2] show that it is the unsteadiness effect in the reaction zone that stabilizes the detonation front.

1. Fickett, N. and Davis, W.C. Detonation 1979

2. Ke,L. and Clavin, P. to be published 1994.

Oran - Klein : *Comment* What do you believe is the interlay beween the 1D longitudinal instability and the multidimensional structure of detonation ? For regular cell structure the size of the longitudinal instability is relatively small. In any cases, the longitudinal instability could provide a perturbation of the front.

JOURNAL DE PHYSIQUE IV
Colloque C4, supplément au Journal de Physique III, Volume 5, mai 1995

Spontaneous Localization of Vibrational Energy

D.W. Brown and L. Bernstein*

Institute for Nonlinear Science, University of California, San Diego La Jolla, CA 92093-0402, U.S.A.
** Department of Mathematics, Box 8085, Idaho State University, Pocatello, ID 83209-8085, U.S.A.*

ABSTRACT --- In this paper we illustrate a number of the characteristic manifestations of soft anharmonicity in the behavior of lattice vibrations, both in and out of thermal equilibrium. In particular, we focus on various ways in which vibrational energy may come to be localized as a consequence of anharmonicity, even in defect-free lattices. These include the "overpopulation" of anharmonic vibrations in thermal equilibrium, the inhibition of dispersion, and the enhancement of spatial coherence. The relevance of the spontaneous localization of vibrational energy in the formation of "hot spots" is discussed, with particular emphasis on the unstable evolution of high-amplitude initial conditions as may be found in initiating shocks.

Research is what I'm doing when I don't know what I'm doing. -- *Werner von Braun*

1. INTRODUCTION

The process of detonation is remarkable in part because of its strong linkage of microscopic events and macroscopic dynamical effects. This cascade across space and time scales has as one of its consequences that no one scientific discipline embraces the phenomenon in its entirety. This paper is addressed to the anharmonic behavior of crystal vibrations in the initiation phase of detonation, defined as the interval between the delivery of a low-amplitude shock into virgin material and the later development of a steady-state detonation front. The phenomenon of greatest interest here is the localization of vibrational energy, particularly whether such localization may facilitate the initiation of chemistry that may ultimately support detonation. While it is possible that such localization may also be involved in the steady-state propagation of the detonation front, the strong role of chemistry in the steady-state problem suggests at least that the space-time interval in which anharmonic vibrational effects may be distinguishable *as such* may be strongly reduced relative to the initiation phase.

In a general sense, the subject to be developed here may be associated with the established concept of "hot spots"; however, it is important to emphasize an essential distinction between the usual conception of hot spots and that of anharmonic localization. While many implementations of the idea could be enumerated, the established concept of hot spots is almost universally associated with material defects that become superheated when stressed by an impinging shock. Though explosive sensitivity is strongly influenced by inhomogeneities of diverse origins, crystalline or nearly defect-free energetic materials are also found to be detonable, albeit at elevated shock pressures. This suggests that even in homogeneous materials processes exist that may be capable of achieving significant energy localization under the influence of a sufficiently energetic drive. This is precisely the nature of soft anharmonic vibrations.

A vibration may be characterized as soft (hard) if the vibrational frequency decreases (increases) with increasing amplitude. In quantum-mechanical terms, a soft (hard) vibration is one whose energy level spacing decreases (increases) with increasing vibrational quantum number. These characterizations apply

equally to symmetric potentials as we use in this paper, or to asymmetric potentials such the Morse or Lennard-Jones [1]. In the case of vibrations whose potentials are symmetric with respect to the equilibrium amplitude, a soft (hard) vibration is one whose potential increases more slowly (rapidly) with increasing amplitude than does the harmonic reference potential describing small oscillations in the same oscillator. These characterizations may change as a function of amplitude; consider, for example, an oscillator whose potential first increases more slowly than harmonic, but which later increases more rapidly than harmonic. For the smooth potentials characteristic of mechanical equilibria, such changes the character of the anharmonicity occur only above some finite amplitude, such that a vibration may be characterized uniquely as soft or hard depending on the *leading* anharmonic correction at low amplitudes; it is this characterization that we apply throughout this paper.

2. THERMODYNAMICS

It will be useful in the following to consider the anharmonic oscillator described by the Hamiltonian

$$H = \frac{1}{2}\dot{x}^2 + \frac{1}{2}x^2 - \frac{\varepsilon}{4}x^4 ; \tag{1}$$

for soft anharmonicity, $\varepsilon > 0$. (It is well to note that this oscillator is thermodynamically unstable, since the potential is unbounded below as $|x|$ increases beyond $x_c = \varepsilon^{-1/2}$, and should be handled with care when used in more than a qualitative sense.)

The equipartition theorem in its general form [2] reads

$$\langle \dot{x}\frac{\partial H}{\partial \dot{x}} \rangle = \langle x\frac{\partial H}{\partial x} \rangle = k_B T . \tag{2}$$

Using the anharmonic oscillator Hamiltonian (1), this yields

$$\langle H \rangle = k_B T + \frac{\varepsilon}{4}\langle x^4 \rangle , \tag{3}$$

which indicates that the equilibrium expectation value of the total energy of a soft anharmonic oscillator exceeds that of a harmonic oscillator. This qualitative conclusion does not depend on the frequency of the harmonic oscillator used for comparison, nor on the degree of freedom underlying the vibration, since all harmonic oscillators in equilibrium at the same temperature share the same energy expectation value. Consequently, we may conclude that any soft anharmonic oscillator will equilibrate to an average energy higher than that of any harmonic oscillator at the same temperature.

The magnitude of this excess is not necessarily large, of course. Clearly, the magnitude of this disparity increases with the strength of the anharmonicity, but for the same value of the anharmonicity (e.g., the same ε), the expected value of the higher moments (e.g. $\langle x^4 \rangle$) will be larger in oscillators having lower frequencies at low amplitude (see below). This suggests that we may expect anharmonicity-driven concentrations of energy to be most pronounced among the lowest-lying vibrational modes of a complex system.

It is well to note that because the principal effect of an impinging shock is to promptly compress material passing under it, energy is first delivered into low-lying vibrational modes associated with volumetric compression; these include the acoustic modes associated with translations of the center of mass of a unit cell, librational modes associated with rigid-body rotations of principal unit cell constituents, and the lowest-lying optical modes associated with relative translations of unit cell constituents. The remaining modes of vibration are associated more essentially with deformations of individual molecules, and being generally substantially higher in frequency, couple less effectively with shocks. (For cautionary observations in this regard, see e.g. Ref. [3].)

Sufficiently far behind the shock, we may assume the material to come to equilibrium at a temperature substantially higher than that of the unshocked material. Under such conditions, the intrinsic anharmonicity of *any* vibration should be more pronounced, with the strongest anharmonic effects evident in the

low-lying vibrations.

In the following, we make use of the notion of a "reference oscillator", by which we mean a hypothetical harmonic oscillator in the same degree of freedom as the anharmonic oscillator in question, such that the frequency of this harmonic oscillator matches the frequency of the anharmonic oscillator at small amplitudes. This allows us to focus on the manner in which the properties of anharmonic oscillators deviate from the harmonic ideal. In such comparisons, quantities associated with anharmonic oscillators are decorated with tildes (e.g., $\tilde{V}$), while harmonic reference quantities are decorated with zeros (e.g., V_0) to indicate that the anharmonicity has been set to zero. Moreover, for simplicity we explicitly consider only vibrational potentials symmetric about the equilibrium.

Since the potential of a soft anharmonic oscillator is less than or equal to that of the harmonic reference oscillator at all amplitudes ($\tilde{V}(x) \leq V_0(x)$), it is evident that the partition function $\tilde{Q}$ of an anharmonic oscillator should be greater than the partition function Q_0 of the harmonic reference oscillator at all temperatures; i.e.,

$$\tilde{Q} = \iint e^{-[\frac{1}{2}p^2 + \tilde{V}(x)]/k_B T}\, dp\, dx \;\geq\; \iint e^{-[\frac{1}{2}p^2 + V_0(x)]/k_B T}\, dp\, dx = Q_0 . \tag{4}$$

Consequently, the free energy of the soft anharmonic oscillator

$$\tilde{A} = E - TS = -k_B \ln Q \tag{5}$$

is lower ($\tilde{A} < A_0$), and (using the equipartition result) the entropy and specific heat higher ($\tilde{S} > S_0$, $\tilde{C}_v > C_v^0$) than in the harmonic reference oscillator.

From such considerations we may draw some conclusions regarding energy fluctuations. The variance of the total energy in thermal equilibrium is related to the specific heat by the relation

$$\langle \Delta E^2 \rangle = k_B T^2 C_v . \tag{6}$$

In view of the equipartition theorem, we may conclude that the normalized variance of the total energy of a single harmonic oscillator at thermal equilibrium is equal to unity

$$\frac{\langle \Delta E_0^2 \rangle}{\langle E_0 \rangle^2} = 1 . \tag{7}$$

On the other hand, the normalized energy variance for our anharmonic oscillator is given by

$$\frac{\langle \Delta \tilde{E}^2 \rangle}{\langle \tilde{E} \rangle^2} = \left[1 + \frac{\varepsilon}{4k_B}\frac{\partial \langle x^4 \rangle}{\partial T}\right]\left[1 + \frac{\varepsilon}{4k_B}\frac{\langle x^4 \rangle}{T}\right]^{-2} > 1 . \tag{8}$$

Expanding the partition function in orders of the anharmonicity parameter ε, we may compute $\langle x^4 \rangle$ approximately as

$$\begin{aligned} \langle x^4 \rangle &\approx \langle x^4 \rangle_0 + \frac{\varepsilon}{4k_B T}[\langle x^8 \rangle_0 - \langle x^4 \rangle_0^2] + O\{\varepsilon^2\} \\ &\approx 3(k_B T)^2 + 24\varepsilon(k_B T)^3 + O\{\varepsilon^2\} , \end{aligned} \tag{9}$$

in which the zero subscript indicates the thermal expectation value in the absence of anharmonicity. From this one may show that the normalized energy variance is greater than unity in the soft anharmonic case, indicating that relative to harmonic oscillators, the energy fluctuations of soft anharmonic oscillators are marked by "higher highs" and "lower lows", or a relative preponderance of high energy fluctuations.

3. DUTY CYCLE AND DISSIPATION

The duty cycle of an oscillation is the ratio of the fractions of a cycle that the oscillator spends in two essentially exclusive states; for example, a square wave may be "on" for one third of a cycle and "off" for

two thirds, for a duty cycle of 1:2. For our purposes, it is useful to consider as exclusive states the conditions that the energy of an oscillation reside a) primarily in the kinetic form, or b) primarily in the potential form. For harmonic oscillators, the energy spends equal times in the two forms, for a duty cycle of 1:1. For soft anharmonic oscillators, the period of oscillation is greater than that of the reference harmonic oscillator, and most of this increase is accounted for by a lengthening of the time that the energy spends in the potential form. This leads to a duty cycle of 1:1+η, where η is a measure of the lengthening of the period due to anharmonicity.

The duty cycle affords a dynamical understanding of our previously-obtained equipartition result. Since the kinetic energy of both harmonic and anharmonic oscillators is a quadratic degree of freedom, the equipartition theorem requires that both harmonic and anharmonic oscillators have the same average kinetic energy. However, since the energy of soft anharmonic oscillators spends relatively more time in the potential form than is the case for harmonic oscillators, the equality of the average kinetic energies forces an inequality of the average total energies such that the greater average energy is found in the soft anharmonic oscillator.

The duty cycle also allows some conclusions to be drawn regarding dissipation. Using the Langevin approach, one may model the dynamics of an oscillator in contact with a heat bath by the equation

$$\ddot{x} = -\frac{\partial V}{\partial x} - \gamma \dot{x} + f(t), \tag{10}$$

in which γ represents the dissipation and $f(t)$ is a zero-centered stochastic force. This implies that energy drains from the oscillator according to

$$\dot{E} = -2\gamma(\textit{Kinetic Energy}) + \dot{x} f(t). \tag{11}$$

Thus, in the case of a freely decaying oscillation ($f(t) \approx 0$), the energy drains nonuniformly in time, and primarily during that fraction of the cycle in which the energy resides primarily in the kinetic form. Since soft anharmonicity extends the time that an oscillator's energy resides in the potential form, we may conclude that softened oscillations decay more slowly than corresponding harmonic oscillations. Since the low amplitude oscillations of a soft oscillator are quite harmonic, we may conclude as well that low amplitude oscillations of a soft oscillator decay more rapidly than do high amplitude oscillations in the *same* oscillator. This suggests a relative preponderance of high energy fluctuations in soft oscillators, consistent with the thermodynamic computation of the energy variance in the preceding section.

All of the foregoing considerations point to a notion of "statistical localization"; that is, that there exists a thermodynamic gradient for concentrating energy in anharmonic vibrations. This concentration may occur spatially if, for example, an anharmonic impurity is embedded in a lattice of harmonic oscillators. Or, in the absence of impurities it may create disparities between classes of modes if, say, librational modes are rich in anharmonicities while acoustic modes (say) are not. Even in our case study of a single soft anharmonic oscillator, we find a tendency for high-energy fluctuations to be damped less vigorously than low-energy fluctuations, resulting in a relative persistence of high-energy fluctuations, allowing one to think of energy localization as occurring in *time* [4].

4. SPATIAL COHERENCE AND THE SOLITON CONCEPT

The localization of energy in time, that is, the anomalous frequency and/or persistence of high energy states, is one factor in promoting the initiation of chemistry as in the hot spot concept; another important factor, however, is the localization of energy in space. The kind of localization discussed to this point could occur in a meaningful way without exhibiting any spatial coherence whatever; e.g., two oscillators that in a random interval of time happen to undergo similar high energy fluctuations might be nearest neighbors or might be widely separated in space. Particularly in energetic materials, quite different consequences might be expected to result if high energy fluctuations were randomly distributed in space or were correlated so as to occur preferentially in a more limited domain.

While there are many ways that energy concentrations may be achieved in the neighborhood of defects,

particularly in non-equilibrium situations such as as the initiation phase of detonation [5,6], we focus here on mechanisms that may support the maintenance of spatial coherence in homogeneous materials.

The most elementary interaction between neighboring oscillators is the harmonic one, as in

$$H\{\dot{x},x\} = \sum_n \left[\frac{1}{2}\dot{x}_n^2 + \frac{c^2}{l^2}(x_n - x_{n-1})^2 + V(x_n) \right], \tag{12}$$

giving rise the propagation of energy through space. In absence of a potential $V(x)$, this represents acoustic vibrations in which c is the speed of sound. The effect of the nearest-neighbor interaction is to drive neighboring oscillators toward the same phase, and thus to establish coherence on the smallest spatial scale. Dynamically, this local drive toward spatial coherence has the effect of dispersing any localized energy distribution, since such a distribution constitutes a deviation from perfect alignment. Thus, the main dynamical consequence of building spatial coherence in vibrational systems is *dispersion.*

Thus we have the tendency of soft anharmonicity to concentrate energy without regard to spatial coherence, and the tendency of spatial coherence to lead to the dispersion of energy. Since these opposing tendencies coexist in the same dynamical system, it is reasonable to expect optimal solutions to achieve some degree of balance between them. Indeed this is the case, and it is this physical need to balance anharmonic focusing against dispersion that gives rise to the concept of solitary waves, and their idealization in the concept of the soliton [7-11]. The relevance of the concept does not depend on the validity of the ideal, however. Figure 1 shows harmonic and anharmonic systems initialized with the same Gaussian pulse in their initial amplitudes. The pulse in the harmonic chain disperses quickly, reaching the (periodic) boundary in just a few frames of this particular "movie". On the other hand, the pulse in the anharmonic chain resists dispersion, retaining its integrity many times longer than in the harmonic case. Though the parameters for this illustration were chosen to make an interesting presentation, it should be noted that nothing about this illustration approaches the soliton ideal; the Gaussian initial condition does not correspond to any soliton solution, the relatively short, discrete chain does not approximate the continuum or infinite-size scenarios typical of soliton systems, and the "leakage" apparent in this solution, albeit small and slow, reflects the non-ideality of the represented phenomenon [12-15].

It is worth noting that the slowly-decaying localized excitation in Figure 1 undergoes a kind of "breathing" motion suggestive of internal modes. This is a general characteristic of soliton-like states that is related to their enhanced lifetimes and dynamical stability; within limits, such anharmonic excitations respond flexibly to perturbations, transiently deforming during interactions with other excitations or defects such that the integrity of the soliton-like state is approximately preserved.

5. PHONONS VS. SOLITONS

"Phonon", as commonly used, denotes a quantum of vibrational energy in any of the normal modes of vibration of an extended medium. ("Phonon" is sometimes reserved for acoustic phonons, and other terms such as "libron" and "vibron" used to denote the quanta of other classes of vibration, but we ignore such distinctions here.) Implicit, however, are a few additional qualifiers; for example, though in principle normal modes can be found for defective crystals, one often restricts "phonon" to the normal modes of perfect crystals, and describes defect effects in terms of phonon-phonon scattering mediated by defects. Moreover, "normal modes" usually implies the harmonic approximation, leaving anharmonic effects to be described in terms of multi-phonon scattering and the finite lifetimes for phonons this implies [5,16,17].

"Solitons" may be viewed as the particle-like subset of the *nonlinear* normal modes of an extended anharmonic system, usually in a classical or semiclassical approximation. Again, some qualifiers are in order. The notion of nonlinear normal modes is exact only for completely integrable systems, and relatively few anharmonic systems of practical interest are completely integrable. Nonetheless, it can be meaningful to regard a practical system as being "nearly" integrable, and to characterize its non-integrability through "scattering" interactions between the nonlinear normal modes (including solitons) of the nearby integrable system, leading to imperfect soliton behaviors including finite soliton lifetimes [18-20].

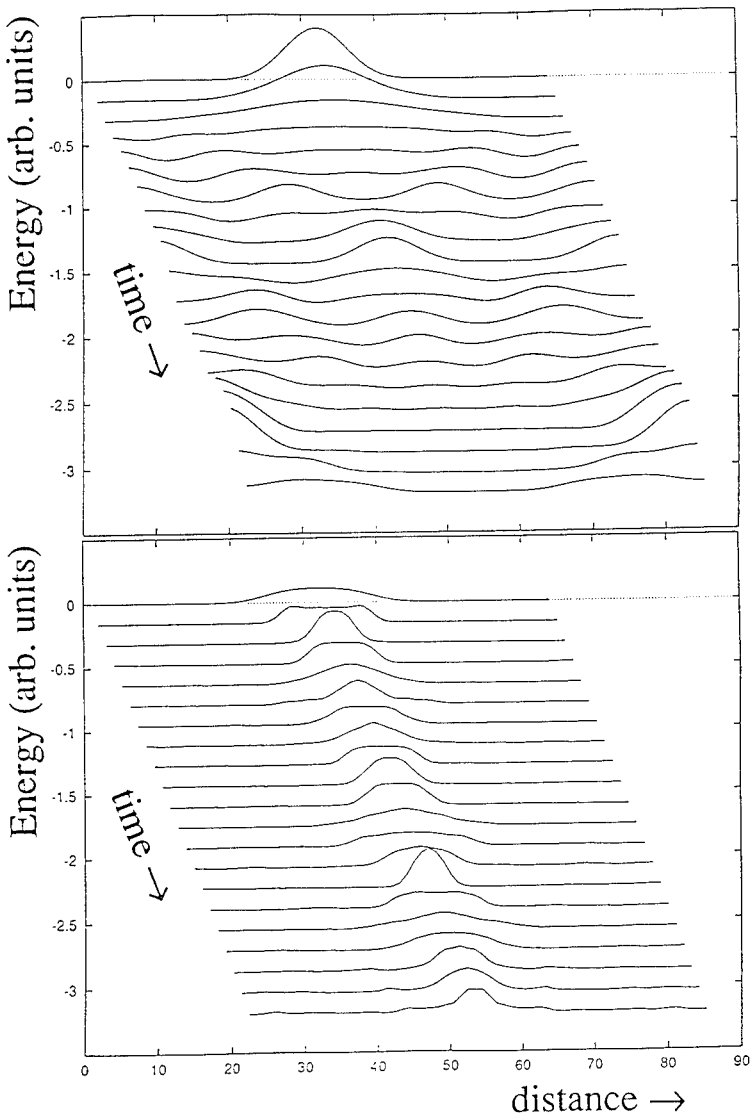

Figure 1. Evolution of identical Gaussian initial conditions in the oscillator amplitudes at zero temperature. Upper panel, harmonic; lower panel, anharmonic. Note that the initial energy profile is different in the two cases; this is because the initial energy is entirely in the potential form, which for a given oscillator amplitude is lower in the anharmonic system than in the harmonic system.

Since most practical scenarios are not perfect fits to either the phonon or soliton picture, it is well to understand what is to be gained by using the generally more-complicated soliton picture. The essential limitation of the phonon picture is that accounting for anharmonic effects by multi-phonon scattering tends to lose information relating to the phonon-phonon coherences such as are involved in the localization of vibrational energy. In the soliton picture, the anharmonicity may be viewed as being separated into a part associated with a "nearby" completely integrable soliton-supporting system and the remainder of the anharmonicity treated as a perturbation, though in a manner that is generally much more complex than in the phonon picture. The advantages are that the soliton picture is well-suited to the description of coherence effects, and the size of the remaining scattering perturbation is smaller than in the phonon picture.

6. THERMAL EQUILIBRIUM SIMULATION

For simulating anharmonic lattices at finite temperature, we need to choose an anharmonic potential that does not suffer the instabilities noted in Eqn. (1). For simplicity, we choose a symmetric potential having a unit frequency at small amplitude, but that saturates monotonically to a constant as $x \to \pm\infty$

$$V(x) = \frac{x^2}{2+\varepsilon x^2} = \frac{1}{2}x^2 - \frac{\varepsilon}{4}x^4 + O\{\varepsilon^2\} . \tag{13}$$

(The first two terms in the Taylor series expansion of this potential are the same as in Eqn. (1).) The system is otherwise as indicated in Eqn. (12), and is simulated using Langevin terms as in Eqn. (10), following Heun's method [21,22]. Each simulation begins with a warm-up phase, during which the system is warmed to the desired temperature from a zero-temperature initial state. Measurement begins only after thermal equilibrium diagnostics fall within required tolerances.

The results of such simulation are quite different from the zero-temperature example of Figure 1. Typical out-takes from thermal equilibrium simulations of both harmonic and anharmonic systems are shown in Figure 2. The outstanding characteristic of these simulations is that the difference between the harmonic and anharmonic simulations is *not* dramatic; it is difficult with the naked eye and a common vocabulary to characterize the differences in texture. One may say that the energy density in the anharmonic simulation is generally more smooth, and marked by a smaller number of high energy excursions that are generally more broad in space; i.e., the anharmonic simulation displays more spatial coherence.

We can be more objective in our characterization by constructing an energy correlation function:

$$C_n = \left[N \left\langle \sum_m E_m E_{m+n} \right\rangle\right]\left[\left\langle \sum_m E_m \right\rangle\right]^{-2} , \qquad \sum_n C_n = N . \tag{14}$$

In the absence of any spatial coherence, this should consist of a central spike above a uniform background

$$C_n = \delta_{n0}\frac{N(C_0-1)}{N-1} + \frac{N-C_0}{(N-1)} . \tag{15}$$

Any deviation from this form indicates the existence of spatial coherence. The result of computing this correlator for the two scenarios of Figure 2 are shown in Figure 3. The result of this computation affirms quantitatively that soft anharmonicity is responsible for an increased spatial coherence in the fluctuating energy density typical of thermal equilibrium.

The contrast between the strong effects shown in Figure 1 and the weak effects shown in Figures 2 and 3 contains and important message. It is often possible to construct long-lived localized excitations in the zero-temperature limit of systems of soft anharmonic oscillators; these excitations tend to decay rapidly at elevated temperatures, however, because strong spatial coherence generally exacts a high cost in entropy that at finite temperatures strongly suppresses the probability of their occurrence.

7. RESPONSE TO SHOCK

The nature of the microscopic response of materials to the passage of a shock front is known only in a rough sense, and primarily in terms of thermodynamic constraints. The nature of the dynamic response on the molecular scale is essentially unknown, and so it is necessary to work from reasonable hypotheses [3,23,24]. To the extent that the shock front may be considered to be "sharp", it would appear reasonable to expect the shock to deliver an impulse to at least the low-lying vibrations associated with the unit cell being traversed. The passage of a shock through a finite piece of material would therefore involve the delivery of a sequence of impulses on the molecular scale. The "initial condition" this provides for the vibrational system consists of a super-thermal energy density, which may, however, be modulated on a length scale related to the sequence of phase delays arising from the finite time elapsing between the delivery of impulses to successive unit cells.

Uniform waves in systems with soft anharmonicities are characteristically vulnerable to modulational

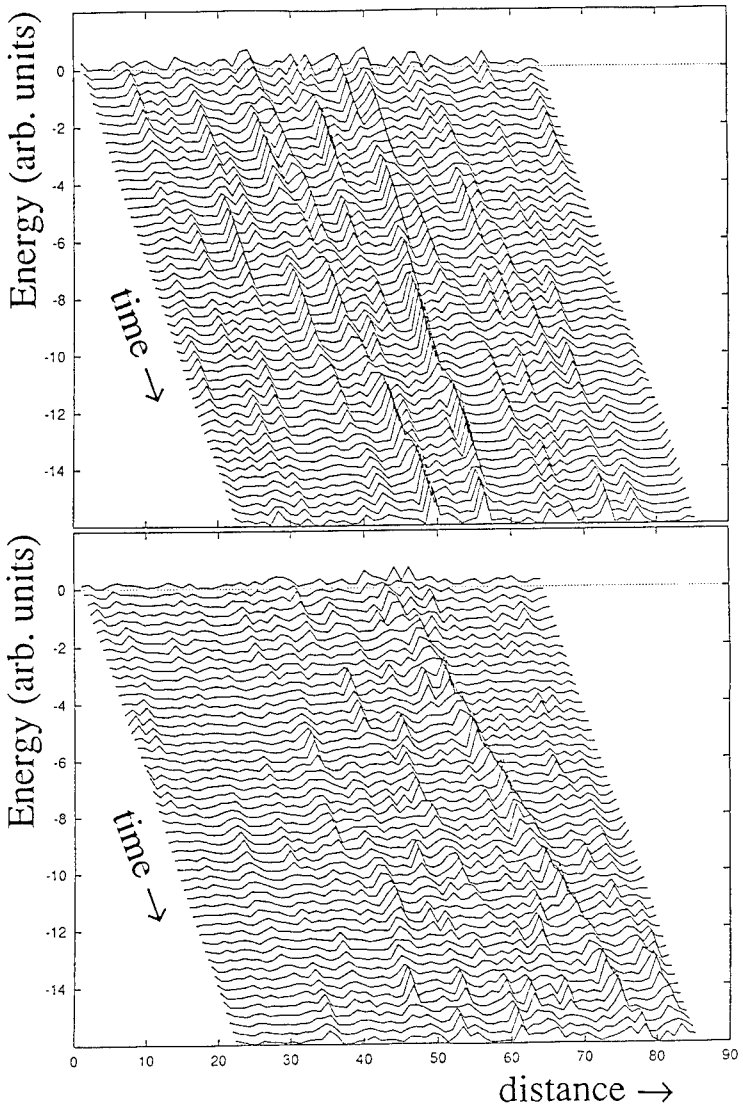

Figure 2. Energy densities at finite temperature. Upper panel, harmonic; lower panel, anharmonic.

instabilities; that is, a monochromatic wave might exist indefinitely, but with the addition of a small spatially-periodic perturbation creating a weak modulation of the fundamental wave, the system may evolve toward a very different state [9,10,15]. Depending on the particular circumstances, monochromatic waves might be unstable to perturbations of any wavelength or only in a limited range (e.g., long wavelengths), or may have an amplitude threshold, and stability may depend on characteristics of the monochromatic wave being perturbed. Characteristically, however, the destabilized wave evolves toward a pulse-train waveform in which the pulses approximate solitary waves of the underlying or "nearby" nonlinear wave equation (if such exist). The *rate* at which perturbations grow typically depends on both the strength of the soft anharmonicity and the amplitude of the fundamental wave, such that perturbations grow much more rapidly in softer modes driven to higher amplitudes. Thus, it would be the more intense shocks that would be more likely to cause initial perturbations to grow, and, recalling earlier discussion, this growth would be more likely to be achieved in the low-frequency modes that couple well

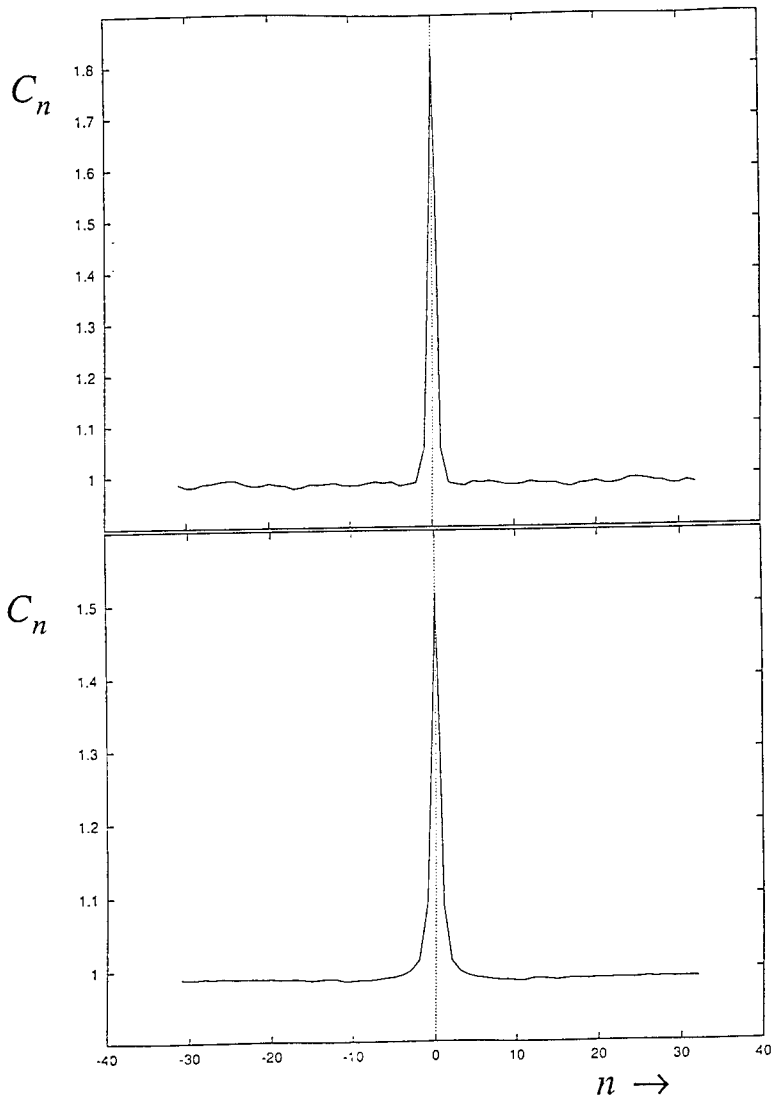

Figure 3. Energy-energy correlation function in site space according to Eqn. (14). Upper panel, result of thermal equilibrium simulation in the harmonic system. Lower panel, result of thermal equilibrium simulation in the anharmonic system at the same temperature. Correlations in the harmonic system are indiscernible from the background beyond the first neighbor; in the anharmonic system, correlations are discernible above background out to fifth neighbors.

with the shock.

In Figure 4 we illustrate the result of initializing chains of oscillators with nearly-uniform initial energy distributions upon which are imposed weak spatially-periodic modulations. The harmonic chain disperses the perturbation as it would any other nonuniformity in amplitude. On the other hand, the modulation in the anharmonic chain grows in time, transforming the original nearly-uniform energy distribution into a train of pulses, each of which spans a number of unit cells within which a several-fold amplification of the original energy density is achieved for a nontrivial interval of time. This could be viewed as local heating, but actually much more coherent, achieving local deformations that much more likely than thermal fluctuations to interact with electronic excitations and perhaps assist in the initiation of chemsitry [25,26]

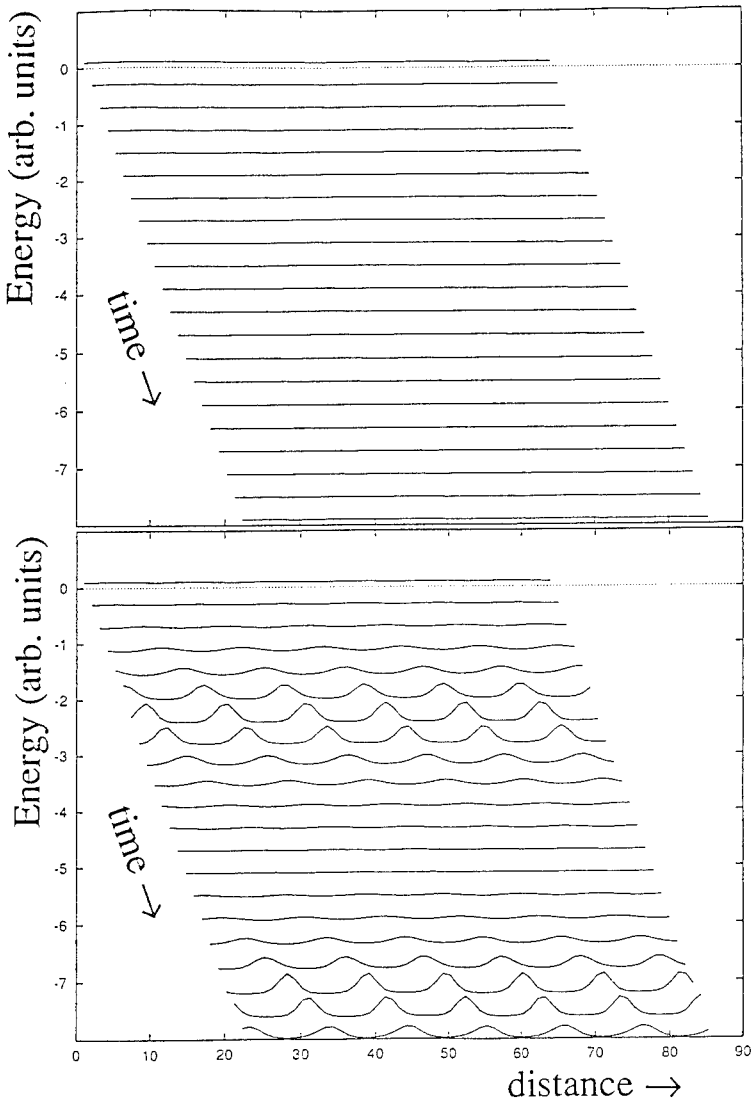

Figure 4. Energy density profile for non-uniform non-equilibrium excitation. Upper panel, harmonic system; lower panel, anharmonic system. The weak sinusoidal perturbation does not grow in the harmonic system, while in the anharmonic system the perturbation is amplified, resulting in transient energy focusing.

This dramatic focusing is a transient phenomenon that is eventually degraded as the shocked material equilibrates to a new local temperature. Anharmonic effects as discussed in previous sections should be more pronounced in the new thermal equilibrium established behind the shock, but cannot be expected to be as dramatic as in the initial transient.

8. CONCLUSION

In this paper we have sketched a number of the characteristic manifestations of soft anharmonicity in systems of oscillators. We have seen how isolated soft anharmonic oscillators at finite temperature have mean energies higher than would be expected for harmonic oscillators, and are distinguished by energy fluctuations that tend to be longer-lived at higher energies than their harmonic counterparts. These characteristics motivate a notion of "statistical localization," the root of which is the entropic drive to

sample the extra phase space rendered accessible by the softening of the vibrational potential.

At zero temperature, entropic effects are frozen out, laying bare the purely dynamical consequences of anharmonicity. The fundamental dynamical phenomena are the tendencies of soft anharmonicity to focus energy and the tendency of harmonic transport terms to disperse it; it is the interplay of these tendencies that is the source of interesting behavior. In its purest form, the balancing of focusing and dispersion leads to the formation of robust particle-like excitations called solitons. Though for the most part solitons are idealizations of practical phenomena, the "nearness" of a practical system to an ideal soliton system tends to show up in "soliton-like" behaviors such as the anomalous persistence of localized excitations (See Figure 1.) or the transient formation of soliton-like pulses during the decay of high-amplitude initial data (See Figure 4).

Thermal equilibrium in vibrational systems is inhospitable to soliton-like excitations in the sense that it is typically difficult to resolve well-defined, long-lived vibrational excitations. The three-fold roots of this difficulty are that 1) the "substance" of which the excitation is made is thermal energy that is not conserved except in a statistical sense, being subject to loss through dissipation and being regenerated only stochastically, 2) solitons are low-entropy states that exact a significant free-energy cost at elevated temperatures, and 3) in order to achieve mean energies sufficiently high to allow a significant penetration of the anharmonic regime, the temperature must be significant as well, such that no thermally generated soliton can ever escape (1) and (2). Thus, soft anharmonic vibrations in thermal equilibrium execute a Sisyphean dance, perpetually driving thermal fluctuations toward a soliton-like order, only to see that growing order continuously degraded by never-ending waves of fluctuations. Consequently, solitonic effects show up not in the major attributes of thermal equilibria, but in the textures and shadings of an otherwise harmonic-looking picture (See Figures 2 and 3).

Of these various perspectives, the one most closely resembling the problem of initiation in energetic materials is that illustrated in Figure 4. It is well to realize, however, that the evolution of "hot spots" from weakly-structured but high-amplitude initial data is just a particularly *dramatic* manifestation of self-focusing; exactly the same mechanisms under thermal equilibrium conditions may appear much less provocative.

Such is the nature of nonlinearity.

9. DISCUSSION

Q. Carl Melius

Is there an upper limit in the space scales and/or time scales for solitons?

A. In principle no. The nonlinear Schrödinger equation, for example, has true infinite-lived soliton solutions of any width in space. In practice, however, the answer depends on parameters and how non-ideal one's circumstance is. Lattice discreteness, for example, has a significant impact on would-be soliton behavior, with effects ranging from scattering to pinning to the total disintegration of localized initial states [12-15].

Q. Elaine Oran

How do you relate this work to that of Bob Wyatt (U. Texas, Austin) on oscillators coupled to a thermal bath? There was a study that tried to compare classical, semi-classical, and full quantum-mechanical results for this case. It seems that body of work is related to the first part of your lecture.

A. I am afraid I am unfamiliar with work to which you refer.

Q. Elaine Oran

What are your thoughts about "rogue waves" causing localization of energy enough to cause ignition in an energetic material?

A. My understanding of rogue waves is casual at best. Perhaps what is most important for us here is that these ship-eating waves that appear "out of nowhere" are *not* normal fluctuations of a fluid in thermal equilibrium, but arise from the interaction of ocean currents in certain parts of the world. Insofar as rogue

waves reflect a driven instability of a medium, one may acknowledge some similarities, but I would be wary of pressing this analogy too far.

Q. Paul Clavin

Is it not possible that the shock change the thermodynamic picture from a double well to a single well?

A. Yes. This is an especially appealing possibility when considering the coupling of "internal" degrees of freedom (librational, vibronic, and molecular motions) with the translational degrees of freedom. It is natural in such considerations for the shape of the double well to be modulated by acoustic vibrations; in such cases the range of possible anharmonic effects is considerably increased. It is conceivable, for example, that a particularly large acoustic deformation might drive a double well to a single well form. But short of such a direct initiation of chemistry, it should be noted that the coupling of acoustic and other vibrations is typically *itself* a source of anharmonicity, as are the bonds supporting the acoustic waves themselves. (In fact, the latter can be credited for the modern discovery of solitons in the famous Fermi-Pasta-Ulam problem [7].) Any one of these several sources of anharmonicity may be active in a particular process, or they may conspire to yield more pronounced effects.

Q. Anatoly Dremin

It is some prolongation of C. Melius' question. It is known that reaction originates under shock effect in liquid EM inhomogeneously (hot spots). My question is--how much time is necessary to generate hot spots by your mechanism in liquid EM?

A. I regret that owing to my unfamiliarity with liquids in general and energetic materials in particular, I cannot give a very satisfactory answer. Typically, however, there are multiple time scales involved in the formation and evolution of anharmonic excitations. In order for anharmonic excitations as we have discussed to be recognized as such, they must exhibit anomalous persistence relative to harmonic dynamics; therefore, the time scales for the harmonic dispersal of energy set lower bounds on the timescales for (soft) anharmonic motions. Having no meaningful numbers in hand for energetic materials, the actual numbers we used in Figure 4 were drawn from another problem of interest to us, the librational dynamics of molecular crystal l-alanine. The librations of l-alanine exhibit a very weak anharmonicity in a weakly dispersive mode, contributing in Figure 4 to a *slow* focusing over about 25 periods of a single harmonic reference oscillator; stronger anharmonicity, together with stronger dispersion and stronger drive would shorten this interval substantially. It should be noted perhaps that energy focusing can occur much more rapidly in three dimensions than in our example of a one-dimensional chain since energy may be drawn from the transverse dimensions as well as from neighbors within the chain, and can result in much *stronger* focusing since anharmonicity in higher dimensions characteristically competes more effectively against dispersion [8].

Q. Dick Miller

On Monday, we heard J. Dick describe the interaction of a shock wave with a PETN single crystal in a particular orientation. He showed experimental evidence of plastic deformation coupled with a chemical possibly fluorescent effect. He then showed a crystallographic representation of the interaction of the shock with the molecules by a shearing mechanism in the lattice that was unperturbed by the shock. You showed similar interactions in the DNA example. How can this type of analysis help us to understand the chemical effects of the shock or the possibly electronically induced chemistry in this experiment?

A. The number of nonlinear effects in the vicinity of the shock front that might contribute to the promotion of chemistry is rather large: there might be local heating, as suggested by Figure 4, "catalysis" might occur as discussed in response to P. Clavin, the formation and movement of dislocations as emphasized by R. Armstrong [23], S. Coffey [24], and J. Dick [3] is certainly a nonlinear phenomenon, to name a few. An important area we have not addressed here is the (strong) interaction of electronic excitations with vibrations; in solid-state physics, this commonly goes by the name of the "polaron problem". In the polaron problem, one is generally concerned with the response of the material to the presence of the electronic excitation; under appropriate circumstances, the self-consistent state of the excitation and the lattice can be viewed as a soliton [12]. The problem you pose is to some extent the

reverse: that is, rather than observing the response of a medium to the injection of an electron, you wish to observe the response of the electronic system to the injection of vibrational excitation. I would say that the theoretical apparatus of both problems should be quite similar, though one's approach would naturally be dictated by one's particular objectives. It should be noted perhaps that the Nobel prize in chemistry recently went to Rudolf Marcus, primarily for his extensive work on electron-transfer reactions, both between individual molecules and between molecules and interfaces such as electrodes; the methodology of this work overlaps considerably polaron theory. One can imagine, as suggested by the work of J. Dick, that the shock front creates a solid-solid interface at which electron transfer might occur in chemically-significant quantities if conditions of the Marcus-type analysis were to apply [25,26].

10. REFERENCES

[1] T. Dauxois, M. Peyrard, and A. R. Bishop, Phys. Rev. E **47**, 684-695 (1993); T. Dauxois, M. Peyrard, and A. R. Bishop, Phys. Rev. E **47**, R44-R47 (1993); T. Dauxois, M. Peyrard, and A. R. Bishop, Physica D **66**, 35-42 (1993); M. Peyrard, Acta Physica Polonica B **25**, 955-992 (1994).

[2] Richard C. Tolman, *The Principles of Statistical Mechanics* (Oxford University Press, London, 1938).

[3] J. J. Dick, J. Appl. Phys. **70**, 3572-3587 (1991); Appl. Phys. Lett. **60**, 2494-2495 (1992); J. Phys. Chem. **97**, 6193-6196 (1993); J. J. Dick and J. P. Ritchie, J. Appl. Phys. **76**, 2726-2737 (1994).

[4] Lisa Bernstein, David W. Brown, and Katja Lindenberg, to be published.

[5] D. D. Dlott and M. D. Fayer, J. Chem. Phys. **92**, 3798-3812 (1990); H. Kim, D. D. Dlott, J. Chem. Phys. **93**, 1696-1709 (1990); D. D. Dlott, J. Opt. Soc. Am. B **7**, 1638-1652 (1990); X. N. Wen, W. A. Tolbert, and D. D. Dlott, Chem. Phys. Lett. **192**, 315-320 (1992); A. Tokmakoff, M. D. Fayer, and D. D. Dlott, J. Phys. Chem. **97**, 1901-1913 (1993); X. N. Wen, W. A. Tolbert, and D. D. Dlott, J. Chem. Phys. **99**, 4140-4151 (1993); S. Chen, W. A. Tolbert, and D. D. Dlott, J. Phys. Chem. **98**, 7759-7766 (1994).

[6] P. Maffre and M. Peyrard, Phys. Rev. B **45**, 9551-9561 (1992); J. Phys. - Condensed Matter **6**, 4869-4878 (1994).

[7] E. Fermi, J. R. Pasta, and S. M. Ulam, in Collected Works of Enrico Fermi, Vol. II (University of Chicago Press, Chicago, 1965), pp. 978-980.

[8] G. H. Derrick, J. Math. Phys. **5**, 1252-1254 (1962).

[9] G. B. Whitham, *Linear and Nonlinear Waves* (John Wiley & Sons, New York, 1974).

[10] R. K. Dodd, J. C. Eilbeck, J. D. Gibbon, and H. C. Morris, *Solitons and Nonlinear Wave Equations*, (Academic Press, New York, 1982).

[11] Alan Newell, *Solitons in Mathematics and Physics* (SIAM, Philadelphia, 1985).

[12] Xidi Wang, David W. Brown, Katja Lindenberg and Bruce J. West, Phys. Rev. A **37**, 3557-3566 (1988).

[13] R. Boesch and M. Peyrard, Phys. Rev. B **43**, 8491-8508 (1991).

[14] H. Feddersen, in *Nonlinear Coherent Structures in Physics and Biology*, Lecture Notes in Physics, Vol. 393, edited by Michel Remoissenet and Michel Peyrard (Springer-Verlag, Berlin, 1991) pp. 160-167.

[15] Y. S. Kivshar and M. Peyrard, Phys. Rev. A, **46**, 3198-3205 (1992).

[16] G. A. Samara and P. S. Peercy, in *Solid-State Physics*, Vol. 36, edited by H. Ehrenreich, F. Seitz, and D. Turnbull (Academic Press, New York, 1981), pp. 1-118.

[17] S. Califano, *Lattice Dynamics of Molecular Crystals*, (Springer-Verlag, New York, 1981).

[18] A. C. Newell and D. J. Kaup, Proceedings of the Royal Society A, **361**, 413-446 (1978).

[19] P. G. Drazin, *Solitons* (Cambridge University Press, New York, 1983).

[20] A. R. Bishop, M. G. Forest, D. W. McLaughlin, and E. A. Overman, Phys. Lett. A **144**, 17-25 (1990); N. M. Ercolani, M. G. Forest, D. W. McLaughlin, and A. Sinha J. Nonlinear Science, **3**, 393-426 (1993); N. M. Ercolani, D. W. McLaughlin, and H. Reitner, J. Nonlinear Science, **3**, 477-539 (1993).

[21] T. C. Gard, *Introduction to Stochastic Differential Equations* (Marcel Dekker, New York, 1988).

[22] J. Honerkamp, *Stochastic Dynamical Systems: Concepts, Numerical Methods, Data Analysis*, (VCH, New York, 1993).

[23] R. W. Armstrong, W. Elban, Mat. Sci. and Eng. A **122**, L1-L3 (1989); H. W. Sandusky, B. C. Glancy, D. W. Carlson, W. L. Elban, et al., J. Propulsion and Power **7**, 518-525 (1991); F. A. Bandak, R. W. Armstrong, and A. S. Douglas, Phys. Rev. B **46**, 3228-3235 (1992); F. A. Bandak, D. H. Tsai, R. W. Armstrong, and A. S. Douglas, Phys. Rev. B **47**, 11681-11687 (1993).

[24] C. S. Coffey, J. Appl. Phys. **66**, 1654-1657 (1989); **70**, 4248-4254 (1991); Phys. Rev. B **49**, 208-214 (1994).

[25] R. A. Marcus and Norman Sutin, Biochimica et Biophysica Acta **811**, 265-322 (1985).

[26] Leon Sanche, IEEE Transactions on Electrical Insulation **28**, 789-819 (1993).

V FROM MICROSCOPIC TO MACROSCOPIC

Chairman : Dr David Jones : Materials Research Laboratory - Ascot Vate

A Transition from a Microscopic to a Macroscopic Approach to Steady State Detonation ; C.S.Coffey

A General Concept Concerning Energetic Material Sensitivity and Initiation; S.A. Shackelford

A Theoretical Approach to Energetic Materials ; M.D.Cook

"Microscopic" and "Macroscopic" Levels of the Errors for Detonation Characteristics Calculations. Pedigree of the Errors ; T.S.Pivina, E.A.Arnautova, M.S.Molchanova and V.V.Scherbukhin

JOURNAL DE PHYSIQUE IV
Colloque C4, supplément au Journal de Physique III, Volume 5, mai 1995

A Transition from a Microscopic to a Macroscopic Approach to Steady State Detonation

C.S. Coffey

Naval Surface Warfare Center, White Oak Laboratory, Silver Spring, MD 20903-5640, U.S.A.

ABSTRACT: Recent efforts to understand initiation of reaction in crystalline explosives on the microscopic level during shock or impact have been extended to the macroscopic case. This allows a different approach to the detonation problem. The initiation portion of the detonation wave is determined and when combined with the reaction zone length completely specifies the detonation wave. Detonation in an unconfined cylinderical charge is treated. This approach should have general application beyond the narrow confines of detonation in predicting the initiation response of crystalline explosives to any arbitrary shock or impact.

1. INTRODUCTION

The classical analysis of a detonation wave propagating in an explosive charge is well known and gives reasonable predictions of both detonation pressure and detonation velocity [1-4]. However, this analysis is highly idealized. The detonation wave is treated as an infinitely thin discontinuity separating the undisturbed material ahead of the wave from the fully reacted material to its rear. Numerous efforts have since been made to account for reaction zone thickness, reaction rate processes, material sensitivity to shock, detonation wave curvature and many of the other attributes of detonation waves [5-8].

Universally, all of these efforts have focussed on pressure as the essential component driving the initiation process. While pressure is important, recent efforts have identified shear as the mechanism by which energy is dissipated and initiation occurs in the detonation wave front. This suggests a different approach to the detonation problem. The shear driven initiation portion of the detonation wave front is first determined. This is then combined with the reaction zone thickness to describe the complete detonation wave. Here we present a determination of the shear wave and initiation front in an unconfined explosive charge. The reaction zone thickness, which can vary across the reaction front, is described in part by the microscopic analysis and in part by the boundary conditions. The results predict that the reaction zone can readily be measured for real charges. In this picture the high pressure portion of the detonation wave is just the end state of the process and supplies some energy to sustain the shear driven initiation process.

This approach resolves a major inconsistency between current detonation theory and experiment, namely

that of dead pressing and similar situations in which it is impossible to initiate crystalline explosives at any pressure when plastic flow is prevented and yet the same material detonates easily at pressures of a few tenths of a GPa when shear and plastic flow occurs. Determining initiation due to the energy dissipated during plastic deformation has the potential of solving a broad range of initiation problems arising from an arbitrary impact or shock stimuli.

1.1 BRIEF REVIEW OF INITIATION AT THE MICROSCOPIC LEVEL

In an effort to understand initiation, we have identified the localized energy dissipation that occurs within the explosive crystals during plastic deformation due to shock or impact as the mechanism responsible for initiation of reaction [9-11]. This is a shear driven process in which the energy dissipated by the moving dislocations responsible for plastic deformation is localized into small regions of sufficient energy density to start chemical reactions. Specifically, during detonation the local lattice distortions produced by the rapidly moving dislocations driven by the shock of the detonation are able to resonantly excite the internal vibrational modes of the explosive molecules. Rapid multiphonon excitation occurs when the energy of the optical phonons generated by the moving dislocations equals the energy required to excite transitions between the internal molecular vibrational levels, typically $\omega \approx 10^{13}$rad/s. The optical phonons generated by the moving dislocations are centered in a band about $\omega = 2\pi v/d$. The quantity d is the molecular spacing, $d \approx 10^{-9}$m, and v is the dislocation velocity. Here $v = v_0 \exp(-\tau_0/\tau)$.[12,13] v_0 is the shear wave speed, $\approx 2 \times 10^3$m/s, τ is the applied shear stress and τ_0 is a characteristic shear stress of the material, $\tau_0 \approx 10$ MPa to about 1.0 GPa. For a high amplitude shock it can easily occur that $\tau >> \tau_0$ and $\omega \approx 2\pi v_0/d \approx 10^{13}$ rad/s. Thus the optical phonons created in this band can resonantly excite the internal molecular modes and cause the rapid molecular dissociation associated with detonations.

Mild impact, $\tau \leq \tau_0$, generates only low velocity dislocations and lower plastic strain rates. These lower velocity dislocations can also produce energy localization and ignition but at a much slower rate and are not of treated here.

2. INITIATION AT THE MACROSCOPIC LEVEL

Since shear stress is the driver of these microscopic processes, it is possible to use the shear stress to extend these concepts to the macroscopic level and obtain predictions of the pressure wave and the shear stress - initiation profile of a steady state detonation wave as well as predictions of other features including the failure diameter.

Consider the case of a steady state detonation wave propagating with a velocity D along the axis of an unconfined cylindrical explosive charge of radius r_0. Let the charge be composed of an aggregate of randomly oriented and sized explosive crystals held in a soft polymer binder. It will be assumed that plastic deformation can always occur since the stresses encountered in a detonation are usually far in excess of the yield strength of any material.

A shear stress can be generated locally within the charge by the contact forces arising from particles pushing against each other due to the shock of the detonation wave [14]. Alternatively, shear stress can arise from the rarefactions originating at the unconfined walls of the charge. For the purposes of this paper it will be assumed that the charge is at or near its theoretical maximum density so that the local shear stresses in the aggregate due to contact forces can be neglected. Here the focus will be on the shear due to the pressure gradient produced by the relief waves that enter the explosive from the unconfined side walls.

Rather than writing the shear stress as the deviatoric elements of a stress tensor, it is more informative to directly write the shear stress in terms of the differential of the forces acting on a crystal element. The shear stress $\vec{\tau}$ can be expressed in terms of the spatial derivative of the force $\vec{F}$ as

$$\vec{\tau} = \frac{1}{A} (\vec{dr} \cdot \vec{\nabla}) \vec{F} \tag{1}$$

where A is the cross sectional area. The differential element $\vec{dr}$ is the size of the active plastic deformation region of the crystal. It is this force gradient applied to a crystal that causes the creation and motion of dislocations and plastic flow to occur. Because of the magnitude of the shear stresses and the plastic flow, the components of the force are strongly coupled to each other which allows the simplification

$$\vec{\tau} \approx (\vec{dr} \cdot \vec{\nabla}) \vec{P} \tag{2}$$

where $\vec{P} = \vec{P}(r,t)$ is the pressure. If the pressure is written as $\vec{P} = P\hat{u}$ where $\hat{u}$ is any unit vector and P is the pressure amplitude, then

$$\vec{\tau} = \hat{u} (\vec{dr} \cdot \vec{\nabla}) P \tag{3}$$

and the amplitude of the shear stress becomes

$$\tau = (\vec{dr} \cdot \vec{\nabla}) P \tag{4}$$

In order for a steady state detonation to develop, initiation must proceed at a constant rate on the surface of the initiation portion of the detonation wave. To achieve this constant rate of molecular excitation and dissociation requires that the shear stress be a constant over the entire surface of the initiation front. Thus on the surface of the initiation portion of a steady state detonation wave $d\tau = 0$ or

$$d\tau = \vec{dr} \cdot \vec{\nabla}\tau = 0 \tag{5}$$

Combining equations (4) and (5) gives the condition for a steady state detonation wave as

$$\nabla^2 P = 0 \tag{6}$$

For a cylinderical charge this has the solution

$$P(r,z) = P_0 J_0(\alpha r) e^{\alpha z} \tag{7}$$

where $J_0(\alpha r)$ is the zero order Bessel function and P_0 is the pressure amplitude of the steady detonation

wave. This closely resembles the form of recent empirical fits to the experimental data for the pressure field of a steady state detonation in a cylindrical charge [15,16].

The magnitude of the shear stress is

$$|\tau| = \alpha P_0 e^{\alpha z} \left(J_1(\alpha r)^2 + J_0(\alpha r)^2 \right)^{1/2} dr \tag{8}$$

For an aggregate of randomly oriented explosives crystals it is only necessary that the magnitude of the shear stress be a constant on the initiation surface ahead of the steady state detonation wave. Thus, on the initiation front the magnitude of the shear stress on the axis of the charge, r = 0, z = 0, and at any other point (r,z) on the constant shear/initiation surface are equal

$$|\tau(r=0, z=0)| = |\tau(r, z)| \tag{9}$$

which reduces to

$$e^{-\alpha z} = \left(J_1(\alpha r)^2 + J_0(\alpha r)^2 \right)^{1/2} \tag{10}$$

It has tactitly been assumed that the shear stress on the surface of interest is sufficient to cause initiation, $\tau \geq \tau_c$, where τ_c is the critical shear stress necessary for initiation.

3. STEADY STATE DETONATION

In order to sustain a steady state detonation the boundary conditions imposed by an unconfined charge require that detonation must exist at the edge of the cylinder. This is necessary in order that the detonation reaction supply energy to the wave front to offset the energy lost to the rarefactions at the edge of the charge. Often in a real charge there appears to be a thin shell of explosive material on the outer edge of the charge that does not undergo reaction [17]. This is probably due to the length of the reaction zone and will not be dealt with further here.

Typically, the charge is driven to detonation by a plane shock wave. Assuming this to be the case, initiation of chemical reaction cannot first occur at the shock front in the interior of the charge since initially the gradient of the pressure is zero in this region and consequently so is the shear stress. Rather, initiation must first occur at the edge of the charge where the rarefaction waves entering from the unconfined side walls create a pressure gradient and consequently a shear stress and plastic flow. A steady state detonation develops as the rarefaction waves progress towards the center of the charge and back to the edge to eventually establish the shear stress profile given by equations (8) or (10).

3.1 REACTION ZONE LENGTH

The reaction zone length, z_0, is determined mainly by the microscopic processes of initiation [9-11,14]. This length is measured from the initiating shear wave front given in equation (8) and extends to the point where the reaction is completed which is usually at the detonation front. Because of the boundary conditions z_0 varies from the center to the edge of the unconfined charge, $z_0 = z_0(r)$. For simplicity, the reaction zone length along the axis of the charge will be taken to be independent of the boundary conditions and is the characteristic reaction length, δ, of the explosive, $z_0(0) = \delta$. At the edge of the charge the reaction zone thickness is controlled in part by the boundary conditions which moderate the

shear stress that drives the reaction.

The shear/initiation front is determined by the shear due to the pressure gradient and is supported by the energy released in the reaction zone. To maximize the shear and associated reaction rate and minimize the energy flow between the interior and the edge of the charge, it is proposed that in the steady state the reaction at a position on the axis of the charge, (0,z), is just completed as the reactions at positions on the edge of the charge with the same z coordinate, (r_0,z), are just initiated. Thus, in a coordinate system centered at the initiation front on the axis of the charge and moving with that front, the shear stress at the edge of the charge is determined from equation (8) with $z = -\delta$. Initiation occurs when a critical shear stress amplitude is achieved, $\tau \geq \tau_c$. The plastic deformation and associated energy dissipation that occur prior to initiation are the same as would occur in a similar inert material and determine the energy required to ignite the sample.

Since shear arising from the rarefactions entering from the edge of the unconfined charge is required to establish a steady state detonation, the reaction at the edge of the charge develops for twice the time interval as the reaction in the center. Thus at the edge of the charge the reaction zone thickness is twice that at the center, $z_0(r_0) = 2\delta$. If it is assumed that the reaction goes to completion at the detonation front then the distance that the steady state detonation front at the edge of the charge lags the detonation front at the center of the charge is 2δ. In a coordinate system centered on the axis of the charge at the detonation front and moving with that front, the pressure at the edge of the charge is determined from equation (7) with $z = -2\delta$.

Equations (7), (8) and (10) along with the reaction zone length, δ, define the surfaces of steady state detonation and initiation waves propagating along the axis of an unconfined cylindrical charge. Table (1) show some comparisons between experimental data obtained from two different explosives, Comp B and an ammonium perchlorate and aluminum, AP/Al, based explosive and predictions obtained from the above equations. This indicates that within the probable accuracy of the data the characteristic reaction zone length, δ, is nearly a constant independent of charge diameter for the AP/Al based explosive. Also, within the accuracy of the data, the detonation front at the edge of the charge lags the detonation front at the center of the charge by the predicted amount 2δ for both explosives.

Finally, consider briefly the case when the cylindrical charge is enclosed in a thick walled tube so that the rarefaction waves from the side walls are reduced. With sufficient confinement the pressure gradient in the charge vanishes and along with it the shear stress within the charge. In the absence of shear and plastic deformation, energy localization and the initiation of chemical reaction cannot occur regardless of the amplitude of the shock introduced into the charge. There exists a substantial amount of experimental data from shock experiments in heavily confined charges at near theoretical maximum density that support this prediction [18-21].

4. SUMMARY

The observation that plastic deformation and the associated shear stress are responsible for energy dissipation and localization and the subsequent initiation of explosive crystals has been carried to the macroscopic level to describe the initiation of a steady state detonation wave in an unconfined cylinderical charge. Together the initiation front and the reaction zone length completely specify the detonation wave. Predictions have been obtained that agree reasonably well with the available experimental data and permit the extension of experimental observations into areas such as reaction zone thickness and the critical shear stress required for initiation.

Since the response of a crystalline explosive to any shock or impact is dependent upon the degree and nature of initiation achieved by the stimulus, it should be possible to extend these results beyond the narrow concerns of detonation and predict the response of an explosive to any arbitrary shock or impact.

5. ACKNOWLEDGEMENTS

This work was supported by the Office of Naval Research and by the Naval Surface Warfare Center Independent Research Funds. The author wishes to thank Dr. Donald H. Liebenberg of the ONR and Mr. Raymond H. Riedl of NSWC for their support and encouragement. In particular, the author wishes to express his appreciation to Dr. E. R. Lemar of NSWC for his comments and insights and for kindly supplying and reducing the experimantal data and to Dr. R. H. Guirguis of NSWC.

Table (1) Comparison of typical experimental data for two explosives, Comp B and an AP/Al based material, with their predicted behavior.

Comp B
Charge radius = 25.43 mm,
Measured from experiment, α = .01134 mm^{-1}, z_0 = 1.86 mm
Reaction zone length calculated from Eq. (10), δ = .93 mm
Predict $z_0 = 2\delta$ = 1.86 mm

AP/Al Explosive
Charge radius = 34.125 mm
Measured from experiment, α = .018367 mm^{-1}, z_0 = 5.48 mm
Reaction zone length calculated from Eq. (10), δ = 2.7 mm
Predict $z_0 = 2\delta$ = 5.4 mm

AP/Al Explosive
Charge radius = 24.06 mm
Measured from experiment, α = .0324 mm^{-1}, z_0 = 4.88 mm
Reaction zone length calculated from Eq. (10), δ = 2.34 mm
Predict $z_0 = 2\delta$ = 4.68 mm

Data was fit to equation (7) and both α and z_0 were determined (Courtesy of E.R. Lemar). Using α the reaction length δ was determined from equation (10) and compared with the prediction $z_0 = 2\delta$. It is not clear why the length of the reaction zone, δ, differs by .36 mm between the two AP/Al explosive entries above. It may be that the assumption that δ = constant independent of charge diameter is not totally correct. It could also be due to slight unintended compositional variations in the material or to experimental error.

6. REFERENCES

[1] Courant, R. and Friedrichs, K., **Supersonic Flow and Shock Waves**, (Interscience Publishers, Inc. New York, 1948).
[2] Zeldovich, Ya. B., Zh. Eksp. Teor. Fiz. **10**, (1940) 542.
[3] Von Neumann, J., (1942) In **Collected Works of John Von Neumann**, Vol. 6, ed. A. J. Taub. (Macmillan, New York, 1963).
[4] Doering, W., Ann. Phys. **43** (1943) 421.
[5] Fickett, W. and Davis, W. C., In **Detonation**, (University of California Press, Berkeley, California, 1979).
[6] Lee, E. L. and Tarver, C. M., Phys. of Fluids **23**, (1980) 2362.
[7] Johnson, J., Tang, P and Forest, C. A., J. Appl. Phys. **57**, (1985) 4323.
[8] Bdzil, J. B. and Stewart, D. S., Phys. of Fluids A, **1** (7), (1989) 1261.
[9] Coffey, C. S., Phys. Rev. B **24**, (1981) 6984.
[10] Coffey, C. S., Phys. Rev. B **32**, (1984) 5335.

[11] Coffey, C. S., J. Appl. Phys. **70** (8), (1991) 4248.
[12] Gilman, J. J., Aust. J. Phys. **13**, (1960) 327.
[13] Gilman, J. J. and Johnston, W. G., in **Solid State Physics**, edited by F. Seitz and D. Turnbull (Academic, New York, 1962), Vol. 13, p. 147.
[14] Coffey, C. S., Submitted Phys. Rev. B. August 1994.
[15] Oeconomos, J.N. and Chaisse, F., To be published in the Proc. of the 10th Symp. on Detonation, (1993).
[16] Lemar, E. R., Private Communication, provided Figures 3 and 4.
[17] Forbes, J. W. and Lemar, E. R. Private Communication.
[18] Price, D. and Liddiard, T. P., NOLTR 66-87, Naval Ordnance Laboratory, White Oak, MD. (1966).
[19] Price, D.; Clairmont, A. R. and Erkman, J. O., NOLTR 74-40, Naval Ordnance Laboratory, White Oak, MD. (1974).
[20] Price, D., Lecture 9, NSWC MP 81-399, (1981).
[21] Spear, R. J. and Nanut, V. in Proc. of the 9th Symp. on Detonation, OCNR 113291-7, (1989) p. 98.

JOURNAL DE PHYSIQUE IV
Colloque C4, supplément au Journal de Physique III, Volume 5, mai 1995

A General Concept Concerning Energetic Material Sensitivity and Initiation [1]

S.A. Shackelford [2]

Alliance Pharmaceutical Corp., 3040 Science Park Road, San Diego, CA 92121, U.S.A.

ABSTRACT. Stimulation and propagation of an energetic material to a catastrophic explosive event could be described as a interactive transfer of mechanistic mechanical, physical, and chemical processes progressing through an "initiation train" sequence, which begins at the bulk material level, next proceeds into the microstructural regime, then to the molecular level, and finally reaches into the atomic region. These mechanistic processes comprising this sequential initiation train serve several functions. First, some create the physically-structured environment and conditions in the initiation train which are needed to house and propagate other mechanisms associated with energy functions and chemical reaction pathways. Secondly, other detailed mechanisms define the orderly transfer and conversion of energy generated during the initiation train sequence, and thirdly, still other detailed mechanisms provide the kinetically-regulated chemical reactions which control energy release rates and provide the intermediate and final chemical product species which drive the detonation wave front. The rate at which these various mechanisms occur in the initiation train defines the sensitivity of an energetic material. This initiation train concept, its potential for controlling sensitivity, and the relevance of certain mechanistic aspects and data as component parts in this initiation train are outlined.

1. INTRODUCTION

Initiation of an energetic material and its accelerator propagation to a catastrophic event like combustion , thermal explosion, or full-scale detonation event occurs when localized self-heating accelerates in the bulk material more rapidly than it can be dissipated within a specific but relatively short time period. Over the past twenty years, a number of scientists have conducted numerous fundamental investigations into various mechanistic processes which appear to contribute to energetic material initiation. Basically, these mechanistic investigations could be divided into three categories: mechanical, physical or physicochemical, and chemical. Various kinds of mechanisms have been theoretically proposed, computationally modeled, or experimentally studied which involve either, the physical environment in which the initiation event occurs, the energy functions associated with energy transfer, conversion and release rates, or chemical pathways associated with molecular structure, reaction rates, and product formation.

Within the past ten years, the energetic materials community also has come to recognize that, during initiation, various mechanisms occur at different levels or scales of energetic material substance composition. These substance composition levels can be described as the macroscopic level involving the bulk material, the microscopic level describing crystal structure considerations, the molecular level describing both the chemical structure and the chemical reactions, and finally, the atomic level involving individual atoms derived from the original energetic compound. These mechanisms, occurring at various compositional levels of an energetic material, each are integral parts of a much larger and complex event. While detailed information still is needed about the mechanistic intricacies of each mechanistic process, there also is a challenge which requires the blending of these into one complete or overall mechanistic

description of the entire initiation event. Simply stated, these individual mechanistic pieces must be properly fit into one large coherent picture which accurately describes the initiation event and which properly describes the interactions occurring among the various mechanistic processes at each of the compositional levels.

This paper introduces a general concept concerning energetic material initiation and sensitivity. It attempts to provide a coherent framework, albeit in a preliminary form, within which this large coherent picture might eventually be assembled. Certain key fundamental research studies involving a number of distinguished scientists are described and cited which illustrate and support various facets of this conceptual initiation train concept. Because of space and time limitations, not all fundamental investigations which might be relevant to this conceptual model, nor the scientific investigators associated with these studies, all can be mentioned, and their omission is not intended to slight the importance of their work nor the contributions of the scientists who conducted them. Additionally, it is anticipated the presentations at this workshop will uncover other new aspects of the initiation event which would nicely dovetail into or require a modification of this preliminary initiation train concept.

2. DISCUSSION

Figure 1 represents a general concept concerning the overall energetic material initiation event. It illustrates an "initiation train" comprised of sequential mechanistic mechanical, physical or

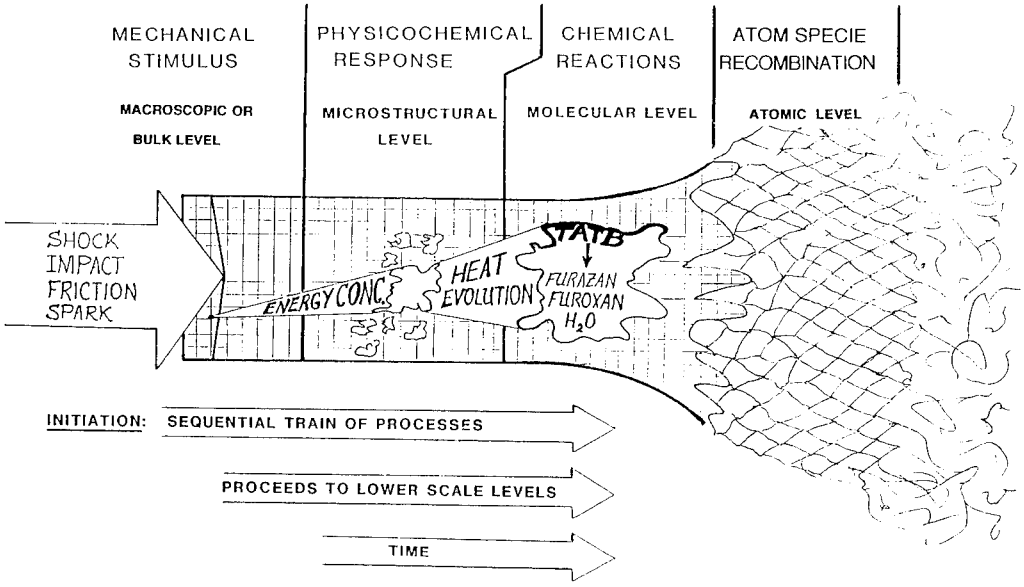

Figure 1. General Pictorial Concept of the Initiation Train Sequence.

physicochemical, and chemical reaction processes which begin with the bulk energetic material at the macroscopic level. It then proceeds into the microscopic level involving the crystal lattice characteristics plus energy behavior of the energetic material. Next, the initiation event moves into the molecular level where chemical reactions generated by a rapid thermochemical decomposition occur; and finally, it proceeds into the atomic level where atomized species form and recombine into the final small gaseous molecules detected as detonation products. It meets the criteria of an event which (a) is sequential in nature, (b) proceeds progressively into more minute material composition levels, and (c) occurs over a very rapid but finite time period. It also contains three other elements which seem to be common with most mechanistic processes studied as part of the initiation event; these would be, (1) the formation of a physical environment in which other mechanisms may proceed, (2) the evolution, conversion, or transfer of heat energy, and (3) the presence of chemical reactions which rapidly decompose the original energetic compound into other chemical compounds with a concomitant energy release.

All types of mechanisms investigated with the initiation event seem to accomplish either one of three functions. Firstly, they ensure formation of the physical environment and resultant conditions which house processes required for the conversion of mechanical energy into heat energy, for the transfer and concentration of heat energy, or for the degradation of the original compound via rapid thermochemical decomposition reactions. Secondly, they provide for the actual conversion of mechanical energy into heat and the transfer and conversion of heat energy. Thirdly, they generate a pathway followed by the heat-generated thermochemical decomposition reactions which produce the intermediate and final product species driving the detonation wave front.

Beginning at the left side of Figure 1, the initiation train scenario might proceed as follows. An external stimulus (impact, shock, friction, spark, heat) on the bulk energetic material at the macroscopic level, introduces a physical response (fracture, shear, viscous flow, plastic deformation, gas bubble pressure and others) [2-21] at the microscopic level which forms new microstructural defects or locates already existing inhomogeneities in crystal lattice of the energetic material. These microstructural defects then each serve as a highly localized nucleation point where mechanical energy is concentrated and converted into heat energy at the microscopic level via some type of physical or physicochemical mechanism. This conversion and concentration of heat in the micron-sized or submicron defect produces a hot spot in which an extremely high pressure and high temperature build up rapidly occurs. Within the hot spot on its inner surface, heat activated thermochemical decomposition reactions begin to occur at the molecular level where some of the heat energy is converted into the kinetic energy needed to activate and drive, perhaps by radical species catalysis, the thermochemical decomposition process and its associated chemical mechanism(s). The kinetically-controlled chemical reactions, generated during the rapid thermochemical decomposition process, produce more sensitive condensed phase intermediate compounds which themselves break down further into gaseous products with more heat evolution. Eventually, this rapid decomposition causes these intermediate condensed phase and gaseous products to reach the atomic structural level by producing atomized species. The recombination of these atomic species into final gaseous detonation products occurs in a cellular-structured environment found to exist behind the detonation shock wave. The fracture, cracking, and shear interfaces occurring at the bulk macroscopic level, the hot spots created at the microscopic level, and the cellular structure inherent with the detonation wave, formed by either mechanical or physical mechanistic responses, represent physically-structured features which define an environment and the parametric conditions where other mechanisms can operate to either generate, transfer, and convert heat energy , or where kinetically-controlled reaction mechanisms provide the necessary chemical species and energy release rates needed to propagate and sustain a detonation event.

A number of theoretical and experimental mechanistic investigations lend support to this concept. Mechanisms (1) by which mechanical stimuli are converted into physical responses at the bulk level, (2) mechanisms by which these physical responses generate and propagate the formation of localized microstructural defects or inhomogeneities; and (3) mechanisms by which these physical responses convert and concentrate their energy into heat to form hot spots have been covered in the literature and at various scientific conferences, workshops, and symposia [2-21]. Some of these mechanistic responses are recognized by the following terms: fracture, shear, viscous flow, plastic deformation, gas bubble pressure, and others. One mechanistic process for which extensive experimental evidence has been gathered, is termed the "Dislocation Pile-Up Avalanche Mechanism" [21]. It describes the conversion of a mechanical stimulus (impact) at the macroscopic bulk level into a physicochemical response known as plastic deformation, which introduces shear bands into the crystalline material. This causes a rapid avalanche type of build-up for microscopic level defects and concentrates heat at these localized points to form hot spots with a concomitant generation of radical species [8,21]. Possibly, these radical species catalyze the initiation of molecular level thermochemical decomposition reactions inside the hot spots.

The potential catalytic role of radicals is illustrated by both theoretical and experimental investigations of crystal structure orientation and sensitivity. Radicals can form along with defects during microscopic level crystal lattice shearing. Theoretical calculations conducted on an initiation model of nitromethane initiation predicted certain crystal orientations of the solid nitromethane crystal lattice would initiate to detonation more easily than others [22]. This effect was noted in an experimental study of solid nitromethane where explosive behavior in a diamond-anvil cell was found to be dependent on crystal orientation [23]. A model invoking steric hindrance in the movement of one molecule of nitromethane past other molecules during shear deformation of the crystal lattice explained this behavior and illustrated that covalent bond rupture occurs more readily in sterically hindered orientations where one molecule

collides with another [23]. PETN also displays a crystal orientation dependence with its shock initiation sensitivity, and this behavior also is attributed to steric hindrance of molecular motion in the shear flow [24]. The dependence of detonation velocity with various crystal orientations in RDX [25], conceivably, also may result in part from radicals being generated as molecules collide in the more sterically hindered orientations and homolytic bond ruptures occur. Thus, microscopic level mechanistic processes produce hot spots and radicals which, in turn, must contribute to starting the molecular level thermochemical decomposition reactions in the hot spots.

The actual existence and role of hot spots was experimentally verified by scanning electron microscopy (SEM) and X-ray Photoelectron Spectroscopy (XPS) analyses of energetic materials which were impacted or shocked just below their initiation threshold [26-29]. Micron-sized (impact) and submicron-sized (shock) quenched hot spots with charred inner surfaces were located by the SEM technique, and XPS analysis of these charred surfaces inside the hot spots revealed new condensed phase intermediate products formed from the original energetic compound. The new condensed phase intermediate compounds resulted from the chemical reactions associated with the rapid thermochemical decomposition process which produced the charred inner hot spot surface. At the molecular level, this thermochemical decomposition process in sub-initiated TATB produced much more sensitive furoxan compounds as well as furazan compounds in this charred hot spot surface (Figure 2). At this point, the chemical kinetics of the rapid thermochemical decomposition process and their role in molecular level chemical reactions must be considered.

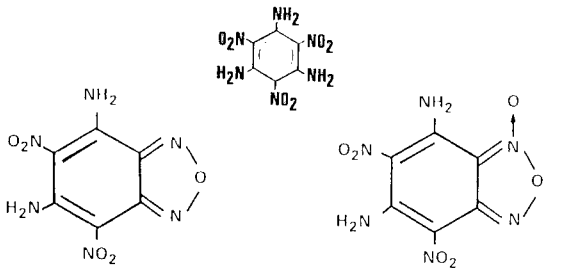

Figure 2. Hot Spot Char Products in TATB Sub-Initiation by Mechanical Impact [29].

The role of chemical kinetics in regulating chemical reaction rates and resultant energy release rates during the thermochemical decomposition process, first was demonstrated with TNT using the kinetic deuterium isotope effect (KDIE) approach [30]. In this mechanistic investigation, the hydrogen atoms in TNT's pendant methyl group were replaced with deuterium atoms (TNT-d_3) and the ambient pressure thermochemical decomposition rate was measured for both the normal TNT and deuterated TNT-d_3 using isothermal differential scanning calorimetry (IDSC) [30]. Introduction of deuterium atoms to form a stronger C-D bond in the TNT-d_3 pendant methyl group (Figure 3), slowed its thermochemical decomposition rate significantly enough to reveal that methyl group C-H bond dissociation (1^0 KDIE) controlled the overall rate of the TNT thermochemical decomposition process. Subsequent KDIE studies with the normal HMX and deuterated HMX-d_8 [31,34] cyclic nitramine compounds indicated the same condensed-phase dependent rate-controlling step exists (C-H bond dissociation), whether HMX is involved in an ambient pressure solid-phase thermochemical decomposition process, a rapid solid-phase pyrolysis process (ambient pressure), or a high pressure/high temperature combustion event [31,35]. KDIE investigations with RDX and RDX-d_6 showed the same rate-controlling C-H bond rupture in both its solid- and liquid-phase thermochemical decomposition processes [32,36-38] and in its high pressure combustion event [39]. KDIE studies with TATB and TATB-d_6 also revealed the same rate-controlling N-H bond rupture in the pendant amino group for the ambient pressure thermochemical decomposition process [40,41] and the initiation sensitivity of its thermal explosion event [40]. Additionally, a shock initiated detonation study with HMX, RDX, and TNT, plus their deuterated analogues (HMX-d_8, RDX-d_6, and TNT-d_3, respectively), revealed a slight yet statistically significant difference in initiation sensitivity; the deuterated analogues were more difficult to initiate indicating a probable contribution

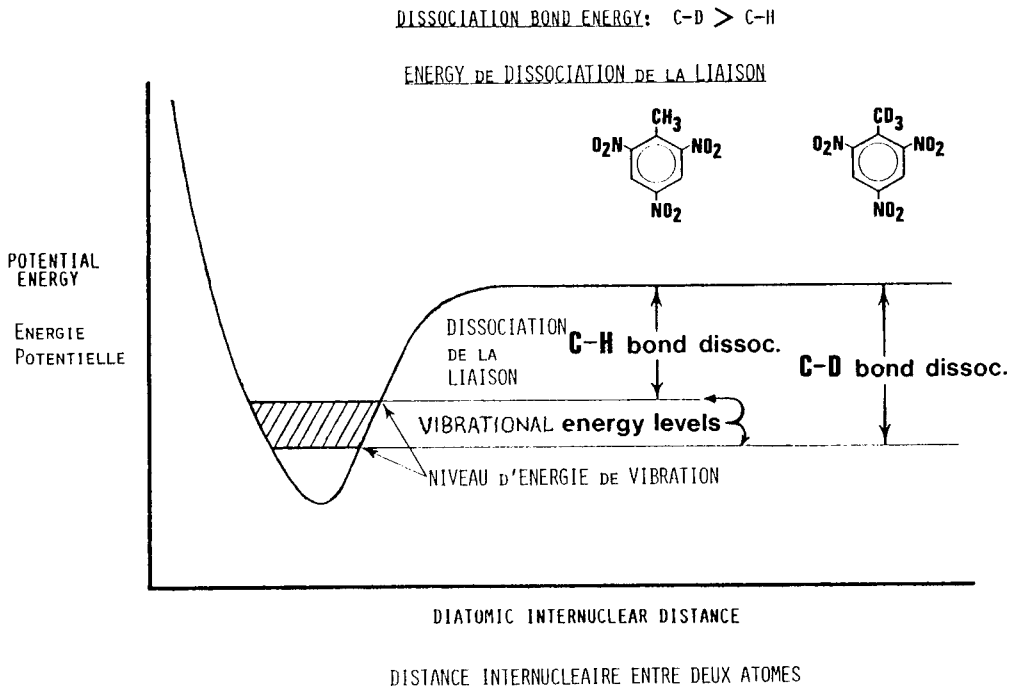

Figure 3. Zero Point Vibrational Energy Difference Between Covalent C-H and C-D Bond Dissociation.

from a rate-controlling C-H bond rupture in the initiation event [32,42]. Figure 4 illustrates the KDIE-determined rate-controlling step in the thermochemical decomposition of the four energetic compounds mentioned. Note the rate-controlling step of HMX apparently varies depending upon its physical state when decomposition is proceeding.

THERMOCHEMICAL DECOMPOSITION RATE-CONTROLLING-STEP (RCS)

COMPOUND	PHASE	KDIE	RCS
TNT	LIQUID	1°	C-H BOND RUPTURE
TATB	SOLID	1°	N-H BOND RUPTURE
RDX	SOLID	1°	C-H BOND RUPTURE
	LIQUID	1°	C-H BOND RUPTURE
HMX	SOLID	1°	C-H BOND RUPTURE
	MIXED MELT	inv.	INTERMOL CRYST. FORCES
	LIQUID	2°	C-N BOND RUPTURE

Figure 4. Rate-Controlling Step in Ambient Pressure Thermochemical Decompositon Process.

Table I summarizes the various KDIE-determined rate-controlling steps detected for a number of energetic materials in different mechanistic processes (thermal decomposition and rapid pyrolysis) and high energy releasing events (combustion, thermal explosion, detonation) [43]. A consideration of all these KDIE results suggests that chemical kinetics play a significant role in controlling the rate of energy release and product formation during the initiation event. It further suggests that chemical kinetics must constitute one significant factor in the initiation train which directly affects the sensitivity of an energetic material toward initiation, and does so by exerting a certain degree of kinetic control on the overall

Table I

Compound	Event	Physical State	KDIE	RCS	Reference
TNT	td	Liquid	1°	methyl C-H	30
TNT	det	?	1°(?)	methyl C-H(?)	42
TATB	td	Solid	1°	amino N-H	40
TATB	te	?	1°*	amino N-H	40
HMX	td	Solid	1°	C-H	31-34
HMX	td	Mixed Melt	Inverse	Internal Cryst Lattice Forces	31
HMX	td	Liquid	2°	Ring C-N	31
HMX	te	Mixed Melt	Inverse*	Internal Cryst Lattice Forces	31
HMX	comb	Solid	1°	C-H	35
HMX	det	?	1° or 2°	C-H or C-N	32
RDX	td	Solid	1°	C-H	32,37
RDX	td	Liquid	1°	C-H	32,36,37
RDX	comb	?	1°	C-H	39
RDX	det	?	1° or 2°	C-H or C-N	32

RCS = Rate-Controlling Step td = thermochemical decomposition
comb = combustion te = thermal explosion
det = detonation * by inference

energy release rate. One computational investigation also lends support to this idea that slower chemical reaction kinetic rates do provide some degree of desensitization for a given energetic material. This theoretical investigation of solid nitromethane's initiation to detonation indicates how effective slowing the rate-controlling step and its associated covalent bond rupture or dissociation can be. Results show that a, 3.45 Kcal/mol increase in a covalent bond's dissociation energy, resulting in a stronger covalent bond, causes a 30 Kcal/mol overall energy decrease in the chemical reactions occurring near the detonation shock front during a specific time interval [44]. Most interestingly, the zero point bond dissociation energy of the stronger C-D bond is 2.3 Kcal/mol [45] more than it is for the analogous C-H covalent bond in the various KDIE mechanistic investigations cited. This 2.3 Kcal/mol energy difference is the basis for the KDIE existence itself. Experimental verification also is needed which demonstrates that the rate-controlling covalent bond rupture of the thermochemical decomposition process is involved with an energetic material's initiation sensitivity. This possibility that the thermochemical decomposition process comprises an integral part of the initiation train sequence strongly was indicated by the charred quenched hot spot surfaces in the sub-initiated TATB, TNT, and RDX samples described earlier [26-29].

Experimental studies, in fact, have been reported which complete this important requirement and establish the rapid thermochemical decomposition process, its kinetically-controlled chemical reactions, and the associated rate-controlling covalent bond rupture are an integral part of the overall initiation train. First, there is correlation between an energetic compound's shock sensitivity and its critical temperature (Figure 5) [46]. Secondly, the critical temperature of an energetic material can be calculated from

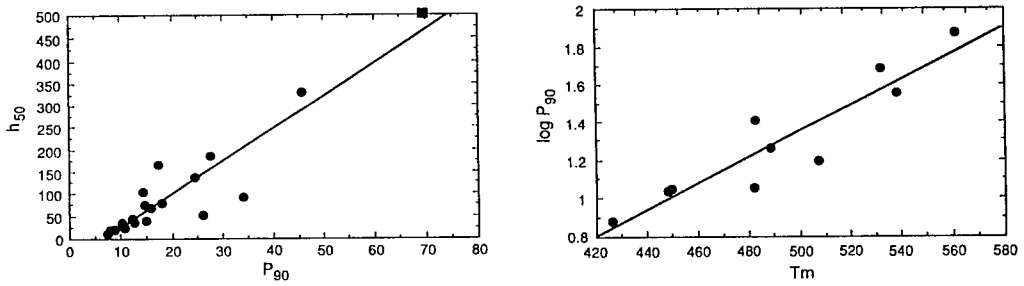

Figure 5. Shock Sensitivity, Impact Sensitivity, and Critical Temperature Correlations [46].

the rate constant obtained by measuring the chemical kinetics of an energy material's ambient pressure slow thermochemical decomposition process. Kinetic measurements made by IDSC analysis, when used in the the Frank-Kamenetskii Equation, provided very accurate critical temperature values [40,47]. The critical temperature of an energetic compound is defined as the lowest constant surface temperature at which a given sample of a specific size and shape will self-heat catastrophically. In other words, below the critical temperature a compound still can undergo a rapid thermochemical decomposition process, but it will not generate enough heat and a high enough concentration of reactive product species to become a self-sustaining entity and propagate into a thermal explosion event. The correlation (Figure 6) of shock

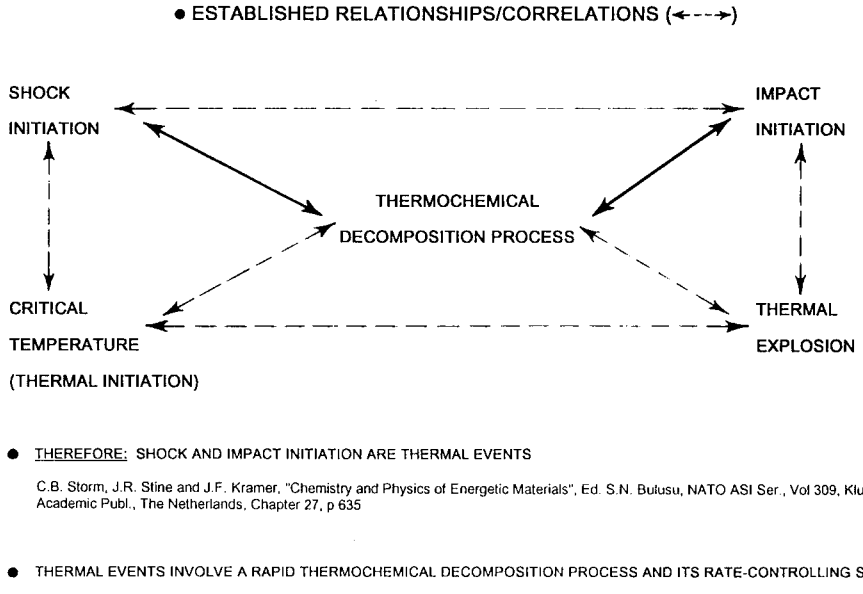

Figure 6. Thermochemical Nature of Shock Initiation, Impact Initiation, and Thermal Explosion [46].

sensitivity to critical temperature (dotted arrow) and the ability to calculate critical temperature from the chemical kinetics of a thermochemical decomposition process (dotted arrow), establish a direct link between the thermochemical decomposition process and shock initiation (solid arrow). The fact that impact initiation produces a thermal explosion event (Figure 6, dotted arrow), that critical temperatures are measured using the thermal explosions of the Henkin Test (dotted arrow), and that the thermochemical decomposition process of a compound (TATB and TATB-d_6) produces the same KDIE-determined rate-controlling step as that found in its thermal explosion [43b], establishes a direct link between the thermochemical decomposition process of a given energetic compound and impact initiation (solid arrow). The correlation (dotted arrow) between shock sensitivity and initiation sensitivity (Figure 6) completes Figure 5 [46] and emphasizes the important role of the thermochemical decomposition process and its kinetically-based rate-controlling chemical reactions in the overall initiation train sequence.

The covalent bond rupture, which constitutes the rate-controlling step for an energetic compound, also depends on its inherent molecular structure. Differences in the chemical environment of a specific covalent bond may determine which structural portion of the molecule provides the rate-controlling covalent bond dissociation (Figure 7). TNT possesses two vastly different types of C-H bonds as illustrated by their large proton NMR shifts between those in the saturated aliphatic pendant methyl

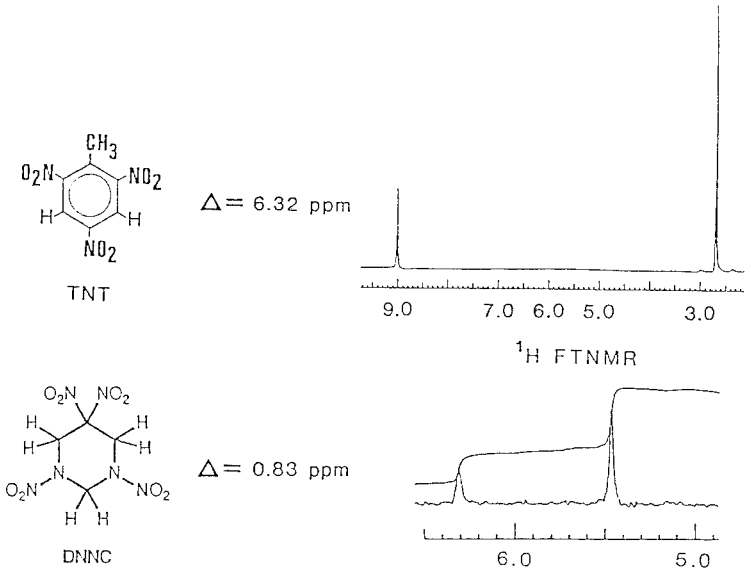

Figure 7. Proton NMR Chemical Shifts in the TNT and DNNC Molecules [1c].

group and those bonded directly to the aromatic phenyl ring. Only aliphatic C-H bond rupture in the TNT methyl group constitutes the rate controlling step during its thermochemical decomposition process [30,43a]. DNNC, however, possesses two methylene groups (4 protons) flanking the geminal dinitro-substituted ring carbon and one methylene group (2 protons) situated between the two ring nitrogen atoms. While the 4 protons in the methylene groups adjacent to the geminal dinitro-substituted are not in an equivalent chemical environment with the 2 protons of the methylene group sandwiched between the ring nitrogen atoms, this difference is very slight as shown by its very small NMR chemical shift. KDIE experiments with DNNC and DNNC-d_6, plus its ADIOL (2,2-dinitropropan-1,3-diol) and ADIOL-d_4 precursors, seem to suggest any of these six protons can participate in DNNC's rate-controlling step during its thermochemical decomposition [48]. In other cases, a slight change in chemical structure greatly can affect an energetic compound's initiation sensitivity, possibly by causing a different rate-controlling step to occur. Vastly different impact sensitivities are seen between 1-picryl-substituted triazoles (**I** and **III**) and the 2-picryl-substituted triazoles (**II** and **IV**) [46,49]. This difference (Figure 8) is explained by compounds **I** and **III** possessing a chemical structure which permits the easy elimination of the gaseous N_2 molecule. Because compounds **II** and **IV** cannot eliminate N_2 in such a labile manner,

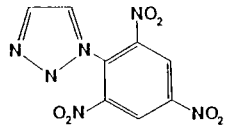

I. 11 cm

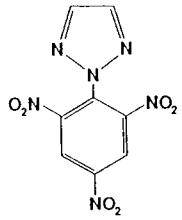

II. 200 cm

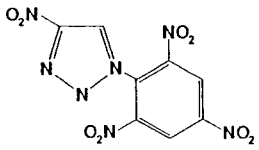

III. 9 cm

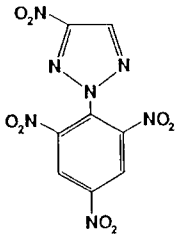

IV. 67 cm

Figure 8. Impact Initiation Sensitivity Comparison of 1- and 2-Picryl-Substituted Triazoles [49].

the chemical reactions leading to its impact initiation probably occur along a different mechanistic pathway, and, therefore, likely would involve a different rate-controlling covalent bond rupture in the rapid thermochemical decomposition portion of its initiation train sequence [2c].

The coupling of condensed phase products, which are derived from rapid thermochemical decomposition in the hot spot, with the KDIE-determined rate-controlling covalent bond dissociation, illustrates the significant role chemical kinetics play in determining the energy release rate during an initiation event. The two condensed phase products, found by XPS analysis in the quenched hot spots of a TATB sample impacted or shocked just below their initiation threshold, were the much less stable furoxan compounds and the furazan compounds (Figures 1 and 2) [26-29]. The furoxans can only form by N-H bond rupture of TATB's pendant amino group, while the furazan compounds must form from [43b]. Mechanistic KDIE thermochemical decomposition investigations with TATB and TATB-d_6 revealed this mechanistic process is controlled by pendant amino group N-H bond rupture [40,41]. The isolation of condensed phase furazan products from the ambient pressure thermochemical decomposition of TATB [26] further supports N-H bond rupture as being the rate-controlling feature. Additionally, a thermal explosion study showed TATB-d_6 was significantly more difficult to initiate as determined by its higher critical temperature [40]. Further evaluation of the TATB and TATB-d_6 critical temperature difference suggests pendant N-H bond rupture to be a significant rate-controlling feature where the kinetics of the normal TATB proceed more at a higher rate and, therefore, provide energy for initiation at a lower temperature [43b]. Similar correlations with TNT [30,50,51] and RDX between the KDIE-determined rate-controlling bond rupture in thermochemical decomposition, plus combustion in the case of RDX [39,43b], and the condensed phase intermediate products formed by analogous bond dissociation in quenched hot spots, also have been detected by XPS analysis [27,29, 43b]. One of the two XPS detected products also was detected from an impacted RDX sample using chromatography and CI mass spectral analyses [52].

Eventually, the kinetically-regulated thermochemical decomposition reactions of the condensed phase move into the gas phase, and it appears these molecular and atomic level gas-phase reactions are housed in a cellular-like physical structure formed in the detonation shock wave (Figure 1). This cellular structure of the shock wave [53-56] appears it might be formed by a physicochemical mechanism at the macroscopic level. Computational studies have simulated the mechanistic formation of this detonation cellular structure and suggested that the cellular shape is affected by energy release rates [56].

Experimental shock tube studies have found a relationship between the size of the macroscopic cellular structure in detonation wave fronts and tubular critical diameter. Detonation is sustained when the critical diameter is 13 times larger than an individual cell structure of the shock wave regardless of the gaseous composition of a fuel/air mixture [53]. Other experimental shock tube studies have shown that cellular structure size can be altered by adding traces of gases into a fuel/oxident mixture which promote or inhibit kinetically-regulated chemical reaction rates, even though the same overall energy of the shocked mixture remains the same [54]. The presence of these trace compounds also alter the induction time, which is defined as the length a shock wave must travel in the shock tube before a critical concentration of reactive species is attained to initiate an explosion event. Therefore, the macroscopic cellular structure size in a gaseous detonation shock wave can be altered by molecular level chemical reaction kinetics; that is, cellular structure size is determined, to some extent, by the kinetically-based rate-controlling step and probably by a specific covalent bond rupture which is present in these gaseous chemical reactions. In turn, cellular structure size is linked to the important physicochemical property of critical diameter. Energy release rates also appear to affect the degree to which an energetic material is converted to gaseous products [57]. This again suggests that chemical reaction kinetics and an associated rate-controlling chemical bond rupture could play a definite role in energy release rates in these gas phase processes. An experimental study of gas products generated by laser pulse heating of RDX showed that energy release rates determined the size of the gaseous product obtained; that is, the degree and extent of energetic material degradation. Higher energy laser pulses generated lower molecular weight gaseous fragments for the RDX molecule, while lower pulsed laser energies produced higher molecular weight gaseous products [57]. It appears the chemical kinetics which regulate the chemical reactions providing the rate-controlling mechanistic step may continue to play a noticeable role in the gas phase, especially in terms of determining energy release rates and the cell structure size in this portion of the initiation train.

Eventually, it appears these gaseous products following the detonation wave breakdown even further until atomization occurs. Traveling behind the shock wave, these atomic species, once formed, must recombine to provide the final gaseous detonation products when the detonation event terminates. The existence and importance of these atomic species achieving a steady-state thermodynamic equilibrium during detonation was determined in two separate experiments using a carbon-14/oxygen-18 labelled homogeneous explosive, BTNEA (Figure 9), and an ^{15}N labeled non-ideal explosive mixture, 20/80 Amatol [20% ammonium nitrate (AN) containing the ^{15}N label and 80% unlabeled TNT) [58]. Even though the BTNEA compound was labeled with ^{13}C and ^{18}O in its two C==O (carbonyl) groups which would favor some retention of its $^{13}C{=}{=}{}^{18}O$ bond in the CO_2 and CO detonation products, no bond retention was found after a full-scale bomb calorimetry detonation experiment [58]. All detonation products (CO_2, CO, CH_4, C_{solid}, and H_2O) gave the same $^{12}C/^{13}C$ and $^{16}O/^{18}O$ ratios contained in the original BTNEA molecule indicating the chemical reaction kinetics were fast enough for all bonds in the

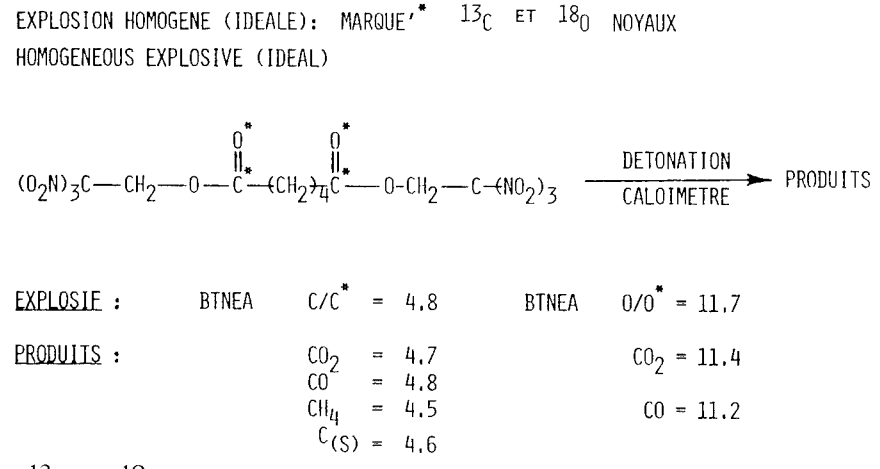

Figure 9. The ^{13}C and ^{18}O Isotopic Distribution in BTNEA Calorimetric Detonation Products [58].

BTNEA to rupture forming a steady-state equilibrium of atomized species prior to their recombination to final detonation products. This might suggest that the KDIE-based differences in the ease of initiation

between TATB/TATB-d_6 during its thermal explosion [40] plus TNT/TNT-d_3,RDX/RDX-d_6, HMX/HMX-d_8 during their detonation event [32,42], come from slower kinetic chemical reaction rate kinetics and their associated rate-controlling covalent bond rupture which occur in the earlier condensed phase rapid thermochemical decomposition process. A previously reported KDIE study conducted with HMX/HMX-d_8 high pressure combustion, suggested the chemical reactions and resultant rate-controlling covalent bond dissociation occurred in the condensed phase portion of the combustion event, rather than in the chemical reactions associated with the gas phase flame portion [35,43b]. With the Amatol, the observed $^{14}N/^{15}N$ ratio, formed only by mixing of atomic ^{15}N species from AN and ^{14}N atomic species from TNT, amounted only to a 12% mixing when one assumes each compound decomposed

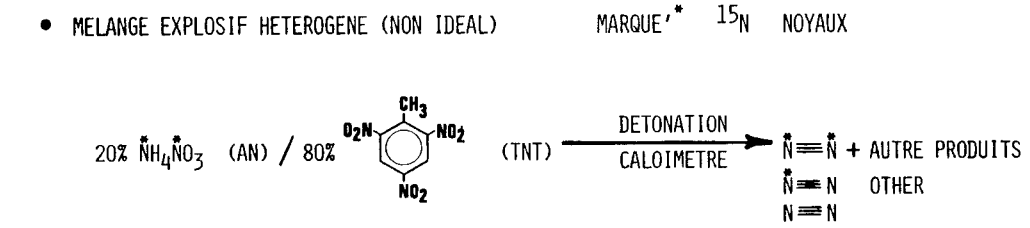

• EXPLOSIF : AMATOL 20/80 (AN MARQUES)
LABELED

• PRODUITS :	ECHANGE AU HASARD (RANDOM)	REEL (ACTUAL)	PAR D'ECHANGES (NONE)
$N^*{\equiv}N^*$	0.086	0.333	0.409
$N^*{\equiv}N$	0.645	0.085	0
$N{\equiv}N$	0.564	0.687	0.887

Figure 10. Isotopic ^{15}N and ^{14}N Exchange of AN and TNT in Amatol Calorimetric Detonation [58].

independently behind the detonation shock wave as did BTNEA. The incomplete mixing of atomic species possibly results from the recombination reaction kinetics proceeding much faster than the microscopic diffusion mechanism of these atomic species into one another [58]. This microscopic diffusion control mechanism explains why the actual macroscopic energy output from the non-ideal Amatol explosive is lower than what theoretical calculations predict.

With the formation and expulsion of final gaseous and solid residue detonation products, the complicated, sequential initiation train is completed. While detailed study must continue on the various component mechanisms, theoretical and experimental studies which reveal the coupling interactions and a possible interdependency of the component mechanisms also require further attention. In some cases, perhaps, where one with the proper insight might recognize their relationship to one another and be able to elucidate how these interactive relationships can provide a better overall understanding of the initiation event. Perhaps this general concept exhibited pictorially by Figure 1 is a starting point.

3. CONCLUSIONS

As discussed in this paper, several key correlations provide new insights into the complex and interactive nature of a sequential initiation train as it proceeds toward an explosive event. Firstly, past kinetic deuterium isotope effect (KDIE) investigations of slow ambient pressure thermochemical decomposition and rapid pyrolytic decomposition processes, plus of other higher pressure/temperature combustion, thermal explosion, and detonation phenomena each reveal a common rate-controlling covalent bond rupture which kinetically regulates the energy release rate of a given energetic material. Secondly, an energetic material's inherent sensitivity has been correlated to it critical temperature, and the energetic compound's critical temperature has been correlated to the kinetics and rate-controlling mechanistic step of the slow ambient pressure thermochemical decomposition process as well as to its higher order thermal explosion phenomenon. Finally, X-ray photoelectron spectroscopy (XPS) analysis with sub-initiatied impact and shock studies of several energetic materials, reveals condensed phase products, generated during hot spot formation, must result from a bond dissociation which provides the rate-controlling step observed during its ambient pressure thermochemical decomposition process. This

suggests that the rate-contolling mechanistic feature of an energetic material's thermochemical decomposition process plays a significant role in its sensitivity characteristics. Additionally, examples have been noted where energy release rates can affect detonation wave's cellular structure, size, and induction times which define when a sufficient concentration of reactive species are generated in the gas phase to effect detonation. The correlation too of chemical kinetics to variations in detonation wave structure during gaseous shock tube detonation, further suggests that kinetically-regulated chemical reactions and their associated rate-controlling bond dissociation step must contribute significantly to determining energy release rates present in the gaseous portion of the initiation train sequence. They may, however, be much faster than the rate-controlling bond dissociations which controls the kinetically-driven chemical reactions of the condensed phase.

These correlations collectively suggest the following: (1) chemical reaction kinetics play a significant role in an initiation train sequence (Figure 1); (2) a slower kinetically regulated rate-controlling mechanistic step can cause noticeable desensitization of an energetic material; and, (c) the kinetically regulated rate-controlling step,usually identified as a covalent bond dissociation or rupture and detected by the condensed phase KDIE approach, is **one** of several desensitizing mechanistic factors found in the initiation train concept. This could mean that by disrupting or altering any one of the several mechanistic processes below its an unspecified threshold, significant desensitization might be achieved for a given energetic material. Alternatively, by collectively altering the pathway or reducing the propagating rate of several mechanistic factors (*eg.* hot spot rate formation or reactive product species threshold concentrations), each by a small degree, an overall additive effect might be achieved which could significantly desensitize a given energetic material. In order to achieve this type of sensitivity control specific mechanisms operating in the explosive train sequence must be more fully elucidated, and just as importantly, the interactions among them and the influence one mechanism has upon another must be determined. Only then will we develop a complete picture of the initiation event which permits explosive sensitivity prediction and design through sound and accurate scientific principles.

4. ACKNOWLEDGEMENTS

The author expresses his sincerest appreciation to Dr.Simone Odiot and her co-chairmen of the 2nd International Workshop on *Microscopic and Macroscopic Approaches to Detonation*, Dr. Ronald Armstrong (USA) and Dr. Anatoly Dremin (Russia), and to members of the Organizing and Scientific Committees for the generous invitation to participate in this scientific gathering. Dr. Frank Walker, an early USA pioneer in hot spot theory and its relevancy, provided the author timely encouragement concerning this initiation train concept. Substantiative scientific discussions with Dr. Jacques Boileau (France) over a number of years also have been very helpful as have been the enthusiasm, encouragement and discussions of Raymond N. Rogers (Los Alamos, NM (USA)] concerning thermal chemistry and the KDIE research the author and his colleagues have conducted during the past 19 years. Alliance Pharmaceutical Corp. provided some needed support in making arrangements to participate at this workshop.

5. REFERENCES and NOTES

[1] Portions of this paper were presented at the following conferences: (a) Shackelford S.A., "Energetic Material Sensitivity and the Rate-Controlling Mechanistic Step", Workshop on Desensitization of Explosives and Propellants", Rijswijk, The Netherlands 11-13 November 1991; (b) Shackelford S.A., "Energetic Material Initiation and Sensitivity. I. Kinetically Regulated Rate-Controlling Mechanistic Steps", Eighteenth International Pyrotechnics Seminar, Breckenridge, Colorado (USA), 13-18 July 1992; and, (c) Shackelford S.A., "Energetic Material Initiation Sensitivity. II. Chemical Structure/Mechanism Relationship to Sensitivity", Eighteenth International Pyrotechnics Seminar, Breckenridge, Colorado (USA), 13-18 July 1992.

[2] Author's new affiliation is Alliance Pharmaceutical Corp. located at the address given on the title header. APC is not involved in any facet of energetic materials research, technology, or development. The sole focus of APC is the use of perfluorocarbon compounds and their derivatives for oxygen transport (synthetic blood substitutes), gas and tissue interchange (liquid breathing), and medical imaging (MRI, X-ray, Ultra-Sound) applications.

[3] Field J.E., Swallowe,G.M., and Heavens S.N., *Proc. R. Soc. Land.*, **A382** (1982) 231-244.

[4] Mohan V.K., Field J.E., and Swallowe G.M., *Combustion Sci. and Tech.*, **40** (1984) 269-278.

[5] Mohan V.K. and Field J.E., *Comb. and Flame*, **56** (1984) 269-277.

[6] Armstrong R.W., Coffey C.S., and Elban W.L., *Acta Metall.*, **30** (1982) 2111-2116.

[7] Elban W.K., Hoffsommer J.C. and Armstrong R.W., *J. Mater. Sci.*, **19** (1984) 552-566.

[8] Armstrong R.W., "Dislocation Pile-Up Mechanism for Initiation of Energetic Crystals", NATO Advanced Study Institute on Chemical Reaction Dynamics, Iraklion (Crete), Greece 25 August-7 September 1985.

[9] Armstrong R.W. and Elban W.L., Microindentation Techniques in Materials Science and Engineering, ASTM STP 889, Eds. Blau P.J. and Lawn B.R. (American Society in Testing and Materials, Philadelphia, 1986) pp. 109-126.

[10] Elban W.L., Armstrong R.W., Yoo K.C. Rosemeirer R.G, and Yee R.Y., *J. Mater. Sci.*, **24** (1989) 1273-1280.

[11] Miller PJ., Coffey C.S., and DeVost V.F., *J. Appl. Phys.*, **59** (1986) 913-916.

[12] Leiber C.O., *J. Hazard Mater.*, **12** (1985) 43-64.

[13] Leiber C.O., *J. Hazard Mater.*, **13** (1986) 311-328.

[14] Leiber C.O., "On Some Shortcomings in the Macroscopic Plane Wave Model of Detonation", Thirteenth International Pyrotechnics Seminar, Grand Junction, Colorado (USA) 11-15 July 1988.

[15] Leiber C.O., "Detonation Model with Spherical Sources Smooth and Rough Pressure Fronts, Dark Waves", Thirteenth International Pyrotechnics Seminar, Grand Junction, Colorado (USA) 11-15 July 1988.

[16] Leiber C.O., "Detonation Model with Spherical Sources C: Quasicontimuum Approach; Slow and Low Velocity Detonation", Fifteenth International Pyrotechnics Seminar, Boulder, Colorado (USA) July 1991.

[17] Leiber C.O., "Detonation Model with Spherical Sources D: Fracture Dynamics of Initiation - Dense Quasihomogeneous Solids", Fifteenth International Pyrotechnics Seminar, Boulder, Colorado (USA) July 1991.

[18] Leiber C.O., "Detonation Model with Spherical Sources E: Dynamic Particle Motion - Initiation of Heterogeneous Materials", Sixteenth International Pyrotechnics Seminar, Jonkoping, Sweden 24-28 June 1991.

[19] Leiber C.O., "Detonation Model with Spherical Sources F: Dynamic Void Mobilities - Alteration of the Hugoniots by Bubble Flow', Seventeenth International Pyrotechnics Seminar, Beijing, China 28-31 October 1991.

[20] Leiber C.O., "Detonation Model with Spherical Sources G: Dynamic Void Mobilities - HVD Initiation of Liquid Explosives", Seventeenth International Pyrotechnics Seminar, Beijing, China 28-31 October 1991.

[21] Armstrong R.W. and Elban W.L.,"Dislocation Mechanics Aspects of Desensitization to Impact or Shock", Workshop on Desensitization of Explosives and Propellants", Rijswijk, The Netherlands 11-13 November 1991.

[22] (a) Odiot S., Peyrard M., and Mijoule C., "Molecular Theory for a Cooperation Mechanism for Shock Induced Detonation Waves in Molecular Crystals: Nitromethane", NATO Advanced Study Institute, Iraklion (Crete), Greece 25 August-7 September 1985; (b) Peyrard M., Odiot S., and Oran E.,

J. de Physique (Colloque C4), **48** (1987) 291-301; and (c) Odiot S. and Peyrard M., *J. de Physique (Colloque C4)*, **48** (1987) 393-395.

[23] Dick J.J., *J. Phys. Chem.*, **97** (1993) 6193-6196.

[24] (a) Dick J.J., Mulford R.N., Spencer W.J., Pettit D.R., Garcia E., and Shaw D.C., *J. Appl. Phys.*, **70** (1991) 3572-3587; and, (b) Dick J.J.,"Orientation Dependence of the Shock Initiation Sensitivity of PETN: A Steric Hindrance Model", Workshop on Desensitization of Explosives and Propellants, Rijswijk, The Netherlands 11-13 November 1991.

[25] Samirant M., *J. de Physique (Colloque C4)*, **48** (1987) 85-98.

[26] Sharma J., Hoffsommer J.C., Glover D.J., Coffey C.S., Santiago F., Stolovy A., and Yasuda S., Shock Waves in Condensed Matter, J. R. Asay , R.A. Graham and G.K. Straub Eds. (Elsevier Science Publishers, Amsterdam, 1983) pp. 543-546.

[27] Sharma J., Hoffsommer J.C., Glover D.L., Coffey C.S., Forbes J.W., Liddiard T.P., Elban W.L., and Santiago F., "Sub-Initiation Reactions at Molecular Levels in Explosives Subjected to Impact and Underwater Shock", 8th Symposium (International) on Detonation (U. S. Government Printing Office, Washngton, D.C., 1987) pp. 725-733.

[28] Sharma J., Forbes J.W., Coffey C.S., and Liddiard T.P., Shock Waves in Condensed Phase Matter, S.C. Schmidt and N.C. Holmes Eds. (Elsevier Science Publishers, Amsterdam, 1987) pp. 565-568.

[29] Sharma J., Forbes J.W., Coffey C.S., and Liddiard T.P., *J. Phys. Chem.*, **91** (1987) 5139-5144.

[30] Shackelford S.A., Beckmann J.W., and Wilkes, J.S., *J. Org. Chem.*, **42** (1977) 4201-4206.

[31] Shackelford S. A., Coolidge M.B., Goshgarian B.B., Loving B.A., Rogers R.N., Janney J.L., and Ebinger, M.H., *J. Phys. Chem.*, **89** (1985) 3118-3126.

[32] Bulusu S.,Weinstein D.I., Autera J.R., and Velicky R.W., *J. Phys. Chem.*, **90** (1986) 4121-4126.

[33] Behrens R.Jr., *J. Phys. Chem.*, **94** (1990) 6706-6718.

[34] Behrens R.Jr. and Bulusu S., *J. Phys. Chem.*, **95** (1991) 5838-5845.

[35] Shackelford S.A., Goshgarian B.B., Chapman R.D., Askins R.E., Flanigan D.A., and Rogers R.N., *Propellants, Explos., Pyrotech.*, **14** (1989) 93-102.

[36] Rodgers S.L., Coolidge M.B., Lauderdale W.J., and Shackelford S.A., *Thermochim. Acta*, **177** (1991) 151-168.

[37] Behrens R.Jr. and Bulusu S., *J. Phys. Chem.*, **96** (1992) 8877-8891.

[38] Behrens R.Jr. and Bulusu S., *J. Phys. Chem.*, **96** (1992) 8891-8897.

[39] Shackelford, S.A., Rodgers S.L., and Askins R.E., *Propellants, Explos., Tech.*, **16** (1991) 279-286.

[40] Rogers R.N., Janney J.L., and Ebinger M.H., *Thermochim. Acta*, **59** (1982) 287-298.

[41] Sharma J., Garrett W.L., Owens F.J., and Vogel V.L., *J. Phys. Chem.*, **86** (1982) 1657-1661.

[42] Bulusu S. and Autera J.R., *J. Energetic Matls.*, **1** (1983) 133-140.

[43] For a Review: (a) Shackelford S.A., Chemistry and Physics of Energetic Materials, S. Bulusu Ed. (Kluwer Academic Press, The Netherlands, 1990) pp. 413-432; and, (b) Shackelford S. A., Chemistry and Physics of Energetic Materials, S. Bulusu Ed. (Kluwer Academic Publishers, The Netherlands, 1991) pp. 433-456.

[44] Odiot S., Chemistry and Physics of Energetic Materials, S. Bulusu Ed. (Kluwer Academic Publishers, The Netherlands, 1991) pp. 102-130.

[45] Allinger N.L., Cava M.P., DeJongh D.C. Johnson C.R., Lebel N.A., and Stevens C.L., Organic Chemistry (Worth Publishers, Inc., New York, 1971) pp.300-301.

[46] Storm C.B., Stine J.R., and Kramer J.F., Chemistry and Physics of Energetic Materials, S. Bulusu Ed. (Kluwer Academic Publishers, The Netherlands, 1991) pp. 605-640.

[47] Rogers R.N., *RCEM Rpt. A-04-87*, (4 Nov 1987) pp. 16-35.

[48] Shackelford S.A. and Goldman J.F.,"Intramolecular Mechanistic Thermochemical Decomposition Studies of 1,3,5,5-Tetranitrohexahydropyrimidine (DNNC) and Its Deuterium Labeled Analogues", 203rd National Am. Chem. Soc. Mtg., San Francisco, CA (USA) 5-10 April 1992.

[49] Storm C.B., Ryan R.R., Ritchie J.P., Hall J.H., and Bachrach S.M., *J. Phys. Chem.*, **93** (1989) 1000-1007.

[50] Rogers R.N., *Anal. Chem.*, **39** (1967) 730-733.

[51] Dacons J.C., Adolph H.G., and Kamlet M.J., *J. Phys. Chem.*, **74** (1970) 3035-3040.

[52] Hoffsommer J.C., Glover D.J., and Elban W.L., *J. Energetic Matls.*, **3** (1985) 149-167.

[53] Lee J., "Combustion and Turbulence I", NATO Advanced Study Institute on Chemical Reaction Dynamics, Iraklion (Crete), Greece 25 August-7 September 1985.

[54] Dupre G., *J. de Physique (Colloque C4)*, **48** (1987) 397-403.

[55] Paillard C., *J. de Physique (Colloque C4)*, **48** (1987) 405-414.

[56] Oran E.S., Kailasanath K., and Guirguis R.H., *J. de Physique (Colloque C4)*, **48** (1987) 105-117.

[57] Pfeil A., Eisenreich N., and Krause H., *J. de Physique (Colloque C4)*, **48** (1987) 209-221.

[58] McGuire R.R., Ornellas D.L., and Askt I.B., *Propellants and Explos.*, **4** (1979) 23-26.

JOURNAL DE PHYSIQUE IV
Colloque C4, supplément au Journal de Physique III, Volume 5, mai 1995

A Theoretical Approach to Energetic Materials

M.D. Cook

Defence Research Agency, Fort Halstead, Sevenoaks, Kent, U.K.

ABSTRACT

This short paper reviews the current theoretical approach to understanding initiation and growth of reaction in energetic materials at Fort Halstead. Theoretical models at the molecular level are used to help develop algorithms at the macroscopic level which can then be used to model real systems.

The study of initiation and growth of reaction in energetic materials has been a rapidly expanding area of research over the last few years. At the microscopic level, many authors have produced decomposition schemes for a wide variety of explosives, but few have provided conclusive experimental evidence to back their predictions. Much of this is due to the great difficulty in experimentally studying fast reactions and identifying each individual step. Despite the difficulties, modern spectroscopic techniques are currently being successfully used to study decomposition reactions at the molecular level.

At the macroscopic level, there have been many many experiments carried out on a whole variety of explosive charges over the last century. However, these experiments have led to only rudimentary mathematical models which have limited application to predicting explosives behaviour. On-the-other-hand the success of the ZND model at predicting the performance of ideal explosives is without question. However, new methodologies still need to be developed to obtain a better understanding and predictive capability particularly in the areas of initiation and growth of reaction, and to describe non-ideal behaviour.

At Fort Halstead we are developing a novel approach to help increase our understanding of the behaviour of explosives and develop predictive models based on well-founded physics and chemical principles. This is an entirely different approach to engineering fits that have been employed to-date. The whole approach is based on theoretical modelling of energetic materials at both the molecular and macroscopic levels.

At the molecular level, it is possible to model decomposition reactions using state-of-the-art Molecular Orbital (MO) codes. These codes have undergone a remarkable transformation within the last ten years or so and, together with ever increasing computing power, that is available at relatively low cost, provide a very powerful tool for investigating decomposition chemistry. MO codes will not replace

experiment, but they can provide a valuable predictive capability which can help the experimentalist. Using such codes it is possible to obtain molecular geometries to within two percent of the experimental values; calculate thermodynamic data; calculate excited states; obtain a whole variety of spectral data; as well as calculate the energetics of reactions. The data obtained from such calculations can be used in other codes both microscopic and macroscopic. It should be noted that MO codes can only be used to perform calculations on at most a few molecules and more commonly only one or two at a time. When two or more molecules are involved in a calculation the whole system is treated as a 'supermolecule'.

Many more molecules can be included in calculations using either Monte Carlo or Molecular Dynamics methods. In these codes hundreds, if not, thousands of molecules can be treated within the model. However, the penalty for including more molecules in the calculation is that, in general, empirical potentials have to be used to describe the interactions between the molecules. However, it has been demonstrated, that it is possible to simulate the essential behaviour of a model explosive using an empirical potential which has an implicit 3-body term. Such models can be used very effectively to study the relationship between the chemistry and physics of explosives. Molecular dynamics calculations on model explosive systems show all the pertinent features that would be expected of real systems. For example, if in the simulation reaction is initiated by means of a flyer plate, then a critical velocity is required to obtain growth to detonation. A steady velocity of detonation is observed, and if the reaction is over-driven then the system still settles to the characteristic velocity of the model. The shock-wave that passes into unreacted material is followed by a zone of highly compressed material, which in turn is followed by the reaction zone, where most of the chemistry takes place. Finally, the reaction zone is succeeded by the gaseous products. This is what is generally observed in real solid explosives.

The gaseous products produced during the detonation are responsible for doing work on the external environment. For example, moving metal. It is important therefore to have a good description of their behaviour at elevated temperatures and pressures. Monte Carlo techniques can, and have been used to study the behaviour of the hot, dense gases in order to aid the development of new improved equations-of-state (EOS). It has been demonstrated using Monte Carlo calculations that many-body terms are required to describe the behaviour of the product gases. These EOS can then, in turn, be used in ideal detonation codes and hydrocodes to predict performance and macroscopic behaviour.

A major goal of any modelling effort must be to predict, from concept of a new energetic molecule its performance, compatibility, stability and sensitivity. Quantum chemistry codes can be used to generate intermolecular potentials which can be used in molecular dynamics codes and monte carlo codes. They can give good predicted geometries which can be used in crystal packing codes to obtain densities. They can also give thermodynamic parameters such as heat of formation. Density information together with heat of formation and an equation-of-state can be used in ideal detonation codes to give an idea of likely performance.

Potentials derived from MO codes can also be used in molecular dynamics simulations. Molecular dynamics simulations of explosives can, in principle, yield reaction kinetics. They can also give very useful physical property data. Both reaction kinetics and material property data can then in principle, be used in hydrocode models to predict sensitivity and other macroscopic properties.

The development of new algorithms to handle the ignition and growth of reaction in explosives is of fundamental importance. Incorporation of suitable routines into existing hydrocodes would allow a much improved predictive capability to model all-up weapon systems. The approach that has been taken at Fort Halstead is to develop an Arrhenius Burn Model that considers the growth of an explosive burn as a series of coupled kinetic steps. The rate of reaction of each step is a function of the concentrations of the constituents, the temperature and the pressure. Each reaction releases energy which fuels the burning process; if the release is sufficiently fast, the burn will run-away to detonation. The model is an attempt to consider the chemistry of the explosive realistically, rather than relying on cruder physical models involving arbitrary parameters. A particular feature of the model is that it employs temperature dependent Arrhenius kinetics. The model is currently being developed to handle both homogeneous and heterogeneous systems. For the latter, hotspots are explicitly considered in a separate routine but are nevertheless assumed to undergo decomposition via the same series of reaction steps.

Discussion

Kondrikov-Cook :

Q : As a result of your calculations you have a critical velocity of a bullet, which can lead to detonation. If you compare the result with the experimental observations, you can precise the equation of state you use, and correspondingly the specific heat value and (V,T) dependence of it, which Dr. Gupta has spoken about.

Did you do this ?

A : Our Arrhenius burn model uses an equation of state for both the products and the reactants. The reactant equation of state is a simple particle velocity shock velocity relationship. The products use the JHWL equation of state. The heat capacity (Cv) used was the published value of the unreacted energetic material at room temperature. The Arrhenius kinetics are adjusted to fit the experimental data. The point that I raised in the presentation was that Cv is temperature dependent and that I had not included the temperature dependence in the calculations to-date. However, the temperature dependent behaviour of Cv can be calculated from stastistical thermodynamics and this will be used in the future.

JOURNAL DE PHYSIQUE IV
Colloque C4, supplément au Journal de Physique III, Volume 5, mai 1995

"Microscopic" and "Macroscopic" Level of the Errors for Detonation Characteristics Calculations: Pedigree of the Errors

T.S. Pivina, E.A. Arnautova, M.S. Molchanova and V.V. Shcherbukhin

N.D. Zelinsky Institute of Organic Chemistry, Russian Academy of Sciences, Moscow 117913, Russia

Abstract

The detonation velocity is one of the principal characteristics of energetic materials. Therefore, computer search for structures of materials with high detonation velocity is a very urgent problem.

We formulated the following task: to elaborate a concept of computer design and subsequent screening of target structures with high detonation velocities.

The present state of this concept and the operation of the program package are illustrated by computer generation of novel energetic compounds, including caged skeletons. Using some optimum gross formulas, we use methods of mathematical chemistry for computer generation of isomeric structural formulas, which may correspond to potentially interesting substances with high detonation velocity. Then, using different methods (mostly original) for estimating the properties of these compounds, we calculate their physicochemical characteristics and recommend some of them for synthesis.

We also analyzed the possible sources of errors during calculation of some detonation characteristics and determined the possible error ranges for the calculated properties at the micro level (enthalpies of formation and molecular crystal densities). As a result, the total (macro level) errors in calculations of detonation parameters were determined.

Introduction

Methods of computer chemistry are presently widely used for predicting structures of substances with the given characteristics. This fact is easy to understand: computer has fantastic potentialities for enumerating structural isomers

generated from the given molecular formula. For example, 217 isomers correspond to the composition C_6H_6. Thus, theoretical computer design and subsequent computer screening turn out to be more efficient (from the economic standpoint) than direct synthetic search.

In addition, the "computer brain" has no accepted stereotypes (which often determine the direction of search for specialists in synthetic chemistry), and we should expect that computer chemistry will provide us with nontrivial structures possessing extremum characteristics.

The objective of this study was computer search for structures of compounds with high detonation velocities.

However, solving the problem of computer screening for compounds with high detonation velocity, we encountered the problem of different errors in velocity calculations. These errors depend on the inaccuracy of estimating the physicochemical characteristics that are used for calculating the velocity: energy content and molecular crystal density of the structures in question. Therefore, we had to study how the errors emerging at the micro level of computer search for compounds with high detonation velocity (i.e., during calculations of formation enthalpies and molecular crystal densities) affect to accuracy of calculations with respect to macro level characteristics (the macro level is the level of computer screening by detonation velocities and subsequent selection of the target structures).

This study does not touch upon the mechanism of such a complex phenomenon as detonation. It only considers, so to say, the purely "pragmatic" aspects of the relationships between the molecular and macroscopic levels of this phenomenon: the relationship between the calculated characteristics of the micro level (enthalpy of formation and molecular crystal density) with the calculated characteristics of the macroscopic level.

So, we analyzed the possible sources of errors in such calculations by several particular examples, trying to trace the "pedigree" of the errors from the micro level to some detonation characteristics of the macro level.

Methodology

The present state of our concept and the program package for computer search of promising structure [1] are illustrated by Fig. 1. Using some optimum gross

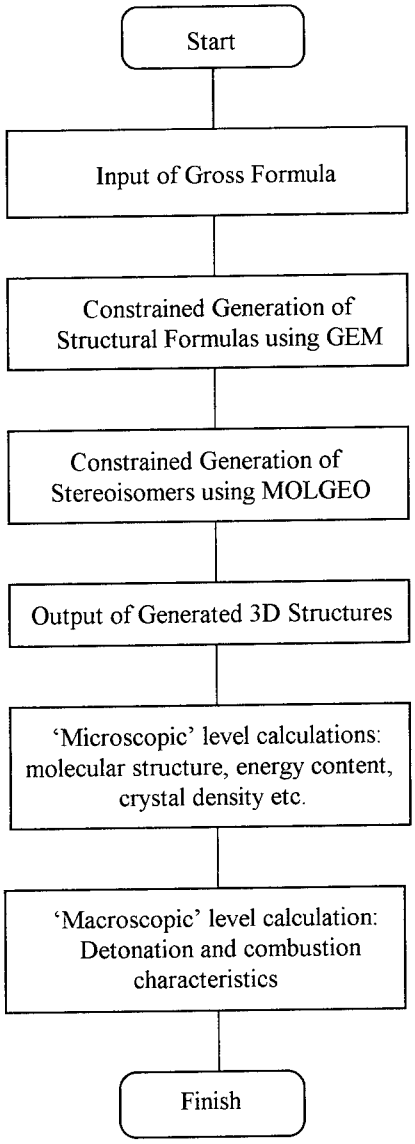

Fif. 1. The flow-chart of computer search for structures of target compounds.

formula, we use mathematical chemistry to perform computer generation of isomeric structural formulas corresponding to potentially interesting substances with possibly high detonation velocity. Then, using different methods for estimating the properties of these compounds, we calculate their physical and chemical characteristics.

This study illustrates the whole concept of search for structures of high-energy compounds with high detonation velocities by the example of caged-type compounds from the adamantane and wurtzitane series.

The problem was formulated as follows: starting from the gross formulas of adamantane $C_{10}H_{16}$ and wurtzitane $C_{12}H_{18}$, find their potentially interesting nitroamino derivatives [2]. The principal parameter characterizing the compounds was their detonation velocity, which is known to be directly related to energy content and crystal density.

From the structural viewpoint, the energy content is determined [3] by the optimum number of quaternary and/or tertiary carbon atoms, tertiary nitrogen atoms, condensed rings, and also by the presence of explosophoric groups. The crystal density depends on the molecule's own symmetry and is usually higher for symmetrical molecules [4].

The first step consisted in the generation of constitutional isomers,represented by molecular graphs. Among all the molecular graphs that could be found for the given gross formulae of the adamantane and wurtzitane series, we considered only those which obeyed the restrictions specified in [2].

Using the GEM program [2] and the conditions for selecting the appropriate structures, we finally sorted out 11 isomers for the adamantane series and 49 isomers for the wurtzitane series. Afterwards, we estimated the energy content of these molecules by computational methods of quantum chemistry and selected 3 isomers from the adamantane series and 5 isomers from the wurtzitane series as the most promising. Then, we considered their hexaazahexanitro derivatives: namely, only those which preserved maximum molecular symmetry after the insertion of six nitroamino groups into the skeleton (Table 1).

At the second step, the MOLGEO [2] program converted the isomers from two-dimensional molecular graphs into possible 3-dimensional molecular models. MOLGEO rapidly generates acceptable 3-dimensional Cartesian coordinates of

Table 1. The calculational parameters of target compounds (● - NNO_2 groups).

No. of Skeleton	Carcasses	Molecular crystal density, g/cm^3	Enthalpy of formation in solid state, kcal/mol	Detonation parameters		Combustion parameters; Δ=0.1 g/cm^3			
				CJ-pressure, kbar	Velosity, m/s	T, K	P, bar	Es, J/g	Qex, J/g
1	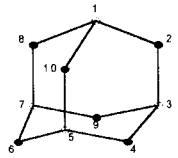	2.000	69.1	378.22 (471.11)	8614 (9948)	4102	1297	1165	1437
2	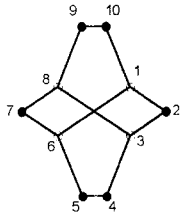	2.054	124.25	410.925 (520.96)	8862 (10444)	4249	1363	1224	1542
3	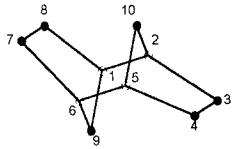	2.067	133.84	422.257 (532.17)	8945 (10550)	4282	1378	1237	1565

Continuation of Table 1.

No. of Skeleton	Carcasses	Molecular crystal density, g/cm^3	Enthalpy of formation in solid state, kcal/mol	Detonation parameters		Combustion parameters; Δ=0.1 g/cm^3			
				CJ-pressure, kbar	Velocity, m/s	T, K	P, bar	Es, J/g	Qex, J/g
4	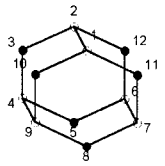	1.915	77.13	376.342 (396.70)	8678 (9170)	4322	1469	1314	1493
5	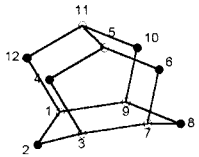	2.023	73.58	421.818 (450.342)	9008 (9609)	4346	1480	1324	1511
6	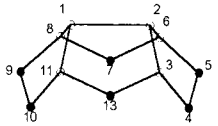	1.984	95.94	410.471 (436.55)	8932 (9529)	4431	1521	1360	1572
7	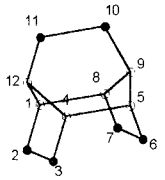	2.000	153.61	430.754 (461.45)	9080 (9819)	4576	1591	1422	1676
8	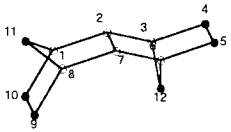	1.89	135.84	376.218 (399.41)	8690 (9271)	4490	1549	1385	1614

atoms according to the molecular connectivity table and the table of standard bond lengths and valence angles.

At the third step, the molecular geometry of the generated structures was refined, and the enthalpy of formation was estimated by subsequent application of the molecular mechanics method - the MM2 program [5] and the PM3 [6] quantum chemical method for the compounds in gas phase.

Then, we calculated molecular crystal densities of the resultant structures and their sublimation enthalpies, using the method of Atom-Atom Potential Functions (AAPF) [7,8]. Calculations of sublimation enthalpy for the crystals of the resultant compounds enabled us to estimate the energy content of these substances in the solid state and, afterwards, to calculate their detonation characteristics and combustion parameters.

However, the accuracy of estimating the detonation characteristics is very much dependent on the accuracy of calculating the energy content and molecular crystal density of the structures in question. Therefore, to reach our principal goal (the search for structures with high detonation velocities), we had to evaluate, so to say, the pedigree of the errors from the micro to the macro level. For this purpose, we first estimated this pedigree of errors by high-energy compounds, where a good experimental basis is available for such estimates and for "tracing" the resultant errors from the micro to the macro level. We selected hexogen (RDX) and octogen (HMX) as such "expert" compounds.

Results and discussion

Table 1 shows some characteristics of our compounds, as well as their principal calculated parameters of detonation and combustion.

On the whole, all the potential skeletons that obtained during directed computer generation have high detonation velocities. Among the compounds from the adamantane series, the hexaazahexanitro substituted frameworks N 3 (D = 8945 m/s) and N 1 (D=8614 m/s) have the highest and lowest detonation velocities, respectively (Table 1). In the wurtzitane series, compounds N 7 (D=9080 m/s) and N 4 (D=8678 m/s) have the highest and lowest detonation velocities, respectively.

Analyzing the results, we may note that hexanitrohexaazaisowurtzitane (CL-20) has the high detonation velocity (9.01 km/s) as calculated by the TIGER program package [9], or 9.61 km/s as obtained by the scheme developed in [10, 11, 12].

However, let us return to the combined effect of the errors in energy content and molecular crystal density calculations on the accuracy of detonation calculations. To consider this problem, let us analyze the calculated results for hexogen and octogen (Tables 2, 3). As follows from the results of our calculations, if the error in the enthalpy of hexogen formation is 1 kcal/mol (the experimental value - 17.0 kcal/mol [13]), the error in the calculated detonation velocity is 4 m/s (the experimental values are 8180 m/s [14] and 8700 m/s [15]). As the same time, if the error in molecular crystal density calculations is 0.02 g/cm^3, the corresponding error in D calculations is up to 68 m/s.

Similar results are also typical for the calculated detonation properties of octogen (the results are obtained for the α-form of this compound): if the error in the calculated enthalpy of formation is 2 kcal/mol (the experimental value is 21.0 kcal/mol [13]) the inaccuracy of D calculations is 6 m/s; if the error in molecular crystal density calculations is 0.04 g/cm^3 (the experimental value is 1.84 g/cm^3 [14]), the inaccuracy of detonation velocity calculations is from 134 to 140 m/s.

Unfortunately, the data on physicochemical properties, combustion and detonation parameters of hexaazahexanitroisowurtzitane (CL-20) are not available from literature; therefore, we cannot estimate the pedigree of errors (at the macro and micro level) for CL-20. The calculated results for this compound are given in Table 4. If we take the calculated density (2.1 g/cm^3 [3]) and the enthalpy of formation (99.3 kcal/mol [16]), then the average inaccurasy of detonation velocity is 4 m/s for the error in formation enthalpy of 2 kcal/mol and 127 m/s for the density error of 0.04 g/cm^3.

Thus, results of our calculations and their analysis let us conclude that errors in the calculated detonation velocity mostly depend on errors in molecular crystal density calculations rather than on errors in energy content calculations.

Conclusion

It may be noted that errors in energy content calculations only moderately affect the resultant errors in calculations of detonation characteristics, whereas the effect of errors in molecular crystal density calculations is very notable. A logical conclusion

Table 2
The results of the TIGER-calculations compared to results of calculations accoding to scheme [10,11,12] (in brackets) for the hexagen (RDX)

$d = 1.75$ g/cm^3				
ΔH°_f, kcal/mol	15.0	16.0	17.0	18.0
P, kbar	334.3 (332.2)	334.7 (332.6)	335.2 (333.1)	335.6 (333.5)
D, m/s	8570 (8650)	8574 (8660)	8578 (8670)	8582 (8670)
T, K	2568	2576	2585	2593
I	(119.1)	(119.2)	(119.3)	(119.4)

$\Delta H^\circ_f = 15$ kcal/mol

d, g/cm^3	1.76	1.78	1.80	1.82	1.84
P, kbar	338.5 (336.6)	347.0 (345.5)	355.7 (354.5)	364.6 (363.7)	373.4 (373.0)
D, m/s	8604 (8690)	8672 (8780)	8740 (8860)	8808 (8940)	8876 (9030)
T, K	2553	2521	2490	2457	2425
I	(119.8)	(121.3)	(122.8)	(124.3)	(125.9)

$\Delta H^\circ_f = 16$ kcal/mol

P, kbar	339.0 (337.0)	347.5 (345.9)	356.1 (355.0)	364.9 (364.1)	373.9 (373.5)
D, m/s	8608 (8700)	8676 (8780)	8743 (8870)	8812 (8950)	8880 (9030)
T, K	2561	2530	2498	2466	2433
I	(119.2)	(121.4)	(123.0)	(124.5)	(126.0)

$\Delta H^\circ_f = 17$ kcal/mol

P, kbar	339.4 (337.5)	347.9 (346.4)	356.6 (355.4)	365.4 (364.6)	374.3 (374.0)
D, m/s	8612 (8710)	8679 (8790)	8747 (8870)	8815 (8960)	8884 (9040)
T, K	2569	2538	2506	2474	2441
I	(120.1)	(121.6)	(123.1)	(124.6)	(126.2)

$\Delta H^\circ_f = 18$ kcal/mol

P, kbar	339.8 (337.9)	348.3 (346.8)	357.0 355.9	365.8 (364.1)	374.8 (374.5)
D, m/s	8616 (8710)	8683 (8800)	8751 (8800)	8819 (8960)	8888 (9050)
T, K	2578	2547	2515	2483	2450
I	(120.2)	(121.7)	(123.2)	(124.7)	(126.3)

Table 3

The results of the TIGER-calculations compared to results of calculations according to scheme [10,11,12] (in brackets) for the octogen (HMX).

ΔH°_f = 20.79 kcal/mol					
d, g/cm^3	1.76	1.80	1.84	1.88	1.92
P, kbar	338.8 (336.8)	355.9 (354.8)	373.7 (373.3)	392.0 (392.5)	410.9 (412.3)
D, m/s	8606 (8700)	8742 (8860)	8878 (9030)	9016 (9200)	9154 (9370)
T, K	2558	2495	2430	2363	2294
I	(119.9)	(122.9)	(126.0)	(129.0)	(132.2)

d = 1.76 g/cm^3				
ΔH°_f, kcal/mol	18	20	22	24
P, kbar	337.9 (335.9)	338.5 (336.6)	339.2 (337.2)	339.8 (337.9)
D, m/s	8598 (8680)	8604 (8690)	8610 (8700)	8616 (8710)
T, K	2540	2553	2565	2578
I	(119.6)	(119.8)	(120.0)	(120.2)

d = 1.80 g/cm^3				
ΔH°_f, kcal/mol	18	20	22	24
P, kbar	355.0 (353.8)	355.7 (354.5)	356.3 (355.2)	357.0 (355.9)
D, m/s	8734 (8850)	8740 (8860)	8745 (8870)	8751 (8880)
T, K	2477	2490	2502	2515
I	(122.6)	(122.8)	(123.0)	(123.2)

d = 1.84 g/cm^3				
ΔH°_f, kcal/mol	18	20	22	24
P, kbar	372.7 (372.3)	373.4 (373.0)	374.1 (373.8)	374.8 (374.5)
D, m/s	8870 (9020)	8876 (9030)	8882 (9040)	8888 (9050)
T, K	2412	2425	2437	2450
I	(125.7)	(125.9)	(126.1)	(126.3)

d = 1.88 g/cm^3				
ΔH°_f, kcal/mol	18	20	22	24
P, kbar	391.0 (391.4)	391.7 (392.2)	392.4 (393.0)	393.1 (394.0)
D, m/s	9008 (9180)	9014 (9200)	9019 (9210)	9025 (9220)
T, K	2345	2358	2370	2383
I	(128.8)	(129.0)	(129.2)	(129.4)

d = 1.92 g/cm^3				
ΔH°_f, kcal/mol	18	20	22	24
P, kbar	409.8 (411.2)	410.6 (412.0)	411.3 (412.9)	412.0 (413.7)
D, m/s	9147 (9360)	9152 (9370)	9158 (9380)	9163 (9390)
T, K	2276	2289	2301	2314
I	(131.9)	(132.1)	(132.3)	(132.5)

Table 4
The results of the TIGER-calculations compared to results of calculations accoding to scheme [10,11,12] (in brackets) for the hexaazahexanitroizowurtzitane (CL-20).

d, g/cm^3	**1.94**	**1.98**	**2.02**	**2.06**	**2.10**
ΔH°_f= 94 kcal/mol					
P, kbar	385.8 (413.5)	403.1 (433.9)	421.0 (454.9)	439.4 (476.6)	458.4 (499.0)
D, m/s	8749 (9330)	8874 (9510)	9002 (9680)	9130 (9850)	9261 (10030)
T, K	2830	2763	2694	2623	2550
I	(131.5)	(134.6)	(137.8)	(140.9)	(144.2)
ΔH°_f = 100 kcal/mol					
P, kbar	387.2 (414.2)	404.6 (435.6)	422.5 (456.7)	440.9 (478.5)	460.0 (500.9)
D, m/s	8761 (9360)	8886 (9530)	9013 (9700)	9141 (9880)	9271 (10050)
T, K	2858	2791	2722	2651	2578
I	(131.9)	(135.0)	(138.2)	(141.4)	(144.6)
ΔH°_f = 106 kcal/mol					
P, kbar	388.7 (416.8)	406.1 (437.3)	424.0 (458.5)	442.5 (480.4)	461.5 (502.9)
D, m/s	8772 (9380)	8897 (9550)	9024 (9730)	9152 (9990)	9282 (10080)
T, K	2886	2819	2750	2679	2606
I	(132.3)	(135.4)	(138.6)	(141.8)	(145.1)
ΔH°_f= 110 kcal/mol					
P, kbar	390.0 (417.8)	407.0 (438.4)	416.0 (459.7)	443.5 (481.6)	462.6 (504.2)
D, m/s	8780 (9390)	8905 (9570)	8968 (9740)	9159 (9920)	9289 (10100)
T, K	2904	2838	2804	2698	2625
I	(132.6)	(135.7)	(138.9)	(142.1)	(145.4)

follows: high-precision calculations of detonation characteristics at the macro level require accurate calculations of the molecular crystal density. To a smaller degree, the errors depend on the inaccuracies in determining the energy content of compounds.

On the whole, we should note that our concept of computer search for structures of compounds with high detonation velocities may be efficiently used both for computer generation (with subsequent screening) by other molecular formulas and for computer search aimed at structures with other desired properties (for example, high impulse of launching ability, definite heat stability, or given sensitivity parameters).

References

(1) T.S.Pivina,V.V.Shcherbukhin, M.S.Molchanova, E.A.Arnautova, A.V.Dzyabchenko, I.A.Suslov. "The Elaboration of an Ab Initio Method for Structural Generation of Synthones Aimed at Creating Energetic Materials", in Proc. of the 20th IPS, Colorado Springs, US, 797(1994).

(2) T.C.Pivina, M.S.Molchanova, V.V. Shcherbukhin, N.S.Zefirov. "Computer Generation of Caged Frameworks Which Can be Used as Synthons for Creating High-Energetic Materisals", Propellants, Explosives, Pyrotechnics 19, 1994.

(3) A.T.Nielsen. Polycyclic Amine Chemistry, in: G.A.Olah and D.R.Squire (Eds.) "Chemistry of Energetic Materials", Academic Press, Inc., 1991.

(4) T.S.Pivina, V.A.Shlyapochnikov. "A Heuristic Model for Computer Prediction of Molecular Crystals with High Density", Zh. Fiz. Khim., 66, 1, 84 (1992).

(5) T.Clark. "A Handbook of Computational Chemistry", John Willey & Sons, Inc., 1985.

(6) AMPAC CODE (Version 1.00).

(7) A.I.Kitaigorodsky. Molecular Crystals and Molecules. Academic Press: New York, London, 1973.

(8) N.E.Kuzmina, N.A.Pirogova, T.S.Pivina, V.A.Shlyapochnikov. "Analysis of Potential Energy Surfaces for Crystals of Poly-Nitro Compounds", Zh. Fiz. Khim., 66, 1, 101 (1992).

(9) M. Cowperthwaite, W.H. Zwisler. "TIGER Computer Program Documentation", SRI Publication, No. Z106, 1973.

(10) V.I. Pepekin, M.N. Makhov, Yu.A. Lebedev. Dokl. Akademii Nauk, 232, 4, 852 (1977).

(11) V.I. Pepekin, N.M. Kuznetsov, Yu.A. Lebedev. Dokl. Akademii Nauk, 234, 1, 105 (1977).

(12) V.I.Pepekin, Yu.A. Lebedev. Dokl. Akademii Nauk, 234, 6, 1391 (1977).

(13) G.Krien, H.H.Licht, J.Zierath. Thermochemische Untersuchungen an Nitraminen, Thermochimica Acta, 6(1973), 465-472.

(14) Properties of Explosives of Military Interest, Army Material Command, AMC pamphlet, 706-177 (1971).

(15) D.R.Hardesty, D.E.Kennedy. Thermochemical Estimation of Explosive Energy Output, Combustion and Flam 28, 45-59 (1977)

(16) S.Bourasseau. A systematic Procedure for Estimating the Standart Heats of Formation in the Condensed State of Non Aromatic Polynitro Compounds. Journal of Energetic Materials, vol.8, 416-441 (1990).

VI TOWARDS A REALISTIC CHEMISTRY OF THE REACTIONAL PROCESSES IN DETONATION

Chairman : Pr Sandor Fliszar, Université de Montréal

When asked where and in what manner quantum chemistry can contribute to the understanding of detonation chemistry and physics, the answer to that surely innocuous question may all too easily get blurred by the diversity of facets offered by detonation : the distinction which is commonly made between its microscopic and macroscopic aspects practically entails the need for (at least) two theoretical approaches.

Basic thermochemical informations about the ground-state reactant - in form of its enthalpy of formation, for example - and of the reaction products is instrumental in macroscopic description, namely, in codes used for the calculation of detonation velocities. In this domain, conventional theory plays in a way the role of a supporting actor, a tool capable of supplying the required numerical input - be it for ground- or excited states - but does not in itself explain why one or another compound explodes.

Microscopic approaches, on the other hand, get at the heart of the matter by explicit consideration of local properties in the molecular fabric, such as individual chemical bonds and the energies required for their cleavage, but this kind of work involves new, less conventional techniques developped from traditional molecular-orbital theory : surely, this adds to our investigative tools, particularly by disclosing in what manner often minute changes in environment do affect individual bond dissociation energies, thus offering new insight into the complex phenomena of detonation.

In short, both the macroscopic and microscopic approaches to the understanding of detonation should greatly benefit from quantum theory. The idea is to ask the right questions. Schrödinger answers the questions but does not volunteer the answers.

1 STUDY OF THE ENERGETIC BEHAVIOUR OF ENERGETIC COMPOUNDS

2 APPLICATIONS FOR ENGINEERING

3 DISCUSSION

1 STUDY OF THE ENERGETIC BEHAVIOUR OF ENERGETIC COMPOUNDS

Etude du comportement énergétique de l'explosif à l'échelle moléculaire. Approche théorique et expérience TRISP ; D.Delpeyroux, C.Lafon, D.Mathieu, **Ph.Simonetti**, F.Cansel, D.Fabre, J.Petitet

Thermochemistry and Reaction Mechanisms of Nitromethane Ignition ; C.F.Melius

Microscopic Experimental Approaches to High Pressure Chemistry ; **T.P.Russell**, T.M.Allen, J.K.Rice and Y.M.Gupta

Reaction Mechanisms in Shocked, Intercalated Graphite and Boron Nitride ; R.D.Bardo

JOURNAL DE PHYSIQUE IV
Colloque C4, supplément au Journal de Physique III, Volume 5, mai 1995

Etude du Comportement Energétique de l'Explosif à l'Echelle Moléculaire. Approche Théorique et Expérience TRISP

D. Delpeyroux, C. Lafon, D. Mathieu, Ph. Simonetti, F. Cansell*, D. Fabre* and J.P. Petitet*

Commissariat à l'Energie Atomique, Centre d'Etudes du Ripault, BP. 16, 37260 Monts, France
** LIMHP-CNRS Institut Galilée, 93430 Villetaneuse, France*

Abstract :

The study of energetic behaviour of explosive in relation with its molecular structure needs the analysis of decomposition mechanisms through Quantum Chemistry calculations. We present methodology and first results. The TRISP technique is developed to detect the intermediate chemical species and the detonation products. And the modelling of IR spectra (theoretical calculations and consideration of (P, T) effects on the vibration bands) is a tool to interpret the experimental results.

1 - Introduction

L'objectif de la recherche de nouvelles molécules explosives est l'obtention d'un compromis satisfaisant, pour l'utilisation recherchée, entre les performances énergétiques et les contraintes de sécurité (sensibilité au choc, stabilité thermique). Les performances dépendent en particulier du travail fourni par les gaz de détonation pendant leur détente.

Ainsi, pour chaque molécule appartenant à une famille donnée, la connaissance des réactions chimiques qui se produisent pendant la décomposition et la caractérisation des espèces formées permettent une meilleure compréhension du comportement énergétique du matériau en relation avec sa structure moléculaire et une simulation plus exacte du comportement macroscopique.

L'étude des mécanismes réactionnels mis en jeu pendant la décomposition de l'explosif est réalisée par l'analyse des Surfaces d'Energie Potentielle des réactions chimiques, obtenues par les méthodes de la Chimie Quantique. Nous recherchons une validation expérimentale des résultats théoriques par la mise en évidence des espèces

formées dans le milieu en détonation à l'aide d'une spectrométrie Infrarouge ultra rapide TRISP [1]. Afin d'aider à l'interprétation de ces spectres Infrarouge expérimentaux, nous utilisons les techniques de calcul de la Chimie Quantique pour leur simulation numérique, et nous exploitons les résultats d'expériences conduites en cellule à enclume de diamant pour évaluer l'influence des effets de forte pression et de température élevée du milieu en détonation sur les bandes de vibration.

2 - Approche théorique

2.1 - Modélisation des mécanismes réactionnels de décomposition de l'explosif

2.1.1 - Méthodologie

Nous nous intéressons tout d'abord à un explosif de la famille des Nitramines, l'Hexogène, sur lequel nous disposons d'un grand nombre de résultats d'études concernant sa décomposition. En nous appuyant sur les données recueillies par une recherche bibliographique, nous établissons le diagramme de décomposition de la molécule avec les différentes voies possibles de cassures de liaison et les espèces chimiques résultantes. Nous voyons sur ce diagramme, représenté sur la figure n° 1, les trois voies essentielles de décomposition du RDX :

- la rupture de liaison simple N-N,
- la cassure concertée des liaisons C-N du cycle,
- le réarrangement intramoléculaire avec élimination de HONO.

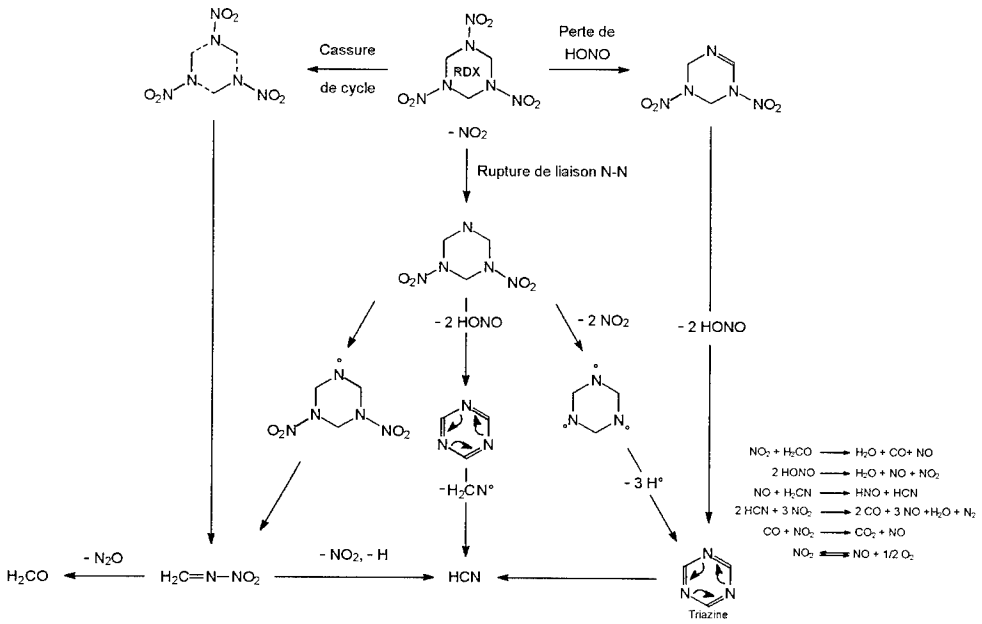

Figure 1 : Schéma de décomposition du RDX

Ces voies conduisent aux espèces chimiques principales suivantes :
$H_2C = N\text{-}NO_2$, triazine, H_2CO, H_2O, HCN, NO_2, HONO, CO_2, CO, N_2O

Notre objectif est de déterminer l'existence de voies préférentielles parmi celles existantes et de proposer les espèces prépondérantes.

Pour cela, nous localisons sur le graphe de la fonction Energie Potentielle du système chimique en cours de dissociation, avec pour variables les coordonnées de réaction le long de la liaison qui se casse, les points stationnaires (géométrie à l'équilibre, état de transition) afin de connaître l'Energie d'activation de dissociation E_a^d de la réaction. Un mécanisme réactionnel est d'autant plus probable, parmi ceux possibles, que l'Energie E_a^d est faible.

La détermination de la fonction Energie Potentielle est réalisée par les méthodes de calcul de la Chimie Quantique. Compte tenu du nombre d'atomes des molécules étudiées et du caractère relatif des résultats que nous recherchons, nous utilisons les méthodes semi-empiriques (AM1, PM3 dans les codes MOPAC6, AMPAC).

D'autre part, nous considérons que même si sous l'effet d'une onde de choc, une certaine population de molécules explosives se trouve dans un état électronique excité [2], la population majoritaire de molécules reste à l'état fondamental. Donc, nous traitons la décomposition des molécules en nous intéressant au paramètre moléculaire, l'Energie d'activation de dissociation, calculé dans l'état électronique fondamental.

Les hypothèses de calcul sont déterminées par une étude préliminaire sur une molécule de la famille des Nitramines, de plus petite taille que l'Hexogène, la Diméthyl-Nitramine DMN [$(CH_3)_2$ $N\text{-}NO_2$]. Ces hypothèses sont les suivantes :

- hamiltonien et paramétrisation AM1,
- description de la structure électronique du système chimique par des méthodes en couches ouvertes (UHF) pour la plupart des réactions, et par des méthodes en couches fermées (RHF) pour les réarrangements (élimination de HONO). Nous représentons sur la figure n° 2 le graphe obtenu pour la cassure $N\text{-}NO_2$ de la Diméthyl-Nitramine.

L'utilisation de l'Interaction de Configurations (IC) permet de traiter correctement un tel problème de réactivité chimique par l'obtention d'une fonction d'onde très flexible et donc apte à représenter celle du système chimique tout au long de son évolution. Cependant nous estimons sa mise en oeuvre trop délicate pour convenir à notre étude à caractère systématique et pour laquelle nous recherchons des résultats relatifs,

- optimisation de la position des autres atomes de la géométrie à chaque pas de la coordonnée de réaction

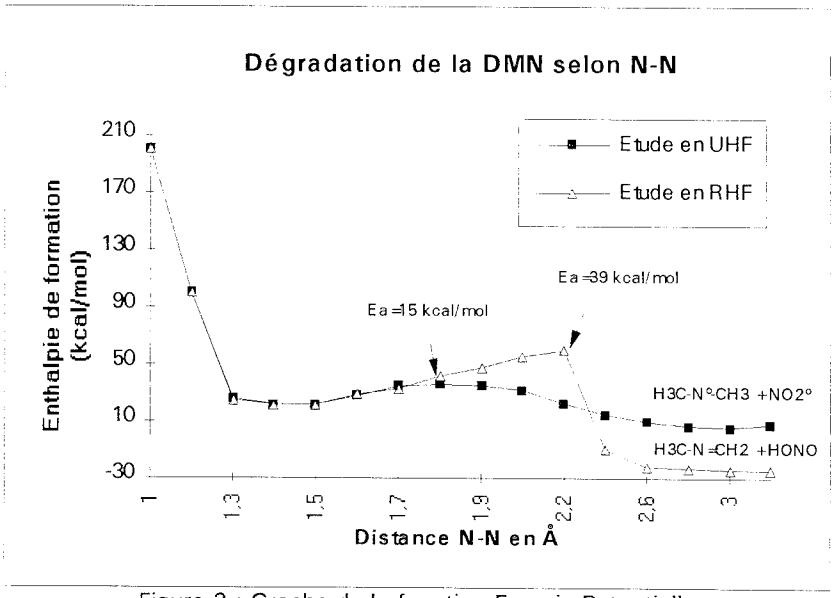

Figure 2 : Graphe de la fonction Energie Potentielle correspondant à la cassure N-NO_2 de la DMN

2.1.2 - Application à l'étude des mécanismes de décomposition de l'Hexogène (RDX)

Nous représentons sur la figure n° 3 le graphe de la fonction Energie Potentielle correspondant à la cassure de liaison simple N-NO_2 de l'Hexogène

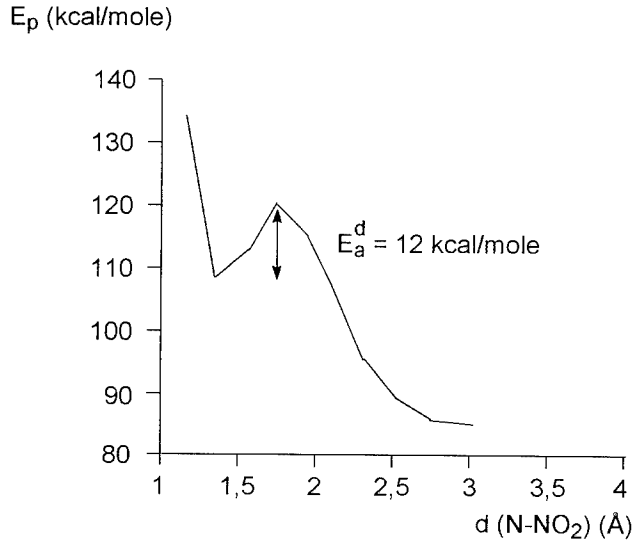

Figure 3 : Graphe de la fonction Energie Potentielle correspondant à la cassure N-NO_2 de l'Hexogène

Nous indiquons sur la figure n° 4 suivante la valeur des Energies d'activation de dissociation pour les réactions chimiques impliquées dans le premières étapes de la décomposition de RDX et dans la dissociation de la Méthylène-Nitramine ($H_2C = N\text{-}NO_2$).

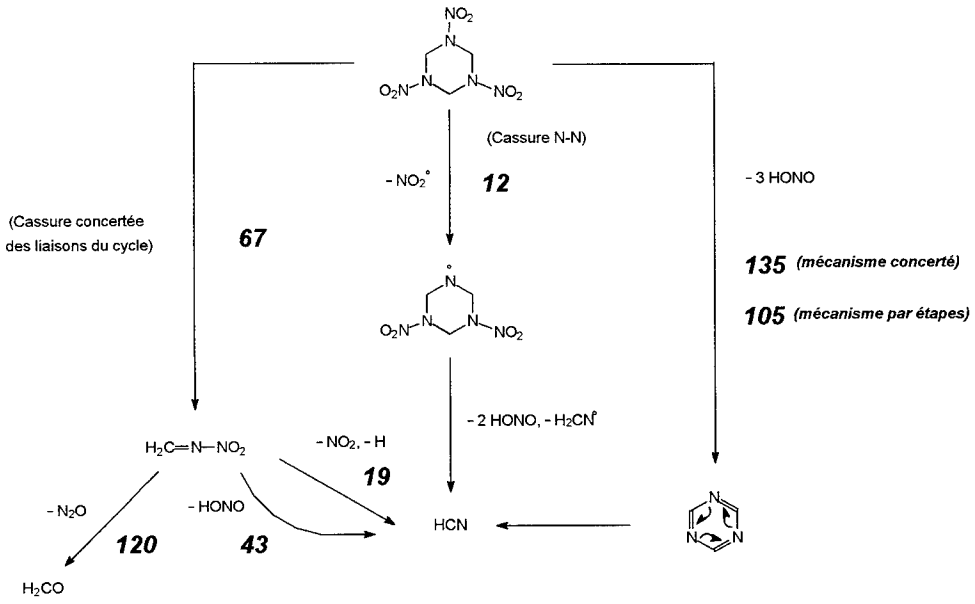

Figure 4 : Schéma de décomposition du RDX
Energies d'activation de dissociation $\left(E_a^d \text{ kcal / mole}\right)$

Selon ces résultats, la voie préférentielle de dissociation du RDX est la cassure de liaison simple $N\text{-}NO_2$, conduisant ensuite à HCN. D'autre part, la décomposition de la méthylène-nitramine, espèce intermédiaire résultant de la cassure concertée des 3 liaisons C-N du cycle, conduit également préférentiellement à HCN plutôt qu'à H_2CO. Ainsi, NO_2 et HCN sont des espèces de petite taille qui se forment très tôt dans le processus. La formation de la triazine, par élimination de HONO après réarrangement intramoléculaire, semble peu probable. Par ordre d'importance décroissante, nous avons donc les espèces suivantes dans le milieu : (NO_2, HCN), (N_2O, H_2CO), (HONO, triazine). Ces conclusions sont en accord global avec les éléments recueillis par notre recherche bibliographique.

2.1.3 - Conclusion

Nous établissons notre démarche théorique, afin d'approfondir notre connaissance des mécanismes réactionnels qui accompagnent la décomposition d'une molécule d'explosif à structure chimique donnée, par l'étude du RDX. Nous appliquons actuellement cette démarche à l'étude de la décomposition d'explosifs avec des formules chimiques et des comportements énergétiques différents : TATB, ANT, ONTA, DANTNP, pour déterminer les réactions les plus probables et les espèces formées prépondérantes en fonction de la structure moléculaire initiale.

2.2 - Modélisation des spectres Infrarouge des espèces formées pendant la décomposition du RDX

La validation des résultats de l'étude théorique concernant les mécanismes réactionnels nécessite la mise en évidence des espèces chimiques formées dans le milieu en détonation. Pour cela, nous recherchons la détection des molécules par leur spectre IR (spectrométrie TRISP). L'interprétation des spectres expérimentaux est facilitée par leur modélisation qui présente deux aspects :

- le calcul numérique des caractéristiques des modes de vibration (fréquence et intensité),

- la prise en compte des effets de forte pression et de température élevée du milieu en détonation sur les modes calculés.

2.2.1 - Simulation numérique des spectres IR

Nous nous intéressons aux spectres Infrarouges des espèces formées pendant la décomposition du RDX. Des spectres de référence existent pour les molécules HCN, H_2CO, NO_2, NO,... Par contre, les temps de vie des espèces intermédiaires sont trop courts pour qu'elles puissent être isolées et caractérisées par spectroscopie.

Pour la simulation numérique de ces spectres, nous utilisons les méthodes ab-initio de la Chimie Quantique au niveau Hartree-Fock et post-Hartree-Fock (MP2) dans le cadre des approximations classiques (Born - Oppenheimer et harmonicité).

Nous distinguons les systèmes à couches fermées (H_2CO, HCN, CO) et ceux à couches ouvertes ou polarisables (NO_2, NO). Pour ces derniers, l'existence d'un électron non apparié nécessite une flexibilité particulière de la fonction d'onde.

Nous présentons dans le tableau n° 1 ci-dessous les résultats concernant les fréquences et les intensités du spectre Infrarouge de la 1,3,5 Triazine, molécule représentative des systèmes à couches fermées. Ces résultats permettent de mettre en évidence les effets de base et de prise en compte de la corrélation électronique. Il apparaît qu'une hypothèse de calcul MP2/6-31G* conduit à des résultats satisfaisants.

4-31G basis set			6-31G* basis set						expérience
HF			HF			MP2			
Freq (cm-1)	Intensity	Δ (%)	Freq (cm-1)	Intensity	Δ (%)	Freq (cm-1)	Intensity	Δ (%)	Freq (cm-1)
751	42	9,3	757	46	10	688	38	0,1	687
800	52	8,3	836	64	13	768	32	- 3,9	739
1076	5	4,1	1082	2	5	920	1	10	1033
1310	2	12	1272	0,2	9	1211	0,04	3,8	1167
1579	213	12	1560	231	10	1469	112	4,2	1409
1810	474	16	1736	274	11,2	1620	154	3,8	1560
3400	74	11,4	3442	30	12,8	3243	42	6,2	3051

Tableau n° 1 : Comparaison des spectres IR expérimental et calculé de la Triazine

Pour les systèmes à couches ouvertes, représentatifs des espèces radicalaires intermédiaires, les méthodes ab-initio testées ne fournissent pas des ordres de grandeur concluants. Cela est illustré par les résultats présentés dans le tableau n° 2 pour NO_2. Quelle que soit l'hypothèse retenue, un écart important subsiste entre les fréquences calculées et expérimentales des trois modes.

	υ1	υ2	υ3
3-21G	1280 (- 341)	1253 (-105)	748 (- 9)
4-31G	1570 (+ 51)	1442 (+ 84)	781 (+ 24)
6-31G*	1880 (+ 259)	1612 (+ 254)	832 (+ 50)
6-31+G*	1865 (+ 244)	1605 (+ 247)	832 (+ 50)
MP2/6-31G*	2272 (+ 651)	1381 (+ 23)	752 (-5)
MP2/6-31+G*	2309 (+ 688)	1370 (+ 12)	752 (-5)
CISD/6-31+G*	2505 (+ 884)	1492 (+ 134)	782 (+ 25)
exp.	**1621**	**1358**	**757**

Tableau n° 2 : Comparaison des spectres IR expérimental et calculé de NO_2 (υ en cm^{-1})

Actuellement, afin de mieux prendre en compte les effets de corrélation dans le calcul de la structure électronique des espèces formées (systèmes à couches ouvertes ou polarisables), nous utilisons les techniques basées sur la Théorie de la Fonctionnelle Densité. Les premiers résultats obtenus avec NO sont encourageants.

2.2.2 - Prise en compte des effets de forte pression et température élevée sur les modes de vibration

La forte pression et la température élevée du milieu en détonation entraînent une modification des caractéristiques (Intensité, Fréquence) des modes de vibration calculés.

Afin de connaître l'évolution de ces modes, une étude est effectuée au LIMHP-CNRS à VILLETANEUSE (93 - FRANCE) sur un banc haute pression pour suivre, jusqu'à 50GPa et 550°C, l'évolution du spectre de vibration du β-HMX. Ce suivi systématique est réalisé par spectroscopie Raman. L'objectif est de collecter un ensemble de données expérimentales afin de développer une modélisation de ces effets.

Les résultats obtenus permettent de mettre en évidence, à température ambiante, trois transitions de phase se manifestant par l'apparition de nouveaux modes, des sauts de fréquence et des changements de pente dans l'évolution des modes en fonction de la pression. De plus, à température ambiante, il n'y a pas de modification chimique de la molécule jusqu'à 40GPa. Les seules modifications dues à la pression sont d'ordre structural ou conformationnel.

3 - Approche expérimentale

Pour la validation des résultats de l'étude théorique, l'intérêt de la spectrométrie TRISP, par rapport aux autres techniques expérimentales existantes, est de sonder directement le milieu en détonation.

Le schéma de l'expérience est représenté sur la figure n° 5.

Le principe du fonctionnement de la chaîne d'analyse, décrit sur la figure n° 6, est le suivant : un faisceau Infrarouge large bande pulsé est généré par effet SERS dans une cellule de conversion de fréquence remplie de métal alcalin (Rb). Le faisceau IR traverse le milieu en détonation où il est modulé par l'absorption des espèces chimiques formées. Il est ensuite reconverti en faisceau visible par effet SERS et par mélange d'ondes dans une seconde cellule de conversion de fréquence. Il est analysé par un monochromateur associé à un détecteur à barrettes de photodiodes et à un analyseur multicanal. Le domaine spectral entre 2 μm et 11 μm est couvert par intervalles de quelques centaines de cm^{-1} ; le positionnement en longueur d'onde dépend du couple colorant/métal alcalin.

Actuellement, nous optimisons les paramètres expérimentaux afin de générer un faisceau IR d'énergie suffisante pour pouvoir sonder le milieu en détonation.

4. Conclusion

La compréhension des mécanismes réactionnels mis en jeu pendant la décomposition de l'explosif et la mise en évidence des espèces formées dans le milieu entraînent une meilleure connaissance de son comportement énergétique.

Par une approche chimique, et par le calcul des Energies d'activation de dissociation à l'aide des méthodes de calcul semi-empiriques de la Chimie Quantique, nous déterminons les principales réactions élémentaires qui se produisent pendant la décomposition. Nous recherchons une validation des résultats par la détection des produits dans le milieu en détonation par la Spectrométrie TRISP. La démarche a été d'abord appliquée au RDX.

Un autre aspect de la modélisation est le calcul théorique, par des techniques ab-initio, des spectres IR des espèces formées afin de faciliter l'interprétation des spectres expérimentaux. La prise en compte des spectres IR des espèces intermédiaires nécessite l'utilisation de techniques basées sur la Théorie de la Fonctionnelle Densité.

En ce qui concerne la prise en compte des effets de pression et température élevées du milieu en détonation sur ces spectres, des expérimentations sont réalisées sur des espèces qui seront présentes dans les produits de détonation à l'aide d'une cellule à enclume de diamant. La modélisation des effets de P et T pourra ainsi être recalée sur des données expérimentales et extrapolée aux espèces transitoires.

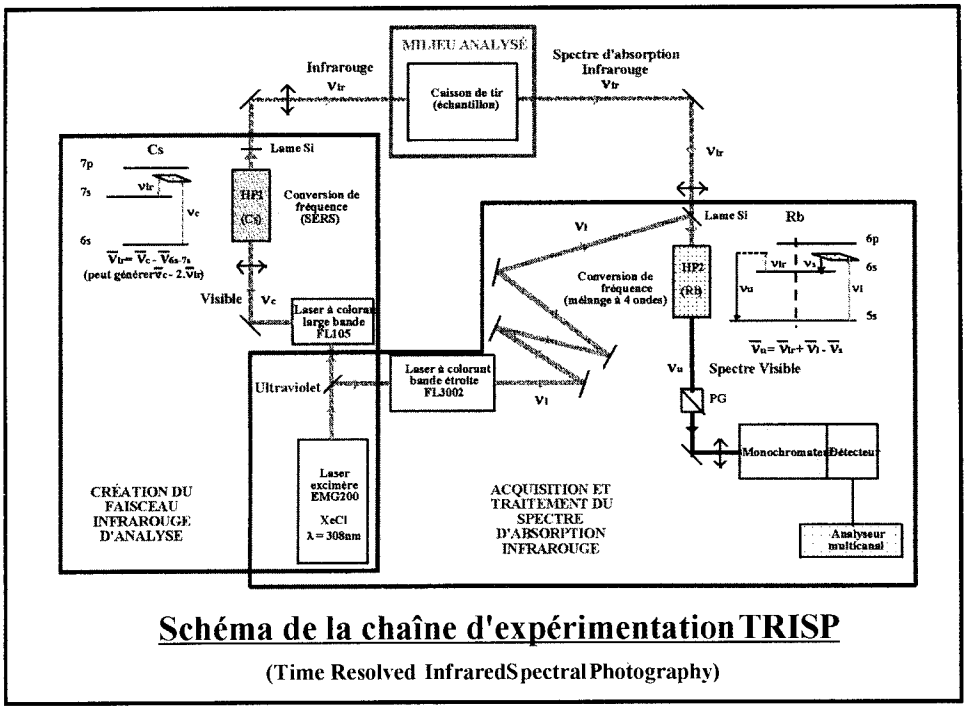

Schéma de la chaîne d'expérimentation TRISP

(Time Resolved Infrared Spectral Photography)

fig. n° 5

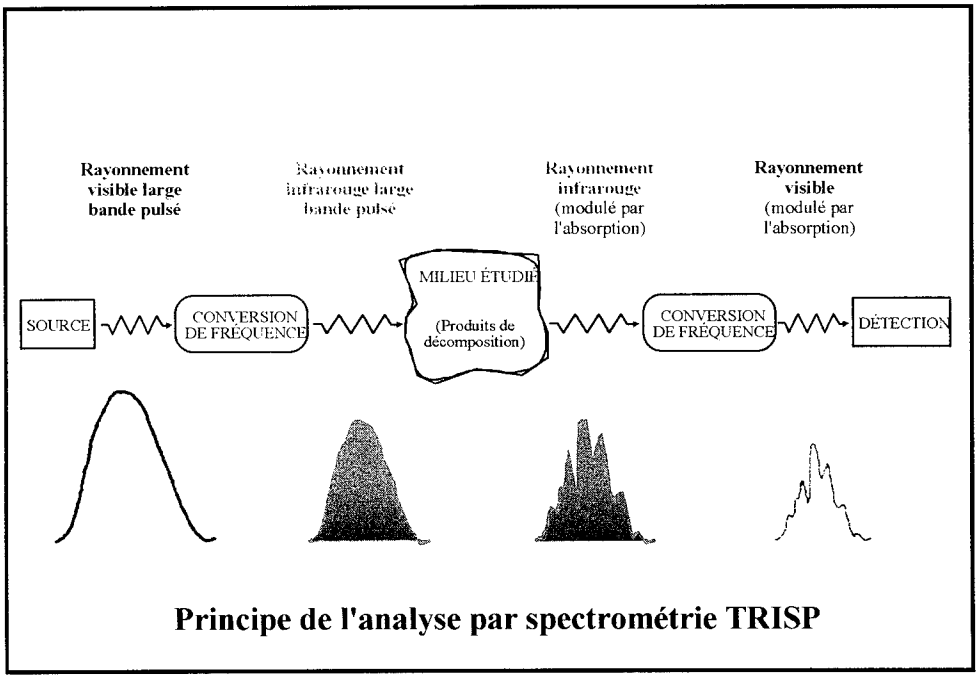

Principe de l'analyse par spectrométrie TRISP

fig. n° 6

REFERENCES

[1] A.M. RENLUND, SA SHEFFIELD, WM TROTT
Time resolved Infra Red Spectral Photography : Study of shock-induced chemistry in CS_2
Shock waves in condensed matter, p. 237, Spokane

Edited by Y.R. GUPTA, PLENUM PRESS (1985)

[2] A. DELPUECH - J. CHERVILLE - C. MICHAUD
7ème Symposium international sur la détonation

ANNAPOLIS (1981)

QUESTIONS/ANSWERS

Gupta :

1 You mentioned that you are working on developing a TRISP method in your work. It was not clear from your remarks whether you will be looking at only the detonation products or whether you wIll also be looking at TRISP measurements during the chemical reactions. Please clarify this point.

2 Is your TRISP method very similar to Anita Renlund's approach or are you making some changes to improve the methodology ?

Simonetti :

1 We are not only interested in the detonation products at the end of the decomposition process, but also in the intermediate chemical species. We think that the temporal resolution of TRISP is suitable for this detection of transient species.

2 Our TRISP technique is quite similar to Anita RENLUND's approach. The main change is about the pyrotechnic arrangement to improve the observation of the detonation gases.

Russel :

What is the pressure transmitting medium ? If it is a powder compact, there will be a large non uniform pressure on the sample. This will effect the spectrum and make IR almost impossible to predict.

Simonetti :

Yes, a detonation medium is at very high pressure with a large gradient. So, we develop studies to help the interpretation of IR spectra : theoretical calculations of characteristics of IR spectra by Quantum Chemistry techniques and consideration of (P,T) effects on vibration bands through IR or Raman spectroscopy in a Diamond Anvil Cell.

Fliszar :

Density functional calculations can be done in a number of ways. Specifically, what DFT approach did you use ?

Simonetti :

These first calculations were made with the UNICHEM-DGAUSS program (Pr A. GRAND - GRENOBLE - FRANCE) in the following hypothesis : exchange -

correlation functional of VOLKO-WILK-NUSAIN (VWN) with non-local corrections of BECKE -PERDEW (BP) and Double-Zeta Polarised basis set extension (DZP).

Odiot :

Just a technical point ? When you build your intramolecular potentials, which approach do you use to take account of correlation effects at large distances, near the dissociation products and at molecular equilibrium distances in order to rely the potential curve ?

Simonetti :

In our study of decomposition mechanisms, we make Quantum Chemistry calculations on an isolated molecule in a gas phase. In this approach, we are interested in relative values of dissociation energies of elementary reactions involved in the main bond breakings. The aim is to propose the main dissociation processes occuring in the detonating medium and the main chemical species which are formed.

Melius :

The experimental spectra that Gupta presented is very significant but needs assistance in interpretation and in suggestions for frequency regions to scan. Your theoretical techniques look extremely promising in helping this effort. Are you and your colleagues able to assist in such calculations ?

Simonetti :

I think that we need personal contacts with Dr Gupta to compare our capabilites in interpretation of experimental spectra with his specific needs. And obviously, if we are able to assit him, we'll be pleased to do that.

Pivina :

I have some questions to you concerning your general conception used for estimating and predicting such phenomena as thermal stability and sensibility. These phenomena depend from a number of parameters, therefore when you declare that you are able to predict these phenomena you should be more precised in making this statement and specify which parameters you mean when saying sensitivity or stability.

Moreover, starting with only your quantum-chemical calculations of some electronic parameters for molecules in the gas phase you cannot extrapolate the

results to crystal state characteristic, particularly to such an "ill-posed" parameter as "hammer's test frequency (H 50 %)".

Simonetti :

In this molecular approach , to study the macroscopic properties (impact sensitivity, decomposition temperature) of explosives we think that, even if other parameters at a different level are important, the electronic structure of molecule and the infering quantities are the main points for the cohesion of the system.

Pivina :

As is known, the modern quantum-chemical semi-empirical methods introduce appreciable errors (about 20-50 kcal/mole) in estimated energy capacity of high nitrogen-oxygen systems. It means that these methods cannot be used for accurate prediction of the energy capacity of these compouds.

Moreover, the results of quantum-chemical calculations for molecules in gas state cannot directly be extrapolated to the solid state because the errors in the estimated enthalpy of sublimation of molecular crystals exceed 60-80 % if we use the method of atom-atom potential functions.

Simonetti :

Indeed, nowadays, with our model and Quantum Chemistry calculations in gas phase, we need an empirical correction to estimate the enthalpy of formation in solid state. This estimation is simple and relatively reliable. Obviously, we work to improve this model in order to extend the application field.

JOURNAL DE PHYSIQUE IV
Colloque C4, supplément au Journal de Physique III, Volume 5, mai 1995

Thermochemistry and Reaction Mechanisms of Nitromethane Ignition

C.F. Melius

Combustion Research Facility, Sandia National Laboratories, Livermore, CA 94551-0969, U.S.A.

Abstract: The thermochemistry and reaction mechanisms of nitromethane initiation are modeled using detailed chemical kinetics. Initial conditions correspond to gaseous nitromethane at atmospheric and liquid-like densities and initial temperatures between 1100 and 2000 K. Global reactions as well as elementary reactions are identified for each of the two stages of ignition. The chemical steps to convert the nitro group to N_2 involve a complex set of elementary reactions. The time-dependence of the ignition steps (ignition delay times) as a function of temperature and pressure is used to determine effective activation energies and pressure dependencies to ignition. The ignition delay times range from several nanoseconds to tens of microseconds. At atmospheric conditions, the delay times for both ignition stages are in excellent agreement with observed experimental data. At the high densities, the ignition times at these elevated temperatures appear to be dominated by the same reaction mechanism that occurs for atmospheric gaseous nitromethane initiation. This is to be contrasted with lower temperature, condensed-phase ignition studies where it appears that solvent-assisted reactions dominate.

1. INTRODUCTION

The ability to identify the chemical reactions involved in the initiation of energetic materials is challenging due to the extremely short time scales involved as well as the high temperatures and pressures that are generated. Furthermore, the chemical intermediates of ignition are highly reactive. The chemistry of nitro compounds, such as nitramines and nitroaromatics, is further complicated by the fact that they may undergo two-stage ignition. We therefore have investigated the initiation of nitromethane as a prototype of an energetic material containing the nitro moiety. The ignition of nitromethane has been studied both experimentally [1-9] and computationally [1,10-15]. In particular, the ignition delay time of gas-phase ignition of nitromethane has been studied by Guirguis *et al.* [1] in which they were able to observe two stages of ignition. Several groups have modeled the ignition process using detailed chemical kinetics [1,9], including previous work by us [13,14]. The modeling was able to treat the first-stage ignition reasonably well, but the second-stage ignition delay times were off by several orders of magnitude. Recent work by Lin and coworkers [16-18] have improved our understanding of the elementary reactions involving the NO, HNO, NO_2, and HCN species. This has enabled us to generate an improved detailed reaction mechanism for nitromethane. We use this improved mechanism to study the initiation of gaseous nitromethane at atmospheric conditions as well as at densities corresponding to that of

*Work supported by the U. S. Department of Energy.

liquid nitromethane. We present the thermodynamics and reaction pathways of the ignition steps. We then use the ignition delay times to determine effective activation energies and pressure dependencies.

2. METHOD

The study of ignition in a uniformly heated system, such as in a shock tube, allows us to study the combustion chemistry of energetic materials in a environment that can provide the initial decomposition and initiation reaction mechanisms. The energetic material can be treated as a homogeneous gas mixture in a closed system, in which we follow the time-dependent evolution of the chemical species. For instance, we can treat an adiabatic system with constant pressure or volume, or we can follow the chemistry under shock detonation conditions. We use the SENKIN program [19], which includes sensitivity analysis, for the integration of the energy and mass conservation equations.

In this section, we study the chemistry of gaseous nitromethane initiation. The ignition of nitromethane is treated as being under constant volume. The governing equations are [14,19]

$$\frac{dY_k}{dt} = v\ \dot{\omega}_k W_k \quad (k = 1, ..., K). \tag{1}$$

and

$$c_v \frac{dT}{dt} = - v \sum_{k=1}^{K} e_k \dot{\omega}_k W_k, \tag{2}$$

In the above equations, T is the temperature, Y_k the mass fraction of the k^{th} species, W_k is the molecular weight of the k^{th} species, t is time, v = V/m is the specific volume, e_k is the internal energy of the k^{th} species, c_v is the constant volume heat capacity of the mixture, and $\dot{\omega}_k$ is the molar rate of production of the k^{th} species. The chemical reaction mechanism included 48 species and 312 elementary reactions. The thermochemical dynamic properties and chemical production rates are evaluated using the Chemkin package [19]. The 48 species and their heats of formation are presented in Table I.

Table I. The chemical species used in the detailed chemical kinetic modeling of nitromethane. Also given are the heats of formation at 298 K (ΔH^o_{f298}), where energies are given in kcal-mol^{-1}.

1	CH_3NO_2	-16.84	2	CH_3ONO	-15.25
3	NO	21.58	4	NO_2	7.91
5	HNO	23.80	6	HONO	-18.34
7	N_2O	19.61	8	H	52.10
9	H_2	0.0	10	O	59.56
11	O_2	0.0	12	OH	9.32
13	H_2O	-57.8	14	HO_2	2.50
15	N	112.96	16	N_2	0.0
16	NH	85.2	18	NH_2	45.50
19	NH_3	-11.97	20	NNH	58.57
21	HNNO	55.20	22	HNOH	21.06
23	H_2NO	15.82	24	N_2H_2	50.90
25	CO	-26.42	26	CO_2	-94.06
27	HCO	10.40	28	CH_2O	-27.70
29	CH_3O	3.90	30	CH_2OH	-4.10

Table I. (Cont.)

31	CH_3OH	-48.06	32	CH_3	34.82
33	CH_4	-17.90	34	CN	104.01
35	HCN	31.89	36	H_2CN	59.11
37	CH_3NH	44.94	38	HCNO	38.43
39	HOCN	-3.53	40	HNCO	-28.22
41	NCO	31.51	42	NCN	107.60
43	CH_3NO	18.95	44	H_2CNO_2	36.47
45	H_2CNO	41.43	46	CH_3NHO	13.32
47	H_2CNOH	5.15	48	CH_2NO_2H	-2.86

3. RESULTS

In Figs. 1 and 2, we present the temperature and species profiles as a function of time for the initiation of 100 per cent gaseous CH_3NO_2 at 7.25 atmospheres and 1131 K. These conditions are representative of the experimental conditions of Guirguis *et al.* [1]. The initiation undergoes two ignition stages, at 13.3 μsec and 25.8 μsec, respectively. The final temperature is 3598 K.

The chemistry can be subdivided by time into several stages: (I) a preliminary stage of slow decomposition followed by (II) a first-stage ignition that undergoes a rapid temperature rise followed by (III) an intermediate stage in which the temperature remains on a plateau followed by (IV) a second-stage ignition where the temperature again rises rapidly to form the final products. The reaction mechanism flow diagrams for the first-stage ignition (II), the intermediate stage (III), and the second-stage ignition (IV) are shown in Figs. 3-5. These reaction pathways show the dominating elementary reactions occurring in each of these stages, with thick arrows being the major pathways while thin arrows are the minor pathways. We have separately shown the reaction chemistry for the carbon atom and the nitrogen atom of nitromethane. The carbon atom must be oxidized, to form CO and, to a lesser extent, CO_2 (note that there is not enough oxygen in nitromethane to oxidize the carbon to CO_2 and the hydrogen to H_2O). Meanwhile, the nitrogen, which is in an oxidized state as part of the nitro group moiety, must be reduced to N_2. The reaction flow diagram for the preliminary decomposition stage (I) is similar to that of the first-stage ignition (II) and thus is not shown. The major difference is that the preliminary stage (I) occurs at the low end of the temperature range, giving rise to slower rates and resulting in a greater variety of minor intermediate species being formed.

In Figs. 6-8, we show the enthalpies and free energies of possible species corresponding to the composition $C_1H_3N_1O_2$. This represents the composition of nitromethane and includes tautomers of nitromethane as well as various product species. Besides the ΔH at 300K (see Table I for individual species heats of formation), we present the ΔG's at 300K and 2000K.

Fig. 1 showed the time profile for nitromethane initiation at 7.25 atmospheres and 1131 K, indicating two rapid temperature rises at 13.6 μsec and 26.1 μsec, designated τ_1 and τ_2 respectively. In Table II, we present these ignition delay times, τ_1 and τ_2, for various initial temperatures and pressures. These results are used to determine activation energies of ignition, defined by the relation $ln\ (\tau_a/\tau_b) \propto (\Delta E/ R)\ (1/T_a - 1/T_b)$. The resulting ΔE's for the first-stage and second-stage ignitions are presented in Table III. In a similar manner, we can define pressure dependencies to the ignition delay time by the relation $ln\ (\tau_a/\tau_b) \propto n\ ln\ (P_a / P_b)$, which corresponds to τ being proportional to P^n. The resulting pressure exponents are given in Table IV.

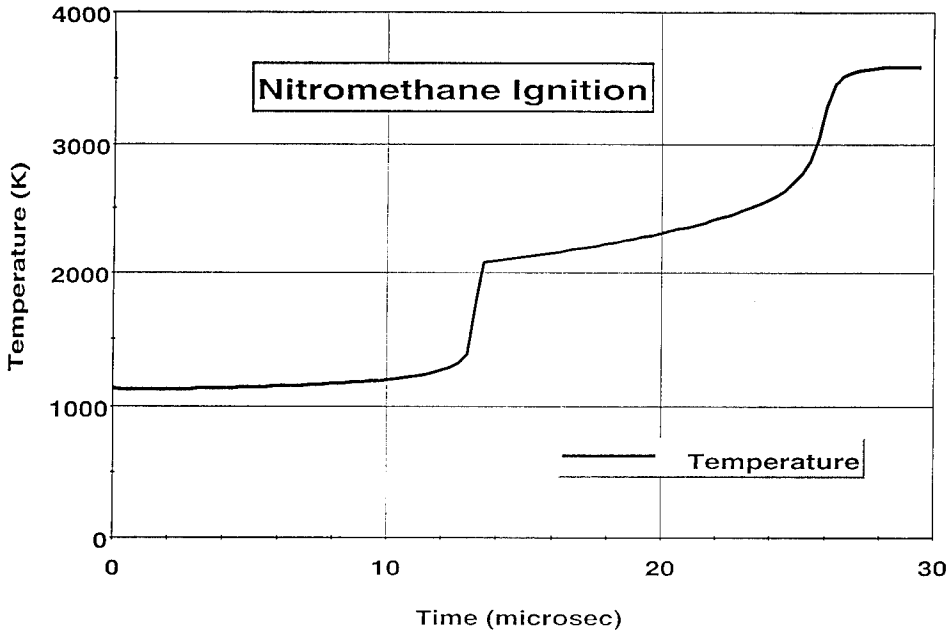

Fig. 1. Temperature vs. time profile for ignition of nitromethane. Initial conditions are 1131 K and 7.25 atm.

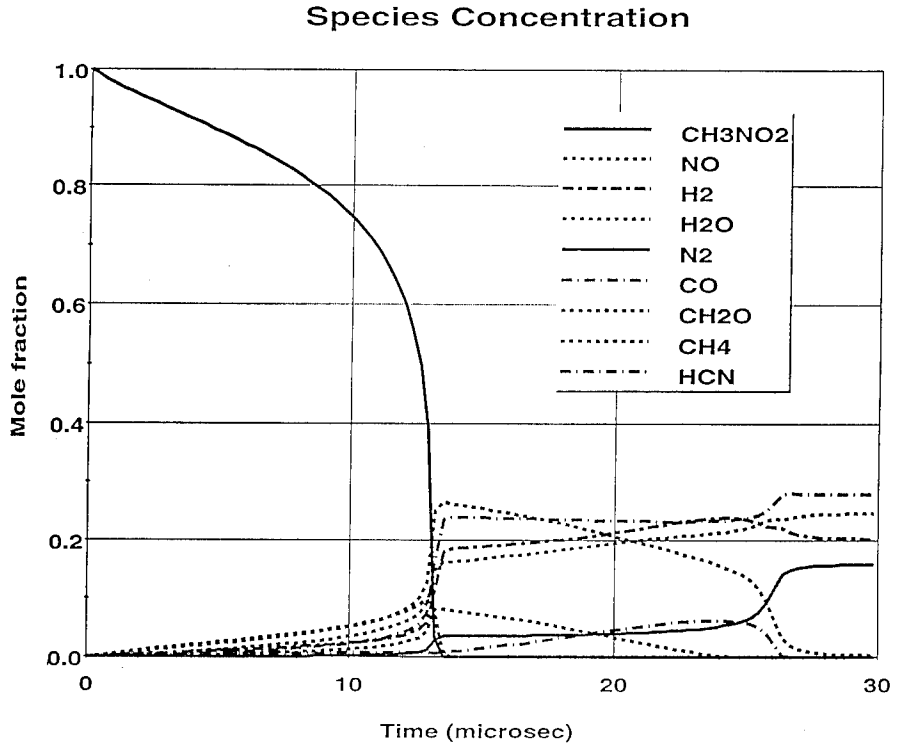

Fig. 2. Species vs. time profile for ignition of nitromethane. Intial conditions are 1131 K and 7.25 atm.

Nitromethane First Stage Ignition Chemistry

Carbon Mechanism

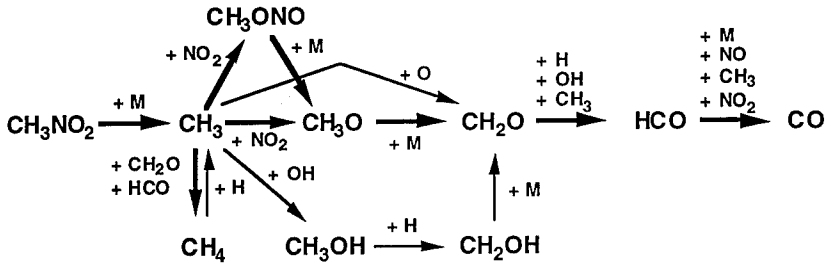

Nitrogen Mechanism

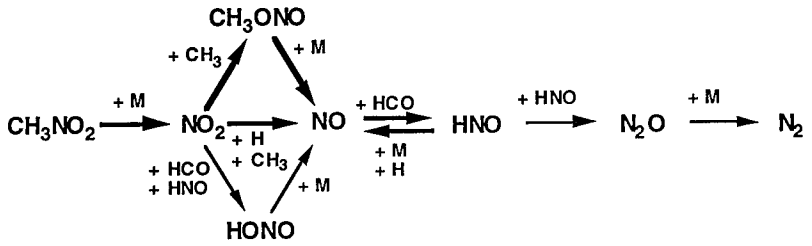

Fig. 3. Reaction mechanism flow diagrams for the first stage-ignition of nitromethane. Thick arrows indicate major pathways. Dominant collision partners for bimolecular reactions are indicated next to arrows. Unimolecular decomposition reactions are indicated by the third-body notation +M. The chemistry of carbon- and nitrogen-containing species are presented separately.

Nitromethane Intermediate Stage Chemistry

Carbon Mechanism

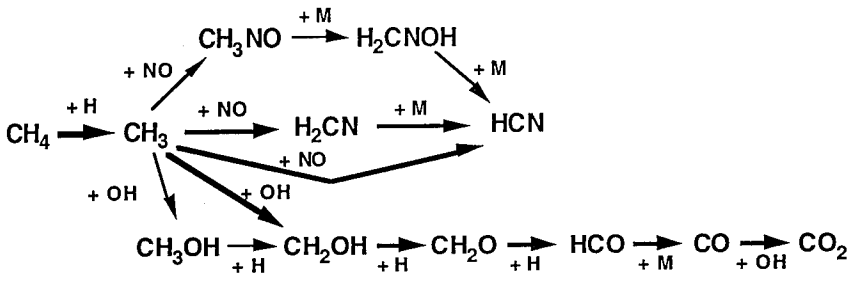

Nitrogen Mechanism

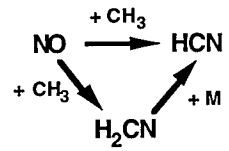

Fig. 4. Reaction mechanism flow diagrams for the intermediate stage (between first- and second-stage) ignition of nitromethane. See Fig. 3 for further caption descriptions.

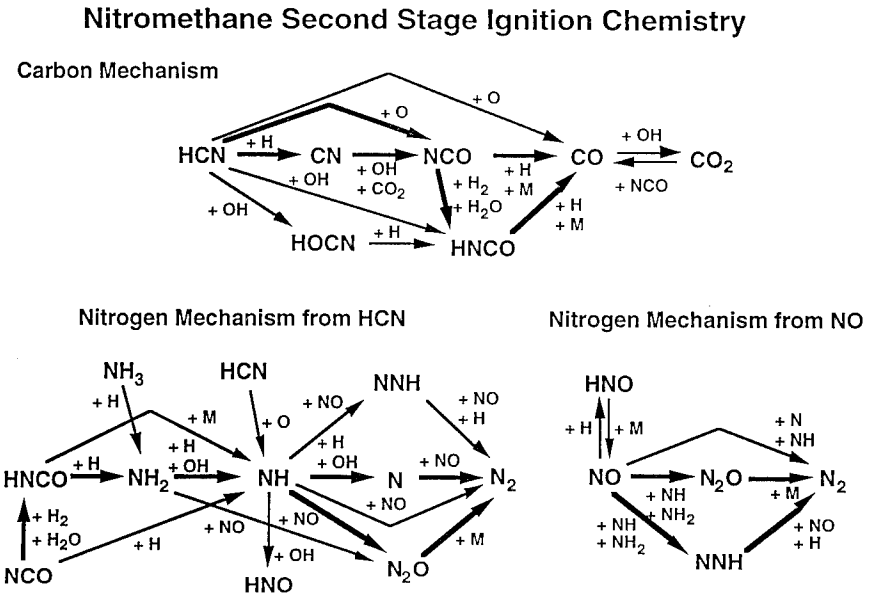

Fig. 5. Reaction mechanism flow diagrams for the second-stage ignition of nitromethane. See Fig. 3 for further caption descriptions.

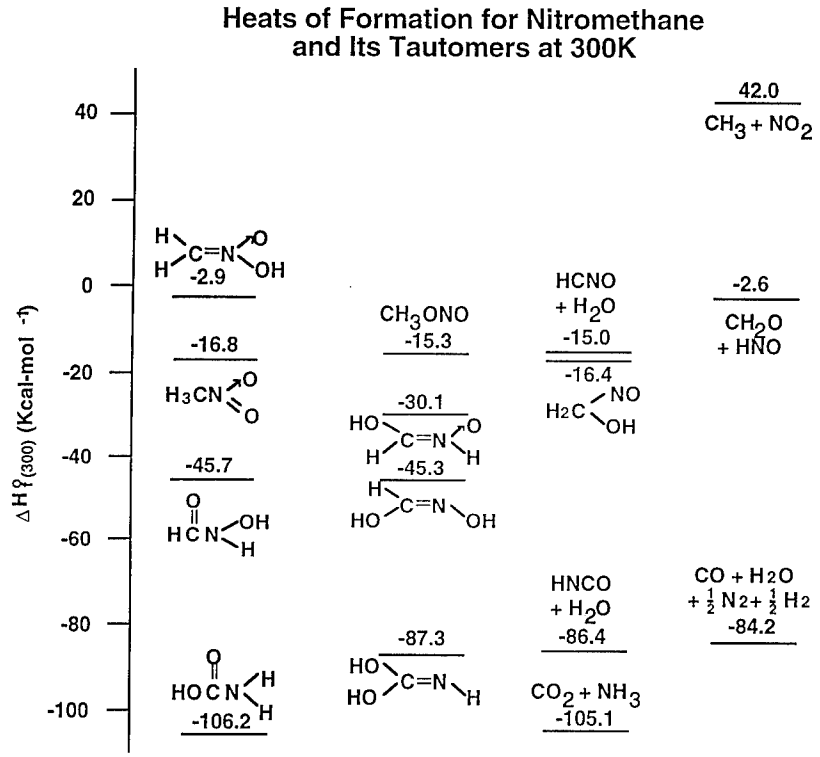

Fig. 6. Heats of formation, ΔH's, at 300 K for nitromethane and its tautomers and other stoichiometric products. Enthalpies are in kcal-mol^{-1}.

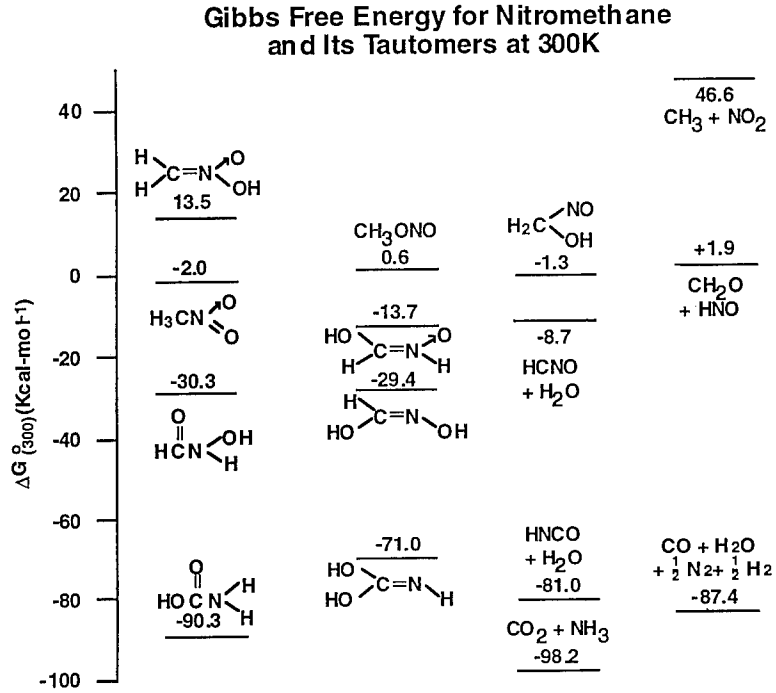

Fig. 7. Free energies, ΔG's, at 300 K for nitromethane and its tautomers and other stoichiometric products. Free energies are in kcal-mol^{-1}.

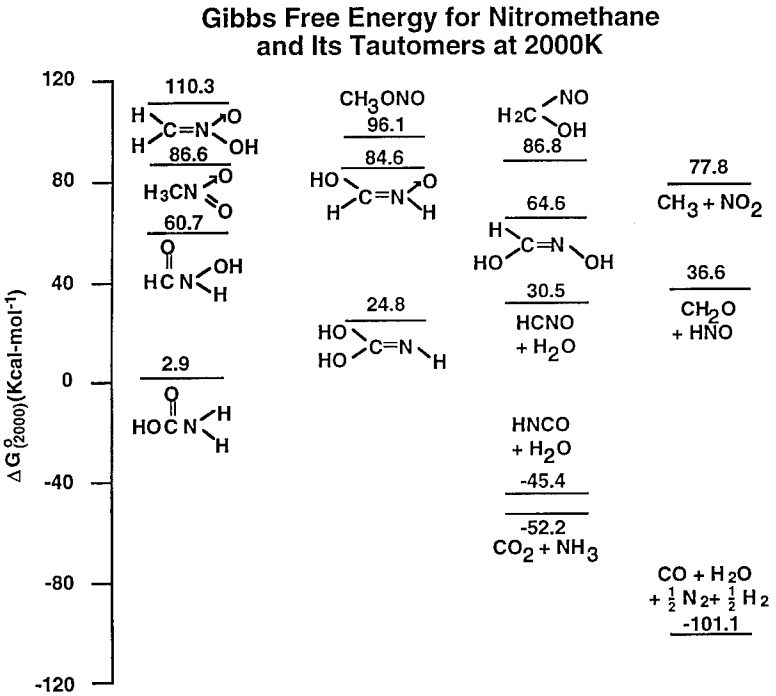

Fig. 8. Free energies, ΔG's, at 2000 K for nitromethane and its tautomers and other stoichiometric products. Free energies are in kcal-mol^{-1}.

Table II. Ignition delay times for gaseous nitromethane for different initial temperatures and pressures.

T (K)	P (Atm)	τ_1	τ_2	$\tau_2 - \tau_1$
1131	5.25	14.9 μs	35.5 μs	20.6 μs
1131	7.25	13.3 μs	25.8 μs	12.5 μs
1331	5.25	1.6 μs	25.3 μs	23.7 μs
1331	7.25	1.2 μs	15.5 μs	14.3 μs
1331	8.53	1.2 μs	12.3 μs	11.1 μs
1131	1574.4	4.352 μs	4.403 μs	.051 μs
1131	1852.8	4.288 μs	4.298 μs	.010 μs
1331	1574.4	0.208 μs	0.219 μs	.010 μs
1331	1852.8	0.202 μs	0.208 μs	.006 μs
1900	2644.8	2.52 ns	4.76 ns	2.24 ns
2000	2784.	1.59 ns	3.59 ns	2.00 ns

Table III. Activation energies of ignition (defined by $ln\ (\tau_a / \tau_b) \propto \Delta E / R\ (1/T_a - 1/T_b)$). Ignition delay times are taken from Table II. Energies in kcal-mol^{-1}.

Constant Pressure	T(K)	P (Atm)	ΔE_1	ΔE_2
	1230	5.25	33.2	7.6
	1230	7.25	35.6	5.1
	1230	1574.4	45.4	44.9
	1230	1852.8	45.7	45.3
Constant Volume	T(K)	P (Atm)	ΔE_1	ΔE_2
	1230	5.25	35.7	11.0
	1230	1574.4	45.9	45.6
	1950	2644.8	34.8	21.3

Table IV. Pressure dependence of ignition delay times for gaseous nitromethane. Pressure dependence is defined by $\tau \propto P^n$ or $ln(\tau_a / \tau_b) \propto n\, ln(P_a / P_b)$. Ignition delay times are taken from Table II.

Low Pressure	T (K)	n_1	n_2
	1131	-0.36	-0.99
	1331	-0.85	-1.52
Low to High	T (K)	n_1	n_2
	1131	-0.22	-0.37
	1331	-0.35	-0.82
High Pressure	T (K)	n_1	n_2
	1131	-0.09	-0.15
	1331	-0.19	-0.32

4. DICUSSION

4 .1 Chemical Reactions

Several points regarding the nitromethane thermochemistry can be observed from Figs. 6-8. First, from the ΔH's presented in Fig. 6, it is seen that indeed nitromethane is an unstable tautomer of $C_1H_3N_1O_2$, lying ~90 kcal-mol^{-1} above the most stable form, $C(O)OHNH_2$. In fact, $C(O)OHNH_2$ is more stable than the major products of detonation, CO, H_2O, N_2, and H_2 (see Fig. 2). Furthermore, as can be seen in Fig. 6, the lowest bond-breaking moiety for CH_3NO_2 is the breaking of the C-N bond to form $CH_3 + NO_2$. which is endothermic by nearly 59 kcal-mol.$^{-1}$ Thus, from an enthalpy view point, CH_3NO_2 would appear to be a reasonable energetic material.

However, while one tends to think of the thermochemistry of the reactions in terms of enthalpies (e.g., heats of reaction), it is the free energy of the system that drives the reaction. Dividing the $C_1H_3N_1O_2$ molecular species into two or more species lowers the free energy, particularly at higher temperatures. As one can see from Fig. 8, at 2000K, the ΔG of $CH_3 + NO_2$ is more stable than that of CH_3NO_2 itself. And the breakup of CH_3NO_2 into its small product molecules, CO, H_2O, N_2, and H_2, forming three molecules from one reactant molecule is extremely exothermic. Thus, it is necessary to have more than the thermostability to bond breaking to make an insensitive energetic material. As we shall see, it is necessary to have a reaction pathway which prevents direct conversion of the energetic material to products.

The overall reaction chemistry converting nitromethane to products is

$$CH_3NO_2 \rightarrow CO + {}^1/_2\, N_2 + H_2O + {}^1/_2\, H_2 \qquad \Delta H_{Rxn} = -67 \qquad (R1)$$

with minor contributions of the following reactions

$CO + H_2O \rightarrow CO_2 + H_2$	$({}^1/_{10})$	$\Delta H_{Rxn} = -10$	(R2)
$H_2O \rightarrow H + OH$	$({}^1/_{15})$	$\Delta H_{Rxn} = +119$	(R3)
$H_2 \rightarrow H + H$	$({}^1/_{30})$	$\Delta H_{Rxn} = +104$	(R4)

Contributions of R2-R4 relative to reaction R1 are given in parentheses. The heats of reaction ΔH_{Rxn} are given in kcal-mol^{-1}.

As stated above, the chemistry can be subdivided by time into several stages: (I) a preliminary stage of slow decomposition followed by (II) a first-stage ignition that undergoes a rapid temperature rise followed by (III) an intermediate stage in which the temperature remains on a plateau followed by (IV) a second-stage ignition where the temperature again rises rapidly forming the final products. This temporal division of chemical reactions, as indicated in Fig. 2, is consistent with the temporal division of the temperature into a preliminary, first-stage ignition, intermediate region, and second-stage ignition, as indicated in Fig. 1. The reaction chemistry during the preliminary stage (I) is

$$9\ CH_3NO_2 \rightarrow 5\ CH_2O + {}^5/_8\ HNO + {}^7/_4\ CO + {}^{35}/_8\ NO + {}^5/_2\ H_2 + 3\ H_2O + {}^3/_4\ N_2O + HCN + CH_4 + {}^5/_8\ NO_2 + {}^1/_4\ CO_2 + {}^1/_4\ N_2 + {}^3/_8\ HONO \qquad \Delta H_{Rxn} = -10, \qquad (R5)$$

the reaction during the first-stage ignition (II) is

$$4\ CH_3NO_2 \rightarrow 3\ CO + CH_4 + 3\ NO + {}^1/_2\ N_2 + 2\ H_2 + 2\ H_2O \qquad \Delta H_{Rxn} = -20, \qquad (R6)$$

the reaction during the intermediate-stage ignition (III) between the first- and second-stage ignitions is

$$4\ CH_4 + 6\ NO + CO \rightarrow 4\ HCN + 5\ H_2O + H_2 + N_2 + CO_2 \qquad \Delta H_{Rxn} = -48, \qquad (R7)$$

while the reaction during the second-stage ignition (IV) is

$$7\ HCN + 13\ NO + {}^5/_2H_2 \rightarrow 6\ CO + 10\ N_2 + CO_2 + 3\ H_2O + 2\ OH + 4\ H \qquad \Delta H_{Rxn} = -54. \qquad (R8)$$

In order to relate the heats of reaction, ΔH_{Rxn}, of the individual reactions to each other, we have normalized the ΔH_{Rxn} for each of the reactions to the CH_3NO_2 molecule. Thus, the ΔH_{Rxn}'s are normalized per CH_3NO_2 (R5 and R6) or NO (R7 and R8) molecule.

The global reactions for each stage in the nitromethane initiation can be further subdivided into subglobal reactions which begin to indicate the reaction mechanism of each stage. While this reaction subdivision is not unique, we have attempted to define those subglobal reactions which represent simple combinations of elementary reactions, as indicated in Figs. 3-5. In addition to the subglobal reaction, we also indicate the relative contribution of each reaction to the net reactions presented above. We also give the absolute heat of reaction, ΔH_{Rxn}, for each of the subglobal reactions.

The preliminary stage (I) global reaction R5 is composed of the subglobal reactions

$CH_3NO_2 \rightarrow CH_2O + HNO$	(4)	$\Delta H_{Rxn} = +13$	(R5a)
$CH_3NO_2 \rightarrow CO + NO + {}^3/_2\ H_2$	(1)	$\Delta H_{Rxn} = +12$	(R5b)
$2\ CH_3NO_2 \rightarrow CH_4 + CO + H_2 + NO + NO_2$	(1)	$\Delta H_{Rxn} = +19$	(R5c)
$2\ CH_3NO_2 + HNO \rightarrow HCN + CH_2O + 2\ H_2O + 2\ NO$	(1)	$\Delta H_{Rxn} = -58$	(R5d)
$2\ HNO \rightarrow N_2O + H_2O$	$({}^3/_4)$	$\Delta H_{Rxn} = -85$	(R5e)
$NO_2 + HNO \rightarrow HONO + NO$	$({}^3/_8)$	$\Delta H_{Rxn} = -28$	(R5f)
$CO + 2\ HNO \rightarrow CO_2 + N_2 + H_2O$	$({}^3/_8)$	$\Delta H_{Rxn} = -173.$	(R5g)

The first-stage global reaction R6 is composed of the subglobal reactions

$CH_3NO_2 \rightarrow CO + NO + {}^3/_2\ H_2$	(3)	$\Delta H_{Rxn} = +12$	(R6a)
$CH_3NO_2 + {}^3/_2H_2 \rightarrow CH_4 + NO + H_2O$	(1)	$\Delta H_{Rxn} = -37$	(R6b)

$H_2 + NO \rightarrow H_2O + {}^1/_2\, N_2$ (1) $\Delta H_{Rxn} = -79.$ (R6c)

The intermediate-stage global reaction R7 is composed of the subglobal reactions

$CH_4 + NO \rightarrow HCN + H_2O + {}^1/_2\, H_2$ (4) $\Delta H_{Rxn} = -30$ (R7a)
$H_2 + NO \rightarrow H_2O + {}^1/_2\, N_2$ (2) $\Delta H_{Rxn} = -79$ (R7b)
$CO + H_2O \rightarrow CO_2 + H_2$ (1) $\Delta H_{Rxn} = -10.$ (R7c)

The second-stage global reaction R8 is composed of the subglobal reactions

$HCN + NO \rightarrow CO + N_2 + {}^1/_2\, H_2$ (7) $\Delta H_{Rxn} = -80$ (R8a)
$CO + H_2O \rightarrow CO_2 + H_2$ (1) $\Delta H_{Rxn} = -10$ (R8b)
$H_2 + 2\, NO \rightarrow N_2 + 2\, OH$ (3) $\Delta H_{Rxn} = -25$ (R8c)
$OH + H_2 \rightarrow H_2O + H$ (4) $\Delta H_{Rxn} = -15.$ (R8d)

The net result of the preliminary (I) and first-stage ignition (II) reactions steps is the conversion of the NO_2 moiety to NO. During the preliminary stage (I), the decomposition of CH_3NO_2 is only slightly exothermic. In fact, the dominant decomposition reaction R5a is endothermic. Subsequent reactions involving the HNO species provide the exothermic heat release. The first-stage ignition (II) chemistry is slightly more exothermic. However, the major exothermic heat release of initiation arises during the second-stage ignition chemistry.

The net result of the intermediate (III) and second-stage ignition (IV) reactions is the conversion of NO to N_2. The NO to N_2 conversion does not occur readily and requires the presence of hydrogen and HCN. The formation of HCN occurs primarily during the intermediate stage (III). This stage (III), which removes the CH_4, is also exothermic but slow. The rapid reaction rates of the second-stage ignition are a result of the high temperatures.

While the net reaction is conversion of CH_3NO_2 to CO, H_2O, N_2, and H_2, the overall chemical process of ignition is complicated. Many steps are required to form the final exothermic products. The chemistry can be divided into two major efforts, (1) conversion of the NO_2 moiety to NO and (2) conversion of the NO moiety to N_2. This process is generic to all nitro-containing energetic materials, including nitrate esters and nitramines [14]. The result is two separated ignition stages, denoted the first or primary stage and the secondary stage.

The primary-stage ignition is conversion of the NO_2 to NO. This can be written stoichiometrically as $CH_3NO_2 \rightarrow CO + NO + {}^3/_2\, H_2$. Note that this reaction is itself endothermic (see reaction R6a). On the other hand, three and a half molecules are formed for each nitromethane molecule, so the entropy of this reaction if favorable, leading to a favorable free energy of reaction as the temperature increases. In order to gain heat release, some of the NO must be reduced. In the preliminary stage (I), N_2O is formed via the HNO intermediate. During the first-stage ignition (II), the temperature rise is sufficient to allow thermal decomposition of the N_2O to form N_2. The relative importance of CH_4 and CH_3OH has changed from our previous investigation [14], with CH_4 now playing the more significant role. The relative importance of CH_4 to CH_3OH is extremely sensitive to the pressure dependence used for various elementary rate constants. In both cases, these species serve to create a temporary heat source (see reaction R6b). The formation of CH_4 occurs earlier in the reaction mechanism (arising from CH_3) than does formation of CH_3OH (arising from CH_3O as indicated in ref. 14).

One can see from Fig. 3 that even the oxidation of the carbon of nitromethane to CO is a multistep process. The major pathway has the CH_3NO_2 breaking the C-N bond to form $CH_3 + NO_2$ which recombines to form CH_3ONO which breaks the O-N bond to form $CH_3O + NO$. The NO then abstracts the H from CH_3O to form $CH_2O + HNO$. Subsequent abstraction of hydrogen atoms

from CH_2O lead to CO. As one can see from Figs. 6-8, this series of reactions is itself endothermic. Thus, the initial set of reactions do not produce significant heat release. This complex set of reactions plays an important role in keeping the nitro compounds from spontaneously decomposing. The heat release from any exothermic reactions is converted into net endothermic reactions. These series of elementary reactions are necessary to move the oxygen atom from the nitrogen atom to the carbon atom, which cannot occur until the C-N bond is first broken.

The secondary stage ignition is the reduction of NO to N_2. This occurs by first reducing one of the nitrogen atoms to a reduced state in HCN. This reduced nitrogen is then oxidized with another oxidized nitrogen of NO to form the formally neutral N_2. The formation of the reduced state of nitrogen, HCN, occurs during the intermediate stage (III). This step is necessary because the NO molecule is very stable, even at the intermediate temperatures.

As noted above, the large free energy release of the reaction is enhanced by the net increase in the entropy of the reaction. The majority of this entropy increase occurs during the preliminary and first-stage ignition, where the decomposition of each nitromethane molecule leads to between two and three new molecules. Thus, while the exothermicity of the preliminary and first stages of the reaction are small compared to that of the intermediate and second stages, the increase in entropy plays an important role in driving the initiation process, allowing the initial reactions to proceed.

4.2 Ignition Delay Times

As discussed in the above section on the reaction mechanism, the nitromethane molecule cannot "spontaneously" decompose to form exothermic products but rather must undergo a series of intermediate steps, many of which are endothermic. These reactions lead to finite ignition delay times, both for the primary and secondary stages. We can analyze these ignition delay times, τ_1 and τ_2, in terms of energies of activation, ΔE_1 and ΔE_2, and pressure dependencies n_1 and n_2, as defined above and in Tables II-IV. The ΔE's and n_i's are define as derivatives of the ignition delay times τ_i's with respect to temperature and pressure, respectively, and thus, have meaning only in the near region of the temperature and pressure specified. We have calculated the ignition delay times for atmospheric pressures as well as a high pressure range corresponding to a nitromethane density of that of liquid nitromethane. The pressure values presented in Tables II-IV are an idealized gas effective pressure with the real gas pressure being much higher. For the constant volume calculations, it is better to view the calculations as constant density calculations.

The atmospheric conditions match the experimental data of Guirguis *et al.* [1]. The ignition delay times are in quite good agreement with the experimental data. The 7.25 atm, 1131 K conditions, for which the experimental was able to separate the two ignition stages, yielded a τ_1 and a τ_2 of 13.3 and 25.8 μsec, which are in remarkable agreement with the experimental data of ~12 and ~25 μsec respectively. These results give us confidence that the elementary reactions for modeling nitromethane are accurate. This represents an improvement over the reaction mechanism used previously [14], which had a reasonable first-stage ignition but a much delayed second stage ignition. The ignition delay times range from microseconds at the low pressure to hundreds of nanoseconds in the high density regime. At the high temperatures and densities, the τ_1's approach the nanosecond time scale.

The effective activation energies of ignition are presented in Table III. The resulting ΔE's indicate that the first-stage ignition has an activation energy ΔE_1 of ~33-36 kcal-mol^{-1} at atmospheric pressures, consistent with the experimental data [1]. At high densities, the ΔE_1 is larger, ~46 kcal-mol,$^{-1}$ though at elevated temperatures (1950 K), the ΔE_1 is ~35 kcal-mol.$^{-1}$ These large activation energies are dominated by the initial C-N bond breaking process, which has a bond dissociation energy of 59 kcal-mol.$^{-1}$ The second-stage ignition delay times, τ_2's, show a wide variation in activation energies. This occurs because the τ_2's decrease significantly faster than the τ_1's with increasing temperature and pressure. Ultimately, the τ_2's approach the τ_1's and are

dominated by the τ_1 times at high densities. However, the difference between the two stages, τ_2 - τ_1, is still several nanoseconds (see Table II).

The effective pressure dependencies of ignition (at constant temperature) are presented in Table IV. The resulting n_i's exhibit varied behavior. At low temperature and pressure, the first-stage n_1 pressure dependence is between zeroth order ($n_1 = 0$) and first order ($n_2 = 1$), corresponding to effective unimolecular and bimolecular behavior. The secondary stage n_2 pressure dependence at the low temperature and pressure is first order and greater. At high pressures, both the n_1 and n_2 pressure dependencies approach zeroth order, indicating the dominance of the first-stage ignition delay time and the high effective activation energy representative of C-N bond breaking. It is difficult to relate these pressure dependencies to shock induced experiments where temperature changes occur simultaneously with pressure changes.

The comparison of our high density results with the experimental ignition delay times at kilobar pressures and low temperatures indicate some significant differences. As an example, we use the experimental ignition delay times measured by Lee *et al.* [3] for 10 and 50 kbar and 400-600 K. Their τ's range from 10 - 100 seconds and have an effective activation energy of ~16 kcal-mol.$^{-1}$ While this activation energy is significantly lower than what we calculate for the higher temperature (1100-1300K) conditions (~45 kcal-mol^{-1}), our pre-exponential rate constants are much larger. Defining the rate constant k as the inverse of the ignition delay time, the effective high temperature rate constant is $k_g = 1.4\ 10^{14}\ exp(-45.4/RT)$ while the effective low temperature rate constant (at 10 kbar) is $2.7\ 10^{4}\ exp(-15.7/RT)$. That is, our ignition delay times are between 200 nsec - 4 μsec while their extrapolated τ's are still longer than 100 μsec. On the other hand, our τ's in the 400-600K range would be longer than theirs. This suggests a switch in mechanism in which at the lower temperatures, the reaction mechanism is "condensed phase"-like, involving proton transfer and hydrolysis reactions, while at high temperatures above 1000 K, the reaction mechanism is "gas phase"-like, involving radical species. We have investigated the inclusion of bimolecular as well as solvent-assisted proton transfer and hydrolysis reactions in our mechanism to mimic the condensed phase reaction process. The results are encouraging. The small pre-exponential rate constants for such reactions (possessing severe entropy constraints) make such reactions important in the 400-600 K temperature range while they have essentially no effect in the 1100-1900 K range. Considerable work remains in order to elucidate the actual elementary reactions for the low temperature, condensed-phase regime.

5. CONCLUSIONS

We have calculated the initiation process for nitromethane using detailed chemical kinetics. The starting conditions were gaseous nitromethane at atmospheric pressures as well as elevated pressures corresponding to liquid density and temperature above 1000 K. The results indicate that the chemical reaction mechanism requires multiple steps, in which many of the initial steps are endothermic. This complex chemical mechanism prevents the energetic nitro-compound from releasing its stored chemical energy immediately as a shock wave passes by. Ignition delay times indicate relatively high activation energies and low pressure dependencies, indicative of initial bond-breaking of the C-N bond. The agreement between our ignition delay times and the experimental data of Guirguis *et al.* [1] is encouraging for the modeling of other nitro-containing energetic material. These systems will have similar NO, HNO, N_2O, and HCN chemistry, particularly for the second-stage ignition. These results indicate that a different mechanism is occurring at elevated temperatures (> 1000 K) compared to lower temperatures.

REFERENCES

[1] R. Guirguis, D. Hsu, D. Bogan, and E. Oran, Comb. and Flames 61, 51 (1985).
[2] D. S. Y. Hsu and M. C. Lin, J. Ener. Mat., 3, 95 (1985).
[3] E. L. Lee, R. H. Sanborn, and H. D. Stromberg, Proc. 5th Symp. (Int) Detonation, 331 (1970).
[4] G. J. Piermarini, S. Block, and P. J. Miller, J. Phys. Chem. 93, 457 (1989).

[5] C. P. Constantinou, T. Mukundan, and M. M. Chaudhri, Phil. Trans. R. Soc. Lond A 339 , 403 (1992).
[6] J. Connor, Chemistry and Physics of the Molecular Processes in Energetic Materials (S. N. Bulusu, ed.), ASI 309, p 545 (1990).
[7] J. C. Mialocq, J. de Phys. C4, 163 (1987).
[8] S. Zeman, Thermochemica Acta, in press.
[9] A. Perche, J. C. Tricot, and M. Lucquin, J. Chem. Res. S, 116 (1979), J. Chem. Res. M, 1555 (1979).
[10] R. D. Bardo, 8th Symp. (Int) Detonation, 855 (1989).
[11] M. D. Cook and P. J. Haskins, 12th Int Pyro Symp., 43 (1987).
[12] S. Odiot, J. de Phys. C4, 225 (1987).
[13] C. F. Melius, Phil. Trans. R. Soc. Lond A 339 , 377 (1992).
[14] C. F. Melius, Chemistry and Physics of the Molecular Processes in Energetic Materials (S. N. Bulusu, ed.), ASI 309, p51 (1990).
[15] C. F. Melius, Chemistry and Physics of the Molecular Processes in Energetic Materials (S. N. Bulusu, ed.), ASI 309, p21 (1990).
[16] C.-Y. Lin, H.-T. Wang, M. C. Lin, and C. F. Melius, Int'l. J. Chem. Kinetics **22**, 455 (1990).
[17] M. C. Lin, Y. He, and C. F. Melius, Int'l. J. Chem. Kinetics **24**, 489 (1992).
[18] M. C. Lin, Y. He, and C. F. Melius, Int'l. J. Chem. Kinetics **24**, 1103 (1992).
[19] A. E. Lutz, R. J. Kee, and J. A. Miller, Sandia Report SAND87-8248 (1987).

Question - Fauquignon

How does the pressure influence the kinetics either as a decomposition or as a recombination in the two-stage process? What is the global influence of the pressure?

Response -
In the model presented here, each of the elementary unimolecular reactions has a pressure dependence in the rate constant, being bimolecular at low pressure ($A+M \leftrightarrow B + C + M$, where M is a third-body collision partner) and becoming pressure independent at high pressure ($A \leftrightarrow B + C$). Each elementary reaction is reversible, so that decomposition and recombination are the forward and reverse directions of the same reaction. At atmospheric pressures, these elementary reactions range from the low pressure limit (e.g., $HCO \leftrightarrow H + CO$) to the high pressure limit ($CH_3NO_2 \leftrightarrow CH_3 + NO_2$). At high densities (> 1 kbar), all these elementary reactions have reached their high-pressure limit, being pressure independent. The global influence on the pressure is influenced by which reactions dominate. To the extent that the unimolecular decomposition of CH_3NO_2 dominates, the kinetics become independent of pressure (e.g., the n_i of table IV approaches 0). Condensed phase bimolecular decomposition process, involving two CH_3NO_2 molecules or a CH_3NO_2 molecule and a water molecule would have a bimolecular pressure dependence (e.g., n_i approaching -1). Our high temperature results of table IV indicate relatively little temperature dependence, dominated by the unimolecular decomposition of nitromethane.

Question - Gupta

In one of your tables, you had a pressure of approximately 2 kbar. At such a pressure, clearly the nitromethane is not a gas. Do your calculations hold for a liquid?

Response -
At the temperatures we consider (> 1000K), we are above the critical point for most of the species involved in the decomposition process. Thus, it is not valid to consider the fluid as either a gas or a liquid. It is best to view the calculations as being at a given density. The real gas equations of state then convert the ideal gas pressure to the real pressure by the compressibility factor Z. In the kilobar range, the compressibility factor should be greater than 1, so the actual pressure will be higher than the corresponding "ideal" pressure given in tables II and III. The reaction rates are a function of the collision frequencies, which depend on the density. We have chosen the pressure to be such that the density of the nitromethane corresponds to that of liquid nitromethane. Given a desired real gas pressure, one can determine an effective "ideal gas" pressure which will reproduce the same density. The important question to ask, then, is does the reaction mechanism contains the appropriate elementary reactions. Our mechanism is strongly biased towards gas-phase reaction mechanisms, e.g., bimolecular radical species. Unimolecular decomposition processes should be appropriate for both condensed phase and gas phase. However, ionic reactions and other solvent-assisted reactions have not been included to a significant degree. We have included some solvent-assisted reactions that normally occur in the liquid phase. Our results indicate that at the high temperatures (> 1000K) studied,

the entropy constraints are too restrictive for such reactions to be important. Thus, we believe that under our conditions, the fluid is behaving more like a gas than like a normal liquid.

Question - Kondrikov

1. How long are the chains in case of the nitromethane decomposition at the very high temperatures (first stage, second stage) without additivity and in the presence of catalysts?
2. Did you try to calculate the self ignition process parameters at pressures of about 10 GPa? (If the chemical equilibria is obviously strongly dependent on the pressure of the equation of state for chemical kinetics, it can be clearly a more or less weak complication).

Response -
1. We have not attempted to determine a chain length. We find that there are no significant chain branching steps and that unimolecular reactions are most important. Radical attack on nitromethane by OH and other radicals is relatively minor < ~5%. We thus believe that at temperatures > 1000K, the chain lengths should be short.

2. With respect to calculations at 10 GPa, we feel very uncomfortable about using a gas-phase model at such high pressures (even the several kbar range is presented only as an indication of what may occur). The issue to be addressed is the mobility and orientation of individual molecules (entropy) which may be restricted at high pressures, counteracting the effects of high temperatures. This would enable concerted condensed phase reaction mechanisms to occur. Also, the role of ionic reactions becomes increasingly important. My belief is that the effects of high temperature will dominate the effects of high pressure in determining the reaction mechanism.

Question - Borisov

Some of the rate constants included in your computation scheme are unknown in the temperature range you used. How did you estimate the missing rate constants?

Response -
The rate constants have an Arrhenius form $k = A\ T^n\ exp(\Delta E/RT)$ which allows the rate constants to be extrapolated to other temperature ranges. Errors can accrue if the mechanism of the reaction changes. Thus, it is important that each reaction be an elementary process involving a single transition state structure. Multiple reaction rates for the same reaction may be included in the overall mechanism for A+B $\rightarrow$ C+D (such as one for an adduct intermediate and one for an abstraction transition state). Each of the elementary reaction rates measured experimentally must be consistent with transition state structures (including entropy changes and activation energies). For reaction rates that have not been measured, estimates of the rate constants can be estimated from analogous reactions where both the experimental and theoretical data are known.

Question - Zeman

Decomposition of nitro-compounds produces radicals. As Prof. Urbanski (Poland) has shown, these radicals can recombine with the nitro-compound. Have you included reactions of this type into your scheme?

Response -
We have included the reaction of radicals on the nitromethane. The radicals include OH, H, CH_3, NO_2, and others. The reactions are relatively unimportant (< ~5% of the unimolecular decomposition rate). The radicals tend to react with the intermediate products of decomposition. In one instance, the reverse of the reaction is observed, whereby the CH_2NO_2 radical abstracts a H atom from CH_3OH reforming the CH_3NO_2, i.e., $CH_2NO_2 + CH_3OH \rightarrow CH_3NO_2 + CH_2OH$. The CH_2NO_2 is formed primarily by H and OH attack on the CH_3NO_2. The attack of CH_3 on CH_3NO_2 yields mostly $CH_3NO + CH_3O$.

Question - Volk

We detonated nitroguanidine containing high explosives (45% TNT / 55% nitroguanidine) in argon atmosphere (1 bar Ar) in a detonation containment (1.5 m^3). We analyzed relatively large amounts of HCN (3-4%) after the detonation. Could you explain this HCN formation? We also found small amounts of HCN (1.5-2.5%) from TATB containing charges.

Response -
We find for nitromethane that HCN is an intermediate in the conversion of the NO to N_2. Furthermore, we find that HCN is a key intermediate in the decomposition of nitramines such as RDX and HMX. It is possible that the expansion process freezes out the HCN species before it has an opportunity to react to completion to form N_2.

Question - Miller

In your calculations on the conversion of the nitromethane to the aci-form, how do you specify the conformation of the H_2O or the other molecules around the CH_3NO_2 reference molecule? If the conformations are specified, is it possible to calculate the change in the polarizability as seen by Presles in shocked liquid CH_3NO_2?

Response -
The geometries of the H_2O molecules participating in bond breaking were treated explicitly in the transition state structures and optimized as part of the overall electronic structure optimization. This required several separate investigations of geometries for orientation of the non-breaking OH bonds, each structure having its own local transition state structure. The rest of the water molecules were treated as a dielectric continuum. Both the explicit water molecules and the continuum solvent molecules contribute to changes in polarizability. The interaction between the

molecular complex's polarizability and that of the dielectric continuum is solved self-consistently to obtain a net polarizability. The extent to which the liquid nitromethane can polarize a given molecule is computationally feasible, given that the response time is sufficient, i.e., that the frequency dependence of the dielectric is small.

Question - Kunz

Dielectric response stabilization to electronic - chemical processes in condensed media dates back at least to Mott-Littleton in 1938. Those approaches based upon a continuum surrounding of the system have been indicative of the size of the issue, but as Gilbert found in 1966, the size-shape of the hole in the dielectric continuum effects the size of the result. More recently, Sangster-Stoneham used atom-based models to avoid this problem. What is your approach to this issue? Secondly, a problem exists with respect to which dielectric constant to use since there is a strong frequency dependence here. Some recent models based upon the shell model of Dick and Overhauser, for example, attempt to model this. What is your approach to the frequency dependency of the dielectric constant?

Response -
Our approach is to use a solvent-accessible surface of the molecule to define the shape of the hole in the continuum. This complex molecular shape is defined by the surface traced out by a solvent molecule rolling around on the Van der Waal's surface of the molecular complex. The approach implemented here is to treat only the static dielectric constant and not the frequency dependence. To the extent that the frequency dependency of the dielectric is important, the effect will be to reduce the solvation contribution to the activation energy lowering. We find that the solvation effect is already greatly reduced at high temperatures due to other entropy effects. This reduces the importance of treating the frequency dependency.

Question - Armstrong

Is there useful information on critical reaction coordinate distances involved in your calculations? My thought is that this information would relate to our interest in solid state decompositions.

Response -
The reaction coordinate distances will be those associated with bond breaking and formation (a general rule of thumb would be a 20-30% stretch in the normal bond distance). A more important question is the required orientation of the molecules during the reaction. These restrictions on molecular orientation impose a severe entropy penalty. At higher temperatures, complex reaction mechanisms usually occurring in the condensed phase (at low temperatures) are no longer important. Of key importance in experimental studies of solid state decomposition is the determination of the temperatures achieved (more specifically time at temperature) at the reaction sites. Specifically, one needs to determine how hot does a hot spot get and for how long. Such results can be used in models like the one presented here to determine ignition delay times.

JOURNAL DE PHYSIQUE IV
Colloque C4, supplément au Journal de Physique III, Volume 5, mai 1995 C4-553

Microscopic Experimental Approaches to High Pressure Chemistry

T.P. Russell, T.M. Allen*, J.K. Rice and Y.M. Gupta*

Naval Research Laboratory, Chemistry Division, Code 6110 Washington, DC 20375-5320, U.S.A.
** Washington State University, Department of Physics, Shock Dynamics Center, Pullman, WA 99164-2814, U.S.A.*

Abstract: The experimental study of the chemistry related to the deflagration/detonation of energetic materials is extremely challenging due to the high pressure, high temperature, and time domain under which the chemical reactions occur. In addition, non equilibrium pressure and temperature conditions temporally effect the reaction pathways and rates during the reaction process. The multiple phases of material present (i.e. the heterogeneous nature of the problem), the multiple reaction pathways (both in series and in parallel), and the temporal dependency of the physical conditions make the assignments of the early reaction products, product sequence, and reaction mechanism an extremely difficult if not nearly unsolvable problem.

Recently, experimental approaches have been developed which permit the spectroscopic identification of products species, reaction sequences, and global reaction rates under simulated detonation conditions. Three experimental techniques: (1) high pressure matrix isolation (2) high pressure time-resolved absorption spectroscopy , and (3) high pressure time-resolved emission spectroscopy are used in conjunction with a gem anvil cell to probe the high pressure chemical processes.

1. INTRODUCTION

The detonation of a condensed explosive is a complex process involving extremely rapid mechanical, physical, and chemical changes. It is convenient to approximate or envision the detonation process in the following sequential steps. First, the materials is subjected to a stimulus, e.g. a shock wave, which transfers energy to the material. Second, the chemically excited material most likely proceeds through an endothermic process (termed reaction initiation) resulting in bond breaking at some threshold deformation and temperature condition. Third, a sequence of endothermic/exothermic processes occur resulting in the liberation of chemical energy. Finally, the released chemical energy supports the propagation wave and results in the continuum or hydrodynamic response of the reacted material. Historically, the last step is the one that has been most commonly studied. Very recently, work has also begun to develop techniques to experimentally access the first two steps. There is, however, little that is known about the third step of the chemical changes following reaction initiation.

The initiated material continues to react over an extended period of time through a variety of reaction pathways until some final product distribution is achieved or reaction quenching terminates the developing processes. This region following initiation is defined as the hot molecule zone. The hot molecule zone includes all endothermic and exothermic reactions after initiation. The hot molecule chemistry supports the detonation wave and is responsible for the conversion of chemical energy into the P/V work. This zone is on the order of nanoseconds to microseconds for an ideal explosive. For a nonideal explosive (such as a composite explosive), this region is on the order of nanoseconds to milliseconds. Despite the importance of the chemical reactions in the hot molecule zone, direct experimental measurements are lacking. All chemical reactions which occur during the detonation process take place under nonequilibrium temperature, pressure, and volume conditions. Our studies focus on the chemistry of the hot molecule region. We recognize that the chemical sequences must be probed under representative pressure, temperature, volume (density) and time conditions. A

microscopic experimental approach has been developed to spectroscopically probe the reaction products, reaction product sequence and global reaction rate related to deflagration/detonation. Three experimental techniques: (1) high pressure matrix isolation (HiPMI) , (2) high pressure time-resolved UV/Vis absorption spectroscopy (HiPTRAS), and (3) high pressure time resolved emission spectroscopy (HiPTRES) are used in conjunction with a high pressure gem anvil cell (GAC).

2. BACKGROUND

In the past, the chemistry taking place in the hot molecule region has been described by applying basic chemical decomposition processes. This information provided the basis for more realistic estimations of thermodynamic parameters and product distributions to describe the explosive behavior. However, the extrapolations made are unreliable and lead to large uncertainties in thermodynamic parameters which are often used to support the theoretical descriptions of the explosion phenomenon. Given the complexity of the reactions involved and the observed temperature and pressure dependent effects an understanding of the hot molecule region is necessary for modeling explosion behavior. Unfortunately, such experiments are difficult to carry out, and therefore, only a few results have been reported. The effects of extreme conditions (high pressure/high temperature) has been applied to energetic materials over the last several years in an attempt to probe the hot molecule region. Several static experimental approaches have been employed to study the structural dependency, decomposition kinetics, and burn rate of energetic materials under high pressure.[1-4] In addition, detonation mass spectrometry has been employed to probed the chemical sequences of the third step. [5] The decomposition kinetics under static high pressures has provided kinetic and thermodynamic data on the decomposition of materials such as, HMX, RDX, and nitromethane. The high pressure decomposition kinetic studies do not provide any chemical information on the reaction intermediates, final products, or reaction mechanisms and the times associated with decomposition are on the orders of minutes to hours. Static high pressure burn rate studies provide a physical measurement of the affects of pressure on the combustion rate. Detonation mass spectrometry has provided limited chemical information on the reaction processes of a detonation. The temporal evolution of the products has been observed. Multiple products with similar masses and poor resolution make product identification a non-trivial process. These experimental approaches have provided a good first approximation to probe structural dependency, global reaction kinetics, burn rate and product formation of the chemistry of a deflagration/detonation. Further advances are necessary to provide additional information of reaction intermediates, product formation sequence and reaction rates under extreme conditions. The approach must probe the chemistry under representative pressure, temperature, volume (density) and time conditions to attempt to identify the dense state chemistry of the hot molecule region.

3. EXPERIMENTAL

The experimental techniques employed in the present work have been reported in detail elsewhere [6-11]. Only a brief description will be given for the sake of clarity.

3.1 High Pressure Cell:

The high pressure apparatus is either a Merrill-Bassett or NIST Anvil cell. [6,7] Two types of gem anvil materials (diamond and cubic zirconia) are employed. The UV/Vis spectroscopy or matrix isolation sample is prepared by compressing a 3-5 micron sample film between two KBr or NaCl salt windows. A tantalum or nickel gasket confines the sample under pressure. (Figure 1). The gasket hole diameter is 250 microns with a 100 or 200 micron thickness. A small ruby sphere, < 15 microns in diameter, is placed within the salt window. The entire sample (salt windows and sample) is compressed in the gem anvil cell (GAC) to the desired initial pressure. Initial temperature is measured by a chromel-alumel thermocouple with the thermocouple bead in contact with the gasket.

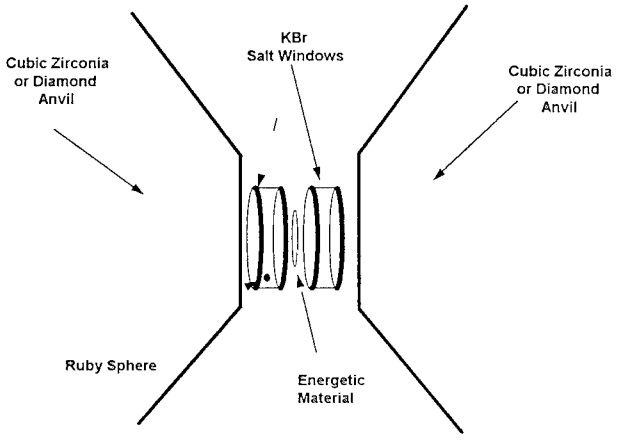

Figure 1. Sample arrangement inside the GAC for HiPTRAS and HiPMI.

In matrix isolation experiments the Merrill-Bassett GAC cell is clamped

in thermal contact with a displex refrigerator head. The GAC (and sample) is cooled to a constant initial temperature of ~40-50 K. The temperature is measured with two gold/chromel thermocouples. One thermocouple is located in a hole drilled in the aluminum mounting plate between the refrigerator and the anvil cell. The second is attached to the gasket surrounding the sample in the GAC cell. Pressure inside the anvil cell is measured by the ruby fluorescence pressure measurement technique originally developed by NIST in 1972 [8,9] and calibrated against the compression of NaCl via the Decker equation of state in 1976.[9] Pressure is evaluated by a peak shift calculation or a line-shape model. The ruby fluorescence measurements are accurate to ± 0.05 GPa when they are made in a hydrostatic environment at room temperature. The material inside the anvil cell is laser heated with either an 8 ns or a 3.5-4.0 microsecond pulse using a visible laser pulse. A first approximation of the bulk thermal response is estimated to be between 700-1200 K.

3.2 High Pressure Matrix Isolation (HiPMI)

The matrix isolation apparatus consists of a closed-cycle helium refrigerator (Air products, Model DE-202) mounted inside a vacuum chamber, a pulsed Nd:YAG laser (Continuum, Model YG 581), and a Nicolet 60 SX FTIR spectrometer employing an MCT-A detector for improved sensitivity.[10]

A single pulse (8 ns) from the frequency doubled Nd:YAG laser (532 nm) is used to heat the sample. The typical laser energies are 15-20 mJ. The laser beam diameters were determined by measuring the spot size burned onto photographic paper loaded in the GAC. Typical values for the beam diameters are ~0.5 mm. The fluence of the laser is ~1 to 1.5 J/cm^2. Under these conditions, an initial temperature between 270 and 740^{o}C (543 and 1013 K) is obtained within the sample. The lower temperature is the minimum required to thermally decompose the sample at this pressure. The higher temperature is the melting temperature of KBr, which is not exceeded. The background pressure of the chamber is ~1.0 x 10^{-7} torr. The sample pressure inside the anvil cell is 3.0 GPa. Vacuum conditions are required to eliminate condensation problems on the anvil cell at ~40-50 K.

The infrared absorption spectra of the starting material and the reaction products are measured before and after the laser pulse. Typical spectra are collected with 500-1000 scans at 2 cm^{-1} resolution. Separate samples are loaded with diamond and cubic zirconia anvils for a complete IR spectral analysis of products in the mid-infrared region (4000-600 cm^{-1}).

3.3 High Pressure Time Resolved UV/Vis and Emission Spectroscopy

The time-resolved apparatus consists of a microscope system employing a 20X Zeiss microscopic objective, a flash lamp pumped dye laser (Candela Model SLL 500), a single monochromator (SPEX 1681), a streak camera (Cordin 160 model No. 5B) and a CCD detector (SPEX Model Spectrum-One). [11]

A single pulse (3.5-4.0 μs) from the flash lamp pumped dye laser, tuned to 514 nm, is used to heat the sample. Typical laser energies are 1.0-6.5 mJ and a measured spot size of ~0.14-0.20 mm. The UV/Vis absorption and emission spectra were collected into the single monochromator and temporally dispersed by the streak camera onto the CCD detector, thus providing an intensity measurement as a function of wavelength and time. The consumption of material by UV/Vis absorption spectroscopy and the detection of products by emission spectroscopy was monitored in the 380-550 nm wavelength region at a maximum temporal resolution of 110 ns.

4. RESULTS

4.1 Matrix Trapping at High Pressure

Matrix experiments have been carried out on hexanitrohexaazaisowurtzitane (HNIW) at 2.7 GPa. Infrared spectra were collected i) before the laser pulse; ii) after the laser pulse; iii) after warming the sample to room temperature at 2.7 GPa; and iv) after the pressure release from 2.7 GPa to ambient pressure. Figure 2 shows selected spectra from the laser initiated reaction of HNIW in a DAC. The same results are observed in the CZAC and DAC experiments. No starting material remains,

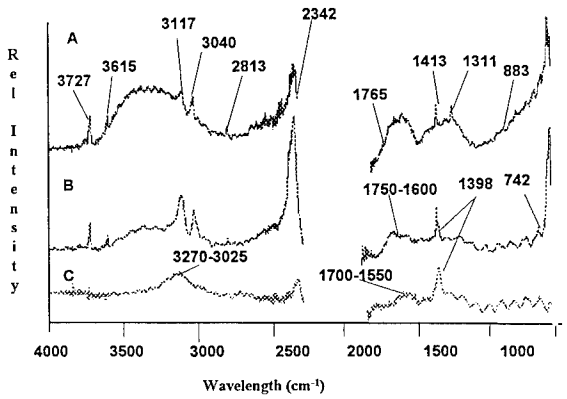

Figure 2. Selected spectra from the HiPMI of HNIW in a DAC.

indicating that the reactant is completely consumed. The products formed are identified by their infrared absorption frequencies. The tentative assignments for the observed reaction products are provided in Table 1. The products observed at 50 K (spectrum A) including unknown (UnK) absorption bands are: CO_2, Unk 3040, H_2O, Unk 1413, NO_2, CO, HNCO, Unk 2813, t-$(NO)_2$, Unk 2015, and N_2O. These products are listed roughly in order of their peak height intensity in the spectra without line strength corrections. The three unknown product absorption bands at 3117, 3040, and 1413 cm^{-1} are tentatively assigned to the formation of at least one product containing NH functionality. The two absorption bands detected at 2813 and 2015 cm^{-1} are assigned to at least one product containing CH and CN functionality. Upon warming the sample to room temperature and 2.7 GPa, the only observed changes (Spectrum B) are: the disappearance of the t-$(NO)_2$ band at 1765 cm^{-1} and the NO_2 symmetric stretching band at 1311 cm^{-1}, and the appearance of a band at 1873 cm^{-1}indicates NO monomer formation. All other products remain the same. After the temperature and pressure are returned to ambient conditions (Figure C) the reaction products observed at 50 K disappear. A visually dark film remains trapped in the matrix. The residue spectrum was determined to have the same functionality observed from decomposition and combustion. Therefore, all product absorption bands which disappear are either volatile products or reactive intermediates.

Table 1. IR Bands and Tentative Assignments of the Observed Products in the CZAC and the DAC.

ν (cm^{-1})	Species	Tentative Assignment (intensity)	in CZ	in DIA
3727	CO_2 or H_2O	$\nu_1+\nu_3$(39) or ν_3(200)	Y	Y
3615	CO_2 or OHCN(?)	$2\nu+\nu_3$(30) or OH str	Y	Y
~3600 (broad)	H_2O	OH str	Y	Y
3117	-NH-[a] or -CH-	NH str or CH str	Y	Y
3040	-NH-[a]	NH str, CH or CH_2 str	Y	Y
2813	CH or CH_2	CH_2 str	Y	Y
2342	CO_2	ν_3(2026)	Y	Y(edge)
2291	HNCO or OHCN	NCO a-str or CN str	Y	
2232	N_2O	ν_3(1285)	Y	
2140	CO	1-0 (235)	Y	
2015	CH or CN(?)		Y	
1765	t-$(NO)_2$	a-str	Y	Y
1413	-NH-[a] or HNO(?) or CH_3NO(?) or H_2CN(?)	NO str CH_3 a-def CH_2 sciss		Y
1311	NO_2(?)[b]	s-str[b]		Y
883				Y
742	CH(?)			Y
~650	CO_2	ν_2^1(194)		Y

[a]Similar to HN_3 decomposition products in Blau and Hochheimer, JCP, 34,1060 (1961) and JCP, 41, 1174 (1964).
[b]Not seen in post-laser fire RT spectrum.

4.2 TIME RESOLVED MEASUREMENTS

4.2.1 UV/Vis Absorption: High pressure time resolved absorption spectroscopy (HiPTRAS) was accomplished with a temporal resolution of 110 ns in the study of $C_6H_6N_{12}O_{12}$, (1,4 trinitroethylamine tetrazine). DTETZ was studied at 0.8, 2.0 and 3.4 GPa. The π - π^* transition at atmospheric conditions at 411 nm of the tetrazine ring was monitored at a 110 ns temporal resolution. A pressure shift was observed for this band. The experiments at 0.8, 2.0 and 3.4 GPa were performed with comparable laser initiation energies. Similar results are observed for all pressures studied. Figure 3 shows selected spectra of the laser initiated DTETZ sample at 0.8 GPa. A decrease in the absorption band is detected after 580 ns and the absorption has reached its minimum value after 1.1 microseconds. The sample maintains a constant transmitance for 1.1 microseconds. After 1.1 microseconds, an increase in absorption is detected between 380-550 nm. The increase in absorption is detected throughout the remaining temporal window (0.66 microseconds) for the experiment.

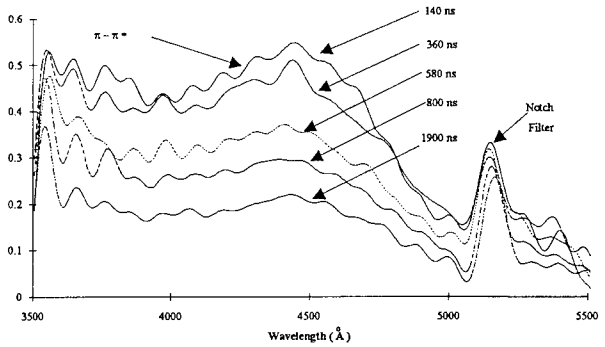

Figure 3: HiPTRAS spectra with 220 ns temporal resolution of the DTETZ π to π^* transition laser initiated at 0.8 GPa.

4.2.2 Emission Spectroscopy:
High pressure time resolved emission spectroscopy (HiPTRES) at a temporal resolution of 110 ns was applied to monitor the reaction sequence for the reaction of Al + H_2O. The Al + H_2O reaction was studied at < 0.1, 0.2, 0.4, and 0.7 GPa. Figure 4 shows selected spectra for the laser initiated Al + H_2O reaction at a pressure < 0.1 GPa. A reaction sequence is identified by the order of appearance of product emissions. The observed emission lines were identified using tables compiled by Pearse and Gaydon. [12] Spectrum A shows the initial emission detected. Al emission superimposed on a low energy continuum spectral background is observed. This continuum spectral background is assigned to the heating process of the H_2O (l). A continuum spectral background equal in intensity is observed at the same time during laser heating of pure H_2O (l). Al atom emission disappears after 330 ns, with the appearance of AlO and AlH emission (Spectra B and C). AlH emission disappears after 220 ns. During the appearance of AlO and AlH, a large continuum background is also detected. An additional species is detected along with AlO and AlH which has not been identified at this time. AlO emission disappears in 1.1 microseconds. The unassigned emission product continues to emit for 0.5 microseconds after the disappearance of AlO. (Spectra D and E) This suggests that the unassigned emission may be produced by the further reaction of AlO. After the unknown emission has disappeared the continuum spectral background continues until the end of the temporal window of the experiment. (Spectrum E) Two products have been reported which may be identified with the continuum emission. [13] These products are Al_2O_2 and Al_2O_3 (l).

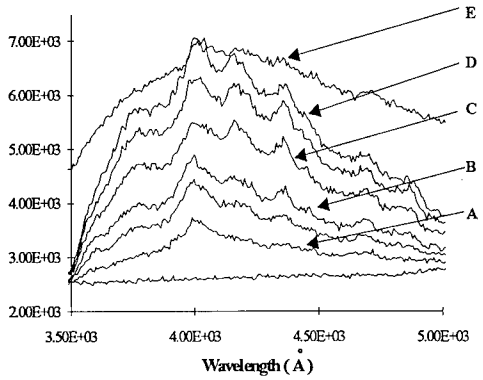

Figure 4: HiPTRES spectra with 110 ns temporal resolution of the laser initiated Al + H2O reaction at < 0.1 GPa.

5.0 CONCLUSIONS

The experimental approaches to the investigation of chemistry at high pressures has been described and preliminary results are presented for each technique. All experiments are initiated by a similar technique in an attempt to model the conditions associated with a deflagration/detonation. However, each experimental approach provides significantly different chemical information which helps to discern the complicated nature of the problem. Three experimental techniques: (1) high pressure matrix isolation(2) high pressure time-resolved UV/Vis absorption spectroscopy and (3)high pressure time-resolved emission spectroscopy have been demonstrated in a GAC. The combined experimental techniques provide multiple spectroscopic probes for the determination of unique chemical information related to the hot molecule zone. The products produced, product formation sequence, and global reaction rate are determined.

6. ACKNOWLEDGMENTS

The authors wish to acknowledge financial support from the Office of Naval Research and Naval Research Laboratory Accelerated Research Initiative on the Heterogeneous Decomposition of Energetic Materials.

7. REFERENCES:

[1] Piermarini G.J., Block S., and Miller P.J., *J. Phys. Chem.*, **91** (1987) 3872. and Piermarini G.J., Block S., and Miller P. J., *J. Phys. Chem.*, **93** (1989) 457.
[2] Miller P. J., Piermarini G. J., and Block S., *Applied Spectroscopy*, **38**, (1984) 680.
[3] Rice Steven F. and Foltz M. F., *Comb. and Flame*, **87** (1991) 109.
[4] Russell T. P., Miller P.J, Piermarini G. J. and Block S., *J. Phys. Chem.*, **97** (1993) 1993.
[5] Blais N.C., *J. of Energetic Mat.*, **6** (1987) 456.
[6] Barnett J.D. Barnett, Block S., and Piermarini G. J., *Rev. Sci. Instrum.* **44** (1973) 1.
[7] Merrill L., and Bassett W.A., *Rev. Sci. Instrum.*, **45** (1974) 290.
[8] Block S., and Piermarini G.J., *Physics Today*, **29** (1976) 44.
[9] Piermarini G.J. Block S., Barnett J.D., Forman R.A., *J. Appl. Phys.*, **46** (1975) 2774.
[10] Rice, Jane K., and Russell T. P., *J. Phys. Chem.* (submitted)
[11] Russell T.P., Allen Theresa M., and Gupta Y.M., (unpublished)
[12] Pearse R.W.B. and Gaydon A.G., The identification of Molecular Spectra (Chapman and Hall, New York, N.Y., (1976)
[13] Brzustowski T. A., and Glassman I., Heterogeneous Combustion, (Progress in Astronautics and Aeronautics Series, Wolfhard H.G., Glassman I., and Green L. eds., Academic Press, New York, NY 1965) Vol 15, p41.

Discussion

Volk-Russell

Q : We detonated high Al - containing composite explosives under water and we were surprised that we could not observe any reaction of the Al with water, even when the explosives contained 30% of Al and even if we found, analyzed, more than 20% of the total Al - content unreacted.
How can you explain this behavior ?

A : The Al + H_2O reaction in our experiment is a model system to understand how the reaction product (H_2O) from the detonation of energetic material reacts with Al. If we consider where the Al particle is located in the detonated system, we can postulate an explanation of the lack of excess Al reaction with the surrounding water medium.
The Al will be consumed initially by the oxidating atmosphere of the explosive. The particle most likely cools and a solid Al_2O_3 layer is on the surface which inhibits or slows the reaction from the surrounding H_2O. Therefore, these reactions will not participate in the Al consumption.

JOURNAL DE PHYSIQUE IV
Colloque C4, supplément au Journal de Physique III, Volume 5, mai 1995

Reaction Mechanisms in Shocked, Intercalated Graphite and Boron Nitride

R.D. Bardo

Naval Surface Warfare Center, 10901 New Hampshire Avenue, Silver Spring, MD 20903, U.S.A.

Abstract: The traditional ways of developing increasingly energetic materials usually lead to an increase in shock and impact sensitivities. It is, therefore, of practical and theoretical importance to design model, highly-energetic polycrystalline systems which will clearly indicate, at the molecular level, the interplay between the shock-induced reaction mechanisms and the associated excited lattice states. Theoretical and experimental studies indicate that such systems may possibly be constructed from special materials such as high-quality pyrolytic, layered graphite and hexagonal boron nitride (BN) crystals. Although each layer of graphite and BN is one of the most stable structures in nature, intercalation of the crystals with various oxidizing agents can yield energetic systems with the desired properties. As an example, intercalation with HNO_3 gives crystals of density 2.20 g/cc. The optimal positioning of the HNO_3 molecules between the BN layers allows the rapid formation of B_2O_3 in a single step with a large release of energy. A possible triggering mechanism is the shock-induced, partial sp^3 hybridization of the layers as a result of kink band formation.

1. INTRODUCTION

New energetic compounds continue to be synthesized which give ever-improving fragment acceleration and blast pressure, but often showing a concomitant increase in sensitivity. Since the traditional "trial and error" methods used in the scale-up of the new materials from laboratory to test conditions continue to show conflicting performance and sensitivity results, it would be of practical and theoretical importance to be able to design, from the ground up, a model highly-energetic system which clearly exhibits the needed insensitivity and performance at all stages of development. It is, therefore, the purpose of this paper to indicate the feasibility of such a program by exploiting the current understanding of the nature of the molecular-level processes governing the behavior of energetic materials at high pressures and temperatures.

Benchmark experiments exist which show profound differences in the way homogeneous and heterogeneous materials initiate under shock. In the case of sustained shock pulse initiation of homogeneous liquid nitromethane (NM),[1] which is free of discontinuities of any kind, fast reaction appears to begin close to the driver plate interface after an induction time of about 10^{-6} sec. No light is emitted directly behind the initiating shock, which at 60 kbar propagates 8 mm before initiation begins at the interface. The absence of light emission indicates no appreciable excitation of electronic states with lifetimes $\leq 10^{-6}$ sec. Similar behavior is observed in molten trinitrotoluene (TNT)[1] as well as in single crystals of pentaerythritol tetranitrate (PETN),[1] cyclotrimethylene trinitramine (RDX)[2] and cyclotetramethylene tetranitramine (HMX).[2] On the other hand, sustained shock pulse initiation of heterogeneous NM containing air and oxygen bubbles and of polycrystalline solids gives rise to initiation close to the initiating shock with negligible induction times.[1] In all of these materials, sensitivity is a function of the defect structure and heterogeneous nature of the medium.

More recently, directional shock sensitivity has been discovered in single crystals of PETN by Dick, et al.[3] who showed that, in the chosen geometry, initiation is difficult to achieve along the crystal direction of greatest slip. Although existing crystals of shock-insensitive, "graphitic" triaminotrinitrobenzene (TATB) are too small to be reliably studied with the techniques used for PETN (crystal size of 1 cm), it is expected that larger specimens would show similar, but more pronounced behavior. In PETN, all three orthogonal directions have van der Waals bonding, whereas the layered structure of TATB has such bonding only in one direction and strong intralayer hydrogen bonding.[4] Other explosives with similarly-pronounced slip systems would be expected to show directional sensitivity properties as well. It should be emphasized that while the above research pertains to the structure of single crystals, an understanding of the effects of polycrystalline interactions are crucial in the final analysis of shock sensitivity. Toward this goal, van der Steen, et al. [5] have, for example, determined that crystalline shapes significantly affect sensitivity.

The present paper discusses the design of high-performance crystals which clearly exhibit directional shock sensitivity properties along specific crystal axes and yet which clearly approach the insensitivity of homogeneous energetics along the other axes. Such materials are being constructed from layered pyrolytic boron nitride (BN) crystals which are intercalated with HNO_3 molecules.

2. INTERCALATION OF BN

Intercalation compounds are formed by insertion of a guest chemical species - an intercalate - between layers in a host material. Because of its simple structure, high-quality pyrolytic graphite is most often the preferred choice of host lattice for purposes of enhancing its electrical conductivity and chemical reactivity.[6] Another simple lattice is pyrolytic BN, the crystal structure of which is closely related to that of graphite and being built of hexagonal layers of the same kind, but arranged so that atoms of one layer lie vertically above those in the layers below.

Although each layer in graphite or BN is one of the most stable structures in nature, intercalation of crystals with various oxidizing agents can yield explosive systems with the desired properties. In the case of BN, highly-energetic reactions are possible with formation of B_2O_3 (ΔH_f = -303 kcal/mol). Under ordinary laboratory conditions, the molecules of intercalate enter the host crystal by exploiting the weak binding energy (1.5 kcal/mol or 0.065 ev) between the layers and increasing the interlayer spacing.[6]

Intercalation proceeds by charge transfer from the host BN layers to the oxidizer molecules, causing bonding within the layers of intercalate. This intercalate-intercalate bonding may be stronger than the intercalate-host bonding, resulting in a large thermal expansion of the intercalate layer relative to that of the host layer, which exhibits almost no thermal expansion. For the oxidizer or acceptor compounds, the intercalate layer becomes negatively charged by extracting electrons predominantly from the host bounding layers. Thus, these host layers have a high concentration of holes, causing the Fermi level to fall and the corresponding cylindrical Fermi surface to shrink.

It is interesting to note here that intercalation of "graphitic" TATB would likely produce a much less stable structure, since the transfer of charge would be small and localized in the vicinity of the carbon rings. As a consequence, the intercalate-intercalate bonding would be weaker than that found in the extended structures with uniform bonding in the host layers.

While ordinary procedures of *doping* give *random* distributions of guest species, *intercalation* produces a *highly-ordered* structure. The resulting process of staging gives a mechanism for controlled variation of the physical properties of the compounds. Stage m compounds have m graphite or BN layers between successive layers of intercalate. For maximum intercalation, m = 1, and the theoretical maximum density (TMD) of the crystal falls in the range $1.80 \leq TMD \leq 2.25$ g/cm^3 for the simple molecular intercalates. In this case, the host and intercalate layers alternate so that the structure is uniform and "homogeneous". In the case of planar NO_3, calculation with the MNDO method[7] gives an equilibrium, horizontal stacking of the BN and NO_3 layers, as shown in Figure 1 for two NO_3 molecules and two truncated structures $B_kN_lH_{13}$. An estimation of the density ρ for the corresponding m=1 system gives ρ = 1.80 g/cm^3, which is much smaller than the value of 2.25 g/cm^3 for hexagonal BN. On the other hand, we find that intercalation of BN in fuming nitric acid gives an m=1 density of 2.20 g/cm^3. The only structure which has this density is the one of optimal vertical packing of HNO_3 molecules shown in Figures 2a and 2b. Calculations with MNDO give the positions of the hydrogen-bonded HNO_3 intercalate indicated in Figure 2b. The entire structure appears to be

stabilized by hydrogen bonding and by the electrostatic forces between the net positive and negative charges on the B and O atoms, respectively. Further calculations of the mechanism of intercalation may indicate that the HNO_3 molecules initially enter the BN lattice horizontally followed by their rotation to the vertical orientation in order to allow macroscopic stabilization of the entire host/intercalate structure.

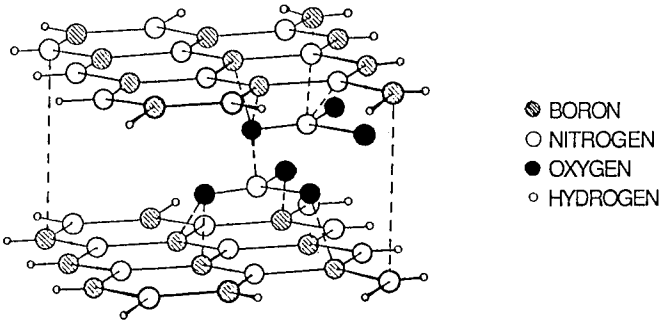

Figure 1. Calculated equilibrium geometry of two HNO_3 molecules between two layers of $B_kN_lH_{13}$.

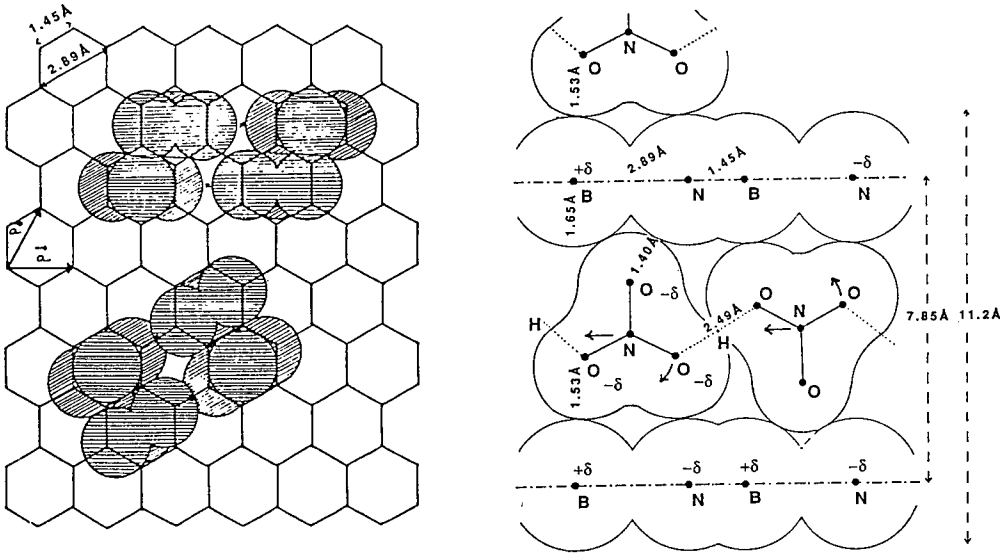

(a) (b)

Figure 2. (a) Two arrangements of HNO_3 molecules perpendicular to the (001) plane of BN. Side-by-side configuration of molecules in lower part of Figure 2a is the most stable one. (b) Side view of the lowest energy arrangement.

Since slip in the layered materials must occur without breakage of the strong B-N bonds, basal dislocations must be present to allow deformation of the hexagons.[8] For stage 1 compounds, maximum slip along the glide planes of dislocations is possible, since the Burgers vectors corresponding to the active basal dislocations of the layers are parallel to the basal plane.[8] In this case, there is minimal slip perpendicular to the basal plane. These dislocations, which split into two partials, have associated with them shear, acoustic modes which are soft (low frequency ω). For stages $m > 1$, regions or galleries of intercalate species are formed between adjacent host layers, resulting in strain of the graphite or BN layers. In graphite the presence of a layer of intercalate causes the two adjacent host layers to undergo relative shear to bring them into eclipsed stacking. The presence of a dislocation at a boundary of a gallery has, then, a Burgers vector with basal and perpendicular components.[8] The presence of the latter component corresponds to an edge dislocation, allowing slip to also occur perpendicular to the basal plane.

3. TIMES TO IGNITION IN SHOCKED, INTERCALATED BN

A theory[9] has been developed by the author which provides a formal framework and guide for the analysis of shock ignition in layered materials. This theory describes the interrelationship among bimolecular chemical reactions and processes for vibrational energy transfer between the crystal lattice and its molecules. Chemical reaction occurs only after sufficient energy is transferred for activation of the molecules. In many cases, this is the slow or rate-determining step, the characteristic time t_{pv} for which is given by

$$t_{pv} = \hbar \sqrt{\rho_a \rho_o}\,, \tag{1}$$

where $\hbar$, ρ_a, and ρ_o are, respectively, Planck's constant and the densities-of-state for the acoustic and optical lattice modes. As indicated in Reference 9, ρ_a and ρ_o may be calculated from the general expression

$$\rho = \left(\frac{2}{\pi n}\right)^{1/2} \frac{(1 - 1/12n)\lambda}{h\langle\nu\rangle(1 + \eta)} \left[\left(1 + \frac{\eta}{2}\right)\left(1 + \frac{2}{\eta}\right)^{\eta/2}\right]^n \tag{2a}$$

where n is the number of vibrational degrees of freedom, <v> is the average of the n frequencies ν_i, and λ and η are defined by the equations

$$\lambda^{-1} = \prod_i (\nu_i/\langle\nu\rangle), \tag{2b}$$

$$\eta = E/E_0. \tag{2c}$$

In Equation (2c), E is the internal energy interval and E_0 is the zero-point energy. Equations (2a)-(2c) apply to both harmonic and anharmonic vibrations.

Calculation of the energy transfer times t_{pv} indicates the important role of slip in the initiation of PETN, as interpreted earlier by Dick, et al.[3] Since excitation of the higher-energy optical modes of the lattice is crucial to ignition,[9] preferential excitation of the long-wavelength acoustic modes corresponding to slip can, by Equation (1), give times t_{pv} which are too slow for the given dimensions of the crystal.

The importance of t_{pv} may be seen in context with other processes occurring in the system which also have characteristic times. These processes and their corresponding rate coefficients pertain to (1) energy transfer from the host lattice into the intercalation molecules $k_{pv} = t_{pv}^{-1}$, (2) energy transfer from the molecules back into the host lattice k_{vp}, and (3) bimolecular reaction k_b between host and intercalate, which combine to give the total rate coefficient[9]

$$k_{tot} = k_{pv}\, k_b/(k_{vp} + k_b)\,. \tag{3}$$

If most of the shock energy is dissipated into the low-frequency acoustic vibrations corresponding to the direction of greatest slip, little reaction is generated so that $k_{vp} >> k_b$ in Equation (3). If, then, $k_{tot}^{-1} > t_r$, where t_r is the time for arrival of rarefaction waves, any reaction is quenched and no ignition is possible, since reduction of the shock pressure P_s below a critical value inhibits the important bimolecular reactions. For the single 1 cm PETN crystals used in Reference 3, calculation shows that $k_{tot}^{-1} \cong 10^{-5}$ sec for $10 \leq P_s \leq 80$ kbar, and $t_r \cong 10^{-6}$ sec for shocks along crystal direction <100>. On the other hand, if $k_{tot}^{-1} \leq t_r$ ($t_{tot} \geq t_r$), ignition is possible. This is the case for orientation <001> where slip is minimized and $k_b >> k_{vp}$, so that $k_{tot}^{-1} = t_{pv}$. Here, calculation shows that $k_{tot}^{-1} < 10^{-10}$ sec for $10 \leq P_s \leq 80$ kbar. These results for PETN are portrayed in Figure 3. It is emphasized here that it is the slow, rate-determining step, identified with t_{pv}, which ultimately determines the ability of the material to ignite at certain critical pressures and temperatures.

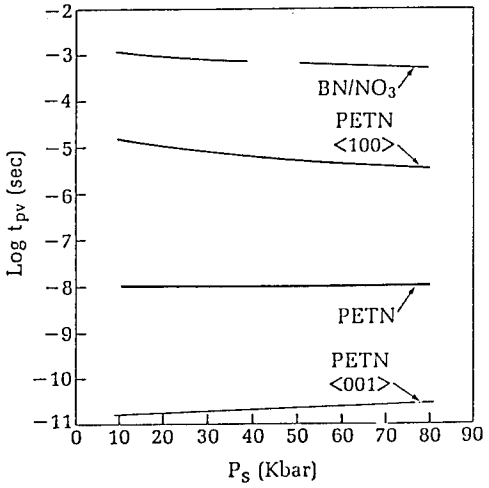

Figure 3. Comparison of shock pressure dependence of t_{pv} for acoustic and optical modes along various crystal directions in BN/NO_3 and PETN. The curve labelled PETN corresponds to the geometric mean of the densities-of-state, Eq.(1), for directions <001> and <100>. Upper two curves for BN/NO_3 and PETN pertain to maximum slip.

For initiation to occur in layered crystals, shocks must have a sufficiently large component of stress P_{cs} along the c-axis of the unit cell. At some critical shock stress P_{cs}, excitation of the initiating optical modes along the c-axis results in bimolecular reaction between the host and intercalate layers, and $t_{pv} < t_r$. For the BN/NO_3 system depicted in Figure 2b, an estimate of t_{pv} is readily obtained from Equations (1) and (2) if the following reasonable assumptions are made: (1) initiation along the c-axis is effectively one-dimensional and (2) $P_{cs} \approx 130$ kbar, which approximates the known minimal pressure required to cause significant distortion of the BN or graphite planes to form the cubic structures.[10] It is assumed here that the lower bound to the optical mode quantum $h\omega$ along the c-axis of BN is about 70 cm^{-1}, which is the value for high-quality graphite.[11] Also, the ratio $\lambda \cong 1$ in Equation (2b) and $E \approx 5 \times 10^9$ ergs/g at $P_{cs} = 130$ kbar,[12] so that in Equation (2c), $\eta \approx 14.3$, since $E_0 \approx 35$ cm^{-1}. The number of atoms per unit cell in the BN/NO_3 structure at stage 1 is 10, and the corresponding number of optical modes n for the one-dimensional problem is 9. Substitution of all of these values into Equation (2a) gives, then, $\rho_0 \leq 1.2 \times 10^{24}$/erg. Accordingly, since n = 1 for the acoustic mode along the c-axis, substitution of the remaining parameters above into Equation (2a) gives $\rho_a \leq 7.8 \times 10^{13}$/erg. Thus, from Equation (1), $t_{pv} \leq 10^{-8}$ sec, which is much shorter than $t_r \cong 10^{-6}$ sec for centimeter-scale crystals.

The effects of sustained shocks of 130 kbar at increasing angles from the c-axis are, to good approximation, two-dimensional in the crystal, corresponding to slip of the host and intercalate planes past each other, because of the relatively weak host/intercalate interaction under shock conditions. In this case, n = 2 and 18 for the acoustic and optical modes, respectively. Substitution of these values as well as the ones above for $\hbar\omega$, λ, and η into Equation (2a) gives $\rho_a \leq 1.1 \times 10^{15}$/erg and $\rho_o \leq 4.7 \times 10^{35}$/erg, and from Equation (1), $t_{pv} \leq 0.02$ sec. Here then, $t_{pv} >> t_r$, and initiation is unlikely. For lower pressures, additional calculations indicate that $t_{pv} \approx 10^{-3}$ sec in the range of $10 \leq P_{cs} \leq 80$ kbar. In Figure 3, these times are seen to be longer than those for PETN, indicating the much greater insensitivity of BN/NO_3 crystals of comparable size.

A similar analysis of TATB, the planar molecules of which form a graphitic structure, is expected to yield times in the range $10^{-5} \leq t_{pv} \leq 10^{-3}$.This is a result of the rigidity (r) of the slip planes for the shock pressures indicated, where r has the order PETN < TATB < BN/NO_3.

4. KINK BANDS AND REACTION

In Figure 2b, the arrows indicate how the NO_3 molecules adjust their positions under compression along the c-axis to form chains of nearest-neighbor B and O atoms. Ignition along the c-axis can then result from reaction between these atoms to form B_2O_3 (O=B-O-B=O) in a single step with high exothermicity. As an example, reaction of BN and HNO_3 for the stage 1 stoichiometry $(BN)_2HNO_3$ would yield 1.57 kcal/g (energy density of 3.45 kcal/cm^3), 6% higher than HMX. Here, the reaction is not diffusion-limited, in contrast to the situation for most known multi-component energetic materials. Thus, the activation energy in k_b of Equation (3) will have the same significance of a homogeneous reaction. The activation parameters have not yet been evaluated for the formation of B_2O_3.

For stage-1 BN/HNO_3 crystals, deformation by slip and the dynamic distortions (vibrations) considered in Section 3 and in Reference 13 do not significantly affect the activation energy. Twinning, on the other hand, which results in the static buckling of the BN planes indicated in Figure 4, can play a role. In contrast fo slip, twinning results from buckling of the BN planes, as indicated in Figure 4 for the basal plane. This source of strain acts as a source of energy for reaction, and so aids the chemical process. The corresponding strain energy, which arises for sp^2 to sp^3 rehybridization, is approximated by $\Delta E \approx 17$ kcal/mol (1420 cal/g).

For many layers of BN, twinning results in kink bands, each of which is defined as the region between two walls of dislocations of opposite sign,[14,15] as shown in Figure 5. Kink bands have been observed in graphite.[8] The shape of the kink band and its size are determined by the integrity of the BN or graphite planes. The size is approximated by the equilibrium condition[15]

$$\frac{w}{L} \ln\left(\frac{L}{w}\right) = \pi (1 - \sigma)\, \theta \left(\frac{\tau_{xy}}{C_{44}}\right) \qquad (4)$$

where σ is the Poisson ratio $\approx 1/3$, θ is the angle of kinking $\leq 20^0$, and the ratio of the shear stress component τ_{xy} to the shear modulus C_{44} is $(\cos\alpha \cos\beta)\, P_{uniaxial} / C_{44}$, which is approximately 1/40. The magnitude of C_{44} for BN is larger than 10 kbar at high stress levels. Equation (4) is obtained by minimizing

$$\frac{U_0}{N} = \frac{C_{44}}{2\pi(1 - \sigma)} \left[(w\theta)^2 \ln\left(\frac{L}{w}\right) - bL\theta \ln\theta \right] \qquad (5)$$

where the Burgers vector magnitude $b \approx 1.45$Å. From Equation (4), $w/L \approx 0.35$ and $U_0 \approx$ 613 cal/g for BN. At $P_{uniaxial} = 300$ kbar, for example, $(1/2)P\Delta V \approx 830$ cal/g from the BN

Hugoniot. The total change in internal energy under shock loading is, therefore, $(1/2)P\Delta V + U_0 \approx$ 1400 cal/g. This elastic strain energy, which approximates the rehybridization energy of 1420 cal/g given above, is stored in the kink bands.

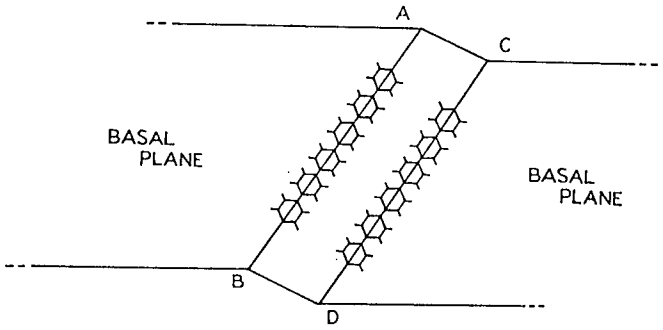

Figure 4. Twin band consisting of two twin boundaries at AB and CD in the basal plane.

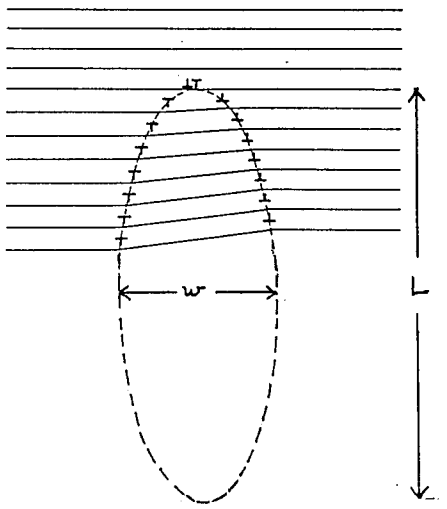

Figure 5. Kink band consisting of twin boundaries in graphite or hexagonal BN.

5. SUMMARY

The important criteria for optimal directional sensitivity in intercalated, layered BN materials are that (1) they must be stage 1 or close to it; (2) the interplanar activation energies for reaction between BN and the intercalate layers must be less than those for reaction within each intercalate layer; and (3) the important interlayer reactions must be bimolecular and exothermic. Criterion (1) addresses the requirement of minimal slip along the crystal axis perpendicular to the basal plane. In this case, $t_{pv\ \parallel} >> t_{pv\ \perp}$, for the parallel and perpendicular directions. Criterion (2) addresses the need to eliminate or minimize reaction in the intercalate layer as a result of energy transfer from the gliding host layers caused by shocks not normal to the basal plane. This requires the careful selection of intercalate. Criterion (3) guarantees that the reactions will occur in times which are short compared to arrival of rarefaction waves caused by shocks. These reactions occur with activation energies that are much lower than those in unimolecular processes. The rates of these reactions given by k_b can be sufficiently fast at the pressures and temperatures of interest in detonations,[9] so that "initiating" energy transfer from the BN lattice into the intercalate molecules is the slow step. Localization of strain energy in kink bands aids the subsequent chemical processes. Reaction occurs at the location of the kink bands. Together, these criteria help to guarantee that the most likely direction of shock initiation is normal or near-normal to the basal plane.

6. ACKNOWLEDGMENT

Special thanks are extended to Prof.R. Armstrong for helpful discussions.

7. REFERENCES

[1] Campbell A.W., Davis W.C., and Travis J.R., Phys. Fluids **4**, 498 (1961).
[2] Campbell A.W. and Travis J.R., in Proceedings of the Eighth Symposium (Int.) on Detonation, NSWC MP 86-194, 15-19 Aug 1985, p.1057.
[3] Dick J.J., Mulford R.N., Spencer W.J., Pettit D.R., Garcia E., and Shaw D.W., J. Appl. Phys. **70**, 3572 (1991).
[4] Cady H.B. and Larson A.C., Acta Cryst. **18**, 485 (1965).
[5] van der Steen A.C., Verbeek H.J., and Meulenbrugge J.J., in Proceedings of the Ninth Symposium (Int.) on Detonation, Vol. 1, OCNR 113291-7, 28 Aug-1 Sep 1989, p. 83.
[6] Bartlett N.and McQuillan B.W., in Intercalation Chemistry, edited by Whittingham M.S. and Jacobson A.J. (Academic Press, New York, 1982), pp. 19-53.
[7] Dewar M.J.S., Thiel W.J.J., J. Am. Chem. Soc. **99**, 4899, 4907 (1977); Stewart J.J.P. MOPAC-MNDO Program in QCPE 1986, 18, p. 455.
[8] Amelinckx S., Delavignette P., and Heerschap M., in Chemistry and Physics of Carbon, Vol. 1, edited by Walker P.L. (Marcel Dekker, Inc., New York,1965), pp. 1-71.
[9] Bardo R.D., Int. J. Quantum Chem. **S20**, 455 (1986); Bardo R.D., in Proceedings of the Ninth Symposium (Int.) on Detonation, Vol. **1**, OCNR 113291-7, 28 Aug-1 Sep 1989, p. 235.
[10] Coleburn N.L. and Forbes J.W., J. Chem. Phys. **48**, 555 (1968).
[11] Green J.F., Bolsaitis P., and Spain I.L., J. Phys. Chem. Solids **34**, 1927 (1973).
[12] Rice M.H., McQueen R.J., and Walsh J.M., in Solid State Physics, edited by Seitz F. and Turnbull D. (Academic Press Inc., New York, 1958), pp. 1-63.
[13] Bardo R.D., in Structure and Properties of Energetic Materials, MRS Vol. **296,** edited by Liebenberg D., Armstrong, R. and Gilman J., (Mat. Res. Soc., May, 1993), p. 186.
[14] Freise E.J. and Kelly A., Proc. Roy. Soc. (London) Ser. **A264,** 269(1961).
[15] Frank F.C. and Stroh A.N., Proc. Phys. Soc. (London) **65**, 811(1952).

Discussion

Kondrikov-Bardo

Q : Did you really obtained the substance you have proposed to produce in our washing machines the layers of BmNn with the molecules of HNO_3 between them ?

A : Density measurements indicated that the maximum packing of HNO_3 molecules between the BN layers was achieved when all intercalant molecules are oriented perpendicular to the host layer. No X-ray crystallography was done, however.

Charrue-Bardo :

Q : Some graphite intercalation compounds are not really stable when stored under air. For example, in such conditions, Lithium - Graphite intercalation compound is a spontaneous flammable product.

So, can you give more details about stability of your nitric acid - graphite compound ?

A : The HNO_3 molecules are bound in the BN interplanar regions by strong electrostatic forces. This is due to the ionic character of the alternating $B(+\delta)$ and $N(-\delta)$ atoms in the planes of the nascent BN crystal. In spite of these forces, liakage of the intercalant does occur over an extended period of time, although to a much smaller extent than in graphite intercalated with HNO_3 where the host lattice / intercalant forces are weaker.

Since much of the BN and HNO_3 character is retained in BN/HNO_3, chemical reactivity should continue to be that of BN and HNO_3 alone.

Melius-Bardo :

Q : In the BN planes, are the empty p orbitals of boron perpendicular to the plane ?

Second, why are the HNO_3 molecules perpendicular to the plane ?

A : The empty p orbitals, perpendicular to the BN plane, combine to form an empty band 2 - 3 ev above the N atom band. The net positive charges on the B atoms attract the net negative charges on the O atoms belonging to the NO_3^- ions. This stabilization, along with the hydrogen bonding, permits optimal packing of the NO_3^- ions perpendicularly to the BN planes in the stage 1 compounds.

Volk-Bardo :

Q : How fast will be the reaction with turbostatic graphite containing small amounts of diamonds, which are the solid reaction products of detonation experiments in Argon atmosphere ?

A : It is very difficult to intercalate turbostatic graphite or BN. This is due to the need for the

intercalant to order itself in extended, near-perfect interplanar regions. Intercalation leads to a highly ordered structure in contrast to doping which is random. It seems likely that the presence of fine diamond particles in turbostatic graphite is random. The high surface energy of these particles may enhance reaction, however.

2 APPLICATIONS FOR ENGINEERING

What Makes a Useable New Energetic Materials, (from Schrödinger to AOP26) ; A.J.Sanderson

The Use of Predictive Methods for the Design of New Explosive Molecules ; A.Delpuech

JOURNAL DE PHYSIQUE IV
Colloque C4, supplément au Journal de Physique III, Volume 5, mai 1995

What Makes a Useable New Energetic Material?

A.J. Sanderson

NATO Insensitive Munitions Information Centre, HQ NATO, 1110 Bruxelles, Belgique

ABSTRACT. In the last 50 years, very many new energetic compounds have been made as potential ingredients for explosive, propellant and pyrotechnic formulations. Of these compounds very few have come to be used in military munitions. To obtain a better understanding of why this has been the case and to help address the discrepancy, the NATO Insensitive Munitions Information Centre (NIMIC) held a workshop in June 1994 open to representatives from government and industry within NIMIC member nations, to study what it is that makes a new energetic material useable. Issues that were addressed included:

-what is currently being used from the current understanding of detonics and molecular modelling in the targeting and preparation of new energetic materials;
-what use is made by the energetic materials designer of present capabilities to predict the performance and safety of new compounds and formulations;
-what do the users require of predictive resources and molecular modelling in order to target more potentially useful new energetic materials;
-what are the user's requirements for useful new energetic materials and can these be interpreted as quantitative properties of energetic molecules.

This paper presents a short summary of those conclusions of this NIMIC workshop that are relevant in the field of the understanding and modelling of detonation at a molecular level.

1. INTRODUCTION

One way of attempting to improve the performance of munitions without compromising safety is to make changes to the energetic materials with which they are filled. A study of the current literature on programmes for research into new ingredients and formulations reveals an apparent lack of an overall, logical and systematic approach to their development, qualification, and assessment of their safety and suitability for use in munition systems. This means that there are significant characteristics missed or overlooked in assessing materials, there are materials discarded when they meet current needs, and there is unnecessary testing. This adds up to time and resources being inefficiently used in the complex route from the conception of a new molecule to the acceptance of a weapon system.

Prediction and modelling of the properties of energetic materials are logically the first steps in the route from the conception to the realisation of energetic materials. However, it is not obvious which attributes of a compound or composition should be modelled in order to try to anticipate whether it is likely or not to be useful in service. One of the purposes of the recent NIMIC workshop was to look at what is available and being used from the current understanding of detonics and molecular modelling in the targeting and preparation of new energetic materials by synthesis and formulation chemists. A further aim was to determine whether what is being predicted coincides with what the users really require of predictive resources and molecular modelling in order to target more potentially useful new energetic materials. In the NIMIC workshop, this followed on from studying the users requirements for new energetic materials and how these can be interpreted as quantitative properties of energetic molecules.

2. PROPERTIES OF ENERGETIC MATERIALS

2.1 Performance

The driving force behind the development (or at least the funding for development) of any new materials for defence use is, and almost certainly always will be, performance. This is readily apparent from almost all recent papers proposing or describing new energetic compounds. An example is found in Olah and Squire [1], where discussion throughout compares performance of new compounds to the current highest energy density materials. This is reasonable, as munition performance requirements are continually increasing, but, however attractive and apparently obvious performance indicators are as a guide to the

most promising materials, there are challenges to this approach that must be considered. These challenges include:

a) what is the most relevant performance indicator to use?
b) will increased 'performance' in a compound lead to increased available performance in a useable composition?
c) will the promotion of new materials on grounds of performance mean that compounds that could be used to give the levels of performance now available but with increased safety be overlooked?

Looking at these points in turn, the first, the question of suitable performance indicators has rarely been addressed. It is common to see lists of detonation velocity or pressure, or theoretical Isp from which conclusions about the highest performance materials are made. However these are not necessarily suitable figures to compare as they oversimplify the estimation of performance [2]. The effect of shaped charges for instance is not solely dependent on detonation velocity, but also on the composition on the product gases and the detonation energy [3]. In fact for widely differing compositions the detonation velocity figures can be completely misleading. A recent example of this came from the study of a LAX112, a new explosive with a very high density and detonation velocity. Comparison of detonation velocities with HMX, RDX etc. implies that this relatively insensitive compound could have wide application because of its high performance, however, comparison of Gurney energies indicates that it will perform relatively poorly in metal accelerating warheads [4]. The situation is at least as complex for propellants, where comparisons can only sensibly be done through the medium of the Isps of optimised compositions containing the compounds of interest. However, optimised compositions may be very dissimilar for different compounds, it is not satisfactory or reasonable to take a baseline formulation and simply replace one oxidiser with the same proportion of another. In comparing nitrate ester and azide containing energetic binders as propellant ingredients for example, there is the possibility of obtaining over-oxidised compositions with nitrate ester binders, which is most unlikely with azide containing ones [5]. In addition, the burning rate, burning rate exponent, and temperature sensitivity etc. are crucial in determining the utility of propellants. There is clearly no single figure that will tell the whole story concerning performance of either explosives or propellants.

The second challenge raised above, that of a compound's performance relative to a useable composition containing that compound, can be illustrated by HMX compositions. The maximum percentage of HMX that can be used in a main charge composition for small warheads is approximately 96% [6]. There is a need for a binder for all HMX compositions to give them some mechanical properties and to make them tolerably safe to use throughout their intended life. Larger warheads need more binder so that they are processable and adequately safe. Some known compounds cannot be processed without using considerably more binder because of the morphology e.g. nitroguanidine, and others need more binder to make them safe enough to process and handle, e.g. PETN. Comparisons of simple performance parameters do not allow for the amount of binder required in different applications to obtain acceptable mechanical, processing or safety properties.

The third difficulty with promoting new compounds on the grounds of performance is that it will miss those materials that might give similar performance when in compositions to those compositions in use today with increased safety. Similarly it will miss those that have intrinsically less performance but, by virtue of the physical and safety properties, might be useable in higher proportions in compositions. A theoretical example might be 'super-TNT', a melt castable compound that has performance less that HMX but that can be used neat like TNT or melt cast with HMX. It's performance when compared to neat HMX would not be attractive, but it could lead to compositions of higher performance.

2.2 Cost

A search of the literature provides scant evidence that cost per se has ever stopped the development of an otherwise suitable new material. However, it may severely limit its application in large or widely used munitions. TATB is an example of this, where its insensitivity and performance have meant that it has found application in a limited range of munitions but its cost prohibits widespread use. Unfortunately this is not necessarily in the best interests of systems costs. Cost/benefit on large rocket systems have

suggested that due to the very high cost of the payloads, relatively small increases in propellant Isp brought about even by using expensive 'exotic' ingredients can reduce the system cost. Cost is strongly related to quantity produced and can frequently be reduced significantly if demand warrants investments to obtain economies of scale.

2.3 Safety

Both explosive and environmental safety issues may prevent the widespread use or even the development of an energetic material. For instance, the concern (however unfounded) about HCl emission from composite rocket motors together with concerns about plume signature for tactical missile motors has lead to a considerable effort to find alternative oxidisers to replace ammonium perchlorate [7]. Regarding material safety, the recent and growing interest in less sensitive munitions and explosives can be seen from the development of national and international insensitive munition policies [8], and additions to UN transport regulations [9]. A significant point about safety in terms of sensitivity, is that unlike performance, it is not a fundamental and unalterable property of most materials. The most insensitive materials can be made to appear relatively sensitive to some stimuli, and conversely sensitive materials can sometimes be made acceptably insensitive. An example of this being HMX, which in certain crystal forms is unusably sensitive to impact, in the normal beta form is less sensitive but still too sensitive to use by itself, and when mixed with a suitable binder is acceptable. Note that the increase of safety is not in this case related to performance [10]. The least sensitive crystal form of HMX is also the one with the highest energy density.

Discussion of compatibility and stability is often noticeably absent in papers presenting new energetic materials. Yet in the literature there are reports on several materials that have appeared very promising in early studies, but after some development have had to be dropped because of compatibility or aging problems. The classic example of this is picric acid which is a more powerful explosive than TNT and was used extensively in WWI, but is not now because of its incompatibility with acid sensitive materials (particularly in the forming of sensitive picrate salts with metals) [11]. More recently, a number of high density compounds containing 2-carbonyl-1,3-dinitramino groups were proposed as high performance explosives until studies highlighted their tendency to hydrolyse in the presence of moisture [12], [13]. One of the most promising materials for high performance low signature solid rockets is ammonium dinitramide, but after several years of research into its synthesis and performance, it has been found relatively unstable (although the reason for this is unclear as yet and it may not be an insoluble problem) [14]. Whatever its performance, it will not be widely used unless it can be used in formulations with a reasonable life expectancy.

As with sensitivity, apparent instability is not always a fundamental property of the material under study. Investigation may show that removable trace impurities may catalyse an otherwise slow decomposition. It is the impurities in low grade TNT that predispose it to decomposition and exudation [15]. In addition the development of polymer microencapsulation where reactive materials can be shielded from moisture and air may make it possible to use materials found too unstable in the past [16].

Another factor with aging and stability is the possible development of stabilisers. It is well known that nitrate ester containing materials usually require stabilisers to prevent autocatalytic decomposition that by reacting with NO_2 radicals give them adequate service lives. Similarly, many synthetic polymers require anti-oxidants.

2.4 User requirements

The conclusion from energetic material users at the NIMIC workshop was that for any material (NB this is the composition and not necessarily the individual ingredients) to be useful it must have:

a) delivered performance at least comparable to materials it might replace;
b) safety characteristics no worse than a compound such as PETN (except possibly within explosive trains of fuzing systems);
c) a reasonable shelf life in a finished article, e.g. 10 years or more.
d) a production cost not significantly greater than TATB, unless a significant cost-benefit can be

demonstrated or it is the only suitable/allowed material for an application;

e) no concerns about its effect on it's manufacturing or the global environment.

3. CODES AND METHODS AVAILABLE TO PREDICT ENERGETIC MATERIAL PROPERTIES

3.1 Performance

Unfortunately, it appears from the NIMIC workshop that the methods used by energetic materials designers in many laboratories do not predict well the attributes required of the energetic materials by their eventual users. The main codes and methods available for the calculation of performance parameters are given in table 1.

Type	Name	Function	pros	cons
Ab initio	Gaussian 8x [17]	Geometry optimisation, Hf, total electronic energy, nuclear repulsion energy, ionisation potential,etc.	No parameterisation necessary.	CPU and memory intensive
	BAC-MP4 [18]	Geometry optimisation, Hf, bond dissociation energies, etc.	Reliable Hf	Relatively little used
Semi-empirical (theory correlated with test data)	MOPAC [17]	Geometry optimisation, Hf, total electronic energy, etc.	Relatively rapid Well known	Accuracy depends on parameterisation
	Molecular Mechanics [19]	Geometry and energy optimisation, can also be used for density [20].	Rapid and simple	Requires parameterisation
	Blake [21]	Impetus or impulse, flame temperature, combustion products	Well known	Needs Hf and δ
	ICT [22]	Impetus or impulse, flame temperature, combustion products		Needs Hf and δ
	NASA-Lewis [23]	Specific impulse, flame temperature, average Mw of combustion products	Well known	Needs δ and Hf, ideal gas
	PEP [24]	Specific impulse, flame temperature, average Mw of combustion products	Simplified NASA-Lewis	Needs δ and Hf
	NOTS	Impetus or impulse, flame temperature, combustion products	PEP code adapted for guns	restricted to ideal gas
	Molpak [25]	Density		needs molecular structure
	Tiger [26]	Dv, Pcj	Well known	need Hf and δ
	ETARC [27]	Dv, Pcj, and other detonation properties		need δ and Hf
Correlations (empirical curve fits of test data)	Stine [28]	Density	Simple and rapid	
	Kamlet & Jacobs [29]	Dv, Pcj and other detonation properties	Well known	need δ and Hf
	Rothstein & Petersen [30]	Dv	needs only molecular formula	
	Stine [31]	Hf	needs only molecular formula	
	QSPR [32]	Hf		
	Stine [33]	Dv		needs Hf and δ
	Akst [34]	Cylinder test data		needs Hdet and δ

Table 1 - Methods for prediction of performance parameters of energetic molecules

Of the empirical curve fits, only Kamlet & Jacobs, and Akst, can be used to give parameters relevant to delivered energy of explosives, and none of them apply to non-ideal explosive compositions and perhaps also to the newer less sensitive compounds. The second drawback also applies to several of the semi-empirical methods. A recent example of this being the low sensitivity explosive NTO, where the delivered energy from detonation is significantly less than that predicted.

3.2 Safety

Using the safety in its broadest sense, it appears that the energetic materials designer has as yet, little assistance from predictive methods. The methods that appear in the literature for predicting some aspects of materials safety are given in table 2. However, it emerged in the NIMIC workshop that these methods

are rarely used by the majority of synthesis and formulation chemists to guide their research. This appears to be due to the fact that there is as yet no complete approach to sensitivity (to shock, impact or heat) as the causes at a molecular level are by no means fully understood [35], [36], [37], [38], [39], [40], [41], [42], [43], [44], [45], [46], [47], [48] in conjunction with the perception that all estimates of sensitivity characteristics of unknown materials tend to be unreliable when applied to unknown compounds depending as they do on the complex interplay of chemical and mechanical factors [49]. As these factors vary for every compound, it was commonly concluded that it will never be possible to find a universally reliable predictive empirical or ab initio method for solid materials. A further complication to this is the
relationship of the sensitivity of the individual ingredients of a composition to the sensitivity of the composition itself. If the sensitivity of a formulation is more dependant on the relative amounts of binder and solids and the porosity of the processed item than on the ingredients, then accurate calculations of the sensitivity of ingredients are only useful for raw material handling and not predicting usefulness.

Method	Function	Requirements	Comments
QSPR [32]	Impact sensitivity and stability used as examples	Numerous predicted or measured parameters	And empirical method for predicting any material characteristic using physical and chemical properties
Ab initio/semi empirical molecular structure (see table 1)	Bond lengths/strengths		Useful indicators, but cannot be directly correlated with any sensitivity properties
Correlation to oxygen balance (Stine) [49]	Impact, shock, critical temperature.	Oxygen balance	Cannot allow for anomalous behaviour caused by other chemical or mechanical properties
Correlation to oxygen balance (Kamlet) [50]	Impact	Oxygen balance	Cannot allow for anomalous behaviour caused by other chemical or mechanical properties
Correlation to bond length/charge distribution (Politze) [48]	Impact	Bond lengths, atomic charges	Cannot alow for anomalous behaviour caused by other chemical or mechanical properties
Statistical/neural network [51]	Impact	Numerous predicted or measured parameters	Relatively poor correlation
Electronic structure/impact sensitivity correlation [52]	Impact	Relative variation of polarity of 'trigger bond' on excitation (from MO calculations)	Takes no account of mechanical influence on sensitivity
Electronic structure/impact sensitivity correlation [53]	Impact	HOMO and LUMO energies	Only correlated for a limited number of compounds

Table 2 - Methods for predicting the sensitivity of energetic compounds

The issue of the prediction of formulation properties based on simple analysis of the gross ingredients, was a major topic of discussion in the NIMIC workshop. It is clear that it is only possible to determine from the analysis of ingredient proportions those formulation properties that depend on the thermodynamics of the mixture, i.e. performance (with only signature being the obvious exception to this rule). It was then agreed that any formulation characteristic that was determined by the mechanical properties or the chemistry of the formulation could not be predicted simply by the proportions of major ingredients, and small proportions of additives (burn rate modifiers, processing aids etc.) could have overwhelming effects on the formulation behaviour. A significant exception to this being those formulations that are almost exclusively made from one ingredient, i.e. very highly filled, pressed, PBXs. This means that it is possible to divide formulation characteristics into three categories as illustrated in table 3. Only those properties that are directly related to ingredient proportions are amenable to prediction by present capabilities in computer modelling.

Characteristics	Detonation parameters Impulse Force Signature	Safety Hazard IM	Stability Compatibility Life Burn rate
Dominant factors in determining characteristics	**Thermodynamics or products of reaction**	**Mechanical properties**	**Chemical reactivity of the formulation**
Relationship to ingredient proportions	Directly related	Some relationship	Little relationship
Effect of additives	Little effect	Significant effect	Significant effect

Table 3. Effect of ingredient and additive proportions on formulation characteristics.

In addition to the above, there appears to be no systematic methods for anticipating most of the properties required of energetic materials by the users, especially important among these being sensitivity to purely thermal threats, ESD, compatibility and stability.

4. CONCLUSIONS

From the NIMIC workshop discussions, it became apparent that the targeting of new energetic materials for synthesis and formulation is in practise largely based on extrapolation from known materials. This is acknowledged not to be ideal, resulting as history shows in far more disappointing materials being made than useful ones. However, it appears that a more successful targeting strategy for the synthesis and formulation of new materials for most applications (small, highly filled, pressed explosive charges being the main exception) will not be realised until it is possible to predict the properties (thermodynamic, chemical and mechanical) of macroscopic mixtures of binders, fillers and additives.

REFERENCES

[1] Chemistry of Energetic Materials, edited by Olah G.A. and Squire D.R., Academic Press, 1991.
[2] Wu Xiong, Sun Jian and Xiao Lianjie, Ninth Symposium (international) on Detonation, August 28, 1989, Red Lion Inn/Columbia River, Portland, Oregon, page 435.
[3] DéFourneaux, M., 'About the Misuse of Detonation Velocities for the Characterisation of High Explosives', 25th International ICT Conference on "Energetic Materials - Analysis, Characterization and Test Techniques" held at the ICT, Karlsruhe (Germany), June 28 - July 1, 1994
[4] Stine, J., Presentation at LANL/ONR workshop on energetic Materials, LANL 1993.
[5] Hordijk, A.C.; Mul, J.M., Meulenbrugge, J.J. and Korting, P.O.A.G.,'Hydrazinium Nitroformate; a 'new' solid oxidizer', PML Technical report, 1992.
[6] DéFourneaux, M. and Sanderson, A., 'A compilation of New Formulations for Insensitive Munitions' NIMIC technical report, NIMIC-MD-168-93, 1993 (NIMIC LIMITED).
[7] e.g. Bennett, R.R., '"Clean" Propellants and the Environment', AIAA/SAE/ASME/ASEE- 28th Joint Propulsion Conference and Exhibit, 6-8 July 1992, Nashville, TN.
[8] DéFourneaux, M., 'Overview of National Policies', ADPA IM Symposium, Williamsburg, June 6-9, 1994.
[9] UN Recommendations on the Transport of Dangerous Goods: series 7 Tests and Criteria.
[10] Sanderson, A., 'New Ingredients and Propellants', AIAA/SAE/ASME/ASEE- 29th Joint Propulsion Conference and Exhibit, Reno, 1994.
[11] Urbanski, T., 'Chemistry and Technology of Explosives', volume 4, Technical University Warsaw, 1985.
[12] Meyer, R., 'Explosives', WASAG-Chemie, VCH, 1993.
[13] Naixing, W., Boren, C., Yuxiang, O., 'Synthesis of N-2,4,6-Trinitrophenyl-N'-2,4-Dinitro-benzofuroxano-3,5-Dinitro-2,6-Diaminopyridine', Propellants, Explosives, Pyrotechnics 17, 265-266, (1992)
[14] Hollins, R., LANL/ONR Workshop on New Explosives and Oxidisers, June 1993.
[15] Fedoroff, B.T. and Sheffield, O.E., 'Encyclopedia of explosives and Related Items', Picatinny Arsenal, 1975.

[16] Dagley I.; Spear R.J. and Nanut V., 'High Explosive Moulding Powders from RDX and Aqueous Polyurethane Dispersions', MRL report MRL-R-1062, May 1987.
[17] Available from Quantum Chemistry Program Exchange (QCPE) at Indiana university.
[18] Melius, C.F. and Binkley, J.S., ACS Combustion Symposium, 249, p103 (1984).
[19] Berkert , U. and Allinger, N.L., 'Molecular Mechanics', ACS series no. 177, Washington DC, 1982.
[20] Delpeyroux, D.; Blaive, B.; Gallo, R.; Becuwe, A.; Piteau, M.;Jacob, G. and Gautier, J.-C., paper 74, 24TH International Annual Conference of ICT 1993; Karlsruhe.
[21] Freedman, E., ARBL-TR-2411, (1982).
[22] Volk, F. and Bartheldt, H., Propellants and Explosives, 1, pp7-14 (1976).
[23] a) Gordon, S. and Zeleznik, F., NASA TN D-1454, (1962). b) Svehl, R. and McBride, B., NASA TN D-7056 (1973)
[24] Cruise, D.R., NWC TP 6037 (1979)
[25] Ammon, H.; Du, Z. and Holden, J.R., 'Prediction of Possible Crystal Structures for C-, H-, N-, O-, and F-Containing Organic Compounds', Journal of Computational Chemistry, Vol.14, No.4, 422-437 (1993).
[26] Cowperthwaite, M. and Zwisler, W.H., Stanford Research Institute Publication No. Z106, 1973.
[27] Bugaut, F.; Bernard, S. and Chirat, R., Ninth Symposium (International) on Detonation, Volume I, August 28-September 1, 1989, Red Lion Inn, Columbia River, Portland, Oregon.
[28] Stine, J.R., 'Prediction of Crystal Densities by Group Additivity', Los Alamos technical report LA-8920, 1991.
[29] a) Kamlet, M.J.; Jacobs, S.J. and Chem, J., Phys., 48, p23 (1968). b) Kamlet, M.J. and Ablard, J.E., Chem, J., Phys., 48, p36 (1968). c) Kamlet, M.J.; Dickinson, C., and Chem, J., Phys., 48, p43 (1968). d) Kamlet, M.J; Hurwitz, H., and Chem, J., Phys., 48, p3685 (1968). e) Short, J.M.; Adolph, H.G. and Kamlet, M.J., 7th Symposium International on Detonation, p952, 1981.
[30] Rothstein, L.R. and Petersen, R., Propellants and Explosives, 4, p56 (1979).
[31] Stine, J.R. and Kramer, J.F., '26th JANNAF Combustion Meeting, held at the Jet Propulsion Laboratory, Pasadena, CA on 23-27 Oct 1989', P 53-56.
[32] Pivina, T.S.; Sukhachev, K.V. and Zefirov, N.S., Proceedings of the 5th International Conference of the 'Groupe de Travail de Pyrotechnie, p71, Jun 6, 1993.
[33] Stine, J.R., Journal of Energetic Materials, vol.8, 041-073 (1990).
[34] Akst, I.B., Ninth Symposium (International) on Detonation, Volume I, August 28-September 1, 1989, Red Lion Inn, Columbia River, Portland, Oregon., page 478.
[35] Cook, M.D. and Haskins, P.J., 'Decomposition mechanisms and chemical sensitization in nitro, nitramine and nitrate explosives' - The Ninth Symposium (international) on Detonation, August 28, 1989, Red Lion Inn/Columbia River, Portland, Oregon, page 427.
[36] Tarver, C. M.; Goodale, T. C.; Cowperthwaite, M. and Hill, M. E. - 'Structure Property correlations in primary explosives' - LLNL Report, 5 Dec 75-4 Dec 76.
[37] Melton, C. E.; Strenzwilk, D. F. and Yedinak, P. D., - 'Microscopic theory of detonation in solids', BRL technical report BRL-TN-1715, 1969.
[38] Delpuech, A.E., - 'The use of time-resolved spectrometries in the study of initiation of explosives at molecular level' - The Ninth Symposium (international) on Detonation, August 28, 1989, Red Lion Inn/Columbia River, Portland, Oregon, page 73.
[39] Chan, M.L.; Lind, C.D. and Politzer, P., - 'Shock sensitivities of energetically substituted benzofuroxans' - The Ninth Symposium (international) on Detonation, August 28, 1989, Red Lion Inn/Columbia River, Portland, Oregon, page 257.
[40] Bardo, R.D., 'The lattice density of states concept and its role in determining the shock sensitivity of PETN and nitromethane' Ninth Symposium (International) on Detonation, Volume I, August 28-September 1, 1989, Red Lion Inn, Columbia River, Portland, Oregon, p235.
[41] Storm, C.B. and Travis, J.R., 'Molecular composition, structure, and sensitivity of explosives', LANL Technical Report, 1992.
[42] Odiot, S., 'Detonation and Investigations on Microscopic Level' Soviet Journal of Chemical Physics, Vol. 12 1994, nbrs 4-5, pp 1005-1020.

[43] Odiot, S.; Blain, M.; Vauthier, E. and Fliszar, S. - 'Influence of the physical state of an explosive on its sensitivity. Is nitromethane sensitive of insensitive' -Journal of Molecular Structure (Theochem), 279 (1933) pp233-238.
[44] Brener, N. E. - Detonations of solid explosives' - Final Report, NTIS no. ADA182934, 1 Feb 85-31 Jan 87.
[45] Storm, C.B.; Stine, J.R. and Kramer, J.F. - 'Sensitivity Relationships in Energetic Materials' - LANL Technical Report, Sep 1989.
[46] Lowe-ma, C. I.,; Nissan, R. A. and Wilson, W. S., - 'The synthesis and properties of picryldinitrobenzimidazoles and the 'trigger linkage' in picryldinitrobenzotriazoles' - NSWC/CL Technical report, Jul 1989.
[47] Melius, C.F. and Binkley, J.S.T., 'Thermochemistry of the Decomposition of Nitramines in the Gas Phase', Twenty-first symposium (INternational) on Combustion/The combustion institute, 1986, pp 1953-1963.
[48] Murray, J.S.; Politzer, P., 'Computational studies of energetic nitramines', Proceedings of the NATO advanced study institute on chemistry and physicsof the molecular processes in energetic materials, 1989.
[49] Storm, C.B.; Stine , J. and Kramer, J.F., 'Sensitivity Relationships in Energetic Materials', Los Alamos Technical Report LA-UR-89-2936, 1989.
[50] Kamlet, M.J., 6th Symposium on detonation, San Diego, California (1976)
[53] Nefati, H.; Legendre, J.J.; Michot, C., Proceedings of the 5th International Conference of the Groupe de Travail de Pyrotechnie' p79, June 6, 1993.
[52] Delpuech, A.; Cherville, J. and Michaud, C., Seventh Symposium (International) on Detonation, Page 65, Jun 16, 1981
[53] Brunet, L; Lombard, J.M.; Blaise, B.; Morin-Allory, L., Proceedings of the 5th International Conference of the 'Groupe de Travail de Pyrotechnie', p 89, June 6th. 1993.

JOURNAL DE PHYSIQUE IV
Colloque C4, supplément au Journal de Physique III, Volume 5, mai 1995

The Use of Predictive Methods for the Design of New Explosive Molecules

A. Delpuech

Commissariat à l'Energie Atomique, Direction des Applications Militaires, France

This speech has two objectives :

- firstly, to show how the use of predictive methods is important during the search for new explosives,
- secondly, to illustrate with an exemple, the reliability of these methods.

Leaving aside considerations linked to the philosophy of individual organizations, the chances of a new molecule being successful involve the combination of at least two factors :

- the first is that it represents a significant advance in comparison with molecules being used at present. There is no doubt that the combination of the energy of HMX and the insensitivity of TATB makes for a major target and an ambitious objective,
- the second is that this new molecule achieves a wide field of application. This raises the factor of cost.

Thus with today's development budgets being more and more reduced, there is a clash between increasingly restrictive specifications :

- high energy performance,
- high safety (shock, heat),
- low cost.

And it is because of this that the need arises to make use of a molecular engineering process, a process based on the use of predictive methods with the double objectives of predicting, a priori and before synthesis, not only the explosive's characteristics (energy and safety), but also of evaluating development costs.

How is it possible to start "blind" on the search for a new molecule, given that the probability of obtaining a molecule which will have high energy performance (calculated as 80% of the energy of HMX) can perhaps be estimated as one chance in ten, a probability which becomes one chance in a million when the molecule has to combine the four requirements of high energy, low shock sensitivity, high thermal stability (> 300°C) and reasonable cost (< 100 $/Kg).

Another consideration must be discussed here.

The substantial advances required in comparison with molecules already in existence mean that those molecules able to respond to these ambitious objectives will belong to new families.

It is thus necessary to consider the use of new predictive methods which are not only empirical but also based on a knowledge of the relationship between the microscopic and the macroscopic. In other words, to develop a large number of tools which are at the same time theoretical or experimental, and which will allow the linking of the molecule's structural parameters with its explosive properties (energy, safety).

We have been engaged on this work at the DAM for close on twenty years. Today this allows us to synthesize new explosive molecules, designed on paper by use of predictive methods and responding to a specification which takes into account all the requirements :

- **safety requirements** : shock sensitivity and thermal stability,
- **energy performance** : detonation pressure and velocity and above all delivered energy,
- **cost**.

Predictive methods associated with each of these requirements have been developed in our laboratories, with the exception of density. Their use enables us to meet the specifications and leads to a proposed molecule.

This proposed molecule is analyzed by use of an expert system for computer-assisted synthesis. This system of course takes into account the chemical reactions involved in this type of synthesis ; above all it combines all the expertise which we have acquired in this field since we began. While the use of this tool allows the research worker to analyse the most likely synthetic paths, it more importantly reveals the difficulties associated with the project, helping to plan for them, and thus to analyze the costs.

The complete process is illustrated in fig. 1.

Before illustrating this with the results, I would like to make two comments :

- the first concerns **the difficulty, according to the property being considered, of achieving a predictive method.**

  The evaluation of this difficulty is of course totally subjective. However it results from a consideration of the efforts which we have had to make to respond to the need. It is thus that it would appear to be more difficult to achieve a predictive tool giving values for detonation velocity and pressure at the CJ point than for density. Even more effort is therefore needed to determine the power supplied by the explosive as a function of time and expansion volume. These two properties relating to safety are in themselves much the most difficult to forecast.

- the second statement concerns **the reliability of these methods**. I am not going to detail here the methods which we use. At the reliability level, I would say that paradoxically, it is the density which poses us the most problems (in particular in the case of new molecules which do not belong to the traditional families). Since we know that this value is fundamental to a determination of the energy properties, this is a real problem.

  In other cases the reliability is good. But this is wholly due to the fact that the methods which we use rely on the study of the true electronic or atomic structure of the molecules and make use of experiments in fundamental physics. It is completely different when we restrict ourselves to the use of empirical methods which indicate the changes in a property in terms of one parameter. Based on the results obtained for a large number of products, these empirical methods are not of any help in predicting the behaviour of a "truly" new product. It seems to me that an important point must be made here. It concerns the difficulty which still remains of evaluating not only the value of the power supplied by the explosive, but the way in which this power is supplied in time (an indispensable parameter for the optimization of the use of an explosive in terms of the munition volume).

Let us return **to one illustration of this step**, by the presentation of the first molecule to be developed with the aid of this process.

This molecule had to respond to three objectives :

- a thermal stability requirement (decomposition temperature > 300°C),
- a shock sensitivity requirement (H50% (5 kg) > 60 cm),
- an energy requirement : energy gain/TATB = 20%.

While the double requirement energy-sensitivity is high, it is the thermal stability requirement which enormously increases the difficulty.

The design of the molecule made use of two molecular engineering steps :

First step : demonstration by quantum chemistry studies of the role played by the ANT unit in the insensitivity. Role confirmed by ultra-fast Raman spectrometry. Thermochemical study of this unit in addition permitted an estimation of its good energetic properties. On the other hand the thermostability of the compound was of the order of 240°C.

Second step : grafting of this type of structure onto thermostable rings. The number of grafted ANT (1, 2 or 3) and the nature of the thermostable ring being optimized with respect to the energy properties.

The DANTNP molecule was constructed in this way. The molecule has been synthesized. An explosive composition of 97% DANTNP and 98% of the theoretical density has been developed.

The objective, the predicted values and the experimental results are shown in fig. 2.

This molecule has of course limitations in application, chiefly its cost and the fact that its energy is delivered very progressively (from which arises the necessity of using large volumes). Its production nevertheless gives a perfect illustration of the contribution of predictive methods in such research.

The value of this contribution becomes even more telling when the changes which can be made to this molecule are considered in terms of different objectives, for example reduction of cost or optimization of the compromise between the different properties sought (sensitivity, thermostability and energy).

Much of the journey remains to be made.

But I firmly believe that only the use of reliable predicative methods will allow the constructive exploration of all four requirements and will enable us to find solutions as a function of the required specifications. Otherwise we shall be continuing to search for molecules "by going fishing". In that case we shall be spending a lot of money for very few results, apart from temporary and short-lived successes. I call temporary success the discovery of a molecule having one or at best two properties and which is then forgotten in a drawer after an ephemeral glory related to an abbreviated presentation of its properties.

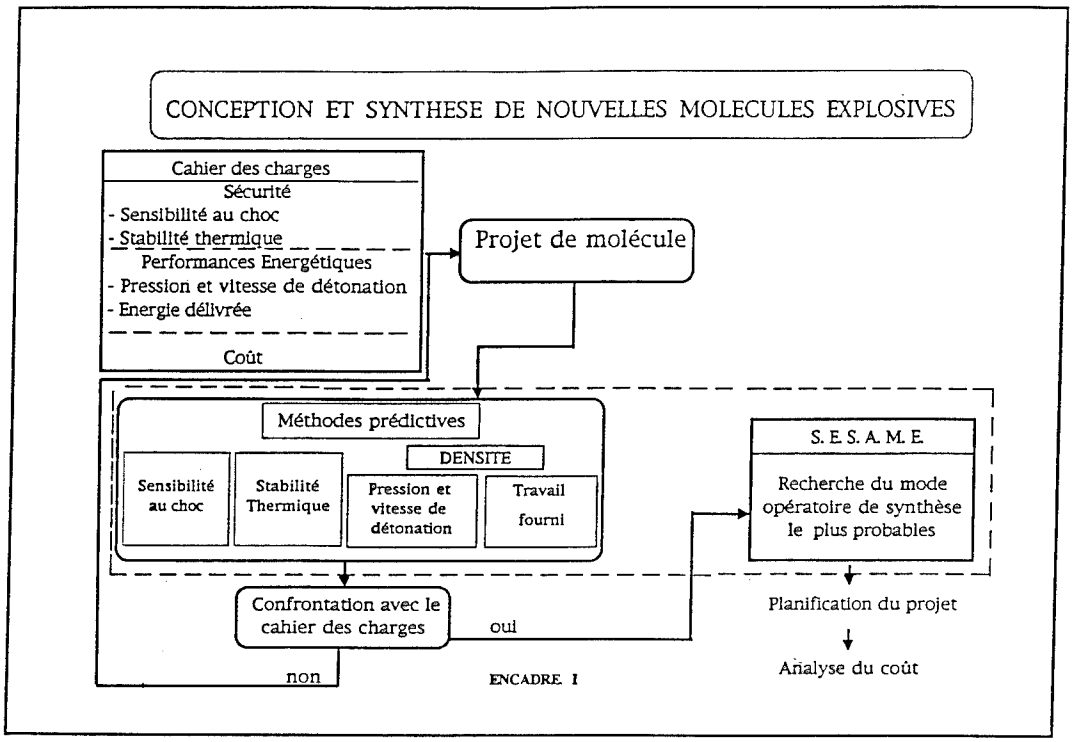

ENCADRE I

DANTNP

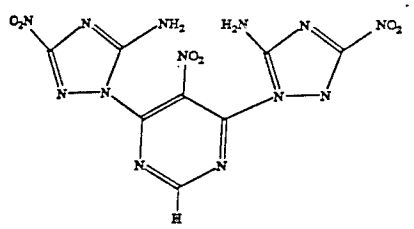

	Objective	Predictive
Shock sensitivity (5 kg) - cm	> 60	60 - 70
Thermal stability	> 300	> 300
P_{CJ} (kbar)	> 330	330
Density		1,85
Detonation velocity (m/s)		8 100 - 8 200
W/W_{TATB}	+ 20 %	+ 18 %

Experimental results

Density (XR)	1,865	Decomposition T° (DSC)	350°C
Detonation velocity	8 200 m/s	Deflagration T°	338°C
P_{CJ}	327 Kbar	Shock sensitivity (powder)	70 cm
W/W_{TATB}	+ 15 %	Friction sensitivity	> 36 kgf

- Fig. 2 -

3 DISCUSSION

Moderator : Malcolm Cook Fort Halstead

Questions - Answers, Comments

Questions-answers, Comments

Dick-Sanderson :

Q : Isn't the reason there are so few explosives in use, a matter of cost (raw materials and synthetic route) ?

A : History has never shown cost to stop the development of an energetic material. In addition it is cost - benefit, not cost per se that is important.

In any case, cost is difficult to predict, as the cost of an explosive charge is very weakly related to the cost of the new materials used in the preparations of the ingredients.

Simonetti-Sanderson *comment* : I don't agree with you when you say that theoretical chemistry is of little help in synthesis of new explosives.

I think that theoretical chemistry helps us to understand at a molecular level, the elementary processes (the excited electronic states, bond breakings ...) that occur during the macroscopic behaviour (shock sensitivity, energetic properties, ...).

And this understanding is necessary to improve our knowledge of explosives. We need both theoretical chemistry and experimental techniques.

A : Whether we like it or not, most synthesis chemists are not using predictions of new compounds properties based on ab initio or semi empirical chemical methods.

This appears to be largely due to the difficulty of relating theoretical chemical calculations to composite explosive systems.

Odiot *comment* : I agree with Philippe Simonetti. There are two engineering ways for trying to predict detonation properties of energetic materials : macroscopic approach - hydrodynamic codes with specific well defined and fitted thermodynamic parameters on one hand, microscopic approach through correlation codes between macroscopic properties and calculated molecular parameters on the other hand. The last one works for predicting relative values of sensitivity inside a same series of energetic compounds, if one chooses an appropriate calculated parameter of the molecule in an excited electronic state. Thus, this correlation code is very useful in practice. Moreover, this result has been important for helping to understand the mechanism of detonation. If it could not be used as a proof that the sensitivity mechanism is governed by this molecular parameter, it means however that among all the conditions, microscopic and macroscopic, which may affect the relative sensitivity test results, the molecule plays a leading role in this phenomenon which should involve a preliminar electronic molecular excitation.

Kondrikov : You have very interesting results of the relative sensitivity of NT1 and NT2 you had mentioned about the correlation in New Hampshire.

Tell us, please, here about the results. They are really very unusual.

Odiot *How is detonation ability of an energetic material affected by electronic structure changes of the molecule, of the molecular chemical bond ?*

At the microscopic level, it is well established that the molecule - its electronic structure and the shape of its chemical bonds energy potentials - confers its detonic nature to the material.

By quantum mechanical calculations* on two nitro triazole compounds, mono and dinitro, we predict opposite nitration effects on shock sensitivity and on thermostability. (Fig.1)

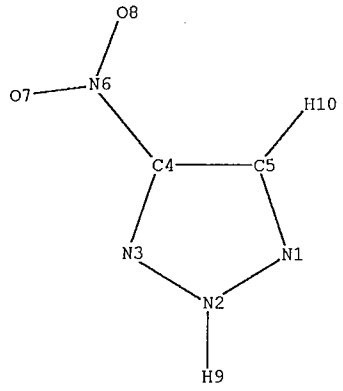

4-nitro-2H-1,2,3-triazole
(NT1).

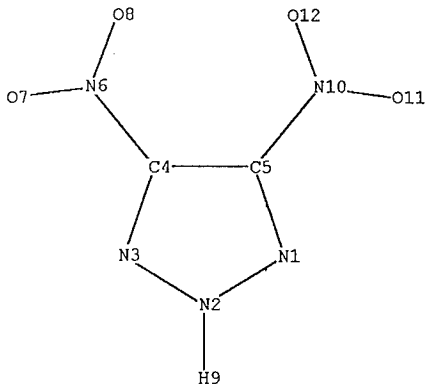

4,5-dinitro-2H-1,2,3-triazole
(NT2)

Fig.1

1- If shock implies in these compounds a molecular electronic excitation, the mononitro compound would be the most shock sensitive, according to results obtained by the Delpuech's sensitivity scale(1) : shock-sensitivity versus chemical-bond polarity in an excited electronic state.
Nitration decreases the sensitivity in this case.

2 - Nitration increases gas-phase formation enthalpy. $\delta\Delta H = 90 kcal.mole^{-1}$ (estimated value in solid phase $\delta\Delta H = 100 kcal/mole$). Calculations have been performed in the frame of modified Xα method(2).The dinitro compound would be more energetic than the mononitro compound and Gamézo estimates, by Kondrikov's and Sumin's code(3), an important increasing detonation velocity - 1500m/s - for the dinitrotriazole, for an assumed density of $1.6 g/cm^3$.

In conclusion for these compounds, nitration increases the explosive performance, the dinitrocompound being the most energetic and the least sensitive. Excellent explosive.

3- But, according to chemical bond strength or chemical bond dissociation energy calculations(4) on the two triazoles in their electronic ground state, the dinitro would be, by far, the least

thermostable. Indeed, its C-N bond dissociation energy decreases by 9kcal/mole together with a weakening of its N-N bonds, thus reducing the thermostability. A hazardous criterion against the dinitro compound.

In conclusion, dinitro triazole compound is not a "kind" explosive.

Let us recall our recent results on nitromethane, gazeous and solid states(5), where we have calculated an increasing of the C-N bond strength of 4.5 kcal/mole in the solid phase relative to the gas phase that conforts the bimolecular mechanism proposed by Bardo to interpret the Piermarini experiments on static high pressure effect on nitromethane.

Who can do experiments to study the relative thermostability and shock sensitivity of these two triazoles, in order to confirm or not the role of the molecular electronic states, ground state and excited state respectively involved in the mechanisms of these two processes ?

*"Theoretical Analysis of the Effects of Nitration on the Explosive Properties of Triazoles : 4-nitro-2H-1,2,3-triazole and 4,5-dinitro-2H-1,2,3-triazole", V.N.Gamezo, S.Odiot, M.Blain, S.Fliszar, A.Delpuech. Theochem, accepted June 1994

(1) A.Delpuech, Thesis, Bordeaux I no. 656 (1980) ; J. Phys., Coll.C4, "Microscopic and macroscopic approaches to detonations" S.Odiot (Ed.), **48**, 353 (1987).

(2) E.Vauthier, M.Blain, S.Odiot and V.Barone, M.Comeau, S.Fliszar; "Xa Local spin density calculations", accepted, Theochem

(3) B.N.Kondrikov, A.I.Sumin, "Selected topics of chemical physics. Calculation of equilibrium processes at high temperature and pressure", B.N.Kondrikov (Ed.), Mendeleev institute of chemical technology, Moscow, 1984.

(4) S.Fliszar, "On the dissociation of chemical bonds" in S.N.Bulusu (Ed.), "Chemistry and Physics of energetic materials", NATO ASI Series, **309**, 143 (1990), Kluwer, Dordech, NL.

(5) S.Odiot, M.Blain, E.Vauthier, S.Fliszar, Theochem **279**, 233, (1993).

Dufort, Nelson-Odiot

Q : Why such a large effect in your two formation enthalpies ?

A : Yes, the calculation shows a very large difference between the formation enthalpy values for these two compounds. A difference is expected, of course, for two reasons. 1) the two molecules differ by one NO_2 group and 2) the two molecules differ by their geometry, the mononitrocompound is planar and the two nitro groups in the second one are twisted out of plane (30°) ; this non planar geometry induces an increasing of the formation enthalpy. But why is it so large ? I don't know.

1) Formation enthalpy $\Delta H_f(T)$ for a molecule in gas phase at T° is correlated to atomization energy ΔE_a by thermodynamic relation :

(1) $\Delta H_f(T) = \Sigma_i n_i (\Delta H_{f(atome\ i)} - 5/2\ RT) + ZPE + E(T)_{vib.}^{mol.} + 4RT - \Delta E_a$

n_i : number of atoms of species i in the molecule

$\Delta H_{f(atome\ i)}$: standard formation enthalpy of atom i (298,15°K)

$\Delta H_{f(atome\ i)}$ kcal/mole = 52.09 for H, 170.89 for C, 113.0 for N, 59.54 for 0.

$ZPE + E(T)_{vib.}^{mol.} + 4RT$ takes account of molecular vibrational, translational and rotational energies at temperature T.

$ZPE = 1/2\Sigma_m h\nu_m$ (Zero Point Energy at 0°K),

$E(T)_{vib.}^{mol.}$: thermal vibrational energy = $N \Sigma_m h\nu_m \exp(-h\nu_m/kT)/(1- \exp(-h\nu_m/kT)$

ν_m : frequency modes of the molecule

ΔE_a : vibrationless atomization molecular energy at 0°K

(2) $\Delta E_a = \Sigma_i n_i E_i - E^{mol}$, E_i: energy of the atom i, E^{mol} : energy of the molecule is the key for calculating $\Delta H_f(T)$.

When one compares (1) for two compounds which like in this study, between NT_2 and NT_1 differ by one H less and one N and two O more, the differences between the two NT_2 and NT_1 terms involved first in $\Sigma_i n_i(\Delta H_{f(atomei)} - 5/2\ RT)$ and second in ΔE_a are respectvely high and opposite i.e. + 177 and - 89 kcal/mole. The first one can be easely predicted, the second one which is a difference between two global molecular energies need to be calculated and we cannot give any a priori estimated value. The difference between the two third terms, $ZPE + E(T)_{vib.}^{mol.} + 4RT$, is small in this case: 2 kcal/mole, it cannot be estimated without knowing experimental or theoretical frequencies.

2) The accuracy of our $X\alpha$ ΔE_a calculations depends strongly on the choice of the molecular α parameter involved in the method. It means that we have to choose the best one. How to do it ? According to Fliszar, first, this molecular parameter is calculated with all the atomic α_i which gives the exact energy of the type of isolated atom i, constituent of the molecule. (i : H, C, N, O, F). We call this α, α_o. However, when i belongs to a molecule, its atomic structure is changed, and its α_i in the molecule cannot be the same. Thus we have to add to α_i of the isolated atom a correction parameter $\Delta\alpha_i$ which will depend on the atomic environment (including hybridization state of the neighbouring atoms) of the atom i inside the molecule. These $\Delta\alpha_i$ have been fitted on about 100 compounds, with all possible environments, found in such HCNO compounds, to obtain the best

molecular α parameter for calculating formation enthalpies (statistical errors less than 4-5 Kcal/mole). Now we are able to calculate a priori new compounds, e.g. calculations of formation enthalpy of ONTA and ANTA in gas phase reproduce some experimental results, but you know that experiments give different values for these two compounds ! We tried to do the best at the lowest cost. However, even if we introduce a systematic error in our two present calculations, I think that the two values will differ stongly. I am waiting for the experimental results.

Nelson : Do you have a physical, qualitative rationalization for why the heats of formation of NT1 and NT2 might be so different ? For example, can you understand why electron withdraw by the second NO_2 group should weaken other bonds in the molecule ?

A : your two questions are different because heat of formation is a molecular property which cannot be resolved in terms of bonds energy.

1 - In a series of nitrocompounds, I tried to correlate heat of formation experimental and theoretical values with NO_2 additional groups in different molecular sites, without any success. No correlation. My answer to a qualitative rationalization is no.

2 - It is easy through theory of dissociation energy bond calculations. A variation of neat charge - 1me - on C and on N, for instance, changes dissociation energy by 1kcal/mole. Thus, with charge calculation results, one analyzes second NO_2 group effect on the other bonds of the molecule.

Shackelford-Odiot

Q : Concerning your result that the NT2 molecule is less sensitive than the NT1 molecule, perhaps one explanation would involve resonance if two conditions exist. Firstly, the NT1 and NT2 molecules would need to be in a planar conformation during their excited state ; and secondly, the unpaired electrons on the central nitrogen atom would need to be aligned properly with the pi bonded electrons found in the two C-N double bonds in this planar conformation. If both these conditions would exist, then the rings of the two molecules would taken on some degree of delocalized aromatic character. One nitro group like that present in NT1 would cause some delocalization in the NT1 ring. With two nitro groups in the NT2 ring, the second electron-withdrawing group would effect some additional delocalization in the NT2 molecule. Since the NT2 molecule would have a higher delocalization energy than the NT1 molecule, the NT2 molecule would be more stable. Did the sensitivity calculations used in your study consider this possibility of delocalization ? There could certainly be other factors involved, but this might be one possibility to account for the sensitivity difference between NT1 and NT2.

A : 1 - We know by geometry optimization calculations of these two compounds that in the ground state the nitro group and NT1 ring are coplanar and that the nitrogroups are twisted out of the ring plane in NT2. Thus in the groundstate, energy calculations of NT2/NT1 take account of delocalization effect which is a balance between two opposite effects : an additional effect of energy

delocalization due to the addition of a nitro group and a reduced one due to the twisting of the nitro groups. Even, if from this point of view NT2 would be more stable on the whole than NT1, it does not mean at all that NT2 would be less sensitive than NT1. Shock sensitivity to detonation is another problem.

2 - We used these two ground state geometries to calculate the excited electronic state polarities according to Delpuech's shock sensitivity-polarities correlation code. It is a strong approximation. However, we have to recall that Delpuech's code has been built in the frame of a semi-empirical quantum chemistry method (CNDO/S) for calculating the molecular electronic states with CNDO/S parameters fitted on UV spectra and that this method adopts the same geometry for all excited states. This method works well for relative sensitivity predictions inside a series of compounds and we have also to adopt the ground state geometry.

VII THE FUTURE OF NUMERICAL SIMULATIONS OF THE DETONATION BY MOLECULAR DYNAMICS

Chairman : Peter Haskins DRA Fort Halstead

Molecular Dynamics Studies of Initiation in Energetic Materials; P.J. Haskins

Molecular Dynamics Analysis of an Energetic System under Thermal and Shock Sollicitations ; Laurent Soulard

The limits of Molecular Dynamics Applied to Condensed-Phase Energetic Materials ; **Elaine Oran** and **Jay Boris**

JOURNAL DE PHYSIQUE IV
Colloque C4, supplément au Journal de Physique III, Volume 5, mai 1995

Molecular Dynamics Studies of Initiation in Energetic Materials

P.J. Haskins

Defence Research Agency, Fort Halstead, Sevenoaks, Kent, U.K.

ABSTRACT

In this paper an overview of Molecular Dynamics simulations of chemically reacting systems is described. In particular, molecular dynamics simulations of shock initiation in a model energetic material are reported. The use of Molecular Dynamics to model thermal initiation and determine reactions rates in energetic materials is also discussed. Finally, the future potential of MD techniques for energetic materials applications is considered.

1. INTRODUCTION

Molecular Dynamics (MD) is the term used to describe the solution of the classical equations of motion (Newton's equations) for a set of molecules. A typical simulation is composed of hundreds, even thousands of atoms. Molecular Dynamics has been used successfully to study the properties of liquids, small rigid molecules, and even large molecules such as proteins. However, it is only very recently that this technique has been applied to the study of energetic materials[1,2,3,4]. A major break-through has been the development of complex inter-atomic potentials such as the Abell-Tersoff potential, which allow chemical reactions to occur through incorporation of a many-body term. This has allowed the study of model reactive systems. Indeed, MD studies offer the prospect of a greatly improved understanding of the coupling between the shock physics and the chemistry of energetic materials.

2. RESULTS AND DISCUSSION

Molecular Dynamics studies at Fort Halstead have involved development of the in-house code DYNAMITE, incorporating a many-body empirical potential, and subsequent use of the code to study detonation phenomena. In particular, the initiation, growth and steady state detonation characteristics have been quantified for a model system. The influence of exothermicity, activation barriers, and inital shock conditions have all been addressed. The work reported in this paper concerns both thermal and shock initiation in a homogeneous system of diatomic molecules. Both 2D and 3D versions of the code have been employed which incorporate the empirical Abell-Tersoff potential. This potential is basically a pair potential and is the sum of a repulsive term, a bonding term, and a non-bonding term. The many-body characteristics of the potential arise through the bonding and non-bonding terms being dependent on third body interactions.

The MD simulations were set up as either regular 2D or 3D (alpha FCC) lattices of heteronuclear diatomic molecules at zero pressure. The atomic mass of nitrogen (14 amu) was used for the atoms in the model. Two sets of binding energies were used in a series of simulations. In one set of simulations a binding energy of 5eV was used for the products A-A and B-B while 2eV was used for the unreacted material. In a further set of simulations, 4eV was used for the products and 1eV for the reactant. The MD code DYNAMITE was written in Fortran 77 and includes periodic boundary conditions, in all dimensions for the thermal initiation studies, but not on the x-axis (shock direction) for shock studies. The code can be run on the DRA Cray or Silicon Graphics computers. Typical run times are a few hours on the Cray YMP for simulations of about 10ps and a few thousand atoms.

The particular aims of the work reported here were to demonstrate that the model system gives chemically reasonable thermal reactions kinetics, and a shock initiation response curve of the correct form for a homogeneous explosive. Considering the thermal initiation studies first, both 2D and 3D simulations were carried out on a square/cubic box of molecules at various inital temperatures. This model was used to study the reaction processes occurring, the times to reaction, and to obtain the specific heats (Cv). The specific heats (Cv) showed a slight increase with increasing temperature. At the highest temperatures (ca. 1500^{o}K) which could be studied (before reaction) the model gave: Cv = 1.28R (0.18 cal/g) for the 2D model, and Cv = 1.69R (0.24 cal/g) for the 3D version. A wide variety of reactions have been observed. The most common are:

$$2AB \text{ ----> } A_2 + B_2, \quad 2AB \text{ ----> } A_2 + 2B, \quad B + AB \text{ ----> } B_2 + A$$

Back reactions and concerted triatomic processes have also been observed. Reaction times have been shown to be very similar in both the 2D and 3D version of the model over a range of temperatures. One feature that is worth noting is that classic "induction time" behaviour is observed at the lower temperatures.

In shock initiation simulations, the initial shocks were introduced by impact of a flyer composed of the same molcules as the acceptor lattice. For the shock initiation studies we have examined the influence of the pulse duration, which is determined by the flyer plate thickness, and the effect of the activation barrier on the threshold pulse amplitudes (flyer velocities) required to achieve "detonation". From these studies it is possible to make some general comments on the properties of the model. Firstly, provided the initial stimulus is sufficient a steady-state chemically sustained shock (detonation) is achieved. This travels at ca. 6 km/s with the parameters used, and is independent of the initial shock. Secondly, detonation results in almost complete conversion of the initial heteronuclear molecules to the more stable homonuclear species.

Initiation in homogeneous explosives is experimentally, observed to show a weak dependence on pulse duration except, for very short high-energy pulses, but to require a minimum particle velocity. For homogeneous systems, it has been widely demonstrated that initiation can be described by use of Thermal Explosion Theory. We have carried out MD calculations to see if our model system is consistent with this behaviour. The essential concept of Thermal Explosion Theory is that after the initial shock heating there is an induction time before significant chemical reaction. Provided the pulse duration is long enough to ensure that no rarefaction cools the material before the induction period is complete, then initiation is assumed to occur. It should be noted that the theory is not strictly valid for very strong shocks since some reaction occurs without an induction period and the hydrodynamics and the chemistry cannot be de-coupled. However, it is still very instructive to base an approximate criterion on the time required to obtain a significant degree (eg. 90%) of reaction. For the 2D simulations five thicknesses of flyer plates ranging between 5 and 37.5 A^{o} were employed. In addition two A-B well depths were considered namely, 2eV and 1eV. For each potential the particle velocity - shock velocity relationship (Hugoniot) was determined. Threshold initiation velocities were ascertained for each flyer thickness and the Hugoniot used to plot the results as threshold energies versus pulse duration. The results of this study showed that the threshold curves had the correct form with a strong dependence on pulse duration for short pulses and weak dependence for longer pulses. Reasonable fits to the MD results were obtained with a simple thermal explosion model based on a single-step exothermic Arrhenius reaction. The threshold condition for the thermal explosion model was taken to be 90% reaction. The Arrhenius parameters needed to provide the fits were shown to be chemically sensible, with the activation energies amounting to about 75% of the unimolecular bond strengths. The model with an A-B well depth of 1eV was fitted with an activation energy of half that of the model with a 2eV well depth, and the same pre-exponential factor. The simulations were repeated with the 3D code using a similar arrangement of molecules. A total of six flyer thicknesses were examined, but only one potential (with an A-B well depth of 2eV) was employed. The results from the 3D simulations were

plotted as threshold energies against pulse duration as for the 2D results. As might be expected, very similar results were obtained to the 2D calculations. Despite the Hugoniot and specific heat being significantly different from the 2D model (as expected), the Arrenhius parameters needed to provide a thermal explosion fit were very similar.

In general, the results obtained with both the 2D and 3D versions of the model gave good agreement with thermal explosion theory. This is despite the fact that the predictions made with thermal explosion theory were strictly outside it's range of validity. Furthermore, an arbitary 90% reaction criterion and single step decomposition scheme were used. Since it is known that there are a number of key reactions this is clearly a gross simplification, and a two step model would be expected to give a much improved fit. It should be noted though, that the agreement between the classical thermal explosion model and the MD results strongly suggests that the MD model supports a classical thermal explosion model for shock initiation. Comparison with 'real' systems can be made by extrapolating the thermal explosion fit to a 2mm thick flyer plate. When this is done a threshold velocity of 2.1 km/s is obtained (for the potential with an A-B well depth of 2eV). This is not an unrealistic value for a real homogeneous explosive. As would be expected for a homogeneous system the Walker-Wasley critical energy (P^2t) criterion does not provide a good fit to the initiation threshold curve. It is interesting to note however, that it does give an approximate fit to the shorter duration pulse results.

3. FUTURE WORK

Looking towards the future, it is hoped that MD studies might be able to address heterogeneous explosives where hotspots are important. For these types of explosives it would be interesting to extend MD studies to lattices with defects. However, the problem of treating realistic hot spot dimensions (ca. 10^{-7} - 10^{-5} m) needs to be resolved before this is achieveable. It should be noted that some apparently heterogeous explosives, for example TATB, appear to have a significant homogeneous behaviour.

Future work will investigate the possibility of including more realistic ab-initio potentials. Ab-initio potentials could be obtained by inclusion of either a Molecular Orbital (MO) or Density Functional (DF) code within the MD code. This could then be used to generate ab-initio potentials directly for all short range interactions and an empirical potential could be used for long-range forces. However, the problems of incorporating either an MO or DF code directly into a MD code are non-trivial. It is hoped that the thermal explosion model might be extended to incorporate a coupled Arrhenius kinetic scheme which could be compared to the MD results. Finally, the ultimate aim of the work is to employ a kinetic model, derived from the MD work, directly into a hydrocode in order to simulate longer time (microsecond) and larger scale behaviour.

4. REFERENCES

[1] P J Haskins and M D Cook, "Molecular Dynamics Studies of Shock Initiation in a model Energetic Material" in Proceedings of the APS Topical Conference on Shock Compression of Condensed Matter, North Holland, 1994, pp 1341-1344.

[2] D W Brenner, M L Elert and C T White, "Incorporation of Reactive Dynamics in Simulations of Chemically-Sustained Shock Waves" in Proceedings of the APS Topical Conference on Shock Compression of Condensed Matter, North Holland, 1989, pp 263-266.

[3] D W Brenner, "Molecular Potentials for Simulationg Shock-Induced Chemistry" in Proceedings of the APS Topical Conference on Shock Compression of Condensed Matter, North Holland, 1991, pp 115-121.

[4] D H Robertson, D W Brenner, M L Elert and C T White "Simulations of Chemically-Sustained Shock Fronts in a Model Energetic Material" in Proceedings of the APS Topical Conference on Shock Compression of Condensed Matter, North Holland, 1991, pp 123-126

JOURNAL DE PHYSIQUE IV
Colloque C4, supplément au Journal de Physique III, Volume 5, mai 1995

Molecular Dynamics Analysis of an Energetic System under Thermal and Shock Sollicitations

L. Soulard

CEV-M, BP. 7, 77181 Courtry, France

We present in this paper molecular dynamics calculations concerning the decomposition of a simple system $A_2 \rightarrow 2A$ under thermal and shock sollicitations. For thermal decomposition, numerical results are consistent with the molecular collision theory. Arrhenius parameters are calculated. For shock decomposition, several regimes of propagation are observed depending upon the initial shock intensity. Analysis of chemical decomposition shows that kinetic parameters are strongly different from thermal decomposition.

I - INTRODUCTION.

The chemical process of decomposition in a reactive shock wave is far from being understood. Because both time and space scales of this phenomenon are very small, experiments must be performed at molecular level with a very high spatial and time resolution. Experiments are then extremely difficult to perform and interpret. Actually, molecular dynamics is the only one technique to provide information on atomic motions in a very small region during a very short time and some promising results are already published (ref. /1/-/6/ for example). In this paper we present first results using molecular dynamics obtained in our laboratory concerning energetic material in homogeneous phase.

The aim of this work is a numerical analysis by molecular dynamics of decomposition of a simple system : $A_2 \rightarrow 2A$ under static (thermal) and dynamic conditions (shock). In the first part, we describe the potential function of the system. In the second part, thermal decomposition is analysed for several initial temperatures. Results are interpreted with the classical molecular collision theory. In part III, decomposition under shock is studied for three shock intensities. As in the second part, kinetic parameters are estimated. Finally, results of thermal and shock decompositions are compared.

II - POTENTIAL FUNCTIONS.

By hypothesis, the potential function depends only upon interatomic distance r_{ij} between atomes i and j. It is consist of two empirical functions ε_1 and ε_2. The ε_1 function is a predissociative potential and describes interaction of atomes in a A_2 molecule, that is $r_{ij}<r_d$, where r_d is the dissociation length. For all other cases, we use the repulsive ε_2 function.

$$\varepsilon_1(r) = \sum_{k=0}^{4} a_k \left(\frac{r_{ij}}{r_0}\right)^{k-n} \qquad r_{ij} \le r_d$$

$$\varepsilon_2(r) = \frac{\alpha}{\left(\frac{r_{ij}}{r_0}\right)^{\gamma}} + \beta, \qquad r_{ij} \le r_d$$

$$\varepsilon_2(r_{ij}) = \varepsilon_1(r_{ij}), \qquad r_{ij} \ge r_d$$

Parameters a_k, α, β and γ are calculated with the following conditions : $\varepsilon_1(r_{eq}) = \varepsilon_0$, $\varepsilon_1'(r_{eq}) = 0$, $\varepsilon_1(r_{act}) = e_{act}$, $\varepsilon_1'(r_{act}) = 0$, $\varepsilon_1(r_d) = 0$, $\varepsilon_2(r_d) = \varepsilon_1(r_d)$, $\varepsilon'_2(r_d) = \varepsilon'_1(r_d)$, $\varepsilon''_2(r_d) = \varepsilon''_1(r_d)$. r_{eq} is equilibrium distance of the A_2 molecule, r_{act} is the position of activation barrier. The parameters used in this work correspond to $r_0=1.10^{-10}$m, $r_{eq}=1.52\ 10^{-10}$m, $r_0=1.710^{-10}$m, $e_{act}=2.73\ 10^{-19}$J and $\varepsilon_0=2.5\ 10^{-19}$J (figure 1). Note that because ε_2 is a repulsive function, any stable intermolecular regular structure exists at thermal equilibrium.

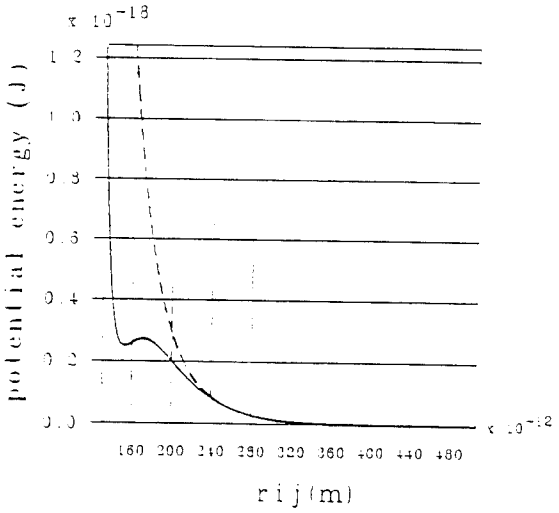

Fig. 1. Potential functions ε_1(—) and ε_2 (---) used in this work.

III - THERMAL DECOMPOSITION.

The overall system is composed of 8×8×8 centred cubic unit cells (2048 atoms) with periodic boundaries on each face. Initial velocities are inferred from a Maxwell-Boltzmann distribution corresponding to a T_i temperature. Then, the evolution of the system is free and calculations are performed until all A_2 molecules are broken. Decomposition fractions are illustrated on figure 2 for five temperatures T_i.

Comparison between the numerical particle velocity distribution and Maxwell Boltzmann distribution calculated from average kinetic energy shows that thermodynamic equilibrium exists at any time; thus thermodynamic parameters are calculated with the usual statistical physics formulation. For example, temperature evolution is shown on figure 3.

Decomposition fraction versus time can be explained with the molecular collision theory. In this topic, two limit cases exist :

- for high temperatures, the decomposition mechanism is of first order : $A_2 \rightarrow 2A$.

- for lower temperatures, the decomposition mechanism is of second order : $2A_2 \rightarrow 2A+A_2$ or $A_2+A \rightarrow 3A$.

The Arrhénius constant k is given by :

$$k(T(t)) = z\sqrt{T(t)}\, exp\left(-\frac{e'_{act}}{k_b T(t)}\right)$$

where e'_{act} is an activation energy, z the frequency factor, T the temperature and k_b the Boltzmann's constant (noting that T is a function of time t). Numerical resolution of differential equations corresponding to different mechanisms shows that decomposition is of first order for the two higher initial temperatures (2121K and 1806K), and second order for the lower temperature (1023K). In the intermediate case, beginning of decomposition is of second order and of first order at the end of reaction. Calculated values of e'_{act} and z (table 1) are pratically identical for all T_i ; this result confirms the choice of theoretical model to describe the numerical results on thermal decomposition.

Table 1. Kinetic parameters deduced from numerical calculations and molecular theory collision.

T_i(K)	e'_{act}(J)	$z(s^{-1}K^{-1/2})$
2121	$8\ 10^{-20}$	$3\ 10^{10}$
1806	$8\ 10^{-20}$	$3\ 10^{10}$
1508	$8\ 10^{-20}$	$2{,}6\ 10^{10}$
1274	$7{,}98\ 10^{-20}$	$3{,}5\ 10^{10}$
1023	$8{,}77\ 10^{-20}$	$3{,}96\ 10^{10}$

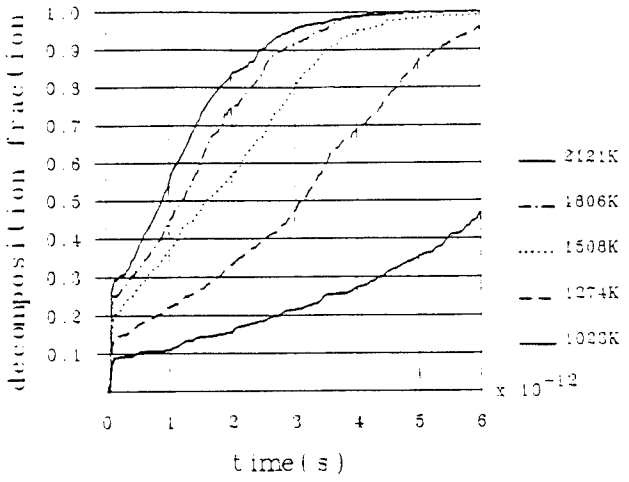

Fig. 2. Decomposition fraction for various initial temperatures.

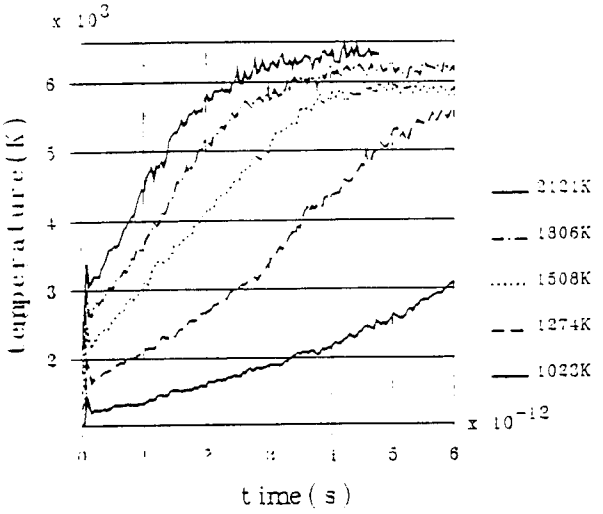

Fig.3. Temperature of system during decomposition.

IV - SHOCK DECOMPOSITION.

The system is made up by 60 unit cells in the x direction, and of 3 unit cells in the y and z directions (2160 atomes). The two faces perpendicular to the x-axis are mirrors, the other faces are periodic. After thermalisation, all particles move at time t_0 in the x direction with a velocity u_0. So, a wave P is generalited in the opposite direction. Three values of u_0 are used : 500m/s, 1500m/s and 2500m/s. The initial temperature is 251K.

For the lower u_0 (500m/s), any decomposition is observed during the calculation. The wave velocity is constant (1463m/s). For u_0=2500m/s, decomposition occurs just on the compression front (figure 4). The wave velocity is constant (5115m/s). The last case (u_0=1500m/s) is more complicated. We observe two regimes : the first one, between t_0 and 4.10^{-12}s, corresponds to a wave velocity of 3097m/s. Reaction of decomposition occurs behind the compressive zone (figure 5). The wave P is thus an inert wave followed by a reactive wave. In the second regime, between $6\ 10^{-12}$s and the end of calculation, the compression zone is overtaken by

reaction zone and, as in the u_0=2500m/s case, decomposition occurs on the compression front (figure 6). The wave velocity is 4479 m/s.

Behind the wave P, the thermodynamic equilibrium is rapidly achieved. Comparison between thermodynamic state behind P deduced from the wave velocity, the particle velocity and Hugoniot

relations and thermodynamic state deduced from statistical physics shows that P is a steady shock wave for u_0=500m/s and u_0=2500m/s (table 2 and 3) . Shock wave is inert in the first case, and reactive in the second one. For u_0=1500m/s, the wave P is not a steady shock wave, because the reaction zone is (relatively) large and unstable in time.

Table 2. Average values for pressure P, density ρ, internal energy e and temperature T behind shock front deduced from statistical physics analysis.

u_0 (m/s)	$\langle P \rangle$(Pa)	$\langle \rho \rangle$(kg/m^3)	$\langle e \rangle$(J/kg)	$\langle T \rangle$(K)
500	8,191 10^8	1275	2,793 10^6	438
2500	1,101 10^{10}	1651	5,788 10^6	8669

Table 3. Pressure P_c, density ρ_c and internal energy e_c calculated from shock and particle velocities and Hugoniot relations.

u_0 (m/s)	P_c(Pa)	ρ_c(kg/m^3)	e_c(J/kg)
500	7,78 10^8	1305	2,800 10^6
2500	1,113 10^{10}	1680	5,824 10^6

The decomposition under shock is a first order mechanism described in part III of this paper, because temperature behind the shock front is high. Kinetic parameters are not the same for the two cases (table 4). Increasing of e'_{act} is probably due to the growth of density with u_0. Similarly, z must theoretically increase with temperature and density, and thus with u_0.

Table 4. Kinetic parameters for shock decomposition.

u_0(m/s)	e'_{act} (J)	z($s^{-1}K^{-1/2}$)
1500m/s	1,78 10^{-19}	1,9 10^{11}
2500m/s	1,85 10^{-18}	1,7 10^{17}

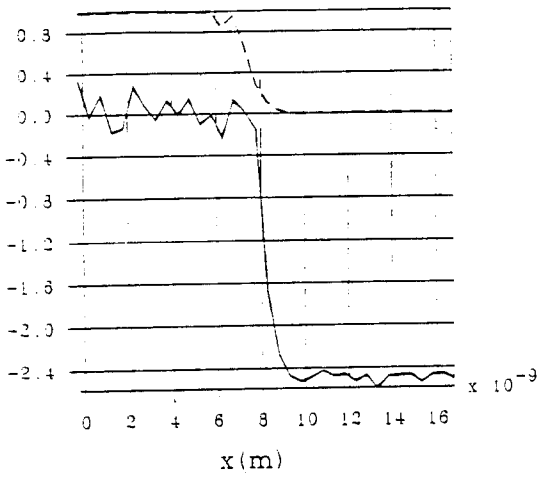

Fig.4. Average x component particle velocity (——) and fraction decomposition (---) for u_0=2500m/s and t=4.430 10^{-12}s. Velocities are divided by 1000.

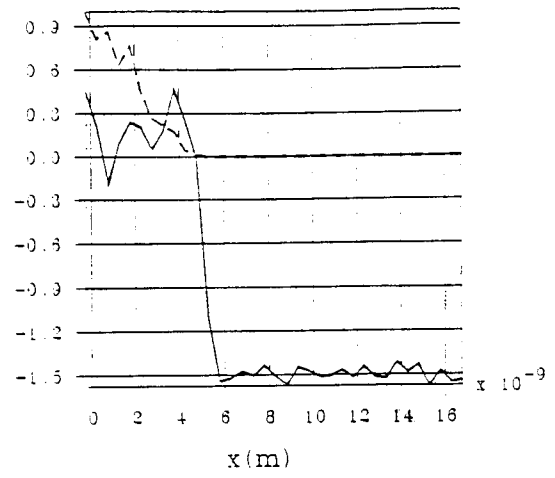

Fig.5. Average x component particle velocity (——) and fraction decomposition (---) for u_0=1500m/s and t=4.430 10^{-12}s. Velocities are divided by 1000.

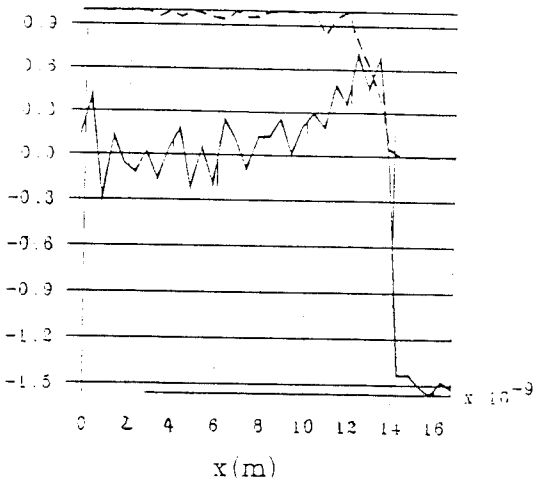

Fig. 6. Average x component particle velocity (——) and fraction decomposition (---) for u_0=1500m/s and t=7.833 10^{-12}s. Velocities are divided by 1000.

V - DISCUSSION.

Two main results of this work concern firstly the structure of the reactive shock wave, and secondly the decomposition kinetic under static and dynamic sollicitations. In homogeneous explosives shocked by a projectile, it is currently admitted that decomposition reactions begin at interface explosive/projectile with a significative delay. The reaction zone overtakes the inert shock wave propagating in explosive at rest. Thus, during a short time, the system is composed of explosive at rest, explosive shocked but not decomposed and a reaction zone behind the inert shock front. This structure is the same as the one observed in our molecular dynamics calculations.

Second point concerns the kinetic parameters for static and dynamic decompositions. Experimental works on PETN single crystal and liquid nitromethane /7-9/ (that are homogeneous explosives) exhibit a strong decay of z and e'_{act} for shock decomposition versus thermal decomposition. Morever, theoretical calculations show that activation energy of nitrogen monoxyde is significantly lowered by intermolecular interaction. Our calculations do not reproduce these results because the potential function used here is too simple. Effect of molecular surrounding on energy activation cannot be taken into account with only a two particles pontential function. Implementation in our code of more realistic potential functions is thus our first aim.

REFERENCES

1. Tai-Guang Wei and Robert E. Wyatt, J. Phys. : Condens. Matter, 2, 9787 (1990).

2. Arnold M. Karo and John R. Hardy, International Journal of Quantum Chemistry, XII, 333 (1977).

3. F.E. Walker, A. M. Karo and J.R. Hardy, The Seventh Symposium (International) on Detonation, 716 (1981).

4. D.H. Robertson, D.W. Brenner and C.T. White, Phys; Rev. Lett., 67(2), 3132 (1991).

5. V. Yu Klimenko and A. N. Dremin, Sov. Phys. Dokl., 25(4), 288 (1980).

6. D.H. Tsai and S.F. Trevino, J. Chem. Phys., 81(12), 5636 (1984).

7. A.J.B. Robertson, J. Soc. Chem. Ind., 67, 221 (1948).

8. J.J. Dick, Shock Waves in Condensed Matter, 545 (1985). NSRDS-NBS21 (U.S. Government Printing Office, Wash., D.C., 1970).

9. R.D. Bardo, The Seventh Symposium (International) on Detonation, 93 (1981).

JOURNAL DE PHYSIQUE IV
Colloque C4, supplément au Journal de Physique III, Volume 5, mai 1995

The Limits of Molecular Dynamics Applied to Condensed-Phase Energetic Materials

E.S. Oran and J.P. Boris

Laboratory for Computational Physics, Naval Research Laboratory, Washington, DC 20376, U.S.A.

The limitations of various methods for computing manybody dynamics are summarized briefly in terms of the physical limits of the specific theory and generally of what can reasonably be computed. This information is then used to assess the current computational limit on using molecular dynamics to describe shocks and detonations in condensed phase energetic materials. This question is addressed by defining the computational requirements of a molecular dynamics simulation of a detonation propagating in an idealized nitromethane crystal lattice. The major questions addressed are: *What is required to compute the properties of the system to obtain reasonable mesoscopic data?* and *What is the size of the system we can now compute, using one of the largest computers available?* From this analysis, we discuss several directions in which future research in this field may proceed.

1. INTRODUCTION

In a manybody-dynamics calculation, a large number of individual particles represent entities such as atoms, molecules, droplets, clusters, stars, or galaxies. These particles move according to prescribed equations of motion and interact according to specified force laws. In principle, the equations of motion can have any form. They could, for example, be classical, quantum mechanical, or relativistic. In the same sense, the interactions among the particles could be, for example, hard-sphere, two-body, manybody, gravitational, or electromagnetic. Once the particles and their interactions are defined, the system is allowed to evolve according to these laws. Applications of manybody dynamics have ranged from studies of phase transitions in liquids and solids, dynamics of large molecules, materials processing in dense systems, and galaxies forming from star clusters.

Several aspects of molecular dynamics are important for making decisions about how and and under what conditions the method can be applied. Molecular dynamics is deterministic, in contrast to any form of Monte Carlo method, in which some elements of a statistical nature are introduced. Molecular dynamics is computer intensive. Computing the behavior of real physical systems, with realistic sizes and interaction, requires a great deal of computer time and memory. Molecular dynamics requires attention to selecting the best algorithms for tracking and evaluating the interactions among large number of particles. Major decisions in setting up the physics

in molecular-dynamics simulations involve defining the nature of the interacting particles and their interactions, given the current knowledge of the interaction and the computational resources available. Usually tradeoffs between accuracy, computational efficiency, and realistic physical complexity must be made to obtain any reasonable results.

The objective of this paper is to clarify the limits, both physical and computational, of using molecular dynamics to describe shocks and detonations in condensed phase energetic materials. This perspective should help determine which directions might profitably be followed in the near future. To help understand these limits, it is first necessary to evaluate the inherent limits of various approaches and therefore how molecular dynamics fits into the scheme of theories for solving manybody interactions. Since molecular dynamics relies on the availability of computational power, we consider what computers can now accomplish, and what they are likely to achieve in the near future. Finally, we use this information to evaluate what can be done in the study of ignition and propagation of shock and detonation waves in energetic materials.

2. APPROACHES TO SOLVING MANYBODY INTERACTIONS

Table 1 shows the heirarchy of mathematical models used to describe the behavior of systems involving many particles and interactions. Molecular dynamics is the most fundamental level of this heirarchy, and the interactions may be as basic as Newton's Law. Both Monte Carlo approaches and the Boltzmann equation are derived from the Liouville equation. At the level where particles can be considered a continuum fluid, the Navier-Stokes equations are generally used.

Some of the information in Table 1 is recast into quantitative form in Figure 1, which shows the physical regimes of validity of the methods (modified from Bird [1]). The regimes of validity are expressed as a function of a characteristic distance in the system L, and the mean molecular spacing, δ. For a fixed molecular diameter, d, as the mean spacing between molecules decreases, the density increases. This is shown on the horizontal axis. The figure shows limits of the Navier-Stokes, DSMC, and molecular dynamics models, methods that can, in principle, be used to describe real physical systems.

Table 1. Levels of Models of Manybody Interactions

Equation	Solution Method
Newton's Laws $f = ma$	Molecular Dynamics
Liouville Equation $F(\mathbf{x}_i, \mathbf{v}_i, t), \quad i = 1, N_p$	Monte Carlo Methods Direct Simulation Monte Carlo
Boltzmann Equation $F(\mathbf{x}, \mathbf{v}, t)$ binary collisions (low density) good for gases	Direct Solution
Navier-Stokes Equation $\rho(\mathbf{x}, t), \quad \mathbf{u}(\mathbf{x}, t)$ short mean free path (small Kn)	Direct Solution: Finite Differences, Finite Volumes, Spectral Methods ...

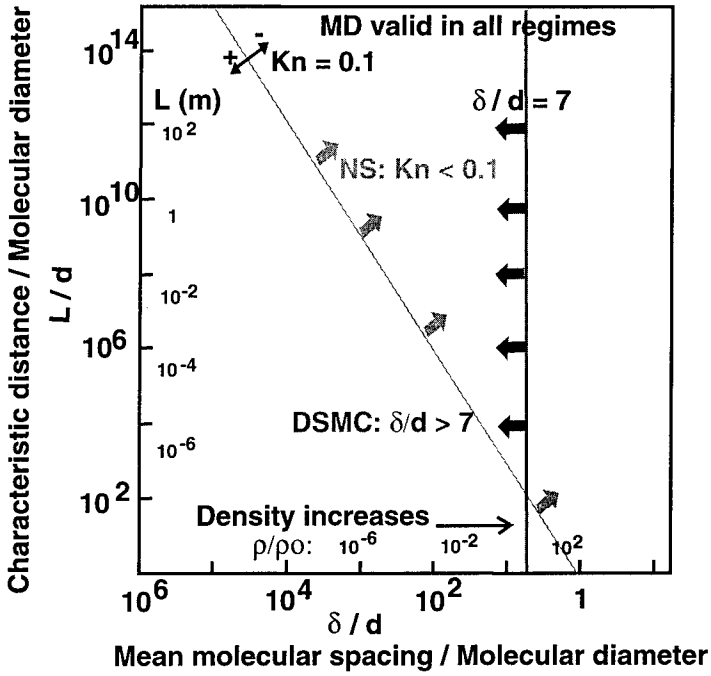

Figure 1. Regimes of validity of molecular dynamics, Direct Simulation Monte Carlo, and Navier Stokes, as a function of the characteristic length scale and mean molecular spacing of a system.

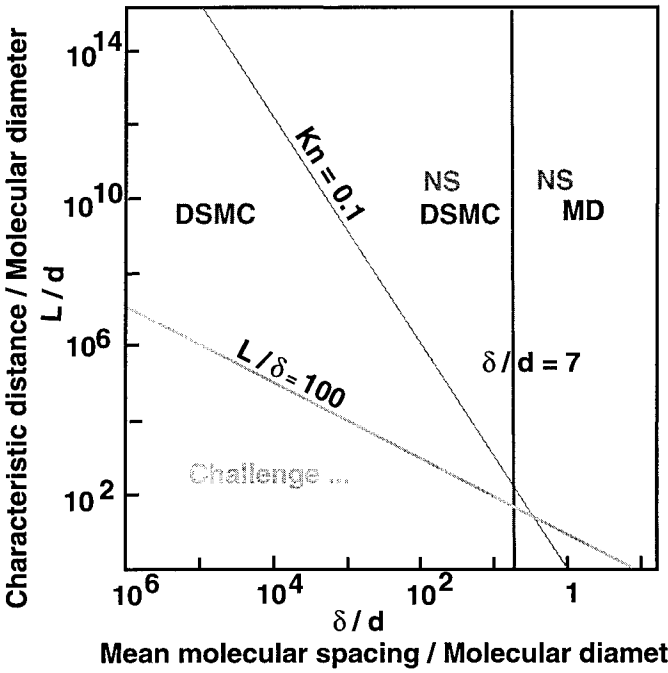

Figure 2. Regimes where various methods can be used, given current computers.

The Navier-Stokes equations are generally applicable when the system behaves as a continuum fluid. This is the case when the Knudsen number, the ratio of the molecular mean free path to a characteristic system length, is small,

$$K_n \equiv \lambda/L < 0.1 \ .$$

The Navier-Stokes equations could be modified to describe flows at higher Knudsen numbers, but to do this it is necessary to reformulate the expressions for heat and mass diffusion. Efforts to do this have been successful in slightly extending the range of validity. Efforts to use continuum approximations for higher Kundsen number situations involve solving equation sets that are mathematically of higher order than the Navier-Stokes equations. Examples of these include the Burnett equations and various moment methods, which are computationally more expensive, more difficult to implement, and less well calibrated than the Navier-Stokes equations.

When the ratio of the mean molecular spacing, δ, to the molecular diameter, d, is large, so that $\delta/d >> 1$, the Direct Simulation Monte Carlo method can be used. It is reasonable to take $\delta/d > 7$ [1]. The DSMC method is statistically based, and generally applied to high-Knudsen-number flows. It has been used extensively for atmospheric reentry problems, where the gas is very dilute, and now it is being used for denser flows in microchannels. The method is based on the same basic approximations from which the Boltzmann equation is derived, but its regime of validity also extends to systems where three-body collisions can occur. Because of the different criteria for validity of Navier-Stokes and DSMC, there is a range in which both methods can be used. Both methods are valid in the triangular domain of Figure 1 where $\delta/d > 7$ but $Kn < 0.1$.

Molecular dynamics is valid throughout the entire range of parameters. This is because it is based on the most fundamental set of equations. There are no *physical* reasons why it cannot be used for all ranges of densities and system sizes.

3. THE COMPUTATIONAL LIMITS

The boundary lines between various methods shown in Figure 1 are based on very general physical principles, unrelated to either the limitations of input data or computational capability. Figure 2 is an attempt to further put limits on the applicability of a method by looking at the computational limits.

Navier-Stokes methods are valid for low Knudsen numbers at high enough densities. When the Knudsen number is close to 0.1, correction terms are necessary. The DSMC methods can be used for high Knudsen number fluids, and again it is still possible to use them for the regimes of overlap with Navier-Stokes, where $K_n < 0.1$ and $\delta/d > 7$, but here the computations become quite expensive.

Molecular dynamics, however, becomes expensive for low density problems. For this method to be useful, we need to compute long enough for the system to evolve on the macroscopic time and space scales while using a specified microscopic particle interaction law. The computational timestep, however, is limited by the timescale of the interaction potential and the method of solution. If the particles are too far apart, it could take thousands or even millions of timesteps to simulate a few collisions. The expense becomes exorbitant. Thus molecular dynamics can be too expensive for dilute systems. This prohibition also extends to very large systems and systems that evolve slowly.

The regime of parameter space in which $L/\delta < 100$ is one in which there are few particles per volume element, and therefore few collisions. When this is the case, there are large fluctuations in the calculations of the mean properties of the system, such as density, pressure, and temperature. A DSMC calculation would require many ensembles to get good statistics. A molecular dynamics calculation would produce large spatial fluctuations in mean quantities. A Navier-Stokes computation would not necessarily show these physically realistic fluctuations, which would have to be

added by other theories. One extreme is the free-molecule limit, where a collisionless Boltzmann equation applies.

4. MOLECULAR DYNAMICS AND THE STUDY OF ENERGETIC MATERIALS

Substantial efforts have gone into using molecular dynamics to study the behavior of shocks and detonations in condensed phase energetic materials. The pioneering work of Karo and Walker [2], Odiot et al. [3-5], and Tsai and Trevino [6] inspired the later work by authors such as Lambrakos et al. [7], White and Brennan [8], and Phillips et al. [9]. All of these molecular dynamics computations used model systems that attempted to incorporate some of the important characteristics of condensed phase energetic materials. In some cases, the systems were treated as two dimensional. Simplified force laws are used, and complex energetic molecules are generally approximated by combining a number of atoms into a smaller number of macroparticles.

These idealized and scaled studies have produced a number of interesting results. The simulations showed that an ordered lattice structure, as in a solid, or a group of more-randomly-oriented dense particles, as in a liquid, can sustain a wave that behaves like a shock wave. Further, if there is energy added close behind the shock wave, the result is a propagating wave structure that looks like a detonation. As in the continuum representation of a detonation, the energy addition contributes to the molecular motion and drives the shock even faster. These results answered some of the first questions about molecular dynamics that were asked by the detonation-physics community: Could a system of particles, interacting in prescribed ways, mimic the understood behavior of a detonation? Once this was shown, it was then possible to ask questions such as how does a supersonic wave pass through a lattice, and what does it do to the lattice as it propagates? Is there a minimum ignition energy required to initiate a detonation? How can you ignite a detonation? What are the differences between a detonation propagating in a lattice and in a liquid? What are the differences between one-dimensional, two-dimensional, and three-dimensional representations of a system? What are the effects of vacancies and mass defects? All of these and other questions have been addressed. Taken together, the simulations performed to answer these questions have given a basic understanding of how a lattice reacts as it is perturbed by highly nonlinear forces and interactions.

5. THE LIMITS OF THESE STUDIES

In the computations discussed above, the system parameters had to be scaled to carry out the simulations. With the resources available, we could not consider simulating detonation ignition or propagation in systems with realistic values of the system size, L, and rates of energy release. To decrease the size of the system and have a viable simulation, the rates at which chemical reactions occur and energy is released must be increased. These types of scaled, approximate models have been used for decades in plasma simulations where much work has been done for proton to electron mass ratios much smaller than the correct value of 1836. This scaling is done with the hope that the same types of effects that occur in actual systems can be studied on a smaller, faster scale. Experimental studies have shown that the sizes and times of the actual effects simulated are orders of magnitude larger than the ones simulated. In such small systems, we can see some of the basic features of wave propagation, but we cannot simultaneously resolve the macroscale processes that we know are important. For example, we can only barely begin to see the effects of coherent waves structures and grain interactions. The question we ask is whether molecular dynamics can be used to compute the kinds of properties of energetic materials that can be compared directly to experimental results? Will we always be confined to "model" systems and scaled parameters?

Consider the more specific question: *How much computational power is needed to model a microscopic system with enough particles to constitute a sample large enough to see macroscopic*

effects? For example, with the largest new computers, we can consider simulating the behavior of a billion individual particles and simultaneously computing their interactions at rates of tens of gigaflops. (One gigaflop is a billion floating point operations per second.) Would a billion particles be enough?

To help address this question, we focus on a specific type of computation that has been optimized on the largest computers: a model system of a nitromethane crystal. The system could also be a liquid, and the same estimates would hold.) We also consider a detonation propagation problem. An ignition problem would require simulating a much larger systems for longer physical times. We assume that the bulk of the energy is released from a shocked element of nitromethane in 5 μm, an estimate that is perhaps too small by a factor of five. An earlier Navier-Stokes computations, describing detonation cells in liquid nitromethane, showed that the detonation cell height is 50 μm, and so the detonation cell length is less than 100 μm.

Therefore, a minimum macroscopic scale (a mesoscale), is at least a couple of detonation cell lengths long, and at least one cell high. The detonation would have to travel further than this in the calculation, but this can be achieved numerically by adding unreacted material ahead of the detonation, and subtracting it from the back. To look at macroscopic phenomena, however, at least one or two cell lengths should be retained in the computer at any on time. Thus our assumption here is that we need to simulate a system that is 100 μm $\times$ 50 μm in two dimensions, and 100 μm $\times$ 50 μm $\times$ 50 μm in three dimensions. We also assume that the detonation travels at about 5000 m/s. Therefore, for the detonation to propagate 100 μm requires that we simulate 2×10^{-8} s of physical time. For a typical computational time step of 10^{-13} s (perhaps too long for realistic simulations), we need to be able to compute 2×10^5 time steps for the detonation to propagate approximately one detonation cell length. A usual computation would require computing for a number of cell lengths, say four or five, or about 10^6 timesteps.

Let us consider the simplest model, the C-N model, in which the C represents CH_3, and the N represents NO_2 [4,7]. The initial shock can create conditions in which the system is electronically excited, and the C-N bond can break. After it has broken, other reactions take place which eventually lead to the formation of final products and energy release. This second process is modeled by a time delay to energy release after the C-N breakup. This extremely simple model contains the essence of what is needed to generate a reaction wave in a system. If the energy release occurs close enough behind the leading shock, it can couple to it dynamically and evolve into a detonation. If the energy release it too slow, a slower deflagration or flame may arise.

Molecular dynamics studies have shown that each pair of C-N's are separated by about 5 A. In two-dimensional studies, the C-N's can form a minimum-energy lattice by aligning with all of the C-N's point in the same direction. In three-dimensions, there are two minimum energy states. In the lowest, the unit cell is 10 A, and the C-N's are aligned in opposite directions every 5 A. In the metastable state, the unit cell is about approximately 5 A, and the C-N's are aligned. We also assume that the relatively simple form of a potential, such as the predissociative potentials [4], are used in the hypothetical calculation.

Recent computations have shown that there are substantial differences between the results of two- and three-dimensional computations [9]. The additional degrees of freedom in three dimensions means that the system can equilibrate more quickly than it would in two dimensions, and so the time scales change. Therefore, anomalous effects occur in simulations in two dimensions, and these effects disappear in three dimensions. For example, in two dimensions, there is a sharp transition from an initial detonation state that depends on initial input energy to one that correspond to the Chapman-Jouguet state. Computations in three dimensions go smoothly to this final state. Our conclusion is that to obtain quantitatively valid simulations involving flows of material in transition, it is necessary to perform three-dimensional calculations. For these particular systems, simulating three-dimensional situations using molecular dynamics may be more important than it

is using a fluid dynamics approach. In fluid dynamics, the equations of state already includes the microscopic effects of three dimensions, even in two-dimensional simulations.

Combining this information about the model lattice and what constitutes a minimum system size to obtain a meaningful mesoscopic simulation, allows us to compute the number for particles that must be included in such a simulation. The result is that a two-dimensional simulation needs at least 4×10^{11} particles, and a three-dimensional simulation should have at least 8×10^{16} particles. This is considerably larger than the billion particles that we can now contemplate simulating and the 600 million particles treated in some simulations to date. These estimates are summarized in Table 2.

For a two-dimensional molecular dynamics simulation using the model given in Table 2, we need approximately 10 arrays. For a three-dimensional calculation, we need to store approximately 12 arrays. These numbers are not exact, because it is often possible to trade off memory storage for computer time. Some variables, that for convenience could be stored in computer memory, can be recomputed from other stored variables. Also, depending on whether the computation is done in single or double precision, approximately 40-80 bytes of storage per particle is required in two dimensions and 50-100 bytes/particle in three dimensions. The result is that 8 terabytes of memory are needed for a two-dimensional calculation, and 4 million terabytes for a three-dimensional computation.

At this point there is a natural question to ask: *What we can simulate now?* First, consider what is actually available in terms of computer resources. These estimates are for the CM-5E at NRL, a massively parallel supercomputer on which most of our molecular dynamics codes are optimized. The CM has 32 Gbytes of memory. Therefore, we definitely do not have the computational memory available to carry out even the 4×10^{11} particle simulation. The CM can reach a theoretical speed of 40 Gflops, and practical programs can achieve about 8 Gflops. This is painfully inadequate. The computation of one time step requires about 500 operations/particle/timestep in two dimensions, and 1000 operations/particle/timestep in three dimensions. Therefore, at a speed of 8 Gflops, one time step of a two-dimensional calculation would take 7 hours to compute, and one timestep of a three-dimensional calculation would take 300 years! We are hardly able to compute for one time step, let alone the 10^5 or 10^6 timesteps it would take for the detonation to propagate a cell length.

Table 2. Summary of Physical Model and Computational Requirements

Physical Model	Modified C-N predissociative model for crystal nitromethane. Intramolecular spacing 5 A. Detonation speed 5000 m/s.		
Minimum Macroscopic Scale			
	2D	100 x 50 μm^2	
	3D	100 x 50 x 50 μm^3	
Number of Simulated Particles			
	2D	4×10^{11}	
	3D	8×10^{16}	
Computational Storage Requirements:			
	2D	40-80 bytes/particle	Total 8 Tbytes
	3D	50-100 bytes/particle	Total 4×10^6 Tbytes

What is close to computable is a system that is 0.2 μm $\times$ 0.2 μm $\times$ 0.4 μm, which, for this physical model, would require 1.6×10^7 particles, or perhaps 0.5 μm $\times$ 0.5 μm $\times$ 1.0 μm, which would require 2.5×10^8 particles. This is about the limit that will fit into a full 32 Gbytes. This larger system would require integrating 2.0×10^{-10} s of physical time for a detonation cell length of 1 μm, which is about 1000 time steps. For 2.5×10^8 particles, and 1000 operations/timestep/particle, a computation requires 2.5×10^{11} operations/timestep. At 8 MFlops, this means that a timestep takes about 40 seconds. Computing the time it takes a detonation to travel 1 μm then requires 40,000 seconds, which is about 11 hours. The problem, then, is finding a realistic physical system with such small detonation cells. This, in turn, means very fast energy release.

Table 3. Current Modeling Limitations

Computer:	CM-5E, 32 Gbytes, 8 Gflops
Physical-System Size:	$0.5 \times 0.5 \times 1.0$ μm^3 (Detonation cell length, 1.0 μm)
Number of Particles:	2.5×10^8
Computational Timestep:	40 s/timestep
Computational Time:	11 hours per detonation cell length

6. CONCLUSIONS

The conclusion from the arguments given above is that even using the classical, model interaction potentials, we cannot easily or directly use molecular dynamics methods to simulate a detonation in nitromethane on current computers for realistic macroscopic sizes and times. Even with a teraflop computer and 100 Gbytes of memory, we could obtain at most a factor of 25 in speed, and a factor of three in particle number over what is now possible. Current rates of improvement in computers indicate that there is about a factor of two increase in speed every two years. Assuming that accessable memory is not a problem, in 10 to 15 years we could perform the computation in a reasonable amount of computer time. We have not yet begun to address the problem of how to deal with the memory and corresponding bandwith problems. These might be answered in 25–30 years. This general conclusion lead to three observations about the applicability of molecular dynamics to energetic materials research.

First, we can continue to do as we have: model scaled systems that represent faster conversion of reactants to products and faster energy release than is correct for actual physical systems. This allows us to examine the qualitative features of interactions potentials, energy transfer, crystal structure, and wave initiation and propagation. This generic approach has been successful for other methods in the past. For example, in the 1960's when the DSMC method was first developed, there were no computers large enough to compute the behavior with realistic scales of physical input data. Today, thirty years later, actual computations are possible and these are regularly compared to experiments. DSMC has entered a stage where it is a practical, useful computational tool for both basic and applied research. This might be the case in 30 years for molecular dynamics of energetic materials.

Second, we could try to find some systems for which direct simulation is possible and meaningful, for which experiments can be done. This would mean working with an explosive with a very fast energy release. Experiments on such a system may not be possible, and if they were, would be very unsafe because the material would be dangerously unstable. The very factors that would make the physical system computable today make it dangerous.

There is a final conclusion that has to be considered very seriously. That is to consider mesoscopic scale particle dynamics in which a particle now represents a cluster of say, C-N's, in a particular configuration. Particles could, for example, represent pieces of crystals that are on the scale of microns. Then we would not be attempting to represent the microscopic scale deterministically from first principles, as we are doing now with molecular dynamics. Instead, we would be attempting to describe a mesoscopic structure. This is a more phenomenological approach that could bridge the current gap between microscopic information and macroscopic behavior. A current argument in favor of this approach is that we do not even properly represent the microscopic behavior in our molecular dynamics computations now. The potentials are not quite correct: we are not quite correctly representing a crystal lattice, and we do not include the full chemical reactions. In some ways, our input data is as crude as the crudest Navier-Stokes computation of a detonation.

In summary, we believe that application of molecular dynamics to simulate the behavior of energetic crystals is truly a grand challenge in computing. We do not believe that we can perform viable direct simulations of such systems, given current computers, for the next 25-30 years. Many of the Grand Challenge problems that have driven the development of modern computing capabilities were in the same situation 20 years ago, and it is that international challenge that has brought us where we are today.

ACKNOWLEDGMENTS

This work is based on observations made during the authors' many years of working with Simone Odiot, who has inspired and guided our research on energetic materials. The authors would like to acknowledge the many helpful conversations with Choong Oh, on the validity of various theoretical approaches to manybody problems, Kay Howell on projections of the future of computational resources, and Robert Sinkovits on the limits of our current computations. This work has been funded by the Office of Naval Research, the Naval Research Laboratory, and the Advanced Research Projects Agency.

REFERENCES

[1] Bird G.A., Molecular gas dynamics and the direct simulation of gas flows (Clarendon Press, Oxford, 1994).
[2] Karo A.M., Walker F.E., DeBoni T.M., and Hardy J.R., *Prof. Aero. Astro* **94** (1983) 405–415.
[3] Peyrard M., Odiot S., and Lavenir E., *C.R. Acad. Sci.* **299**, Śŕie II, 917 (1984).
[4] Peyrard M., Odiot S., Lavenir E., and Schnur J.M., *J. Appl. Phys.* **57**, 2626 (1985).
[5] Peyrard M., Odiot S., Oran E., Boris J., and Schnur J., *Phys. Rev. B* **33** (1986) 2350–2363.
[6] Tsai D.H. and Trevino S.F., *J. Chem. Phys.* **81** (1984) 5636–5637.
[7] Lambrakos S.G., Peyrard M., Oran E.S., and Boris J.P., *Phys. Rev. B* **39** (1989) 993–1005.
[8] Elert M.L., Deaven D.M., Brenner D.W., and White C.T., *Phys. Rev. B* **39** (1989) 1453–1456.
[9] Phillips L., *J. Phys.: Cond. Matter* 5, 473–6376 (1993).

Discussion

Questions - Answers, Comments

Odiot - Oran *Comment*

Input data - intramolecular and intermolecular excited electronic potentials, have to be given at the same level of accuracy than your calculation possibilities to simulate a realistic phenomenon which may involve electronic excitation, as you want. Till now one mixes intramolecular potentials of excited electronic state with intermolecular potentials of the ground state, each one as accurate as possible ! It is wrong, but you cannot do anything else, today.

Progress in intermolecular data and chemistry in excited states are definitly needed to be coherent and realist.

Oran - Clavin

Q : Why are you so interested in so small time scale as 10^{-10} second when you deal with 10^{-6} second as characteristic reaction time for exothermic reaction ? Why don't you put all this short time inside the leading shock structure ?

A : I thought that initial effects of shock on lattice structure might influence the subsequent chemical reactions, i.e. provide different initial conditions for subsequent chemistry, that occurs at longer timescales.

Kondrikov - Boris :

Q : In june, in New Hampton, I asked to Dr Haskins about the possible reasons of separation of the products of detonation at the Molecular Dynamic Calculations. Now I see the same phenomenon at decomposition of nitromethane. It is a very important effect, at first, relatively the F.Ree suggestion at forming of two-phase liquid at detonation of explosives, the model which this morning reported in a poster session a very nice girl (Marie Turkel). On the other hand the effect is connected with the mechanism of chemical reaction of nitromethane in presence of catalysts, which are usually heavy molecules of amines or acids, and probably form the more heavy complexes with nitromethane. If, say, heavy molecules push out of the group were light ones, it can lead to formation of "the clusters" the dimension of which is sufficient for ignition and the quick burning of the mass of nitromethane. The gas bubbles formed can give the system which will be able to DDT and so on. Thank you.

A : The apparent separation of the "nitro" and the "methane" groups you refered to in my viewgraph is caused by the periodic boundary conditions and the regular (diagonal) placement of the particles. As we plotted the graphs when one species goes out the top it gets moved to the bottom. The effect we see is certainly mostly an optical illusion.

Boileau - Oran :

Q : Àre you able to calculate the liquid nitromethane detonation propagation velocity with following assumptions :

- molecules are moving, rotating, etc
- the propagation is only possible in some geometric spatial respective positions (solid angle) and stopped in other directions target : verify why the difference of detonation velocity in liquid and solid states is about 600m/s, that was observed with some high explosives.

A : We have, in fact, carried out some molecular dynamics calculations of shock-initiation of detonations in liquid nitromethane. These used the same pre-dissociative potential we have used for the solid. We have some preliminary values of the detonation velocity, which seems lower than the solid-detonation velocity. But before anything conclusive can be said, we need to check the results much more carefully. We should have a "prediction" in a few months time.

Jones - Boris :

Q : Why aren't cellular automata useful for studying detonation in condensed phase explosives at the mesoscopic level ?

A : Cellular automata require a set of simple (i.e. logical - not algebraic) rules to define the behaviour of the system. They rely on statistical behavior of the set of automata to give the same global behavior as the "real" system. For detonations 1) we do not know the "rules" (cellular automata will be no help in uncovering them), 2) we already have a global / macroscopic model that works well.

When we understand the microscopic details of molecular configuration sensitivity, defects, grain boundaries, phonon up pumping, etc - we will already have solved the problem with suitable input for the existing macroscopic models.

Melius - Oran :

Q : You have presented an excellent overview of the capabilities as well as limitations of molecular dynamics as an approach to study shock detonation. I would like to see a discussion on what experiments on explosives can be performed which can better couple with the MD calculations. In preparation of this discussion, could you provide us with a reasonable upper size limit on MD calculations in the for seeable future ?

A :

1- Assume a very simple molecular interaction that has the basic features of the interaction and parameters are fit to experiment (similar to early approaches in gas phase cellular structure calculations.)

2 - If we have a system that's 0.1 * 0.1 * 0.5 m^3, need $8*10^7$ particles (OK!) and 13 Gbytes memory (OK!)

3 - If need about 100 s/timestep, and a detonation travels $5*10^5$ cm/s, currently need 300 hours of computer time. In 5 years (may be), with teraflop speeds, will need 15 hours (OK!)

4 - But this implies energy release must occur in about $1/20*0.1\ \mu = 5*10^{-7}$ cm ∿10 unit cells !
This is probably not reasonable.
5 - We need to have about a micron, I think, not 0.1 μ. I think we need to consider a series of models to get us through the scales problem.
6 - This says nothing about thermal ignition - just shocks.

CONCLUSION

Chairman ; Jacques Boileau

Some suggestions on experimental ways to explore in Detonics

I personnaly think, to go farther more quickly in the detonation mechanisms understanding, that it is necessary to imagine and to build experiments as simple and unsophisticated as possible, in order to ascertain an idea or to verify an hypothesis or a theory ; it is necessary to avoid to mean : I have a high sophisticated apparatus (or I may obtain it) : what can I do with it ?

So it is possible to save money and time.

In this mind, I present you four suggestions :

1- The synchronization between initiation phenomena and usable subnanosecond observation methods, e.g. with a subpicosecond laser :

Two ways may to be conceived, to monitor the both simultaneously :

- a unique detonation source

- a unique laser pulse source

***Unique detonation source** : it seems to be difficult to obtain with a detonator a precise management of the laser emission in the right timing to observe the detonation phenomena (delays : Kerr cells or Pockels door seem to be not precise enough) (Is it true ?)*

***Unique laser pulse source** : to initiate and to observe with a good synchronization.*

A laser pulse could correctly initiate some explosives, but is it the same mechanisms than by shock ? (e.g. mixtures CH_3NO_2 - HN_3). To avoid this objection, it is necessary to find a precise and reproductible shock initiation by a laser pulse at the picosecond level : by slapper ? by surdetonation ? by gaseous mixture detonation ?

It may be possible to imagine a liquid explosive initiation device, by a laser initiated detonation of a gaseous mixture acetylene - oxygen. This device must be in vertical position (fig. 1) to obtain the direct contact of the gaseous detonation wave and the liquid.

2 - Precise and fixed localization of the detonation phenomena

It seems to be interesting, and often cheap, to use a Dautriche-type differential arrangement, giving a shock between two quasi-planar detonation waves, with a precise location : an unique

detonator initiates a high precision explosive cord, which is splitted in two ways ; both initiate at both ends a tube containing a liquid high explosive, producing the formation of two quasi-planar waves running in opposite direction, and collide at a precise shockpoint (possible precision 0.2 mm ?). (fig 2)

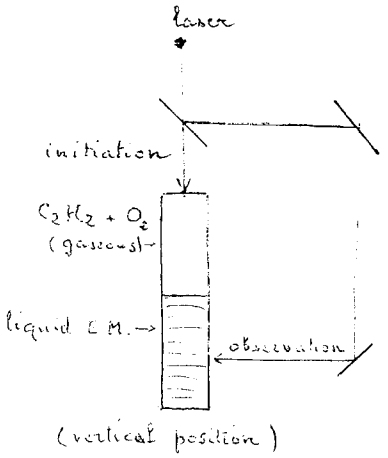

Fig 1

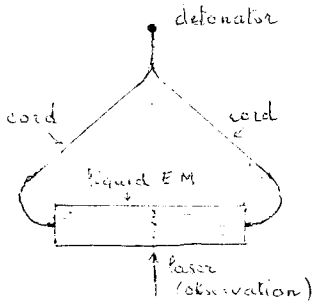

Fig 2

Consequently, the laserbeam used for observation can be located with precision, and it would be possible to observe at this fixed point the sequence of the colliding, especially before the detonation fronts. The study in-time of the pop-plot, of the effect of a curvature of the detonation front may be possible. If necessary, for instance for high precision (picosecond measurements), it is possible to combine this device with the precedent, with for the liquid explosive a vertical U-tube, and for the gaseous mixture an inverted - Y - shaped tube, with laser initiation.

3 - Choice of the EM (if liquid)

- If a large critical diameter is allowed, nitromethane. If it is necessary to use a product with a small critical diameter, I suggest to try NEN nitroethylnitrate : $O_2NCH_2CH_2ONO_2$.

NEN is a liquid easy to obtain (for instance by nitration of nitroethanol) with fair purity by distillation, stable, middle sensitive, and probably with a low critical diameter (I did not measure it, the properties are not far from nitroglycerine or glycoldinitrate in some extend). This product has both linkages C-NO_2 (so as nitromethane) and O-NO_2. Perhaps it can be sensitized by traces of amines (to verify, verify also if the stability is lowered with these traces).

- With nitromethane, it is interesting to study mixtures with ethylnitrate (EN) $H_3CCH_2ONO_2$; this energetic liquid material is relatively not very sensitive, in contradistinction to methyl nitrate, to be totally avoided. Pure EN is probably not sensitized by amines (to verify). Are the mixtures EN-nitromethane sensitized by amines ? May a sensitization occur with an

addition of x% molar nitromethane + x% molar triethyl amine ? Target : is nitromethane in form of clusters, does a complex nitromethane-amine exist ? If yes, how the dispersion of the complex or the clusters occurs inside the EN ? It is necessary to work with tertiary amines, to avoid H-N linkages. What does occur with other tertiary amines, e.g. tristearylamine (steric hindrance ?).
What does occur when we add some HN_3 (hydrogen azide) (1) to nitromethane ? Sensitization ?
The potential curves of HN_3 in fundamental and electronic excited states are known, one of them is a dissociative triplet which crosses the fundamental one and may be populated under shock. Because HN_3 is a very sensitive liquid (BP. 37°C) which may explode if one introduces a needle quietly through the surface of the liquid, does the surface tension energy play a role ? (a two-dimension effect ?). What properties vary linearly with the composition of binary mixtures CH_3NO_2 - HN_3 ?
Is it an interaction between nitromethane and cryptands (a kind of tertiary amines) with sensitization ? Quid with the 2.2.2 cryptand with Na inside the cryptand ?
According to the results, quid with NEN + cryptands ?
(1) H.D.Fair and R.F.Walker : Energetic Materials I, 25 (1977) Plenum Press.

4 - <u>Detonation mechanisms in biphasic v/s monophasic energetic materials</u>
The goal is to study the influence of surfaces and interfaces on detonation. I suggest the study of a <u>same</u> energetic material (explosive) existing in two forms, biphasic (crystals embedded in a binder), or monophasic (the same crystals in the same proportion, but so tiny that they become nanocrystals or disappear in an X-rays Debye-Scherrer spectrum) ; this monophasic material is often transparent.
Exemples : polyvinylnitrate + PETN or RDX.
(Recently, I heard that such kinds of monophasic transparent mixtures were prepared by Dr.H.Licht (ISL, Saint Louis) some years ago, with a nitramine and an energetic binder)..
The idea is to verify, perhaps by differential methods, what is changing when with a same composition, we go from a biphasic to a monophasic system.
It may be a way to understand the detonation mechanisms in non-ideal explosives, e.g. containing ammonium nitrate, when this product becomes ultratiny (nanometric size).

Dick : Summary comments
I believe that this has been a very good meeting with the free exchange of many viewpoints and presentation of much good work on microscopic and macroscopic aspects of initiation and detonation of explosives. It was especially good to have presentations by workers from other fields of research. This brought new ideas to our field. The concept of soliton-like focussing or localization presented by Dave Brown seems especially intriguing. It might be worth pursuing whether this has application to shock and detonation waves. In general anharmonic, nonlinear processes may be very important for initiating molecular decomposition in detonations.

Anatoly Dremin presented his hypothesis that nonequilibrium excitation of explosive molecules occurs in the detonation shock wave. This is followed by reaction of these excited molecules with other neutral molecules behind the front. This is a modification of the Zeldovich or ZND model. I agree with this hypothesis of excitations occuring in the shock wave. Furthermore, I believe that the mechanism of excitation is the sterically hindered shear process that has explained the orientation-dependence of shock sensitivity of PETN monocrystals. This process occurs due to the uniaxial strain of a plane shock wave. It assumes that the strength of the explosive is still important at detonation pressure. In other materials it has been shown that the strength of a solid increases as the shock strength increases. Measurements of the melting temperature of explosives as a function of pressure using static high pressure techniques would be helpful in determining details of the mechanism and importance of deformation. Very little information of this kind exists.

The conventional viewpoint is that molecular excitation and bond breaking occur by thermal processes. However, in our studies of initiation of PETN monocrystals we found that fluorescence from excited electronic states began immediatly at the onset of the plastic wave with a time resolution of a few nanoseconds. Furthermore, our estimate of the speed of molecular deformation in the sterically hindered shear is that large deformations occur on times scales of the order of 50 femtoseconds.These observations lead us to believe in that direct electronic excitation in the shock wave may occur, even though this requires much more energy than thermal excitation.

Elaine Oran gave an assessment of the possibility of using molecular dynamics computations to model "real" materials given an estimate of the size and speed of computers in the forseeable future. I would like to reinforce that in noting that the shear process at 45 degrees to the shock is suppressed by the periodic boundary conditions for small computation sizes. Brad Holian at Los Alamos has found that a computation about 1000 unit cells wide was needed before dislocations were nucleated at 45 degrees of the shock in a perfect lattice. Smaller computations using an imperfect lattice, containing voids for example, can still probably give useful insights on deformation processes.

I conclude with a few small observations. (1) In general in the response of explosives to shock waves we are concerned with two regimes, initiation and detonation. The detailed physical mechanisms may be different in the two cases. (2) We must remember that we stand on a foundation of thermodynamics and hydrodynamics. This can keep us from going in unproductive directions. (3) I have optimism that by doing research combining shock wave experiments, static high-pressure experiments, and theory good progress on understanding initiation and detonation on a more detailed level will be made.

I express my gratitude to the organizers of the workshop, especially Mme Odiot, for bringing together such a fine group of workers from a number of countries for an intensive interaction on these subjects.

Questions and Recommendations

Dick :
Does the shock and shear process cause the excited state ?

Delpuech : We have listened to many propositions of theoretical models at the molecular level. I think that the question for the next years is to obtain experimental informations in order to valid these models.
The question is what are the possibilities of picosecond spectroscopies ?
How is it possible to use these technics in front shock with the problem of chronometry ?
The first step to get over is perhaps to use these technics in lab at high static pressure and high temperature. It's very hard but how extrapolate results obtained at room temperature and at atmospheric pressure ?

Pivina *a comment to Delpuech* : I do not agree with the statement by Alain Delpuech that now we have the model describing the detonation phenomenon at the micro-level and the problem reduces only to finding an adequate experiment.
In my opinion, we only know some details, some aspect of this phenomenon at the macro-level and we believe that these details can be connected with some characteristics of molecular systems at the micro-level.
Generally, it seems to me that here we speak in different languages about what we mean by these different levels. Therefore, I am thankful to Dr Cheret for his comment to my poster session report about necessity to use the definitions of so to say "meso"- level for connection of the notions and models at these different levels.

Ramsay to Delpuech
It is essential that, the theorist and the experimentalist cooperatively design experiments and calculations to determine where agreement and differences occur. Future meetings could examine the results of comparisons between experiments with condensed phase explosives and calculational parameter studies.

Melius : What is temperature being developed in 100 nanosecond time scale just before ignition in a detonation process ?

Van der Steen : I would like to stress that in obtaining experimental proof for the many models presented this week it is essential to do these experiments on very well defined solid materials. Experiments have shown that sensitivity could be shifted by an order of magnitude for the same material with different defect structures.

Odiot *a comment to Van der Steen* : According to Califano's study on isotopic impurity effects, impurities, defect structures modify energy exhange ways in solid phase and sensitivity may be shifted.

Coffey : What kind of timeframes, temperatures and pressures exist in shear bands as a mechanistic process to detonation ?
What can we learn from comparing the detonation of solids, liquids, and gases ?

Borisov : How can we correlate the ZND model with 3-D calculations to 2-D calculations at least? I would like to make three suggestions for future studies.

The first concerns steady-state gaseous and two phase detonations. Since many people still use the ZND model for explaining most of their observations, because of its simplicity, we have to build a bridge between the ZND model and truly three-dimensional calculations of cellular detonation waves. This can be achieved by averaging the calculated parameters over the tube cross section and by deriving the correlation between the pure chemical effects and the effective quasi-onedimensional heat release profiles behind (and within) the detonation front. This will enable one to modify the heat release kinetics to obtain reasonably accurate results in ZND calculations of the wave structure and the critical phenomena.

The second suggestion pertains to DDT processes in gases and two-phases (dusty gases and sprays) media. This is an essencially three-dimensional process. The models for starting and terminal parts of this process (turbulent flame and detonation) are well developed and the computation results are available. But the range between these two parts of the transient process is studied extremely poorly (particularly by computation modeling). Development of a proper model for incipient detonation from hot spots surrounded by the mixture with the needed temperature gradients based on the physical principles (the nature of which is quite known) will shed light on this complicated process and lead to a closed model providing adequate quantitative results. So, we need a good computational model (three- or at least two-dimensional) capable of predicting formation of hot spots and reactive shock development from them.

Finally, I would like to suggest the computer modellers to start studies at DDT phenomena in solids in three-dimensional formulation. Because the processes responsible for DDT comprise accelerated convective burning behind the compaction wave, and formation, development and decay of hot spots, fragmentation of the material by penetrating gases or by combustion products which are three-dimensional, we badly need this model to support quantitatively the qualitative conclusions derived from quasi-onedimensional calculations.

S.Zeman and P.Vavra

The workshop gave very good summary of contemporary ideas about phenomena present in front of the detonation wave and just behind it. We have found introduced simulating computer programs very useful and helpful in studying these phenomena. We suppose that this approach

could help to clarify the influence and role of induction period before front of the detonation wave (i.e. Dremin's induction period) : according to one from us (1) the primary fragments of an explosive produced by endothermic homolysis in this period. The character and amount of these fragments can significantly influence the process and kinetics of reactions in reaction zone of the detonation wave, i.e. they can influence the detonation course (2). For instance, F.E.Walker's results from his study (3) on diethylenetriamine influence on initiation and detonation of nitromethane (*about homolysis of nitromethane and its aci-form see re.4*) may be well interpreted on the basis of above-mentioned idea.

Construction of a model describing the initiation of detonation based on phenomena in liquids (*on example in nitromethane*) or in ideal crystals (*for example PETN*) is primary necessary. On the assumption, that initiation mechanism is unchanging, this model should be suitable even for other, non-homogeneous setting (*i.e. ANFO, emulsions-*). For facility of this problem solution two basic systems should be recognized here :

- individual energetic material (*RDX, TNT, PETN etc*)
- mixture oxidizer-fuel

The phenomena in the front of detonation wave, in these different systems, will probably be also different. Dividing line between these two systems could be represented by intramolecular explosives (*i.e. eutectics on the basis of ammonium nitrate*).

The workshop was very inspiring and all of us were quite impressed. We would like to put emphasis on three topics we are concentrated now :

a) clarification of relationship between low-temperature thermolysis and detonation phenomena of individual explosives ;

b) detailed observation of the relationship between structure of energetic materials and their initiation pressure ;

c) the relationship between molecular structure of the individual explosives and their explosive properties, especially sensitivity to various external stimuli.

We suppose that some of found relation would be convenient for construction of some of detonation initiation micro-models.

1 . S.ZEMAN, M.DIMUN and S.TRUCHLIK : *The relationship between Kinetic Data of the Low-Temperature Thermolysis and the Heats of Explosion of organic Polynitro Compounds.* Thermochim. Acta 78, 181-209 (1984).

2 . S.ODIOT : *The detonation Study in the Microscopic Level.* Khim.Fiz. 12, 684-693 (1993)

3 . F.E.WALKER : *Initiation and Detonation Studies in Sensitized Nitromethane.* Acta Astronautica 6, 807-813 (1979)

4 . S.ZEMAN : *New Application of Kinetic Data of the Low-Temperature Thermolysis of Nitroparaffins.* Thermochim. Acta (1995) - in press.

Boileau : Proposals for the future

I give here a short summary of some proposals presented by the participants.

- Promote a better mutual understanding between theoreticians and experimentalists.
- At the experimental level, improve the ultrashort (e.g. picosecond) delays chronometry, for instance in high speed spectroscopy under high pressure and temperature conditions.
- Study the optical aspects of the detonation (light emission) in order to link the results with the theories.
- Study the electrical phenomena linked to the detonation : role of electrons, of electrical charges, dipoles, perhaps cold plasma, with the corresponding measurements.
- Go more deeply in understanding and modeling 3D inside and behind the detonation front.
- Overcome the present limitation in Molecular Dynamics, e.g. boundary conditions, shear bands ...
- Not forget to take into account some more macroscopic phenomena, so as thermo or hydrodynamic ones (e.g. turbulence).
- Have a reflection about an approach by fractals and by percolation theories.
- Extend the studies to biphasic energetic materials (crystalline load with a binder) where the crystal size decreases to nanophases and till a monophasic material. It may be a way to understand the behavior of some non-ideal explosives (e.g. ammonium nitrate explosives).

Armstrong : Topics for "Critical issues to be addressed in the future"

1 - What can be learned from comparisons of detonations in gases, liquids and solids ?

2 - What are the comparative challenges from either a physics, chemistry, mathematics or engineering viewpoint ?

3 - How to obtain more information than comes from "classical shock theory" ?

4 - How to be more specific about electronic vs thermal vs thermomechanical vs mechanical aspects of initiation of detonations ?

Dremin : So the end of our workshop has come. The workshop seems to be not bad. And the feelings or regretment of most if not all of the participators as to the termination of the workshop are in fact some manifestation of the opinion.

Our workshop has definitely shown that detonation wave physical model proposed by hydrodynamic detonation theory needs farther development even for ideal condensed explosives. We have also realized that the development has to be directed to the study of the problem of the

shock mechanical energy transfer to EM's molecules. The study is believed to be the line of the detonation community activity during the next decade. Some hypothesis have been already proposed for the process, however, they are rather qualitative due to the lack of reliable information on EM's molecules behaviour under the shock effect. We need especially experimental information on the problem and in this respect the detonation community can hope that investigations of A.Delpuech's, Y.Gupta's, D.Dlott's, K.Nelson's groups will provide necessary data. Molecular Dynamics simulations of the process are also of great importance for the problem study.

It is a general opinion that private discussions are especially important and interesting during the meetings and we have to be thankful to all our french colleagues who arrange the workshop and gave us this opportunity. At present I'd like to give all of you best wishes of good health and success in your study of the problem.

Odiot : Now that the end has come, I am glad with this work. I want to thank everyone who transformed this workshop into a lively fruitful tribune.

I take the opportunity to thank the C.N.R.S. in the persons of Paul Rigny, one of the chairmen of this meeting, and Claude Cohen-Tannoudji, chairman of "the Atomic and Molecular Physics" commission of the C.N.R.S. to which I belonged, who let me absolutely free to work a long time with happiness on my own research subject choice : "Why does an explosive explode ?"

While I was listening to you, I thought of my first steps in Detonics about twenty years ago. I did not know anything on Detonics but I was familiar with all aspects of molecular crystals and large size molecules.Thus, my quiet walk inside the Detonation field, was extremely free, without any constraint either scientific or administrative. Of course, I considered an Energetic Material as an explosive molecule, as an explosive crystal and I asked myself the following question :

What can differenciate two series of molecules, explosive and non-explosive, two series of molecular crystals, explosive and non-explosive ?

1) By very useable "hand" quantum chemistry calculations (Hückel Method) on such two series of aromatic compounds I could realize that the two series differ strongly only through a high increase of the chemical bond polarity in the first π electronic excited state of the explosive molecule, while no increase appears in the non explosive molecule. I thought that such an electronic excitation could be induced by shock, the initiation, and that the increase of the bond polarity could further intermolecular forces and hence the propagation of the shock wave by a cooperative effect inside the crystal.

2) The propagation inside the crystal must also be easier in an explosive than in an inert crystal. Thus we analyzed a lot of cristalline structures of these two series of crystals for comparison. Unquestionably, a chain structure appeared in energetic crystals that we did not find in non energetic crystals. Moreover these chain structures, could explain the anisotropy of the

detonation as well as the steric effect observed in PETN.

3) To obtain a detonation, the chemical bond must dissociate under shock and produce energy to sustain the detonation through chemical reactions, it is all the more efficient since they occur near the shock front i.e.with fast kinetics. I tried to compare the two series of molecules in order to look after a predissociative chemical bond potential, without great success, they had too large size to be calculated accurately in 1980 without the approximations of the semi empirical methods of the theoretical chemistry. But CH_3NO_2, HNF_2, N_3H could be treated very accurately. We calculated the two first ones and found that in nitromethane an exothermic predissociative potential appeared in the first singulet excited electronic state, while for difluoramine as well as for hydrogen azide this kind of potential appeared in the ground state crossed by the first dissociative triplet, that could explain the high sensitivity difference of nitromethane on one hand and the two other compounds on the other hand.

4) Electronic excitation, predissociative intramolecular potentials and chain crystalline structure have been the fundations to build a model for propagating a detonation in a molecular crystal like nitromethane by molecular dynamics.With the help of Michel Peyrard, specialist of soliton propagation in crystals and numerical simulations by molecular dynamics, we could propose a 1D and a 2D model. This last one was rich enough to observe a "window" showing the three main regions, initial state in front of the shock wave, then induction zone where can be seen the intramolecular C-N bond deformations followed by the first dissociations called reaction front and the reaction zone, where most of the C-N bonds are broken and chemical energy transfer may occur. It can be observed that dissociation end follows the shock front with very little delay. This structure of shock detonation wave is compatible with the present Dremin's pressure profile of shock detonation wave ; shock front, sharp increase of pressure, endothermic zone, soft increase of pressure, exothermic zone, regular decrease of pressure.

I allowed me some time to comment on my works. Why ? Of course the obvious pleasure of speaking of oneself ! But above all to transmit my own conclusion.

This naive simple microscopic approach to detonation, founded on theoretical comparison between explosive and non explosive molecules or crystals, gave "a priori" macroscopic concepts in agreement with previous Delpuech's conclusions founded on correlations and experiments, with experimental observation of shock induced polarization of Presles, with works of Samirant and Dick on the anisotropy of detonation. It means that this approach seems fruitful.

Thus for the next decade, where much work has to be devoted to study deeply the EM's molecules behaviour under the shock effect, I suggest strongly to study this shock effect on two similar explosive and non explosive molecules. Experimentally by spectroscopy, in real time, and I remember that it is the idea formulated by Rullière in his paper (this workshop) to do this comparison on nitro-stilbene derivaties. Theoretically, nowadays or in the near future, a much

more 'realist' Theoretical Chemistry is able to study carefully excited electronic states, intermolecular potentials and chemistry in these states and one day, shock effect. But one has to pay attention to the size of the choosen compounds for treating them accurately. It means that theoreticians and experimentalists have to think together, even if they work in different laboratories, even in different countries. One of the greatest success of these two workshops 1987 and 1994 has been to build a wall-less Detonics laboratory among our community. The communications between us by Fax or e-mail are so easy to day !

I am sure that one will soon find a strong difference between the shock behaviour of explosive and non explosive molecules, because I am sure that the detonic gene is encoded in the molecule. But which one ?

Nevertheless, it goes without saying that these molecules are also building blocks of the detonation fluid flow, and that with these new microscopic informations in mind, it is always a highly performing hydrodynamics which will lead to the knowledge of the macroscopic effect of detonation.

Good bye.

Author Index

Allen T.M. C4-553
Armstrong R.W. C4-89
Arnautova E.A. C4-505
Bardo R.D. C4-561
Belmas R. C4-61
Bernstein L. C4-461
Boris J.P. C4-609
Borisov A.A. C4-129
Bouton E.C4-49
Braithwaite M. C4-209
Bratos S. C4-283
Brown D.W. C4-461
Brun L. C4-225
Byers Brown W. C4-191
Califano S. C4-279
Cansell F. C4-359? C4-521
Chaisse F. C4-57
Charlet F. C4-407
Chevalier J.M.C4-25
Chung D.D. C4-289
Clavin P. C4-431
Coffey C.S. C4-477
Cook M.D. C4-501
Courtecuisse S. C4-359
Davis W.C. C4-3
Delpeyroux D. C4-521
Delpuech A. C4-379, C4-581
Desbordes D. C4-155
Dhar L. C4-289
Dick J.J. C4-103
Dlott D.D. C4-337
Doyle R.J. C4-417
Dremin A.N. C4-259
Dufort S. C4-303
Dunlap B.I. C4-417
Eloy J.F. C4-379
Fabre D. C4-359, C4-521
Fauquignon C.C4-3
Feng Z. C4-209
Fourkas J.T. C4-289
Gamezo V.N. C4-395
Goldwasser J.M. C4-189
Gupta Y.M. C4-445, C4-553
Haskins P.J. C4-595
He L. C4-431
Jonusauskas G. C4-365
Kasimov A.R. C4-129
Kennedy D.L. C4-191, C4-220
Khasainov B.A. C4-129
Khoroshev S.M. C4-395
Klein R. C4-443
Kondrikov B.N. C4-163, C4-395
Kosenkov V. C4-129
Kozak G.D. C4-395
Lafon C. C4-521
Mathieu D. C4-521
McAfee J.M. C4-179
Mel'nichuk O.I. C4-129
Melius C.F. C4-535
Miller R.S. C4-189
Molchanova M.S. C4-505
Nelson K.A. C4-289
Oran E.S. C4-609
Petitet J.P. C4-359, C4-521
Pivina T.S. C4-505
Plotard J.P. C4-61
Presles H.N. C4-49, C4-143
Rajchenbach C. C4-365
Rice J.K. C4-553
Rulliere C. C4-365
Russell T.P. C4-553
Sanderson A.J. C4-573
Shackelford S.A. C4-485
Shcherbukhin V.V. C4-505
Simonetti Ph. C4-521
Soulard L. C4-599
Swift D.C.C4-37
Troshin K.Ya. C4-129
Turkel M.L. C4-407
van der Steen A. C4-107
Van Tiggelen P.J. C4-127
Vidal P.C4-49, C4-143
Volk F. C4-383
Walker F.E. C4-231, C4-309
Wang W. C4-289
White S.J.C4-37